BRITISH COLUMBIA

Ministry of Energy and Mines
Resource Development Division

Geological Fieldwork 2002

A Summary of Field Activities and Current Research

DOC
BC
G41
D:G4
2002
c.3

Paper 2003-1

LEGISLATIVE LIBRARY OF BRITISH COLUMBIA
3 3298 00274 2485

103-03281/

BRITISH
COLUMBIA

Ministry of Energy and Mines
Resource Development Division
Geological Survey Branch

Paper 2003-1

GEOLOGICAL FIELDWORK 2002

A Summary of Field Activities and Current Research

Geological Survey Branch
New Ventures Branch

LIBRARY
[illegible]
FEB 18 2003

Energy and Minerals Division
Geological Survey Branch

Parts of this publication may be quoted or reproduced if credit is given. The following is the recommended format for referencing individual works contained in this publication:

Mihalynuk, M.G. and Lowe, C. (2003): Atlin TGI Part I: Atlin targeted geoscience initiative - summary of accomplishments and project closure; *in* Geological Fieldwork 2002, *BC Ministry of Energy and Mines*, Paper 2003-1, p. 1-12.

British Columbia Cataloguing in Publication Data

Main entry under title:

Geological Fieldwork: - 1974 -

Annual.

Issuing body varies

Vols. For 1978-1996 issued in series: Paper / British Columbia. Ministry of Energy, Mines and Petroleum Resources; vols for 1997- 1998, Paper / British Columbia. Ministry of Employment and Investment; vols for 1999- , Paper / British Columbia Ministry of Energy and Mines.

Includes Bibliographical references.

ISSN 0381-243X=Geological Fieldwork

1. Geology - British Columbia - Periodicals. 2. Mines and mineral resources - British Columbia - Periodicals. 3. Geology - Fieldwork - Periodicals. 4. Geology, Economic - British Columbia - Periodicals. 5. British Columbia. Geological Survey Branch - Periodicals. I. British Columbia. Geological Division. II. British Columbia. Geological Survey Branch. III. British Columbia. Geological Survey Branch. IV. British Columbia. Dept. of Mines and Petroleum Resources. V. British Columbia. Ministry of Energy, Mines and Petroleum Resources. VI. British Columbia. Ministry of Employment and Investment. VII. British Columbia Ministry of Energy and Mines. VIII. Series: Paper (British Columbia. Ministry of Energy, Mines and Petroleum Resources). IX. Series: Paper (British Columbia. Ministry of Employment and Investment). X. Series: Paper (British Columbia Ministry of Energy and

Cover photo by Fil Ferri- Looking northwest near Eaglenest Creek at thick, resistive conglomerate lenses interbedded with sandstone and siltstone within the Eaglenest Assemblage. This unit is part of the Bowser Lake Group and represents deltaic facies. These conglomerates, as with other clastics of the Bowser Lake Group, are composed of chert clasts derived from the Cache Creek Terrane.

VICTORIA
BRITISH COLUMBIA
CANADA

JANUARY 2003

FOREWORD

The British Columbia Ministry of Energy and Mines annually publishes **Geological Fieldwork: a Summary of Fieldwork and Current Research** to present the results of provincial geoscience surveys completed in the previous year. This is the twenty-eighth edition. British Columbia Geological Survey staff contribute most of the articles in the volume. This year, the Ministry's New Ventures Branch provided articles on energy-related topics, in addition to those articles contributed by Geological Survey of Canada, university and industry authors.

This year's volume is shorter than those published in recent years, reflecting reduced government funding for geoscience field activities. The Ministry initiated formal partnership programs with industry in 2002 to partially address this problem. These private-public partnerships have produced four articles and additional data will be released as separate publications later this year. As in previous years, the Geological Survey of Canada was a strong partner with respect to field surveys. Their staff have co-authored or written seven of the articles, which discuss results from major projects in the Atlin, Bella Coola and Bowser Basin areas of the province. Eight articles on energy and industrial minerals complete the volume. Some of the highlights of this year's volume are:

- Reports on bedrock mapping activity from the Atlin and Bella Coola projects completed jointly with the Geological Survey of Canada as part of their Targeted Geoscience Initiative.
- A description and interpretation of the Joss'alun mineral occurrence discovered by a Ministry of Energy and Mines field crew, which led to a mini-staking rush in the northwest.
- Discussions of the styles of gold mineralization on the Axelgold, Hawk and Kena gold properties with comments regarding regional exploration implications.
- The identification of mineral exploration targets using the recently released, Regional Geochemical Survey data from the Bella Coola area, another Targeted Geoscience Initiative co-funded by the Geological Survey of Canada.
- An extension of new stratigraphic and structural interpretations for the Snowshoe Group from the Cariboo Lake area into the Wells gold mining camp.
- An overview of the coalbed methane potential of British Columbia's Tertiary basins.
- A review of potential CO_2 sequestration techniques.
- Preliminary description and characterization of live oil staining in Bowser Lake sediments.

Over the past year the Ministry of Energy and Mines published 2 new bulletins, 16 Open Files including three maps covering the Ecstall belt near Prince Rupert, 4 new Geoscience Maps, Exploration and Mining in BC 2001, 2 Regional Geochemistry Survey data releases, 7 GeoFiles and other brochures and products. The British Columbia Geological Survey also continued to improve and add new data layers and features to MapPlace, its web-based interactive mapping system.

A former employee of the British Columbia Geological Survey Branch, Dr. Trygve Höy, received the Provincial Geologists Medal in 2002 in recognition of a career devoted to documenting and deciphering the geology of southeastern British Columbia. This medal is awarded to recognize major contributions to geoscience research by a staff member of a provincial or territorial survey. Trygve Höy is the first British Columbian and only the fourth recipient of this prestigious national award. During his 28 years with the British Columbia Geological Survey he was a prolific producer of maps and insightful scientific reports that have illuminated our understanding of the geology and mineral deposits of the southeastern Canadian Cordillera.

Our thanks to all the authors whose professional skills in the field and office make this publication possible. The articles have been improved by peer and management review. Special thanks go to Janet Holland and Brian Grant who combine their publications duties with many other responsibilities and have worked long hours to meet difficult deadlines.

Dave Lefebure
A/Director – Chief Geologist
BC Geological Survey

TABLE OF CONTENTS

MAPPING

ATLIN

M.G. Mihalynuk and C. Lowe: Atlin TGI, Part I: Atlin Targeted Geoscience Initiative - Summary of Accomplishments and Project Closure 1

M.G. Mihalynuk, S.T. Johnston, J.M. English, F. Cordey, M.E. Villeneuve, L. Rui and M.J. Orchard: Atlin TGI, Part II: Regional Geology and Mineralization of the Nakina Area 9

M.G. Mihalynuk, E. Villeneuve and F. Cordey: Atlin TGI, Part III: Geological Setting and Style of Mineralization at the Joss'alun Occurrence, Atlin Area 39

A. Bath: Atlin TGI, Part IV: Middle Jurassic Granitic Plutons Within the Cache Creek Terrane and their Aureoles: Implications for Terrane Emplacement and Subsequent Deformation 51

H. Sano, T. Igawa and T. Onoue: Atlin TGI, Part V: Carbonate and Siliceous Rocks of the Cache Creek Terrane, Southern Sentinel Mountain 57

BELLA COOLA

L.J. Diakow, J.B. Mahoney, J.W. Haggart, G.J. Woodsworth, S.M. Gordee, L.D. Snyder, T.P. Poulton, R.M. Friedman and M. Villeneuve: Geology of the Eastern Bella Coola Map Area, West-Central British Columbia 65

BARKERVILLE

P. Schiarizza and F. Ferri: Barkerville Terrane, Cariboo Lake to Wells: A New Look at Stratigraphy, Structure and Regional Correlations of the Snowshoe Group 77

ECONOMIC GEOLOGY

J. Nelson, R. Carmichael and M. Gray: Innovative Gold Targets in the Pinchi Fault/Hogem Batholith Area: The Hawk and Axelgold Properties, Central British Columbia 97

G.T. Nixon: Use of Spinel in Mineral Exploration: The Enigmatic Giant Mascot Ni-Cu-PGE Deposit - Possible Ties to Wrangellia and Metallogenic Significance 107

J.M. Logan: Iron Mask Project, Kamloops Area 129

J.M. Logan: Kena Mountain Gold Zone, Southern British Columbia 139

R. Lett and P. Friske: National Geochemical Reconnaissance Surveys in the BC Cordillera Identify New Mineral Exploration Targets 155

INDUSTRIAL MINERALS

M. Bustillo and G.J. Simandl: Marilla Perlite - Volcanic Glass Occurrence, British Columbia 169

Z.D. Hora: Feldspathic Sandstone Flagstone from Near Hudson Hope, Northern British Columbia - Potential for Sandstone Production in British Columbia 175

ENERGY

J.M. English, M.G. Mihalynuk, S.T. Johnston, M.J. Orchard, M. Fowler and L.J. Leonard: Atlin TGI, Part VI: Early to Middle Jurassic Sedimentation, Deformation and a Preliminary Assessment of Hydrocarbon Potential, Central Whitehorse Trough and Northern Cache Creek Terrane 187

B. Ryan: Pseudovitrinite: Possible Implications for Gas Saturation in Coals and Surrounding Rocks 205

B. Ryan: Overview of the Coalbed Methane Potential of Tertiary Coal Basins in the Interior of British Columbia 215

B. Ryan: Cleat Development in Some British Columbia Coals 237

K.G. Osadetz, C.A. Evenchick, F. Ferri, L.D. Stasiuk and N.S.F. Wilson: Indications for Effective Petroleum Systems in Bowser and Sustut Basins, North-Central British Columbia 257

D.A. Voormeij and G.J. Simandl: Geological and Mineral CO_2 Sequestration Options: A Technical Review 265

Atlin TGI, Part I: Atlin Targeted Geoscience Initiative - Summary of Accomplishments and Project Closure

By Mitchell G. Mihalynuk[1] and Carmel Lowe[2]

KEYWORDS: Geology, aeromagnetic survey, mineral potential, hydrocarbon, organic maturation, coal, volcanogenic massive sulphide, placer-related gold, geochemistry, fossil, geochronology, Cache Creek Terrane, Atlin, Yukon.

INTRODUCTION

A third and final season of geoscience field studies under the aegis of the Targeted Geoscience Initiative (TGI) was completed in the Atlin area in 2002. Jointly funded by the federal and provincial governments, the TGI is designed to deliver timely, high-quality geoscience data as a lasting stimulus for mineral resource exploration and economic development. The Atlin region was selected from other national proposals for three principal reasons: the regional economy is mineral resource dependent, with a single commodity focus on placer gold; the existing regional geological framework predates plate tectonic theory; and the area is well endowed with geological environments prospective for other types of mineral deposits.

TGI geoscience data collection began in 2000 with a federally funded, high-resolution aeromagnetic survey covering the entire project area (GSC 2001; Figure 1). Joint federal and provincially supported mapping studies began in 2001. Aided by the aeromagnetic data, mapping provided on-the-ground evaluation of geological environments for their potential to host different deposit types, for example, volcanogenic massive sulphide accumulations. Proof of concept is in the discovery of a magnetite [illegible] in 2001, and in 2002, semi-massive pyrite-chalcopyrite lenses (see Sure Shot occurrence in TGI, Part III, this volume).

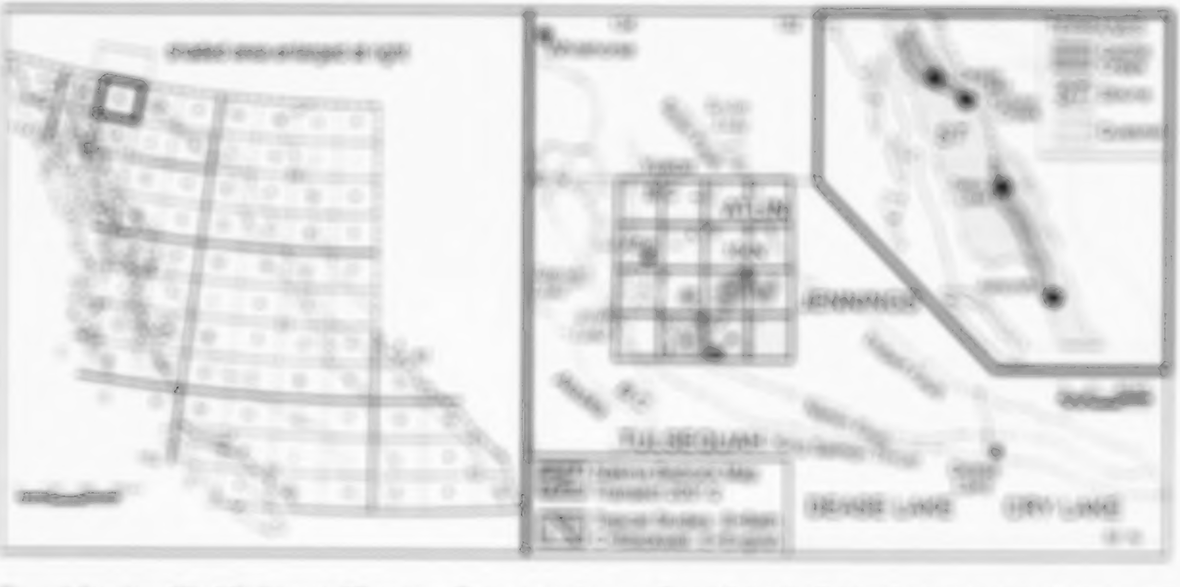

Figure 1. Location of the Atlin Integrated Geoscience Project in northwestern British Columbia. [illegible]

---

[1] BC Geological Survey Branch
Mitch.Mihalynuk@gems1.gov.bc.ca

[2] Geological Survey of Canada, Sidney, BC

[illegible]
[illegible]
[illegible]

[illegible]	[illegible]	[illegible]	[illegible]
[illegible]	[illegible]	[illegible]	[illegible]
[illegible]	[illegible]	[illegible]	[illegible]
[illegible]	[illegible]	[illegible]	[illegible]
[illegible]	[illegible]	[illegible]	[illegible]
[illegible]	[illegible]	[illegible]	[illegible]
[illegible]	[illegible]	[illegible]	[illegible]
[illegible]	[illegible]	[illegible]	[illegible]
[illegible]	[illegible]	[illegible]	[illegible]
[illegible]	[illegible]	[illegible]	[illegible]
[illegible]	[illegible]	[illegible]	[illegible]
[illegible]	[illegible]	[illegible]	[illegible]
[illegible]	[illegible]	[illegible]	[illegible]
[illegible]	[illegible]	[illegible]	[illegible]
[illegible]	[illegible]	[illegible]	[illegible]
[illegible]	[illegible]	[illegible]	[illegible]
[illegible]	[illegible]	[illegible]	[illegible]
[illegible]	[illegible]	[illegible]	[illegible]
[illegible]	[illegible]	[illegible]	[illegible]
[illegible]	[illegible]	[illegible]	[illegible]
[illegible]	[illegible]	[illegible]	[illegible]
[illegible]	[illegible]	[illegible]	[illegible]
[illegible]	[illegible]	[illegible]	[illegible]

[illegible]

[illegible]	[illegible]	[illegible]	[illegible]	[illegible]
[illegible]	[illegible]	[illegible]	[illegible]	[illegible]
[illegible]	[illegible]	[illegible]	[illegible]	[illegible]
[illegible]	[illegible]	[illegible]	[illegible]	[illegible]
[illegible]	[illegible]	[illegible]	[illegible]	[illegible]
[illegible]	[illegible]	[illegible]	[illegible]	[illegible]
[illegible]	[illegible]	[illegible]	[illegible]	[illegible]
[illegible]	[illegible]	[illegible]	[illegible]	[illegible]

[illegible]

[illegible]

[illegible]

[illegible]

- [illegible]
- [illegible]
- [illegible]

[illegible]

[illegible]

[illegible]

[illegible]

Provincial funding had less impact on portions of the program that relied only on federal funding. Carmel Lowe continued to synthesize and model the aeromagnetic data set collected in 2000 and 2001, and Bob Anderson conducted a field evaluation of magnetic bodies with more than 40 traverses.

MAP COVERAGE AND HIGHLIGHTS

A second season of mapping the Nakina Transect (104N/1, 2 & 3) permitted complete coverage of Mapsheet 104N/2 and about 75% of 104N/3 (Figure 2). Incomplete areas include the river valleys of the Nakonake, the Nakina, below its confluence with the Silver Salmon River, and the Sloko, downstream of the Nakonake River. Incomplete coverage also exists in lower Goldbottom Creek (above and below "Psychobear Ridge", note that informal names appear in quotes), the western slopes of Chikoida Mountain, and the alpine area west of an unnamed peak in southwest 104N/2.

Highlights of the mapping and preliminary analysis of samples include:

- discovery of massive sulphide mineralization at the Joss'alun occurrence. Apparently stratiform sulphide lenses occur within a pillow basalt succession that is interbedded with Permian chert along strike and overlain by a coarse clastic unit containing chert breccia fragments of Middle Triassic age and sandstone containing Permian zircons (Mihalynuk *et al.*, 2003b; Figure 2, star).
- an increase in the width of the serpentinite melange belt extending it to the northeast, almost as far as the Silver Salmon River (Figure 2 diagonal hatch west of Silver Salmon River).
- recognition of intense thrust repetition of strata in the canyon walls of Tayana Creek, "Tumblepack Creek" and Nakina River of northeast 104N/2W (Figure 2, highlighted creek sections).
- discovery of a broad zone of quartz-sericite-pyrite alteration in siliceous argillaceous strata exposed along upper "Tumblepack Creek" (Figure 2, solid box).
- preliminary hydrocarbon assessment of the southern Whitehorse Trough (English *et al.*, 2003, this volume).
- recognition of a magnetic unit within the Laberge Group (SI ~15-25 x 10^{-3}). This unit includes several percent orange garnet as well as sparse, fresh olivine crystals. It may record exposure of the Cache Creek mantle during Cache Creek emplacement (Figure 2, stippled belt).

Geological setting, stylized stratigraphy, isotopic and micropaleontologic age, and chemical analyses from the Joss'alun occurrence and environs are presented in greater detail in Atlin TGI, Part III (Mihalynuk *et al.*, 2003b, *this volume*). Details of Nakina Transect mapping results, micropaleontological and isotopic age, and lithogeochemical and stream sediment data are presented in TGI, Part II (Mihalynuk *et al.*, 2003a, this volume).

MAGNETIC SURVEY STUDIES

Approximately 12 000 line-kilometres of aeromagnetic data covering the entire Atlin 104N mapsheet were collected as part of the regional aeromagnetic survey in 2000 and early 2001 (for survey parameters and details see Lowe and Anderson, 2002). Survey results have been published at 1:50 000 scale as a series of sixteen aeromagnetic anomaly maps (Dumont *et al.*, 2001a, b, c and 13 others). The survey benefited from augmentation by magnetic susceptibility measurements taken in the field during the course of geological mapping.

One of the most striking features of the aeromagnetic data set is a strong positive aeromagnetic anomaly that extends far northeast of the previously mapped extent of ultramafic rocks. A two-dimensional model of magnetic data (Lowe *et al.*, 2002a) showed that the observed data could be explained by a series of steeply northeast-dipping, ultra-

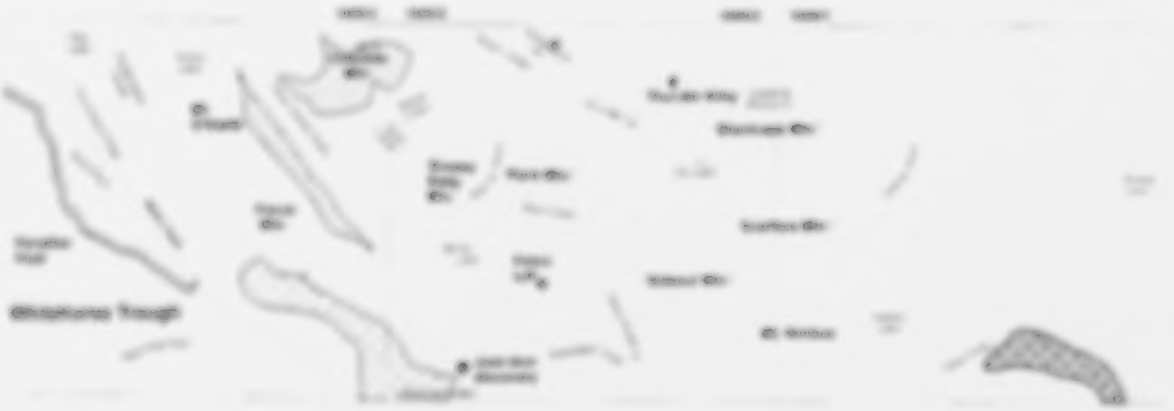

Figure 2. Nakina transect physiographic features, major intrusive bodies (patterned) and serpentinite mélange (diagonal hatch). Symbols show location of mineralized zones.

mafic lenses. Efficacy of modelling was limited by a lack of direct magnetic susceptibility measurements within and adjacent to the ultramafic rocks. To remedy this problem, Lowe and Canil (UVic) sampled and measured magnetic susceptibilities across the Nahlin ultramafic body and adjacent rocks in southwestern 104N/2 (Figure 1). In that area, ultramafic rocks are mainly serpentinized harzburgite, with pods of serpentinized dunite. They demonstrated an expected correlation between magnetic susceptibility and degree of serpentinization. However, the most intense aeromagnetic anomaly values (>2000 nT) correspond with rocks that are only moderately serpentinized at the surface. It would appear that either the ultramafic rocks are more pervasively and intensely serpentinized at depth, or that ultramafic bodies may persist to depths of >7 km. Lowe is now utilizing the new *in situ* susceptibility measurements in constructing a more detailed model to explain the airborne anomalies. New map data also will bear on the model because we now know that ultramafite *DOES* extend farther to the northeast as a series of serpentinite melange belts (Figure 2, hatched area west of Silver Salmon River).

JURASSIC AND CRETACEOUS PLUTONIC ROCKS

Granitoid batholiths and stocks of Jurassic and Cretaceous age are widespread in the Atlin area (Figure 1, shaded). Middle Jurassic bodies are temporally and spatially associated with known lode gold veins (Ash, 2001). According to Ash, the veins are usually near the Middle Jurassic stocks or other high- level intrusions assumed to be comagmatic, but hosted by oceanic crustal rocks, mainly gabbro and diabase, of the Cache Creek terrane. This association is mimicked by regional geochemical stream sediment gold values: most Atlin mapsheet samples that are 90th percentile and above (, are from streams that drain the margins of Middle Jurassic plutons. Despite these encouraging geologic and geochemical relationships, no significant past production (in excess of 1 kg) has been recorded from any gold lode vein discovered thus far in the Atlin camp.

Enrichments of uranium, molybdenum, tin, tungsten, beryllium, fluorine and other granophile elements are typical of the Surprise Lake batholith. Molybdenum in particular, is enriched in a part of the Batholith called the "Mount Leonard Boss" stock (*e.g.* Christopher and Pinsent, 1982). The stock underlies the headwaters of Ruby Creek from which placer gold is recovered (Figure 1); near 'H' in 104N/11.

In 2002, R. Anderson built upon a 2001 reconnaissance study of Middle Jurassic and Cretaceous plutonic bodies (Lowe and Anderson, 2002). Objectives of the study are:

- to map compositional heterogeneity;
- correlate composition with magnetic signature;
- establish timing of different phases;
- look at contacts with deformed Cache Creek country rocks;
- look for alteration and evidence for late-stage magmatic volatiles;
- evaluate their potential for enrichments in gold and granophile elements. In particular, scrutinize plutons where they underlie the headwaters of creeks from which gold placers are won, or from which anomalously high base or precious metal values have been recorded in stream sediment samples.

Work on plutonic rocks was about equally divided between presumed Middle Jurassic bodies originally mapped and named by Aitken (1959) as Mount Llangorse batholith and Mount McMaster stock, and the Surprise Lake batholith of Late Cretaceous age (Christopher and Pinsent, 1982; Mihalynuk *et al.*, 1992).

Modal analyses of the Mount Llangorse batholith by Aitken (1959) show it to be mainly diorite and tonalite. According to Aitken, the core is more felsic than the rim, consistent with a coreward decrease in the aeromagnetic response. Aitken also showed that the country rocks having been shouldered aside by the batholith producing a foliation within the batholith and within the adjacent 1.2km-wide thermal aureole.

Mount McMaster stock (Aitken, 1959) is a composite of irregularly distributed quartz monzodiorite and hornblende-biotite granodiorite and monzogranite. It is unfoliated and more felsic and leucocratic than the Mount Llangorse batholith. Miarolitic cavities occur along one contact. The nearly circular outline of this stock is mimicked by an annular aeromagnetic anomaly.

Surprise Lake batholith is compositionally homogeneous, especially when contrasted with its high degree of textural variability. Overall, it is biotite granite with numerous local concentrations of uranium and other granophile elements (Cu, Zn, Mo, Sn, W). It is the best studied of all intrusions in the Atlin area, due to numerous contained mineral occurrences, including the Adanac molybdenum deposit. Mineralization at Adanac occurs in several phases of the "Mount Leonard Boss" stock, which is separated from the main batholith by a belt of country rocks on its eastern side. Defined, open pit-able reserves at the Adanac deposit are 152 million tonnes grading 0.063% Mo (Christopher and Pinsent, 1982). Most mineralization is associated with porphyritic or megacrystic phases. Miarolitic cavities up to decimetre size are common in scattered zones. Cavities are lined with alkali feldspar, smokey quartz and tourmaline. These features record late vapour phase evolution during high-level emplacement.

Most of the Surprise Lake batholith is characterized by magnetic susceptibility values less than 0.1 x 10-3 SI and correspondingly low magnetic anomaly values. However, a series of northwest-trending magnetic lineaments with peak amplitudes of 20-30 nT is imaged over the eastern portion of the batholith and adjacent aureole (Lowe and Anderson, 2002).

SURFICIAL GEOLOGY AND PLACER POTENTIAL

Despite a focus on geological environments other than placer gold, the TGI program also serviced this mainstay of the Atlin economy. An enhanced surficial geology map of the Atlin mining district was produced on a digital elevation base. It will be formally published in early 2003, together with placer potential information as Levson *et al.* (2003). The map is an updated, coloured and visually enhanced version of an earlier publication by Levson and Kerr (1992). Updates include recent research on the Quaternary geology of the area (Levson and Blyth, 2001); new field and geochemical data bearing on platinum in placer deposits (Levson *et al.*, 2002); and revised map units together with chrono-stratigraphic and surficial materials data. Marginal notes discuss placer gold potential of both buried-channel and Holocene deposits, as well as potential of the bedrock to supply gold for placers.

UNIVERSITY THESIS STUDIES

One measure of Atlin TGI success is the high proportion of student geoscientists who, through the initiative, have pursued theses or directed studies on geological aspects of the Atlin area. Seven of the eight student members of 2001/2002-field mapping crews completed, or are currently working on, advanced study topics under the auspices of the Atlin TGI.

Two thesis studies begun in 2001 were completed in 2002. Y. Merran completed his M.Sc. thesis, supervised by F. Cordey at Université Claude Bernard, entitled Mise en Place et Environnement de depot d'une Plate-Forme Carbonatee Intraoceanique: Exemple du Complexe d'Atlin, Canada (Merran, 2002). Under the supervision of J.Mortensen at The University of British Columbia, F. Devine completed her B.Sc. thesis entitled "U-Pb geochronology, geochemistry and tectonic implications of oceanic rocks in the northern Cache Creek terrane, Nakina area, Northwestern British Columbia" (Devine, 2002). J. English began work on a M.Sc. study in 2001 under supervision of S. Johnston at the University of Victoria. His study of volcanic environments and petrogenesis, has evolved into one component of a Ph.D. on the evolution of the Whitehorse Trough and evaluation of its hydrocarbon potential. Also under the supervision of S.Johnston at the University of Victoria, is a B.Sc. thesis on the structural setting of a gabbro allochthon by J. Blackwell, and a directed study on characterization of aureoles around Middle Jurassic plutons by A. Bath. A Ph.D. thesis study supervised by D. Canil at the University of Victoria, was to compare Cordilleran ultramafites, including the bodies near Atlin. Unfortunately, it has been suspended and Canil is synthesizing the Atlin data collected thus far.

Atlin TGI also supports components of post-doctoral study by T. Igawa and a Ph.D. thesis by T. Onoue, supervised by H. Sano, Kyushu University, Japan. Logistical support has also been provided for 2 M.Sc. theses at The University of British Columbia. L. Hansen, supervised by G. Dipple, is investigating carbonatized ultramafite as a natural analogue for application in industrial *in situ* CO_2 sequestration. M. Harder, under the supervision of K. Russell, initiated an investigation of erosional remnants of Quaternary diatremes and comagmatic pyroclastic and lava flow successions that pepper the Atlin area. One focus of their study is the use of abundant mantle xenoliths as probes of the subcrustal lithosphere (*see* Lowe *et al.*, 2003 for preliminary findings). Table 1 provides a summary of Atlin TGI participants, their affiliations and products.

PUBLIC OUTREACH

Public outreach is recognized as a key component of the Atlin TGI. A public outreach program in the townsite of Atlin began as a series of free public lectures in 2001. In 2002, C. Lowe continued the program with a workshop on the use of handheld magnetic survey devices for fun and profit. Sshe also presented a poster at the PDAC meeting in Toronto in March, 2002 and gave a seminar on the magnetic component of the project in April. Elsewhere, public presentations have been delivered at six venues within and outside Canada. Continued delivery of project results will be by a combination of public lectures, poster sessions and conventional maps and reports (*see* Table 1). Anderson is currently working on Atlin Geoscape, a wall poster product aimed at public education. Geoscape posters have proven to be a popular teaching tool in schools.

PROJECT WRAP-UP

Atlin TGI funding terminates at the end of the 2002/3 fiscal year, in the spring of 2003. In accordance with the original design of TGI programs, all products are to be delivered by that time. It is apparent, however, that not all project generated data will be available for synthesis in time for the spring deadline. In addition, J. English has plans for fieldwork in 2003, as part of his Ph.D. study. Clearly, the rollout of future TGI-generated products will extend past the spring of 2003, with an impact that lasts well beyond.

ACKNOWLEDGMENTS

Success of the Atlin TGI is attributable to the combined efforts of many contributing geoscientists. In 2002, these were: Joe English, Steve Johnston, Adam Bath, Jacqueline Blackwell, Lucinda Leonard and Dante Canil (UVic); Fabrice Cordey (UCB, Lyon); Bob Anderson, Mike Villeneuve, Mike Orchard, Wayne Bamber and Martin Fowler (GSC); Oliver Roenitz (SFU); Lyle Hansen, Margaret Harder and Kelly Russell (UBC); Hiroyoshi Sano, Toshie Igawa and Tetsuji Onoue (Kyushu University); Fionnuala Devine (YGO), and Paul Wojdak (BC MEM). Jim Monger supplied his original field maps, which helped to direct our work.

Heartfelt thanks are owed to the community of Atlin for their unflagging passion for geoscience. More than any single person, the success of the program hinged on our helicopter pilot, Norm Graham of Discovery Helicopters in

Atlin. We regularly entrusted our lives to Norm, in the face of adverse weather and terrain - and he always delivered.

REFERENCES CITED

Aitken, J.D. (1959): Atlin map-area, British Columbia, *Geological Survey of Canada*, Memoir 307, 89 pp.

Bath, A. (2003): Atlin TGI, Part V: Middle Jurassic granitic plutonswithin the Cache Creek terrane and their aureoles: Implications for emplacement and deformation; *in* Geological Fieldwork 2002, *BC Ministry of Energy and Mines*, Paper 2003-1, this volume.

Christopher, P.A. and Pinsent, R.H. (1982): Geology of the Ruby Creek and Boulder Creek area near Atlin (104N/ 11W); *BC Ministry of Energy, Mines and Petroleum Resources*, Preliminary Map, 52, 10 pages.

Cordey, F. (2001): Preliminary report on radiolarians, August 2001, 3 pages (unpublished report).

Cordey, F. (2002):Report on radiolarians, Atlin, winter 2001-2002, 5 pages (unpublished report).

Devine, F. (2002): U-Pb geochronology, geochemistry and tectonic implications of oceanic rocks in the northern Cache Creek terrane, Nakina area, Northwestern British Columbia; unpublished B.Sc. thesis, *The University of British Columbia*, Vancouver, 50 pages.

Dumont, R., Coyle, M. and Potvin, J. (2001a): Aeromagnetic total field map British Columbia: Nakina Lake, NTS 104N/1; *Geological Survey of Canada*, Open File 4091.

Dumont, R., Coyle, M. and Potvin, J. (2001b): Aeromagnetic total field map British Columbia: Nakina, NTS 104N/2; *Geological Survey of Canada*, Open File 4092.

Dumont, R., Coyle, M. and Potvin, J. (2001c): Aeromagnetic total field map British Columbia: Sloko River, NTS 104N/3; *Geological Survey of Canada*, Open File 4093.

English, J.M., Mihalynuk, M.G., Johnston, S.T. and Devine, F.A.M. (2002): Atlin TGI, Part III: Geology and Petrochemistry of Mafic Rocks within the Northern Cache Creek Terrane and Tectonic Implications; *in* Geological Fieldwork 2001; *BC Ministry of Energy and Mines*, Paper 2002-1, pages 19-29.

English, J.M., Mihalynuk, M.G and Johnston, S.T., Orchard, M.J., Fowler, M. and Leonard, L. (2003): Atlin TGI, Part II: Lower to Middle Jurassic sedimentation, deformation and a preliminary assessment of hydrocarbon potential of the central Whitehorse Trough and northern Cache Creek terrane; in Geological Fieldwork 2002; *BC Ministry of Energy and Mines*, Paper 2003-1, this volume.

Jackaman, W. (2000): British Columbia Regional Geochemical Survey, NTS 104N - Atlin; *BC Ministry of Energy and Mines*, BC RGS 51.

Levson, V.M. and Blyth, H. (2001): Formation and preservation of a Tertiary to Pleistocene fluvial gold placer in northwest British Columbia; *Quaternary International*; Volume 82, pages 33-50.

Levson, V.M. and Kerr, D.E. (1992): Surficial geology and placer fold settings of the Atlin - Surprise Lake area, NTS 104N/11, 12; *BC Ministry of Energy and Mines*, Open File 1992-7, Scale 1:50 000.

Levson, V.M., Mate, D. and Ferbey, T. (2002): Platinum-group-element (PGE) placer deposits in British Columbia: characterization and implications for PGE potential; in Geological Fieldwork 2001; *BC Ministry of Energy and Mines*, Paper 2002-1, pages 303-312.

Levson, V. M., Kerr, D.E., Lowe, C. and Blyth, H. (2003): Quaternary geology of the Atlin area, British Columbia; *BC Ministry of Energy and Mines*, Geoscience Map 2003-1, Scale 1: 50 000.

Lowe, C. and Anderson, R.G (2002): Preliminary Interpretations of new aeromagnetic data for the Atlin mpa area, British Columbia; in Current Research; *Geological Survey of Canada*, Paper 2002-A17, pages .

Lowe, C. and Mihalynuk, M.G (2002): The Atlin Integrated Geoscience Project, northwestern British Columbia - an overview; in Current Research, Part A; *Geological Survey of Canada*, Paper 2002-A17, pages .

Lowe, C., Dumont, R., Coyle, M. and Potvin, J. (2002): Interpretation of new aeromagnetic data, Atlin map area (NTS 104N); Cordilleran Exploration Roundup 2002, Vancouver, British Columbia.

Lowe, C., Mihalynuk, M.G., Anderson, R.G , Canil, D., Cordey, F., English, J.M., Harder, M., Johnson, S.T., Orchard, M., Russell, K., Sano, H. and Villeneuve, M. (2003): Atlin TGI Project overview, northwestern British Columbia, year three; *in* Current Research, *Geological Survey of Canada*, Paper 2003-A11, 10 p.

Merran, Y. (2002): Mise en place et environnement de depot d'une plate-forme carbonatee intraoceanique: exemple du complexe d'Atlin, Canada; Université Claude Bernard, Lyon, France, unpublished M.Sc. Thesis.

Mihalynuk, M.G (1999): Geology and Mineral Resources of the Tagish Lake Area; *BC Ministry of Energy and Mines*, Bulletin 105, 117 pages.

Mihalynuk, M.G., Bellefontaine, K.A., Brown, D.A., Logan, J.M., Nelson, J.L., Legun, A.S. and Diakow, L.J. (1996): Geological compilation, northwest British Columbia (NTS 94E, L, M; 104F, G H, I, J, K, L, M, N, O, P; 114J, O, P); *BC Ministry of Energy, Mines and Petroleum Resources*, Open File 1996-11.

Mihalynuk, M.G and Lowe, C. (2002a): Atlin TGI, Part I: An Introduction to the Atlin Targeted Geoscience Initiative; in Geological Fieldwork 2001, *BC Ministry of Energy and Mines*, Paper 2002-1, pages 1-4.

Mihalynuk, M.G., Johnston, S.T., Lowe, C., Cordey, F., Devine, F.A.M., English, J.M., Merran, Y. and Larson, K. (2002b): Atlin TGI Part II: Regional mapping highlights from the Nakina area (104N/1, 2) northwestern BC; *in* Geological Fieldwork 2001; *BC Ministry of Energy and Mines*, Paper 2002-1, pages 5-18.

Mihalynuk, M.G., Johnston, S.T., English, J.M., Cordey, F. Bath, A., Blackwell, J. Villeneuve, M., Roenitz, O., Leonard, L., Devine, F.A.M. and Canil, D. (2003a): TGI Part II: Regional geology and mineralization of the Nakina area, (NTS 104N/2W and 3); *in* Geological Fieldwork, *BC Ministry of Energy and Mines*, Paper 2003-1, this volume.

Mihalynuk, M.G., Cordey, F., Villeneuve, M. and Devine, F.A.M. (2003b): TGI Part III: Geological setting of Massive Sulphide mineralization at the Joss'alun occurrence; *in* Geological Fieldwork, *BC Ministry of Energy and Mines*, Paper 2003-1, this volume.

Monger, J.W.H. (1975): Upper Paleozoic rocks of the Atlin Terrane, northwest British Columbia and south-central Yukon, *Geological Survey of Canada*, Paper 74-47, 63 pages.

Nassichuk, W.W. (1975): Upper Permian ammonoids from the Cache Creek Group in western Canada; *Journal of Paleontology*, Volume 51, pages 557-590.

Orchard, M.J., Cordey, F., Rui, L., Bamber, E.W., Mamet, B., Struik, L.C., Sano, H. and Taylor, H.J. (2001): Biostratigraphic and biogeographic constraints on the Carboniferous to Jurassic Cache Creek Terrane in central British Columbia; *Canadian Journal of Earth Sciences*, Volume 38, pages 551-578.

Atlin TGI, Part II: Regional Geology and Mineralization of the Nakina Area (NTS 104N/2W and 3)

By Mitchell G. Mihalynuk[1], Stephen T. Johnston[2], Joseph M. English[2], Fabrice Cordey[3], Michael E. Villeneuve[4], Lin Rui[5] and Michael J. Orchard[6]

KEYWORDS: Geology, mineralization, volcanogenic massive sulphide, exhalite, sepiolite, talc, geochronology, fusulinacean, radiolarian, fossil, aeromagnetic survey, Cache Creek terrane, Nahlin fault, Nakina, Atlin.

INTRODUCTION

We report on the second and final year of geological mapping in the Nakina area, conducted under the Atlin Targeted Geoscience Initiative (TGI). Principal aims of the TGI are to create a legacy of high quality geoscience data that will stimulate geological resource exploration, and regional economic development (*see* Atlin TGI - Part I). Geological maps produced as part of the project portray base-line data required for informed land-use decisions or other studies where bedrock geology is a consideration.

Since 1898, when Fritz Miller and his partner Kenneth McLaren discovered rich placers on Pine Creek (Bilsland, 1952), the economic well-being of the Atlin region has been largely tied to the price of gold. Yet, good potential for economic diversification in the mining sector exists because the Atlin area contains a diversity of prospective geological environments. Results of geological mapping in the Nakina area in 2001 (Mihalynuk *et al.*, 2002) affirmed such potential. Results included the discovery of submarine felsic volcanic rocks and extensive hydrothermal deposits of exhalative magnetite; deposits that are common in mining camps where copper, lead and zinc are produced from volcanogenic massive sulphide accumulations. A key host rock in many of these camps is submarine dacite or rhyolite. Felsic volcanic rocks, and the sediments derived from them, have long been considered uncharacteristic of the Cache Creek rocks in the Atlin area. Our mapping showed that clastic strata derived from felsic volcanic rocks are relatively common. Further evidence for prospectivity of Cache Creek rocks comes from discoveries during 2002. Mineralization includes massive sulphide lenses in submarine mafic volcanic rocks at the new Joss'alun discovery (*see* Atlin TGI -Part III), massive pyrrhotite that is probably related to Eocene skarn, a broad zone of quartz-sericite schist in a side canyon of the Nakina River, and industrial mineral occurrences of sepiolite near Mount O'Keefe and talc near Chikoida Mountain.

Results of geological studies presented arise from collaborative partnerships between the BC Ministry of Energy and Mines, Geological Survey of Canada, University of Victoria, Université Claude Bernard, Simon Fraser University, and the Yukon Government.

LOCATION, ACCESS AND PHYSIOGRAPHY

In 2001, Regional geologic mapping at 1:50 000 scale was conducted across the southeast corner of the Atlin mapsheet, covering the Nakina Lake area and about 70% of the Nakina River area (Figure 1); NTS mapsheets 104N/1 and 2, respectively. Fieldwork in 2002 was originally planned to complete mapping of NTS mapsheet 104N/2 as well as the Sloko River mapsheet, 104N/3. Reduced financial support for field programs in 2002 hampered mapping progress, resulting in incomplete mapping over about 25% of the 104N/3 sheet. Mapsheet 104N/1, 2 and 3 together cover an area of approximately 2400 km^2 (28 km from north to south and 84 km east to west) that spans a region between 38 and 115 kilometres southeast of the town site of Atlin (Figure 1). It is herein referred to as the "Nakina transect".

Access to the Nakina transect is most effectively achieved using a helicopter charter based out of Atlin. Parts of the transect can also be accessed from lakes large enough for floatplanes. There are no all-season roads within the area. One rough, fire abatement road extends to Kuthai Lake at the northern limit of 104N/3; about a 2.5-hour drive from Atlin. It is suitable for four wheel drive or all-terrain vehicles and requires fording the O'Donnel River and Dixie Lake outflow.

Travel by foot is relatively easy within the Nakina transect. Two heritage footpaths cross the area: the Telegraph and Taku trails. Telegraph Trail was cut diagonally across 104N2 and 3 between 1900 and 1902 as part of an ill-fated telecommunication syndicate (Bilsland, 1952). Most of the durable telegraph wire has been scavenged and put to good use, and much of the route is still well maintained by guide-outfitters. Other parts are overgrown and

---

[1] *BC Ministry of Energy and Mines*
[2] *University of Victoria*
[3] *Université Claude Bernard, Lyon France*
[4] *Geological Survey of Canada, Ottawa*
[5] *Paleontological Consultant, Calgary*
[6] *Geological Survey of Canada, Vancouver*

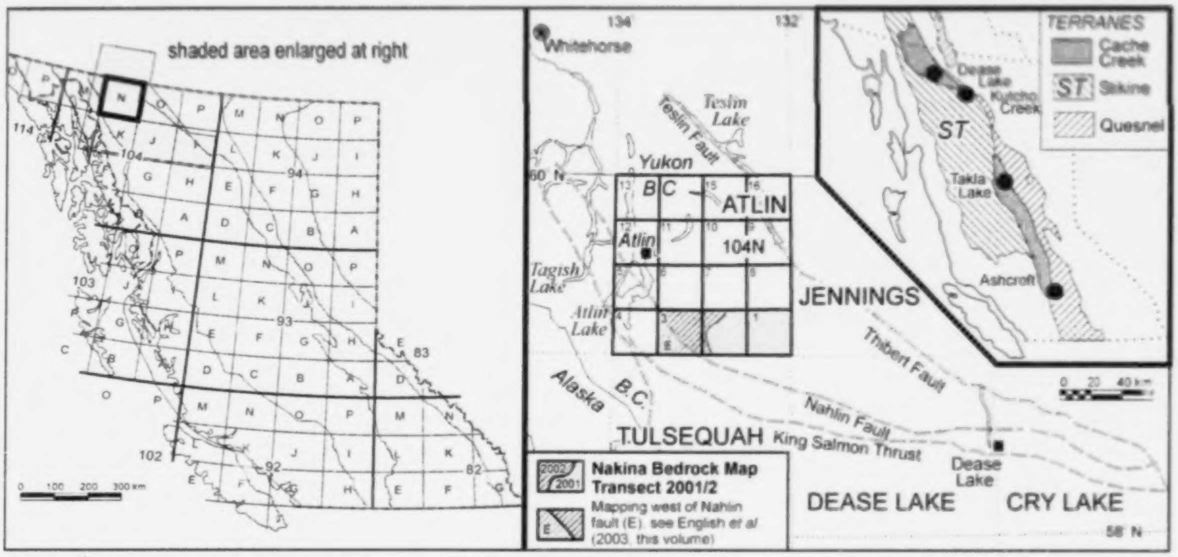
shaded area enlarged at right
114
104
94
93
83
103
102
92
82
0 100 200 300 km
134
132
Whitehorse
Teslin Lake
Teslin Fault
Yukon
60 N
ATLIN
104N
Atlin
Tagish Lake
Atlin Lake
JENNINGS
Thibert Fault
Alaska
B.C.
Nahlin Fault
TULSEQUAH
King Salmon Thrust
Dease Lake
DEASE LAKE
CRY LAKE
58 N
0 20 40 km
Nakina Bedrock Map Transect 2001/2
Mapping west of Nahlin fault (E), see English et al (2003, this volume)
TERRANES
Cache Creek
ST Stikine
Quesnel
ST
Dease Lake
Kutcho Creek
Takla Lake
Ashcroft

Figure 1. Location of the Atlin Targeted Geoscience Initiative (TGI) Project in northwestern British Columbia. Bold outlined box (104N) shows extent of Atlin TGI aeromagnetic survey. Regional geological mapping surveys were conducted over the eastern and central Nakina transect (104N/1, 2) in 2001 and extended into 104N/3 in 2002.

recognizable only by weathered blazes and beleaguered relicts (Photo 1).

Atlin was linked with tidewater on Taku Inlet by the Taku Trail, which followed the Silver Salmon River in the Nakina area (Figure 2). Except where the route coincides with game trails, it has overgrown with the ebb of foot traffic in the post gold rush era. Off trail, foot passage is easy on dry or well-drained south-facing slopes, which generally have open forest floors between fir, spruce, aspen and pine; or in recent forest fire scars that have yet to establish willow, alder and dwarf birch growth. Foot travel is more challenging on slopes that are north facing and poorly drained, especially near treeline where they can be a tangle of stunted fir and spruce. Canyons along the lower Nakina River and its major tributaries are negotiated with difficulty; parts are impassable without technical climbing equipment. However, travel along canyons rims is a spectacular treat and many parts are lined with well-trodden goat trails. These canyons are part of the elevated Taku Plateau in the western Nakina transect area; they drain to the Pacific. Topography subsides eastward to the low, swampy Kawdy Plateau (Photo 2), which mainly drains to the Arctic. Most of the Nakina transect area is below tree line, which is around 1400 metres elevation. Mountains are less than 1900 metres elevation, and are relatively easily negotiated on foot. One exception is Paradise Peak at 2100m, which lies just beyond the western boundary of the Nakina transect.

Photo 1. Reminders of a bygone era, horseshoes hang along the overgrown Telegraph Trail.

PREVIOUS WORK

Previous regional map coverage of the Nakina transect is of early to mid 1950s vintage (Aitken, 1959), pre-dating the advent of plate tectonics. Thematic revision mapping in the mid to late 1960's by Monger (1975) covered much of

Photo 2. View over the eastern two thirds of the Nakina transect area, from Focus Mountain in east-central 104N/3.

the carbonate-dominated rocks in the central transect area. Monger (1975) pieced together a biostratigraphy and used igneous geochemistry, map relationships, and the recognition of a disrupted ophiolitic succession to show that the Atlin area is composed largely of relict ocean basin crust and oceanic islands. Terry (1977) confirmed this assertion and suggested an analogue in the Pindos ophiolites of Greece. Ash (1994) drew similar conclusions from the ophiolitic ultramafic rocks near the town site of Atlin.

In 1996, a compilation of Atlin geology was completed as part of a provincial mineral potential evaluation (Mihalynuk *et al.*, 1996) available for viewing or download at www.em.gov.bc.ca/Mining/Geolsurv/MapPlace. Sources of information drawn upon for the compilation included mineral tenure assessment reports, 1:50 000-scale revision mapping (Bloodgood and Bellefontaine, 1990; Lefebure and Gunning, 1988; Mihalynuk and Smith, 1992) and 1978 Regional Geochemical Survey (RGS) results (BCMEM, 1978). Archival stream sediment samples were reanalysed for a broad range of elements, including gold, and published in 2000 (Jackaman, 2000; available for download at www.em.gov.bc.ca/Mining/Geolsurv/rgs/sheets/104n.htm). In the same year, a regional aeromagnetic survey of the entire Atlin map sheet, about 14 000 square kilometres was conducted (*e.g.* Dumont *et al.*, 2001a, b, c; Lowe and Anderson, 2002) as the first phase of the Atlin TGI. Evaluation of the aeromagnetic data is ongoing with future publication anticipated, together with publication of results from other branches of the TGI project (*see* TGI Part I).

REGIONAL GEOLOGY

Rocks of the Nakina transect area can be broadly separated into one of four distinct packages. From oldest to youngest (and most to least abundant), they are: Mississippian to Early Jurassic Cache Creek oceanic rocks; Early to Middle Jurassic Laberge wacke and shale; Middle Jurassic, post-tectonic intrusions; and Early Eocene continental arc volcanic, comagmatic plutonic, and sedimentary rocks of the Sloko Group.

Most of the eastern transect area is underlain by Cache Creek oceanic crustal and supracrustal strata and Middle Jurassic bodies that intrude them. They are separated by the crustal-scale Nahlin fault from strata the Laberge Group an overlying Sloko Group in southwest 104N/3. Sloko basalt may also occur east of the Nahlin fault in the Pike Lake area. All rocks older than the ~172Ma Jurassic plutons have been folded and faulted; most recently by southwest-verging folds and thrusts, between 174 and 172 Ma.

Geological observations reported here are new or updated in 2002, mainly for mapsheets 104N/2 and 3. For information on the geology of 104N/1, including an overview on nomenclature for Cache Creek rocks, refer to (Mihalynuk *et al.*, 2002) and sources therein.

CACHE CREEK ROCKS

As early as 1953, M.L. Thompson recognized the Tethyan affinity of fusulinid faunas collected from Cache Creek rocks in the Atlin area (*in* Harker, 1953); clearly exotic with respect to the adjacent non-Tethyan rock packages. This demonstrably exotic aspect of the Atlin rocks was pivotal to the development of the "Terrane Hypothesis" (Coney *et al.*, 1980). Cache Creek rocks continue to play a leading role in our understanding of the Canadian Cordillera, and perhaps the best exposures are in the Nakina transect.

Within the transect, Cache Creek rocks comprise four domains (Figure 2): eastern and western domains are dominated by basalt, chert and ultramafite (Disella and Goldbottom domains); a central domain is dominated by carbonate and lesser chert (Sinwa domain); and a northern heterolithologic domains are comprised of well bedded, folded and faulted chert (Chikoida doman), and carbonate and volcanic rocks (Blackcaps domain). Most of the eastern

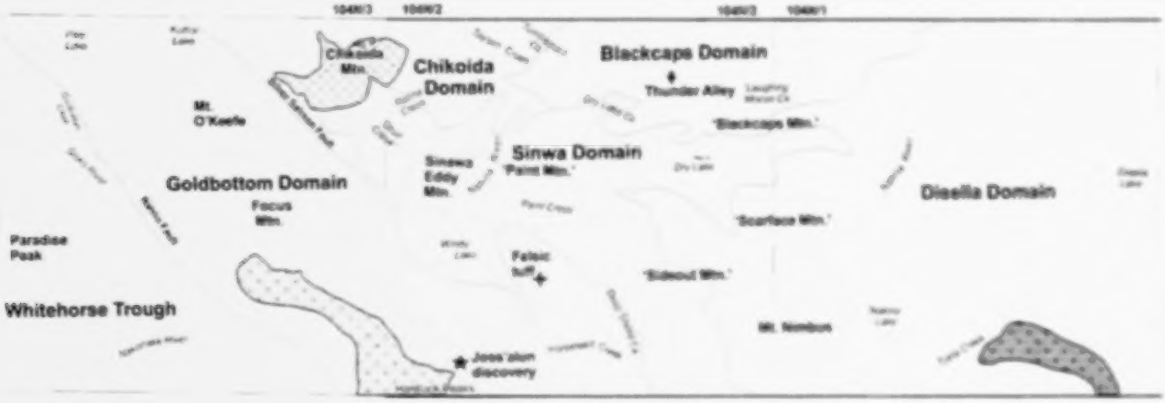

Figure 2. Geologic domains of the Nakina transect area in relation to key geographic and geological features.

domain lies within 104N/1 and is described by Mihalynuk *et al.* (2002).

Regional metamorphic grade of the Northern Cache Creek terrane is prehnite-pumpellyite facies, although thermal upgrading to biotite and, rarely, garnet-grade is observed around large plutons. Local blueschist grade metamorphism is known from the Dease Lake area (Monger, 1969), but is not known in the Nakina transect. Sparse conodont alteration indices (CAI) from Cache Creek rocks in the Nakina area are generally slightly higher than the metamorphic grade as indicated from authigenic mineralogy (*see* English *et al.*, 2003, this volume).

We address new observations in a stratigraphic context, from lowest (mantle) to highest (platformal carbonate) as they would appear in an undisturbed, idealized oceanic crustal section.

MANTLE: SERPENTINIZED HARZBURGITE

Harzburgite is an ultramafic rock composed mainly of olivine and orthopyroxene with accessory clinopyroxene and chromite. Orthopyroxene and chromite grains commonly form streaky clusters outlining a high temperature fabric interpreted as having a mantle origin (Photo 3a). This fabric is cut by undeformed pyroxenite dikelets (Photo 3b), also of presumed mantle origin. Harzburgite is the dominant protolith within the Nahlin ultramafic body and forms a coherent 1.5 x 15 km, dun-weathering body, best exposed south of the Nakina River in 104N/2W (Figures 2, 3). At that locality, it is bound to the west by gabbro, which passes upwards into submarine basalt, host to massive sulphide mineralization at the Joss'alun occurrence (*see* Mihalynuk *et al.*, 2002b, this volume). To the east are fault panels of wacke and mafic volcaniclastics with lesser serpentinite lenses interpreted as part of an accretionary prism. North of the Nakina River, the harzburgite body is structurally interleaved with panels of bright green serpentinite. Bright orange quartz-carbonate (listwanite) alteration of serpentinite occurs where it has been extensively veined, commonly near faults (*see* structural styles following). Within the main harzburgite body, there is no deformational fabric that post-dates emplacement of pyroxenite dikelets, indicating that strain was highly partitioned, or that the harzburgite acted as a rigid body during emplacement.

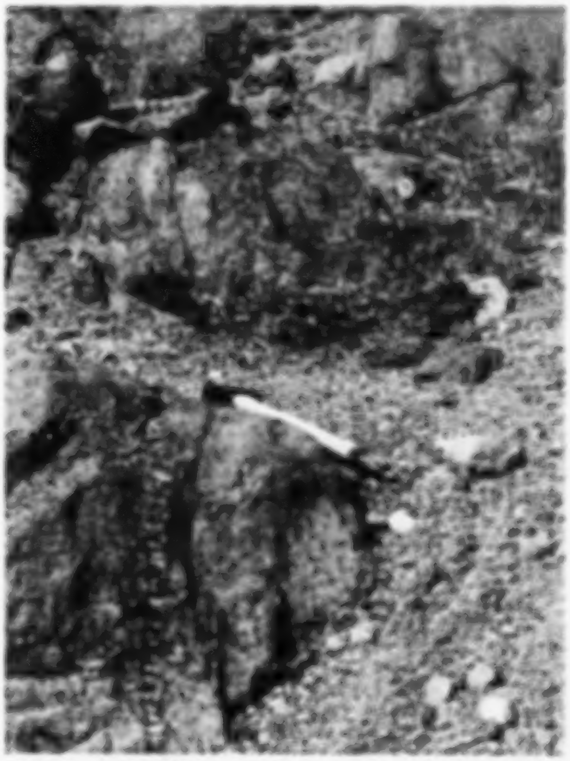

Photo 3. (a) mantle tectonite fabric outlined by serpentinized relicts of sheared orthopyroxene. (b) undeformed pyroxenite dikelet cuts mantle fabrics.

SERPENTINITE MÉLANGE

Much of the low-lying area between the Sloko and Silver Salmon rivers is underlain by serpentinite mélange (Figure 3). Knockers up to several square kilometres in area vary in a relatively consistent manner from west to east. A western belt contains mainly of harzburgite and gabbro knockers; followed by diorite and basalt knockers, then chert with minor basalt, and finally, basalt with minor chert. In both the eastern and western-most belts, serpentine may comprise more than 50% of areas several square kilometres in size. In the intervening belts, serpentine is estimated to comprise less than 10% of the rock volume.

Near with the easternmost limit of the serpentinite-rich mélange belts are panels of thinly bedded siltstone. Immediately west, mint green volcaniclastic rocks abruptly increase in abundance, comprising blocks up to mountain-size. Sparse exposures in valleys between the blocks are comprised of scaly serpentine. Swampland west of the Silver Salmon River in central 104N/3E is underlain mainly by serpentinite. Knockers, some more than 400 metres across, stick up out of the swamps. They are resistant buttress to rat-tails of serpentinite that point in the direction of ice flow during the last continental glaciation; lakes occupy the scoured up-ice side of the knockers (see Lowe *et al.*, 2003).

Chert is subordinate to mafic volcanics, but it also comprises blocks the size of entire mountainsides. Focus Mountain is part of one such block, which is composite of many fault-bounded panels that are intermittently exposed over an area of 3.5 km by 10 km. Serpentinite occurs along the boundaries of the Focus Mountain domain as it does along all major blocks. Serpentine becomes increasingly dominant towards the west, so that the mélange belt near the Nahlin Fault is composed mainly of serpentinite, and knockers generally less than 1 or 2 km in maximum dimension. An exception is the harzburgite at Hardluck Peaks, south of the Nakina River, which forms a semi-coherent, 1.5 km-wide body that parallels the structural grain for ~15 km. North of the Nakina River, the harzburgite body is structurally disaggregated, and comprises the dominant knocker type within the western part of the mélange belt. Gabbro, and hornblende diorite are subordinate to the harzburgite, increasing in abundance to the east. The large size of some knockers argues against entrainment of knockers as "xenoliths" during serpentine diapirism or subduction zone backflow, at least when compared to modern analogues. Rather, tectonic juxtaposition within a subducting margin setting probably occurred by two processes: first, by exhumation of the mantle (but not necessarily to the level of subaerial-subaqueous exposure) during initiation of subduction; and later, by offscraping of oceanic sediment and crustal protruberances such as ocean islands from the subducting slab.

GOLDBOTTOM CREEK GABBRO

Gabbro crops out over several square kilometres at the headwaters of Goldbottom Creek, south of Mount O'Keefe. It is a folded, sheet-like body that displays an intrusive contact with overlying mafic volcanic rocks and fault contact with underlying ultramafic, mafic and quartz-rich clastic rocks. It is interpreted as an allochthonous sheet. Chert in the footwall of the allochthon is carried on a southwest-verging thrust that has been deformed by open folds; similar to in style to those that control the map pattern distribution of the allochthon. Gabbro within the allochthon appears to have been attenuated by dilatent, high-angle faults that are invaded by serpentinite. Dilatent faults are probably kinematically linked to motion on the Nahlin Fault (*see* Nahlin fault).

SHEETED DIKE COMPLEX?

Nowhere in the northern Cache Creek terrane has an intact-sheeted dike complex been found. However, crowded sets of mafic dikes occur within the gabbro-basalt succession southwest of Mount O'Keefe. Knockers composed of multiple dikes may also be relicts of a sheeted dike complex, but they are generally less than 10m across; too small to permit confirmation.

MAFIC PLUTONS AND PLAGIOGRANITE

Hornblende diorite or tonalite, representatives of the intrusive magmatic parts of the crustal section, are also found as knockers together with relicts of harzburgite within serpentinite mélange. Below tree line near Tsenu Creek (104N/1), a >1 km² area of diorite is intruded by an irregular network of pegmatitic plagiogranite dikes. These rocks may be part of an intact oceanic crustal section. Plagiogranite dikes are generally less than 0.5 m thick. They are composed mainly of plagioclase and hornblende with about 10% interstitial quartz and accessory titanite and zircon. They are undeformed and weakly metamorphosed. Plagioclase is partly altered to prehnite and, possibly, the zeolite phillipsite (Photo 4a). Hornblende is nearly pristine, with only the slightest traces of chlorite alteration (Photo 4b).

BASALTIC VOLCANICLASTICS 'BLACKCAPS' ASSEMBLAGE

Basaltic volcaniclastic rocks are the dominant Cache Creek unit within the Nakina transect. Monger (1975) included such rocks within the Nakina Formation. English *et al.* (2002) recognized geochemically distinct volcanic units that probably formed in different tectonic environments. The most abundant mafic volcaniclastic unit they called the 'Blackcaps' assemblage, we use their terminology here (Figure 3).

'Blackcaps' assemblage basaltic volcaniclastics commonly display well-preserved, aphanitic lapilli and ash-sized fragments despite widespread replacement by prehnite, pumpellyite, calcite and chlorite. Colour of fresh surfaces is distinctive: mint green with a grey or pinkish cast caused by filaments (fine shear bands) of clay and iron oxides. Weathered outcrop surfaces are orange, dark brown or olive green. Gabbro and rare plagiogranite intrude the basalt (*see above*). Near 'Blackcaps Mountain', volcaniclastics are interbedded with Middle Triassic chert (Table 1). Disrupted chert beds or olistostromal layers, with

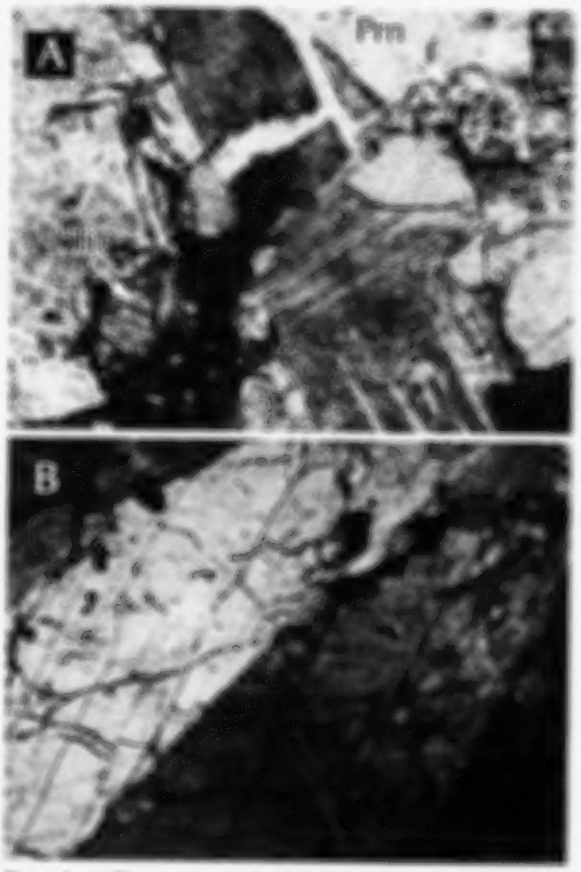

Photo 4. (a) Photomicrograph of plagiogranite. Quartz and feldspar dominate the section, accessory titanite (Ti) and authigenic prehnite (Prn) are labelled. (b) Basal section of hornblende (Hb) shows only the slightest traces of chlorite alteration; most hornblende in the sample is less altered.

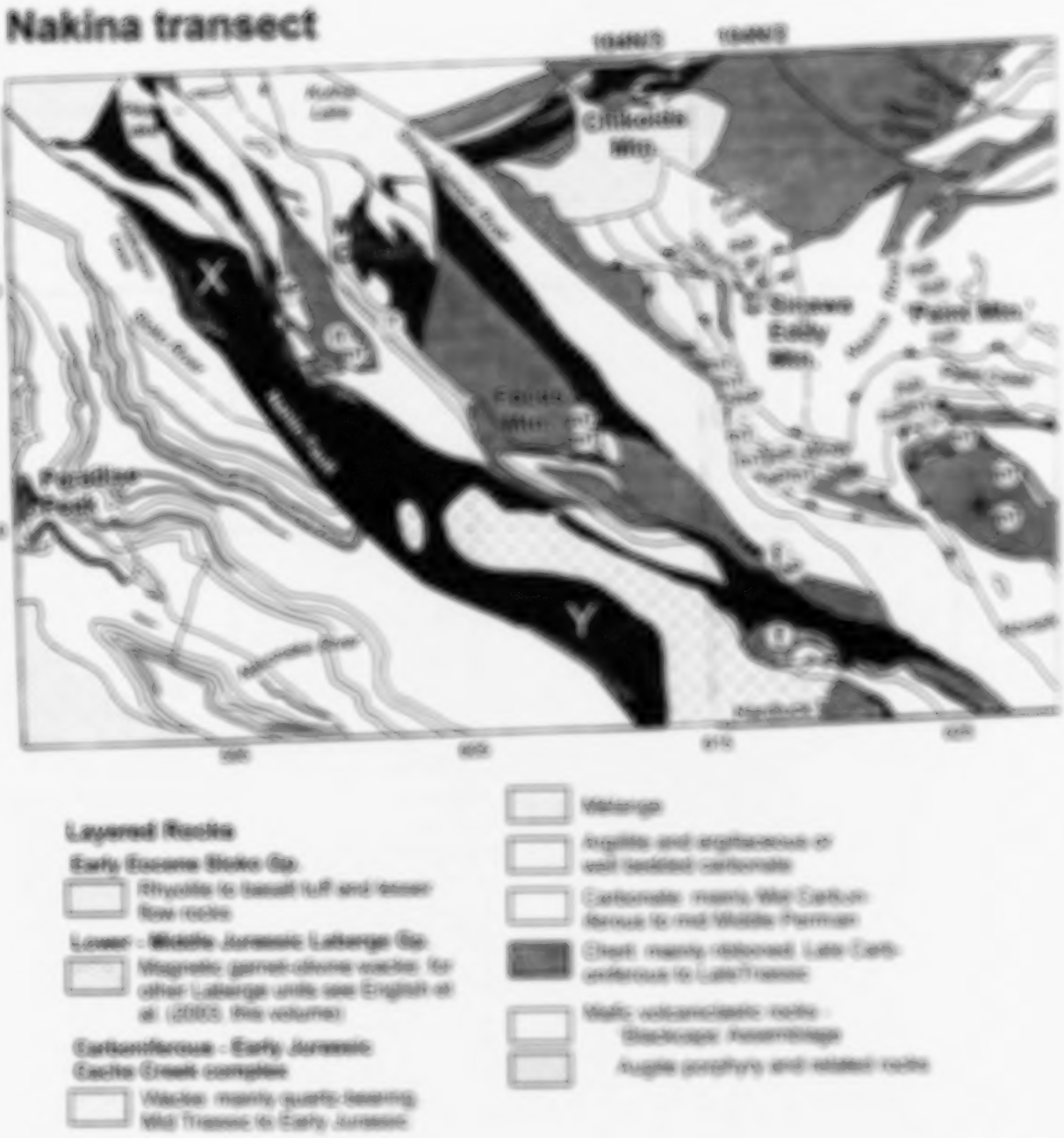
Nakina transect
X
Y
Chikoida Mtn.
Paint Mtn.
Layered Rocks
Early Eocene Sloko Gp.
Rhyolite to basalt tuff and lesser flow rocks
Lower - Middle Jurassic Laberge Gp.
Magnetic garnet-chrome wacke; for other Laberge units see English et al. (2003, this volume)
Carboniferous - Early Jurassic Cache Creek complex
Wacke: mainly quartz-bearing Mid Triassic to Early Jurassic
Mélange
Argillite and argillaceous or well bedded carbonate
Carbonate: mainly Mid Carboniferous to mid Middle Permian
Chert: mainly ribboned; Late Carboniferous to Late Triassic
Mafic volcaniclastic rocks:
[illegible] assemblage
Augite porphyry and related rocks

Figure 5: Simplified geology map of the Nakina transect

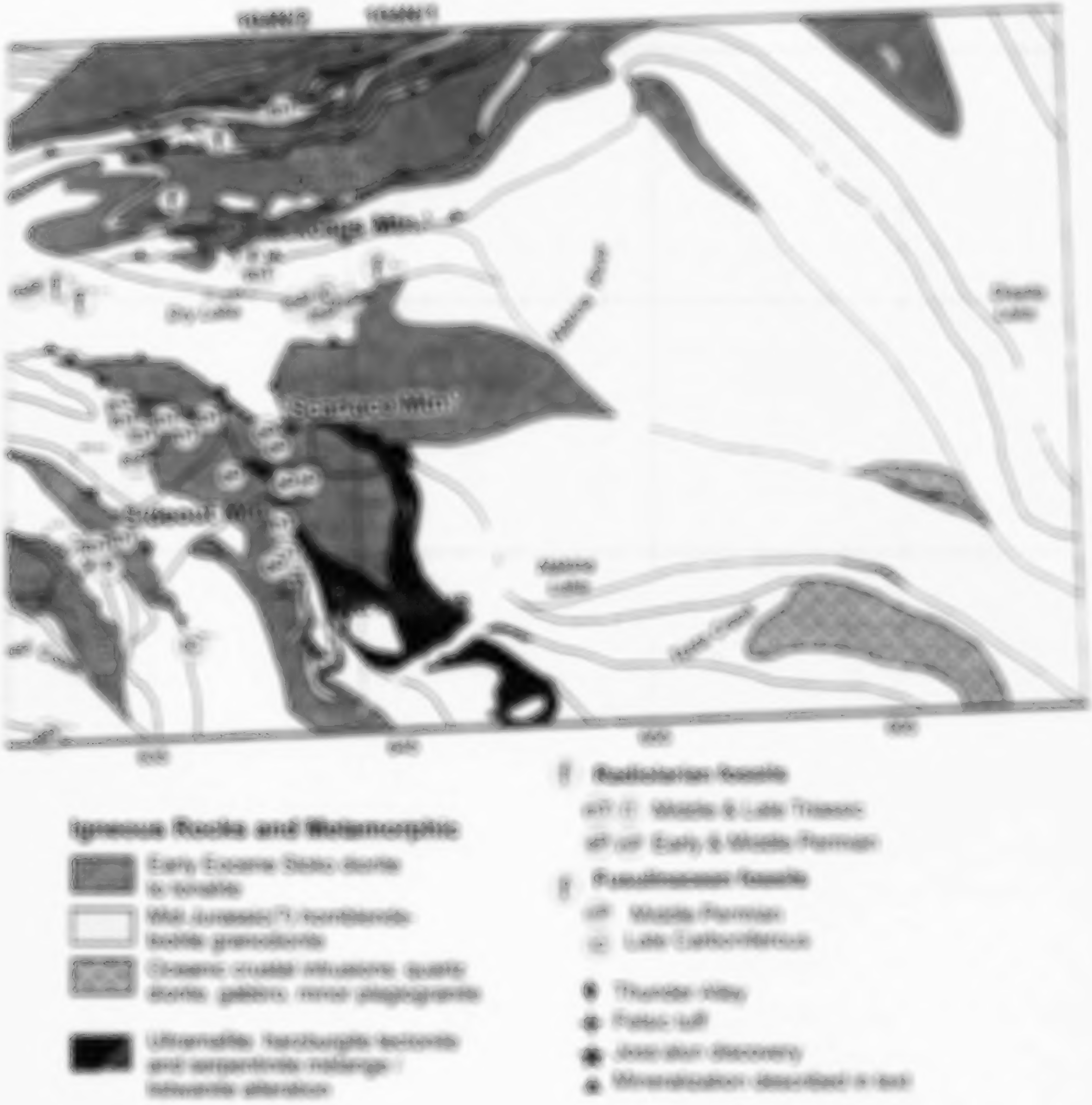
Scarface Mtn
Dry Lake
Igneous Rocks and Metamorphic
Early Eocene Sloko diorite to tonalite
Mid Jurassic(?) hornblende-biotite granodiorite
Oceanic crustal intrusions: quartz diorite, gabbro, minor plagiogranite
Ultramafite: harzburgite tectonite and serpentinite mélange / listwanite alteration
Radiolarian fossils
Middle & Late Triassic
Early & Middle Permian
Fusulinacean fossils
Middle Permian
Late Carboniferous
Mineralization described in text

Figure 3 continued

Table 1, continued

Station Number	NAD 83 UTM E	NAD 83 UTM N	Lithology	Preservation	Radiolarian taxa / Observations	Age
[illegible]	[illegible]	[illegible]	grey siliceous chert from isolated outcrop in fault zone	poor to moderate	Pseudostylosphaera sp., Triassocampe sp., Yeharaia sp., fragments of Oertlispongidae	Middle Triassic
[illegible]	[illegible]	[illegible]	fine-grained tuffaceous argillite (protolith?)	very poor	rare spheromorphs and sponge spicules, matrix fragments	Indeterminate
[illegible]	[illegible]	[illegible]	grey siliceous chert	good	Pseudostylosphaera sp., Triassocampe sp., Yeharaia sp., [illegible] sp.	Middle Triassic
[illegible]	[illegible]	[illegible]	dark grey siliceous chert	moderate	Entactinia sp., [illegible] sp., Latentifistula sp., Pseudoalbaillella u-forma	Early Permian
[illegible]	[illegible]	[illegible]	green [illegible] siliceous	very poor	spheromorphs and sponge spicules, matrix fragments	Indeterminate
[illegible]	[illegible]	[illegible]	black siliceous chert	moderate	[illegible] sp., Pseudostylosphaera compacta, Yeharaia sp., Triassocampe sp.	Middle Triassic
[illegible]	[illegible]	[illegible]	black siliceous chert	good	Entactinia sp., Latentifistulidae fragments, [illegible]	Late Paleozoic
[illegible]	[illegible]	[illegible]	grey chert, broken bx	moderate	Oertlispongids, Pseudostylosphaera sp., Triassocampe sp., Yeharaia sp.	Middle Triassic
[illegible]	[illegible]	[illegible]	grey chert, broken bx	good	Pseudostylosphaera japonica, Triassocampe sp., Yeharaia sp.	Middle Triassic; late Anisian-Ladinian
[illegible]	[illegible]	[illegible]	[illegible] argillite	poor	rare spheromorphs	Indeterminate
[illegible]	[illegible]	[illegible]	dark green shale interbedded with silt [illegible]	n/a	abundant black and dark green crystals of various sizes, clays	Indeterminate
[illegible]	[illegible]	[illegible]	brown mudstone [illegible]	n/a	silica fragments, clays, small-size dark crystals	Indeterminate
[illegible]	[illegible]	[illegible]	mudstone interbedded with fine silt	n/a	silica fragments, abundant brown clays	Indeterminate
[illegible]	[illegible]	[illegible]	fine siliceous silt	n/a	silica fragments, clays, spheromorphs, round quartz crystals	Indeterminate
[illegible]	[illegible]	[illegible]	fine siliceous silt	n/a	black and dark green crystals of various sizes, silica fragments, clays	Indeterminate
[illegible]	[illegible]	[illegible]	grey siliceous chert with [illegible] tuff	moderate	[illegible] sp., Pseudostylosphaera magnispinosa, Triassocampe sp., Yeharaia elegans	Middle Triassic; Anisian-early Ladinian
[illegible]	[illegible]	[illegible]	grey siliceous chert interbedded with siliceous argillite	poor	Triassocampe sp., pyrite crystals	Middle or Late Triassic
[illegible]	[illegible]	[illegible]	grey siliceous chert, small [illegible]	moderate	Capnodoce sp., Canoptum sp., Sarla sp.	Late Triassic; late Carnian to Middle Norian
[illegible]	[illegible]	[illegible]	grey siliceous chert, [illegible]	moderate	Pseudotriassocampe sp., Oertlispongus sp., Pseudostylosphaera sp., Triassocampe sp.	Middle Triassic
[illegible]	[illegible]	[illegible]	grey siliceous chert	moderate	Capnodoce sp., Pachus sp.	Late Triassic; late Carnian to Middle Norian
[illegible]	[illegible]	[illegible]	grey siliceous chert	poor to mod	Capnuchosphaera sp., Triassocampe sp.	Late Triassic; Carnian to Middle Norian
[illegible]	[illegible]	[illegible]	black siliceous argillite	n/a	abundant clays, silica fragments	Indeterminate
[illegible]	[illegible]	[illegible]	grey siliceous chert	moderate	Latentifistula sp., Pseudoalbaillella u-forma	Early Permian; Sakmarian-Artinskian
[illegible]	[illegible]	[illegible]	fine-grained [illegible]	n/a	abundant quartz crystals, some pyrite, silica fragments	Indeterminate
[illegible]	[illegible]	[illegible]	grey siliceous chert	poor	Eptingium sp., Pseudostylosphaera sp., Triassocampe sp.	Middle Triassic
[illegible]	[illegible]	[illegible]	[illegible]	poor	[illegible]	Indeterminate

Table 1, continued

Station Number	NAD 83 UTM E	[illegible] UTM N	Lithology	Preservation	Radiolarian taxa Observations	Age
[illegible]	[illegible]	[illegible]	black-grey siliceous chert unit #1 within thick volcaniclastic unit	poor	*Oertlispongus* sp., *Pseudostylosphaera* sp., *Triassocampe* sp.	Middle Triassic
[illegible]	[illegible]	[illegible]	black-grey siliceous chert unit #1 within volcaniclastic unit	poor	*Triassocampe* sp., indeterminate spumellarians	Middle or Late Triassic
[illegible]	[illegible]	[illegible]	grey siliceous chert unit #2 within volcaniclastic unit	poor	*Plafkerium* sp., *Pseudostylosphaera* sp., *Triassocampe* sp.	Middle or Late Triassic
[illegible]	[illegible]	[illegible]	grey siliceous chert	poor	*Oertlispongus* sp., *Pseudostylosphaera* sp., *Triassocampe* sp., moderately abundant sponge spicules	Middle Triassic
[illegible]	[illegible]	[illegible]	grey siliceous chert	moderate	*Annulotriassocampe* sp., *Oertlispongus* sp., *Pseudostylosphaera nazarovi*, *Triassocampe* sp.	Middle or Late Triassic; late Ladinian-middle Carnian
[illegible]	[illegible]	[illegible]		poor	abundant recrystallized sphaeromorphs	indeterminate
[illegible]	[illegible]	[illegible]		poor	sphaeromorphs, recrystallized spumellarians	indeterminate
[illegible]	[illegible]	[illegible]		poor	sphaeromorphs, recrystallized spumellarians	indeterminate
[illegible]	[illegible]	[illegible]	[illegible]	poor	sphaeromorphs, probable spumellarians	indeterminate
[illegible]	[illegible]	[illegible]	[illegible]	poor	*Plafkerium* sp.	Triassic
[illegible]	[illegible]	[illegible]	well bedded black siliceous chert with continuous layers	poor to moderate	*Pseudostylosphaera* sp., narrow *Triassocampe* sp., *Yeharaia* sp.	Middle Triassic
[illegible]	[illegible]	[illegible]		poor	recrystallized sphaeromorphs, silica fragments	indeterminate
[illegible]	[illegible]	[illegible]		poor	abundant recrystallized silica rods (sponge spicules), black clays, sphaeromorphs	indeterminate
[illegible]	[illegible]	[illegible]		poor	sphaeromorphs, recrystallized spumellarians, sponge spicules, [illegible]	indeterminate
[illegible]	[illegible]	[illegible]	very well bedded black and grey siliceous chert	poor	*Pseudostylosphaera* sp., narrow *Triassocampe* sp., recrystallized spumellarians	Middle Triassic
[illegible]	[illegible]	[illegible]	tan and grey siliceous chert adjacent limestone [illegible]	poor	*Entactinia* sp., *Quinqueremis* sp., *Pseudoalbaillella* sp. cf. *lomentaria*, sponge spicules	Permian
[illegible]	[illegible]	[illegible]	chert from [illegible]	poor	*Pseudostylosphaera* sp., narrow *Triassocampe* sp.	Middle Triassic
[illegible]	[illegible]	[illegible]	well bedded black siliceous chert	good	*Entactinia* sp., *Latentifistula texana*, *Polyfistula* sp., *Pseudoalbaillella* sp. cf. *longicornis*, *Pseudoalbaillella lomentaria*	Early Permian
[illegible]	[illegible]	[illegible]	brown siliceous chert with very tough and [illegible] layers	good	*Canoptum* sp., *Capnuchosphaera* sp., *Capnodoce* sp.	Late Triassic, late Carnian-mid Norian
[illegible]	[illegible]	[illegible]	black siliceous chert, continuous [illegible] beds	good	*Pseudostylosphaera compacta*, *Triassocampe* sp.	Middle Triassic
[illegible]	[illegible]	[illegible]		poor	abundant sphaeromorphs	indeterminate
[illegible]	[illegible]	[illegible]	pod in carbonaceous argillite matrix	poor to moderate	*Pseudoalbaillella lomentaria*, fragments of *Latentifistulidae*	Early Permian
[illegible]	[illegible]	[illegible]		poor	rare sphaeromorphs, silica fragments, black clays	indeterminate
[illegible]	[illegible]	[illegible]	semi-continuous black siliceous chert interlayered with [illegible]	poor	*Capnodoce* sp.	Late Triassic, late Carnian-mid Norian
[illegible]	[illegible]	[illegible]	dark grey well bedded	moderate	abundant *Tritortis* sp., *Triassocampe* sp.	Middle Triassic
[illegible]	[illegible]	[illegible]	black massive to laminated chert	poor	*Entactinia* sp., *Pseudoalbaillella*, abundant sphaeromorphs	Paleozoic, possibly Permian
[illegible]	[illegible]	[illegible]	[illegible] chert with volcaniclastics	poor	*Albaillella* sp., abundant sponge spicules	possibly Paleozoic
[illegible]	[illegible]	[illegible]	diverse, fine grained volcaniclastics	good	[illegible]	indeterminate
[illegible]	[illegible]	[illegible]	grey siliceous chert	moderate	*Hegleria mamilla*, *Pseudoalbaillella* sp.	Middle Permian; Wordian-Capitanian

Table 1. continued

Station Number	NAD 83 UTM E	Zn8 UTM N	Lithology	Preservation	Radiolarian taxa Observations	Age
MMI-02-15-07-3	587129	6558443	siliceous, fine-grained volcaniclastics	moderate	*?Entactinosphaera* sp. cf. *sashidai, ?Parentactinia* sp., various forms of primitive *?Pseudostylosphaera* sp., sponge spicules	**possibly late Early Triassic or earliest Middle Triassic**
MMI-02-28-10	592250	6560914	siliceous, fine-grained volcaniclastics	very poor	highly recrystallized elements, silica fragments, quartz crystals	**indeterminate**
MMI-02-30-09	624516	6566125	siliceous, fine-grained volcaniclastics	poor	abundant small-size spumellarians, clays	**indeterminate**
MMI-02-34-02-1*	621980	6543778	jasperoid radiolarian chert within pillow breccia unit	poor	*Entactinia* sp., *?Follicucullus* sp., *Pseudoalbaillella* sp., *Latentibifistula* sp., fragments of *Latentifistulidae*	**Permian**
MMI-02-34-02-2*	621980	6543778	jasperoid radiolarian chert within pillow breccia unit	poor	Sphaeromorphs, probable spumellarians	**indeterminate**
MMI-02-34-07*	620383	6544147	30cm x15m rusty black ribbon chert block above unconformity	moderate	*Eptingium* sp., *Pseudostylosphaera* sp. aff. *tenuis, Pseudostylosphaera coccostyla compacta, Triassocampe* sp., *Yeharaia* sp.	**Middle Triassic, late Anisian or early Ladinian**
VME01-23-03b	630968	6560595	silicified limestone (stratigraphic contact between pillows and limestone)		silica fragments	**indeterminate**

* as Station Number suffix indicates a sample from the Joss'alun discovery area, see Mihalynuk ***et al.*** (2003b, this volume)

ble size and range up to 1 m in long dimension. The unit may be repeated by a series of south-verging folds that have imparted a pervasive flattening fabric that dips moderately to the north. Structurally above the breccia are pillowed feldspar porphyry basalt flows (*see* following). The basalt-breccia contact is not exposed.

Breccia probably records tectonic instability of the Cache Creek chert-carbonate complex, possibly during off-scraping at an accretionary margin. Lack of evidence for rounding or sorting of clasts by alluvial processes argues against extensive subaerial exposure of the source area.

PORPHYRITIC FLOWS AND TUFF

Feldspar porphyry occurs both as pillowed flow and volcaniclastic facies less than 10m thick. Its contact with underlying limestone-chert breccia is not exposed, but it displays a slightly disrupted, probable stratigraphic contact with overlying well-bedded limestone having chert interlayers.

Porphyritic flows, together with under- and overlying units may be the stratigraphically equivalent to a succession in northwestern 104N/1 where mapping in 2002, revealed a highly indurated pyroxene-porphyritic flow unit at approximately the same stratigraphic interval, between a great thickness of chert and carbonate (Mihalynuk *et al.*, 2002), in the east-central part of the Blackcaps domain. Near treeline in "Laughing Moose Creek" valley, a sequence of chert, overlying breccia, and submarine pyroxene-porphyritic volcanic rocks may also be correlative. Magmagenesis of the augite-porphyritic unit displays a within-plate geochemical signature (English *et al.*, 2002). It was probably formed in an ocean island or plateau setting. Chemical analysis of the feldspar porphyritic unit is pending. Age of the unit is not known. Interpillow lime mudstone and the overlying interbedded chert-limestone unit were both sampled for conodonts, but results were not available at the time of writing.

CARBONATE-DOMINATED STRATA

Carbonate rocks comprise much of the central part of the Nakina transect, here called the Sinwa domain (in the local Tlingit dialect "sinwa" means limestone). Most of the carbonate domain was mapped as part of the 2001 field program, with findings reported in Mihalynuk *et al.* (2002) and detailed in the M.Sc. thesis study by Merran (2002). In Late Carboniferous and Permian times (Table 2) these carbonate strata may have been deposited in a laterally extensive tract of shallow-water, massive limestone that interfingered with well-bedded lagoonal facies and talus to turbidite facies on the platform margins.

New observations, mainly from the Nakina River canyon and its tributaries, and from Mount Sinawa Eddy, are reported here.

NAKINA AND BRANCH CANYONS

Carbonate strata mapped within the Nakina River Canyon in northern 104N/2 are structurally interleaved with panels of ribbon chert 1 to 3 km thick (Figure 3). Various carbonate lithologies are well exposed. Most are the same or similar to units that have been previously reported (Mihalynuk *et al.*, 2002; Merran, 2002) from areas to the south and east. Typical lithologies include light grey, well-bedded, bioclastic (turbiditic?) limestone; coarse

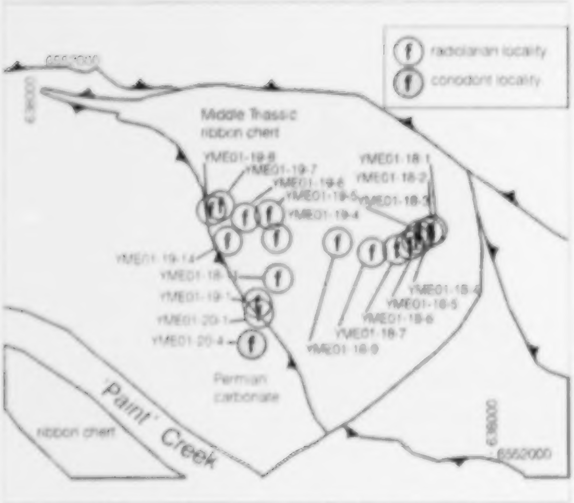

Figure 4. Major antiform north of Paint Creek is cored by Middle Triassic chert and overthrust by Permian carbonate. Fossil numbers prefixed by YME01 correspond with FCO01 prefix in Table 1.

limestone breccia which occurs as sheets and channels decimetres to several metres thick; indistinctly thick to medium-bedded, cream-coloured limestone about 80-120 m thick; and distinctly medium to thin-bedded, dark grey to black, fetid and/or argillaceous limestone ~40m thick. The latter two units are of particular note as they are primary constituents of a thrust-repeated section with a structural thickness of nearly 1 km (*see* Structural Styles, below).

Nakina River canyon in central 104N/2W, east and south of Sinawa Eddy Mountain, is precipitous. Observations of outcrops above the rim of the canyon and vantage point mapping of the canyon walls below, suggest that the dominant lithology is massive, very poorly bedded limestone, such as that which comprises the peak of Sinawa Eddy Mountain. However, a flight down the axis of this part of the canyon revealed moderately well-layered, thick to medium-bedded sections, commonly disrupted by complex subhorizontal faults and folds that mainly have <10m amplitudes and <100m wavelengths. Canyon walls provide the best exposures from which to gain an understanding of the details of the sedimentary and structural complexity of the Cache Creek within the Nakina Transect. Unfortunately, many parts of the main Nakina River canyon are difficult to access.

SINAWA EDDY

Massive limestone at Sinawa Eddy Mountain probably accumulated in an intra-oceanic platformal setting (Monger, 1975; Merran, 2002). Many cubic kilometres of this unit are featureless except for sparse crinoid ossicles and fragments of bivalves, bryozoa, rare corallites, pisoids or limestone clasts. In stark contrast, are well-bedded strata exposed along "Skull Creek" that incises the northern flanks of Sinawa Eddy Mountain. Most conspicuous is a ~40m thick succession of well-layered dark-coloured strata, including volcanic beds, between massive light grey limestone units. Contacts between beds are well exposed in cliff-faces which are oriented perpendicular to the bedding. Only in such locations is it apparent that many of the contacts are either faults or sheared bedding planes. Nevertheless, the succession can be traced for about two kilometres across a shallow cirque. Part of this succession is in fault contact with the massive peak limestone (Photo 6). Exposed at the fault contact are vesicular, strongly fractured, rusty-weathering, dark green mafic flow rocks. They are cut by many high angle faults, making an estimation of thickness difficult. Overlying the mafic volcanics is about two metres of sooty limestone, which is also strongly faulted. This is in fault contact with beds of medium to dark grey limestone with thinner irregular layers of black chert. Bed thickness is variable, up to 1 m thick, but is typically 5 to 20 cm. Some of these beds (especially along strike to the north) contain silicified rugosan corals. The ?base of one bed is packed with 5-8 cm orbicular bivalves (Photo 7). In faulted (originally stratigraphic?) contact is a conspicuous 1-2m thick layer of red and green tuffite; in one place containing a 80cm thick limestone interbed. Very fine laminae display cross stratification and slump structures that suggest a north-dipping paleoslope (Photo 8). Northernmost

Photo 6. Well layered strata in fault contact with massive limestone that comprise the peak of Mt. Sinawa Eddy.

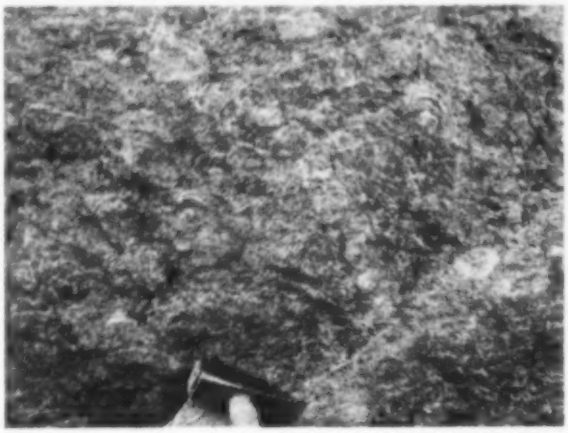

Photo 7. Articulated, orbicular bivalves are packed tightly at the base (?) of the limestone bed.

TABLE 2
FUSULINACEAN FORAM IDENTIFICATIONS BY LIN RUI FROM SAMPLES COLLECTED WITHIN THE NAKINA TRANSECT

GSC Locality Number	BCGS Sample No.	UTM Coordinates (Zone 08V)	Fusulinacean Identification	Age
C220456	MMI01-20-4	631625E, 6550247N	*Sphaeroschwagerina* sp., *Triticites* sp., *Schwagerina* sp.	Early Permian, Asselian
C220457	MMI01-20-6	632197E, 6550113N	*Schwagerina* sp.	Late Carboniferous-Early Permian
C220460	MMI01-21-5	632255E, 6548980N	*Schubertella* sp., *Daixina* sp.	Late Carboniferous-Early Permian
C220461	MMI01-21-6	632268E, 6549033N	*Sphaeroschwagerina* sp., *Schwagerina* sp.	Early Permian, Asselian
C220462	MMI01-21-7	632305E, 6549191N	*Sphaeroschwagerina* sp., *Triticites* sp., *Schwagerina* sp.	Early Permian, Asselian
C220462	MMI01-21-7B	632305E, 6549191N	*Sphaeroschwagerina* sp., *Triticites* sp.	Early Permian, Asselian
C220463	MMI01-21-8B	632352E, 6549607N	?*Eostaffellina* sp., ?*Eoschubertella* sp.	Middle Carboniferous, Moscovian
C220464	MMI01-21-9C	632326E, 6549629N	*Mediocris* sp., *Eoschubertella* sp., ?*Profusulinella* sp.	Middle Carboniferous, Moscovian
C220464	MMI01-21-9D	632326E, 6549629N	?*Pseudostaffella* sp., *Profusulinella* sp.	Middle Carboniferous, Moscovian
C220465	MMI01-23-11	641824E, 6559764N	*Parafusulina* sp., *Pseudodoliolina* sp.	Middle Permian, Roadian (Kubergandian)
C220466	MMI01-23-12	641306E, 6559781N	*Pseudoendothyra* sp., *Schubertella* sp.	Early Permian-Middle Permian
C220467	MMI01-23-13	641176E, 6559686N	*Schubertella* sp., ?*Schwagerina* sp.	Early Permian-Middle Permian
C220468	MMI01-28-8D	654178E, 6564091N	*Schubertella* sp.	Early Permian-Middle Permian
C220469	MMI01-29-1A	622764E, 6554988N	*Parafusulina* sp.	Permian, Leonardian-Rodian
C220469	MMI01-29-1B	622764E, 6554988N	*Parafusulina* sp.	Permian, Leonardian-Rodian
C220499	MMI01-29-18	625936E, 6552249N	*Parafusulina* sp.	Permian, Leonardian-Rodian
C220470	MMI01-30-6C	626779E, 6551009N	No fusulinaceans were found in this sample	
C220470	MMI01-30-6D	626779E, 6551009N	?*Schubertella* sp.	?Permian
C220472	MMI01-31-11A	622642E, 6553662N	*Colania* sp.	Middle Permian, Wordian
C220472	MMI01-31-11B	622642E, 6553662N	*Colania* sp.	Middle Permian, Wordian
C220472	MMI01-31-11C	622642E, 6553662N	*Schubertella* sp., *Nodosaria* sp., *Pachyphloia* sp.	Middle Permian, Wordian
C220473	MMI01-31-12A	622600E, 6553670N	*Schwagerina* sp.	Middle Permian, Wordian
C220473	MMI01-31-12G	622600E, 6553670N	?*Schubertella* sp., ?*Schwagerina* sp.	Middle Permian, Wordian
C220475	MMI01-31-14A	622580E, 6553695N	*Colania* sp.	Middle Permian, Wordian
C220475	MMI01-31-14E	622580E, 6553695N	*Schwagerina* sp.	Middle Permian, Wordian

TABLE 3
PRODUCTIVE CONODONT SAMPLES COLLECTED FROM THE CACHE CREEK COMPLEX DURING THE 2001 FIELD SEASON (36 SAMPLES, 9 PRODUCTIVE)[1]

Field Number	UTM east	UTM north	GSC number	Fossils	Preservation	CAI	Age & comments
FDE01-16-5,	622689	6564368	C-306173	undiagnostic ramiform elements	poor	5	probably Triassic
YME01-16-6	620615	6558443	C-306178	***Neogondolella inclinata*** together with ***Metapolygnathus polygnathiformis***	poor	5	Ladinian-early Carnian (M-Late Triassic)
YME01-19-11	633081	6555787	C-306186	***Neogondolella szaboi***	poor	5	Anisian (Middle Triassic)
YME01-20-4	633980	6553859	C-306187	***Sweetognathus*** ? and ***Hindeodus*** ? occur together with indeterminate ellisonids	very poor	5-5.5	Permian
YME01-21-6	632100	6560081	C-306189	***Sweetognathus*** ? and ***Hindeodus*** ? occur together with indeterminate ellisonids	very poor	5-5.5	Permian
YME01-22-9	630381	6560265		undiagnostic ramiform elements	poor	5	probably Triassic
YME01-23-3	630968	6560595	C-306191	***Idiognathoides*** sp. and ***Neognathodus?*** sp.	very poor	5.5-6	probable Bashkirian to Moscovian (Late Carboniferous)[2]
YME01-24-1	647466	6554472	C-306192	***Sweetognathus*** ? and ***Hindeodus*** ? occur together with indeterminate ellisonids	very poor	5-6	Permian
YME01-31-7	637065	6550442	C-306195	undiagnostic ramiform elements	poor	5	probably Triassic

[1] Identifications by M. Orchard, Geological Survey of Canada

[2] In Nechako region they characterize the first major carbonate (Orchard ***et al***., 2001)

outcrops of this unit are very different in character. They are dun-weathering calcareous volcanic sandstone (Photo 9a), commonly containing decimetre angular blocks of fine-grained carbonate (Photo 9b). Trough cross stratification indicates paleoflow to the south, opposite to paleoflow in the red tuffite. Dun volcanic sandstone is apparently conformably overlain by light grey, poorly layered, thick-bedded limestone, which becomes massive 5-20 metres up section. In one place, at or near the upper volcanic sandstone contact, a breccia with clasts up to the size of small rooms, occurs near the base of the massive unit (Photo 10a). Other such breccia zones can be mapped within the massive unit. They may be collapse breccias related to tectonism.

On the ridge east of `Skull Creek' a similar coarse breccia apparently grades laterally into a homogneous breccia with pebble-sized clasts of limestone, sparse chert and rare, ochre tuff clasts, forming a persistent layer up to 20 m thick (Photo 10b). In places the breccia is well bedded and graded, but more commonly it is massive. This unit is apparently in the immediate hangingwall of a gently west-dipping thrust that most commonly juxtaposes the light grey, massive carbonate with more steeply dipping, well-bedded, dark grey carbonate. The pebble breccia may represent a synorogenic clastic wedge that is overridden by the massive carbonate. A similar unit of possibly synorogenic breccia was mapped between the thick chert unit and well-bedded carbonate in northern 104N/2E.

FELSIC VOLCANIC AND INTERCALATED UNITS

Mapping in 2001 identified bimodal volcanic rocks within a package of dominantly Middle Triassic chert (Figure 3; Mihalynuk et al., 2002). Mapping in 2002 traced the felsic volcanic unit and associated thinly-bedded, platey limestone across the alpine ridges between the lower stretches of `Paint' and Horsefeed creeks. This interval can

Photo 8. Cross stratified tuffite indicates northward paleoflow.

be followed for ~800 m before it is lost beneath cover in a tributary valley of Horsefeed Creek. An exposure of coarse, feldspar-phyric breccia of probable intermediate composition crops out ~600m to the west.

Felsic tuffite forms beds centimetres to decimetres thick. Reworked volcanic detritus, including euhedral quartz grains, are intercalated with green and maroon chert that contains radiolaria of "Paleozoic, possibly Permian" age and abundant sponge spicules (Table 1, MMI01-30-5b). Additional microfossil age determinations are pending. A U-Pb age determination of a sample of quartz-phyric tuff is also pending. Reworked fusulinaceans from the platey limestone are "?Permian" (Table 2, MMI01-30-6D). Two conodont samples collected from sooty limestone were barren. Along strike to the southeast, chert structurally above the volcanic unit contain Middle Triassic radiolaria (FCO01-17-5 to 14, 9 samples; Table 1). The age of the volcanic strata is most likely Permian to Middle Triassic. Volcanic rocks of the Kutcho Formation and associated massive sulphide mineralization were deposited within this time interval (241 - 253 Ma; Childe and Thompson, 1997). Coarse, euhedral quartz phenocrysts are also a characteristic of the Kutcho Formation. Based on these criteria a tenuous correlation with the mineralized Kutcho Formation is suggested. Elevated base metal values in the RGS survey results (Jackaman, 2000) further points to potential for mineralization in the drainage basins where this stratigraphy occurs (*c.f.* Mihalynuk *et al.*, 2002). However, a re-evaluation in 2002 detected no sign of base metal sulphide mineralization in association with the felsic tuff.

COARSE CLASTIC UNIT

Coarse, polymictic conglomerate are known from three separate localites. Two isolated areas are southeast of Mt. O'Keefe where their area of exposure totals less than ~0.2 km^2. A more widespread unit north of Hardluck Peaks crops out across an area of ~4.5 km^2. In all areas the unit appears to rest atop mafic volcaniclastic strata. Clasts include granitoid boulders as well as other clasts that are derived lithologies within the Cache Creek complex: chert, mafic volcanics, limestone, and ultramafite (in order of decreasing abundance). Near Hardluck Peaks, chert blocks range up to the size of small houses, probably deposited as landslide debris near a fault scarp. Middle Triassic radiolaria collected from one such block provide a Middle Triassic maximum age for deposition of that part of the unit (*see* Mihalynuk *et al.*, 2003, this volume).

LATE TRIASSIC TO EARLY JURASSIC CACHE CREEK WACKE

Wacke of the Cache Creek complex was divided into two main units by Mihalynuk *et al.* (2002): a common variety comprised largely of a siliceous mud matrix (a clastic-rich variant of Type 4a chert), and less common variety that is mainly silt and sand-sized grains. Similar relative abundances of these units are mapped in the western Nakina transect. Siliceous mud-rich wacke is brown and less commonly dark grey, black or blue-grey. It commonly contains chert grains and rare cobbles, and volcanic clasts from ash to lapilli size. Rare quartz grains may be derived from quartz diorite, which occurs as, foliated granules. Locally, the unit grades into chert or volcaniclastic rocks. Where this occurs near 'Blackcaps Mountain' the chert is of Middle or Late Triassic age (Table 1).

Photo 9. (a) Distinctive, dun-weathering, volcaniclastic limestone. (b) Angular limestone blocks of boulder size indicate high energy, rapid deposition.

Photo 10. (a) Coarse breccia within otherwise massive light grey limestone. (b) Laterally persistent limestone pebble breccia is remarkably uniform in character.

Sand or silt-sized grains are common within some wacke beds; however, quartz grains locally comprise a significant proportion of the beds. Three of these areas are described in Mihalynuk *et al.* (2002). They are on the north flank of `?Scarface Mountain', on the western ridge of Mount Nimbus, and between lower Horsefeed and `Paint' creeks. At these localities, monocrystalline quartz can comprise as much as 20-30% of the grains.

At `Scarface Mountain,, a chert-dominated fault panel was described by Mihalynuk *et al.* (2002) as containing between 1 and 3 metres of well-bedded, coarse, olive coloured, quartz-rich volcanic sandstone that caps a section of basalt flows and conformably overlying corals within a carbonate buildup about 18m thick. These authors suggested that the clastic rocks smothered the corals, but this interpretation is not supported by new age data. Preliminary fossil identification of the reef fauna indicates a probable Early Carboniferous age, probably late Tournaisian or Early Viséan, according to W. Bamber at the Geological Survey of Canada (personal communication, 2002); whereas, detrital zircons from the overlying wacke are as young as Early Jurassic (*see* Isotopic Age Determinations). A major hiatus is indicated.

West of Mount Nimbus, thinly bedded, silty wacke comprises a 5 to 20+m thick fault-bounded panel between kilometre-thick panels of mafic volcanic and carbonate rocks. Thin beds and lamellae have been strongly disrupted by synsedimentary micro-faults. Populations of detrital zircons extracted from this unit are Middle to Late Triassic in age (Devine, 2002). An adjacent succession of cherty argillite and ribbon chert displays very consistent, straight layering (Type 3 chert). It is brown weathering, and contains Late Triassic radiolaria (MMI01-20-8; Table 1).

Between lower Horsefeed and `Paint' creeks, fault-bounded panels of quartz-rich wacke are tectonically interleaved chert and lesser carbonate. Fault panels are a few metres to a few hundred metres in thickness, and display abundant evidence for soft-sediment deformation. Middle Triassic radiolaria were extracted from a carbonaceous cherty argillite unit (MMI01-29-2), which is concordant with adjacent carbonate containing Leonardian-Roadian fusulinids (Early-Middle Permian; MMI01-29-1A, 1B; Table 2). Approximately 1km away, across strike, is a disrupted argillaceous chert unit containing semi-continuous beds and bulbous layers of chert. Radiolaria extracted from the latter (MMI01-29-4b, Table 1) reveal an Early Permian age. These beds are presumably in thrust contact with ribbon chert and quartz-bearing wacke. Radiolarian chert occurs within the wacke as subangular blocks and semi-continuous beds up to 30 cm thick. Radiolaria from one block returned a Late Triassic age (MMI01-29-5b, Table 1), one of the youngest ages obtained from chert of the Cache Creek complex. Farther across strike, in another fault panel, ribbon chert from a locality with unusually straight beds (Type 3 chert), contain Middle Triassic radiolaria (MMI01-29-8).

LABERGE GROUP

Laberge Group is restricted to the western end of the Nakina transect, west of the Nahlin Fault (Figure 3). Laberge group stratigraphy within the transect area, together with a preliminary assessment of its hydrocarbon potential, is presented by English *et al.* (2003, this volume). Here we outline only observations that are not included by those authors.

CHERT PEBBLE CONGLOMERATE

Chert pebble conglomerate is known from immediately southwest of the Nahlin Fault along the informally named `Psychobear' ridge. A resistant band of listwanite along the Nahlin fault forms the ridge crest and conglomerate is exposed in a series of low outcrops covering about 100 m^2 within open forest just a few metres west of the ridge crest (southeast of Goldbottom Creek, too small to show on Figure 3). Chert pebbles are well-rounded, dominantly grey in colour and comprise about 80% of the unit.

This unit is tentatively correlated with Middle Jurassic (Bajocian) chert pebble conglomerate known from the Tulsequah area (Mihalynuk *et al.*, 1995).

MAGNETIC GARNET-OLIVINE WACKE

A distinctive wacke unit within the Laberge Group contains up to 3% detrital garnet and sparse, very fresh olivine grains (Photo 11). Plagioclase-hornblende porphyry

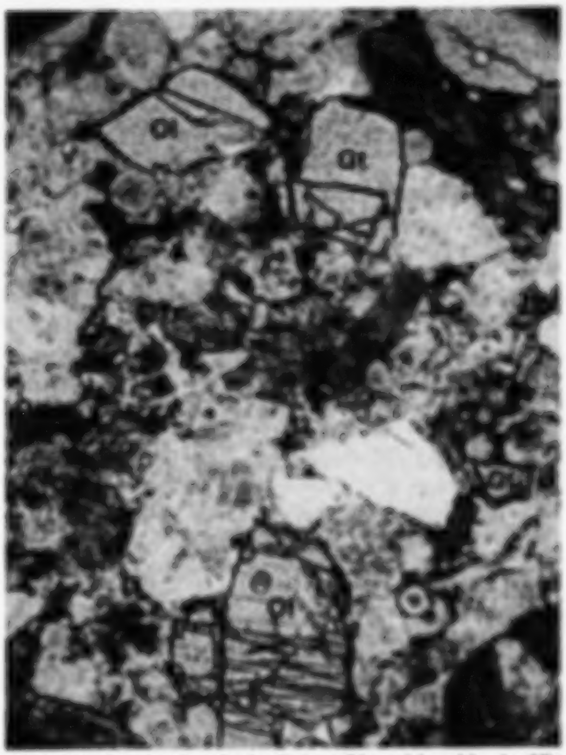

Photo 11. Garnet (Gt), fresh olivine (Ol) and hornblende (Hb) within magnetic, tuffaceous wacke of the Laberge Group. Length of photo represents ~2mm.

clasts of sand to pebble size are common. The unit is abnormally magnetic (15-22 $x10^{-3}$ SI) and correlates with magnetic anomaly that is well portrayed on the regional aeromagnetic survey map (Dumont *et al.*, 2001c). It is one of the few marker units within the Laberge Group of the Nakina transect and has been sampled for detrital zircon separation and dating in order to help constrain its maximum age. Microprobe analyses of the garnet and olivine grains are in progress.

SLOKO VOLCANIC STRATA

Mafic to felsic continental arc volcanic rocks of the Sloko Group are restricted to the western margin of the transect area. Common units include white and rust felsic tuff, green lapilli tuff and coarse breccia, and dense, feldspar-phyric flows and sills. Unconformable or fault contacts with the Laberge Group strata are well exposed. A basal conglomerate is locally well developed. South of Paradise Peak, the basal conglomerate unit is more than 30 metres thick (Photo 12). Throughout the lower half of the unit are seams of coal up to 15cm thick. Some seams are relatively pure. More commonly, they have a significant ash component. Clasts within the conglomerate are mainly derived from the Sloko Group or the Laberge Group strata.

Polymictic ash tuff is a common constituent within the lower Sloko Group. Pyroclasts are commonly light green lapilli, but range to dark-coloured bombs up to a metre or more across (Photo 13). Another common lithology is cream coloured lapilli and ash tuff with local rust weathering.

Photo 12. Basal conglomerate of the Sloko Group south of Paradise Peak, contains coal seams, especially in its lower half.

Dense, dark green to black, feldspar-porphyritic flows and sills are minor constituents within the volcanic stratigraphy, except for where they crop out west of Pike Lake. At this locality, fresh basalt is tentatively included with the Sloko Group as originally suggested by Aitken (1959) because it appears to be much less altered than basaltic rocks

Photo 13. Course angular bombs in Sloko Group pyroclastic unit, note sledge head for scale.

of the Cache Creek complex. However, the unit displays a magnetic character indistinguishable from the adjacent Cache Creek complex, and like the older units, it is also truncated by the Nahlin fault.

LATE SYN- TO POST-ACCRETIONARY INTRUSIVE ROCKS

Three semicircular to elongate intrusions lie northeast of the Nahlin fault. All are composed of hornblende > biotite granodiorite and quartz diorite. Internal schlieren or contact zones of quartz diorite are common. Aitken (1959) mapped them as Middle Jurassic age. All major bodies have been sampled for isotopic age determinations, but at the time of writing, only the Nakina River stock age has a confirmed Middle Jurassic age by $^{40}Ar/^{39}Ar$ dating of biotite (see Mihalynuk *et al.*, 2003 in the following paper).

Nakina River stock (named by Aitken, 1959) is the largest and most elongated, with its long axis oriented parallel to the regional structural grain. It extends ~18 km from south of the Atlin 104N map area to the southern flank of Focus Mountain. Within the map area, it averages about 4 km across.

In northeastern 104N/3, the Chikoida Mountain stock (Aitken, 1959) is a composite body that is slightly east-northeast elongated, with maximum continuously exposed dimension of 7.5 km. However, outcrops up to 2.5 km west of the continuous exposures of the body appear from a distance to also be intrusive. It is about 4 km wide, although discontinuous outcrops on its treed northern slope probably belong to an apophysis that extends a further 7 km from the main body. An annular positive magnetic anomaly that occupies the centre third of the stock may be a late intrusive phase. However, an isolated occurrence (~2 Ha) of Quaternary basalt with abundant mantle xenoliths occurs on the inner margin of the anomaly annulus.

A small, ~1km^2 granodioritic body centred 3.5 km east-southeast of Focus Mountain, had not been previously mapped. It is herein called the Focus Mountain stock.

All intrusive bodies cut across pre-existing structures, but also appear to have intruded with a force that has shouldered aside and warped structural trends in the country rocks. Such relationships are well described by Aitken (1959) and are the subject of detailed mapping and petrographic studies by Bath (2003, this volume).

SLOKO DIORITE

A subcircular diorite stock underlies the precipitous terrain around Paradise Peak. It intrudes and thermally alters both Laberge Group and Sloko Group strata. Like other Sloko suite intrusive bodies, this stock is believed to be broadly comagmatic with the volcanic carapace into which it intruded.

ISOTOPIC AGE DETERMINATIONS

We report here on successful $^{40}Ar/^{39}Ar$ age dating of the mafic oceanic crustal rocks and detrital zircon age determinations from overlying coarse clastic strata. No age determination of the mantle rocks has yet been attempted from the Cache Creek in the Nakina transect, primarily because harzburgite normally lacks mineral species that are amenable to conventional dating techniques. However, Gordey *et al.* (1998) were apparently successful in recovering a small amount of broken, clear, colourless zircon from peridotite in the Teslin map area. They reported an age 245.4 +/-0.8 Ma and interpret it as the age of uplift and quenching of the mantle, possibly a few million years after being brought to the surface by sea floor spreading.

PROCEDURES FOR $^{40}AR/^{39}AR$ ANALYSIS

Laser $^{40}Ar/^{39}Ar$ step-heating analysis was carried out at the Geological Survey of Canada laboratories in Ottawa, Ontario. Selected samples were processed for 40Ar-39Ar analysis of hornblende phenocrysts by standard heavy-liquid mineral separation techniques, followed by hand picking of clear, unaltered crystals in the size range 0.5 to 1 mm. Individual mineral separates were loaded into aluminum foil packets along with a single grain of Fish Canyon Tuff Sanidine (FCT-SAN) to act as flux monitor (apparent age = 28.03± 0.1 Ma; Renne *et al.*, 1998). The sample packets were arranged radially inside an aluminum can. The samples were then irradiated for 12 hours at the research reactor of McMaster University in a fast neutron flux of approximately 5×10^{16} neutrons/cm^2. Neutron flux gradients throughout the sample canister were evaluated by analyzing the sanidine flux monitors included with each sample packet. We then interpolated a linear fit for calculated J-factor versus sample position. The error on individual J-factor values is conservatively estimated at ±1.0% (2 sigma).

Upon return from the reactor, samples were split into several aliquots and loaded into individual 1.5 mm-diameter holes in a copper planchet. The planchet was then placed in the extraction line and the system was evacuated. Heating of individual sample aliquots in steps of increasing temperature was achieved using a Merchantek MIR10 10W CO_2 laser equipped with a 2 mm x 2 mm flat-field lens. The released Ar gas was cleaned over getters for ten minutes, and then analyzed isotopically using the secondary electron multiplier system of a VG3600 gas source mass spectrometer; details of data collection protocols can be found in Villeneuve and MacIntyre (1997) and Villeneuve *et al.* (2000).

Corrected argon isotopic data are listed in Table 4, and presented as gas release spectra shown on Figure 5. Such plots provide a visual image of replicated heating profiles, relative gas volumes per heating step, evidence for Ar-loss in the low temperature steps, and the error and apparent age of each step.

Because the error associated with the J-factor is systematic and not related to individual analyses, correction for this uncertainty is not applied until calculation of dates from isotopic correlation diagrams (Roddick, 1988). No evidence for excess ^{40}Ar was observed in any of the samples and, therefore, all regressions are assumed to pass through the $^{40}Ar/^{36}Ar$ value for atmospheric air (295.5). All errors are quoted at the 2 sigma level of uncertainty.

PROCEDURES FOR U/PB ANALYSIS

Following the separation of heavy minerals using heavy liquids, samples were passed through a Frantz LB-1 magnetic separator to purify zircon, titanite and monazite. Zircon crystals were selected for analysis based on criteria that optimized for their clarity, lack of cloudiness and colour, and lack of fractures. All zircons were abraded prior to analysis to increase concordance by removing the outer portions of the grains where much of the Pb loss and alteration take place (Krogh, 1982).

Following abrasion, photography, and final mineral selection, mineral fractions were analyzed according to methods summarized in (Parrish *et al.*, 1987). Data have been reduced and errors have been propagated using software written by J.C. Roddick; error propagation was done by numerical methods (Parrish *et al.*, 1987; Roddick, 1987). Error ellipses on concordia diagrams are shown at the 2 sigma (95%) confidence level of uncertainty. Final errors are indicated on Table 5. Fraction letters shown on concordia diagrams are keyed to the fraction letters in Table 5.

AGE OF OCEANIC CRUSTAL ROCKS

Of all magmatic rocks sampled within the Nakina transect, the contacts between the Tsaia Creek plagiogranite and mafic volcanic and diabase rocks that it intrudes has been least affected by faulting. Dating of the Tsaia Creek plagiogranite by both $^{40}Ar/^{39}Ar$ and U-Pb age methods at the GSC's Geochronology Laboratory in Ottawa yielded ages that compare favourably despite problems with $^{40}Ar/^{39}Ar$ determination of hornblende due to a high Ca/K ratio (>70), and abundant Cl, leading to larger than typical uncertainties (Table 4, Figure 5). A second of two Ar analyses produced a preferred $^{40}Ar/^{39}Ar$ age of 265 ± 25 Ma, as determined from a plateau representing 98% of Ar released.

Abundant, high quality zircons were recovered from the plagiogranite. Four concordant to near concordant, overlapping analyses result in an interpreted age of 261.6 ± 0.7 Ma, with MSWD of 0.6 (Table 5, Figure 6). This is the oldest directly dated oceanic crust in the northern Cache Creek terrane and is coeval with a 263.3 ± 0.4 Ma age determination (Mihalynuk *et al.*, 1999) from adamellite granodiorite in the French Range (Figure 1). The crustal age data are corroborated by unpublished age data from ibbotsonites near Mount Nimbus (located in 92P/14NW 1), which also returned Late Permian ages as reported by Devine (2002).

QUARTZ-RICH CLASTIC ROCKS

Quartz-rich strata were sampled at two localities for detrital zircon age determinations. Two samples were collected from an olive green, quartz-rich sandstone that overlies fossiliferous limestone interbedded with mafic tuff on the north side of Sentinel Mountain.

Seven samples were collected from a succession of immature, quartz-rich clastic rocks that unconformably overlies the oceanic crustal section north of Hardluck Peaks (above the Jesse? occurrence; see Mihalynuk *et al.*, 2003, this volume). One sample was collected from coarse sandstone, and six granitoid boulders were taken from a very coarse conglomerate.

Zircons were extracted and single zircon grains were analyzed by the SHRIMP (Super High Resolution Ion

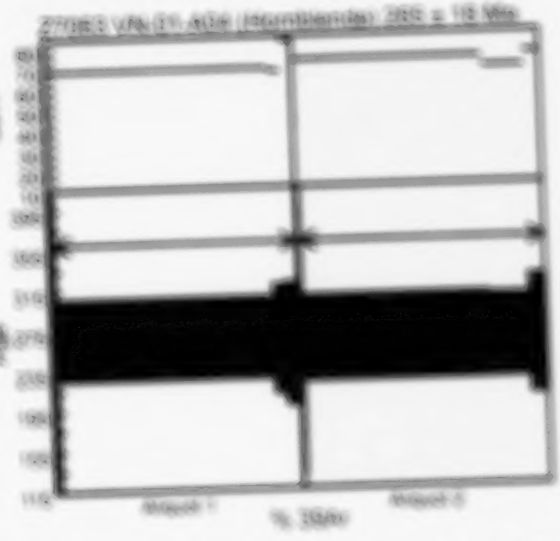

Figure 5. Stepwise heating and $^{40}Ar/^{39}Ar$ release spectrum for hornblende from the Tsaia Creek plagiogranite.

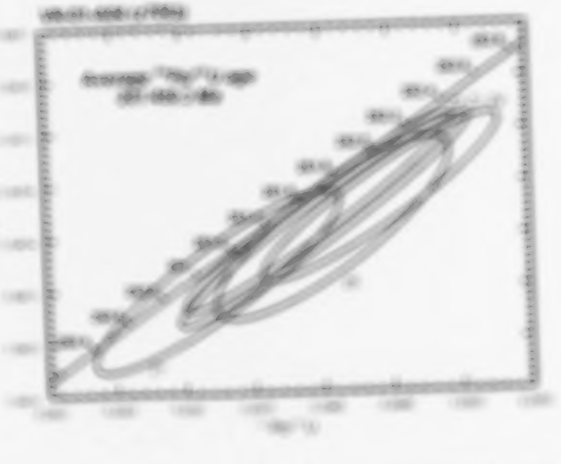

Figure 6. Concordia plot of U-Pb isotopic compositions of zircon populations extracted from the Tsaia Creek plagiogranite. A weighted average of four concordant fractions yields a best interpreted age of 261.6 ± 0.7 Ma.

TABLE [illegible]

[illegible]

[illegible]

Aliquot A

[illegible]

Aliquot B

[illegible]

[illegible]

MicroProbe at the Geological Survey of Canada in Ottawa ([illegible] Williams *et al.*, 2003, this volume).

Analysis of one of the [illegible] sandstone samples revealed a [illegible] age population. [illegible]

Analysis of the [illegible] sandstone samples [illegible] Williams *et al.* (2003, this volume).

STRUCTURAL STYLES

[illegible]

[illegible]

[illegible]

[illegible]

[illegible]

[illegible]

[illegible]

[illegible]

[illegible]

[illegible]

[illegible]

[illegible]

[illegible]

biotite zone were not mapped out in detail, but it is estimated as less than 1 km across. Biotite is not deformed (Photo 15); therefore, it may have formed subsequent to latest regional deformation in the Middle Jurassic. The thermal alteration zone is coincident with the southern margin of a weak positive magnetic anomaly on the aeromagnetic survey map (Dumont *et al.* 2001b). It is noteworthy that the Thunder Alley occurrence is not imaged on the aeromagnetic survey, indicating that substantial accumulations of magnetite are unlikely to be present in the subsurface. Analysis of stream sediments (Table 6) did not reveal metal values in concentrations significantly above background values reported by Jackaman (2000) as part of the regional geochemical survey; however, sampling focused on drainages north of the occurrence.

QUARTZ-SERICITE-PYRITE MINERALIZATION

A rust-weathering zone of intermittently developed quartz-sericite-pyrite mineralization crops out along ~200m of the upper canyon section of Tumbleypack Creek (Photo 16; location Z on Figure 3). Pyrite comprises up to 15% of the most altered outcrops (MMI02-12-7); although, geochemical analysis of the alteration zone did not reveal base metal concentrations of economic interest.

The cause of this mineralization is not known; however, it occurs on the margin of a positive magnetic anomaly, near the terminus of an eastward-extending salient (Figure 7). The cause of the magnetic anomaly is assumed to be related to an unexposed intrusion. Outcrops closest to the heart of the anomaly are hornfelsed chert cut by a single 2m thick, light pink, feldspar porphyritic dike.

PARADISE PEAK PYRRHOTITE

Boulders of massive pyrrhotite occur on the southeast flank of the group of steep ridges comprising Paradise Peak (Figure 3). Boulders range in size up to 30 by 20 by 15 cm within a talus fan (Photo 17). Part of the talus debris is derived from the thermally metamorphosed contact between Slocko diorite and well-bedded calcareous wacke and argillite of the Laberge Group. Geochemical analysis of the boulder did not return base or precious metal values of interest.

Photo 16. A view up Tumbleypack Creek of quartz-sericite-pyrite altered zone.

CHIKOIDA MOUNTAIN TALC

Tabular bodies of orange-weathering talc occur near the contact between ultramafic rocks and chert on east flank of Chikoida Mountain. These bodies parallel the fabric within the serpentinite. They are exposed for several metres along strike and are up to a metre or more thick. Talc purity has not been established.

TABLE 5
U-PB ISOTOPIC AGE DATA DETERMINED BY THERMAL IONIZATION MASS SPECTROMETRY
AT THE GSC OTTAWA GEOCHRONOLOGY LABORATORY

F[1]	Wt[2] mg	U ppm	Pb[3] ppm	$^{206}Pb/^{204}Pb$[4]	Pb[5] pg	$^{208}Pb/^{206}Pb$[3]	Radiogenic ratios (±1σ, %)[6] $^{206}Pb/^{238}U$	$^{207}Pb/^{235}U$	$^{207}Pb/^{206}Pb$	Age (Ma, ±2σ) $^{206}Pb/^{238}U$	$^{207}Pb/^{235}U$	$^{207}Pb/^{206}Pb$
VN-01-A04 (Z7063: 59.0110°N 132.2279°E)												
Z1 (Z)	307	90	6	22150	0	0.080	0.2911±0.15	0.04113±0.14	0.05149±0.07	265.1±0.7	259.9±0.7	263±3
Z2 (Z)	015	93	4	50179	1	0.110	0.2942±0.18	0.04016±0.17	0.05152±0.04	261.7±0.8	261.5±0.9	264±2
Z3 (Z)	032	98	4	64523	2	0.110	0.2942±0.17	0.04016±0.15	0.05153±0.04	261.7±0.8	261.5±0.8	264±2
Z4 (Z)	283	120	5	38732	2	0.110	0.2942±0.15	0.04016±0.15	0.05153±0.06	262.4±0.7	261.8±0.7	266±3
Z5 (Z)	173	222	6	29890	1	0.110	0.2942±0.16	0.04016±0.16	0.05154±0.08	261.8±0.7	261.4±0.7	265±4

[1] Fraction: all zircon fractions are abraded. (Z) = Zircon

[2] Error on weight = ±0.001 mg

[3] Radiogenic Pb

[4] Measured ratio corrected for spike and Pb fractionation of 0.09±0.03%/AMU

[5] Total common Pb on analysis corrected for fractionation and spike, of blank model Pb composition

[6] Corrected for blank and spike Pb and U and common Pb (Stacey Kramers model Pb equal to the 206Pb/238U age)

Figure 7. Strong positive magnetic anomaly in north-central 104N/2. Near the eastern limit of the anomaly is the alteration zone on "Tumblepack Creek".

GREMLIN'S CASTLE SEPIOLITE

Sepiolite occurs along a spiked ridge informally named 'the Gremlin's Castle' 5.6 km south of Mount O'Keefe. Mineralogical identification was made via X-ray diffraction at Teck Cominco Laboratories, Vancouver.

Sepiolite is a hydrated magnesium silicate: $Mg_4Si_6O_{15}\cdot 2H_2O$. It has a hollow, tube-like molecular structure, producing a lightweight molecular sieve. Industrial applications are numerous: environmental absorbants, paint thickeners, deodorizers, livestock feed supplements, carriers for fertilizers and pesticides, rubber strengtheners, among others. Sepiolite normally occurs as compact earthy masses, rarely in crystalline form with fibres up to 2cm in length. In this regard, the Gremlin's Castle sepiolite is unusual. Parallel fibres nearly 20 cm long comprise veins that occur as gashes within quartz-carbonate-chromian mica-altered ultramafite (listwanite). The veins are light grey-green and look like splintered and weathered wood (Photo 18). Sepiolite veins comprise up to ~3% of the outcrops in which they were observed; however, no accurate assessment of either the extent or abundance of sepiolite veining was made in the field. Because of its unusually fine state of crystallization, the Gremlin's Castle sepiolite may be useful in specialized applications, or as museum specimens.

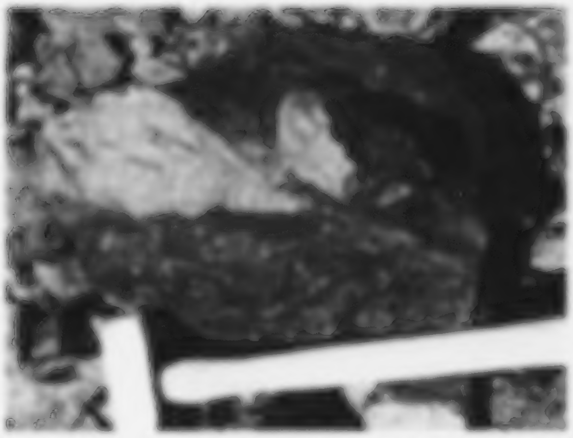

Photo 17. Talus block of massive pyrrhotite southeast of Paradise Peak.

Photo 18. Sepiolite vein within listwanite.

SUMMARY AND FUTURE WORK

Geological field studies under the aegis of the Targeted Geoscience Initiative have shown that the Nakina transect area contains geological environments that are prospective for a variety of deposit types. This work has also begun to unravel the structural complexities of the Cache Creek complex and it has forever changed the way that we view its paleotectonic origins.

Of key importance has been the discovery of submarine felsic volcanic rocks of Late Permian to Middle Triassic age; coeval with those hosting volcanogenic massive sulphide accumulations at Kutcho Creek. Volcanic quartz in detrital sediments from a variety of places across the map area points to widespread felsic volcanism within or on the margins of the ancient Cache Creek ocean basin. Indeed, most of the volcanic rocks within the northern Cache Creek terrane are now known to have an intra-oceanic arc affinity. The possibility that Cache Creek felsic or mafic volcanic successions might be associated with mineralised exhalites is demonstrated by vigorous fossil hydrothermal system

TABLE 6
ANALYTICAL RESULTS FROM STREAM SEDIMENTS

Station Number	NAD 83 UTM East	Zone 9 UTM North	Mo ppm	Cu ppm	Pb ppm	Zn ppm	Ag ppb	Ni ppm	Co ppm	Mn ppm	Fe %	As ppm	U ppm	Au ppb	Th ppm	Sr ppm	Cd ppm	Sb ppm	Bi ppm	V ppm
FDR02-02-06*	629718	6541346	1.12	77.45	3.28	88.7	74	482.0	44.2	794	4.14	2.8	0.9	1.7	0.9	37.5	0.26	0.22	0.06	88
FDR02-02-07*	629136	6541305	1.26	90.39	5.66	162.0	263	157.2	80.2	1346	3.91	5.2	1.7	3.8	2.0	59.2	0.06	2.76	0.17	102
FDR02-02-10*	629117	6541720	1.19	72.06	3.41	93.9	90	95.7	34.4	994	4.19	3.3	0.3	1.8	0.8	54.5	0.26	0.41	0.06	80
JEN02-14-01	634833	6561399	4.58	69.04	6.08	88.7	300	50.1	17.1	1044	2.97	29.1	1.0	8.9	2.4	30.6	0.63	2.31	0.13	54
JEN02-14-03	632947	6563483	1.84	61.50	8.04	111.0	178	53.3	9.8	995	1.46	6.9	2.2	2.6	0.4	50.7	1.91	0.91	0.08	33
JEN02-14-07	632882	6563220	2.43	60.98	5.52	98.1	89	62.1	16.8	977	2.82	6.1	1.0	3.6	2.2	35.4	0.89	0.68	0.11	57
JEN02-14-09	631915	6563659	0.90	18.45	2.65	102.8	154	18.8	5.1	355	0.92	3.0	1.0	1.2	0.1	76.6	1.88	0.59	0.06	21
MMI02-11-05	636985	6568772	0.96	43.82	5.13	145.1	79	76.2	17.8	899	2.08	6.5	0.6	3.8	1.5	32.3	1.17	0.48	0.09	60
MMI02-11-11	636792	6567485	1.54	39.80	4.90	128.3	52	77.7	18.0	2004	2.04	5.1	0.7	1.3	1.1	28.0	1.00	0.39	0.10	58
MMI02-11-14	636318	6566381	1.56	72.30	8.88	190.3	90	60.6	14.8	1364	2.58	6.3	1.7	1.8	1.2	28.9	2.64	0.77	0.15	39
MMI02-11-15	636306	6566279	1.00	45.70	5.83	155.5	44	82.3	16.8	884	3.10	5.1	0.5	2.1	1.1	32.4	1.40	0.48	0.10	69
MMI02-12-07sc	626552	6568582	14.90	70.65	25.89	95.2	866	29.7	7.9	330	7.60	15.2	2.8	< .2	8.1	1014.6	0.58	0.87	2.83	47
MMI02-12-11	625919	6568900	1.29	6.18	1.36	25.0	20	9.4	3.0	229	0.80	0.9	3.4	0.6	1.4	25.1	0.09	0.09	0.02	21
MMI02-14-05*	630872	6548094	2.05	57.55	4.09	126.0	56	67.9	24.5	1066	4.32	5.5	0.4	0.9	0.4	65.5	0.50	0.46	0.06	106
MMI02-15-10	602970	6565290	0.64	24.11	2.60	59.7	37	188.8	29.8	1019	3.31	3.0	0.3	0.9	1.2	21.7	0.14	0.20	0.05	61
ORC02-28-08	636207	6568194	0.98	47.83	5.50	92.7	104	77.2	16.6	498	2.80	15.9	0.6	10.1	1.9	29.1	0.56	0.89	0.11	67
ORC02-30-02	629503	6568438	0.42	3.66	1.54	18.3	19	5.6	2.1	188	0.77	0.6	0.7	0.2	0.6	17.0	0.11	0.08	< .02	22
Red Dog Standard			13.91	863.65	7.42	54.1	84	12.6	11.7	438	4.38	6.0	0.4	22.0	1.1	48.9	0.22	0.21	0.55	99

Station Number	Ca %	P %	La ppm	Cr ppm	Mg %	Ba ppm	Ti %	B ppm	Al %	Na %	K %	W ppm	Sc ppm	Tl ppm	S %	Hg ppb	Se ppm	Te ppm	Ga ppm
FDR02-02-06*	1.30	0.046	5.0	395.0	5.49	114.2	0.130	11	2.17	0.016	0.07	< .1	9.0	0.06	0.04	41	0.9	0.03	6.6
FDR02-02-07*	0.63	0.075	9.0	215.1	3.51	689.5	0.113	2	2.08	0.022	0.22	< .1	7.9	0.24	0.08	67	2.1	0.08	7.6
FDR02-02-10*	1.14	0.063	6.6	88.3	1.72	367.3	0.053	5	1.69	0.015	0.11	< .1	10.3	0.11	0.09	47	0.6	0.05	5.4
JEN02-14-01	0.89	0.071	11.6	38.9	0.79	170.1	0.105	1	1.10	0.006	0.08	< .1	4.4	0.11	0.04	105	0.8	0.08	4.0
JEN02-14-03	4.88	0.124	9.3	110.1	1.45	204.1	0.048	8	0.75	0.010	0.09	< .1	3.9	0.26	0.18	150	5.5	0.03	3.0
JEN02-14-07	1.31	0.119	14.2	65.6	1.33	115.6	0.126	1	1.36	0.006	0.11	< .1	4.1	0.10	0.03	66	0.9	0.05	4.9
JEN02-14-09	16.75	0.077	7.0	41.7	1.38	111.8	0.026	1	0.41	0.006	0.05	< .1	1.4	0.12	0.08	61	1.6	0.03	1.6
MMI02-11-05	1.21	0.115	11.4	104.8	1.57	208.0	0.114	2	1.51	0.007	0.13	< .1	4.7	0.09	0.07	81	1.7	0.02	5.5
MMI02-11-11	0.99	0.088	10.7	98.6	1.45	277.3	0.105	1	1.41	0.008	0.11	< .1	8.0	0.10	0.06	39	2.4	0.05	5.3
MMI02-11-14	1.58	0.228	21.3	41.6	1.01	231.1	0.041	2	1.45	0.004	0.15	< .1	3.7	0.20	0.05	99	0.4	0.06	5.0
MMI02-11-15	1.01	0.113	15.0	98.2	1.70	175.8	0.105	3	1.75	0.006	0.17	< .1	4.9	0.10	0.06	42	0.8	0.05	6.2
MMI02-12-07sc	0.31	0.171	18.3	19.9	0.72	125.3	0.139	1	0.82	0.141	0.62	8	2.3	0.58	1.64	21	15.9	0.24	4.0
MMI02-12-11	0.41	0.095	8.2	17.7	0.27	382.7	0.044	< 1	0.70	0.018	0.05	< .1	1.3	0.05	0.02	8	0.3	< .02	2.4
MMI02-14-05*	0.83	0.041	3.7	69.9	2.19	36.0	0.157	4	2.35	0.026	0.05	< .1	9.7	0.19	0.04	35	0.6	0.03	7.8
MMI02-15-10	0.67	0.060	7.5	367.9	3.74	93.0	0.107	4	1.14	0.007	0.04	< .1	5.4	0.05	0.92	171	0.3	0.02	4.6
ORC02-28-08	1.00	0.117	13.1	110.6	1.68	183.6	0.111	3	1.56	0.010	0.15	< .1	6.3	0.12	0.04	120	0.9	0.03	5.3
ORC02-30-02	0.40	0.069	5.0	14.4	0.17	87.0	0.035	< 1	0.41	0.018	0.03	< .1	0.7	0.03	0.02	7	0.4	< .02	1.3
Red Dog Standard	0.68	0.057	4.6	22.5	0.69	53.6	0.138	< 1	1.84	0.021	0.04	0.1	4.8	0.01	0.65	17	3.2	0.41	6.0

Analyses by ACME Analytical Laboratories, Vancouver

Sediment sample sieved to -80 mesh @ ACME
Aqua regia digestion; ICPMS (1 gram sample)

* as station number suffix indicates a sample collected in the drainage underlying the Joss'alun discovery

'sc' as station number suffix indicates a soil composite (mainly fine talus) that comprises the Thunder Alley occurrence. Thermal metamorphism of Cache Creek strata northeast of Thunder Alley may be related to the hydrothermal system responsible for the exhalite. Our follow-up mapping and stream sediment sampling around Thunder Alley focused on the area north of the occurrence. More prospecting and geochemical evaluation of the area is required to properly assess the potential for mineralization in the area.

The origin of massive copper sulphide at the new Joss'alun discovery is uncertain, but sulphide lenses appear to be at least partly concordant, and possibly syngenetic with submarine volcanic rocks (more discussion in the following paper).

Structural and stratigraphic advances in our understanding of the Nakina transect have benefited from the rapid expansion of paleontological and isotopic age data. Production of 1:50 000 scale maps will be aided by ~140 new radiolarian collections; ~65 new collections of Carboniferous to Permian fusulinids; 9 Carboniferous, Permian and Triassic conodont collections, and numerous macrofossil collections including Permian ammonoids and Carboniferous corals. New structural, stratigraphic and age data, in combination with petrochemical studies (*e.g.* (English *et al.*, 2002), permit as to suggest the following tectonic history:

- Late Permian rupture of oceanic crust and formation of the intra-oceanic Kutcho arc, perhaps more than 2500 km long. Submarine massive sulphide mineralization accumulates within the arc setting. A lack of rocks older than Early Carboniferous suggests that the rupture occurred across oceanic crust of this age and younger.
- Strata incorporated into the forearc and accretionary complex retain an oceanic signature until Middle or Late Triassic time when quartz-rich detritus is derived from exhumation of the Kutcho arc.
- By Early Jurassic time, detritus carries Devono-Mississipppian zircons signalling influx from Stikine, Quesnel and/or Yukon-Tanana terranes (may all be broadly considered parts of the same arc complex; *e.g.* Mihalynuk *et al.*, 1994). The northern Quesnel arc segment amalgamated with an ancestral continental margin assemblage at 186 Ma (Nixon *et al.*, 1993).
- In Early Middle Jurassic time (~173 Ma Mihalynuk *et al.*, 1999) the Stikine arc segment and intervening Cache Creek complex collided with the Quesnel arc segment. Because the Quesnel arc was already welded to an inboard continental domain (North America or an outboard ribbon continent; *e.g.* Johnston, 2001), it acted as a rigid backstop, and drove the intervening Cache Creek accretionary complex southwest over the forearc Laberge Group strata of the Stikine arc segment. Southwest-verging fold and thrust belt deformation in the previously undeformed Laberge Group records the collision. Superposition of this deformational episode on thrust faulted accretionary complex resulted in (re)folding, reactivation, and or reimbrication by younger thrust faults.
- Emplacement-related structures in Cache Creek terrane are extensively cut by Middle Jurassic plutons ~172Ma. Hydrothermal alteration of ultramafite adjacent to the Chikoida stock may have facilitated formation of tabular bodies of talc.
- Dextral motion on the Nahlin fault occurred, at least intermittently, until Eocene time. Motion around 55 Ma may have facilitated crustal transit of Sloko Group magma and eruption of continental arc volcanic rocks and comagmatic plutons. Extensive zones of listwanite at deflections in the fault trace may record hydrothermal fields related to Sloko magmatism. Post Sloko dilation resulted in gash veins infilled with sepiolite.
- By ~46 Ma the Nahlin fault is plugged by the Birch Mountain pluton.

ACKNOWLEDGEMENTS

Success of the Nakina transect mapping program is due to the combined effort of a dedicated mapping team who made full use of the midnight sun (or lack thereof). Those not acknowledged through co-authorship are: Adam Bath, Jacqueline Blackwell, Oliver Roenitz, Lucinda Leonard and Fionnuala Devine; all delivered a rock-solid effort. Sincere thanks to the Atlin TGI leader, Carmel Lowe of the Pacific Geoscience Centre (GSC), who took care of endless paperwork in order to secure the TGI funding for mapping in 2002. Jim Monger thoughtfully offered us the use of his unpublished field maps. Numerous individuals aided in geological mapping or contributed to our work through stimulating discussions (at times slurred) at our base camp in Atlin.

For a second consecutive field season, Norm Graham of Discovery Helicopters in Atlin extended service beyond the limits of our budget, and beyond the limits of reasonable flying conditions. Rita Scott and Nora (Kuya) Minogue shared with us their home and folklore. Thanks also to the many other people of Atlin who offer their continued enthusiastic support of our field programs.

REFERENCES CITED

Aitken, J.D. (1959): Atlin map-area, British Columbia; *Geological Survey of Canada*, Memoir 307, 89 pages.

Ash, C.H. (1994): Origin and tectonic setting of ophiolitic ultramafic and related rocks in the Atlin area, British Columbia (NTS 104N); *B.C. Ministry of Energy, Mines and Petroleum Resources*, Bulletin 94, 48 pages.

Bath, A. (2003): Atlin TGI, Part IV: Middle Jurassic granitic plutons within the CacheCreek terrane and their aureoles: Implications for terrane emplacement and deformation; *in* Geological Fieldwork 2002, *BC Ministry of Energy and Mines*, Paper 2003-1, this volume.

BCMEM (1978): Atlin Regional Geochemical Survey, 882 sites plus 160 lake sites; *BC Ministry of Energy and Mines and the Geological Survey of Canada*, RGS 51.

Bilsland, W.W. (1952): Atlin, 1898-1910: The story of a gold boom; *British Columbia Historical Quarterly*, Volume 16, Numbers 3 and 4 (Reprinted in 1971 by the Atlin Centennial Committee, 63 pages with pictorial supplement).

Bloodgood, M.A. and Bellefontaine, K.A. (1990): The geology of the Atlin area (Dixie Lake and Teresa Island) (104N/6 and parts of 104N/5 and 12); *in* Geological Fieldwork, 1989, *B.C. Ministry of Energy, Mines and Petroleum Resources*, Paper 1990-1, pages 205-215.

Childe, F.C. and Thompson, J.F.H. (1997): Geological setting, U-Pb geochronology, and radiogenic isotopic characteristics of the Permo-Triassic Kutcho Assemblage, north-central British Columbia; *Canadian Journal of Earth Sciences* , Volume 34, pages 1310-1324.

Childe, F.C., Thompson, J.F.H., Mortensen, J.K., Friedman, R.M., Schiarizza, P., Bellefontaine, K. and Marr, J.M. (1998): Primitive Permo-Triassic volcanism in the Canadian Cordillera tectonic and metallogenic implications; *Economic Geology and the Bulletin of the Society of Economic Geologists*, Volume 93, pages 224-231.

Coney, P.J., Jones, D.L. and Monger, J.W.H. (1980): Cordilleran suspect terranes; *Nature (London)*, Volume 288, pages 329-333.

Cordey, F., Gordey, S.P., Orchard, M.J. and Canada, G.S. (1991): New biostratigraphic data for the northern Cache Creek Terrane, Teslin map area, southern Yukon; *in* Current research; Part E—Recherches en cours; Partie E., *Geological Survey of Canada*, pages 67-76.

Devine, F.A.M. (2002): U-Pb geochronology, geochemistry, and tectonic implications of oceanic rocks in the northern Cache Creek terrane, Nakina area, northwestern British Columbia; *The University of British Columbia*, Vancouver, unpublished B.Sc. thesis, 50 pages.

Dumont, R., Coyle, M. and Potvin, J. (2001a): Aeromagnetic total field map British Columbia: Nakina Lake, NTS 104N/1; *Geological Survey of Canada*, Open File, 4091.

Dumont, R., Coyle, M. and Potvin, J. (2001b): Aeromagnetic total field map British Columbia: Nakina, NTS 104N/2; *Geological Survey of Canada*, Open File, 4092.

Dumont, R., Coyle, M. and Potvin, J. (2001): Aeromagnetic total field map British Columbia: Sloko River, NTS 104N/3; *Geological Survey of Canada*, Open File, 4093.

English, J.M., Mihalynuk, M.G., Johnston, S.T. and Devine, F.A. (2002): Atlin TGI Part III: Geology and Petrochemistry of mafic rocks within the northern Cache Creek terrane and tectonic implications; *in* Geological Fieldwork 2001, *B.C. Ministry of Energy and Mines*, Paper 2002-1, pages 19-29.

English, J.M., Mihalynuk, M.G., Jonhnston, S.T., Orchard, M.J., Fowler, M. and Leonard, L.J. (2003): Atlin TGI, Part VI: Early to Middle Jurassic sedimentation, deformation and a preliminary assessment of hydrocarbon potential, central Whitehorse Trough and northern Cache Creek terrane; *in* Geological Fieldwork 2002, *BC Ministry of Energy and Mines*, Paper 2003-1, this volume

Gordey, S.P., McNicoll, V.J. and Mortensen, J.K. (1998): New U-Pb ages from the Teslin area, southern Yukon, and their bearing on terrane evolution in the northern Cordillera; *in* Radiogenic age and isotopic studies; Report 11., *Geological Survey of Canada*, pages 129-148.

Harker, P. (1953): Report on fossil collections submitted by R.L. Christie and J.D. Aitken from the Bennett Lake and Atlin Lake area; *Geological Survey of Canada*, unpublished Fossil Report, P7, 2 pages.

Hart, C.J.R., Dickie, J.R., Ghosh, D.K. and Armstrong, R.L. (1995): Provenance constraints for Whitehorse Trough conglomerate: U-Pb zircon dates and initial Sr ratios of granitic clasts in Jurassic Laberge Group, Yukon Territory; *in* Jurassic magmatism and tectonics of the North American Cordillera., Miller, David, M.; Busby and Cathy (Editors), *Geological Society of America*, Special Paper 299, pages 47-63.

Jackaman, W. (2000): British Columbia Regional Geochemical Survey, NTS 104N/1 - Atlin; *BC Ministry of Energy and Mines*, BC RGS, 51.

Johnston, S.T. (2001): The Great Alaskan Terrane Wreck: reconciliation of paleomagnetic and geological data in the northern Cordillera; *Earth and Planetary Science Letters*, Volume 193, pages 259-272.

Krough, T.E. (1982): Improved accuracy of U-Pb ages by the creation of more concordant systems using an air abrasion technique; *Geochimica et Cosmochimica Acta*, Volume 46, pages 637-649.

Lefebure, D.V. and Gunning, M.H. (1988): Gold lithogeochemistry of Bronson Creek area, British Columbia; *in* Exploration in British Columbia; 1987., Anonymous (Editor), *British Columbia Ministry of Mines and Petroleum Resources*, 1987, pages B71-B77.

Lowe, C. and Anderson, R.G. (2002): Preliminary interpretation of new aeromagnetic data for the Atlin Map area, British Columbia; *in* Current Research, Part A, *Geological Survey of Canada*, Paper 2002-A17, page 10.

Lowe, C., Mihalynuk, M.G., Anderson, R.G., Canil, D., Cordey, F., English, J.M., M, H., Johnston, S.T., M, O., Russell, J.K., Sano, H. and Villeneuve, M. (2003): Atlin TGI Project overview, northwestern British Columbia, year three; *in* Current Research, Part A, *Geological Survey of Canada*, Paper 2003-, this volume.

Merran, Y. (2002): Mise en place et environnement de depot d'une plate-forme carbonatee intraoceanique: exemple du complexe d'Atlin, Canada; *Université Claude Bernard*, Lyon, France, unpublished M.Sc. thesis, 50 (and appendices) pages.

Mihalynuk, M.G. and Smith, M.T. (1992): Highlights of 1991 mapping in the Atlin-West Map area (104N/12); *in* Geological fieldwork 1991; a summary of field activities and current research., Grant and B.; Newell (Editors), *Province of British Columbia, Ministry of Energy, Mines and Petroleum Resources*, pages 221-227.

Mihalynuk, M.G., Nelson, J. and Diakow, L.J. (1994): Cache Creek Terrane entrapment: oroclinal paradox within the Canadian Cordillera; *Tectonics*, Volume 13, pages 575-595.

Mihalynuk, M.G., Meldrum, D., Sears, S. and Johannson, G. (1995): Geology and mineralization of the Stuhini Creek area (104K/11); *in* Geological fieldwork 1994; a summary of field activities and current research., Grant and B.; Newell (Editors), *BC Ministry of Energy, Mines and Petroleum Resources*, pages 321-342.

Mihalynuk, M.G., Bellefontaine, K.A., Brown, D.A., Logan, J.M., Nelson, J.L., Legun, A.S. and Diakow, L.J. (1996): Geological compilation, northwest British Columbia (NTS 94E, L, M; 104F, G, H, I, J, K, L, M, N, O, P; 114J, O, P); *BC Ministry of Energy and Mines*, Open File, 1996-11.

Mihalynuk, M.G. and Cordey, F. (1997): Potential for Kutcho Creek volcanogenic massive sulphide mineralization in the northern Cache Creek Terrane: a progress report; *in* Geological fieldwork 1996; a summary of field activities and current research., Lefebure, V.; McMillan and J.; McArthur (Editors), *BC Ministry of Energy, Mines and Petroleum Resources*, Paper 1997-1, pages 157-170.

Mihalynuk, M.G., Erdmer, P., Ghent, E.D., Archibald, D.A., Friedman, R.M., Cordey, F., Johannson, G.G. and Beanish, J. (1999): Age constraints for emplacement of the northern Cache Creek Terrane and implications of blueschist metamorphism; *BC Ministry of Energy, Mines and Petroleum Resources*, Paper 1999-1, 127-142 pages.

Mihalynuk, M.G. (2002): Geological setting and style of mineralization at the Joss'alun discovery, Atlin area, British Columbia; *BC Ministry of Energy and Mines*, Geofile, GF2002-6, 4 (plus digital presentation) pages.

Mihalynuk, M.G., Johnston, S.T., Lowe, C., Cordey, F., English, J.M., Devine, F.A.M., Larson, K. and Merran, Y. (2002): Atlin TGI Part II: Preliminary results from the Atlin Targeted Geoscience Initiative, Nakina Area, Northwest British Columbia; *in* Geological Fieldwork 2001, *BC Ministry of Energy and Mines*, Paper 2002-1, pages 5-18.

Monger, J.W.H. (1969): Stratigraphy and structure of Upper Paleozoic rocks, northeast Dease Lake map-area, British Columbia (104J): Ottawa, ON, Canada, Geological Survey of Canada, 41 pages.

Monger, J.W.H. (1975): Upper Paleozoic rocks of the Atlin Terrane, northwestern British Columbia and south-central Yukon; *Geological Survey of Canada*, Paper 74-47, 63 pages.

Nixon, G.T., Archibald, D.A. and Heaman, L.M. (1993): (^{40}) Ar-(^{39}) Ar and U-Pb geochronometry of the Polaris alaskan-type complex, British Columbia; precise timing of Quesnellia-North America interaction; *in* Geological Association of Canada; Mineralogical Association of Canada; annual meeting; program with abstracts, *Geological Association of Canada*, page 76.

Okulitch, A.V. (1999): Geological time scale, 1999; *Geological Survey of Canada*, National Earth Science Series, Geological Atlas, Open File 3040, wall chart - revision pages.

Parrish, R.R., Roddick, J.C., Loveridge, W.D. and Sullivan, R.W. (1987): Uranium-lead analytical techniques at the Geochronology Laboratory, Geological Survey of Canada; *in* Radiogenic Age and Isotopic Studies: Report 1, *Geological Survey of Canada*, Paper 87-2, pages 3-7.

Renne, P.R., Deino, A.L., Walter, R.C., Turrin, B.D., Swisher, C.C.I., Becker, T.A., Curtis, G.H., Sharp, W.D. and Jaouni, A.R. (1994): Intercalibration of astronomical and radioisotopic time; *Geology*, Volume 22, pages 783-786.

Roddick, J.C. (1987): Generalized numerical error analysis with applications to geochronology and thermodynamics; *Geochimica et Cosmochimica Acta*, Volume 51, pages 2129-2135.

Roddick, J.C. (1988): The assessment of errors in 40Ar/39Ar dating; *in* Radiogenic Age and Isotopic Studies, Report 2, *Gelological Survey of Canada*, Paper 88-2, pages 7-16.

Schiarizza, P., Massey, N. and MacIntyre, D.G. (1998): Geology of the Sitlika Assemblage in the Takla Lake area (93N/3, 4, 5, 6, 12), central British Columbia; *in* Geological fieldwork 1997; a summary of field activities and current research., Smyth (Editor), *British Columbia Geological Division*, pages 4.1-4.19.

Terry, J. (1977): Geology of the Nahlin ultramafic body, Atlin and Tulsequah map-areas, northwestern British Columbia; *in* Current Research, Part A, *Geological Survey of Canada*, pages 263-266.

Villeneuve, M.E. and MacIntyre, D.G. (1997): Laser 40Ar/39Ar ages of the Babine porphyries and Newman Volcanics, Fulton Lake map area, west-central British Columbia; *in* Radiogenic Age and Isotopic Studies, Report 10, *Geological Survey of Canada*, Current Research 1997-F, pages 131-139.

Villeneuve, M.E., Sandeman, H.A. and Davis, W.J. (2000): A method for the intercalibration of U-Th-Pb and 40Ar/39Ar ages in the Phanerozoic; *Geochimica et Cosmochimica Acta*, Volume 64, pages 4017-4030.

Atlin TGI, Part III: Geological Setting and Style of Mineralization at the Joss'alun Occurrence, Atlin Area (NTS 104N/2SW), MINFILE 104N136

By Mitchell G. Mihalynuk[1], Michael E. Villeneuve[2] and Fabrice Cordey[3]

KEYWORDS: Massive sulphide, geologic mapping, geochronology, U-Pb, 40Ar/39Ar, radiolarian, Kutcho, intraoceanic arc, Joss'alun, Cache Creek terrane.

INTRODUCTION

Ministry of Energy and Mines personnel encountered massive, copper-rich sulphide mineralization during regional geological mapping in the southern Atlin area. Now named the Joss'alun occurrence, its discovery is a direct consequence of the joint federal and provincially funded Atlin Targeted Geoscience Initiative (Lowe and Mihalynuk, 2002). We report here on updates to map data released following the discovery (Mihalynuk, 2002) as well as new petrographic, isotopic age and micropaleontological age data.

GEOGRAPHIC LOCATION

The Joss'alun discovery is located approximately 75 kilometres southeast of the placer mining town of Atlin (Figure 1). Access is by helicopter, which can be chartered in Atlin. Float planes can land at a 1.4 km long lake, locally known as "Windy Lake", about 7.5 km north of the occurrence. Atlin is 92 km south of the Alaska Highway, and 182 km from Whitehorse, which is the nearest major center with a national airport. Closest road access to the Joss'alun is a very rough, fire abatement road that ends at Kuthai Lake, 30 km northwest of the occurrence. A proposed road route to the Tulsequah Chief minesite (50 km southwest of Joss'alun) is within about 22 km of the occurrence. Redfern Resources, operator of the Tulsequah project, was issued a project approval certificate in December 2002. Nearest tidewater is Taku Inlet, about 70 km to the southwest, and accessible by barge from the confluence of the Tulsequah and Taku rivers, about 12 km downstream from the Tulsequah Chief deposit.

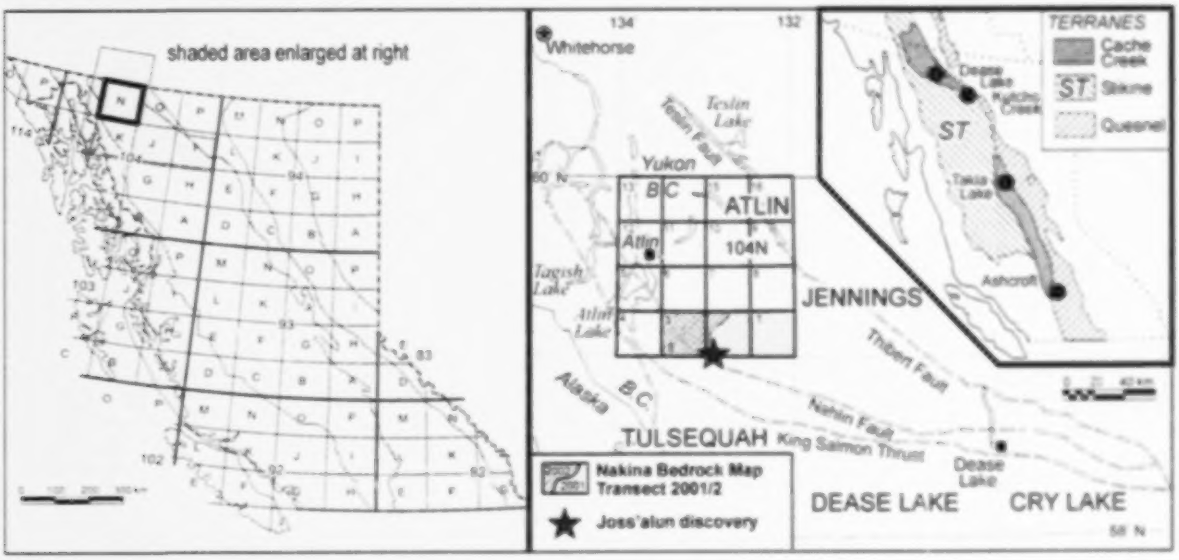
shaded area enlarged at right
Whitehorse
Teslin Lake
Teslin Fault
Yukon
BC
60 N
ATLIN
104N
Atlin
Tagish Lake
Atlin Lake
JENNINGS
Alaska
BC
TULSEQUAH
Thibert Fault
Nahlin Fault
King Salmon Thrust
Dease Lake
DEASE LAKE
CRY LAKE
58 N
Nakina Bedrock Map Transect 2001/2
Joss'alun discovery
TERRANES
Cache Creek
ST Stikine
Quesnel
ST
Dease Lake
Kutcho Creek
Takla Lake
Ashcroft
134
132
104
94
103
93
102
92
83
82
114

Figure 1. Location of the Joss'alun discovery and Nakina mapping transect in northwestern British Columbia.

---

[1] *BC Ministry of Energy and Mines*

[2] *Geological Survey of Canada, Ottawa*

[3] *Sciences de la Terre, Université Claude Bernard, Lyon, France*

EXPLORATION OF JOSS'ALUN AND REGION

At the time of discovery, there were no signs of previous work at the Joss'alun occurrence. One prior claim block was staked in 1985, located 2.5 km southwest, near the head of the valley. It was recorded as the NOW claims by Noranda Mining and Explorations Inc. (ARIS Report Number 14364), but follow-up geochemical surveys failed to detect base or precious metal anomalies and the claim was left to lapse with no further wock recorded. Nearest mineral claims in good standing were located approximately 30 km to the northwest (104N/3) and an equal distance to the south in the northern Tulsequah map area (104K/10). Nearest known mineralization recorded in MINFILE is more than 10 km to the southeast in the Tulsequah map area. Known as "Inklin" or "Yeth Creek" (MINFILE 104K022), it is a series of galena-sphalerite-chalcopyrite-bearing quartz veins, hosted by submarine volcanic rocks correlated with the Late Triassic Stuhini Group. Within the Atlin map area, the nearest mineral occurrences are: an asbestos occurrence 17 km to the northwest, known as "Focus Mountain" (MINFILE 104N071); a magnesite occurrence, 19 km northwest, known as "Sloko River" or "Nahlin Fault" (MINFILE 104N083); and the "Nakina River" limestone occurrence, 20 km to the northeast (MINFILE 104N094).

A public announcement of the discovery was made a 14:00 on September 13. By 15:00, Aurum Geological (Whitehorse) had staked the KNACK claims (2 units) over the main mineralized zone, on behalf of Copper Ridge Explorations Inc. (Carleson, 2002). While the Aurum crew was at work, the Northair Group arrived and staked the adjoining 12 unit D claims to the northwest, on behalf of Tennajon Resources Ltd. Beset by Friday the 13th problems, the Imperial Metals Corp. crew arrived the following day, and staked the 16 unit DARK claims to the southeast of the main mineralized zone. Immediately prior to the release date, the Northair Group staked 3 claim blocks within 13 km northeast of Joss'alun: the 20 unit, HF #1 block, the 4 unit, TOP #1, and the 8 unit VM claims. At the tail end of the staking activity, the 18 unit Bobit 3 block, located by Peter Burjowski, was staked 8 km to the west-southwest. No further activity was recorded prior to the date of publication in December.

DISTRIBUTION AND CHARACTER OF MINERALIZATION

Photo 1. An overview of mineralization at the Joss'alun taken from about 1 km to the southeast at about the same stratigraphic/structural position. Shading indicates the approximate extent of known mineralization.

Mineralization is exposed at and below tree line on the western side of a broad valley containing a north-flowing stream. Mineralized outcrops are low and rubble-strewn. They occur within, and south of, a shallowly incised, east-flowing creek that joins the main stream about 0.5 km (map distance) below tree line (Photo 1). Mineralization that was encountered farthest to the northwest is a 30 cm wide, copper stained and gossanous zone on the northern side of the creek cut near UTM 620271,6544371N, EPE: 4m (Note that EPE = estimated position error that is calculated by a proprietary algorithm). Mineralization occurs intermittently over a distance of about 255 m, across the area of low scattered outcrops containing massive sulphide lenses (UTM 620381N 6544322N, EPE: 5m) to a very low, isolated, and competent outcrop amongst the trees and brush above a gossanous seep. Here (UTM 620460E 6544252N, EPE: 10m), discordant chalcopyrite veins (3-4 cm thick) cut the outcrop, and several pieces of fist-sized float of semi-massive sulphide were found resting on the outcrop. Sulphide float presumably tumbled down slope from above, but a crisscross traverse through subalpine fir upslope did not reveal the source. Southeast of the veined outcrop, the mineralized zone disappears beneath cover in the broad valley.

Across the valley axis, about one kilometre to the east-southeast, blebs of chalcopyrite, up to 0.5 cm across, occur within mafic breccia, along the trend of the host rocks in the discovery zone, and at approximately the same stratigraphic level.

Mineralization consists of a series of stacked lenses of semi-massive chalcopyrite, lesser pyrite, and quartz-chlorite gangue in gossanous outcrops with weak copper staining. Host rocks are dominantly mafic volcaniclastics: pillow breccia and aquagene lapilli to ash tuff and tuffite. Lens thickness ranges up to approximately 1m. Thicknesses of 30cm are more typical. Lateral extent of the lenses is difficult to determine due to the generally low and rubbly nature of the outcrops. However, some are exposed for more than 3m. Both chalcopyrite and pyrite within the lenses appear brecciated (Photo 2). Pyrite clasts display a variety of textures including framboidal and having angular intergrowths of chalcopyrite (Photo 2a). Bedding within the mafic volcanic unit is not everywhere obvious, but the lenses appear to be concordant. Chalcopyrite also occurs as veins up to 5cm thick that are clearly discordant.

Mineralization is strongest in a ~10 x 30 m area near the center of the known limits of the mineralized zone. Mihalynuk (2002) reported analytical results from two chip and three grab samples from near the center of the strongly mineralized area. These occur in a digital publication for-

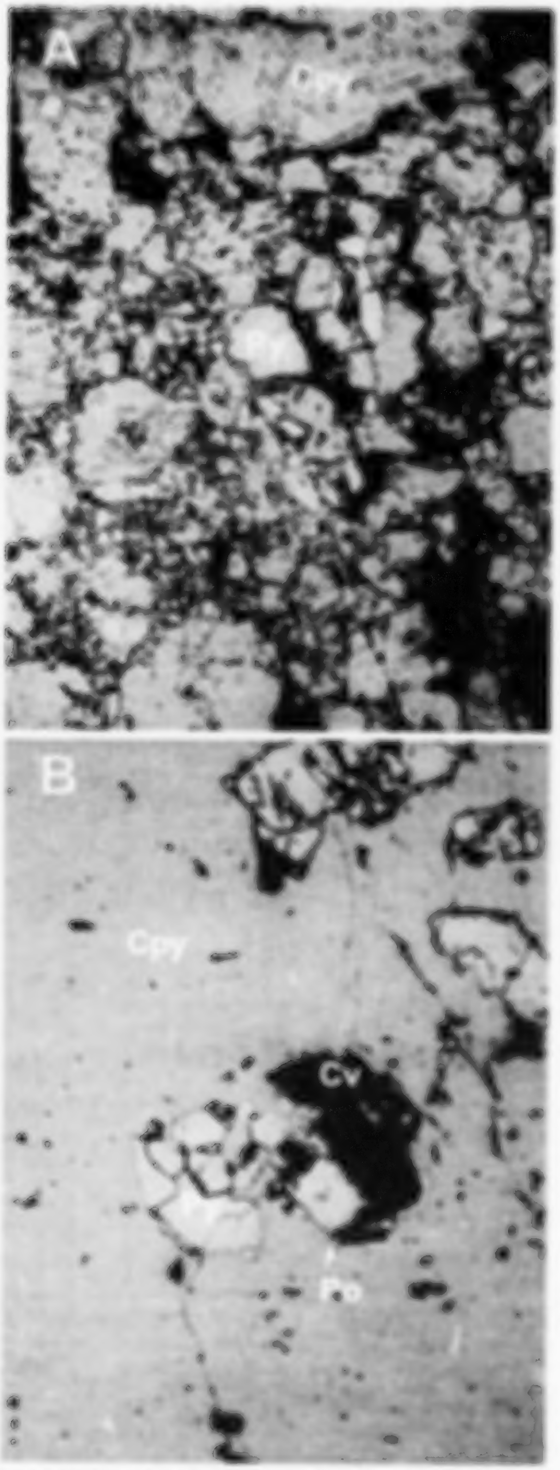

Photo 2. Reflected light photomicrograph of massive sulphide textures, A) brecciated textures with pyrite having various textures. B) Representative mineralogy: Cpy = chalcopyrite, Py = pyrite, Cv = covellite, Po = minor blob of pyrrhotite. Length of photo represents about 5mm.

mat and are reproduced here in Tables 1 and 2 for the benefit of clients who do not have on-line access.

GEOLOGICAL SETTING

Rocks underlying the Joss'alun discovery are part of the oceanic Cache Creek terrane. In the area around the Joss'alun stratigraphic and structural contacts parallel the general northwestern structural fabric of the Cordillera. However, some low angle contacts display variable directions because of interplay with topography. Dominant rock units are: harzburgite, gabbro, submarine basalt flows, flow breccia, and tuffaceous rocks and coarse, quartz-rich clastic strata. They are exposed in this same approximate order from north to south (Figure 2) and deepest to shallowest crustal level.

HARZBURGITE

Bright orange to dun-weathering harzburgite is a conspicuous, very dense and magnetic ultramafic rock that comprises a large part of the Nahlin ultramafic body. It is a resistant unit that crosses the valley about 300 m north of the Joss'alun occurrence (Figure 2). It has a characteristic knobby weathering appearance due to resistant orthopyroxene crystals and crystal trains in a less resistant olivine matrix. Shearing of orthopyroxene to produce crystal trains is a texture produced at mantle temperatures, and supports an interpreted origin as part of the ancestral Earth's mantle. It has been variably serpentinized, and now comprises up to 100% serpentine. Strongly serpentinized zones are exceptionally magnetic and produce an extreme positive aeromagnetic anomaly (Dumont *et al.*, 2001).

GABBROIC ROCKS

Gabbro occurs as resistant, blocky, grey outcrops between harzburgite and basalt. Contacts with the harzburgite are not exposed; they are inferred to be faults. Gabbro contacts with basalt are intrusive with evidence for multiple episodes of intrusion. Zones of intense epidote alteration are common, suggesting vigorous hydrothermal alteration.

MAFIC VOLCANICLASTIC ROCKS

Dark green pillow breccia, and lapilli and ash aquagene tuff dominate the unit. Ferruginous chert and laminated, muddy limestone are minor components. Bedding is poorly displayed, as the volcanic rocks tend to be massive. Where chert and ash tuff or tuffite beds occur, the bedding is well displayed. The unit on the east side of the valley displays good pillow textures. Steeply dipping dark green dikes up to one metre thick, cut the volcaniclastic rocks, but have not been observed in the unconformably overlying coarse quartz-rich clastic unit.

Age of the volcaniclastic unit is Permian as determined by identification of radiolaria extracted from interbedded ferruginous chert from the east side of the valley (Figure 2, Photo 3, Table 3). A submarine origin for the unit is indicated by pillows, radiolarian-bearing Fe-rich chert, and

TABLE 1

[illegible]

Field Number	UTM Easting	UTM Northing	sample type	Cu ppm	Cu %	Mo ppm	Pb ppm	Zn ppm	Ag ppb	Ni ppm
[illegible]	[illegible]	[illegible]	grab	[illegible]	[illegible]	[illegible]	[illegible]	[illegible]	[illegible]	[illegible]
[illegible]	[illegible]	[illegible]	grab	[illegible]	[illegible]	[illegible]	[illegible]	[illegible]	[illegible]	[illegible]
[illegible]	[illegible]	[illegible]	grab	[illegible]	[illegible]	[illegible]	[illegible]	[illegible]	[illegible]	[illegible]
[illegible]	[illegible]	[illegible]	[illegible] chip	[illegible]	[illegible]	[illegible]	[illegible]	[illegible]	[illegible]	[illegible]
[illegible]	[illegible]	[illegible]	[illegible] chip	[illegible]	[illegible]	[illegible]	[illegible]	[illegible]	[illegible]	[illegible]

	Mn ppm	As ppm	U ppm	Au ppb	Th ppm	Sr ppm	Cd ppm	Sb ppm	Bi ppm	V ppm	Ca %
[illegible]	[illegible]	[illegible]	[illegible]	[illegible]	[illegible]	[illegible]	[illegible]	[illegible]	[illegible]	[illegible]	[illegible]
[illegible]	[illegible]	[illegible]	[illegible]	[illegible]	[illegible]	[illegible]	[illegible]	[illegible]	[illegible]	[illegible]	[illegible]
[illegible]	[illegible]	[illegible]	[illegible]	[illegible]	[illegible]	[illegible]	[illegible]	[illegible]	[illegible]	[illegible]	[illegible]
[illegible]	[illegible]	[illegible]	[illegible]	[illegible]	[illegible]	[illegible]	[illegible]	[illegible]	[illegible]	[illegible]	[illegible]
[illegible]	[illegible]	[illegible]	[illegible]	[illegible]	[illegible]	[illegible]	[illegible]	[illegible]	[illegible]	[illegible]	[illegible]

	Fe %	P %	La ppm	Cr ppm	Mg %	Ba ppm	Ti %	B ppm	Al %	Na %	K %
[illegible]	[illegible]	[illegible]	[illegible]	[illegible]	[illegible]	[illegible]	[illegible]	[illegible]	[illegible]	[illegible]	[illegible]
[illegible]	[illegible]	[illegible]	[illegible]	[illegible]	[illegible]	[illegible]	[illegible]	[illegible]	[illegible]	[illegible]	[illegible]
[illegible]	[illegible]	[illegible]	[illegible]	[illegible]	[illegible]	[illegible]	[illegible]	[illegible]	[illegible]	[illegible]	[illegible]
[illegible]	[illegible]	[illegible]	[illegible]	[illegible]	[illegible]	[illegible]	[illegible]	[illegible]	[illegible]	[illegible]	[illegible]
[illegible]	[illegible]	[illegible]	[illegible]	[illegible]	[illegible]	[illegible]	[illegible]	[illegible]	[illegible]	[illegible]	[illegible]

	Co ppm	W ppm	Sc ppm	Tl ppm	S %	Hg ppb	Se ppm	Te ppm	Ga ppm	Sample g
[illegible]	[illegible]	[illegible]	[illegible]	[illegible]	[illegible]	[illegible]	[illegible]	[illegible]	[illegible]	[illegible]
[illegible]	[illegible]	[illegible]	[illegible]	[illegible]	[illegible]	[illegible]	[illegible]	[illegible]	[illegible]	[illegible]
[illegible]	[illegible]	[illegible]	[illegible]	[illegible]	[illegible]	[illegible]	[illegible]	[illegible]	[illegible]	[illegible]
[illegible]	[illegible]	[illegible]	[illegible]	[illegible]	[illegible]	[illegible]	[illegible]	[illegible]	[illegible]	[illegible]
[illegible]	[illegible]	[illegible]	[illegible]	[illegible]	[illegible]	[illegible]	[illegible]	[illegible]	[illegible]	[illegible]

UTM = Universal Transverse Mercator, Zone [illegible], NAD[illegible]

Analysis by Acme Analytical Laboratories Ltd.

Analysis by [illegible], aqua regia digestion, [illegible] g sample [illegible]

TABLE 3
FIRE ASSAY ANALYTICAL RESULTS

Field Number	UTM E	UTM N	% Cu
WMB02-[illegible]	[illegible]	[illegible]	[illegible]
WMB02-[illegible]	[illegible]	[illegible]	[illegible]
WMB02-[illegible]	[illegible]	[illegible]	[illegible]
WMB02-[illegible]	[illegible]	[illegible]	[illegible]
WMB02-[illegible]	[illegible]	[illegible]	[illegible]
detection limit			0.001

UTM = Universal Transverse Mercator, Zone 8, NAD 83

Analysis by Acme Analytical Laboratories Ltd.

Analysis by ICP, aqua regia digestion, 1 g sample (Group 7AR)

laminated [illegible] [illegible] (condition results from the [illegible] are pending).

COARSE QUARTZ-RICH CLASTIC UNIT

Quartz-rich clastic rocks comprise the peak 1500 m west of the [illegible] discovery (here informally called "the Peak", el. 1865m), and extend over 5 km to beyond the southern border of the map area (Figure 2). This unit is highly variable. It includes well laminated siltstone, thin to thick-bedded clean sandstone to wacke, coarse boulder conglomerate, fault scarp debris with blocks in excess of 10m long, and clastic carbonate layers. At "the Peak", a very well exposed section of coarse quartz wacke displays an angular unconformable relationship with underlying basalt. A red-weathering basal conglomerate containing oxidized cobbles of basalt grades rapidly upwards into

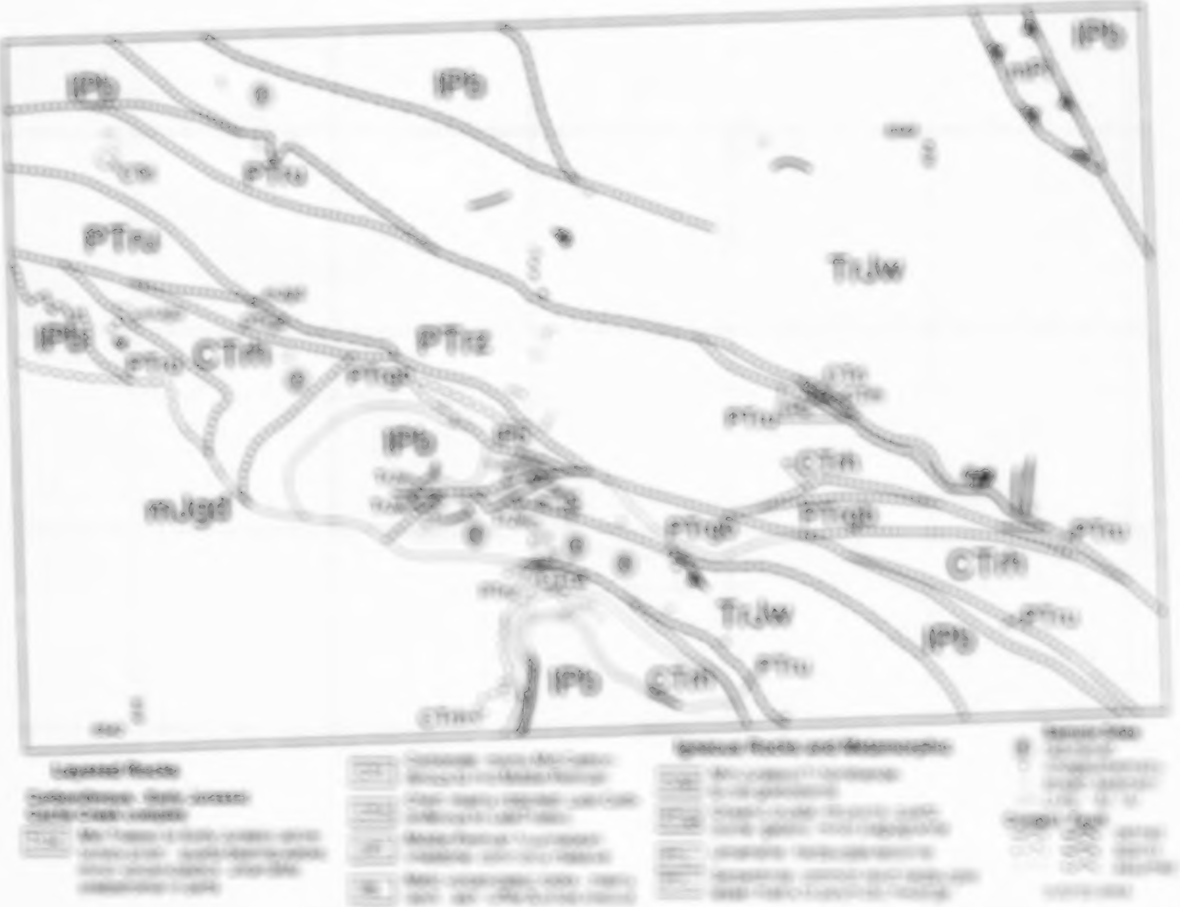

Figure 2. Geologic setting of the [illegible] discovery.

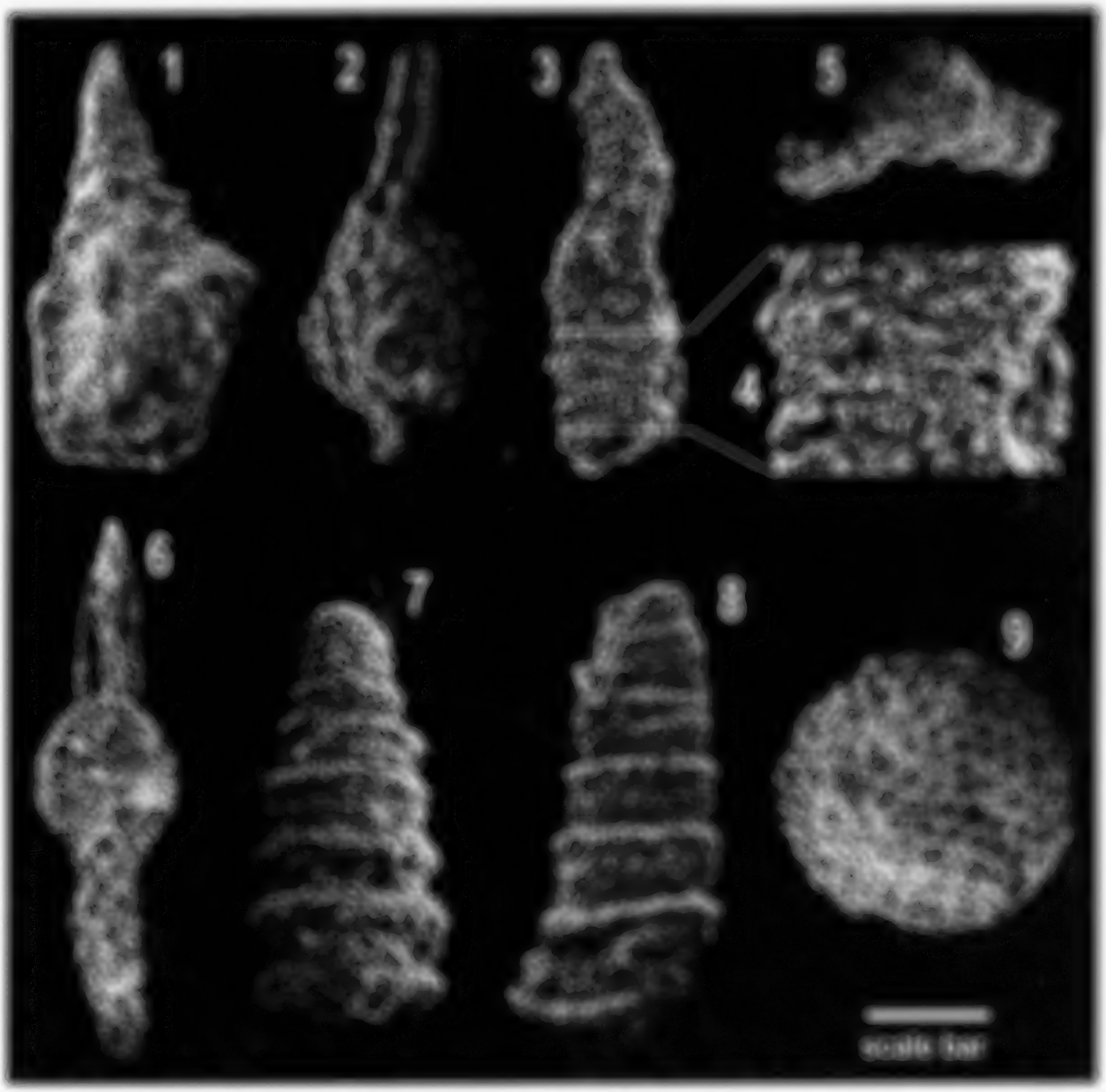
1
2
3
4
5
6
7
8
9
scale bar

[illegible]

[illegible]

TABLE 4
U-Pb ISOTOPIC DETERMINATIONS FROM DETRITAL ZIRCONS OF SAMPLE VN01-A03

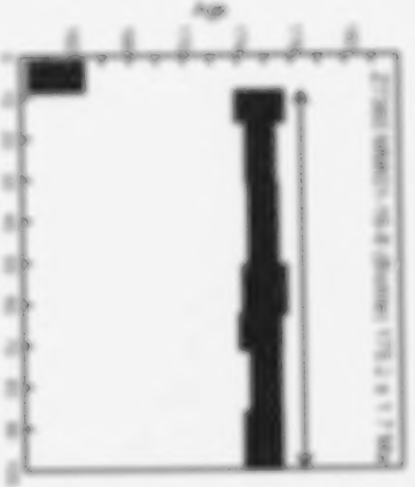

Figure 4. Ar-release spectra for sample MM01-16-8.

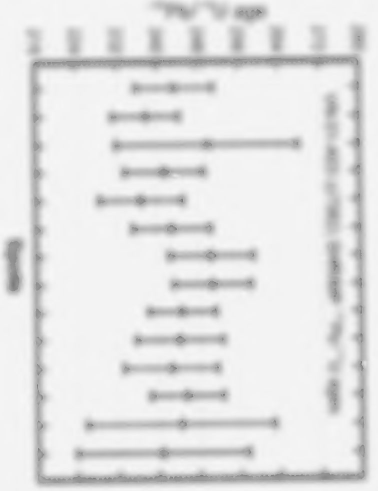

Figure 3. ^{206}Pb/^{238}U age data plots detrital zircon grains from sample VN01-A03.

made to separate or select grains on the basis of morphology. Grains were polished and examined in cathodoluminescent (CL), transmitted and reflected light. The former method enhances details of the internal growth structures of the zircon and can highlight the presence of xenocrystic cores that, unless avoided, may skew individual results to apparently older ages. Analyses use O⁻ as primary beam, the 563.5 Ma zircon standard, BR266 and data reduction techniques outlined in Stern (2000). All uncertainties are quoted and displayed at 1σ level of uncertainty and all quoted ages represent ^{207}Pb/^{206}Pb ages (Table 4), unless otherwise noted.

AGE OF DETRITAL ZIRCONS

Results of the analyses gave concordant results and thus the data is displayed in terms of ^{206}Pb/^{238}U age (Figure 3, Table 4). The data has a surprisingly unimodal age population. If there are multiple age sources, they cannot be resolved at the uncertainty levels present. It is clear that all grains are derived from a Permian-age body (or bodies) with no indication of other sources. This small population has a 33% probability of missing components that represent less than 1 in 10 of the overall population (Sircombe, 2000). Nevertheless, the results would indicate that other sources, if present, represent a minor component only

NAKINA RIVER STOCK

The methodology for the ^{40}Ar/^{39}Ar isotopic age dating reported here is the same as that in Mihalynuk *et al.* (2003, this volume), except that biotite was dated instead of hornblende. Biotite from the Nakina River stock gave a good plateau age (Table 5) with only slight evidence of Ar-loss in the earliest steps (Figure 4). A plateau age based upon ~91% of ^{39}Ar released in the high temperature steps is 175.2 ± 1.7 Ma concordant with ages determined from other Middle Jurassic plutons in the Atlin area (*e.g.* Symons, 1998).

DISCUSSION

Deposit type and mode of genesis of the mineralization at the Joss'alun occurrence are undetermined at this time. However, the host rocks were clearly deposited in a submarine setting as is shown by pillow textures in flow breccia, radiolarian chert, and laminated lime mud. Within the mineralized zone, submarine textures are more equivocal; however, tuffaceous chert (lacking easily identified radiolaria) and vague bedding in lapilli ash tuffite support a submarine origin. Massive sulphide lenses are apparently stratabound. Some of the geochemical characteristics of the mineralization, particularly the elevated cobalt, are typical of submarine massive sulphide deposits, like Cyprus and Besshi-types (Lefebure and Ray, 1995). On the basis of the above, we tentatively interpret the sulphide lenses as syngenetic. However, discordant chalcopyrite veins are relatively common, and an epigenetic origin for the sulphide lenses cannot be ruled out at this preliminary stage in our investigation.

Results of trace and major element analyses are pending. However, the textural and mineralogical characteristics of pillow breccia are similar to those observed elsewhere in the Nakina Transect, and these dominantly show a tholeiitic arc affiliation (English *et al.*, 2002). It is likely that the host rocks of the Joss'alun massive sulphide are primitive volcanic arc strata as well. Furthermore, detrital zircons from the overlying quartz-rich coarse clastic unit suggest a nearby felsic volcanic/intrusive center that was exhumed between Middle Triassic and Middle Jurassic times. The most likely source of magmatic rocks of only Permian age is Cache Creek terrane itself, probably from felsic arc component, coeval with French Range - Kutcho Creek volcanism (*see* age tabulation in Mihalynuk *et al.*, 1999); petrochemistry in Mihalynuk and Cordey (1997)

TABLE 5
AR ISOTOPIC DATA FOR SAMPLE MM001-16-8

MM001-16-8 Biotite; J=.00293400 (Z7360; 59.0169°N 132.9121°E)

Aliquot: A

Power^a	Volume ^{39}Ar x10^{-11} cc	^{36}Ar/^{39}Ar	^{37}Ar/^{39}Ar	^{38}Ar/^{39}Ar	^{40}Ar/^{39}Ar	%^{40}Ar ATM	^{40*}Ar/^{39}Ar	f$_{39}$^b (%)	Apparent Age Ma^c
2.4	0.1912	0.0246±0.0060	0.111±0.015	0.123±0.011	24.442±1.100	30.2	17.063±1.800	1.4	88.13±9.08
2.8	1.0187	0.0083±0.0009	0.022±0.004	0.102±0.011	33.582±0.368	5.6	31.717±0.404	7.3	160.52±1.98
3.0	1.0451	0.0010±0.0009	0.020±0.002	0.104±0.011	35.022±0.315	0.9	34.723±0.380	7.5	175.02±1.73
3.5	2.0508	0.0012±0.0005	0.021±0.002	0.100±0.011	35.086±0.191	1	34.727±0.211	14.8	175.04±1.02
3.8	2.7579	0.0018±0.0004	0.013±0.002	0.099±0.011	35.286±0.201	1.5	34.761±0.212	19.9	175.21±1.02
4.2	1.653	0.0022±0.0009	0.017±0.002	0.109±0.011	35.418±0.213	1.8	34.778±0.320	11.9	175.29±1.54
4.6	1.2107	0.0015±0.0008	0.026±0.003	0.104±0.011	35.151±0.254	1.3	34.707±0.308	8.7	174.94±1.47
5.5	2.0505	0.0009±0.0005	0.022±0.002	0.103±0.011	35.049±0.183	0.8	34.777±0.221	14.8	175.28±1.08
12.0	1.8989	0.0017±0.0006	0.035±0.002	0.101±0.011	35.234±0.238	1.4	34.741±0.272	13.7	175.11±1.31

a: As measured by laser in % of full nominal power (10W)

b: Fraction 39Ar as percent of total run

c: Errors are analytical only and do not reflect error in irradiation parameter J

d: Nominal J, referenced to FCT-SAN=28.03 Ma (Renne *et al.*, 1994)

All uncertainties quoted at 2σ level

and English *et al.* (2002). Terranes adjacent to the Cache Creek contain numerous Mesozoic and Late Paleozoic sources of magmatic arc zircons, as well as older zircons derived from adjacent continental masses, or recycled from pericratonic sediments, and therefore are unlikely source terrains.

Extreme facies changes, abundant intraclasts and fault scarp debris that characterize the quartz-rich coarse clastic unit indicate rapid deposition in a tectonically active environment. Lack of any trace of an *in situ*, exposed source for coarse granitoid boulders is puzzling. Perhaps the granitoid source was removed by translation on an arc-parallel fault? The same fault, or series of faults, may be responsible for creation of the basin in which the coarse clastics were deposited, and synsedimentary deformation. Transcurrent faults with similar characteristics are common features of along the axes of most modern arcs.

SUMMARY AND FUTURE WORK

Our work around the Joss'alun discovery, which amounts to less than one full day of field mapping, leaves many questions unanswered. The proposed syngenetic origin for the mineralization requires testing. Analysis of the Pb isotopic signature of chalcopyrite will be undertaken at the Pacific Isotopic and Geochemical Research for isotopic and Geochemical Research (UBC) in order to determine if the mineralization is coeval with Permian host rocks, and to compare with the lead isotopic composition of the Kutcho Creek massive sulphide deposit.

More detailed mapping is required to understand the interplay of synsedimentary faulting and mineralization. Detailed mapping should be extended to the western flank of "Jos Peak" and southeast of the main valley where mafic volcanic rocks are in contact with the coarse clastic unit, but have not been walked over. Age constraints for the coarse clastic unit need to be improved in order to understand the duration of sedimentation and its role, if any, in the mineralizing event. To this end, a ~1m thick granitic dike that cuts the upper part of the coarse clastic unit will be processed for U-Pb age dating. Plus, detrital zircon age determinations on five boulders are in progress. Geochronologic results from the boulders may provide a fingerprint of the source terrain. Could they be remnants of the Kutcho arc?

Northern Cache Creek terrane has long been considered unprospective for volcanogenic deposits. However, the possibility of arc-related volcanogenic massive sulphide mineralization at the Joss'alun discovery forces us to reevaluate this large region of northern British Columbia and southern Yukon. Given that these rocks comprise one of the most common rock types in the Nakina-Atlin area (Aitken, 1959; Mihalynuk *et al.*, 1996; Mihalynuk *et al.*, 2002; English *et al.*, 2002), there is much exploration still to be done.

ACKNOWLEDGEMENTS

Several people were instrumental in the discovery of the Joss'alun occurrence and successful release of the data. Fionnuala (Nula) Devine volunteered her considerable skills, and in so doing, enabled us to return to the far southern edge of the map area where the Joss'alun discovery was made during the last hours of the last day of the field season. Rod Hill of the Yukon Territorial Government generously consented to loaning us Fionnuala for the final critical days of our field program. Steve Johnston, Joe English, Yann Merran, Kyle Larson, Jacqueline Blackwell, Adam Bath, Oliver Roenitz and Lucinda Leonard laboured on upgrading the regional geological framework through miles of soggy bush and mosquito-infested swamp, and always managed a smile at the end of the day. Norm Graham, our trusty and honourable helicopter pilot shouldered the cloak of silence prior to the data release date. Larry Jones and Alan Wilcox triple checked the originality of the Joss'alun discovery. Jim Logan helped to organize the data release in Vancouver.

REFERENCES CITED

Aitken, J.D. (1959): Atlin map-area, British Columbia; *Geological Survey of Canada*, Memoir, 307, 89 pages.

Bath, A. (2003): Atlin TGI, Part IV: Middle Jurassic granitic plutons within the CacheCreek terrane and their aureoles: Implications for terrane emplacement and deformation; *in* Geological Fieldwork 2002, *BC Ministry of Energy and Mines*, Paper 2003-1, in press.

Carleson, G.C. (2002): Copper Ridge acquires new high grade copper discovery; *KRX TSX Venture Exchange*, Press Release, No. 25/2002, 1 page.

Dumont, R., Coyle, M. and Potvin, J. (2001): Aeromagnetic total field map British Columbia: Nakina, NTS 104N/2; *Geological Survey of Canada*, Open File, 4092.

English, J.M., Mihalynuk, M.G., Johnston, S.T. and Devine, F.A. (2002): Atlin TGI Part III: Geology and Petrochemistry of mafic rocks within the northern Cache Creek terrane and tectonic implications; *in* Geological Fieldwork 2001, *BC Ministry of Energy and Mines*, Paper 2002-1, pages 19-29.

Lefebure, D.V. and Ray, G.E. (1995): British Columbia mineral deposit profiles, Volume 2 - metallics and coal; *BC Ministry of Energy and Mines*, Open File, 1995-20, 135 pages.

Lowe, C. and Mihalynuk, M.G. (2002): The Atlin Integrated Geoscience Project, northwestern British Columbia - an overview; *in* Current Research, Part A, *Geological Survey of Canada*, Paper 2002-A.

Mihalynuk, M.G., Bellefontaine, K.A., Brown, D.A., Logan, J.M., Nelson, J.L., Legun, A.S. and Diakow, L.J. (1996): Geological compilation, northwest British Columbia (NTS 94E, L, M; 104F, G, H, I, J, K, L, M, N, O, P; 114J, O, P); *BC Ministry of Energy and Mines*, Open File, 1996-11.

Mihalynuk, M.G. and Cordey, F. (1997): Potential for Kutcho Creek volcanogenic massive sulphide mineralization in the northern Cache Creek Terrane; a progress report; *in* Geological fieldwork 1996; a summary of field activities and current research., Lefebure, V ; McMillan and J ; McArthur (Editors), *BC Ministry of Energy, Mines and Petroleum Resources*, Paper 1997-1, pages 157-170.

Mihalynuk, M.G., Erdmer, P., Ghent, E.D., Archibald, D.A., Friedman, R.M., Cordey, F., Johannson, G.G. and Beanish, J. (1999): Age constraints for emplacement of the northern Cache Creek Terrane and implications of blueschist metamorphism; *in* Geological Fieldwork 1998, *BC Ministry of Energy, Mines and Petroleum Resources*, Paper 1999-1, pages 127-142.

Mihalynuk, M.G. (2002): Geological setting and style of mineralization at the Joss'alun discovery, Atlin area, British Columbia; *BC Ministry of Energy and Mines*, Geofile, GF2002-6, 4 pages (plus digital presentation).

Mihalynuk, M.G., Johnston, S.T., Lowe, C., Cordey, F., English, J.M., Devine, F.A.M., Larson, K. and Merran, Y. (2002): Atlin TGI Part II: Preliminary results from the Atlin Targeted Geoscience Initiative, Nakina Area, Northwest British Columbia; *in* Geological Fieldwork 2001, *BC Ministry of Energy and Mines*, Paper 2002-1, pages 5-18.

Mihalynuk, M.G., Johnston, S.T., English, J.M., Cordey, F., Villeneuve, M.J., Rui, L. and Orchard, M.J. (2003): Atlin TGI Part II: Regional geology and mineralization of the Nakina area (NTS 104N/2W and 3); *in* Geological Fieldwork 2002, *BC Ministry of Energy and Mines*, Paper 2003-1, in press.

Sircombe, K. (2000): The usefulness and limitations of binned frequency histograms and probability density distributions for displaying absolute age data; *in* Current Research, *Geological Survey of Canada*, Paper 2000-F2, 11 pages.

Stern, R. (2000): A new istopic and trace-element standard for the ion microprobe: preliminary thermal ionization mass spectrometry (TIMS) U-PB and electron-microprobe data; *in* Radiogenic age and isotopic studies, *Geological Survey of Canada, Current Research*, Report 14, 2001-F1, 10 pages.

Symons, D.T.A., Harris, M.J., Hart, C.J.R. and Blackburn, W.H. (1998): Geotectonics in the Northern Cordillera from paleomagnetism and geobarometry; progress report and recent results from the Eocene White Pass dikes and Jurassic Fourth of July Batholith; *in* Slave-NORthern Cordillera Lithospheric Evolution (SNORCLE) and Cordilleran tectonics workshop; Cook, F. and Erdmer, P. (Editors), *University of British Columbia, Lithoprobe Secretariat [for the] Canadian Lithoprobe Program*, pages 171-180.

Atlin TGI, Part IV: Middle Jurassic Granitic Plutons Within the Cache Creek Terrane and their Aureoles: Implications for Terrane Emplacement and Deformation

By Adam Bath

KEYWORDS: regional mapping, granite pluton, terrane emplacement, Atlin, Jurassic, age dating, Cache Creek, Fourth of July batholith, Nakina River stock, Chikoida Mountain stock, thermal aureole.

INTRODUCTION

The timing of oceanic terrane obduction within orogenic belts provides important constraints in the evolution of convergent-plate margins. Middle Jurassic plutons, which intrude Cache Creek Terrane in northwestern British Columbia, provide a means to tightly constrain the timing of obduction and the nature of post obduction deformation.

Blueschist ages ($^{40}Ar/^{39}Ar$) from the French Ranges in northwestern British Columbia (Figure 1) indicate that the Atlin complex within the Cache Creek terrane was subjected to blueschist grade metamorphism around 173.2±7.6 Ma (Mihalynuk *et al.*, 1999). The youngest chert, dated by radiolarians from the Atlin complex, indicates an age of between 192+3.8/-5.2 Ma and 178+1.0/-1.5Ma (Cordey *et al.*, 1987; Cordey *et al.*, 1991; Cordey, 1998). These dates, together with isotopic ages, best constrain the timing of obduction of Cache Creek terrane to be between 183-171Ma (Mihalynuk, *et al.*, 1992, 1999).

Crosscutting plutons within the Atlin complex have been dated using reliable methods such as U-Pb zircon and $^{40}Ar/^{39}Ar$ of hornblende and biotite. An example of this is the Fourth of July batholith, which crystallized at 171.7±3Ma (U-Pb; Mihalynuk *et al*, 1992) or 172.7±0.7 Ma from hornblende ($^{40}Ar/^{39}Ar$; Symons *et al.*, 1998). This batholith intruded and thermally metamorphosed the deformed rocks of the Cache Creek terrane and has itself only been subjected to relatively minor, brittle deformation (Mihalynuk *et al.*, 1992). The age of this intrusion, and others within the terrane, constrain the youngest date of Cache Creek terrane obduction to within 9.8 m.y. of crystallization of the Fourth of July batholith (although a compilation of new isotopic data requires obduction within 2.5 m.y. of

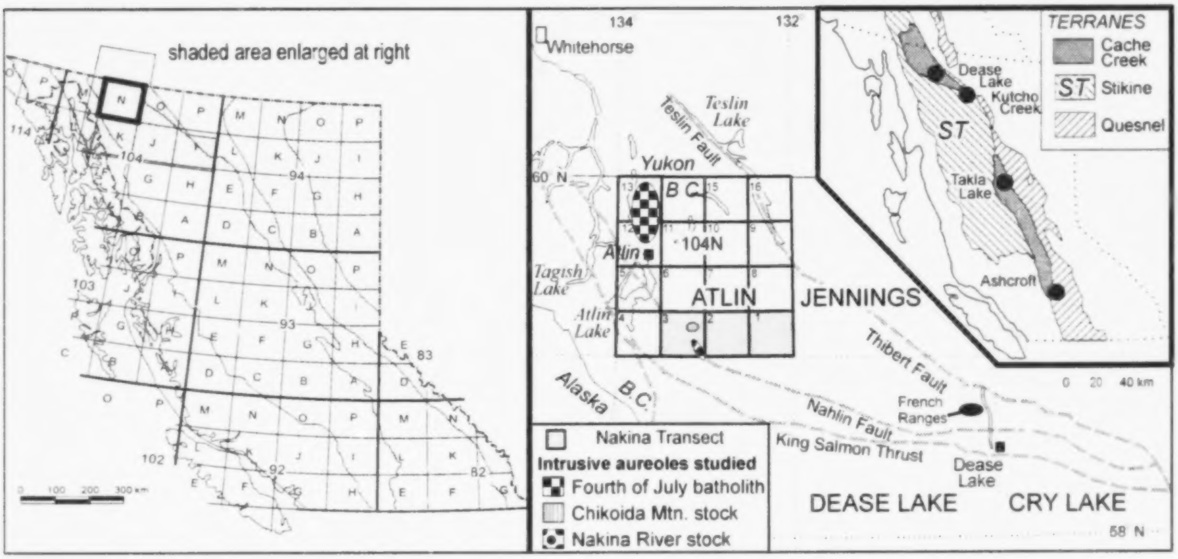
shaded area enlarged at right
114
104
94
103
93
83
102
92
82
0 100 200 300 km
134
132
Whitehorse
Teslin Lake
Teslin Fault
Yukon
60 N
B.C.
104N
Atlin
Tagish Lake
Atlin Lake
ATLIN
JENNINGS
Alaska
B.C.
Thibert Fault
Nahlin Fault
King Salmon Thrust
French Ranges
Dease Lake
DEASE LAKE
CRY LAKE
58 N
Nakina Transect
Intrusive aureoles studied
Fourth of July batholith
Chikoida Mtn. stock
Nakina River stock
TERRANES
Cache Creek
ST Stikine
Quesnel
Dease Lake
Kutcho Creek
ST
Takla Lake
Ashcroft
0 20 40 km

Figure 1. Study area within the northern Cache Creek Terrane, also referred to as the Atlin Complex. The top right hand insert shows adjacent terranes Stikina (ST) to the west and Quesnel (QN) to the east. These three terranes together make up the Intermontane Superterrane. All studied intrusive bodies are within the Atlin map area (104N), while the study area used by Mihalynuk (1998) to date blueschist is further to the southeast in the French Ranges.

intrusion; Mihalynuk, pers. comm., 2002). This paper presents field and petrographic observations from three intrusions of known or suspect Middle Jurassic age (Aitken, 1959; Mihalynuk *et al.*, 2003 (this volume); Figure 1) and their thermally metamorphic aureoles, which overprint the deformed Atlin complex. Detailed petrographic observations provide a test for the relative timing of regional deformation and Middle Jurassic intrusion. Studied intrusive bodies include: Fourth of July (Creek) batholith, Nakina River, and Chikoida Mountain stocks. All intrusive bodies are exposed within the Atlin map area (104N) and their relative locations are shown on Figure 1.

FOURTH OF JULY BATHOLITH

The Fourth of July batholith is a heterogenous intrusive complex, which varies from diorite to granite and alaskite (Mihalynuk *et al.*, 1992). The batholith occupies more than 770 square kilometres in 104N; Aitken, 1959) and is dominantly granite, with biotite- to hornblende-rich and K-feldspar megacrystic to equigranular phases (Mihalynuk *et al.*, 1992). A well-exposed contact along the Atlin Road (Highway 7) south of Como Lake, is the southern most extent of the batholith (Figure 2). At that location the body is a K-feldspar megacrystic hornblende granite. A lateral variation in K-feldspar abundance is common and the rock ranges from that of a sparse to a crowded porphyry. Mafic xenoliths are rare. Euhedral K-feldspar phenocrysts range in size from 1-4cm and typical grain size of groundmass is 2-4mm. No preferred orientation of K-feldspar phenocrysts or xenoliths was observed. Anhedral quartz grains within the groundmass are unstrained, and exhibit little to no undulatory extinction. Common accessory phases include titanite and apatite.

Wallrock metabasites consist of amphibole, plagioclase, quartz and chlorite. Calcite exists predominantly as veinlets 0.05mm wide. Grain size is 0.05 to 1 mm, and no preferred orientation of grains is evident. Many of the quartz grains display undulatory extinction. However, grain boundaries have sharp, straight contacts and quartz grains intersect with 120 degree junctions. The contact between the intrusive and wall rocks is vertical, trending 040 degrees.

Metachert, which has been thermally altered by the batholith, is exposed 100m south of the contact. Minerals include quartz, tremolite and calcite. Grain size is between 0.02 to 0.5 mm. Tremolite grains are acicular and have no preferred orientation. Anhedral quartz grains have undulatory extinction and grain boundaries are serrated. Bedding is sub-vertical, striking 040 degrees. Metacherts, 150m away from the contact, are also thermally altered, but are less so than those at 100metres distance.

CHIKOIDA MOUNTAIN STOCK

The Chikoida Mountain stock is semicircular and relatively homogeneous in mineralogy and grain size. The stock occupies more than 36 square kilometres and is composed of quartz, K-feldspar, plagioclase, biotite and hornblende. Two areas of the stock were studied, including both the southern and northern contacts (Figure 3). The

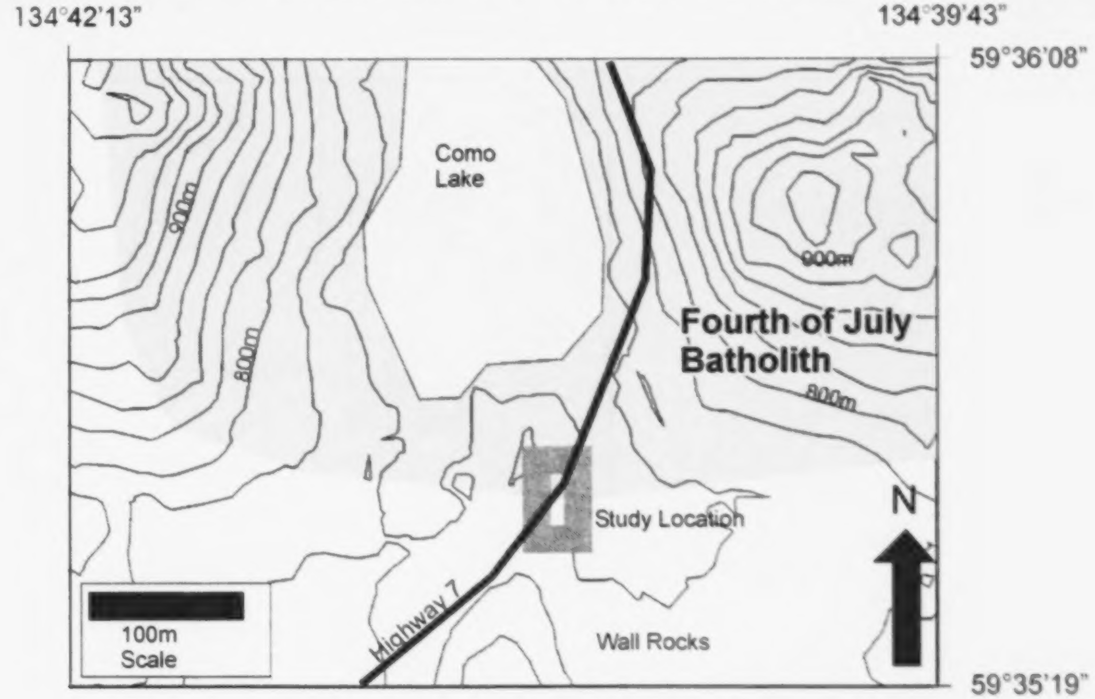

Figure 2. Studied location for the Fourth of July Batholith.

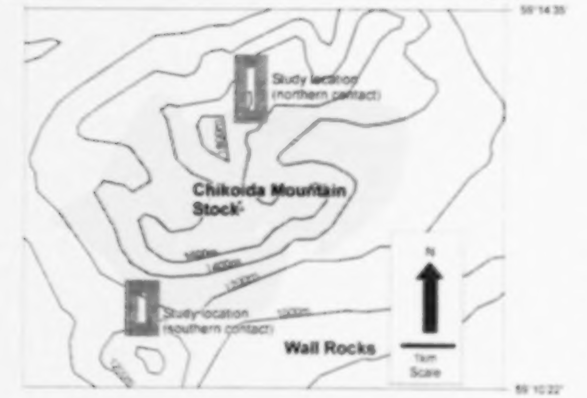

Figure 3. Studied areas of the Chikoida Mountain stock.

rock type at both contacts is hornblende biotite granodiorite. Grain size ranges between 1-4 mm. Both plagioclase and K-feldspar grains are subhedral, but other grains are anhedral with no preferred orientation. Quartz grains have little or no undulatory extinction. Alteration of hornblende to chlorite and alteration of plagioclase to sericite is evident. Accessory phases include zircon and apatite.

NORTHERN AUREOLE

Metapelites at the northern contact are characterized by biotite, quartz, muscovite, sericite, apatite and zircon. Biotite grains have a preferred orientation, while quartz grains have more equant shapes. Quartz grains overprint foliation, which indicates hornfels postdate regional metamorphism (Photo 1). Grain size is 0.1-0.3 mm and grain boundaries are straight to embayed. Quartz grains are not strained. Bedding and foliated fabric are sub-parallel and vertical trending 100 degrees, while the contact is 080/90. Hornfels texture becomes difficult to detect more than 100m from the contact. Regionally metamorphosed volcanoclastics, about 400m from contact, contain strained quartz.

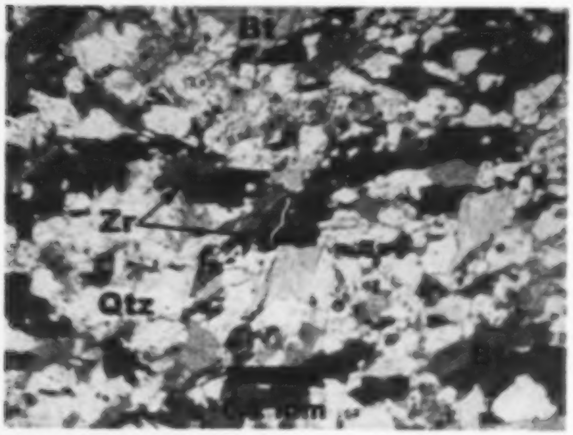

Photo 1. Thin section of hornfelsed metapelite under plane polarized light. This sample was taken within one meter of the contact on the nothern side of the Chickoida pluton. Note that the hornfels fabric is outlined by biotite.

SOUTHERN AUREOLE

Recrystallised calcite (100%) occures within 100 metres of the southern contact of the Chikoida Mountain stock. Calcium carbonate grain boundaries are sharp and intersect at 120-degree junctions. Grain sizes are 0.1-2mm. Pervasive dark and light banding which has a thickness of 4-5mm is orientated parallel to the inferred contact at 090/90. Carbonate rocks 300m farther south are not recrystallised and fossil debris is preserved.

NAKINA RIVER STOCK

The Nakina River stock is an elongated body (trending NW-SE) comprised of two intrusive rock types. It occupies over 97 square kilometres within the 104N mapsheet and is characterized by an inner granodiorite main body with a 200m thick quartz diorite outer rim. The stock is composed of quartz, plagioclase, K-feldspar, biotite, and hornblende, as well as minor epidote. Contacts of the Nakina River stock were investigated at three localities: one on the east side of the body at the southern limit of the Atlin map sheet, and two localities at the northern contacts west of Focus Mountain (Figure 4). The main intrusive body is a homogenous hornblende-biotite granodiorite with grain sizes of 1-3mm, and the outer rim is a relatively finer grained (0.5-2mm) hornblende-biotite-quartz diorite. Both rock types consist of subhedral zoned plagioclase grains, while other grains are typically anhedral. Quartz diorite rocks have sericite-altered plagioclase grains, as well as hornblende altered to chlorite. Granodiorite rocks are typically less altered. A weakly foliated hornblende fabric parallel to the contact is evident in quartz diorite rocks at the northwestern contact. Foliation does not occur in the main inner zone or at the southeastern contact. Strained quartz is present in the quartz diorite rocks at the southwestern contact. Intrusive rocks at the northern margin contain little or no strained quartz. Accessory phases in all rock types include zircon and apatite.

SOUTHEASTERN AUREOLE

Metachert occurs along the southeastern contact. Grains consist dominantly of quartz with fine muscovite inclusions. Quartz grains are 0.05-1mm and have embayed grain boundaries. Undulatory extinction is not evident. Quartz grains are finer in size away from the contact, to <0.01mm at 50 metres. A metamorphosed, quartz diorite dike which has a grain size of 0.1-1mm, occurs 150 metres from the contact. Quartz grains within the dike have undulatory extinction, but no alignment of hornblende or preferred orientation of biotite is evident. A limestone body lo-

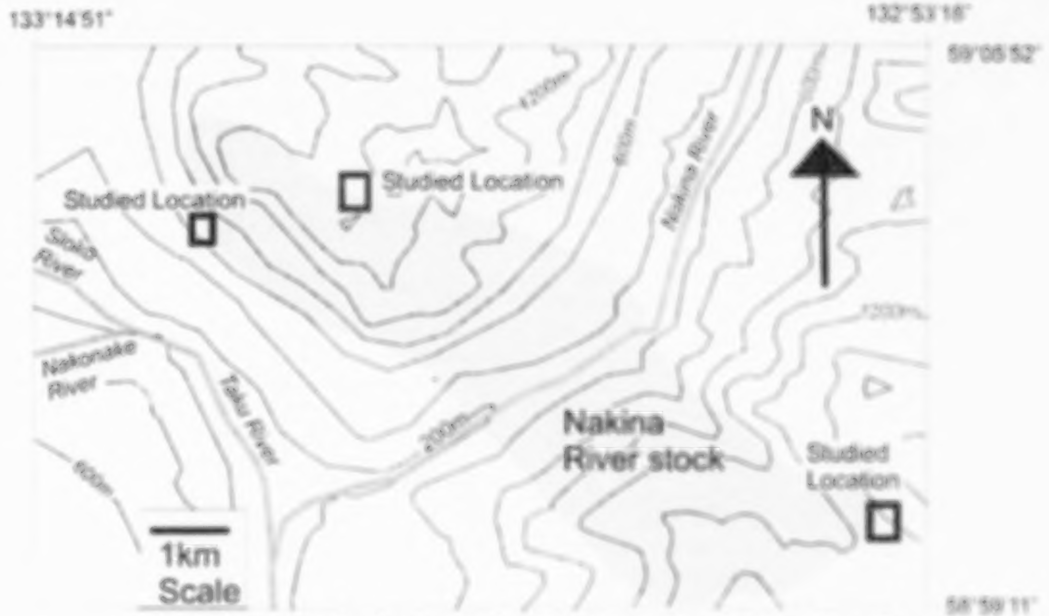

Figure 4. Areas studied at the margin of the Nakina River stock and its thermal aureole.

cated approximately 300m from the contact is fine-grained with little evidence of recrystallisation.

NORTHWESTERN AUREOLE

Metabasite rocks exposed at the northwestern contact are characterized by amphibole, quartz, plagioclase and biotite. Grains are 0.05-1mm with sharp, straight grain boundaries. Biotite is kinked and quartz displays undulatory extinction. Alignment of amphibole grains defines a foliation. Aligned biotite inclusions, within amphibole, may define a pre-existing fabric at a high angle to the fabric defined by amphibole alignment (Photo 2). Late biotite is orientated 90 degrees to hornblende and reflects a shift in direction of the major stress field. Delta-type amphibole porphyroclasts indicate a dextral vorticity (Photo 3). Foliation is orientated sub vertical with a trend of 140 degrees and is sub parallel to the intrusive contact, which is vertical, trending 135 degrees.

Northern Aureole

Like the northwestern aureole, metabasite includes quartz, amphibole and biotite. Grain size is very fine (0.01-0.05mm) and amphibole grains are well aligned. Stress kinking and mild undulatory extinction is observed in biotite and quartz respectively. Grain boundaries are

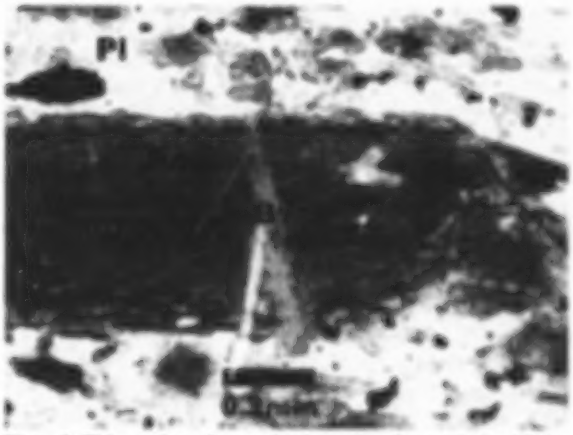

Photo 2. Thin section of a metabasite under plane polarized light. This sample was taken from within one meter of the contact on the south eastern side of the Nakina River stock. Note that amphibole grains have overgrown biotite which is typically orientated with its long axis 90 degrees to the dominant foliation.

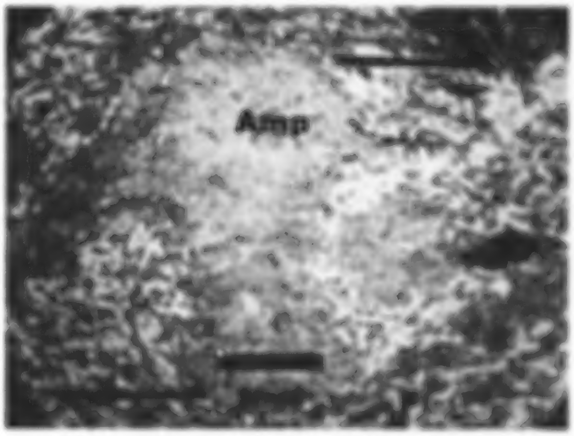

Photo 3. Thin section of metabasite under plane polarized light. This sample was taken from within one meter of the contact on the southwestern side of Nakina River stock. Hornblende porphyroblast is delta-form, indicating dextral vorticity (arrows).

sharp and straight. Quartz grains intersect at 120-degree junctions.

DISCUSSION AND CONCLUSIONS

Features common to all of the intrusions and intrusive aureoles investigated indicate that ductile deformation, during or following pluton emplacement was not significant. These features include: a general increase in the frequency of stressed minerals away from intrusive contacts, a lack of foliation in intrusive rocks, and the presence of hornfels texture overprinting foliation in aureole rocks. In addition, a smooth annular aeromagnetic anomaly within the Chikoida Mtn. stock, and magnetic contact aureoles around semicircular bodies, such as Mount McMaster, appear undeformed. Minor, brittle faulting is common near the contacts of most bodies, but nowhere is a fault offset of an aureole identified, nor has folding of a contact aureole been observed.

One exception may be the northwestern contact of the Nakina River stock where delta-type porphyroclasts (Photo 3) and the presence of an internal fabric outlined by biotite within amphibole porphyroblasts (Photo 2) indicates deformation along the southwestern margin occurred during emplacement. Orientation of delta-type porphyroclasts implies subvertical dextral shear subparallel to the intrusion margin. This fabric could be related to regional stresses or, more likely, to local stresses attending magma emplacement. Intrusion-generated fabrics are shown by Aitken (1959) to be a common feature of Middle Jurassic intrusions. The common occurrence of biotite grains that define an overprinting fabric perpendicular to an earlier, growth-defined fabric of amphibole (Photo 2) may indicate a transient stress field that switches abruptly during retrograde metamorphism related to cooling of the intrusion. The data suggest a principle stress that changes from a sub-horizontal to a sub-vertical orientation. Systematic study of cooling ages from amphibole and biotite grains, which define fabric in aureoles, should be conducted to help to better define the history of deformation within Cache Creek rocks.

ACKNOWLEDGMENTS

This paper was supported and funded by a TGI research mapping grant. The author owes many thanks to M. Mihalynuk, S. Johnson, J. English, O. Roentz, J. Blackwell and F. Cordey for their shared knowledge and friendship during field mapping. Extra special thanks goes to M. Mihalynuk, J. English, B. Grant and S. Johnson for their time and efforts in reviewing this paper, with which this paper has benefited greatly.

REFERENCES

Aitken, J.D. (1959): Atlin map-area, British Columbia; *Geological Survey of Canada*, Memoir 307, 89 pages.

Cordey, F., Mortimer, N., DeWever, P. and Monger, J.W.H. (1987): Significance of Jurassic radiolarians from the Cache Creek Terrane, British Columbia; *Geology (Boulder)*, Volume 15, pages 1151-1154.

Cordey, F., Gordey, S.P. and Orchard, M.J. (1991): New biostratigraphy data for the northern Cache Creek terrane, Teslin map area, southern Yukon; *in* Current Research, Part E, *Geological Survey of Canada*, Paper 91-1E, pages 67-76.

Cordey, F. (1998): Radiolaires des complexes d'accretion de la Cordillère canadienne (Colombie-Britannique). Translated Title: Radiolaria from accretion complexes in the Canadian Cordillera, British Columbia; Ottawa, ON, Canada, *Geological Survey of Canada*, 209 pages.

Mihalynuk, M.G., Smith, M.T., Gabites, J.E., Runkle, D. and Lefebure, D. (1992): Age of emplacement and the basement character of the Cache Creek Terrane as constrained by new isotopic and geological data; *Canadian Journal of Earth Sciences*, Volume 29, pages 2463-2477.

Mihalynuk, M.G., Erdmer, P., Ghent, E.D., Archibald, D.A., Friedman, R.M., Cordey, F., Johannson, G.G., Beanish, J. (1999): Age constraints for the emplacement of the northern Cache Creek Terrane and implications of blueschist metamorphism; *in* Geological Fieldwork 1998, *BC Ministry of Energy, Mines and Petroleum Resources*, Paper 1999-1, 127-141 pages.

Mihalynuk, M.G., Johnston, S.T., English, J.M., Cordey, F., Villeneuve, M.J., Rui, L. and Orchard, M.J. (2003): Atlin TGI Part II: Regional geology and mineralization of the Nakina area (NTS 104N/2W and 3); *in* Geological Fieldwork, *BC Ministry of Energy and Mines*, Paper 2003-1, this volume.

Symons, D.T.A., Harris, M.J., Hart, C.J.R. and Blackburn, W.H. (1998): Geotectonics in the Northern Cordillera from paleomagnetism and geobarometry: progress report and the recent results from the Eocene White Pass dikes and Jurassic Fourth of July Batholith; *in* slave-NORthern Cordillera Lithospheric Evolution (SNORCLE) and Cordilleran tectonics workshop, Cook Fredrick, Erdmer and Philippe (Editors), *The University of British Columbia, Lithoprobe Secretariat [for the] Canadian Lithoprobe Program*, pages 171-180.

Atlin TGI, Part V: Carbonate and Siliceous Rocks of the Cache Creek Terrane, Southern Sentinel Mountain, NTS 104N/5E and 6W

By H. Sano[1], T. Igawa[1] and T. Onoue[1]

KEYWORDS: Cache Creek terrane, Atlin, Sentinel Mountain, basalt, carbonate, chert, radiolaria, fusulinid, biostratigraphy

INTRODUCTION

Cache Creek terrane is a subduction-generated accreted terrane within the Canadian Cordillera (Struik *et al.*, 2001). It is characterized by an oceanic rocks including Lower Mississippian to upper Middle Permian shallow-marine carbonates containing Tethyan-type fusulinid-bearing limestones, often occurring as huge tectonic slabs. Lower Mississippian to Middle Jurassic radiolarian chert, argillite, greywacke, basic volcanic rocks and ultramafic rocks are other major constituents (Monger *et al.*, 1991). Tethyan fusulinids imply paleobiogeographic allochthoneity to North America (Monger and Ross, 1971; Carter *et al.*, 1991; Orchard *et al.*, 2001). Cache Creek terrane is, therefore, a key terrane which contains remnants of the Mississippian to Jurassic, long-lived Panthalassan Ocean, and contains a record of much of the late Mesozoic tectonic evolution of the Canadian Cordillera (Mihalynuk *et al.*, 1994).

The most extensive and best exposures of Cache Creek terrane occur within a wedge-shaped region centered on the Atlin area (Figure 1; Monger *et al.*, 1991). As in the other major exposure areas, such as near Pavilion (Figure 1), Cache Creek terrane near Atlin comprises a highly complicated structural aggregate of the Lower Mississippian to Upper Triassic oceanic rocks. During the Atlin Targeted Geoscience Initiative (TGI) (Mihalynuk *et al.* 2003; Mihalynuk and Lowe, 2002), Mesozoic and Paleozoic oceanic rocks of Cache Creek terrane were investigated (Figure 1) within the area southwest of Sentinel Mountain. We discuss the stratigraphic relationship of the deep-marine siliceous rock facies to the shallow-marine carbonates, historically referred to as the Kedahda and Horsefeed formations, respectively (Monger, 1975), and how this bears on the evolution of the Cache Creek as a whole.

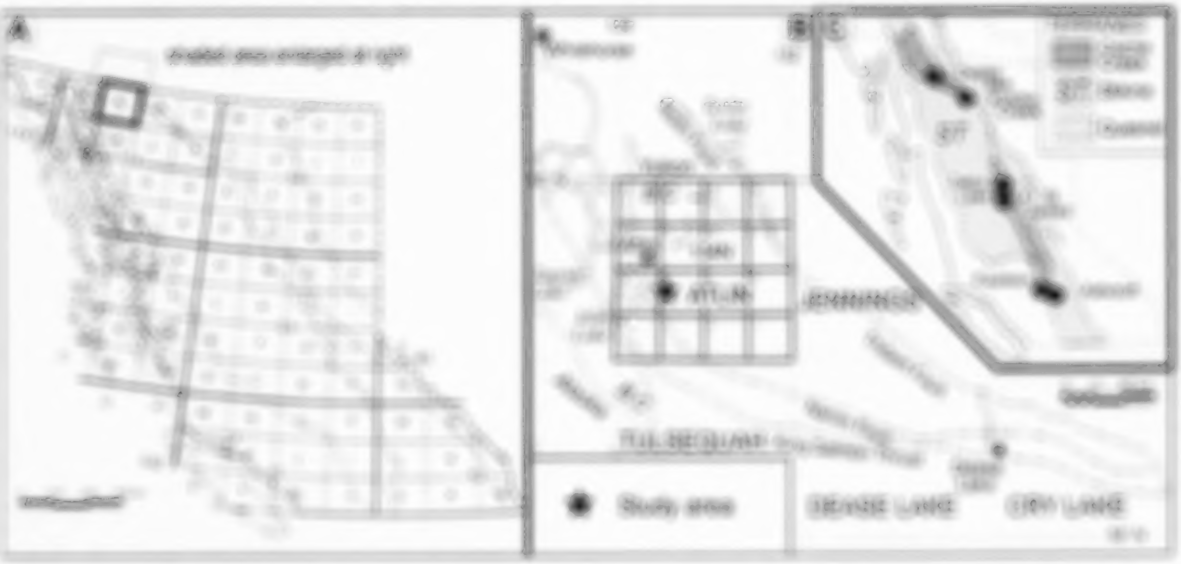

Figure 1. The location of Atlin TGI bedrock mapping, in northwestern British Columbia (A), and location of our field area, on the southern flank of Sentinel Mountain (B).

---

[1] *Department of Earth & Planetary Sciences, Kyushu University, Fukuoka 812-8581 Japan*

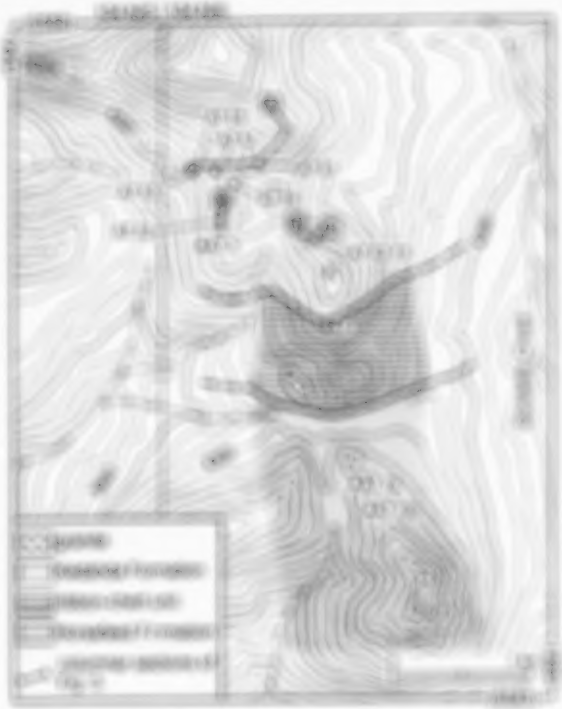

[illegible]

[illegible]

[illegible]

[illegible]

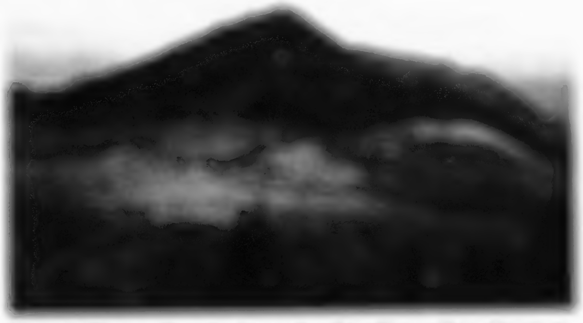

[illegible]

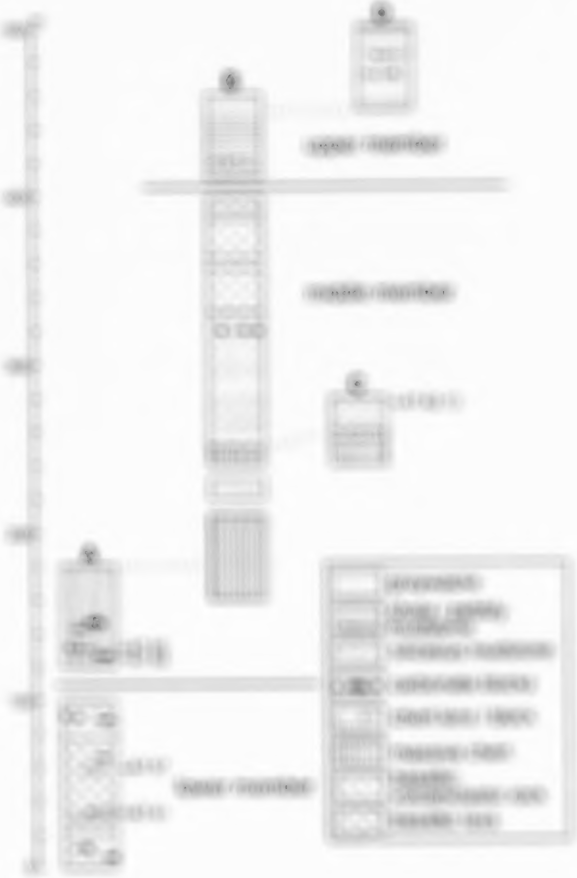

[illegible]

[illegible]

[illegible]

[illegible]

[illegible]

[illegible]

[illegible]

[illegible]

[illegible]

[illegible]

[illegible]

[illegible]

[illegible]

[illegible]

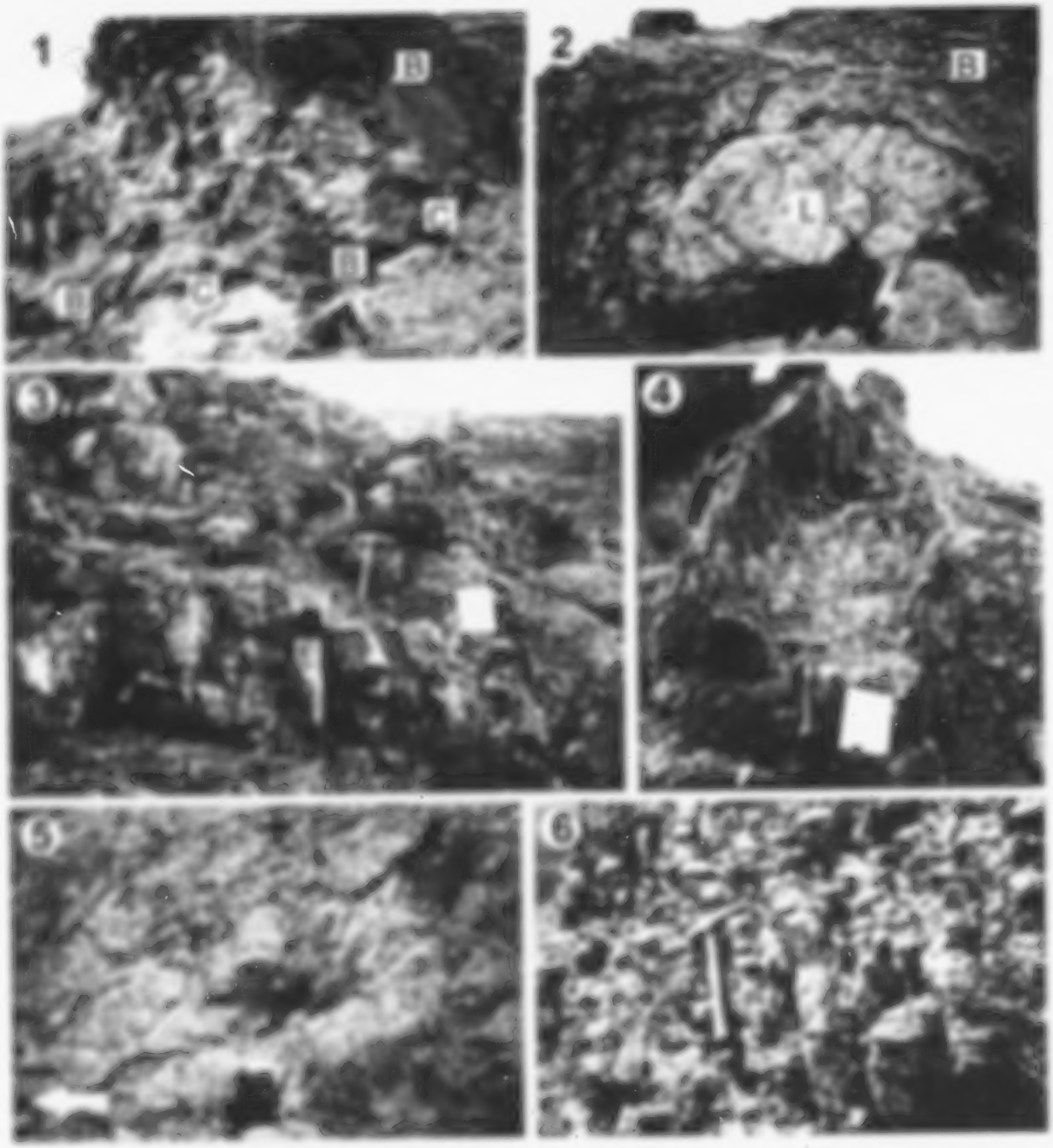

Photo 2. Kedahda Formation basaltic rocks and ribbon-bedded chert. Localities are indicated on Figure 2.
1. Lenticular beds of chert (C) intercalated in basaltic flow rocks (B) with minor volcaniclastic rocks. Locality AT 61. See Figure 3 for approximate stratigraphic level.
2. Isolated block of siliceous limestone (L) wholly embedded in a basaltic lava (B), which also contains small blocks of chert and limestone breccia. Locality AT 57. See Figure 3 for approximate stratigraphic level.
3. Dark grey, massive chert, entirely devoid of bedding surfaces, cut by nearly vertical joints. Locality AT 8.
4. Folded and fractured, siliceous mudstone having locally crowded, pebble-sized limestone debris. Locality AT 12.
5. Penetratively and pervasively cleaved, pale green, tuffaceous shale of Kedahda Formation. The scaly cleavage is anastomosing and moderately inclined to northwest. Arrow at lower left indicates north. Locality AT 59.
6. Weakly contorted, ribbon-bedded, radiolarian chert with clayey partings. Locality AT 66.

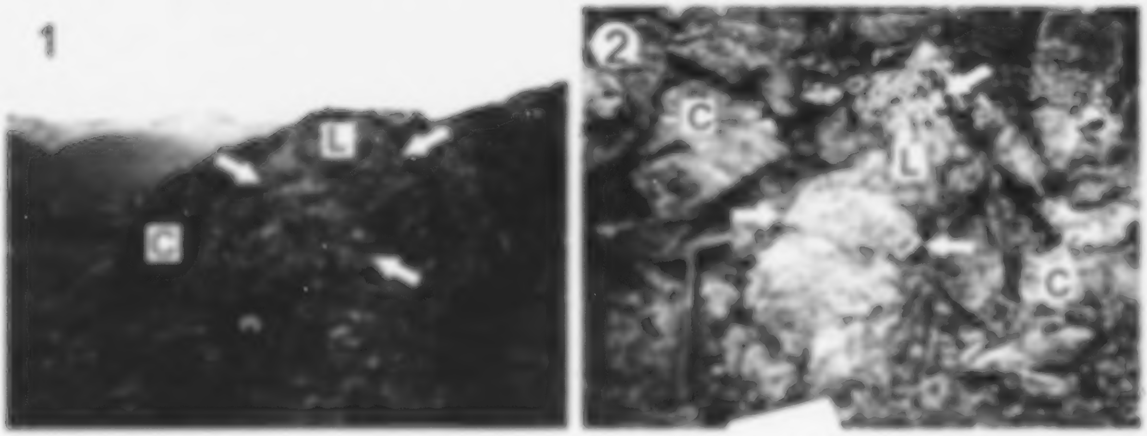

Photo 3. Various-sized, displaced limestone blocks (L) embedded in massive chert (C) of the Kotcho Formation. Arrows denote lithologically sharp, rugged and knobby boundary surface between limestone blocks and massive chert. All localities are shown on Figure 2. See Figure 3 for approximate stratigraphic levels.

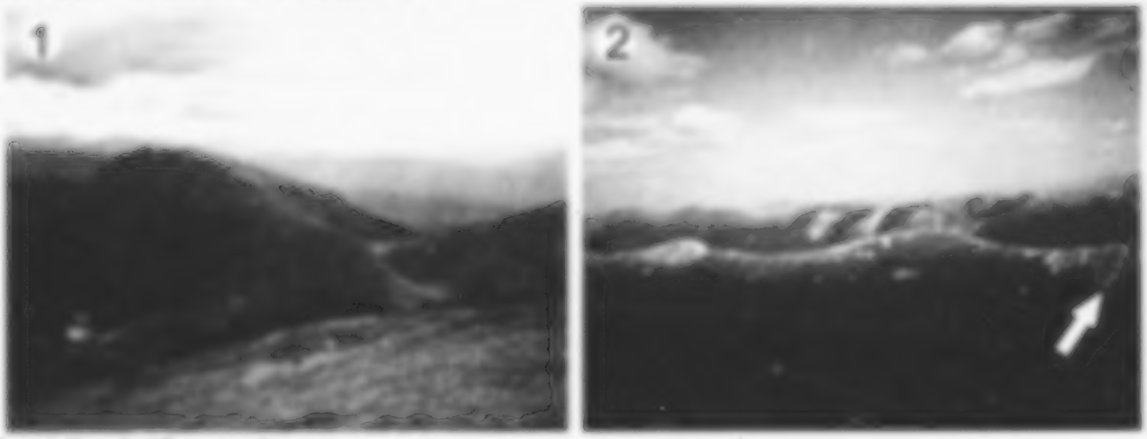

Photo 4. Horsefeed Formation limestone.
1. North-northwest-trending ridge underlain mostly by massive limestone of the Horsefeed Formation. View to south from small peak underlain by Kotcho Formation siliceous rocks. Densely-vegetated, western slope of Burdette Creek is at left edge of view.
2. Horsefeed Formation limestone exposed on north-trending ridge. View is to east across Burdette Creek. Note moderately north-dipping, thick limestone beds, indicated by arrow. Beyond this ridge is the southern part of Laurie Range, which is underlain by Horsefeed Formation limestone.

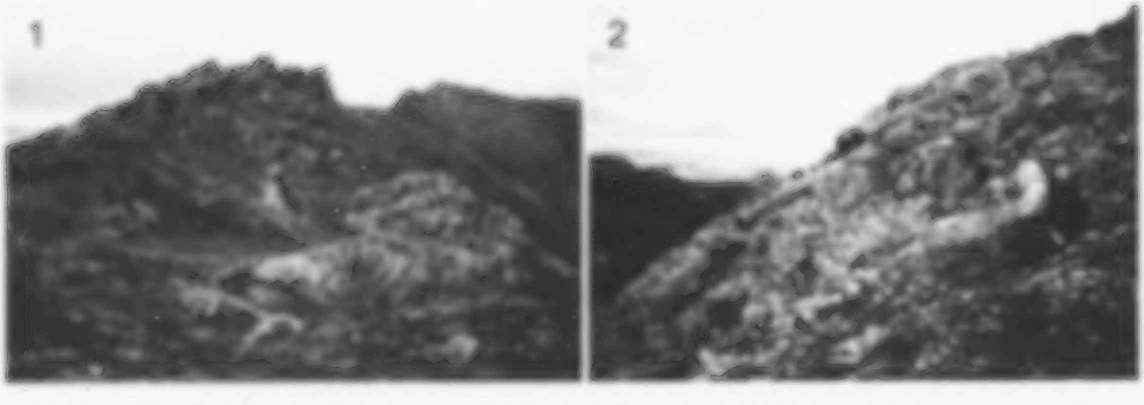

Photo 5. Views of Horsefeed Formation limestone in southern Sentinel Mountain area.
1. View of strongly fractured, massive limestone exposed at peak, denoted as H in Figure 2.
2. Style of bedded limestone with intercalation of thin, highly carbonaceous marl layers. Locality AT 100 in Figure 2.

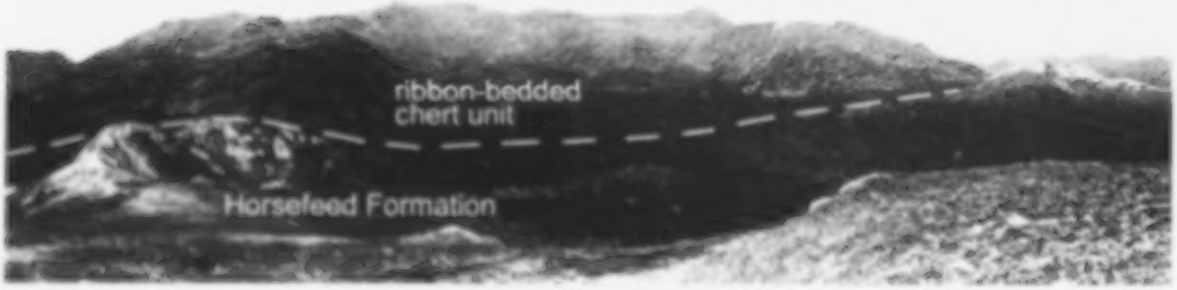

Photo 6. Panoramic view of fault boundary, indicated by dashed line, between Triassic radiolarian-bearing ribbon-chert unit and Horsefeed Formation carbonate rocks. Fault boundary trends east-northeast. Thickly vegetated, upper reaches of Burdette Creek at center of view.

beds are usually a few tens to several tens of centimetres thick, dominate the marl beds, which are commonly less than 5 centimeters thick. Siliceous limestone is dark grey to black, probably rich in carbonaceous matter. Carbonaceous marl is dark grey, occasionally jet black, weakly fissile, and smells putrid when broken. Bedding surfaces are gently undulated and knobby, due to stylolitization. The rocks trend approximately southwest, with moderate northwest dips. This structural trend extends outside of the study area, to the east (Photo 4-2).

All Horsefeed limestone contains shallow-marine bioclasts. Boundstone is not observed. Fossils preserved are fusulinids, crinoids, gastropods, bivalves, ostracods, and dasycladacean algae; all are indicative of carbonate accumulation in shallow water. These skeletal debris are in many cases supported by a micritic matrix, but in places the rock is grain supported (Photo 7).

Although fusulinids were found at many localities throughout the outcrop area, their preservation is poor. Preliminary identifications support an upper Lower Permian (upper Artinskian) age for the highly carbonaceous limestone (AT 100 in Figure 2). On the basis of the upper Artinskian fusulinids, plus the lower Lower and upper Middle Permian fusulinids previously reported by Monger (1975), the Horsefeed Formation in the Sentinel Mountain probably rangesin age from Lower to Middle Permian.

DISCUSSION

REVISION OF KEDAHDA FORMATION STRATIGRAPHY AND ITS SEDIMENTOLOGICAL IMPLICATION

Kedahda succession of the Sentinel Mountain area probably represents stratigraphy formed in a deep marine environment. We consider that the stratigraphic change from massive chert to greywacke, records a lateral shift from a deep-marine basin ideal for the chert accumulation, to a hemipelagic environment, then to a trench-environment, where land-derived clastic sediments and intermediate volcaniclastic debris were deposited.

Kedahda massive chert is interpreted to be a deep-water siliceous facies, characterized by an abundance of siliceous sponge spicules, which accumulated in a pelagic setting in an open-ocean. This would place it far beyond the reach of terrigenous clastics.The argillaceous character of the siliceous mudstone is interpreted to represent accumulation in a hemipelagic setting. Deposition of the tuffaceous shale suggests a nearby volcanic source; however, the siliceous rocks suggest sedimentation in a pelagic to hemipelagic setting, succeeded by a deep-marine environment. The Lower Permian, radiolarian-bearing greywacke is possibly a distal trench-fill sediment.

HORSEFEED AND KEDAHDA FACIES INTERPRETATION

Horsefeed Formation rocks are shallow-marine bioclastic carbonate sediments. Carbonaceous and siliceous properties, and predominance of the micritic matrix, imply deposition in a slightly stagnant, lagoonal setting within the deep subtidal zone. An absence of terrigenous materials in the Horsefeed Formation suggests deposition on a topographic high in an open-ocean setting. According to Monger *et al.* (1991), the Horsefeed Formation carbonates formed a cap upon a basaltic seamount, or an oceanic plateau.

Massive chert of the Kedahda Formation is similar to the Bashkirian to Moscovian chert of the Pope succession within the Cache Creek Complex of the Mt. Pope area near Fort St. James, central British Columbia (Sano and Struik, 1997; Orchard *et al.*, 1998) as both contain siliceous sponge spicules and displaced shallow-marine carbonates. Although they differ in age, the Kedahda and Pope cherts are commonly interpreted as siliceous facies formed in a deep-water setting, where shallow-marine carbonates could have been introduced by density flows (olistostromes), most probably sourced from the nearby Horsefeed and Pope buildups, respectively.

Following the sedimentary model of Monger *et al.* (1991) and Sano and Rui (2001), we consider that the Kedahda massive chert accumulated on the lower flank of a seamount, or an oceanic plateau, the top of which was capped by the Horsefeed carbonate buildup. We infer that

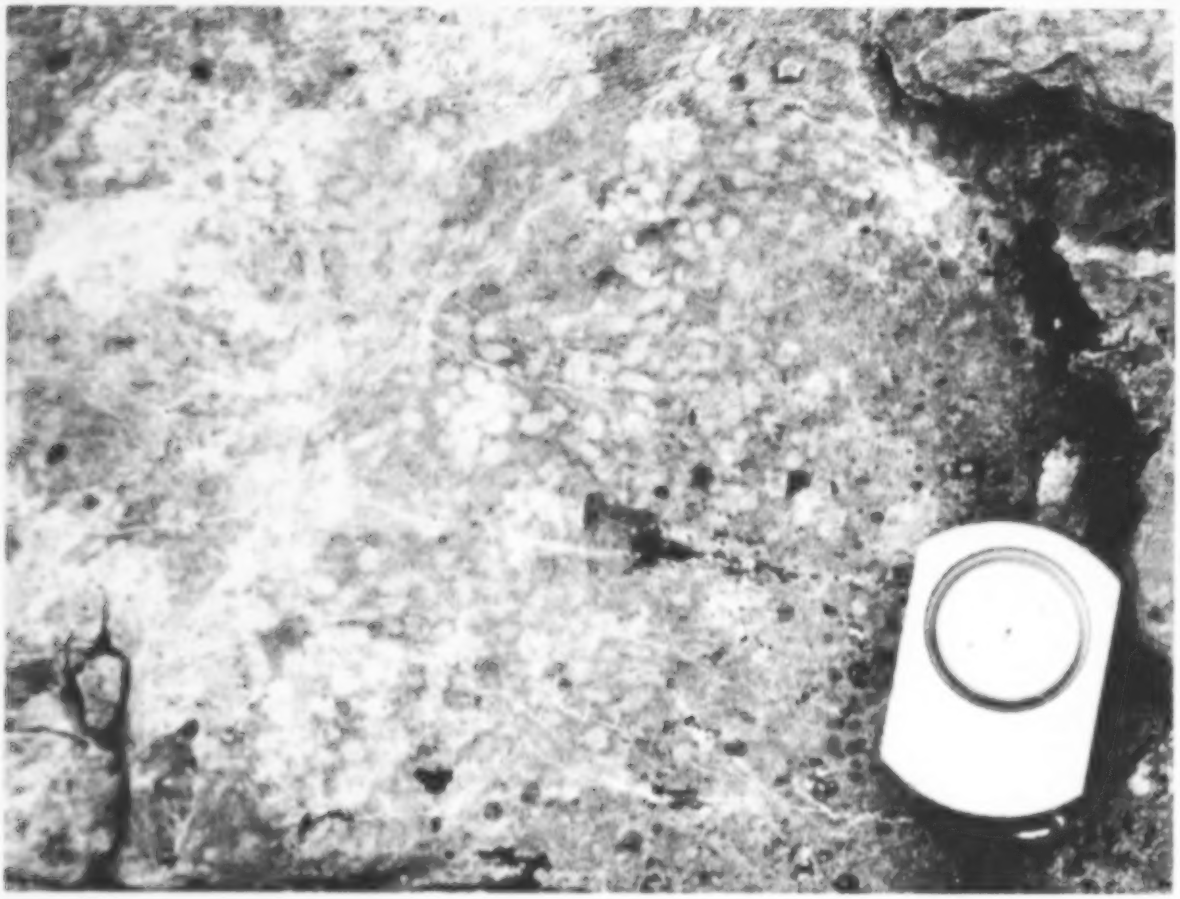

Photo 7. Local, dense accumulation of fusulinids in dark grey, micritic limestone. Location AT 78 in Figure 2.

their deposition was nearly synchronous; Horsefeed shallow-marine and Kedahda deep-marine facies pass laterally into each other, linked by olistostromal carbonate blocks and debris. Analogous facies occur in the Upper Carboniferous to Middle Permian spicular chert of the Akiyoshi terrane (Uchiyama *et al*., 1986; Sano and Kanmera, 1988), a subduction-generated Permian accretionary complex in southwest Japan. It is characterized by remnants of a Lower Carboniferous to Middle Permian shallow-marine carbonate buildup atop a seamount (Kanmera and Nishi, 1983; Kanmera *et al*., 1990).

Siliceous sponge spicules, instead of radiolaria, are the common biogenic component of the Carboniferous to Permian Kedahda, Pope, and Akiyoshi cherts. It is uncertain what this similarity implies. It is probably a facies controlled rather than age-related. Sano and Kanmera (1988) suggest that the Akiyoshi spicular chert exhibits proximal facies with respect to the carbonate capped seamount, whereas time-equivalent radiolarian chert is a distal facies without olostostromal carbonate.

SUMMARY

The Kedahda and Horsefeed oceanic rocks of Cache Creek terrane were investigated within the southern part of the Sentinel Mountain area, southeast of Atlin Lake, BC. Kedahda Formation consists of basaltic lavas and volcaniclastic rocks, massive chert, siliceous mudstone, tuffaceous shale, dark grey shale and pebbly mudstone, and greywacke, in ascending order. Isolated blocks and resedimented debris of shallow-marine carbonate occur at several levels embedded in the siliceous and argillaceous rocks. The succession is interpreted as oceanic stratigraphy formed by a shift from accumulation of the massive chert in an open-ocean realm, through hemipelagites in a possible trench setting. The massive chert yields Middle to Upper Permian radiolaria. Horsefeed Formation is composed entirely of locally dolomitized, but mostly siliceous, dark grey and carbonaceous, bioclastic limestone. It is mainly thick- bedded with thin, highly carbonaceous marl beds, and contains fusulinids, bivalves gastropods, and crinoids, all having a shallow-marine affinity. The fusulinids are preliminarily dated as the upper Lower Permian (Artinskian).

We interpret the Kedahda and Horsefeed oceanic rocks as having been deposited beside or atop a basaltic seamount, or oceanic plateau in an open-ocean realm. The Horsefeed shallow-marine facies and Kedahda deep-water facies pass laterally into each other, linked by olistostromal, shallow-marine carbonates.

ACKNOWLEDGMENTS

We express our sincere thanks M. Mihalynuk (BCGS, Victoria), who provided important suggestions on the geology of Cache Creek terrane within the study area and offered outstanding support and advice for fieldwork. Special thanks are due to Bert Struik (GSC, Vancouver), who encouraged us to participate in Atlin TGI. F. Cordey (Univerisité Claude Bernard Lyon 1, France) is acknowledged for his fruitful discussion on the siliceous rocks of the Kedahda Formation. This paper was reviewed by B. Grant and M.G. Mihalynuk.

REFERENCES

Carter, E.S., Orchard, M.J., Ross, C.A., Ross, J.R.P., Smith, P.I. and Tipper, H.W. (1991): Part B. Paleontological signatures of terranes; *in* Gabrielse, H. and Yorath, C.J. (Editors); Geology of the Cordilleran orogen in Canada -Geology of Canada. Number 4, Chapter 2, 28-38, Geological Survey of Canada.

Kanmera, K. and Nishi, H. (1983): Accreted oceanic reef complex in southwest Japan; *in* Hashimoto, M. and Uyeda, S. (Editors); Accretion tectonics in the circum-Pacific regions, Terra, Tokyo, pages 195-206,.

Kanmera, K., Sano, H. and Isozaki, Y. (1990): Akiyoshi terrane. *in* Ichikawa, K. *et al.* (Editors), *Pre-Cretaceous terranes of Japan.* Publication of IGCP Project 224, pages 49-62.

Mihalynuk, M.G., Nelson, J.-A., Diakow, L.J. (1994): Cache Creek terrane entrapment: Oroclinal paradox within the Canadian Cordillera; *Tectonics*, Volume 13, pages 575-595.

Mihalynuk, M.G. and Lowe, C. (2002): Atlin TGI, Part I: An introduction to the Atlin Targeted Geoscience Initiative; *in* Geological Fieldwork 2001, *B. C. Ministry of Energy and Mines*, Paper 2002-1.

Mihalynuk, M.G., Johnston, S.T., Lowe, C, Cordey, F., English, J.M., Devine, F.A. M., Larson, K. and Merran, Y. (2002): Atlin TGI Part II: Preliminary results from the Atlin Targeted Geoscience Initiative, Nakina area, northwest British Columbia; *in* Geological Fieldwork 2001, *B.C. Ministry of Energy and Mines*, Paper 2002-1, pages 1-4.

Monger, J.W.H. (1975): Upper Paleozoic rocks of the Atlin Terrane, northwestern British Columbia and south-central Yukon; *Geological Survey of Canada*, Paper 74-47, 63 pages.

Monger, J.W.H. and Ross, C.A. (1971): Distribution of fusulinaceans in the western Canadian Cordillera; *Canadian Journal of Earth Sciences*, Volume 8, pages 259-278.

Monger, J.W.H., Wheeler, J.O., Tipper, H.W., Gabrielse, H., Harms, T., Struik, L.C., Campbell, R.B., Dodds, C.J., Gehrels, G.E. and O'Brien, J. (1991): Part B. Cordilleran terranes; *in* Gabrielse, H. and Yorath, C.J. (Editors): Geology of the Cordilleran orogen in Canada, *Geology of Canada*, Number 4, Chapter 8, Geological Survey of Canada, pages 281-327.

Nelson, J.A. and Mihalynuk, M.G. (1993): Cache Creek ocean: Closure or enclosure?; *Geology*, Volume 21, pages 173-176.

Orchard, M.J., Struik, L.C. and Taylor, H. (1998): New conodont data from the Cache Creek Group, central British Columbia; *in* Current Research, *Geological Survey of Canada*, Paper 1998-A, pages 99-105.

Orchard, M.J., Cordey, F., Rui, L., Bamber, E.W., Mamet, L.C., Struik, L.C., Sano, H. and Taylor, H.J. (2001): Biostratigraphic and biogeographic constraints on the Carboniferous to Jurassic Cache Creek Terrane in central British Columbia; *Canadian Journal of Earth Sciences*, Volume 38, pages 535-550.

Sano, H. and Kanmera, K. (1988): Paleogeographic reconstruction of accreted oceanic rocks: Akiyoshi, southwest Japan; *Geology*, Volume 16, pages 600-603.

Sano, H. and Struik, L.C. (1997): Field properties of Pennsylvanian-Lower Permian limestones of Cache Creek Group, northwest of Fort St. James, central British Columbia; *in* Current Research, *Geological Survey of Canada*, Paper 1997-A, pages 85-93.

Sano, H. and Rui, L. (2001): Facies interpretation of Middle Carboniferous to Lower Permian Pope succession limestone of Cache Creek Group, Fort St. James, central British Columbia; *Canadian Journal of Earth Sciences*, Volume 38, pages 535-550.

Struik, L.C., Scharizza, P., Orchard, M.J., Cordey, F., Sano, H., MacIntyre, D.G., Lapiere, H. and Tardy, M. (2001): Stratigraphy, structural stacking, and paleoenvironment of the Cache Creek Group, central British Columbia; *Canadian Journal of Earth Sciences*, Volume 38, pages 495-514.

Uchiyama, T., Sano, H. and Kanmera, K. (1986): Depositional and tectonic settings of cherts around the Akiyoshi Limestone Group; *Faculty of Science, Kyushu University*, Memoir, Ser. D, Volume 26, pages 51-68.

Geology of the Eastern Bella Coola Map Area (93 D), West-Central British Columbia[1]

By L.J. Diakow[2], J.B. Mahoney[3], J.W. Haggart[4], G.J. Woodsworth[4], S.M. Gordee[3],
L.D. Snyder[3], T.P. Poulton[5], R.M. Friedman[6] and M. Villeneuve[7]

KEYWORDS: Regional mapping, mineral potential, Bella Coola, Early Cretaceous, Bathonian rocks, Monarch assemblage, Hazelton Group, Stikine Terrane, volcanogenic massive sulphide, Regional Geochemical Survey.

INTRODUCTION

Eastern Bella Coola map area (NTS 093D), in west-central British Columbia, is a rugged part of the Coast Mountains, and includes the topographic divide and transition zone between the Coast and Intermontane morphogeological belts. The principal objectives of the Bella Coola Targeted Geoscience Initiative (TGI) are to assess little known Mesozoic volcanic assemblages in eastern Bella Coola map area for their massive sulphide (VMS) potential, and to improve understanding of the geologic evolution of this part of the central Coast region. A significant component of the TGI program was a bedrock mapping study. It was undertaken during 2001-2002 and covered an area greater than 5000 km^2 between the Dean Channel and South Bentinck Arm on the west and the western boundary of Tweedsmuir Provincial Park on the east (Figure 1). The Geological Survey of Canada and the British Columbia Geological Survey in conjunction with the University of Wisconsin-Eau Claire and the University of British Columbia conducted the Bella Coola program.

This report briefly describes the geology of the eastern Bella Coola map area, which includes regions south of the Bella Coola River (093D/01, 02, 07, 08) and north of the Dean River (093D/15). Geological results from the first season are presented in a series of reports, including Diakow *et al.*, (2002), Hrudey *et al.*, (2002), Israel and Kennedy (2002), Mahoney *et al.*, (2002), Sparks and Struik (2002) and Struik *et al.*, (2002). Nomenclature used in this report, particularly that of the plutonic rocks, supersedes that utilized in those reports.

GENERAL GEOLOGY

The area eastern part of Bella Coola map area marks the transition from the Coast Plutonic Complex into the Intermontane Belt (Figure 1 inset). In general, the geology of the study area is dominated by two, northwest-trending, belts of volcanic and sedimentary rocks representing Jurassic and Cretaceous island arcs, elements of the Stikine tectonostratigraphic terrane of the Intermontane Belt (Figure 1). These rocks are intruded by westerly-increasing volumes of plutonic rocks, some considered comagmatic with Mesozoic arc assemblages and others comprising part of the Coast Plutonic Complex. The Coast Plutonic Complex is cut by the Coast Shear Zone, a major transpressional structure that may have accommodated significant early Tertiary displacement (Andronicos *et al.*, 1999).

Geology in the eastern Bella Coola map area (Figure 2), is dominated by three lithostratigraphic successions, including, from east to west: the Jurassic Hazelton Group (Baer, 1965; Diakow *et al.*, 2002); the Early Cretaceous, informally named, Monarch volcanics (van der Heyden, 1990, 1991; Rusmore *et al.*, 2000; Struik *et al.*, 2002), herein referred to as the Monarch assemblage; and contrasting suites of Late Jurassic(?), Early Cretaceous, and Tertiary plutons (Baer, 1973; Hrudey *et al.*, 2002). Additionally, spatially restricted volcanic rocks of Late Jurassic age may also be present within the region, but have yet to be identified. The plutonic rocks are subdivided into a plutonic suites based on textural and compositional characteristics, crosscutting relations, xenoliths, degree of alteration, and weathering character.

LOWER(?) AND MIDDLE JURASSIC HAZELTON GROUP

The oldest known rocks in the eastern Bella Coola region consist of Lower(?) to Middle Jurassic sedimentary and volcanic rocks which correlate regionally with the youngest part of the Hazelton Group. These rocks expand the known distribution of the Early-Middle Jurassic magmatic arc sequence, exposed extensively to the north in central Stikine terrane, south-southeast from Whitesail Lake map area (93 E) into the northeastern Bella Coola map area. North of the Bella Coola River, exposures of these rocks crop out intermittently east of the broad belt of Lower Cre-

---

[1] *Contribution of the Bella Coola Targeted Geoscience Initiative Project, #000025*

[2] *BC Geological Survey Branch*

[3] *Department of Geology, University of Wisconsin at Eau Claire, Wisconsin*

[4] *Geological Survey of Canada, Vancouver*

[5] *Geological Survey of Canada, Calgary*

[6] *Department of Earth & Ocean Sciences, The University of British Columbia, Vancouver*

[7] *Geological Survey of Canada, Ottawa*

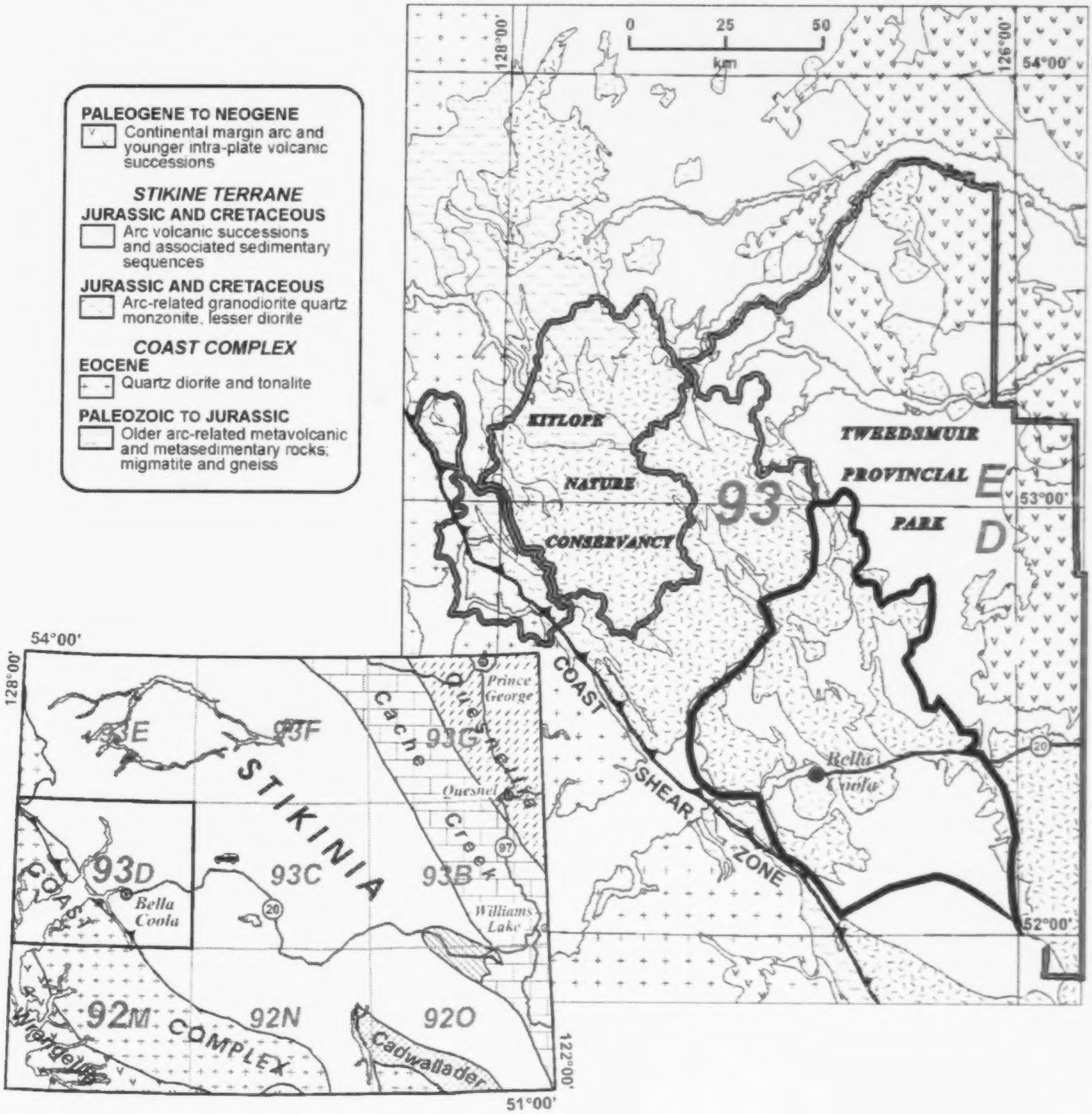
PALEOGENE TO NEOGENE
Continental margin arc and younger intra-plate volcanic successions
STIKINE TERRANE
JURASSIC AND CRETACEOUS
Arc volcanic successions and associated sedimentary sequences
JURASSIC AND CRETACEOUS
Arc-related granodiorite quartz monzonite, lesser diorite
COAST COMPLEX
EOCENE
Quartz diorite and tonalite
PALEOZOIC TO JURASSIC
Older arc-related metavolcanic and metasedimentary rocks; migmatite and gneiss
0
25
50
km
128°00'
126°00'
54°00'
53°00'
52°00'
KITLOPE
NATURE
CONSERVANCY
TWEEDSMUIR
PROVINCIAL
PARK
93
E
D
COAST
SHEAR
ZONE
Bella Coola
20
54°00'
128°00'
93E
93F
STIKINIA
93G
Prince George
Cache Creek
Quesnellia
Quesnel
97
93D
93C
93B
COAST
Bella Coola
20
Williams Lake
92M
92N
92O
COMPLEX
Wrangellia
Cadwallader
122°00'
51°00'

Figure 1. Schematic regional geologic map of Bella Coola (NTS 93D), Whitesail Lake (NTS 93E), and adjoining map areas. The black bordered polygon within eastern 93 D delimits the region mapped in 2001 and 2002. The inset map shows morphogeologic belts and tectonic terranes for west-central Canadian Cordillera.

taceous (Valanginian, in part) volcano-sedimentary rocks, within a northwest-trending corridor coinciding with the western boundary of Tweedsmuir Provincial Park. Also within this corridor, an unconformable contact between Middle Jurassic and a presumed Lower Cretaceous succession, that is not necessarily as old as the Valanginian stratigraphy farther west, is suspected; however, this relationship requires verification from isotopic dating in progress (*see* Upper Lower Cretaceous Volcanic Rocks, herein).

Along the northern margin of the Bella Coola map area, centered on Jumble Mountain, near continuous Jurassic stratigraphy consists of a superbly layered, east-dipping homocline more than 4 kilometres thick. The lower part of this succession is dominated by maroon and green, massively bedded basalt and basaltic andesite flows, intercalated with crudely stratified fragmental rocks. Dacitic to quartz-bearing rhyolitic block and finer tuffs comprise volumetrically significant deposits near Sakumtha Crag and immediately west of East Sakumtha River. Felsic rocks at these localities have been sampled for uranium-lead-zircon geochronometry in order to ascertain the age of deposits which are stratigraphically low in the homocline. We speculate that the lower part of this stratigraphic succession passes well down into the Lower Jurassic, possibly into the Pliensbachian.

Up-section of the mafic to intermediate volcanic sequence that forms the distinctly layered western slopes of Jumble Mountain, is a thick sedimentary succession composed of coarse-grained volcanic lithic arenite, arkosic sandstone and conglomerate. Rhyolitic tuff forms distinctive, light-weathered interbeds. Sedimentary structures within lithic arenites include crude parallel laminae, graded bedding, and rare trough cross-stratification. Minor medium to thickly bedded calcareous sandstone and sandy limestone occur, and are richly fossiliferous locally, yielding a diverse assemblage of gastropods, bivalves, and ammonites. The earliest Aalenian ammonite *Troitsaia westermanni* and the accompanying bivalve assemblage in the middle part of the homoclinal succession, resembles that reported at Troitsa Peak, Whitesail Lake map area (Poulton and Tipper, 1991). Farther east, near Sigutlat Lake, stratigraphically higher sedimentary beds contain Early Bajocian stephanoceratid ammonites and the type specimens of *Myophorella dawsoni* (Whiteaves), characteristic of the Smithers Formation, which is widespread in the Whitesail Lake map area.

YOUNGER MIDDLE JURASSIC VOLCANIC ROCKS

A unique, comparatively young Middle Jurassic (Bathonian and Callovian?) sequence composed of volcanic and volcaniclastic-epiclastic rocks crops out between the Dean and Bella Coola rivers, and is mainly exposed in a small area between Stack Peak, Mount Collins, and Tzeetsaytsul Peak. These rocks are significant for several reasons. Firstly, stratabound massive sulphide lenses of volcanogenic origin are associated with silica-bimodal volcanic rocks of this succession at the Nifty property, hence they are a prospective stratigraphic unit for mineral exploration. Secondly, volcanic rocks of Bathonian age are not known anywhere else in Stikinia. They record an eruptive pulse that may either represent the last "gasp" of the Hazelton magmatic arc, or vestiges of a more extensive, but previously-unrecognized volcanic event marking terminal arc magmatism in Stikinia, prior to widespread basinal sedimentation of the Bowser Lake Group.

The nature of the contact separating Lower Bajocian from Bathonian rocks is unknown in the study area. Aphanitic rhyolitic flows and associated quartz-phyric dikes, and basalt to andesitic volcanic rocks, occupy topographically low-lying terrain east of the headwaters of Noosgulch River. Felsic country rocks near the Nifty VMS prospect dated as part of this project have yielded a U-Pb age similar to that for a previously dated crosscutting dike (164.2+1.2/-0.9 Ma; Ray *et al.*, 1998). Farther north, toward Mount Collins, aphanitic rhyolitic volcanic rocks are succeeded up section by several hundred metres of felsic, volcanic-derived turbidites and volumetrically minor interspersed pyroclastic flows. Welded rhyolites from this sequence yield a U-Pb date on zircons of 164.7±2.0 Ma, indicating rapid aggradation of submarine fan deposits proximal to a contemporaneous subaerial rhyolite volcanic center. Near Mount Collins, more than 500 metres of massive, parallel bedded, dark grey-black siltstone, sandstone and subordinate grit beds represent a deeper water, more distal sedimentary facies. Still farther north, in the vicinity of Stack Peak, thence to the Dean River, laminated black mudstone and siltstone alternating with distinctive white ash-tuff layers and sparse arkosic sandstone interbeds, dominate a moderately deep water, partly turbiditic facies. Belemnoids occur throughout all sedimentary facies, but are particularly abundant in darker, more organic-rich, siltstone beds, which in places are accompanied by sparse limey beds and lenses containing rare bivalves and ammonites. Rare and poorly preserved ammonite fragments from a limestone lens in black siltstone (GSC Loc. C-306159) are not firmly identified, but resemble Middle Bathonian to Middle Callovian *Cadoceras* or *Lilloettia*. This unit resembles the Bowser Lake Group in its probable age and abundance of belemnites. However, the prominence of Bathonian volcanic rocks in the Bella Coola area distinguishes them from exclusively marine and younger, Lower Callovian sedimentary rocks assigned to the Bowser Group in the adjacent Whitesail Lake and Nechako River map areas.

LATE JURASSIC (?) MICRODIORITE-BASALT INTRUSIVE-EXTRUSIVE COMPLEX

A belt of undivided mafic rocks, mapped primarily as microdiorites, is situated in the easternmost part of the study area between Sea Lion Peak and the eastern Dean River area. It is difficult to discern the origin of many of these rocks as either intrusive hypabyssal *versus* an extrusive origin and this relates to their characteristic fine-grained, felted appearance, as well as the absence of significant textural variations or associated bedded rocks.

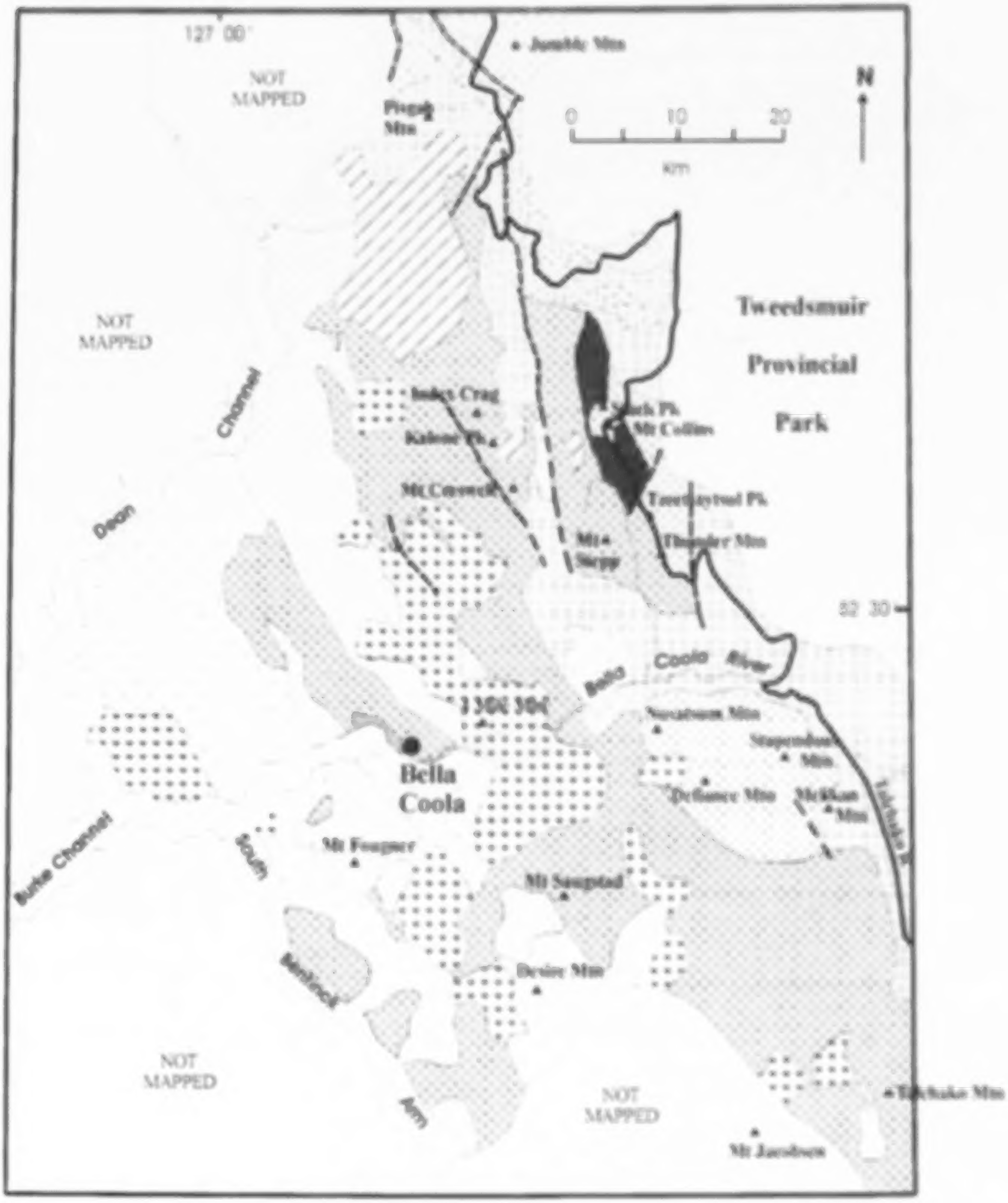

127°00'
NOT MAPPED
Jumble Mtn
Pogg Mtn
0
10
20
km
N
NOT MAPPED
Tweedsmuir
Provincial
Park
Channel
Index Crag
Kalone Pk
Stack Pk
Mt Collins
Mt Cresswell
Tszetlaytsul Pk
Dean
Mt Stepp
Thunder Mtn
52°30'
Bella
Coola
River
Nusatsum Mtn
Stupendous Mtn
Bella
Coola
Defiance Mtn
McKlan Mtn
Burke Channel
South
Mt Fougner
Mt Saugstad
Talchako R.
Bentinck
Desire Mtn
NOT MAPPED
Arm
NOT MAPPED
Talchako Mtn
Mt Jacobsen

Figure 2. Schematic geological map of the eastern portion of the Bella Coola map area bordering Tweedsmuir Provincial Park.

Nooskulla plutonic suite
Four Mile plutonic suite
Fougner plutonic suite
Desire plutonic suite
Monarch assemblage
Stick Pass plutonic suite
Microdiorite
Early(?) Cretaceous volcanic rocks
Middle Jurassic volcanic rocks
Hazelton Group

Legend for Figure 2.

Rock exposures are typically dark green, massive, and most commonly exhibit minute plagioclase laths and anhedral intercrystalline mafic grains. Also included within this unit is medium grained hornblende diorite, cut by a north-south set of basaltic dikes, forming Sakumtha Crag and extending to the northwest across the East Sakumtha River. Similar smaller bodies of medium-grained diorite occur elsewhere in gradational contact with more widespread microdiorite. Near Mount Bernhardt, dikes of white weathered aphanitic felsite and chloritized hornblende-biotite granodiorite trend northwest and cut the microdiorites. The granodiorite dikes closely resemble rocks comprising the Stick Pass plutonic suite.

Immediately north of Sea Lion Peak, a rare, distinctive white quartz porphyritic rhyolite flow dome underlies a thick sequence of basaltic volcanic rocks. About 25 metres of massive rhyolite, containing potassium feldspar megacrysts and abundant phenocrysts of quartz and biotite, are directly overlain by a block-lapilli tuff that contains fragments of the underlying rhyolite. Samples of this quartz-rich rhyolite flow have been collected for isotopic dating to provide a crystallization age for the mafic rocks. A Late Jurassic age is possible for the succession, if crosscutting biotite-hornblende granodiorite dikes are, in fact, part of the Early Cretaceous Stick Pass suite.

EARLY CRETACEOUS STICK PASS PLUTONIC SUITE

Probable Jurassic microdiorite and volcanogenic strata are intruded by a suite of medium grained, equigranular biotite-hornblende granodiorite to diorite, referred to as the Stick Pass suite after exposures on Stick Pass Mountain. The suite appears restricted to the eastern part of the map area between Pogah Mountain north of the Dean River, and Melikan Mountain south of the Bella Coola River. It is characterized by extensively chloritized biotite and hornblende, saussuritized plagioclase, and dark pink interstitial and phenocrystic potassium feldspar. The mineralogy and alteration result in a mottled green and pink coloration. Quartz and epidote veins are common. The suite contains abundant xenoliths of microdiorite, and is cut by abundant basaltic and microdiorite dikes. North of the Bella Coola valley and east of Noosgulch River, a swarm of north-trending microdiorite dikes cutting older granodiorite accounts for up to 70% of exposure. The mafic dikes exhibit chilled margins grading inward to porphyritic or sparsely amygdaloidal textures.

Basal conglomerates of the Lower Cretaceous Monarch assemblage nonconformably overlie rocks of the Stick Pass suite. The suite includes the Firvale pluton of van der Heyden (1991), which yields several U-Pb ages of circa 134 Ma.

LOWER CRETACEOUS MONARCH ASSEMBLAGE

A thick succession of andesitic flows, fragmental rocks, volcaniclastic sandstone, tuffs and argillites occupy a northwest-trending belt between Noosgulch River-Kalone Creek and Christenson Creek-Jump Across Creek (Struik *et al.*, 2002). This succession is herein referred to as the Monarch assemblage. It is dominated by olive green amygdaloidal dacite to basaltic andesite flows and associated breccias and tuff breccias, and contains intercalated argillite, siltstone and volcanic lithic sandstone that form locally continuous stratigraphic sections up to 2.5 kilometres thick. Stratigraphy, within this sequence, is complex, a result of abrupt lateral facies changes complicated by structural deformation. The Monarch assemblage nonconformably overlies several plutons assigned to the Stick Pass suite. Nowhere in the study area are the oldest stratigraphic units of the Monarch assemblage observed resting on Jurassic strata. This may be due, in part, to differential uplift within an intervening belt of Early Cretaceous intrusions that separates older Cretaceous strata in the west from Jurassic rocks in the east, in the region north of the Bella Coola River valley. The erosional base of the Monarch assemblage is exposed in four localities, listed from north to south:

1. South of Stick Pass Mountain. The base of the section here consists of polymict boulder conglomerate nonconformably overlying granodiorite of the Stick Pass suite. The conglomerate contains boulder-sized clasts of altered biotite granodiorite identical to the underlying pluton, and is overlain by a succession of sandy limestone, lapilli tuff, tuff breccia and volcanogenic sandstone and thick amygdaloidal flows.
2. Necleetsconnay headwaters. At this locale, a thick succession of highly cleaved argillite overlies a leucocratic granodiorite that yields a U-Pb date indicating Early Cretaceous intrusion. Numerous basaltic dikes intrude the granodiorite and overlying argillite. The contact is interpreted as a nonconformity that has been subsequently faulted.
3. North of Saloompt Peak. Polymictic plutonic and volcanic conglomerate overlies a quartz diorite pluton yielding several U-Pb zircon dates of circa 154 Ma. Plutonic detritus is identical to the subjacent pluton. The conglomerate passes up-section into thin to medium bedded feldspathic sandstone and argillite, which is in turn overlain by a thick succession of amygdaloidal andesite flows.
4. Eastern flank of Mount Ratcliff. Boulder conglomerate at this locality, just southeast of the map area, nonconformably overlies an altered granodiorite pluton that yielded a U-Pb age of approximately 155 Ma (van der Heyden, pers. comm., 2002), and contains clasts lithologically identical to the subjacent pluton. The conglomerate is locally overlain by basalt to andesite lava flows, breccias and intercalated volcaniclastic rocks. Laminated siltstone and argillite interbeds indicate stratigraphic facing to the west (Israel and Kennedy, 2002). About 5 kilometres farther north of Mount Ratcliff a very thick succession (~3 km) of massive, basalt to andesite lava flows, fragmental rocks and bedded argillite-sandstone-siltstone units presumably occur up section from the basal conglomerate.

Several particularly well-exposed sections of the Monarch assemblage demonstrate its lithological variability. Near Mount Creswell (093D 10) approximately 1000 metres of aphanitic andesite and crystal tuff are interstratified with argillite in its uppermost part. The section lacks fossil control, however it is correlated with fossiliferous rocks of the Monarch assemblage based on lithologic content and structural relationships (Sparks and Struik, 2002). Probably the most extensive continuous section recognized, approximately 2500 metres thick, is found west of Kalone Peak, 8 kilometres northwest of the Mount Creswell section. The lower half of this section consists almost exclusively of fine-grained basaltic andesite lava flows with very rare sedimentary intercalations. In contrast, the upper half includes similar flows, but with substantial amounts of interstratified fine to coarse grained volcanic-lithic sandstone, rich in feldspar. The uppermost 500 metres of this section is composed almost entirely of these sandstones, which show grading, convolute laminations, shale rip-up clasts, flame structures, and fossilized wood and plant fragments. The sandstones likely represent proximal facies in a fan delta system adjacent to an active arc. Black argillite beds up to 15 metres thick are interstratified with sandstones in the upper part of the section west of Kalone Peak. At least 10 distinct argillite units were identified interstratified with the sandstones at the top of this section. The stratigraphically highest argillite is succeeded by approximately 100 metres of amygdaloidal pillow basalt.

The Monarch assemblage mapped in the Bella Coola region is interpreted to be Valanginian (Early Cretaceous) in age, in part based on sparse ammonite collections made from several localities in 2001 (Struik *et al.*, 2002). One argillite bed near the top of the section west of Kalone Peak, studied in 2002, also yielded Valanginian fossils. These biostratigraphic data are the only firm age control at present for the Monarch assemblage, which is widespread in the Bella Coola area. Correlative strata, albeit slightly younger Lower Cretaceous beds, extend southward into Rivers Inlet map area (92M; Rusmore *et al.*, 2000), and farther east into Waddington map area. Lower Cretaceous volcanic rocks have also been mapped to the north in adjoining Whitesail Lake map area (Woodsworth, 1980; van der Heyden, 1989).

UPPER LOWER CRETACEOUS(?) VOLCANIC ROCKS

Bathonian strata are unconformably overlain by a massive volcanic sequence dominated by basaltic lava flows, associated primary and reworked autoclastic breccias. Basaltic flows are dark green to purplish, locally amygdaloidal, and include aphanitic as well as medium-grained, plagioclase-phyric varieties. Rounded to irregular amygdules are filled with quartz and chlorite. Rhyolitic tuffs and lesser flows occupy widely separated intervals tens of metres thick within the mafic sequence. This succession forms the distinctive crudely layered, precipitous topography at Stack Peak, Mount Collins, and the Tzeetsaytsul-Thunder massif and, south of the Bella Coola valley, the rugged mountains of Nusatsum, Defiance and Stupendous. It is estimated to be in excess of 1500 metres thick south of the Bella Coola River valley, thinning gradually northward to its apparent terminus immediately south of the Dean River valley.

The unconformity with underlying probable Bathonian strata is marked by either volcanic boulder conglomerate, such as those superbly exposed in the headwall of a southeast-facing cirque at Mount Collins, or a sequence of pyroxene-bearing sandstone and grits containing quartz and mudstone particles found nearby to the south-southwest. The conglomerate is composed of oxidized reddish basaltic clasts that are characterized by a 'crowded porphyritic' texture imparted by 1-3 mm plagioclase and subordinate pyroxene grains. Conglomerate is monomictic and clast supported, composed of well rounded clasts as large as 2 metres in diameter. Locally, volcanic sandstones, siltstones and red mudstones within the conglomerate comprise variegated red-green, parallel-bedded intervals up to

50 metres thick. These fine clastic rocks commonly contain angular pyroxene and plagioclase grains, presumably derived locally from contemporaneous mafic-intermediate lava flows.

On the north flank of Tzeetsaytsul Peak, the basaltic sequence rests on monomictic volcanic boulder conglomerate, which in turn unconformably overlies a dacite flow dome. A Middle Jurassic U-Pb zircon date of 171.0±2.5 Ma from the dome provides a maximum age for the basaltic sequence. A U-Pb date on zircons from welded rhyolite collected high in the basaltic succession exposed at Tzeetsaytsul Peak has provided an inconclusive minimum age of 113 Ma. The implication of this provisional date is that the thick, mafic volcanic sequence may represent a younger, discrete eruptive episode of the Monarch assemblage, possibly as young as Aptian. Alternatively, this succession could conceivably be Middle to Late Jurassic, part of little known and poorly exposed Bathonian stratigraphy documented during this program, or correlative perhaps with the Upper Jurassic (Oxfordian) Hotnarko volcanics recognized by van der Heyden (1991) in Anahim Lake map area (NTS 93C). Distinctive volcanic conglomerates marking the bottom of the mafic lava sections at Tzeetsaytsul Peak and Mount Collins, also crop out along a ridge trending north of Mount Stopp, where they also contain thin, discontinuous interbeds of rhyolitic tuffs and quartz-phyric flows. Quartz rhyolite lava flows from this section have been sampled for U-Pb zircon geochronometry.

EARLY CRETACEOUS DESIRE PLUTONIC SUITE

Metavolcanic rocks interpreted as part of the Monarch assemblage are intruded in several localities by a heterogeneous diorite to granodiorite intrusive complex referred to as the Desire suite. The suite is extensively exposed south and east of Desire Mountain and west of Clayton Falls Creek, from Howe Lake to the southern end of the map area. It is texturally and compositionally diverse, ranging from a fine to medium-grained hornblende diorite-quartz diorite to a medium to coarse-grained biotite-hornblende granodiorite. The suite is characterized by numerous metavolcanic pendants, and xenoliths of mafic, commonly amphibolitic composition. A weak to pronounced foliation is widespread. Internal crosscutting relationships within the suite are complex, with metavolcanic screens intruded by hornblende diorite, which is cut by hornblende-quartz diorite that in turn is cut by hornblende granodiorite to tonalite dikes, and themselves cut by quartz-porphyritic felsic dikes.

Rocks assigned to the Desire suite yield a U-Pb age of 110±2 Ma (Gehrels and Boghossian, 2000).

MID- TO LATE CRETACEOUS FOUGNER PLUTONIC SUITE

The Fougner suite is a distinctive, homogeneous hornblende-biotite tonalite to granodiorite that is widely exposed in the western part of the map area, west of Thorsen Creek and the Necleetsconnay River. The suite is named for excellent exposures on Mount Fougner, at the head of Clayton Falls Creek. The Fougner suite is characterized by medium to coarse-grained, equigranular hornblende-biotite tonalite to granodiorite that contains minor (1-2%), yet conspicuous, honey brown sphene. Stretched dioritic xenoliths with a medium-grained equigranular texture are widespread. Massive exposures display prominent exfoliation joint sets.

Sub-vertical, high-strain shear zones locally cut and deform plutons of the Fougner suite. Apparent flattening within the shear zones is moderate to intense, as observed by locally abundant protomylonite and mylonite. Shear fabric is defined by very attenuated mafic enclaves and fractured, elongate to rotated plagioclase and flattened to smeared biotite and quartz. Shear fabric within tonalite is commonly gradational along shear zone margins into the undeformed pluton. Tonalite dikes assigned to the Fougner suite also cut the shear zones and, the Mount Fougner pluton clearly plugs a major high-angle shear zone near Clayton Falls Creek. The Fougner suite is thus believed to be syn- to post-kinematic with respect to development of these shear zones.

The age of the Fougner suite is presently unconstrained. Quartz diorite along the south side of the Bella Coola estuary, dated at 110±2 (Gehrels and Boghossian, 2000), was considered to be part of the Fougner suite by Hrudey *et al.* (2002); however, the character and field relationships demonstrate that this pluton belongs to the Desire suite. The Fougner suite intrudes the Desire suite, requiring it to be younger than 110 Ma. Moreover, the Fougner suite is cut by the Four Mile suite, dated at 73 Ma. The syn- to post-kinematic nature of the Fougner suite suggests a mid- to Late Cretaceous age.

LATE CRETACEOUS TO EOCENE FOUR MILE PLUTONIC SUITE

Coarse-grained, muscovite-biotite granite forming spectacular exfoliated exposures on both sides of the Bella Coola Valley is assigned to the Four Mile suite, named after Four Mile Mountain (Hrudey *et al.*, 2002). The Four Mile suite extends to the north and south of the Bella Coola valley, underlying large areas between Mount Creswell and Big Snow Mountain. These plutons are characterized by parallel, steeply dipping joints that lend a sheeted, exfoliated appearance.

The suite consists of homogeneous, coarse-grained, equigranular biotite granite to granodiorite, containing large, fresh books of biotite up to 7 mm in diameter. Muscovite is diagnostic, and comprises up to 5 volume percent. Rare scattered maroon to red, semi-opaque garnet (0.5-1.5 mm) is also diagnostic, but a minor component. The suite is locally inequigranular, containing potassium feldspar phenocrysts. Aplite dikes with pegmatitic segregations containing garnet, muscovite and tourmaline are associated with the suite.

[illegible]

[illegible]

[illegible]

[illegible]

STRUCTURE

[illegible]

[illegible]

[illegible]

[illegible]

[illegible]

MINERAL EXPLORATION TARGETS

[illegible]

[illegible]

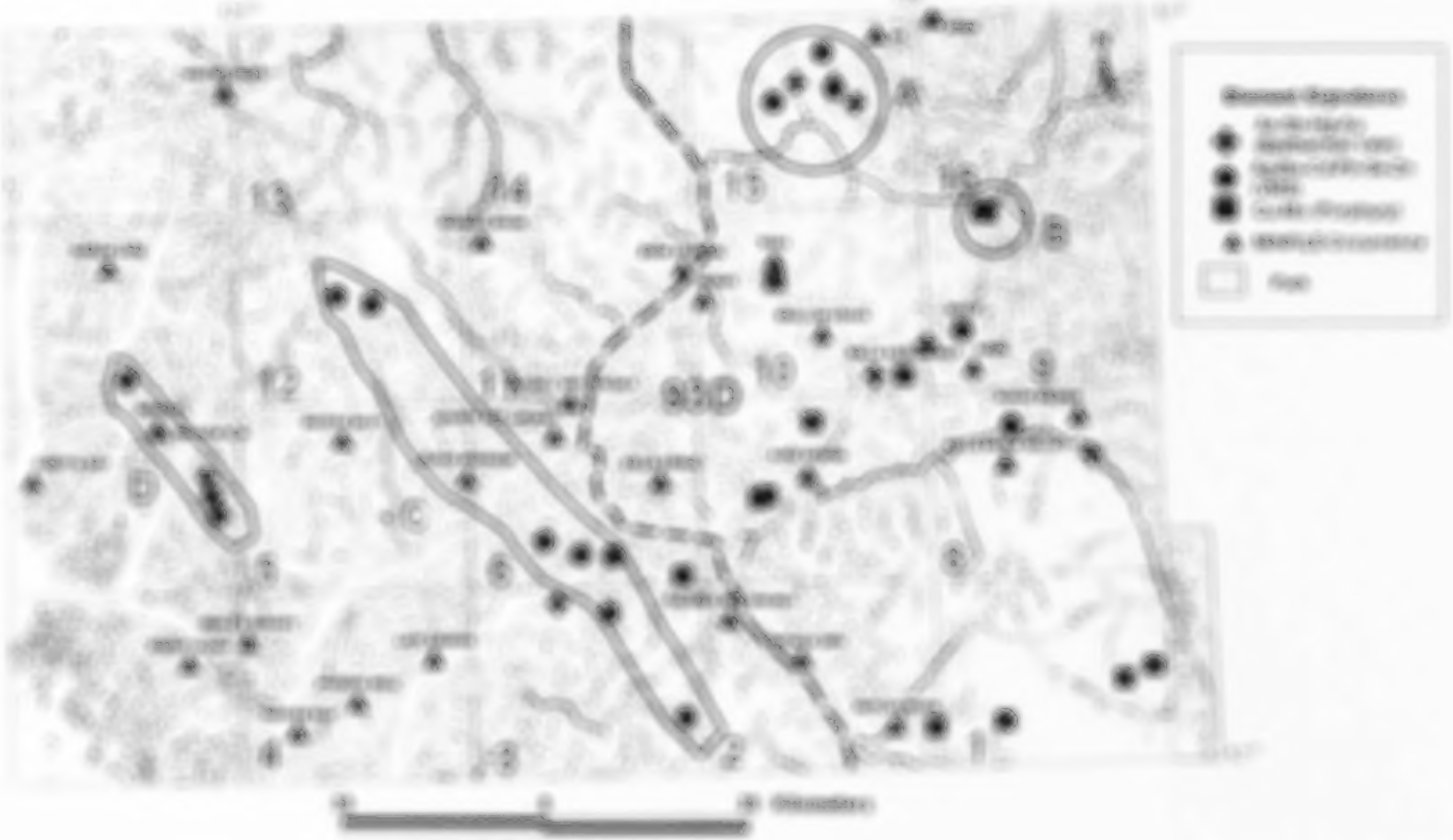
A
B
16
15
14
13
12
11
10
9
8
7
6
5
4
3
2
1
93D
C
D

[illegible]

procedure ranking geochemical anomalies according to groupings of elements commonly associated with epithermal vein, massive sulphide and porphyry mineralization (Lett and Friske, this volume), highlights several areas that warrant follow-up work (Figure 7).

North of the Dean River, in map sheet 93D/15 (A in Figure 7), a number of drainages contain anomalous epithermal vein or VMS signatures. In general within this area, near Pygah Mountain, intrusive rocks tentatively assigned to the Early Cretaceous Stick Pass suite crop out above treeline. The anomalies, however, are presumably associated with volcanic rocks that may be exposed on vegetated slopes at lower elevations within the various watersheds. The most northerly of the anomalous VMS sites at location A, situated 11 kilometres due west of Sakumtha Crag, is positioned within a drainage containing a large gossan. Although rocks at this locality were not mapped, immediately to the south of Sakumtha Crag, a succession of rhyolite breccias intermixed with reworked pyroclastic debris and mafic flows, believed to be part of the Jurassic Hazelton Group, may be extrapolated to the west into this gossanous zone.

The majority of prospects documented in the MINFILE database in the eastern Bella Coola region are copper-molybdenum prospects associated with various granitoids. They appear to be related to mainly Early Cretaceous and lower Eocene biotite-hornblende bearing granodiorite and tonalite stocks. At locality B in Figure 7, two high-ranking copper-molybdenum anomalies occur in parallel drainages sourced in granodiorite that is assigned to the Stick Pass suite and cut by an en echelon north-south set of diabase dikes.

West of the Dean Channel, outside of the area mapped during the Bella Coola TGI program, a series of RGS anomalies with a pronounced VMS signature define two parallel belts (areas C and D in Figure 7). These anomalies correspond with tracts of undivided metasedimentary and metavolcanic rocks, informally named the Burke Channel assemblage (Rusmore *et al.*, 2000). Regionally, these metamorphic rocks may be equivalent to those that host numerous Kuroko-type VMS occurrences in the Ecstall Belt (Alldrick, 2001), located about 300 kilometres to the northwest.

CONCLUSIONS

Geologic and geochronologic relationships obtained through regional mapping conducted during the Bella Coola TGI provides an improved geologic framework for the eastern Bella Coola region that aids mineral exploration and broader-based geoscience. Some important results from the program include:

- The best known stratiform massive sulphide-barite mineralization in the region is associated with a previously unknown and poorly exposed Middle Jurassic (Bathonian) bimodal volcanic sequence. Regionally, these rocks are thought to represent a brief subaerial to submarine eruptive event that marks the end of Hazelton island arc construction in Stikinia.
- Lower Cretaceous volcanic rocks informally named the Monarch assemblage and comagmatic plutonic suites occupy a northwest trending belt in the east-central Bella Coola region. The layered rocks consist of marine clastic rocks interlayered with mafic to intermediate and subordinate felsic volcanic rocks which are interpreted as units of island arc volcanoes that formed along the western fringe of Stikinia during Valanginian to possibly Aptian time.
- Multi-element geochemical anomalies, with a massive sulphide signature, cluster in volcanic rocks tentatively assigned to the Monarch assemblage north of the Dean River. Many of the copper showings in the region are spatially associated with diorite to granodiorite plutons assigned to either Early Cretaceous or Eocene suites. Porphyry-style mineralization in the region lacks the broad colored gossans and alteration associated with large mineralized systems.
- Structural events in the region include Early Cretaceous uplift that resulted in widespread erosion and deposition of conglomerates at the base of the Monarch assemblage. Substantial east-west crustal extension, manifest as north trending swarms of diabase dikes and potentially related eruption of significant volumes of mafic lava flows may record the latest magmatic pulse of the Monarch assemblage. A contractional event imparts northeast vergent folds and thrust faults in Lower Cretaceous strata in the western part of the study area. An episode of high-strain strike-slip shearing overprints the folded rocks within a series of parallel, northwest-trending zones. Plutons that show variable degrees of strain or truncate deformed rocks broadly bracket the timing of ductile deformation between 123 and 73 Ma.

ACKNOWLEDGMENTS

We thank Luke Beranek, Nicky Hastings, Ben Paulson, Chantal Saunders, Chantal Venturi and Sarah White for their superb field assistance. Discussions and unpublished geochronology data provided by Peter van der Heyden have benefited the program. Richard Lapointe and Rob Skelley of West Coast Helicopters, and Danny Hodson of Rainbow West Helicopters gave expert helicopter support. Brian Grant and Steve Gordey provided helpful reviews of the manuscript.

REFERENCES

Alldrick, D.J. (2001): Geology and mineral deposits of the Ecstall greenstone belt, northwest British Columbia (NTS 103H/14W); *in* Geological Fieldwork 2000, *BC Ministry of Energy and Mines*, Paper 2001-1, p. 279-305.

Andronicos, C., Hollister, L.S., Davidson, C. and Chardon, D. (1999): Kinematics and tectonic significance of transpressive structures within the Coast Plutonic Complex, British Columbia; *Journal of Structural Geology*, v. 21, p. 229-243.

Baer, A.J. (1965): Bella Coola (93 D) map-area, British Columbia; *in* Report of Activities, Field 1964, *Geological Survey of Canada*, Paper 65-1, p. 39-42.

Baer, A.J. (1973): Bella Coola-Laredo Sound map-areas, British Columbia; *Geological Survey of Canada*, Memoir 372, 122 p.

Diakow, L.J., Mahoney, J.B., Gleeson, T.G., Hrudey, M.G., Struik, L.C. and Johnson, A.D. (2002): Middle Jurassic stratigraphy hosting volcanogenic massive sulphide mineralization in eastern Bella Coola map area (NTS 093 D), southwest British Columbia; *in* Geological Fieldwork 2001, *British Columbia Ministry of Energy and Mines*, Paper 2002-1, p 119-134.

Gehrels, G.E. and Boghossian, N.D. (2000): Reconnaissance geology and U-Pb geochronology of the west flank of the Coast Mountains between Bella Coola and Prince Rupert, coastal British Columbia; *in* Tectonics of the Coast Mountains, southeastern Alaska and British Columbia, H.H. Stowell and W.C. McClelland editors, *Geological Society of America*, Special Paper 343, p 61-75.

Hrudey, M.G., Struik, L.C., Diakow, L.J., Mahoney, J.B., Woodsworth, G.J., Sparks, H.A., Kaiser, E.A. and Gleeson, T.P. (2002): Plutonic rocks of the eastern Bella Coola map area, southwest British Columbia; *in* Current Research 2002-A09, *Geological Survey of Canada*, 10 p.

Israel, S.A and Kennedy, L.A. (2002): Reconnaissance of structural geology of the Atnarko Complex, southern Tweedsmuir Park, British Columbia; *in* Current Research 2002-A12, *Geological Survey of Canada*, 9 p.

Israel, S.A. and Kennedy, L.A. (2003): Geology of the Atnarko metamorphic complex, south Tweedsmuir Park, west-central British Columbia; *in* Current Research 2003, *Geological Survey of Canada*.

Lett, R. and Fiske, P. (2003): National Geochemical Reconnaissance Surveys in the B.C. Cordillera can Encourage Mineral Exploration; *in* Geological Fieldwork 2002, *British Columbia Ministry of Energy and Mines*, Paper 2003-1, this volume.

Lett, R., Jackaman, W. and Fiske, P.W.B. (2002): Regional stream sediment and water data, Bella Coola, British Columbia (NTS 93C, 93D, 103A); British Columbia Regional Geochemical Survey 56 or Geological Survey of Canada Open File 4414.

Mahoney, J.B., Struik, L.C., Diakow, L.J., Hrudey, M.G., and Woodsworth, G.J. (2002): Structural geology of eastern Bella Coola map area, southwest British Columbia; *in* Current Research 2002-A10, *Geological Survey of Canada*, 9 p.

Poulton, T.P. and Tipper, H.W. (1991): Aalenian ammonites and strata of western Canada; *Geological Survey of Canada*, Bulletin 411, 71p.

Ray, G.E., Brown, J.A., Friedman, R.M., and Cornelius, S.B. (1998): Geology of the Nifty Zn-Pb-Ba prospect, Bella Coola District, British Columbia; *in* Geological Fieldwork 1997, *British Columbia Ministry of Energy and Mines*, Paper 1998-1, p 20-1 to 20-28.

Rusmore, M.E. and Woodsworth, G.J. (1994): Evolution of the eastern Waddington thrust belt and its relation to the mid-Cretaceous Coast Mountains arc, western British Columbia; *Tectonics*, v 13, p 1052-1067.

Rusmore, M.E., Woodsworth, G.J., and Gehrels, G.E. (2000): Late Cretaceous evolution of the eastern Coast Mountains, Bella Coola, British Columbia; *in* Tectonics of the Coast Mountains, southeastern Alaska and British Columbia, H.H. Stowell and W.C. McClelland editors, *Geological Society of America*, Special Paper 343, p 89-106.

Rusmore, M.E., Gehrels, G. and Woodsworth, G.J. (2001): Southern continuation of the Coast shear zone and Paleocene strain partitioning in British Columbia–southeast Alaska; *Geological Society of America Bulletin*, v 113, p 961-975.

Sparks, H.A. and Struik, L.C. (2002): Stratigraphy of the Early Cretaceous Monarch sequence at Mount Creswell in east-central Bella Coola map area, west-central British Columbia; *in* Current Research 2002-E1, *Geological Survey of Canada*, 11 p.

Struik, L.C., Mahoney, J.B., Hrudey, M.G., Diakow, L.J., Woodsworth, G.J., Haggart, J.W., Poulton, T.P., Sparks, H.A. and Kaiser, E.A. (2002): Early Cretaceous stratigraphy and tectonics of eastern Bella Coola map area, southwest British Columbia; *in* Current Research 2002-A8, *Geological Survey of Canada*, 10 p.

van der Heyden (1989): U-Pb and K-Ar geochronometry of the Coast Plutonic Complex, 53°N to 54°N, British Columbia, Ph.D. thesis, *University of British Columbia*, Vancouver, 392 p.

van der Heyden, P. (1990): Eastern margin of the Coast Belt in west-central British Columbia; *in* Current Research, Part E, *Geological Survey of Canada*, Paper 90-1E, p 171-182.

van der Heyden, P. (1991): Preliminary U-Pb dates and field observations from the eastern Coast Belt near 52°N, British Columbia; *in* Current Research, Part A, *Geological Survey of Canada*, Paper 91-1A, p 79-84.

Woodsworth, G.J. (1980): Geology of Whitesail Lake (93E) map area, British Columbia; *Geological Survey of Canada*, Open File 708, 1:250 000 scale.

Barkerville Terrane, Cariboo Lake to Wells: A New Look at Stratigraphy, Structure and Regional Correlations of the Snowshoe Group

By Paul Schiarizza and Filippo Ferri

KEYWORDS: Barkerville Terrane, Snowshoe Group, Downey succession, Bralco limestone, Hardscrabble Mountain succession, Harveys Ridge succession, Agnes conglomerate, Goose Peak succession, Kootenay Terrane, nappe, gold, besshi.

INTRODUCTION

The area underlain by the Barkerville Terrane has an important exploration and mining history dating from the discovery of placer gold on Keithley Creek in 1860. Placer gold production peaked in the 1860s, but continues at a modest scale to the present time. Lode gold production came mainly from the Wells mining camp, located near some of the richest placer streams in the district, between 1933 and 1987. The more recent discoveries of the Ace and Frank Creek occurrences near Cariboo Lake has attracted attention to the massive sulphide potential of the Barkerville Terrane, whereas the discovery of high-grade gold mineralization within the Bonanza Ledge zone in March 2000 rejuvenated interest in the lode-gold potential of the Wells mining camp.

The BC Geological Survey Branch conducted regional mapping programs near Cariboo Lake in 2000 and 2001 (Figure 1), directed mainly at examining the stratigraphic and structural setting of massive sulphide mineralization within the Snowshoe Group of Barkerville Terrane (Ferri, 2001; Ferri and O'Brien, 2002). This work led to a revised interpretation of the Snowshoe Group stratigraphy that had previously been established by Struik (1988). The purpose of the 2002 Barkerville bedrock mapping project, reported on here, was to evaluate this revised stratigraphic interpretation farther north, with the aim of providing a better framework for evaluating the potential of individual units within the Snowshoe Group to host precious or base metal mineralization. This mapping project is a P3 partnership with International Wayside Gold Mines Limited, who are conducting a major exploration program for gold mineralization in the Wells-Barkerville area.

The 2002 mapping program was carried out from July 9 to September 7. An area of about 600 km^2, including portions of NTS sheets 93A/13 and 14 and 93H/3 and 4, was covered, but much of this was at reconnaissance scale (Figure 1). More detailed coverage was obtained in a relatively small area (100 km^2) extending from Jack of Clubs Lake southeastward to Grouse Creek. This area encompasses the Barkerville gold belt of Hanson (1935), and provided insights into correlations between the detailed stratigraphy that Hanson established within this belt and the regional stratigraphy of the Snowshoe Group. Furthermore, this area provides juxtaposition of three units within the Snowshoe Group (Harveys Ridge, Downey and Hardscrabble Mountain) whose mutual relationships are critical and contradictory in the stratigraphic schemes of Struik (1988) *versus* Ferri and O'Brien (2002).

The 2002 map area is located near the north end of the Quesnel Highlands, an area of moderate relief bounded by the Interior Plateau to the west and the rugged Cariboo Mountains to the east. Fieldwork was conducted from a base in the town of Wells, located along Highway 26 about 75 kilometres east of Quesnel. Forest Service, logging and mining roads, as well as historic mining trails and modern snowmobile and ski trails, provide good access to much of the eastern part of the map area. Access to the northern part of the area is from logging and mining roads along Lightning and Peters creeks, which extend southward from Highway 26 west of Wells. The Swift River Forest Service Road branches southward from Highway 26 about 25 kilometres east of Quesnel, and provides access to the western part of the area via major logging road networks that extend up Fontaine Creek and the Little Swift and Swift rivers.

REGIONAL GEOLOGIC SETTING

Barkerville Terrane is represented mainly by the Snowshoe Group, a package of predominantly siliciclastic rocks with local intercalations of carbonate and metavolcanic rocks. It was defined by Struik (1986, 1988) who correlated it with the Kootenay Terrane of southern British Columbia. These Hadrynian and Paleozoic rocks display some similarities to strata of the North American miogeocline, but differ in the presence of Paleozoic grit, volcanic and intrusive rocks, and local indications of Paleozoic deformation and metamorphism, not evident in age-equivalent rocks to the east. They are generally interpreted as an outboard facies of the North American continental margin (*eg.* Struik, 1987; Colpron and Price, 1995).

Barkerville Terrane is contacted to the east by a succession of Hadrynian through late Paleozoic clastic sedimentary rocks and carbonate represented mainly by the Kaza, Cariboo and Black Stuart groups. These rocks are assigned to the Cariboo Terrane (Figure 1; Struik, 1986). They are at

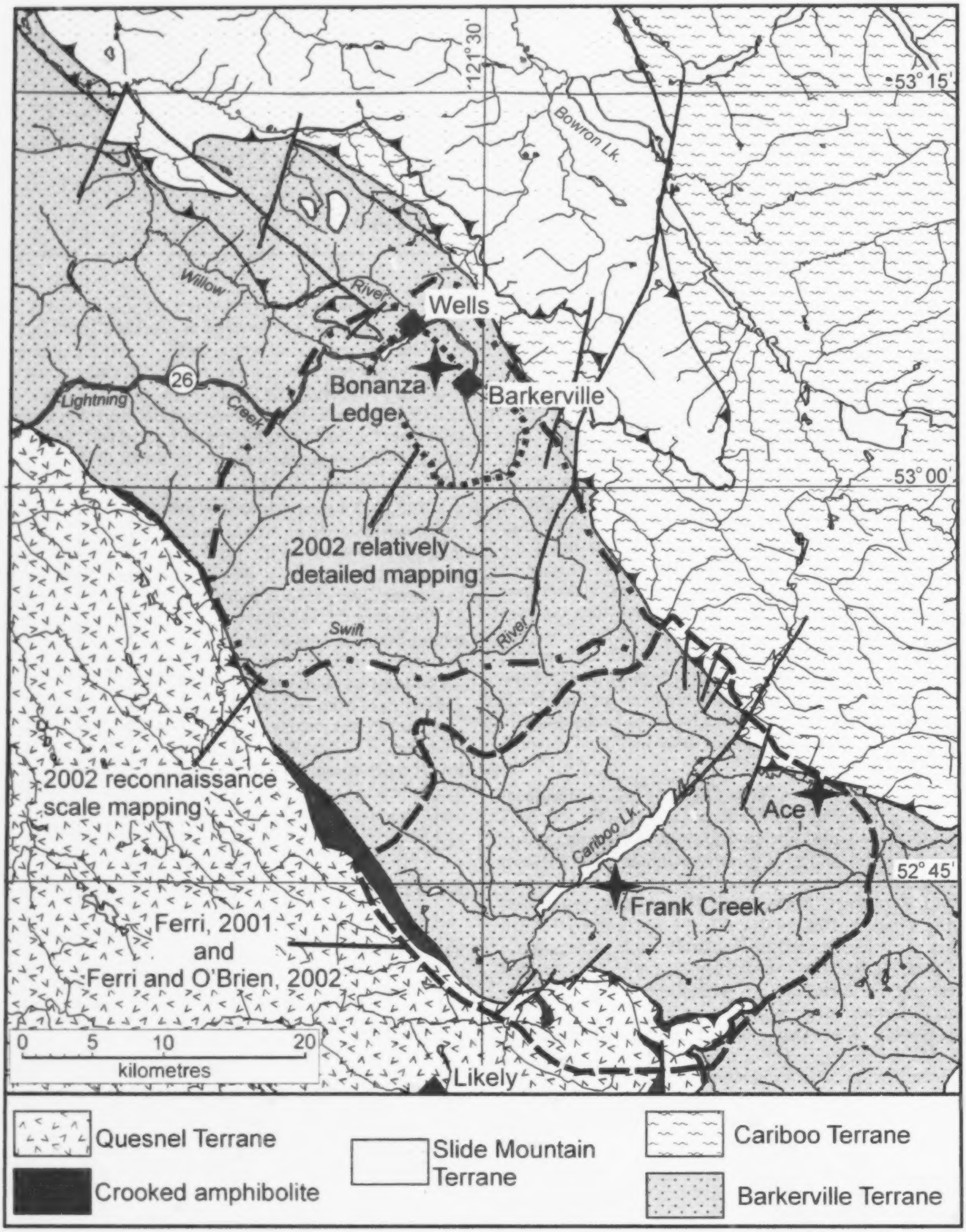
121°30'
53° 15'
Bowron Lk.
Willow
River
Wells
Bonanza
Ledge
Barkerville
26
Lightning
Creek
53° 00'
2002 relatively
detailed mapping
Swift
River
2002 reconnaissance
scale mapping
Cariboo Lk.
Ace
52° 45'
Frank Creek
Ferri, 2001
and
Ferri and O'Brien, 2002
0
5
10
20
kilometres
Likely
Quesnel Terrane
Crooked amphibolite
Slide Mountain
Terrane
Cariboo Terrane
Barkerville Terrane

Figure 1. Simplified terrane map of the Cariboo Lake - Wells area, showing areas mapped by the B.C. Geological Survey Branch in 2000 through 2002.

least partially age-equivalent to rocks of the adjacent Barkerville Terrane, but contain facies that suggest a more proximal continental shelf setting. The two terranes are separated by the east-dipping Pleasant Valley thrust fault (Struik, 1986).

East of Wells, the Cariboo Terrane is structurally overlain by oceanic rocks of the Slide Mountain Terrane, represented by Lower Mississippian to Lower Permian basalt and chert of the Antler Formation. The Antler Formation is internally thrust-imbricated (Struik and Orchard, 1985), and is separated from the underlying Cariboo Terrane by the gently-dipping, presumably east-directed Pundata thrust fault. The age of the Pundata thrust is not well constrained, but thrust-imbrication and emplacement of the Slide Mountain Terrane elsewhere in the region has been interpreted to be a Permo-Triassic event (Schiarizza, 1989; Ferri, 1997). To the northwest of Wells, the western boundary of the Antler allochthon also overlaps the eastern edge of Barkerville Terrane (Figure 1). This relationship can be interpreted to reflect fault juxtaposition of Barkerville and Cariboo terranes prior to emplacement of the Antler allochthon (Struik, 1986, 1988). However, a similar geometry could result from early emplacement of the Antler allochthon above Cariboo Terrane, followed by west-directed thrusting of Cariboo above Barkerville Terrane, provided the Pleasant Valley thrust cut up-section in its hangingwall through the Pundata thrust and into the Antler Formation.

The Barkerville Terrane is bounded to the west by the Quesnel Terrane, represented mainly by Middle Triassic to Lower Jurassic arc-derived sedimentary, volcanic and intrusive rocks (Struik, 1988; Panteleyev *et al.*, 1996). The contact is the predominantly west-dipping Eureka thrust fault. Slivers of ultramafic rock, gabbro, amphibolite and ocean-floor basalt that occur along this thrust fault are assigned to the Crooked amphibolite unit; these rocks have been correlated with the Slide Mountain Terrane and inferred to represent part of the basement to the Quesnel volcanic arc (Rees, 1987; Struik, 1988).

Studies along the western edge of the Barkerville Terrane document Early to Middle Jurassic east-directed thrusting of Quesnel Terrane above Barkerville Terrane along the Eureka thrust fault, followed by southwest-vergent folding of the terrane boundary (Ross *et al.*, 1985; Brown *et al.*, 1986; Rees, 1987). This deformation was accompanied by amphibolite to greenschist facies metamorphism. The metamorphic peak was attained prior to (Fillipone and Ross, 1990) or during (Rees, 1987) the southwest-directed folding, and is dated as Middle Jurassic on the basis of a 174±4 Ma U-Pb age on metamorphic sphene from near Quesnel Lake (Mortensen *et al.*, 1987). Similar southwest-vergent, synmetamorphic folds are prominent structural features thoughout much of Barkerville, Kootenay and western Cariboo terranes (Raeside and Simony, 1983; Schiarizza and Preto, 1987; Murphy, 1987; Struik, 1988; Ferri and O'Brien, 2002), and are constrained or interpreted to be of late Early to Middle Jurassic age (Murphy *et al.*, 1995; Colpron *et al.*, 1996). Younger folds within Barkerville Terrane are upright to northeast or southwest-vergent, and mainly late to post-metamorphic (Rees, 1987; Struik, 1988; Ferri and O'Brien, 2002). However, studies within and adjacent to the southern Cariboo Mountains, near the Barkerville/Cariboo terrane boundary, indicate that structures which postdate the major southwest-vergent folding there are associated with a younger metamorphic event of Early Cretaceous age. (Currie, 1988; Digel *et al.*, 1998; P.S. Simony, personal communication, 2002).

Among the youngest structures in the region are orogen-parallel dextral strike-slip faults and related folds that are documented within the Cariboo Mountains east of Barkerville Terrane (Reid *et al.*, 2002). These structures are thought to be Late Cretaceous to Eocene in age, and thus coeval with other major dextral strike-slip fault systems in the Canadian Cordillera (Struik, 1983; Umhoefer and Schiarizza, 1996).

HISTORY OF NOMENCLATURE

The first major study of bedrock geology in the region was by Bowman (1889) who assigned rocks presently included in Barkerville terrane to the Cariboo schists. Johnston and Uglow (1926) mapped the Barkerville area and subdivided the Cariboo Series into several formations. Hanson (1935) mapped the area between Island Mountain and Grouse Creek, referred to as the Barkerville gold belt for its numerous lode-gold occurrences, in more detail. This belt is underlain mainly by Johnston and Uglow's Richfield Formation, which Hansen subdivided into the Baker, Rainbow, B.C., Lowhee and Basal members; these names are still widely used in the Wells mining camp. Lang (1938) mapped farther to the south and presented a different subdivision of the Richfield Formation as well as several new formation names. Holland (1954) mapped the Yanks Peak and Rountop Mountain areas, changed Cariboo Series to Cariboo Group and introduced new formation names that completely revised the stratigraphy of the group. This revised stratigraphy included the Snowshoe Formation, named for the Snowshoe plateau of the Quesnel Highlands, as the upper formation of the group. Sutherland Brown (1957) extended Holland's Cariboo Group terminology northward to Wells, completely replacing the terminology of Johnston and Uglow (1926) and Hanson (1935), and then eastward, far into the Cariboo Mountains (Sutherland Brown, 1963).

The Cariboo Group of Holland (1954) and Sutherland Brown (1957, 1963) encompassed rocks of both the Cariboo Mountains and Quesnel Highlands. Campbell *et al.* (1973) suggested that some formations assigned to the group in the Quesnel Highlands might not be equivalent to formations with the same name in the Cariboo Mountains. They also suggested that the Snowshoe Formation, interpreted as the uppermost formation of the Cariboo Group in the Quesnel Highlands, might actually be equivalent to the Kaza Group, which underlies the Cariboo Group in the central Cariboo Mountains. These questions were addressed in subsequent regional mapping programs undertaken by L.C. Struik of the Geological Survey of Canada. Struik (1986, 1987, 1988) concluded that the Quesnel Highlands stratigraphy was indeed different from that in the Cariboo Mountains. He retained the term Cariboo Group, as well as most of the original formational names (excluding Snowshoe Formation) for the stratigraphic succession of the Cariboo Mountains, and coined the term Cariboo Terrane for the larger package of rocks, or facies belt, that contains the group. Struik assigned most of the Quesnel Highlands succession to the Snowshoe Group, and introduced the name Barkerville Terrane for the facies belt that includes the group.

LITHOLOGIC UNITS

SNOWSHOE GROUP

Overview

Struik (1988) assigned most rocks of the Barkerville Terrane to the Snowshoe Group. He subdivided the Snowshoe Group into 14 informal units, allowing that some of the units might be lateral equivalents. Struik considered the lower part of the group to be Hadrynian and higher stratigraphic units to be Paleozoic, possibly extending into the upper Paleozoic. His distribution of stratigraphic units defined a general younging from southwest to northeast across the Barkerville Terrane.

Ferri (2001) and Ferri and O'Brien (2002) proposed major revisions to Struik's stratigraphic interpretation based on their mapping of the Snowshoe Group near Cariboo Lake (Figure 1). They suggested that the Ramos succession along Keithley Creek was actually part of the Keithley succession and, most importantly, that these Keithley plus Ramos rocks correlated with the Downey succession, which formed much of the eastern edge of the Barkerville Terrane. They also suggested that the Harveys Ridge and Hardscrabble Mountain successions were correlative. These correlations reduced that number of stratigraphic units within the Snowshoe Group by about 50 percent (Figure 2), and implied major stratigraphic repetitions across the Snowshoe belt.

Observations made during the 2002 field season were generally consistent with the revised stratigraphic interpretation of Ferri and O'Brien (2002). Specifically, rocks mapped as Harveys Ridge succession east of Cariboo Lake (Struik, 1988; Ferri and O'Brien, 2002) were traced northwestward to the Barkerville area, where they interfinger with rocks of the Hardscrabble Mountain succession. The Harveys Ridge and Hardscrabble Mountain successions therefore appear to be part of the same stratigraphic unit, and relationships in both the southern (Ferri and O'Brien, 2002) and northern (Struik, 1988; this study) parts of this belt indicate that this unit rests structurally beneath the Downey succession to the east across an overturned stratigraphic contact. Further corroboration comes from the western part of the study area, where the northwestern extension of the belt mapped as as Keithley and Ramos by Struik (1988), but correlated with the Downey succession by Ferri and O'Brien (2002), was found to comprise rocks that are lithologically identical to those of the Downey succession.

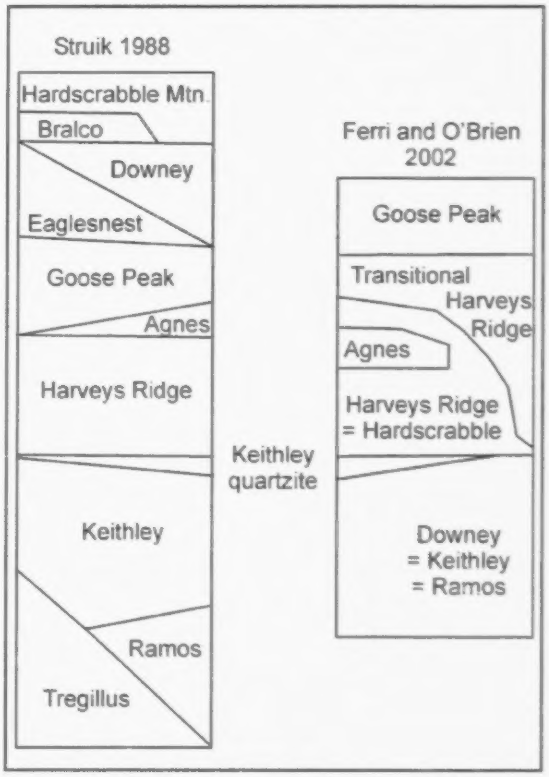

Figure 2. Stratigraphic charts comparing the Snowshoe Group stratigraphy defined by Struik(1988) and the revised interpretation suggested by Ferri and O'Brien (2002).

The stratigraphy of the Snowshoe Group in the Cariboo Lake – Wells area, as interpreted in this study, is summarized in Figure 3, and the generalized distribution of map units within the group is shown in Figure 4. Correlation of the Downey succession with the Keithley and Ramos successions requires a major structural repetition across the area, which we attribute to a large southwest-vergent nappe that has subsequently been folded across the upright Lightning Creek antiform. The axial trace of this late antiform separates the area into a northeast domain of mainly northeast-dipping strata and a southwest domain of mainly southwest-dipping strata (Figure 5). Individual map units within the Snowshoe Group are discussed in the following sections.

DOWNEY SUCCESSION AND CORRELATIVE ROCKS

Rocks assigned here to the Downey succession crop out in two belts on opposite sides of the Lightning Creek antiform (Figure 4). Both belts are flanked by younger rocks on either side, and are therefore inferred to core isoclinal anticlines; in the interpretation preferred here these are different parts of the same anticline folded across the

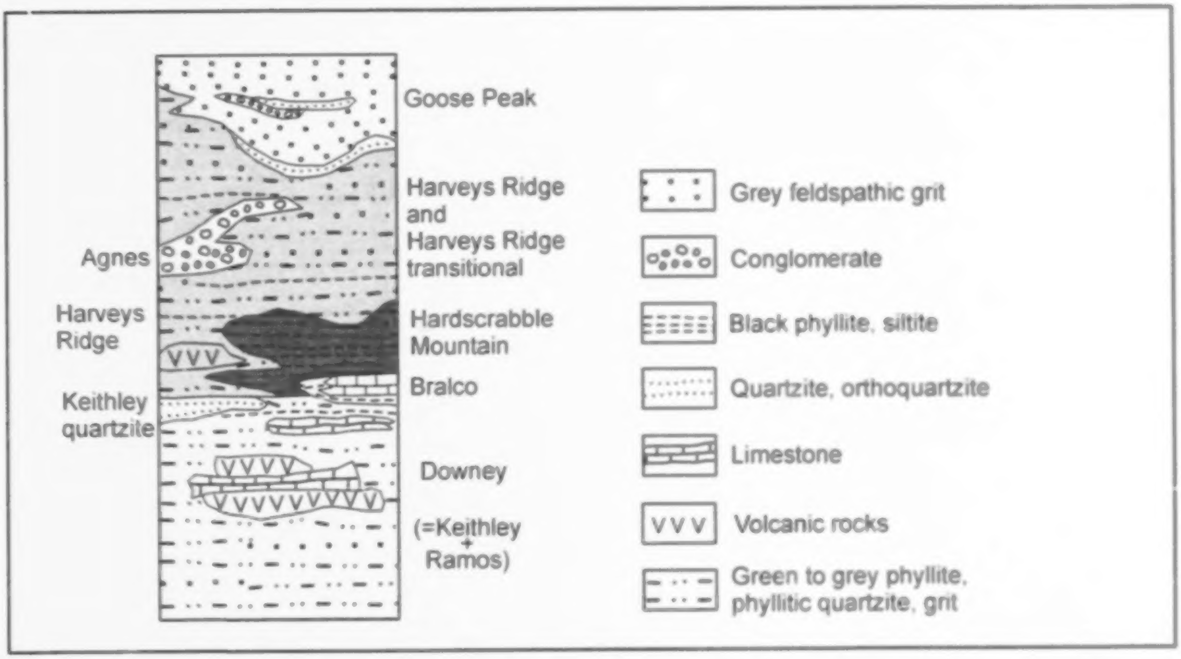

Figure 3. Generalized stratigraphic column summarizing the stratigraphy of the Snowshoe Group in the Cariboo Lake – Wells area, as interpreted in this study.

Lightning Creek antiform (Figure 5). The eastern belt, extending from the east end of Cariboo Lake to Wells, comprises the Downey succession as defined and mapped by Struik (1988). The southern end of the western belt includes rocks assigned to the Keithley and Ramos successions by Struik (1988), which were remapped and tentatively correlated with the Downey succession by Ferri and O'Brien (2002). The northern part of the western belt includes rocks assigned to the Keithley succession and undifferentiated Snowshoe Group by Struik (1988). These rocks were examined during the 2002 field season and are included in the Downey succession on the basis of their lithologic similarity to the eastern belt of Downey rocks. Higher grade metasedimentary and metavolcanic rocks that occur above the Keithley thrust, west of Keithley Creek, are also assigned to the Downey succession following Ferri and O'Brien (2002).

The Downey succession is in part characterized by mafic metavolcanic rocks and limestone that are not common within other parts of the Snowshoe Group. However, the unit is dominated by phyllites, siltites, phyllitic quartzites and phyllitic grits that resemble rocks in many other units of the group. The most common lithology is pale to medium green to grey-green phyllite and silty phyllite that typically displays a distinct silvery sheen on cleavage surfaces. Coarser grained phyllitic quartzite and grit are also common. These may occur as distinct thin to thick beds intercalated with phyllite, or as intervals many tens of metres thick in which bedding is not easily discerned. These coarser rocks, like the associated phyllites, are commonly green to grey-green in colour. In places, however, and particularly near the top of the succession, they are light to medium grey and associated with medium grey to black phyllite, in which case they are not distinct from quartzites and grits found in the Harveys Ridge transitional or Goose Peak successions. Relict detrital grains in the quartzites and grits are mainly clear, grey or blue quartz, but may include up to several percent feldspar.

Massive, mainly light grey quartzite to orthoquartzite forms the top of the Downey succession (formerly Keithley succession) in the vicinity of Yanks Peak, and along strike to the northwest, on the north side of the Swift River. This quartzite is referred to as the Keithley quartzite by Struik (1988). Similar relatively pure quartzite forms the top of the Downey succession in exposures east of Cariboo Lake, forming part of the rationale for correlating the Downey and Keithley successions (Ferri, 2001; Ferri and O'Brien, 2002).

Light to medium grey, commonly orange, brown or dark-grey weathered limestone is a subordinate but distinctive component of the Downey succession. In the eastern belt good exposures are found near Cunningham Creek, along lower Lowhee Creek and on the lower slopes west of Cow Mountain. Ferri and O'Brien (2002) identified limestone within the western belt, in rocks previously mapped as Ramos succession along upper Keithley Creek, and limestone was encountered farther to the north, along the Swift River, during our 2002 mapping program. The limestone within the Downey succession forms massive to well-bedded units ranging from a few metres up to many

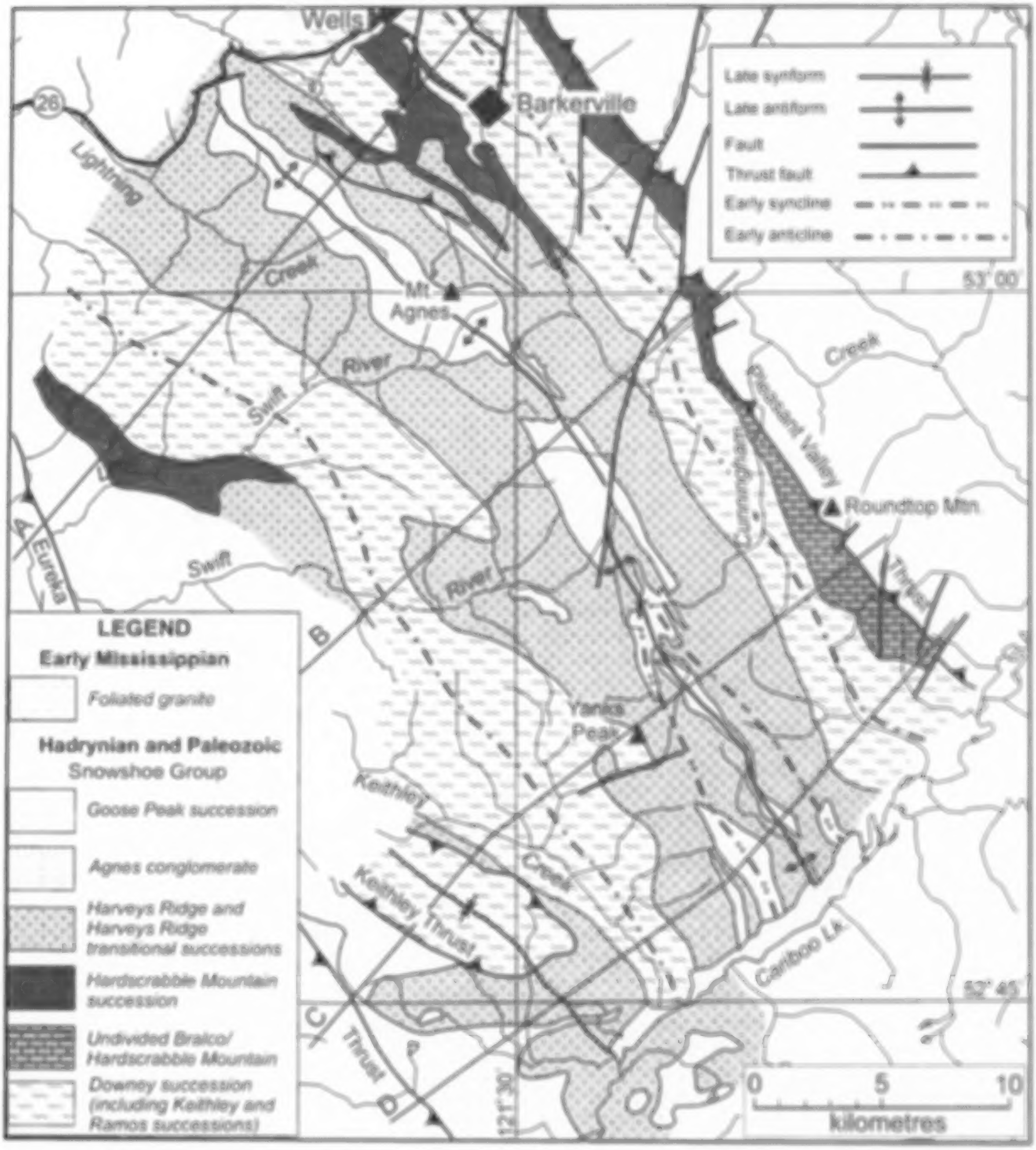
Wells
Barkerville
26
Lightning
Creek
Mt Agnes
Swift
River
Eureka
Swift
River
Creek
Pleasant Valley
Cunningham
Roundtop Mtn
Thrust
Yanks Peak
Keithley
Creek
Keithley Thrust
Cariboo Lk.
Thrust
A
B
C
D
53° 00'
52° 45'
121° 30'
0
5
10
kilometres
Late synform
Late antiform
Fault
Thrust fault
Early syncline
Early anticline
LEGEND
Early Mississippian
Foliated granite
Hadrynian and Paleozoic
Snowshoe Group
Goose Peak succession
Agnes conglomerate
Harveys Ridge and Harveys Ridge transitional successions
Hardscrabble Mountain succession
Undivided Bralco/ Hardscrabble Mountain
Downey succession (including Keithley and Ramos successions)

Figure 4. Generalized geology of the Cariboo Lake - Wells area, based on the work of L.C. Struik (1984, 1988), Ferri and O'Brien (2002) and this study.

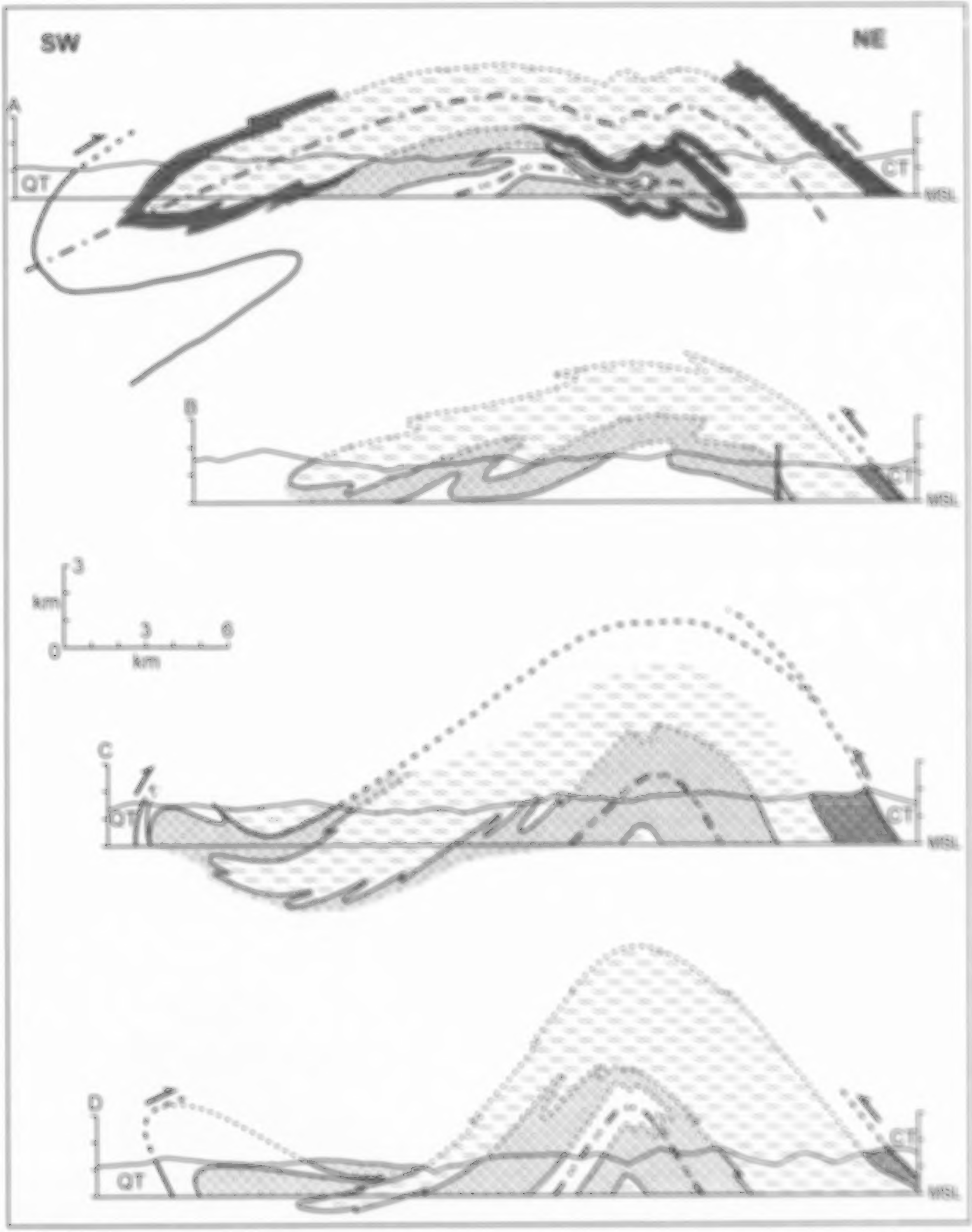
SW
NE
A
QT
CT
MSL
B
CT
MSL
3
km
0
3
6
km
C
QT
CT
MSL
D
QT
CT
MSL

Figure 5. Schematic vertical cross sections illustrating the main structural features of the Snowshoe Group, as interpreted in this study. Cross section lines and legend are shown in Figure 4. Sections C and D are from Ferri and O'Brien (2003). CT = Cariboo Terrane; QT = Quesnel Terrane.

tens of metres thick. These limestone units are in part intercalated with clastic rocks typical of the Downey succession, although immediately adjacent phyllites and quartzites are in many places distinctly calcareous. Commonly, however, limestone occurs in sections that include abundant chloritic phyllite of probable volcanic or volcaniclastic origin.

The thickest section of mafic volcanic and volcaniclastic rocks known within the Downey succession occurs in the Mount Barker area, east of Cariboo Lake and south of the present study area. There, Ferri (2001) describes chloritic schists and bedded mafic tuffs, intercalated with limestone, phyllite and quartzite, that are the dominant lithology over a stratigraphic interval of several hundred metres near the structural base (stratigraphic top) of the Downey succession. Ferri and O'Brien (2002) traced this interval northwestward across the Cariboo River to Simlock Creek, where it is represented by less than 100 metres of chlorite schist structurally overlain by interbedded limestone and phyllite. Still farther along strike to the northwest, along Cunningham Creek, chloritic phyllite occurs as several narrow units, each less than ten metres thick, intercalated with quartzite, phyllite and limestone over a stratigraphic interval that may be several hundred metres thick. Chloritic phyllite was noted at a number of widely scattered localities elsewhere within both eastern and western Downey belts but, with the exception of a thick mafic package included in the Downey succession above the Keithley thrust (Ferri and O'Brien, 2002), does not appear to constitute a major proportion of the succession. Furthermore, although a mafic igneous origin is reasonably inferred, most exposures do not display relict textures that demonstrate a volcanic or volcaniclastic origin; it is possible that a significant proportion are derived from intrusive rocks associated with younger foliated dioritic bodies that are common within the Downey succession (described in a later section).

Struik (1988) considered the Downey succession to be Paleozoic. Fossils collected from limestone tentatively included in the Downey succession north of Wells indicate a Paleozoic, probably Late Cambrian or younger, age. However, the fossils were collected from a fault panel along the Pleasant Valley thrust fault that is not in continuity with the main belt of Downey rocks. This panel is only tentatively assigned to the Downey succession (Struik, 1988), and therefore the fossils may not provide a valid age constraint for the unit.

HARDSCRABBLE MOUNTAIN SUCCESSION

The Hardscrabble Mountain succession consists almost entirely of black siltite and phyllite that is here considered to be a fine-grained facies within the Harveys Ridge succession (Figure 5). It is best exposed in the Wells - Barkerville area, where it flanks the Downey succession to both the northeast and southwest (Figure 6). Most of these rocks were also mapped as Hardscrabble Mountain succession by Struik (1988), although he included part of the southwestern belt in the Harveys Ridge succession. The Hardscrabble Mountain succession is also mapped as a belt that crosses the Little Swift River along the western boundary of the map area. These rocks are structurally above the Downey succession on the southwest flank of the western Downey belt. They were mapped mainly as Harveys Ridge succession by Struik (1988).

Bedding-cleavage relationships, fold asymmetry and sedimentary tops indicators in both Downey and Hardscrabble Mountain successions west of Barkerville and Wells, where the Downey is structurally above the Hardscrabble Mountain, indicate that this contact is overturned and the Hardscrabble Mountain succession is stratigraphically above the Downey succession (Benedict, 1945; Alldrick, 1983; Struik, 1988; this study). South and west of Barkerville, both along and across strike, the fine-grained rocks of the Hardscrabble Mountain succession interfinger with, and eventually become a subordinate facies within, a succession dominated by medium to dark grey quartzites and gritty quartzites assigned to the Harveys Ridge succession (Figure 6). The Hardscrabble Mountain succession has a greater strike length on the northeast flank of the Downey succession, but there its stratigraphic top is not seen because it is structurally overlain by the Pleasant Valley thrust.

The most common lithology within the Hardscrabble Mountain succession is dark grey to black siltite that occurs as thin to locally medium beds separated by partings or thin films of black phyllite. The siltite commonly contains thin bedding-parallel laminae of white quartz. In places black siltite is intercalated with planar to wavy laminae or very thin beds of light to medium grey siltite to very fine-grained quartzite. Elsewhere, the unit consists mainly of well-foliated black phyllite.

BRALCO LIMESTONE

A prominent limestone unit that occurs stratigraphically above the Downey succession along the western edge of the Barkerville Terrane between Cunningham Creek and the north arm of Quesnel Lake is referred to as the Bralco limestone by Struik (1988). At the north end of this belt the Bralco is repeated several times across northeast-dipping thrust faults and associated folds (Struik, 1988) and is structurally interleaved with black phyllite, and locally pale green phyllite and phyllitic quartzite. These associated rocks are assigned to the Hardscrabble Mountain succession by (Struik, 1988), although some rocks in the western part of the belt may be upper Downey. This area was only examined briefly during the present study, and is designated as undivided Bralco-Hardscrabble on Figure 6.

Struik (1988) reports that a specimen of Bralco limestone from this belt, west of Roundtop Mountain, contains echinoderm fragments, suggesting a Paleozoic age. This is the only fossil control known within the entire Cariboo Lake - Wells study area.

HARVEYS RIDGE SUCCESSION

Struik (1988) defined the Harveys Ridge succession to consist mainly of black and dark grey siltite, quartzite and phyllite. He showed that it occurred stratigraphically above the Keithley and Ramos successions, and was in turn overlain by a variety of units, including the Goose Peak, Eaglesnest and Downey successions. Ferri (2001) showed that the Downey succession is overturned where it occurs structurally above the Harveys Ridge succession east of Cariboo Lake, suggesting that the Downey is actually stratigraphically beneath the Harveys Ridge and equivalent to the Keithley and Ramos successions. Ferri (2001) also introduced the term "Harveys Ridge transitional" for thick sections in which typical Harveys Ridge rocks are interbedded with feldspathic grits and quartzites similar to those of the overlying Goose Peak succession.

Here we use Harveys Ridge in an expanded sense that includes both the Harveys Ridge and Harveys Ridge transitional units of Ferri (2001). This succession dominates an extensive belt, flanked on both sides by older rocks of the Downey succession, which extends from Cariboo Lake to Highway 26. The Harveys Ridge succession is also mapped on the west side of the western Downey belt in the vicinity of Cariboo Lake. The rocks mapped as Harveys Ridge on Figure 3 include both the Harveys Ridge succession of Struik (1988), and extensive belts of rock mapped by Struik as undifferentiated Snowshoe Group. Struik noted that most of these undifferentiated rocks belonged to the Harveys Ridge through Eaglesnest part of the Snowshoe Group stratigraphy, in accord with the interpretation presented here.

The Harveys Ridge succession, as mapped here, consists mainly of medium to dark grey, locally black or light grey, quartzite and grit intercalated with variable proportions of dark grey to black siltite and phyllite. The siltite and phyllite are lithologically identical to those of the Hardscrabble Mountain succession, and mapping at a more detailed scale than that of Figure 3 could likewise present some of the more extensive occurrences as separate mappable units. The base of the succession corresponds to a change from predominantly light coloured rocks of the Downey, mainly in shades of green to grey green, to grey rocks that invariably include significant dark grey to black varieties. Commonly the contact is marked by a thin unit of black quartzite that forms the base of the Harveys Ridge succession. The upper contact is harder to define as light and medium grey grits and quartzites, together with dark to black grey siltite and phyllite, are commonly interbedded over substantial intervals. Thus the base of the overlying Goose Peak succession is somewhat arbitrarily defined, but is placed where light grey grit and quartzite predominate over darker varieties, and interbedded phyllite and siltite are only a minor component of the succession.

Although clastic rocks predominate, the Harveys Ridge succession locally includes carbonate and volcanic rocks. Dark grey limestone is apparently widespread, but forms local thin units that make up a very small proportion of the succession. Mafic to intermediate volcanic and volcaniclastic rocks locally form substantial thicknesses, but seem to be common only around Cariboo Lake. These volcanic rocks are described by Ferri (2001) and Ferri and O'Brien (2002).

AGNES CONGLOMERATE

Relatively thin units of quartzite-clast conglomerate within the Snowshoe Group were mapped as Agnes conglomerate by Struik (1988), who considered them a lateral equivalent of the Goose Peak succession. The conglomerate units around Cariboo Lake were also mapped by Ferri (2001) and Ferri and O'Brien (2002) who thought they were internally within the Harveys Ridge succession. Conglomerate units encountered during the 2002 mapping program were mainly within the Harveys Ridge succession, but similar conglomerate occurs locally in rocks we assign to the Goose Peak succession.

Most of the mappable units of Agnes conglomerate shown on Figure 3 are after Struik (1988) and Ferri and O'Brien (2002). The one north of Mount Agnes was encountered during our 2002 mapping. It comprises more than 50 metres of section that is about 50 percent pebble conglomerate, as beds or lenses ranging from a few tens of centimetres to almost 10 metres thick. The conglomerate beds are intercalated with intervals of mainly dark grey phyllite, siltite and sandy phyllite. The flattened clasts are mainly light to dark grey, fine grained quartzite, but also include pink quartzite and medium to dark grey siltite, as well as minor phyllite and vein quartz. The conglomerate matrix varies from phyllitic to sandy, and in some beds changes from one to the other along strike.

GOOSE PEAK SUCCESSION

Struik (1988) assigned predominantly coarse grained feldspathic quartzite and grit that crops out discontinuously along or near the trace of the Lightning Creek antiform between Cariboo Lake and Mount Agnes to the Goose Peak succession. Northwest of Mount Agnes he mapped a more continuous unit of quartzite, phyllite and grit, which he assigned to the Eaglesnest succession, in the core of the antiform. Struik thought that both the Goose Peak and Eaglesnest successions were stratigraphically above the Harveys Ridge succession, and that in the small area of overlap near Mount Agnes the Eaglesnest was above the Goose Peak.

Traverses across Struik's (1988) Eaglesnest succession between Mount Agnes and Highway 26 suggest that parts of the succession, including dark grey to greenish grey phyllite and siltite with intercalations of light to dark grey phyllitic quartzite and grit, should be included within the Harveys Ridge (transitional) unit. The remaining part is dominated by thin to thick-bedded light grey phyllitic quartzite and feldspathic grit, commonly with thin partings or interbeds of medium to dark grey phyllite and siltite. Also within this succession are units of relatively pure, light grey quartzite, and local lenses of conglomerate comprising flattened light grey quartzite clasts within a matrix of dark grey phyllite. This part of Struik's (1988) Eaglesnest succession, as well as similar rocks mapped at the headwaters of the Swift River to the south, are here correlated with the Goose Peak succession (Figure 3). They, together with Goose Peak exposures mapped farther southwest at the head of Cunningham Creek by Struik (1988), form a discontinuous belt that follows the trace of the Light-

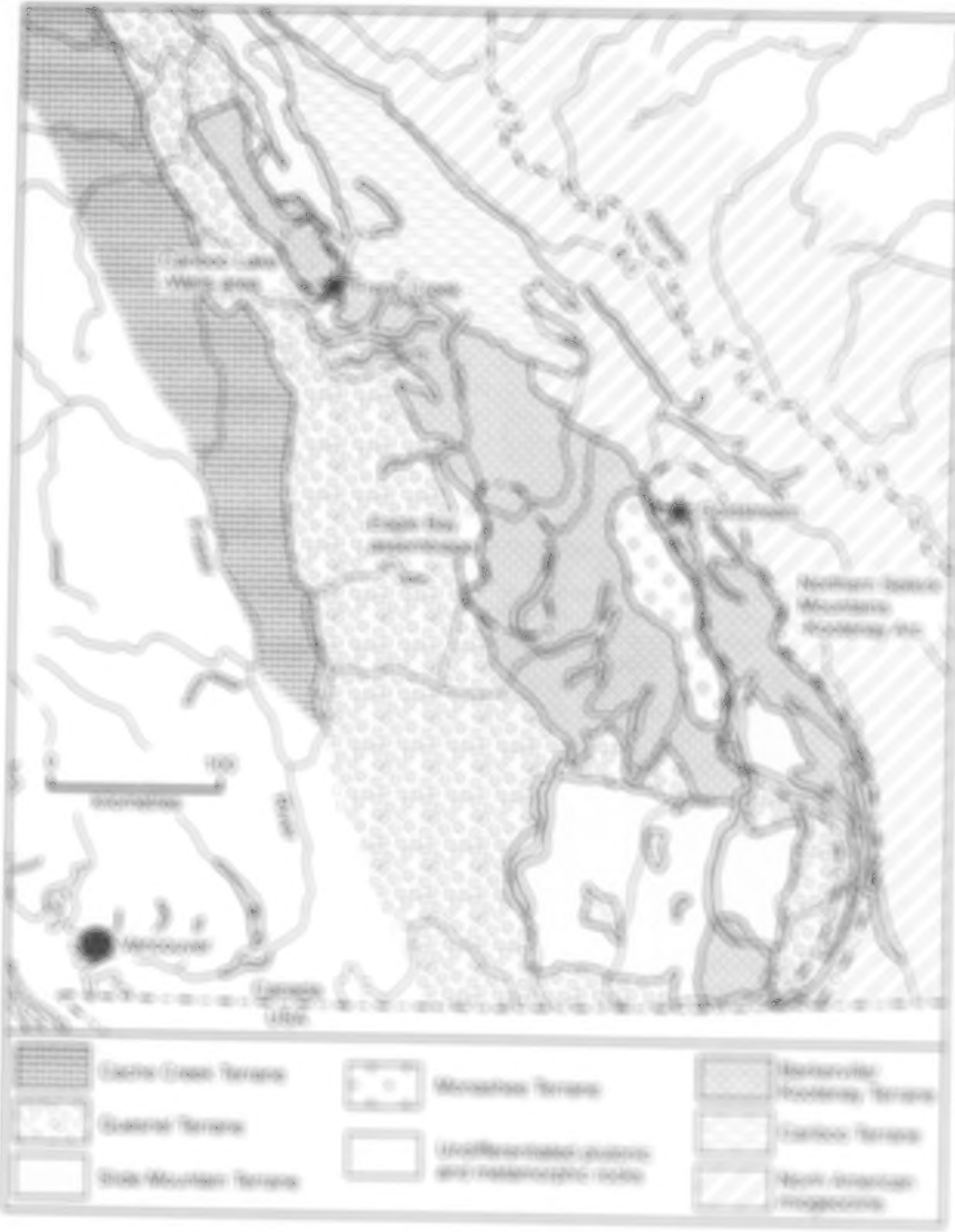
Cariboo Lake
Wells area
Frank Creek
Eagle Bay
assemblage
Goldstream
Northern Selkirk
Mountains
Kootenay Arc
0
100
kilometres
Vancouver
Canada
USA
Cache Creek Terrane
Quesnel Terrane
Slide Mountain Terrane
[illegible] Terrane
Undifferentiated plutonic
and metamorphic rocks
Barkerville/
Kootenay Terrane
Cariboo Terrane
North American
Miogeocline

Figure 4. Terrane map of southern British Columbia [illegible] the stratigraphic sections correlated in Figure 7.

[illegible]

[illegible]

REGIONAL CORRELATIONS

[illegible]

[illegible]

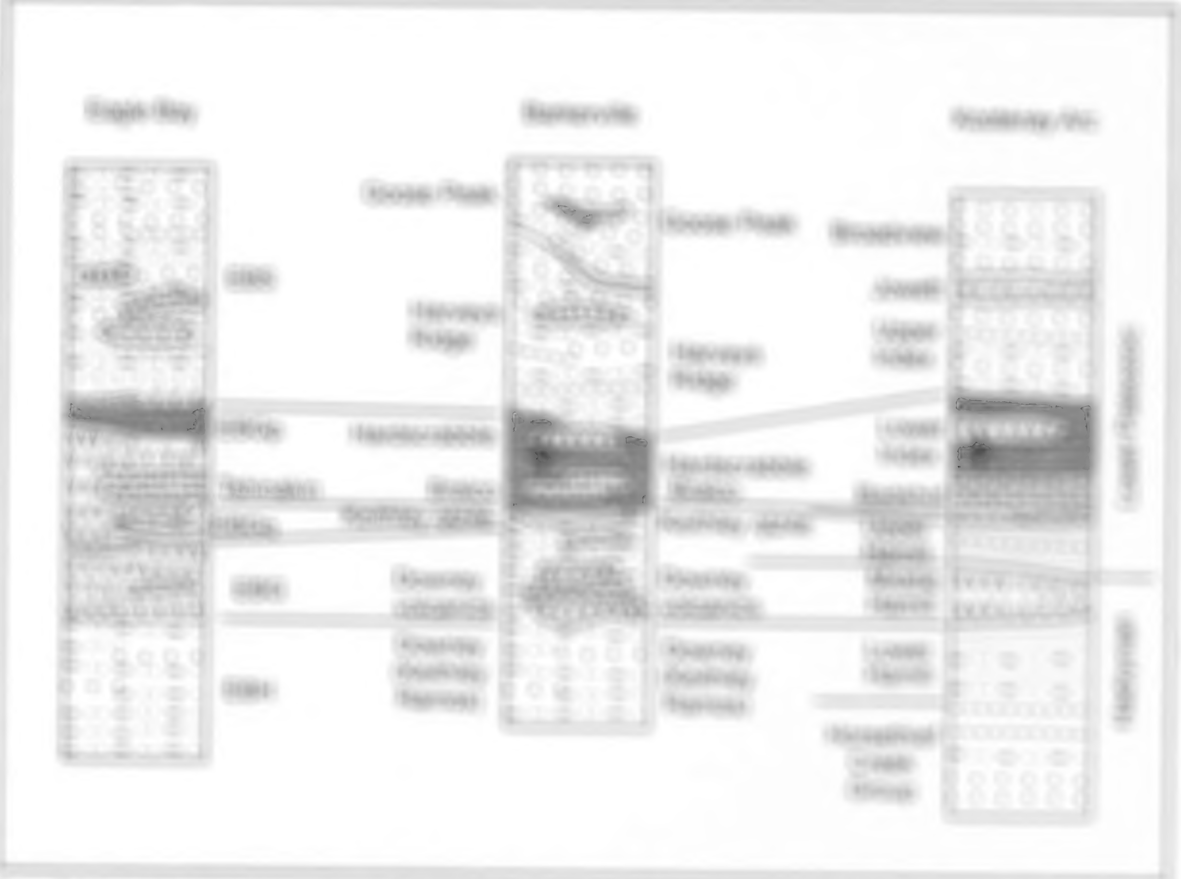

Goose Pond
Goose Pond
Harvey Ridge
Harvey Ridge
Upper
Lower

[illegible]

found in the Downey succession, but the middle Hamill does include a substantial mafic volcanic component that may correlate with the volcanic rocks of the Downey (Devlin, 1989). The Hamill volcanics have yielded a latest Hadrynian U-Pb zircon date of 569.6±5.3 Ma (Colpron *et al.*, 2002). The clean quartzite at the top of the Hamill is overlain by the archaeocyathid-bearing Badshot limestone, which we correlate with the Brilco limestone. The Badshot is in turn overlain by the Index Formation of the Lardeau Group, the lower unit of which comprises black phyllite that is readily correlated with the Hardscrabble Mountain succession and correlative facies within the Harveys Ridge succession. This correlation is enhanced by the presence of mafic volcanic rocks within the lower Index that may correlate with the Harveys Ridge volcanics. In the northern Selkirk Mountains, black phyllite of the lower Index Formation is overlain by quartzite, phyllite, grit and minor carbonate of the upper Index, mafic volcanic rocks of the Jowett Formation, and an upper grit-dominated package assigned to the Broadview Formation (Figure 7). The Jowett Formation is not apparently represented in the Snowshoe Group, but the upper Index and Broadview formations are reasonably correlated with the Harveys Ridge transitional and Goose Peak successions, respectively.

Figure 7 shows only the lower and middle parts of the Eagle Bay assemblage. The upper part comprises Devono-Mississippian felsic to mafic volcanic rocks and clastic sedimentary rocks that are not apparently represented in the Snowshoe Group, although Struik (1986) suggested that the Hardscrabble Mountain succession might correlate with Mississippian clastic rocks within the upper package. The lower part of the Eagle Bay assemblage differs from the Snowshoe Group and Kootenay Arc successions in that it contains a much higher proportion of mafic volcanic rocks. These mafic volcanics dominate a heterogeneous package assigned to Unit EBG by Schiarizza and Preto (1987). The Tshinakin limestone is a discontinuous but commonly very thick carbonate unit within this mafic volcanic succession; it contains Lower Cambrian archaeocyathids at one locality and therefore correlates with the Badshot Formation of the Kootenay Arc and probably with the Brilco limestone of the Snowshoe Group. A discontinuous but widespread sedimentary succession beneath the Tshinakin invariably includes a unit of very pure quartzite (Unit EBGq) that is here correlated with the Keithley quartzite. Underlying rocks comprise limestone intercalated with mafic volcanics and may correlate with the mafic volcanic/limestone intervals found within the Downey succession. This lower part of Unit EBG is gradationally underlain by grey to green quartzites, phyllites and grits (Unit EBH) that are similar to, and here correlated with, the typical clastic rocks of the Downey succession (Figure 7). The upper part of Unit EBG, above the Tshinakin limestone, includes a continuous unit of black phyllite, with local intercalations of dark grey limestone and quartzite (Unit EBGp), that we correlate with the Hardscrabble Mountain/Harveys Ridge succession of the Snowshoe Group and the lower Index Formation of the Lardeau Group. If this is the case, then the mafic volcanic rocks of Unit EBG may actually represent two or more pulses of volcanism that correlate with Downey and Hamill volcanics at the base of the unit, and with Index and Harveys Ridge volcanics at the top of the unit (Figure 7).

The upper part of Unit EBG is truncated by a thrust fault in some areas and by a suspected unconformity beneath Devono-Mississippian rocks in others, so the stratigraphic top of the unit is not well understood. Elsewhere within the Eagle Bay exposure belt, however, is a heterogeneous unit dominated by phyllitic grits, quartzites and subordinate phyllites, that also underlies Devono-Mississippian rocks and is suspected to be younger than Unit EBG. This unit (Unit EBS of Schiarizza and Preto, 1987) is lithologically similar to, and tentatively correlated with, the Harveys Ridge transitional and/or Goose Peak successions of the Snowshoe Group (Figure 7).

INTRUSIVE ROCKS

EARLY MISSISSIPPIAN GRANITE

Foliated granite to granodiorite, locally grading to orthogneiss, crops out in the southwestern corner of the map area, south and west of the west end of Cariboo Lake (Figure 4). These rocks intrude the Harveys Ridge succession, and locally form the footwall to the Eureka thrust fault. Ferri and O'Brien (2002) show that the main granitic exposures comprise a transgressive sill-like body that is folded by a late upright synform. The granitic rocks are assigned an Early Mississippian age on the basis of a U-Pb zircon date of 357.2±1.0 Ma obtained by Ferri *et al.* (1999).

The Early Mississippian granite near Cariboo Lake is at the north end of a discontinuous belt of similar intrusions that extends for more than 100 kilometres southeastward within western Barkerville Terrane (Mortensen *et al.*, 1987). Similar Devono-Mississippian granitic rocks are also found in the correlative Kootenay Terrane farther south, where they are in part associated with apparently co-magmatic Devono-Mississippian volcanic rocks of the Eagle Bay assemblage (Schiarizza and Preto, 1987). Ferri *et al.* (1999) suggest, on the basis of geochemistry, that the Early Mississippian granitic rocks near Cariboo Lake are the products of arc magmatism.

PROSERPINE INTRUSIONS

Johnston and Uglow (1926) introduced the term "Proserpine sills and dikes" for a suite of altered and foliated felsic intrusions found locally within rocks now assigned to the Snowshoe Group in the Antler Creek - Barkerville area. Rocks that probably belong to this suite were encountered in a few localities near Barkerville during the course of the 2002 mapping program, within rocks of the Downey, Hardscrabble Mountain and Harveys Ridge successions. These rocks comprise moderately foliated, brown-weathering quartz-feldspar-ankerite-sericite schists and semischists, in which feldspar and/or quartz were in part derived from relict igneous phenocrysts. One exposure of sericite-feldspar-quartz semischist within the upper part of the Downey succession near the head of Stouts Gulch displays hints of relict texture that suggest it was derived from an equigranular, medium-grained granitic rock. The

Proserpine intrusions are not dated, but this rock bears some similarity to the Early Mississippian granitic rocks near Cariboo Lake, suggesting that the two suites may, at least in part, be related. A sample of the foliated granitoid rock at the head of Stouts Gulch has been submitted for U-Pb dating of zircons in an attempt to determine its age. The results are not yet available.

METADIORITE

Medium to dark green variably foliated metadiorite, grading to feldspar-chlorite schist, is scattered widely within the Snowshoe Group, but typically forms sills, dikes and irregular intrusive masses that measure only a few metres to tens of metres in size. Metadiorite is most common in the Downey succession, but is also found in other units of the group. The largest body of diorite in the region forms a mappable sill-like unit, up to several hundred metres thick, that intrudes the Downey succession near Mount Barker, east of Cariboo Lake (Ferri and O'Brien, 2002). Ferri and Friedman (2002) report U-Pb zircon dates from two separate samples of this large diorite unit, and another date from a diorite sill that intrudes the Harveys Ridge succession southwest of Keithley Creek. The samples from the diorite body near Mount Barker yielded dates of 277.3±4.8 Ma and 281.0±5.2 Ma, respectively, and the sill southwest of Keithley Creek yielded a similar date of 281±12 Ma. It is suspected that most other metadiorite bodies within the Snowshoe Group are of similar Early Permian age.

STRUCTURE

MESOSCOPIC STRUCTURES

Most rocks within the study area are at lower (sub-biotite) greenschist facies metamorphic grade. The mesoscopic structure is dominated by a synmetamorphic cleavage that is axial planar to northwest or southeast plunging mesoscopic folds of bedding (Photo 1). This cleavage is penetrative within slates and phyllites, but is typically less pervasive within metasandstones and coarser rocks. It is commonly accompanied by a stretching or rodding lineation that is approximately parallel to the axes of the associated folds (Photo 2). This synmetamorphic cleavage and associated structures are related to predominantly southwest-vergent macroscopic folds that commonly form the dominant map-scale structures within the Snowshoe Group.

Locally it is apparent that the dominant synmetamorphic cleavage within the area is a composite fabric element that overprints, or is parallel to, one ore more earlier bedding-parallel cleavages. These earlier cleavages are typically only evident in the hinge zones of folds, where they are folded and cross-cut at a high angle by the predominant cleavage. No folds were observed to be associated with these earlier cleavages, although relationships documented in the underground mines at Wells suggest that such structures might exist (Robert and Taylor, 1989; Rhys and Ross, 2001). Studies elsewhere in the region suggest that these early fabric elements within the Snowshoe Group are related to Early Jurassic east-directed overthrusting by the Quesnel Terrane (Ross *et al.*, 1985; Rees, 1987; Ferri, 2001), and/or to an earlier deformation event that affected the Snowshoe Group after intrusion of Early Mississippian granitic rocks (Ross *et al.*, 1985; Fillipone and Ross, 1990; McMullin *et al.*, 1990).

Photo 1. Recumbent fold in the Harveys Ridge (transitional) succession, Jack of Clubs Creek. View is to the west-northwest.

Photo 2. Strong linear fabric in folded siltite of the Hardscrabble Mountain succession, south of Wells.

In most exposures in the map area, the dominant synmetamorphic cleavage is cut by one or two generations of younger structures. Most common is a single crenulation cleavage that dips steeply to the northeast or southwest (Photo 3). The associated crenulation lineations and upright mesoscopic folds plunge gently to the northwest or southeast, more or less parallel to the older fold axes and lineations. Locally, this steeply-dipping crenulation cleavage overprints an intermediate generation of folds that also deform the dominant synmetamorphic cleavage. These mesoscopic folds are most common in the area between Lightning and Barkerville, where they are typically tight and asymmetric, with vergence to the south-southwest. The

Photo 3. Upright crenulation cleavage cutting phyllitic cleavage, Harveys Ridge succession east of Lightning Creek.

fold axes, together with an associated crenulation lineation, plunge gently to the west-northwest or east-southeast, and the north-northeast-dipping axial surfaces are commonly followed by narrow quartz veins.

MAP-SCALE STRUCTURES

Our interpretation of the macroscopic structure of the map area is summarized in the schematic vertical cross-sections of Figure 5. The distribution of geologic units within the Snowshoe Group is controlled by a large southwest-vergent nappe structure (Ferri and O'Brien, 2003) that is folded across the younger, upright, Lightning Creek antiform. The Downey succession forms the core of the early recumbent anticline. The axial trace of this structure had previously been recongnized within the eastern belt of Downey rocks, because the Hardscrabble Mountain succession occurs on both sides of the Downey succession (Struik, 1988). Furthermore the western part of the Downey succession in this belt has long been known to be overturned on the basis of detailed work in the Well mining camp (Benedict, 1945; Skerl, 1948), where bedding/cleavage relationships and fold asymmetry show that the structure is related to formation of the regional synmetamorphic cleavage. The interpretation that this fold is actually the root zone of a large nappe, however, is based on the revised stratigraphic interpretation presented here, and in particular the interpretation that the Downey succession (together with flanking Hardscrabble Mountain/Harveys Ridge successions) is repeated to the west, in part as rocks that had previously been mapped as Keithley succession (Figure 4). Struik (1982) inferred similar recumbent fold structures based on a preliminary stratigraphic interpretation that correlated the Harveys Ridge and Hardscrabble Mountain successions; his later cross sections (*e.g.* Struik, 1988) do not show such structures because he subsequently interpreted the Hardscrabble Mountain succession to be younger than the Harveys Ridge (Figure 2).

Stratigraphic symmetries within the Harveys Ridge succession and associated rocks north of Cariboo Lake suggest that the hinge of the associated syncline structurally beneath the anticlinal nappe breaches the topographic surface in that area. The synclinal hinge apparently closes to the north, around the axial trace of the late antiform, reflecting a gentle northward plunge of the antiform (Figures 4 and 5).

The recumbent, southwest-vergent fold pair interpreted to be the dominant structural feature of the map area is related to the main synmetamorphic cleavage within the area, and is suspected to be early Middle Jurassic in age (Mortensen *et al.*, 1987). These folds are correlated with similar southwest-vergent folds and nappes, of known or suspected Middle Jurassic age, that have been documented throughout much of Barkerville and correlative Kootenay terrane (Raeside and Simony, 1983; Ross *et al.*, 1985; Schiarizza and Preto, 1987; Brown and Lane, 1988). Many of these folds have overturned limbs comparable in size to the structure inferred here.

The most conspicuous map-scale structure of the area is the Lightning Creek antiform, which extends from Cariboo Lake northwestward to beyond the limits of the present map area (Struik, 1988). The axial trace of the fold separates predominantly northeast-dipping bedding and synmetamorphic cleavage on its northeast limb from predominantly southwest dipping orientations to the southwest. Although it is clearly an antiform, the fold contains the youngest units of the Snowshoe Group in its core because it is superimposed on the overturned limb of the older southwest-vergent nappe structure. As shown in Figure 5, the antiform is a well-defined open fold in the southeast, but becomes a broad arch to the northwest. The antiform is thought to be the same age as the steeply-dipping crenulation cleavage that is a common mesoscopic fabric element in the area. Other structures that may be the same age include an open synform west of Keithley Creek (Figure 4), and upright folds that repeat and warp the overturned Downey/Hardscrabble contact southwest of Wells (Figure 5, section A).

The Keithley thrust fault (Struik, 1988) is preserved in the core of the late synform west of Keithley Creek (Ferri and O'Brien, 2002; Figure 5, section C). The fault carries biotite and garnet-bearing rocks tentatively correlated with the Downey succession, and places them above younger Harveys Ridge and Goose Peak successions that are at lower metamorphic grade. Ferri and O'Brien (2002) describe highly deformed rocks along the eastern trace of the thrust, suggesting the presence of a large ductile shear zone. The movement direction along the thrust is unknown. In Figure 5 it is show to root to the east, beneath the Pleasant Valley thrust, but alternatively it might be related to the Eureka thrust to the west. A system of thrust faults and ductile shear zones has also been mapped north of Wells, placing the Crooked amphibolite and Tom succession of Struik (1988) above the Downey succession. Like the Keithley thrust, these faults carry rocks that are, at least in part, at higher metamorphic grade than the footwall rocks. The significance and origin of these ductile shear zones and higher grade rocks in the upper structural levels of Barkerville Terrane has not been addressed.

MINERAL OCCURRENCES

Bedrock mineral occurrences in the study area, extracted from the B.C. Geological Survey Branch's MINFILE database, are shown in Figure 8. Most are quartz veins, containing variable amounts and combinations of pyrite, galena, cosalite, sphalerite and scheelite, that have been explored for gold. In the Wells mining camp, pyritic replacement bodies in limestone are associated with the gold-quartz veins and have contributed substantially to the gold production. Massive sulphide occurrences in the Harveys Ridge succession around Cariboo Lake are relatively recent discoveries that are currently being explored by Barker Minerals Ltd. Stratabound lead-zinc and bedded barite showings in rocks that belong to the upper Downey or overlying Hardscrabble Mountain succession along upper Cunningham Creek may be sedimentary exhalative deposits (Höy and Ferri, 1998).

MASSIVE SULPHIDE OCCURRENCES

Massive sulphide mineralization is represented in the present study area by the Frank Creek occurrence and nearby Big Gulp and Unlikely showings, all within the Harveys Ridge succession near the southwest end of Cariboo Lake. The Besshi-style mineralization and host rocks are described by Höy and Ferri (1998), Ferri (2001) and Ferri and O'Brien (2002). Here, we point out that the regional correlations presented in Figure 7 show that the host rocks to the Frank Creek occurrence correlate with rocks that host Besshi-style massive sulphide mineralization at the past-producing Goldstream deposit in the northern Selkirk mountains (Höy, 1979; Logan and Colpron, 1995).

LODE GOLD OCCURRENCES

Almost all of the historic lode-gold production in the area has come from the Cariboo Gold Quartz, Island Mountain and Mosquito Creek mines of the Wells Mining camp (Figure 8). These three mines produced a combined total of 1.23 million ounces of gold from 3.03 million tons of ore between 1933 and 1987 (Hall, 1999). International Wayside Gold Mines Ltd. started exploring the Wells – Barkerville area in 1994 and discovered the Bonanza Ledge zone in March 2000. The zone is about 2 kilometres southeast of the main workings of the Cariboo Gold Quartz mine, although the B.C. vein, structurally above the zone, was accessed by an underground extension of the mine's main haulage level in 1941. A recent resource estimate by Giroux Consultants Ltd. of Vancouver shows indicated resources of 372 000 tons grading 0.239 oz/ton Au in Bonanza Ledge and 326 000 tons grading 0.155 oz/ton Au in the B.C. vein, using a 0.02 oz/ton cutoff. Inferred resources, using the same cutoff, are 44 000 tons grading 0.179 oz/ton Au in Bonanza Ledge and 321 000 tons grading 0.070 oz/ton in the B.C. vein. An estimate for the nearby Cow Mountain zones (Cariboo Gold Quartz mine) made in 2000 showed indicated and inferred resources of 6 629 000 tons grading 0.065 oz/ton Au and 1 684 000 tons grading 0.054 oz/ton Au, respectively. A scoping study is currently underway to examine the possibility of open-pit mining all three areas utilizing a central milling facility (Press Release by International Wayside Gold Mines Ltd., November 2002).

Detailed descriptions of the past-producing mines of the Wells camp are provided by Benedict (1945), Skerl (1948), Sutherland Brown (1957), Alldrick (1983) and Robert and Taylor (1989). Descriptions of the Bonanza Ledge zone are provided by Rhys and Ross (2001) and Ray *et al.* (2001). Historic gold production has come from two different types of ore: auriferous pyrite in quartz veins, and massive auriferous pyrite lenses, referred to as replacement ore, associated with limestone. The main producing vein systems (mainly Cariboo Gold Quartz mine) comprise diagonal and transverse veins adjacent to northerly striking faults. The overall geometry of the system, together with the structural characteristics of the two vein sets, suggest that the diagonal veins and north-striking faults are part of a conjugate fault system, and the transverse veins fill extensional fractures related to this system (Figure 9; Sutherland Brown, 1957; Rhys and Ross, 2001). The replacement ore (mainly Island Mountain and Mosquito Creek mines) occurs in carbonate-bearing stratigraphy that is structurally above (stratigraphically below) the main vein systems. It occurs within and adjacent to limestone units, commonly as linear bodies localized in the hinge zones of synmetamorphic folds. The fold hinges are perpendicular to the transverse (extensional) veins of the structurally lower vein-hosted ore, and ore-bearing veins are locally seen to extend into and terminate in replacement ore (Skerl, 1948; Alldrick, 1983).

Historic production from the Wells camp has come from a restricted stratigraphic range, and stratigraphy has consequently been an important guide to exploration in the area. The critical stratigraphic units are the Rainbow and Baker members of the Richfield formation, as defined by Hanson (1935). Most producing vein systems are in quartzites and phyllites of the Rainbow member, while replacement ore occurs in limestone bodies at or near the base of the structurally overlying (stratigraphically underlying) Baker member. As shown in Figure 10, both of these units are in the upper part of the Downey succession. The structurally underlying B.C. member of Hanson comprises the base of the Hardscrabble Mountain succession. Hanson's structurally lower Lowhee and Basal units are probably structural repeats of the Rainbow and B.C. members, respectively, as suggested by Skerl (1948).

The most prominent and continuous quartz veins in the Wells area, the so-called strike veins, are more or less parallel to the regional strike of the host strata, but dip more steeply. One of these, the B.C. vein, produced a modest amount of gold in the 1940s. Exploratory drilling on the B.C. vein led to the discovery of Bonanza Ledge, in the footwall of the vein, in March 2000. According to Rhys and Ross (2001) gold within the Bonanza Ledge zone occurs in discrete pyrite-rich areas within a zone of intense and pervasive sericite-iron carbonate-pyrite alteration that ranges from 20 to 100 metres wide. Gold-bearing zones are locally more than 30 metres thick and comprise veinlets, concor-

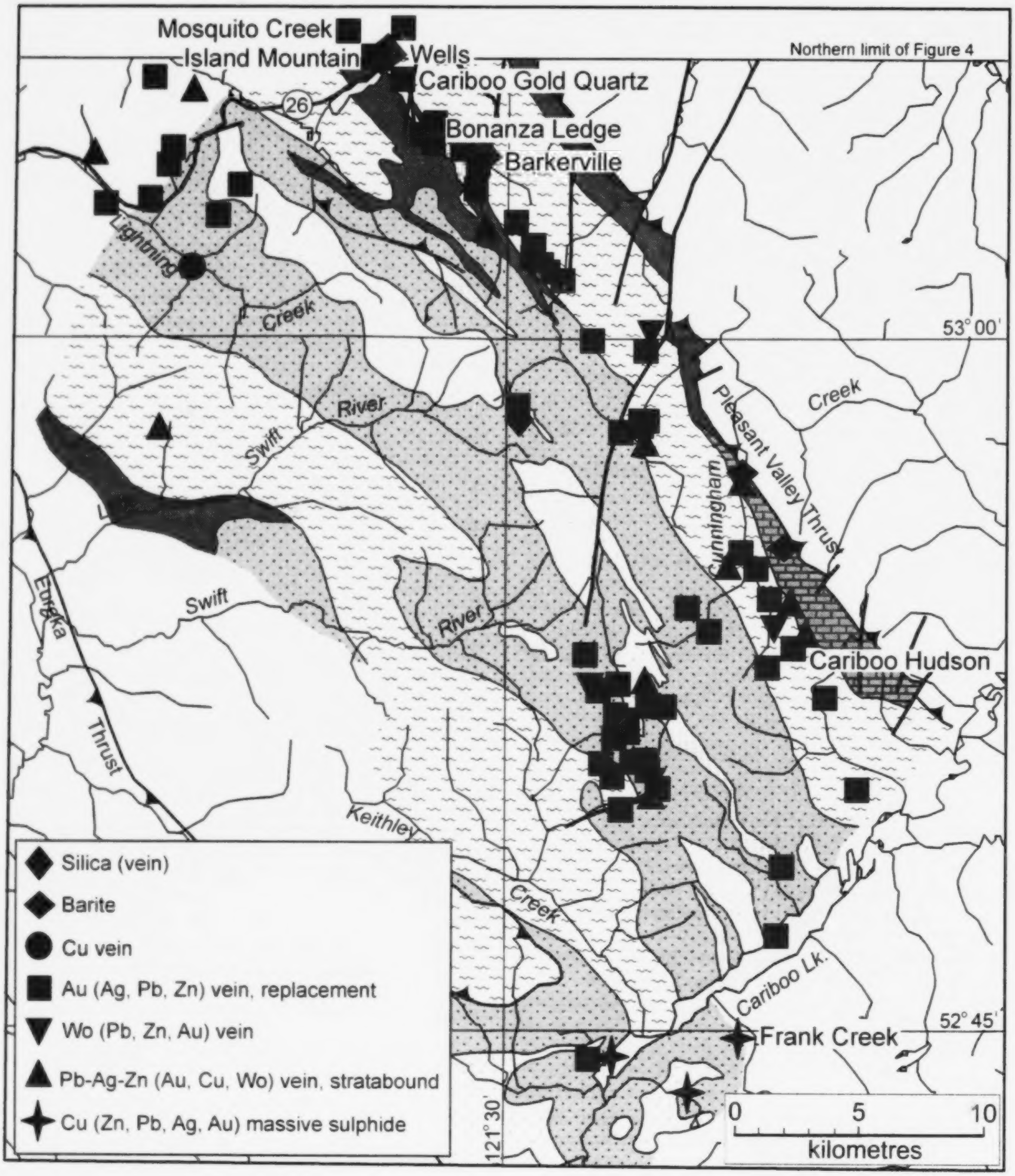
Mosquito Creek
Island Mountain
Wells
26
Cariboo Gold Quartz
Bonanza Ledge
Barkerville
Northern limit of Figure 4
Lightning
Creek
53° 00'
River
Swift
Creek
Pleasant Valley Thrust
Cunningham
Swift
River
Eureka
Thrust
Cariboo Hudson
Keithley
Creek
Cariboo Lk.
52° 45'
Frank Creek
121° 30'
0
5
10
kilometres
◆ Silica (vein)
◆ Barite
● Cu vein
■ Au (Ag, Pb, Zn) vein, replacement
▼ Wo (Pb, Zn, Au) vein
▲ Pb-Ag-Zn (Au, Cu, Wo) vein, stratabound
✦ Cu (Zn, Pb, Ag, Au) massive sulphide

Figure 8. Locations of MINFILE occurrences in the Snowshoe Group, Cariboo Lake - Wells area.

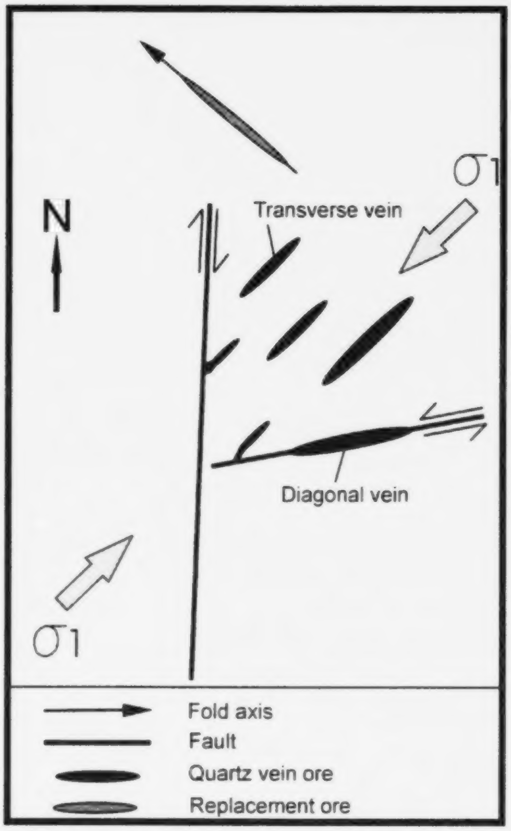

Figure 9. Schematic summary of the geometric relationships of ore-hosting veins and structures in the Wells mining camp, after Sutherland Brown (1957) and Rhys and Ross (2001).

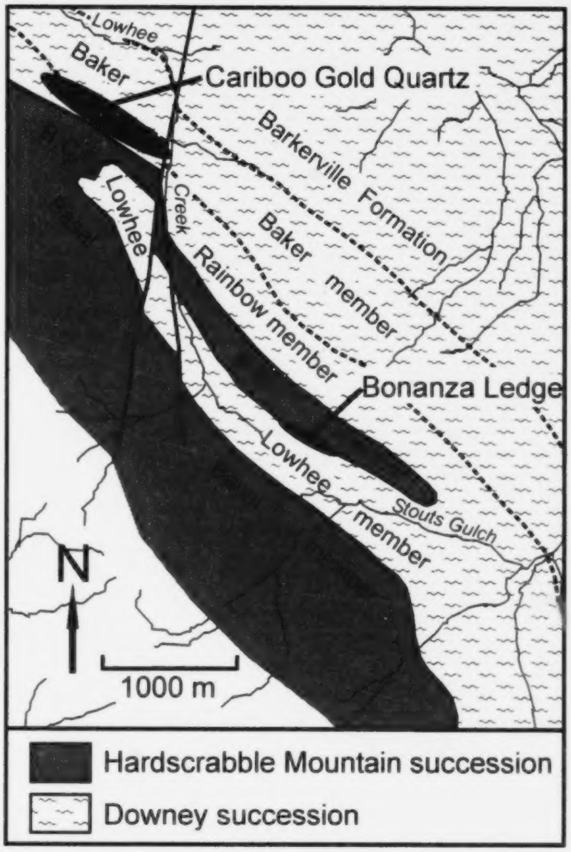

Figure 10. Geology of the Lowhee Creek – Stouts Gulch area, showing relationship between Hanson's (1935) stratigraphic units and the regional stratigraphy, as well as stratigrahic/structural position of Bonanza Ledge relative to past-producing lodes, as represented by the Cariboo Gold Quartz mine.

dant laminations and massive bands of pyrite in a gangue of muscovite, dolomite/ankerite and quartz. Veinlets and pyrite bands are folded and locally elongated parallel to the fold axes. Rhys and Ross suggest that the mineralization and alteration style at Bonanza Ledge is similar to that associated with the replacement bodies that were historically mined in the Wells camp. However, the Bonanza Ledge bodies are larger, and structurally lower than the past-producing lodes (Figure 10) so present an important new exploration target.

On a regional scale, the Wells Mining camp is here interpreted to occur on the overturned limb of a large southwest-vergent nappe structure (Figure 5, section A). This structure is thought to be Jurassic in age, and a Jurassic component of deformation and metamorphism is corroborated by a whole rock K-Ar date of 179±8 Ma obtained from phyllite near Wells (Andrew *et al.*, 1983). Lead isotope data suggest that the gold has a host-rock upper crutstal source (Andrew *et al.*, 1983) and may have been mobilized by prograde regional metamorphic fluids and then deposited in structurally higher and cooler parts of the orogen (Struik, 1988). The gold-bearing lodes of the Wells camp were deposited after the stratigraphy was overturned (given that the replacement deposits seem to be fed by the structurally underlying vein systems), but formed in a strain regime compatible with the one that formed the main regional structures (Figure 9). The few K-Ar dates on muscovite from veins in and near the Wells camp cluster around 140 Ma (Andrew *et al.*, 1983; Alldrick, 1983; Hall, 1999). A similar Early Cretaceous age has been documented for regional metamorphism in the southern Cariboo Mountains (Digel *et al.*, 1998), and near the Barkerville/Cariboo terrane boundary at Hobson Lake this metamorphism is associated with southwest-vergent structures that overprint, and are not easily distinguished from, synmetamorphic southwest-vergent folds of Middle Jurassic age (P.S. Simony, personal communication, October 2002). It is suspected that a similar Early Cretaceous structural/metamorphic overprint may extend northwestward to the Wells-Barkerville area. This might explain some of the structural observations made by Robert and Taylor (1989) and Rhys and Ross (2001) that suggest there is more than one episode of synmetamorphic deformation within the Wells mining camp.

SUMMARY OF MAIN CONCLUSIONS

Observations made during the 2002 mapping program are generally consistent with the revised stratigraphic interpretations presented by Ferri (2001) and Ferri and O'Brien (2002). The lowest stratigraphic unit of the Snowshoe Group is the Downey succession, which includes rocks previously mapped by Struik (1988) as Keithley and Ramos successions. The Downey is overlain by the Harveys Ridge succession, which includes the Hardscrabble Mountain unit as an internal mappable facies in its lower part, and the Agnes conglomerate as a mappable unit at higher stratigraphic levels. The Goose Peak succession is the highest stratigraphic element of the group and includes some rocks mapped by Struik as Eaglesnest succession.

The stratigraphic interpretation adopted here requires major across-strike repetitions of mappable units within the Snowshoe Group. We interpret this map pattern to reflect the presence of a major southwest-vergent nappe that is folded by the younger Lightning Creek antiform. The early fold nappe is correlated with southwest-vergent folds and nappes, of mainly Middle Jurassic age, that are a prominent feature of other parts of Barkerville/Kootenay terrane. The Lightning Creek antiform changes from an open fold in the southeast to a broad arch in the northwest, and contains the youngest rocks of the Snowshoe Group in its core. This otherwise enigmatic feature is explained by the presence of the older nappe since, at the present level of erosion, the antiform is developed in the overturned limb of the early structure.

The Keithley quartzite at the top of the Downey succession is correlated with the upper unit of the Hamill Group in the northern Selkirk Mountains and with Unit EBGq of the Eagle Bay assemblage. Underlying rocks of the Downey are correlated with the middle and lower units of the Hamill Group, and with the lower part of Unit EBG and underlying Unit EBH. The Bralco limestone, which overlies the Downey succession locally, is correlated with the Badshot Formation of the Northern Selkirks and the Tshinakin limestone of the Eagle Bay assemblage. The overlying Hardscrabble Mountain facies of the Harveys Ridge succession is correlated with prominent black phyllite units comprising the Lower Index Formation of the northern Selkirks and Unit EBGp of the Eagle Bay assemblage. The upper Harveys Ridge and Goose Peak successions are correlated with similar Paleozoic grit-bearing successions comprising the upper Index and Broadview formations of the northern Selkirks and Unit EBS of the Eagle Bay assemblage.

The regional correlations presented here show that the host rocks to the Frank Creek massive sulphide occurrence correlate with rocks that host Besshi-style massive sulphide mineralization at the past-producing Goldstream deposit in the northern Selkirk Mountains.

ACKNOWLEDGMENTS

We thank Frank Callaghan and International Wayside Gold Mines Ltd. for providing the financial support required to conduct fieldwork. Discussions in the field with Godfrey Walton, Richard Hall and Dave Lefebure were very helpful and much appreciated. We particularly thank Judy Cushman for being an excellent field assistant and Fran MacPherson for very efficiently handling many of the logistical aspects of the field program. Bert Struik led Fil Ferri on a field trip through the Snowshoe Group in June 2000, and provided us with his field notes and maps from the project area. Brian Grant provided editorial comments on the manuscript and Janet Holland formatted it for publication.

REFERENCES

Alldrick, D.J. (1983): The Mosquito Creek Mine, Cariboo Gold Belt (93H/4); *in* Geological Fieldwork 1982, *British Columbia Ministry of Energy, Mines and Petroleum Resources*, Paper 1983-1, pages 99-112.

Andrew, A., Godwin, C.I. and Sinclair, A.J. (1983): Age and genesis of Cariboo gold mineralization determined by isotope methods (93H); *in* Geological Fieldwork 1982, *British Columbia Ministry of Energy, Mines and Petroleum Resources*, Paper 1983-1, pages 305-313.

Benedict, P.C. (1945): Structure at Island Mountain Mine, Wells, B.C.; *Canadian Institute of Mining and Metallurgy*, Transactions, Volume 48, pages 755-770.

Bowman, A. (1889): Report on the geology of the mining district of Cariboo, British Columbia; *Geological Survey of Canada*, Annual Report for 1887-1888, Volume III, part 1, pages 1-49.

Brown, R.L. and Lane, L.S. (1988): Tectonic interpretation of west-verging folds in the Selkirk Allochthon of the southern Canadian Cordillera; *Canadian Journal of Earth Sciences*, Volume 25, pages 292-300.

Brown, R.L., Journeay, J.M., Lane, L.S., Murphy, D.C. and Rees, C.J. (1986): Obduction, backfolding and piggyback thrusting in the metamorphic hinterland of the southeastern Canadian Cordillera; *Journal of Structural Geology*, Volume 8, pages 255-268.

Campbell, R.B., Mountjoy, E.W. and Young, F.G. (1973): Geology of McBride map-area, British Columbia; *Geological Survey of Canada*, Paper 72-35, 104 pages.

Colpron, M. and Price, R.A. (1995): Tectonic significance of the Kootenay terrane, southeastern Canadian Cordillera: An alternative model; *Geology*, Volume 23, pages 25-28.

Colpron, M., Price, R.A., Archibald, D.A. and Carmichael, D.M. (1996): Middle Jurassic exhumation along the western flank of the Selkirk fan structure: Thermobarometric and thermochronometric constraints from the Illecillewaet synclinorium, southeastern British Columbia; *Geological Society of America*, Bulletin, Volume 108, pages 1372-1392.

Colpron, M., Logan, J.M. and Mortensen, J.K. (2002): U-Pb zircon age constraint for late Neoproterozoic rifting and initiation of the lower Paleozoic passive margin of western Laurentia; *Canadian Journal of Earth Sciences*, Volume 39, pages 133-143.

Currie, L.D. (1988): Geology of the Allan Creek area, British Columbia; unpublished M.Sc. thesis, *University of Calgary*, 152 pages.

Devlin, W.J. (1989): Stratigraphy and sedimentology of the Hamill Group in the northern Selkirk Mountains, British Columbia: evidence for latest Proterozoic - Early Cambrian extensional tectonism; *Canadian Journal of Earth Sciences*, Volume 26, pages 515-533.

Digel, S.G., Ghent, E.D., Carr, S.D. and Simony, P.S. (1998): Early Cretaceous kyanite-sillimanite metamorphism and

Paleocene sillimanite overprint near Mount Cheadle, southeastern British Columbia: Geometry, geochronology, and metamorphic implications; *Canadian Journal of Earth Sciences*, Volume 35, pages 1070-1087.

Ferri, F. (1997): Nina Creek Group and Lay Range Assemblage, north-central British Columbia: Remnants of late Paleozoic oceanic and arc terranes; *Canadian Journal of Earth Sciences*, Volume 34, pages 854-874.

Ferri, F. (2001): Geological setting of the Frank Creek massive sulphide occurrence near Cariboo Lake, east-central British Columbia (93A/11, 14); *in* Geological Fieldwork 2000, *British Columbia Ministry of Energy and Mines*, Paper 2001-1, pages 31-49.

Ferri, F. and O'Brien, B.H. (2002): Preliminary geology of the Cariboo Lake area, central British Columbia (093A/11, 12, 13 and 14); *in* Geological Fieldwork 2001, *British Columbia Ministry of Energy and Mines*, Paper 2002-1, pages 59-81.

Ferri, F. and O'Brien, B.H. (2003): Geology of the Cariboo Lake area, central British Columbia; *British Columbia Ministry of Energy and Mines*, Open File 2003-1.

Ferri, F. and Friedman, R.M. (2002): New U-Pb and geochemical data from the Barkerville subterrane; *in* Slave-northern Cordillera lithospheric evolution (SNORCLE) transect and cordilleran tectonics workshop meeting, Lithoprobe Report No. 82, pages 75-76.

Ferri, F., Höy, T. and Friedman, R.M. (1999): Description, U-Pb age and tectonic setting of the Quesnel Lake gneiss, east-central British Columbia; *in* Geological Fieldwork 1998, *British Columbia Ministry of Energy and Mines*, Paper 1999-1, pages 69-80.

Fillipone, J. A. and Ross, J.V. (1990): Deformation of the western margin of the Omineca Belt near Crooked Lake, east-central British Columbia; *Canadian Journal of Earth Sciences*, Volume 27, pages 414-425.

Hall, R. D. (1999): Cariboo Gold project at Wells, British Columbia; prepared for *International Wayside Gold Mines Limited* at http://www.wayside-gold.com/i/pdf/RHall_report.pdf, 52 pages.

Hanson, G. (1935): Barkerville Gold Belt, Cariboo District, British Columbia; *Geological Survey of Canada*, Memoir 181, 42 pages.

Holland, S.S. (1954): Geology of the Yanks Peak - Roundtop Mountain area, Cariboo District, British Columbia; *British Columbia Department of Mines*, Bulletin 34, 102 pages.

Höy, T. (1979): Geology of the Goldstream area; *British Columbia Ministry of Energy, Mines and Petroleum Resources*, Bulletin 71, 49 pages.

Höy, T. (1999): Massive sulphide deposits of the Eagle Bay assemblage, Adams Plateau, south central British Columbia (082M/3, 4); *in* Geological Fieldwork 1998, *British Columbia Ministry of Energy and Mines*, Paper 1999-1, pages 223-245.

Höy, T. and Ferri, F. (1998): Stratabound base metal deposits of the Barkerville subterrane, central British Columbia (093A/NW); *in* Geological Fieldwork 1997, *British Columbia Ministry of Energy and Mines*, Paper 1998-1, pages 13-1 - 13-12.

Johnston, W.A. and Uglow, W.L. (1926): Placer and vein gold deposits of Barkerville, Cariboo District, British Columbia; *Geological Survey of Canada*, Memoir 149, 246 pages.

Lang, A.H. (1938): Keithley Creek map-area, Cariboo District, British Columbia; *Geological Survey of Canada*, Paper 38-16, 48 pages.

Logan, J.M. and Colpron, M. (1995): Northern Selkirk project - geology of the Goldstream River map area (82M/9 and parts of 82M/10); *in* Geological Fieldwork 1994, *British Columbia Ministry of Energy, Mines and Petroleum Resources*, Paper 1995-1, pages 215-241.

Logan, J.M., Colpron, M. and Johnson, B.J. (1996): Northern Selkirk project, geology of the Downie Creek map area (82M/8); *in* Geological Fieldwork 1995, *British Columbia Ministry of Employment and Investment*, Paper 1996-1, pages 107-125.

McMullin, D.W.A., Greenwood, H.J and Ross, J.V. (1990): Pebbles from Barkerville and Slide Mountain terranes in a Quesnel terrane conglomerate: Evidence for pre-Jurassic deformation of the Barkerville and Slide Mountain terranes; *Geology*, Volume 18, pages 962-965.

Mortensen, J.K., Montgomery, J.R. and Fillipone, J. (1987): U-Pb zircon, monazite and sphene ages for granitic orthogneiss of the Barkerville terrane, east-central British Columbia; *Canadian Journal of Earth Sciences*, Volume 24, pages 1261-1266.

Murphy, D.C. (1987): Suprastructure/infrastructure transition, east-central Cariboo Mountains, British Columbia: Geometry, kinematics and tectonic implications; *Journal of Structural Geology*, Volume 9, pages 13-29.

Murphy, D.C., van der Heyden, P., Parrish, R.R., Klepacki, D.W., McMillan, W., Struik, L.C. and Gabites, J. (1995): New geochronological constraints on Jurassic deformation of the western edge of North America, southeastern Canadian Cordillera; *in* Jurassic magmatism and tectonics of the North American Cordillera, edited by D.M. Miller and C. Busby, *Geological Society of America*, Special Paper 299, pages 159-171.

Panteleyev, A., Bailey, D.G., Bloodgood, M.A. and Hancock, K.D. (1996): Geology and mineral deposits of the Quesnel River - Horsefly map area, central Quesnel Trough, British Columbia; *British Columbia Ministry of Employment and Investment*, Bulletin 97, 155 pages.

Raeside, R.P. and Simony, P.S. (1983): Stratigraphy and deformational history of the Scrip Nappe, Monashee Mountains, British Columbia; *Canadian Journal of Earth Sciences*, Volume 20, pages 639-650.

Ray, G., Webster, I., Ross, K. and Hall, R. (2001): Geochemistry of auriferous pyrite mineralization at the Bonanza Ledge, Mosquito Creek Mine and other properties in the Wells-Barkerville area, British Columbia; *in* Geological Fieldwork 2000, *British Columbia Ministry of Energy and Mines*, Paper 2001-1, pages 135-167.

Reid, L.F., Simony, P.S. and Ross, G.M. (2002): Dextral strike-slip faulting in the Cariboo Mountains, British Columbia: A natural example of wrench tectonics in relation to Cordilleran tectonics; *Canadian Journal of Earth Sciences*, Volume 39, pages 953-970.

Rees, C.J. (1987): The Intermontane-Omineca belt boundary in the Quesnel Lake area, east-central British Columbia: tectonic implications based on geology, structure and paleomagnetism; unpublished Ph.D. thesis, *Carleton University*, 421 pages.

Robert, F. and Taylor, B.E. (1989): Structure and mineralization at the Mosquito Creek gold mine, Cariboo District, B.C.; *in* Structural environment and gold in the Canadian Cordillera, *Geological Association of Canada, Cordilleran Section*, Short Course No. 14, pages 25-41.

Ross, J.V., Fillipone, J., Montgomery, J.R., Elsby, D.C. and Bloodgood, M. (1985): Geometry of a convergent zone, central British Columbia, Canada; *Tectonophysics*, Volume 119, page 285-297.

Rhys, D.A. and Ross, K.V. (2001): Evaluation of the geology and exploration potential of the Bonanza Ledge zone, and adjacent areas between Wells and Barkerville, east-central British Columbia; internal report prepared for International Wayside Gold Mines Ltd. by Panterra Geoservices Inc., 110 pages.

Schiarizza, P. (1989): Structural and stratigraphic relationships between the Fennell Formation and Eagle Bay Assemblage, western Omineca Belt, south-central British Columbia: Implications for Paleozoic tectonics along the paleocontinental margin of western North America; unpublished M.Sc. thesis, *University of Calgary*, 343 pages.

Schiarizza, P. and Preto, V.A. (1987): Geology of the Adams Plateau-Clearwater-Vavenby area; *British Columbia Ministry of Energy, Mines and Petroleum Resources*, Paper 1987-2, 88 pages.

Skerl, A.C. (1948): Geology of the Cariboo Gold Quartz Mine, Wells, B.C.; *Economic Geology*, Volume 43, pages 571-597.

Struik, L.C. (1982): Snowshoe Formation (1982), central British Columbia; *in* Current Research, Part B, *Geological Survey of Canada*, Paper 82-1B, pages 117-124.

Struik, L.C. (1984): Outcrop geology, Cariboo Lake, Spectacle Lakes, Swift River, and Wells map areas, Cariboo District, British Columbia; *Geological Survey of Canada*, Open File 1109.

Struik, L.C. (1986): Imbricated terranes of the Cariboo gold belt with correlations and implications for tectonics in southeastern British Columbia; *Canadian Journal of Earth Sciences*, Volume 23, pages 1047-1061.

Struik, L.C. (1987): The ancient western North American margin: an Alpine rift model for the east-central Canadian Cordillera; *Geological Survey of Canada*, Paper 87-15, 19 pages.

Struik, L.C. (1988): Structural geology of the Cariboo Gold Mining District, east-central British Columbia; *Geological Survey of Canada*, Memoir 421, 100 pages.

Struik, L.C. (1993): Intersecting intracontinental Tertiary transform fault systems in the North American Cordillera; *Canadian Journal of Earth Sciences*, Volume 30, pages 1262-1274.

Struik, L.C. and Orchard, M.J. (1985): Late Paleozoic conodonts from ribbon chert delineate imbricate thrusts within the Antler Formation of the Slide Mountain terrane, central British Columbia; *Geology*, Volume 13, pages 794-798.

Sutherland Brown, A. (1957): Geology of the Antler Creek area, Cariboo District, British Columbia; *British Columbia Department of Mines*, Bulletin 38, 105 pages.

Sutherland Brown, A. (1963): Geology of the Cariboo River Area, British Columbia; *British Columbia Department of Mines and Petroleum Resources*, Bulletin 47, 60 pages.

Umhoefer, P.J. and Schiarizza, P. (1996): Latest Cretaceous to Early Tertiary dextral strike-slip faulting on the southeastern Yalakom fault system, southeastern Coast Belt, British Columbia; *Geological Society of America*, Bulletin, Volume 108, pages 768-785.

Innovative Gold Targets in the Pinchi Fault/Hogem Batholith Area: The Hawk and Axelgold Properties, Central British Columbia (94C/4, 94N/13)

By JoAnne Nelson[1], Bob Carmichael[2] and Michael Gray[3]

KEYWORDS: British Columbia, gold, intrusion-related, alkalic-hosted, Hogem batholith, Pinchi Fault, Axelgold

INTRODUCTION

The Pinchi Fault and Hogem Batholith are major geological elements of central British Columbia (Figure 1).

Both have been long known to localize significant mineral deposits, such as the Lorraine porphyry copper-gold deposit in the Hogem Batholith, and mined mercury deposits such as Takla Bralorne and the Pinchi Mine along the Pinchi Fault. Traditional models for mineralization, derived from past exploration successes and the general geological history of the area, have focused on porphyry copper-gold in the Hogem Batholith, and precious metal and mercury vein and stockwork styles along the Pinchi Fault. Two novel mineral deposit models are currently being tested on the Hawk and Axelgold properties, intrusion-related and alkalic-related styles of gold mineralization respectively. This project, a partnership between the B.C. Ministry of Energy and Mines, Redcorp Ventures Ltd. and Rubicon Minerals Corporation, aims at substantiating the validity and applications of these innovative exploration concepts to other prospects in the area.

REGIONAL GEOGRAPHY AND GEOLOGY

The Hawk and Axelgold properties are located in central British Columbia, about 150 km northeast of Smithers and 300 kilometres north of Fort St. James (Figure 1). Hawk is either ATV or helicopter accessible from a secondary branch of the Thutade-Osilinka road, which departs the Omineca Mining Road 16 kilometres south of the Osilinka Camp, and Axelgold is a short helicopter flight from a logging spur road west of Mt. Ogden. The two properties lie on opposite sides of the Omineca River, which has developed a deep valley in shattered bedrock around the main strand of the Pinchi Fault. The Axelgold is located west of the river, in the Axelgold Range, next to a subsidiary strand of the Pinchi system shown as the Axelgold Fault on Figure 1. The Hawk lies east of the river, in the prominent mountains underlain by granitoids of the northern Hogem Batholith.

The Pinchi Fault, one of the major structural lineaments of the Cordillera, separates the arc terrane, Quesnellia, with its Triassic-Jurassic volcanic and epiclastic strata and related plutons, from the oceanic Cache Creek accretionary complex to the southwest. The fault has had a protracted, complex and still imprecisely constrained history of displacement. Some strands, such as the Pinchi Fault near Pinchi Lake, may be remnants of the southwest-vergent mid-Jurassic collision that trapped the Cache Creek complex between Quesnellia and the outboard Stikinia arc terrane (Struik *et al.*, 2001). The main strand truncates Cretaceous and even Tertiary units. Based on offsets to the north on the Finlay and Kutcho faults (Gabrielse, 1985), the Pinchi probably accommodated on the order of a hundred kilometres of dextral motion in Cretaceous-Early Tertiary time. The Pinchi Fault and its splays, as well as zones of distributed strain in the rocks around it, provide likely structural controls for mineralization. A number of mineral prospects are localized along and near the main fault, including the Pinchi and Takla Bralorne mercury mines, and gold-bearing quartz-stibnite veins at the Snowbird and Indata prospects. The Lustdust skarn-manto system lies 8 kilometres west of the fault (Figure 1).

The Hogem Batholith is a northwest-elongate composite body 160 kilometres long and up to 35 km wide, that intrudes Mesozoic arc-related strata of Quesnellia. It is truncated to the southwest by the Pinchi Fault (Figure 1). It comprises a highly variable Early Jurassic suite of plutons (Hogem intrusive suite; Nelson and Bellefontaine, 1996) that range in age from 206 to 171 Ma by K-Ar methods, (Garnett 1978; converted to new decay constants), and a set of later, cross-cutting granite bodies that are identical in texture and composition to the mid-Cretaceous Germansen Batholith. K-Ar ages of 120 to 100 Ma (Figure 1; Woodsworth *et al.*, 1991, Garnett, 1978) evidence this younger intrusive event. The Early Jurassic phases tend to mildly alkalic, shoshonitic compositions, equivalent to coeval volcanic units of the Quesnellia arc (Nelson and Bellefontaine, 1996). The Lorraine porphyry copper-gold deposit is hosted by one of the youngest Jurassic phases, the Duckling Creek syenite. Similar in style and age to

---

[1] BC Geological Survey Branch
[2] Redcorp Ventures Ltd.
[3] Rubicon Minerals Corporation

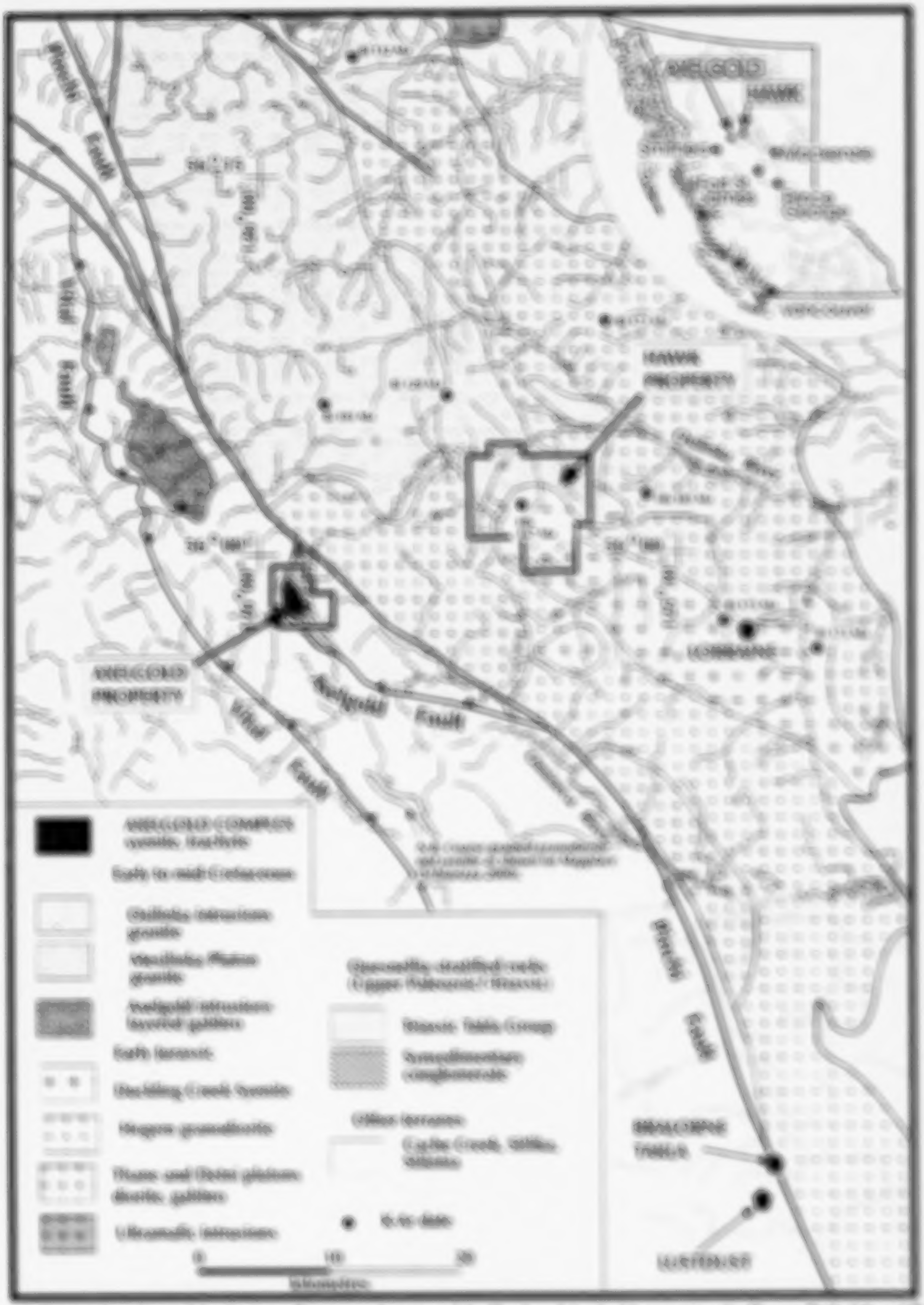
Pinchi Fault
Vital Fault
AXELGOLD
HAWK
HAWK PROPERTY
AXELGOLD PROPERTY
LORRAINE
Vital Fault
Pinchi Fault
Early terranes
Hogem granodiorite
Duckling Creek Syenite
Ultramafic intrusions
Other terranes
Takla Group
U-Pb date
0
10
20
kilometres

Figure 1. Regional geology of the Omineca River area; location of the Hawk and Axelgold properties, the Hogem Batholith and Pinchi Fault. Sources: Woodsworth (1976), Garnett (1978), Irvine (1976), Paterson (1974), Schiarizza (2000).

Lorraine, the Mt. Milligan porphyry system is associated with a small crowded porphyry monzonite stock southeast of the Hogem Batholith.

THE HAWK VEIN SYSTEM: PERIPHERAL TO PORPHYRY, OR INTRUSION-RELATED AU?

The Hawk property was originally explored for porphyry-style mineralization in the early 1970's by Amoco, and for porphyry-related vein targets by Cyprus and Castlebird in the 1990's (Stevenson, 1991). The Hawk veins are roughly centered on the contact between the Duckling Creek syenite to the south and a granite body to the north (Figure 2). They cut both syenite and granite. Woodsworth (1976; Woodsworth et al., 1992) considered the granite body to be of mid-Cretaceous age, based on textures, field relationships and K-Ar dating (Figure 1). If correct, this interpretation implies that the Hawk veins are mid-Cretaceous or younger, and thus unrelated to Jurassic porphyry-style mineralization in the syenite.

The veins are quartz-rich, with pyrite, chalcopyrite, galena, sphalerite, rare large clumps of scheelite in the Zeta vein and in a few instances, visible gold. Elevated gold values are accompanied by silver, bismuth, and tungsten (Redcorp internal report). This geochemical signature, along with the possible Cretaceous host granite, suggests that this may be an intrusion-related Au system, with parallels in the Tombstone plutonic suite in Alaska and the Yukon. One goal of this study is to test the applicability of intrusion-related models to the Hawk veins.

THE AXELGOLD PROPERTY: ALKALIC-RELATED, BUT WHICH INTRUSIVE SUITE?

Geological maps of the Axelgold property show polymetallic mineralization hosted within and adjacent to a small syenite body, which intrudes mixed volcanogenic and sedimentary rocks (Jiang and Bailey, 1996; McGann, 1998; Figures 1, 7). The intrusion and its country rocks are cut off by the Axelgold fault to the southwest, which juxtaposes them with the oceanic Cache Creek complex. To the northeast, in the northern Axelgold Range, the Cache Creek rocks are intruded by the Axelgold layered gabbro body (Irvine, 1976), which Armstrong et al. (1985) assigned a mid-Cretaceous age, based on K-Ar and Rb-Sr dating. Irvine (1976) mapped very small syenites and [illegible] within the Axelgold gabbro. However, the [illegible] intrusion on the Axelgold property is separated from the gabbro complex by a major fault, and its host rocks, conglomerate, siltstone, wacke and lapilli tuff, are considered part of Quesnellia rather than the oceanic Cache Creek Terrane (Paterson, 1974; Taylor, 1987). The Axelgold syenite, described as a multiphase fine grained to K-spar megacrystic body, could be part of the [illegible] Ma (Garnett, 1978) Duckling Creek syenite on the Lorraine property (G. Nixon, personal communication August 2002; Nixon, this volume). A third possible correlation is with the Eocene monzonite of the Glover Stock on the Lustdust property, which like the Axelgold syenite is a composite of felsic phases with strong structural control, and is associated with gold mineralization (Ray et al., 2002). Each of these three possible ages, Jurassic, Cretaceous and Eocene, suggests a different exploration strategy for regional equivalents.

GEOLOGY AND MINERALIZATION ON AND NEAR THE HAWK PROPERTY

GRANITOID HOST ROCKS

The Hogem Batholith in the vicinity of the Hawk property, as elsewhere, is highly heterogeneous, comprising a range of compositions from ultramafic to syenite and diabase (Figure 2). The northern part of the property is underlain by a distinctive mafic-poor granite. This body, one of the Osilinka intrusions of Woodsworth (1977), is unusual within the Hogem intrusive suite. It is a pale pink to pale greenish, white weathering, medium grained, equigranular to somewhat inequigranular granite that is homogeneous over tens of kilometres. Sparse mafic minerals include biotite and euhedral sphene. Near its southern contact with the Duckling Creek syenite, the granite contains very sparse pink K-spar megacrysts, possibly xenocrysts derived from the syenite. A decrease in grain size towards the contact suggests that it is chilled.

In contrast to the homogeneity of the granite, the Duckling Creek "syenite" is characterized by a plethora of textures and compositions, including K-spar megacrystic and crowded megacrystic porphyry phases, as well as phases containing abundant mafic inclusions and/or mafic schlieren, and equigranular granodiorite and monzonite. The degree of foliation ranges from strong to weak. Most foliation textures - crystal alignment and flattening of mafic inclusions - reflect magmatic flow and/or [illegible]. Local zones of subsolidus deformation occur, with most northwesterly orientations parallel to the contact with the granite.

Figure 3 shows rare earth element signatures from five samples of the Osilinka granite (Table 1), plotted with a field of granodiorite and the data of Barrie (1993) for the southern Hogem Batholith. The mainly intermediate Hogem phases, which are moderately LREE enriched and generally similar to average upper continental crust. The Osilinka granite, although showing relative LREE enrichment with respect to chondrite, is markedly depleted in all REE compared to average upper crust, with a strong negative Eu anomaly that reflects the fractionation of plagioclase. The rare earth elements were probably depleted during extensive fractional crystallization of phases such as titanite.

GOLD-BEARING QUARTZ VEINS

The Hawk property contains gold-bearing quartz veins of several orientations. Originally explored in the early 1970's by Amoco, it was later surveyed and drilled for vein targets by Cyprus and Castlebird in the 1990's (Stevenson,

[illegible]

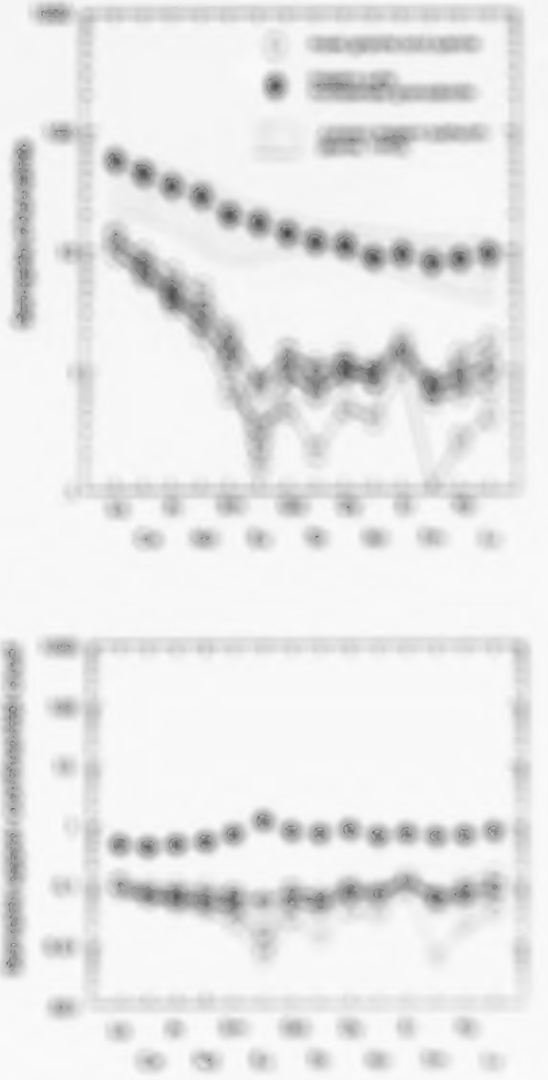

[illegible]

[illegible]

[illegible]

TABLE 1
[illegible]

Sample	Description	UTM east	UTM north	SiO2	TiO2	Al2O3	Fe2O3	MnO	MgO	CaO	Na2O	K2O	P2O5	LOI	SUM	Y*	Zr*	Nb*	[illegible]
[illegible]-01	Granodiorite - coarse, 25%hb	334712	6217085	56.52	0.7	17.77	7.65	0.15	3.63	7.73	3.66	2.4	0.25	1.46	99.46	17	74	3	[illegible]
[illegible]-05	Granite - mg, alaskitic	331975	6216558	71.8	0.16	15.46	1.17	0.02	0.16	1.27	5.13	2.91	0.02	0.67	99.28	4	76	<3	[illegible]
[illegible]-10	Quartz syenite	336785	6216113	73.65	0.07	14.67	0.93	0.02	0.09	1.2	5.09	3.25	0.01	0.46	99.09	<3	56	<3	[illegible]
[illegible]-26	Granite - mg, alaskitic	332795	6213240	72.29	0.1	15.16	0.93	0.02	0.07	1.1	5.21	3.33	0.01	0.8	99.23	3	80	<3	[illegible]
[illegible]-41	Granite - mg, alaskitic	332505	6213750	72.66	0.1	15.05	0.87	0.02	0.15	1.28	5.17	3.4	0.01	0.46	99.37	5	85	4	[illegible]
[illegible]-42	Granite - mg, alaskitic	330605	6216620	70.31	0.16	16.43	1.2	0.02	0.23	1.72	5.63	2.71	0.01	0.95	99.58	3	107	<3	[illegible]

Sample	Ba	Y	Zr	Hf	Nb	Ta	Th	La	Ce	Pr	Nd	Sm	Eu	Gd	Tb	Dy	Ho	Er	Tm	Yb	Lu
[illegible]-01	1545.756	13.595	109.801	2.396	5.386	0.419	4.071	13.559	26.407	3.247	13.16	3.094	0.077	2.826	0.437	2.751	0.49	1.53	[illegible]	1.43	0.24
[illegible]-05	1551.263	2.151	78.864	1.675	3.695	0.128	0.226	2.296	4.211	0.45	1.536	0.28	0.045	0.277	0.04	0.322	0.06	0.29	[illegible]	0.159	0.03
[illegible]-10	1411.634	1.161	50.162	1.252	3.14	0.052	0.143	2.335	3.602	0.34	0.955	0.101	-0.01	0.1	0.006	0.128	0.02	0.16	[illegible]	0.044	0.01
[illegible]-26	1698.25	1.958	83.763	1.973	5.006	0.195	0.509	2.389	3.611	0.42	1.31	0.204	0.009	0.201	0.025	0.244	0.05	0.26	[illegible]	0.147	0.03
[illegible]-41	2163.571	2.225	76.763	2.071	4.969	0.222	1.817	3.16	4.36	0.395	1.246	0.18	-0.01	0.206	0.026	0.254	0.05	0.29	[illegible]	0.223	0.04
[illegible]-42	2304.39	1.89	66.019	1.900	4.256	0.030	0.373	3.042	5.002	0.609	2.159	0.315	0.041	0.286	0.034	0.272	0.05	0.28	[illegible]	0.112	0.02

Oxides: Fused Disc - X-ray fluorescence, Cominco Laboratories * = Pressed pellet XRF, Cominco Laboratories Other traces: Peroxide fusion-ICPMS, Memorial University

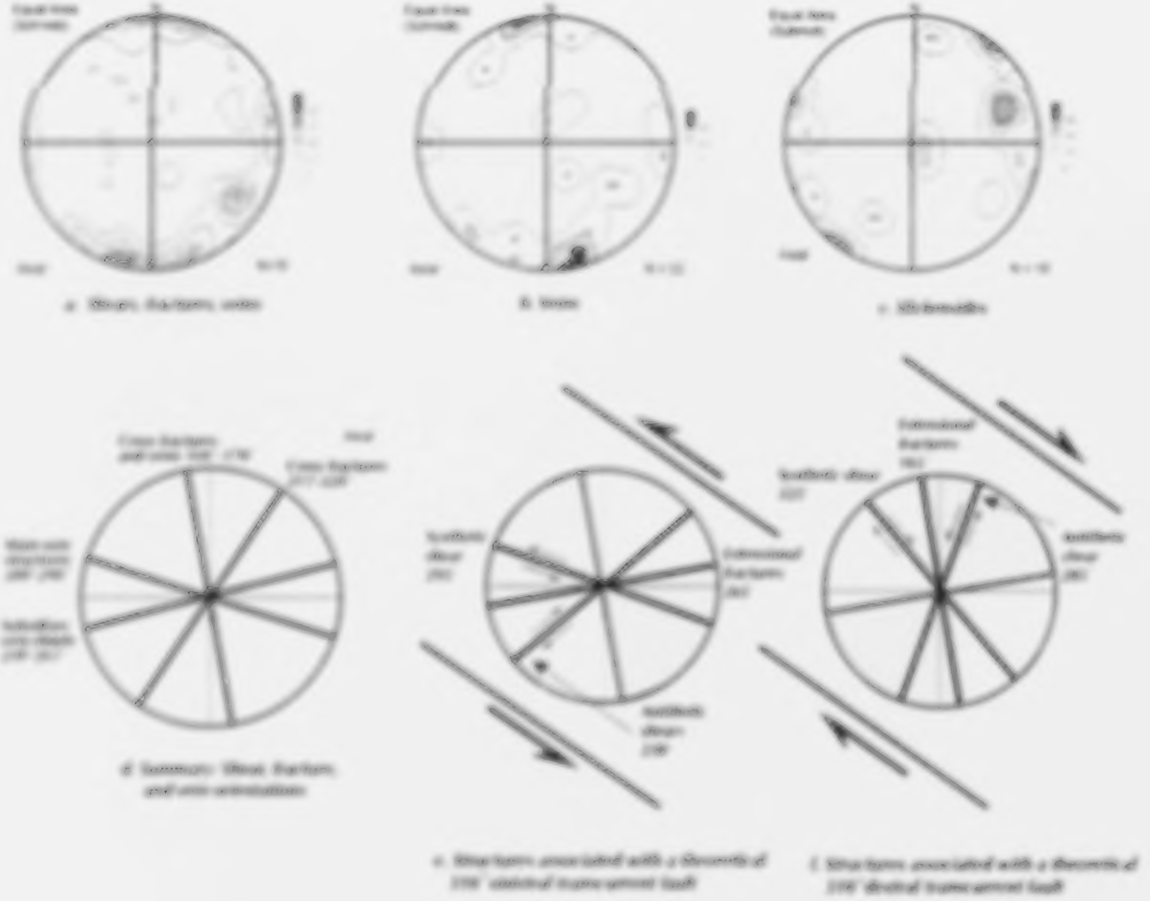
Equal Area (Schmidt)
N
Axial
Extensional fractures
Synthetic shear
Antithetic shear
Main vein structures 280°-290°
Subsidiary vein sheets 250°-265°
Cross fractures 215°-220°
Cross fractures and veins 160°-170°

a. Shears, fractures, veins

b. Veins

c. Slickensides

d. Summary: Shear, fracture, and vein orientations

e. Structures associated with a theoretical 310° sinistral transcurrent fault

f. Structures associated with a theoretical 310° dextral transcurrent fault

	Shear sense (number of measurements)	*Shear sense pre-mineralization*	*Shear sense syn-mineralization*	*Shear sense Post-mineralization*
Main vein structures 280°-290°	*Sinistral N-up* (2) *Dextral S-up* (3) *Dravnsby (Pl. 19)*	*Dextral S-up* *Splays in dextrally deflected 280 foliation (Pl. 28)* *Zulu vein (Pl. 29)*	*Dextral S-up* *South vein (Pl. 27)*	
Subsidiary vein sheets 250°-265°	*Sinistral N-up* (1) *Dextral S-up* (3)			
Cross fractures 215°-220°	*Sinistral N-up* (3) *Dextral S-up* (2)			*Sinistral N-up* *Offsets Raft's vein (Pl. 28)*
Cross fractures and veins 160°-170°	*Sinistral N-up* (2) *Dextral S-up* (2)		*Sinistral N-up* *Vein-bearing structure offsets 220 cross fractures (Pl. 40)*	*Dextral S-up* *Dextral shear bands offset vein sheets (Pl. 41)*

Figure 4. Structural analysis of veins, shears and fractures on and near the Hawk property.

shears is predominantly transcurrent, except for downdip catalastic fabric lineation on one prominent 280° shear south of the main vein system.

The Hawk vein set is located 10 kilometres from the Pinchi Fault: sets of local shears may have developed as subsidiary structures to it. Figures 4e and 4f show the predicted orientations and offsets of shears and extensional fractures associated with, respectively, sinistral and dextral transcurrent motion on a 310 degree-striking master fault such as the Pinchi. Each accounts for part but not all of the observed features. Given this, and the observed opposite senses of motion on each shear set, a model of fault reactivation is reasonable. Fault reactivation occurs when new motion takes place on a pre-existing shear plane which is near but not at the ideal orientation for failure in the ambient stress field. The main 280-290° vein-hosting shears could have initially formed as sinistral faults related to sinistral motion on the Pinchi, because they closely correspond to the 295° predicted orientation of synthetic shears. This would explain the sinistral sense of motion on them. During later dextral motion, they could have been reactivated as dextral faults proxying for the ideal 325° synthetic shears. Similarly, northeast-striking shears show both sinistral and dextral motion. The sinistral motion, which post-dates veining, corresponds to antithetic shears in a dextral system (Figure 4f). The north-northwesterly shears correspond best to extension features developed in a dextral system (Figure 4f); there is also minor dextral motion on them.

The veins post-date most, but not all, offsets on shears. For instance, in the Radio vein, undeformed 250° splays feather into dextrally deflected shear fabric in the main 290° structure (Figure 4). On the other hand, sinistral motion on the 220° shear set (resulting from dextral motion on the 310° master fault) postdates mineralization, because it offsets the Radio vein; and shear bands related to dextral motion on the 160-170° set offset vein shoots. This suggests that veining took place after the transition from sinistral to dextral regional shear couples, but before dextral motion on the Pinchi Fault ceased.

INTRUSION-RELATED GOLD MODELING: GEOLOGICAL, GEOCHEMICAL AND ISOTOPIC INDICATORS

The apparent localization of the Hawk gold-quartz veins along the margins of the Osilinka pluton is an indirect argument for relating mineralization to the granite. On the other hand, a direct connection cannot be demonstrated. None of the mineralized veins grade into pegmatites. White, flat-lying, barren quartz veins do show this relationship, but they may belong to an earlier generation. The strong structural control of the gold-bearing veins could indicate that they formed significantly later than the intrusive bodies that host them. Unlike many deposits of the Tombstone belt and Fairbanks district, fracture-controlled sheeted veins are not observed.

Intrusion-related gold mineralization is associated with a characteristic suite of elements, including Bi, W, As, Mo, Te, Sb and low concentrations of base metals (Lang and Baker, 2001). Bismuth, molybdenum and tungsten in particular may indicate the role of high-temperature magmatic fluids. In Figure 5, log-log cross-plots based on analyses from quartz veins on the Hawk property show that Ag, Bi, and Pb correlate positively with Au. Copper, tungsten, molybdenum and tungsten are elevated but do not correlate with gold. This is probably due to the uneven distribution of mineral phases in the veins. For instance, scheelite has only been recognized in a single clot 10 cm across in the Zulu vein. Arsenic and antimony occur only in trace amounts. Significantly, the field of Au/Bi values from the Hawk veins overlaps the field of analyses from gold-bearing, plutonic related quartz veins in southern B.C. (Logan, 2001).

Lead isotopic analyses were performed on two galena samples from the Hawk veins by Janet Gabites at the University of British Columbia Geochronological Laboratory (Table 2). Figure 6 shows this data. Also plotted are fields for the Cretaceous, continental, intrusion-related(?) gold vein system at Cassiar (Bradford, 1988), feldspar leads from the mid-Cretaceous Tombstone intrusive suite (J. Mortensen, unpublished data), Jurassic veins of Stikinia and the Copper Mountain copper-gold porphyry deposit of southern Quesnellia (Godwin *et al.*, 1988). The lead in the Hawk veins is most similar to that from Jurassic Snip and Sulphurets veins. It is more radiogenic than Copper Mountain, but considerably less radiogenic than leads associated with the Cretaceous, continental gold deposits of the Tombstone suite and at Cassiar. This signature is consistent with 1) a Jurassic age for the Hawk veins and 2) their location within the Intermontane belt, which is partially underlain by thick, pericontinental crust. The unradiogenic Copper Mountain leads may reflect more mantle input.

A uranium-lead date for the host granite is now in progress.

Hart *et al.* (2002) divided the deposits of the Tintina gold province, which includes both the Fairbanks and Tombstone districts, into three end-member types: intrusion-related, such as Fort Knox, epizonal, such as Donlin Creek, and shear-related, such as Longline and Pogo. The shear-related deposits, because they are structurally focussed, contain much higher gold grades than the other categories. They tend to have equivocal or distal relationships with causative plutons, although they may have plutonic hosts. Their location within shear zones, and features such as tensile vein arrays and ductile shears, ally them with orogenic vein deposits. The Hawk veins fit most closely into this class.

ARE THERE OTHER HAWK VEIN SYSTEMS IN THE NORTHERN HOGEM BATHOLITH?

Regional prospecting in 2002 led to the discovery of two significant, previously undocumented veins hosted by granite of the Osilinka pluton; in a cirque 5 kilometres north of the Hawk property, the Lazy Boy and Far North veins (Figure 2). The Lazy Boy vein strikes 100-125 degrees and

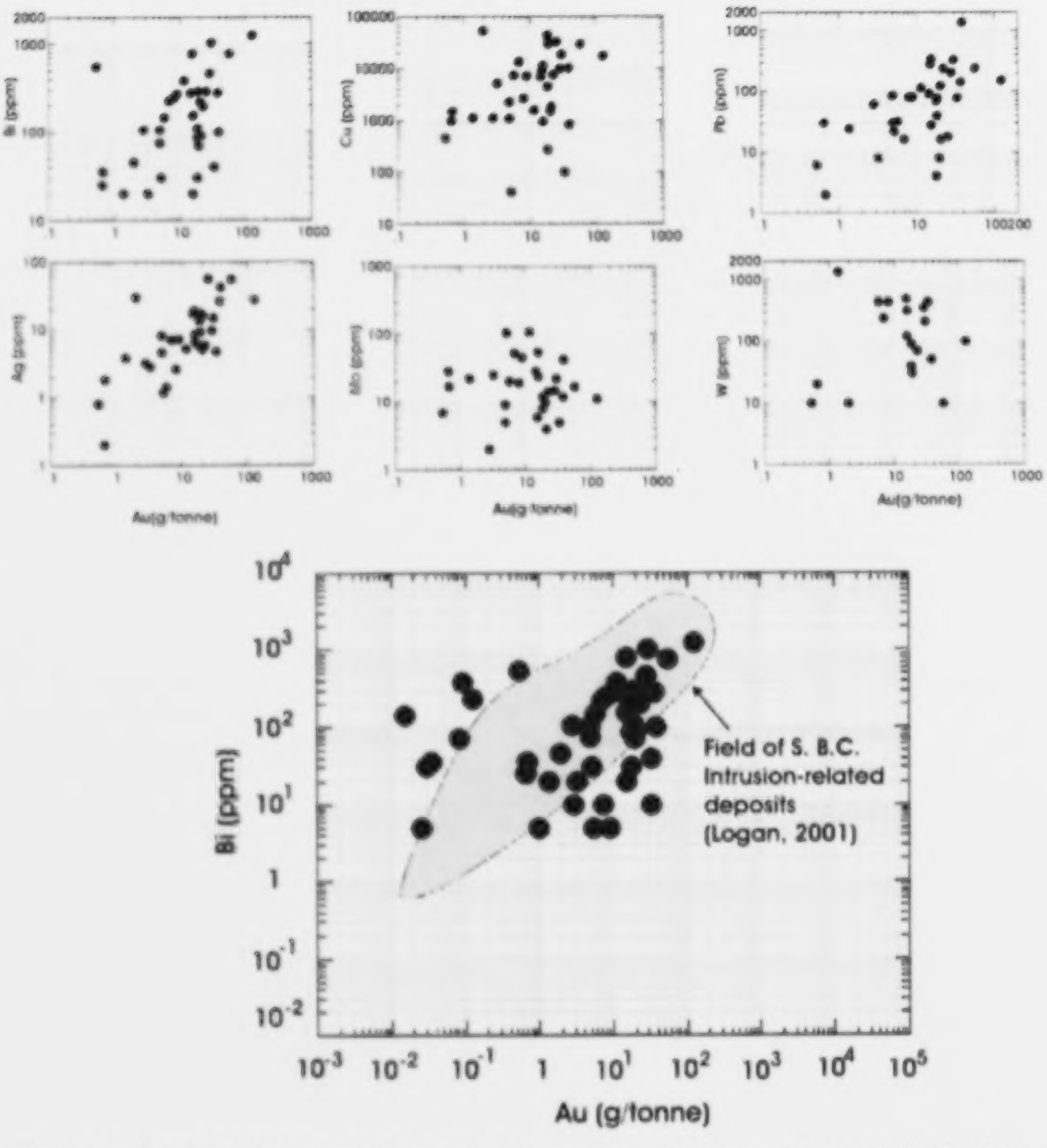

Figure 5. Geochemical correlation diagrams: Hawk vein samples: plotted vs. Au. Data from Redcorp Ventures Ltd.; Eco-Tech Laboratories analysis.

dips gently at 15 to 30 degrees to the south. It forms a low knob in the flat bottom of a subsidiary cirque with a total exposure of approximately 15 by 25 metres and a thickness of between 0.50 and 0.75 metres. White quartz in the vein contains pyrite and traces of galena. The highest grab sample assay from this vein returned 1.78 g/tonne Au and 10.4 g/tonne Ag. The Far North vein occupies a prominent 170° striking shear zone that can be traced over a kilometre. In its main exposure, the quartz vein attains widths of 15 metres, and contains streaks and laminae of pyrite. Extensions can be seen in the cirque floor to the south, and in the headwall of the adjacent cirque to the north. Although only containing trace amounts of gold, a few samples from this outcrop contain anomalous Bi (to 140 ppm) and W (to 340 ppm).

So far, all known vein occurrences are located either within or near one of the granitic Osilinka plutons (Figure 2). This setting may or may not stand up as a "hard" constraint on their distribution. Further exploration should employ air-photo analysis for identifying possible vein-hosting linear structures, in combination with detailed geochemical sampling and prospecting. In comparison to copper-gold porphyry systems, Hawk-type gold-quartz vein systems, with their spatially limited geochemical ha-

TABLE 2
LEAD ISOTOPIC DATA FROM HAWK VEINS

Sample Number	UTM East	UTM North	Mineral	206Pb/ 204Pb	Pb64 %err	207Pb/ 204Pb	Pb74 %err	208Pb/ 204Pb	Pb84 %err	207Pb/ 206Pb	Pb76 %err	208Pb/ 206Pb	Pb86 %err
Flat Vein	332432	6212856	galena	18.8793	0.045	15.6511	0.066	38.6353	0.087	0.8290	0.022	2.0465	0.044
BCR-003	330783	6216117	galena	18.8385	0.043	15.6248	0.065	38.5162	0.087	0.8294	0.022	2.0446	0.043
HK-42	329803	6220532	sphalerite?	18.8940	0.043	15.7579	0.065	38.9881	0.087	0.8340	0.022	2.0635	0.044

Analyses by Janet Gabites, Geochronology Laboratory, Department of Earth and Ocean Sciences, The University of British Columbia.

Results have been normalized using a fractionation factor of 0.15% based on multiple analyses of NBS981 standard lead.

loes and negligible alteration effects, may have been overlooked.

GEOLOGY AND MINERALIZATION ON AND NEAR THE AXELGOLD PROPERTY

On the Axelgold property, disseminated and vein-style, gold-enhanced polymetallic mineralization coincides with a small syenite body. The syenite and its country rocks are bounded to the southwest by the Axelgold Fault (Figures 1, 7). Geological mapping in 2002 focussed on three issues: the extent and nature of the syenite body, the nature and regional correlations of its host rocks, and the displacement history of the Axelgold Fault and its relation to the syenite.

STRATIGRAPHIC FRAMEWORK

The southern Axelgold Range northeast of the Axelgold Fault is underlain by a three northwesterly-elongate fault slivers, each of which comprises a distinct rock unit (Figure 7).

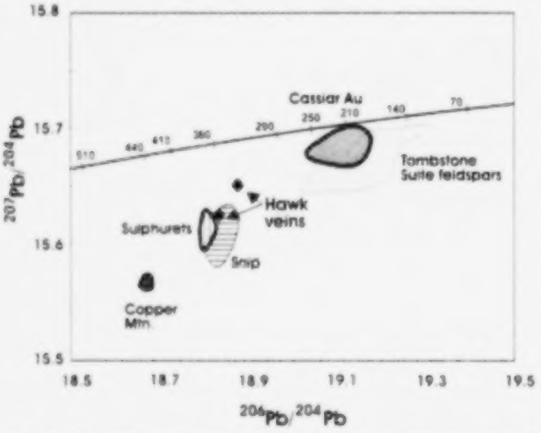

Figure 6. Pb isotopic analyses from Hawk veins. Data sources: Table 2; Bradford (1988), Godwin *et al.* (1988), Mortensen (unpublished data).

They are: 1) synsedimentary breccia, which hosts the syenite; 2) regularily bedded, grey shale and siltstone and green volcanic sandstone and 3) grey, brachiopod-bearing siltstone/shale/pebble conglomerate. All of these units have analogues within Quesnellia. As first noted by Paterson (1974), they do not belong within the Cache Creek Terrane.

The synsedimentary breccia unit is coarse, immature, matrix-supported in areas of relatively low clast density, and rarely bedded. Clasts of grey radiolarian chert and black radiolarian-bearing argillite, limestone, volcanics and ultramafites, occur in a dark grey, graphitic matrix. Sparse, bright green micaceous clasts are probably fuchsite. The argillite clasts tend to be subangular, irregular and flattened, features that suggest they are intraclasts. In one area this sediment-dominated unit grades into a volcanic-dominated facies, in which green and red volcanic and orange-weathering carbonate clasts are surrounded by a green to maroon, tuffaceous matrix. The sedimentary breccia is characterised by significant ductile strain throughout, with strong flattening and elongation of the clasts. Its affinity is uncertain. It differs from the Triassic units of Quesnellia in several significant respects. Most notable is the presence of ultramafic clasts. Some of these are quartz-carbonate altered. Others are remarkably fresh, with clinopyroxene(-spinel) cumulate textures and serpentinized interstitial olivine. They could be derived from the Cache Creek Terrane, as could the radiolarian cherts. Ultramafic clasts occur in the Triassic Tezzeron succession near Pinchi Lake, which Struik *et al.* (2001) included within the Cache Creek Terrane. The volcanic clasts include plagioclase-phyric and equigranular, plagioclase-rich lithologies. Although of probable intermediate island arc affinity, they lack the augite and hornblende phenocrysts that are nearly ubiquitous in the Takla Group. No clasts similar to Cache Creek basalts were seen.

The degree of penetrative strain displayed in the sedimentary breccia unit exceeds both that of the Takla Group regionally, and the degree of strain in the other

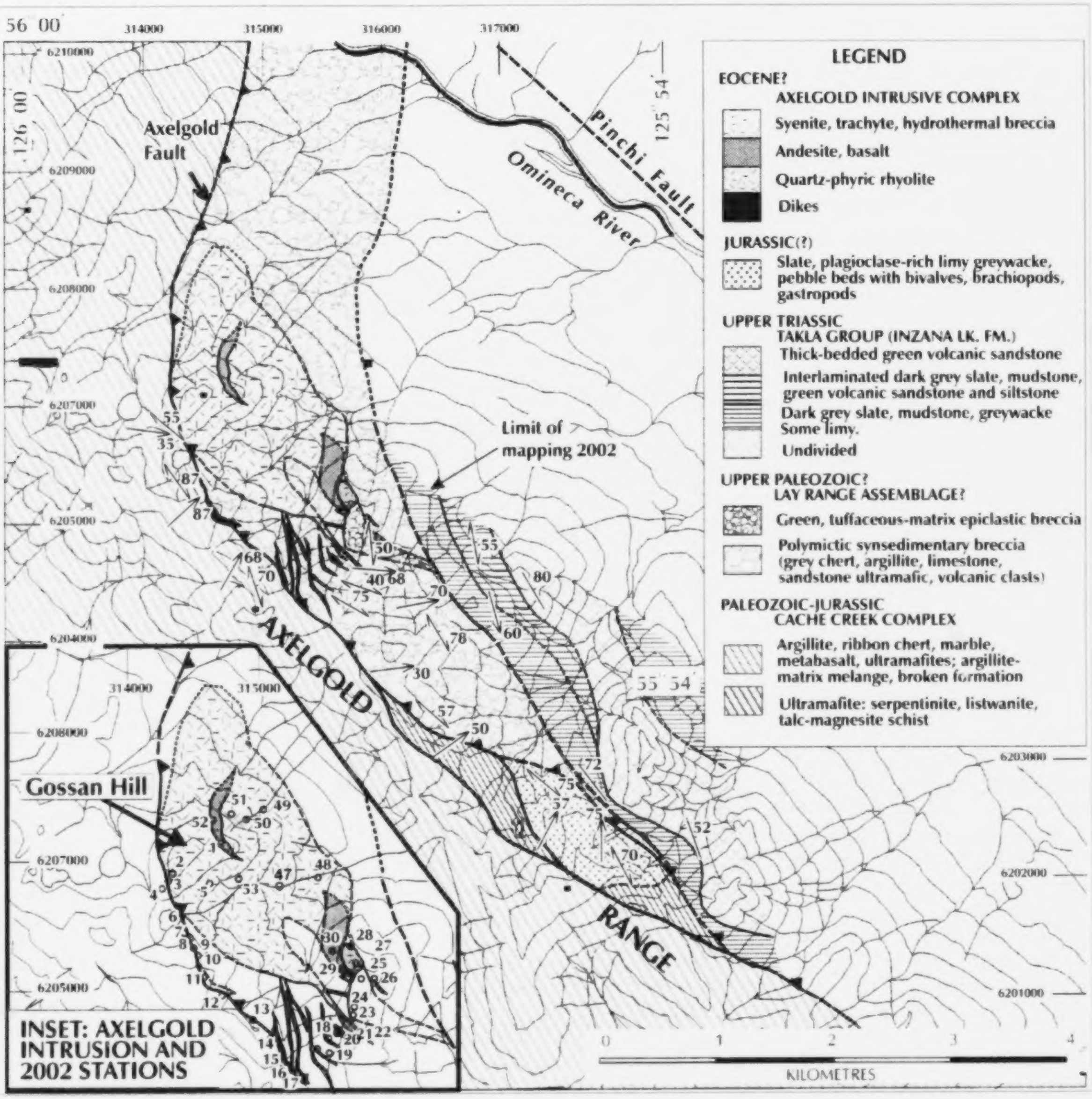
56 00
126 00
125 54
55 54
Axelgold Fault
Pinchi Fault
Omineca River
Limit of mapping 2002
AXELGOLD
RANGE
Gossan Hill
INSET: AXELGOLD INTRUSION AND 2002 STATIONS
KILOMETRES
LEGEND
EOCENE?
AXELGOLD INTRUSIVE COMPLEX
Syenite, trachyte, hydrothermal breccia
Andesite, basalt
Quartz-phyric rhyolite
Dikes
JURASSIC(?)
Slate, plagioclase-rich limy greywacke, pebble beds with bivalves, brachiopods, gastropods
UPPER TRIASSIC
TAKLA GROUP (INZANA LK. FM.)
Thick-bedded green volcanic sandstone
Interlaminated dark grey slate, mudstone, green volcanic sandstone and siltstone
Dark grey slate, mudstone, greywacke Some limy.
Undivided
UPPER PALEOZOIC?
LAY RANGE ASSEMBLAGE?
Green, tuffaceous-matrix epiclastic breccia
Polymictic synsedimentary breccia (grey chert, argillite, limestone, sandstone ultramafic, volcanic clasts)
PALEOZOIC-JURASSIC
CACHE CREEK COMPLEX
Argillite, ribbon chert, marble, metabasalt, ultramafites; argillite-matrix melange, broken formation
Ultramafite: serpentinite, listwanite, talc-magnesite schist

Figure 7. Geology on and near the Axelgold Property. Mapping by J. Nelson 2002.

fault-bounded units locally. It may be of Paleozoic age, part of the Harper Ranch subterrane of Quesnellia. Its provenance requires proximity to sources of oceanic detritus: perhaps it represents the Paleozoic forearc region of Quesnellia, as the Tezzeron succession represents the Triassic forearc.

The second unit is identical to the Inzana Lake formation, the lower unit of the Takla Group in the Nation Lakes area of central Quesnellia (Nelson and Bellefontaine, 1996). Interbedded dark grey shale, siltstone and limy siltstone at its base coarsen upward through thinly interbedded green volcanic sandstone and grey siltstone, into a resistant, cliff- and summit-forming unit dominated by thick-bedded volcanic sandstone (Figure 7). In marked contrast to the homogeneous synsedimentary breccia unit, this sequence is very well bedded. The volcanic sandstones are in places graded, and some of their bases show load casts. They are turbiditic in origin, as evidenced by the incorporation of wispy black shale intraclasts as well as sparse pebble-sized volcanic detritus. They are rich in plagioclase, with fresh, black hornblende and augite grains visible in some samples. Although cleaved, this unit does not show penetrative ductile deformation.

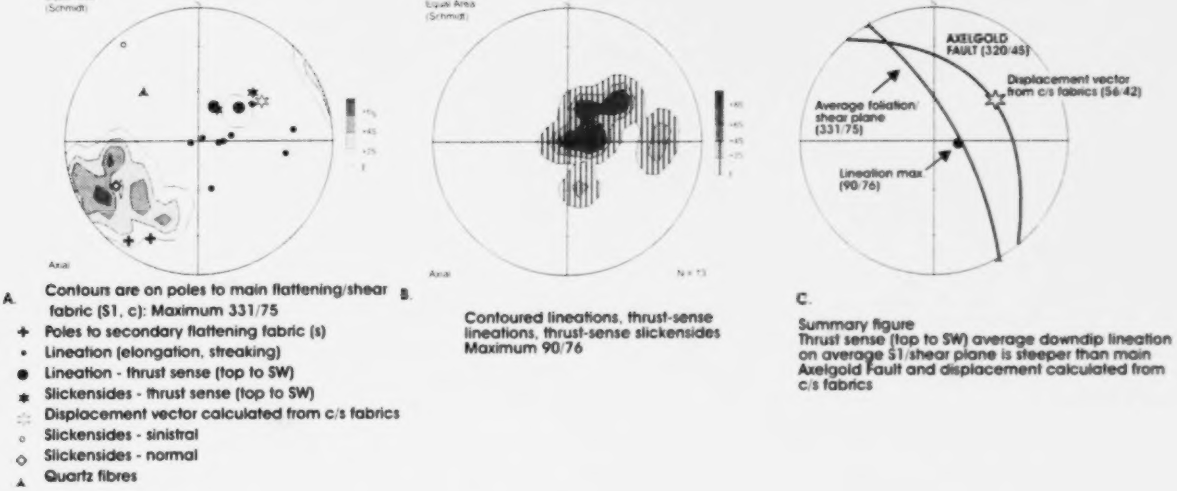

A. Contours are on poles to main flattening/shear fabric (S1, c): Maximum 331/75

- ✚ Poles to secondary flattening fabric (s)
- • Lineation (elongation, streaking)
- ● Lineation - thrust sense (top to SW)
- ✱ Slickensides - thrust sense (top to SW)
- ✡ Displacement vector calculated from c/s fabrics
- ∘ Slickensides - sinistral
- ◇ Slickensides - normal
- ▲ Quartz fibres

B. Contoured lineations, thrust-sense lineations, thrust-sense slickensides Maximum 90/76

C. Summary figure
Thrust sense (top to SW) average downdip lineation on average S1/shear plane is steeper than main Axelgold Fault and displacement calculated from c/s fabrics

Figure 8. Structures on and near the Axelgold property.

The third unit is entirely sedimentary, with no volcanogenic detritus. It comprises limy shale, siltstone, sandstone/greywacke and sandstone with rounded chert pebbles. Fragments of bivalves, brachiopods, and gastropods are very common in parts of this unit, particularily in the coarser, sandy beds. It is cleaved, but neither fossil fragments nor clasts show any flattening. T. Poulton (personal communication, October 2002) notes that the brachiopods, probably rhynchonellids or spiriferids, appear to be generalized, non-diagnostic forms; however a Lower or Middle Jurassic age is reasonable. In central Quesnellia and the Cache Creek Terrane, pre-Jurassic shallow-water shelly faunas are rare. This unit occurs in a structural panel with Cache Creek ultramafic rocks, west of the main Axelgold Fault (Figure 7). It could be a late-stage, syn-accretionary overlap sequence similar to the Bowser Lake Group, or Toarcian sedimentary rocks of central Quesnellia (Nelson and Bellefontaine, 1996).

STRUCTURE

The most prominent structure in the southern Axelgold Range is the steeply northeast-dipping Axelgold Fault, which here separates Quesnellia from the Cache Creek Terrane. Numerous shear and subsidiary faults imbricate the rocks on both sides of the main fault. Regional geological relationships (Figure 1) imply that the Axelgold Fault is an early structure, cut off by the main strand of the Pinchi Fault.

Small-scale linear features range from ductile to brittle in origin. They include clast elongation in the synsedimentary breccia, mineral lineations in carbonatized ultramafites, and slickensides. With rare exceptions, these lineations plunge steeply to the northeast, indicating primarily dip-silp movement (Figure 8).

Where motion sense indicators are present, such as steps on slickensided surfaces, c-s fabrics and shear bands, they indicate top-to-the-southwest, thrust-sense motion on the Axelgold Fault and within the rock masses around it. A few shallowly-plunging sinistral, and no dextral indicators were observed. Given that the Cretaceous-Tertiary history of the Pinchi Fault involved regional dextral motion (Gabrielse, 1985), it is reasonable that the Axelgold Fault and its surrounding rocks preserve the record of an earlier, proto-Pinchi thrust motion history, perhaps analogous to the area around Pinchi Lake (Struik *et al.*, 2001).

Rocks of the Axelgold intrusive complex are unfoliated and unsheared. Dikes of the complex follow and fill shears developed within the synsedimentary breccia unit (Figure 9).

On the other hand, the complex is confined to the panel northeast of the Axelgold Fault. Dikes approach the fault but do not cross it. This may be due to late reactivation of the fault, rock competency contrasts between the Cache Creek argillites and serpentinites *versus* the brittle synsedimentary breccia, or both.

THE AXELGOLD INTRUSIVE COMPLEX AND ITS ASSOCIATED ALTERATION AND MINERALIZATION

The Axelgold intrusion is a northwesterly-trending, composite intrusive body, 3 kilometres long by over a kilometre wide, centred on a ridge informally called "Gossan Hill", where spectacular iron-streaked ridge-top exposures rise out of heaps of orange talus. The margins of the body dip steeply northeast, controlled by the structural fabric of its country rocks. Dike swarms both cut and extend southeastward from the main body, in some cases following shear planes in the host synsedimentary breccia. Syenitic phases are predominant, ranging from porphyryitic with Kspar megacrysts, through finer grained to aphanitic. Small biotite books distinguish the later dikes from the main intrusion. One unusual phase, a quartz-phyric rhyolite with square to rounded, embayed phenocrysts, forms a small pluglike body in the southeastern part of the complex (Figure 7).

Intrusive rocks tend to be strongly altered, with abundant secondary sericite, ankeritic carbonate and Kspar (C. Leitch, petrographic report for Rubicon Minerals, October, 2002). Green microporphyritic andesite or trachyandesite phases show comparatively weaker alteration. A significant proportion of the intrusion shows breccia textures, in which intrusive fragments are surrounded by a clastic matrix. The breccias range from coarse-textured (fragments > 10 cm) to very finely comminuted. Some are monolithologic; others are polymictic, containing a mixture of clasts from different intrusive phases, for instance megacrystic and fine grained equigranular syenites and trachytes. Crystal clasts of Kspar and lesser embayed, igneous quartz are also present, particularily in the finer grained breccias. Multi-episodic brecciation is shown by breccia clasts surrounded by breccia matrix.

The microscopic textures of these breccias are compatible with either an intrusive-hydrothermal, or alternatively a surface, pyroclastic origin (C. Leitch, petrographic report for Rubicon Minerals, October, 2002). Field characteristics and relationships of the breccias clearly favor the hydrothermal, intrusive option. The breccias occur wholly within the Axelgold intrusive complex, and their clasts are solely derived from syenites, trachytes and rhyolites of the complex. They share alteration assemblages with the rest of the complex. Overall morphologies of the breccia bodies are roughly tabular and steeply northeast-dipping, similar to the shapes of individual intrusions of the complex (Allen, 2002). In detail, breccia zones in core cut across unshattered syenite. So far, the only dikes that have been observed to cross-cut the breccias belong to the late-stage, relatively unaltered andesite group; although the biotite-phyric trachytes do not appear to be brecciated. These characteristics suggest that hydrothermal brecciation occurred within the syenite complex, probably during the later stages of its emplacement.

Gold mineralization within the Axelgold syenite complex is of disseminated to stringer, and rarely vein style. Higher gold values tend to be associated with the Kspar-biotite-plagioclase monzonite dikes. Mineralization comprises quartz, carbonate, fluorite, pyrite, chalcopyrite, chalcocite, ?tetrahedrite, galena, stibnite, and a bright green micaceous mineral that has not yet been positively identified. Microscopically, it consists of fine grained, greenish sericite-like masses that in some cases surround opaque material, possibly magnetite replacing chromite grains. A rock sample containing roughly 5% of this mineral returned low values of vanadium (9 ppm) and chromium (68 ppm). These low abundances fail to support identification of either the vanadium mica roscoelite or the chromium mica fuchsite. On the other hand, anomalous gold values in surface rock samples correlate with vanadium (*see* below).

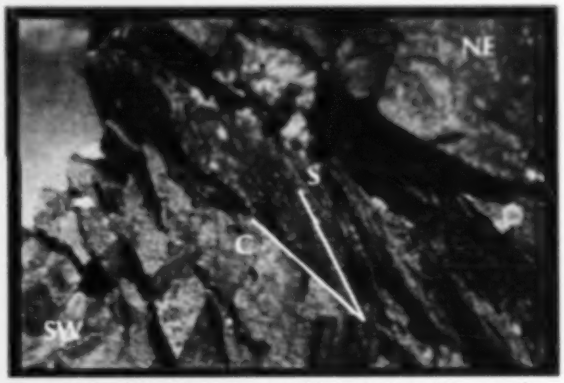

Figure 9. Trachyte dike cutting c-s fabrics in the sedimentary breccia unit, Axelgold property.

PETROCHEMISTRY OF THE AXELGOLD INTRUSIVE COMPLEX

Because of the intense, pervasive alteration within the Axelgold complex, whole-rock analytical data is of little use for igneous rock characterization. Mineralogically, the complex is dominantly syenitic with subordinate monzonite and granite phases. Relict igneous features indicative of felsic alkalic composition include the predominance of orthoclase phenocrysts with little quartz and plagioclase; and trachytic as well as equigranular, Kspar-rich matrix textures. However , to characterize these rocks in detail, immobile trace element chemistry is the tool of choice. Five representative samples were analysed for immobile elements, including rare earths (Table 3). Key plots are shown on Figure 10.

On the Zr/Ti vs. Nb/Y discrimant diagram of Winchester and Floyd (1977), Axelgold syenites plot in the alkalic, comendite-pantellerite field. They contrast with the mildly alkalic, shoshonitic arc rocks of Quesnellia, which plot in the subalkaline field on this diagram. The Axelgold syenites are highly enriched in light rare earths (Figure 10). They are similar to monzonites of the Eocene Glover stock on the Lustdust property, but unlike the more mildly LREE-enriched Jurassic Hogem batholith. This evidence, although not conclusive, suggests that the Axelgold complex and Glover stock are part of an Eocene alkalic belt that parallels the Pinchi Fault.

DEPOSIT MODELLING

Gold mineralization within the Axelgold syenite complex offers intriguing parallels with other alkalic-related

TABLE 3
PETROCHEMICAL DATA FROM AXELGOLD SYENITE

Sample	Description	UTM-east	UTM-north	SiO2	TiO2	Al2O3	Fe2O3	MnO	MgO	CaO	Na2O	K2O	P2O5	LOI	SUM	Y*	Zr*	Nb*	Rb*	Sr*
AX02-11-22.86 m	Syenite; medium to coarse-grained porphyry	314607	6206694	69.50	0.30	14.69	2.24	0.03	0.89	0.32	4.29	4.63	0.08	2.53	99.83	19	230	20	150	600
AX02-14-25.91 m	Syenite intrusion breccia	314375	6206680	63.03	0.63	15.06	4.38	0.08	1.76	0.73	1.65	6.81	0.29	5.03	99.44	36	370	30	244	600
AX02-14-174.69 m	Syenite; medium to coarse-grained porphyry	314391	6206764	71.22	0.29	14.44	2.01	0.01	0.31	0.24	4.31	4.72	0.09	2.09	99.90	20	240	20	137	700
AX02-09- 56.2 m	Orthoclase-plagioclase-biotite porphyry	315549	6206606	56.86	0.88	14.48	5.79	0.08	3.09	4.49	4.16	5.18	0.48	4.12	99.22	30	230	20	140	1200
AX02-13- 53.5 m	Syenite; megacrystic	314336	6206955	59.19	0.51	16.76	3.93	0.07	1.15	1.79	3.74	7.56	0.16	4.51	99.38	40	620	40	196	1600

Sample	Ba*	V	Th	La	Ce	Pr	Nd	Sm	Eu	Gd160	Tb	Dy	Ho	Er	Tm	Yb	Lu
AX02-11-22.86 m	2000	11.4	20	51.5	93.9	9.7	34.8	5.9	1.7	5.4	0.6	2.3	0.3	1	0.1	0.8	0.1
AX02-14-25.91 m	3700	24.9	28	82.5	156.5	17.1	65.2	11.5	3.3	10.6	1.2	5.1	0.8	2.3	0.3	1.8	0.3
AX02-14-174.69 m	2500	10.3	19	41.6	75.2	7.7	27.7	4.6	1.3	4.3	0.5	2	0.3	0.9	0.1	0.7	0.1
AX02-09-56.2 m	1300	22.2	19	67.1	134	15.6	62.1	11.6	3.1	9.6	1.1	4.8	0.7	2.1	0.2	1.5	0.2
AX02-13-53.5 m	1200	27.7	61	104.5	183	19.3	68.8	11.6	3.1	10.1	1.1	4.9	0.8	2.5	0.3	2.2	0.3

Oxides: X-ray fluorescence, ALS CHEMEX Laboratories * = Pressed pellet-XRF; ALS CHEMEX

Other traces: Lithium metaborate fusion, Mass spectrometer, ALS CHEMEX

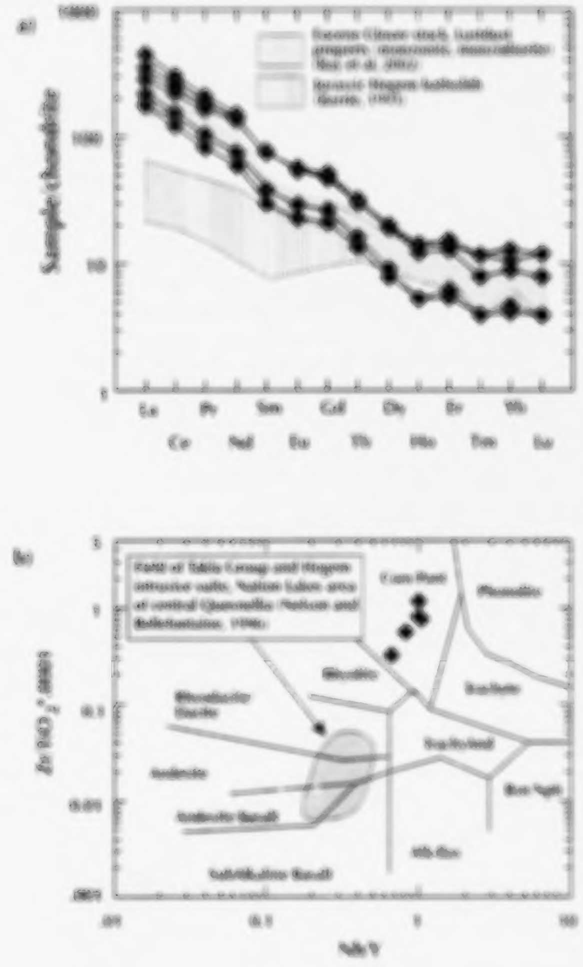

Figure 10. Petrochemical characterization of the Axelgold syenite complex. b) Winchester and Floyd, 1977.

Au deposits worldwide (Mutschler and Mooney, 1993; Schroeter and Cameron 1996). Most important are the well-developed hydrothermal breccias, similar to those described in the Tertiary epithermal systems at Cripple Creek (Thompson *et al.*, 1985), Golden Sunlight (Porter and Ripley, 1985), and Montana Tunnels (Sillitoe *et al.*, 1985). Additional features include widespread carbonate alteration (Taylor, 1987); the presence of green sericite, which may be in part the vanadium mica roscoelite; Au associated with quartz, carbonate, fluorite, pyrite, chalcopyrite, tetrahedrite, galena and stibnite; and a geochemical association with Sb, As, Cu, Zn, Mo, and Pb (Kaip, 2002; and this paper). The geochemical signature of the Axelgold system shows moderately anomalous gold correlating with V, Sb, As, Cu, and Zn (Figure 11).

The alkalic-related suite embraces a wide variety of deposit types and associations, from epithermal mineralization at Lihir, the Emperor Mine (Anderson and Eaton, 1990), Porgera (Richards, 1992) and Cripple Creek, to mesothermal Au-quartz veins at Kirkland Lake (Cameron, 1990), to a possible linkage with Au-Cu porphyries. The locus of mineralization may be within intrusive rocks, as at Porgera, in calderas as at Lihir , the Emperor Mine, and Cripple Creek, or along regional structures, as at Kirkland Lake. Evaluation of exploration parameters rests entirely on the geological setting of the individual deposit: the alkalic association alone is not predictive in terms of local controls on mineralization or the discovery of additional prospects.

Petrochemical affinities between the Axelgold syenite and Glover stock suggest that they could represent a belt of small, high-level intrusions, possibly a previously-unrecognized eastern, alkalic extension of the Babine porphyry belt (Ray *et al.*, 2002; J. Oliver, personal communication, August 2002). A number of small felsic and porphyritic intrusions near Humphrey Lake (*see* Schiarizza, 2000) may also belong to this group. Two known prospects establish the gold potential of the belt: Au skarns and mantos at the Lustdust (Ray *et al.*, 2002), and diffuse, low-grade gold at Axelgold. Given the small footprints of the host intrusions, it is entirely possible that others may be found.

CONCLUSIONS: NEW IDEAS, NEW DIRECTIONS

This project has added to the repertoire of gold exploration target types in central British Columbia. A series of vein discoveries on the Hawk property in 2002 demonstrates the potential of the northern Hogem batholith for high grade, gold-only, in addition to porphyry-style copper-gold targets. The geochemical character of the veins, for instance the gold-bismuth correlation, suggests that they may fit broadly into the category of intrusion-related gold occurrences. Significant differences between the Hawk and well-documented Cretaceous deposits of the Fairbanks and Tombstone districts, for instance location within a primarily Jurassic batholith, lack of associated arsenic and strong structural control, may expand the search parameters for intrusion-hosted gold in the Canadian Cordillera.

The dating of the Glover stock as Eocene (Ray *et al.*, 2002) and the recognition in this study of affinities between it and the Axelgold syenite offers a new potential belt of Au-enriched alkalic intrusions west of the Pinchi Fault.

ACKNOWLEDGEMENTS

Gord Allen and Dave Kamisi, consulting geologists for Rubicon, contributed significantly to the development of ideas on the Axelgold property, particularly the extent and significance of the intrusive breccias. We thank Janet Gabites for timely and important lead isotopic analyses that have advanced our knowledge of the Hawk vein system. Wes Luck, third generation pilot, provided safe, efficient helicopter service between clouds and crags.

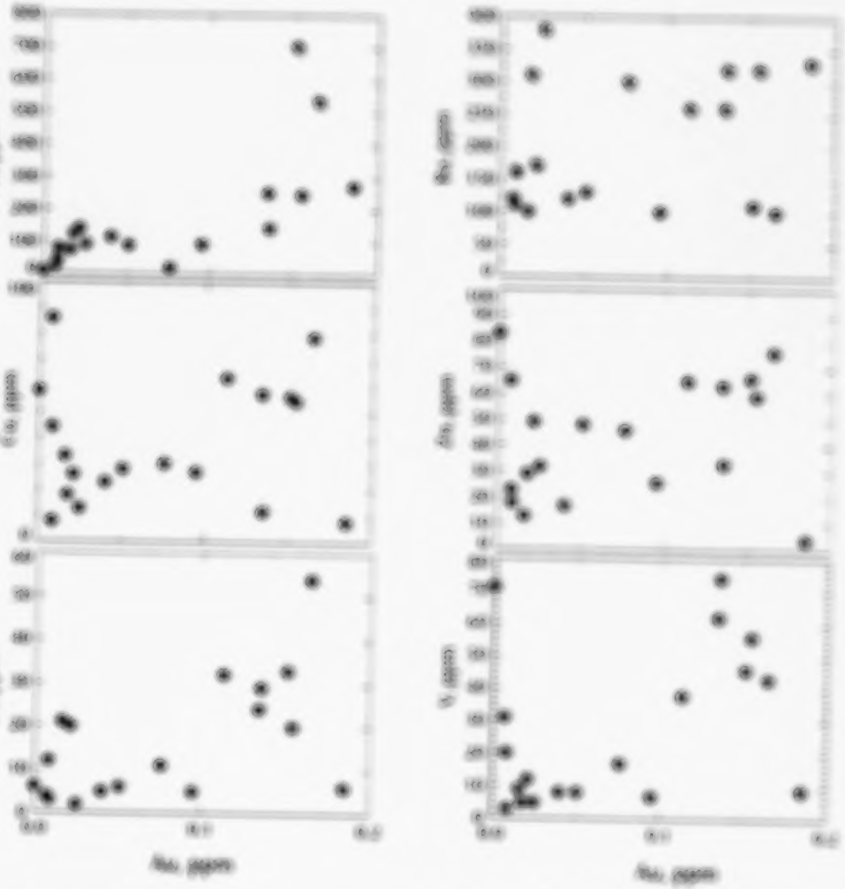

Figure 11. Geochemical correlation diagrams: Voelgold vein samples plotted vs. Au. Data from surface grab samples, Rubicon Minerals Corp. Intermediate values only plotted; actual gold values up to 4.95 ppm (analyses by ALS CHEMEX).

REFERENCES

Allen, G. (2002): Report on the 2002 diamond drilling program on the Voelgold Property, Omineca Mining Division, B.C. NTS 93N/11W, for Rubicon Minerals Corp.; *B.C. Ministry of Energy and Mines* Assessment Report, submitted.

Anderson, W.B. and Eaton, P.C. (1990): Gold mineralization at the Emperor Mine, Vatukoula, Fiji; *Journal of Geochemical Exploration*, Volume 36, pages 267-296.

Armstrong, R.L., Monger, J.W.H. and Irving, E. (1985): Age of magnetization of the Voelgold Gabbro, north-central British Columbia; *Canadian Journal of Earth Sciences*, Volume 22, pages 1217-1222.

Barrie, C.T. (1993): Petrochemistry of shoshonitic rocks associated with porphyry copper-gold deposits of central Quesnellia, British Columbia, Canada; *Journal of Geochemical Exploration*, Volume 48, pages 225-258.

Bradford, J.A. (1988): Geology and genesis of the Midway silver-lead-zinc deposit, north-central British Columbia; Unpub. M.Sc. thesis, *The University of British Columbia*, 290 pages.

Cameron, E. (1990): Alkaline magmatism at Kirkland Lake, Ontario: product of strike-slip orogenesis; *in* Current Research, Part C, *Geological Survey of Canada*, Paper 90-1C, pages 261-269.

Gabrielse, H. (1985): Major dextral transcurrent faults along the northern Rocky Mountain Trench and related lineaments in north-central British Columbia; *Geological Society of America* Bulletin, Volume 96, pages 1-14.

Garnett, J.A. (1978): Geology and mineral occurrences of the southern Hogem Batholith; *British Columbia Ministry of Mines and Petroleum Resources*, Bulletin 70, 67 pages.

Godwin, C.I., Gabites, J.E. and Andrew, A. (1988): Leadtable: a galena lead isotope data base for the Canadian Cordillera, with a guide to its use by explorationists; *British Columbia Ministry of Energy, Mines and Petroleum Resources*, Paper 1988-4.

Hart, C.J.R., McCoy, D.T., Goldfarb, R.J., Smith, M., Roberts, P., Hulstein, R., Bakke, A.A. and Bundtzen, T.K. (2002): Geology, exploration and discovery in the Tintina Gold Province, Alaska and Yukon; *Society of Economic Geologists*, Special Publication 9, pages 241-274.

Irvine, T.N. (1976): Studies of Cordilleran gabbro and ultramafic intrusions, British Columbia; *in* Current Research Part A, *Geological Survey of Canada*, Paper 76-1A, pages 75-81.

Jiang, X.D. and Harley, T.D. (1996): Voelgold prospect: Report on the 1996 exploration program for Cyprus Canada Inc.; *B.C. Ministry of Energy and Mines*, Assessment Report 24,726, 17 pages.

Kemp, R. (2002): Exploration memo and data synthesis: Verdigold property, north-central British Columbia; private report for Redhawk Minerals Corporation.

Lang, J.R. and Baker, T. (2001): Intrusion-related gold systems: the present level of understanding; *Mineralium Deposita*, Volume 36, pp. 477-489.

Logan, J.M. (2001): Prospective areas for intrusion-related gold-quartz veins in southern B.C.; in Geological Fieldwork, *British Columbia Ministry of Energy and Mines*, Paper 2001-1, pages 231-252.

McAdam, R. (1998): Geological and lithogeochemical report on the Verdigold property: 1997 exploration program for Redhawk Minerals Corporation; *British Columbia Ministry of Energy and Mines*, Assessment Report 25407, 17 pages.

Mutschler, F.E. and Mooney, T.C. (1993): Precious-metal deposits related to alkalic igneous rocks: provisional classification, grade-tonnage data and exploration frontiers; in Kirkham, R.V., Sinclair, W.D., Thorpe, R.I. and Duke, J.M., eds., Mineral Deposit Modeling, *Geological Association of Canada*, Special Paper 40, pages 479-520.

Nelson, J.L. and Bellefontaine, K.A. (1996): The geology and mineral deposits of north-central Quesnellia; Tezzeron Lake to Discovery Creek, central British Columbia; *British Columbia Ministry of Energy, Mines and Petroleum Resources*, Bulletin 99, 112 pages.

Paterson, I.A. (1973b): Geology of the Cache Creek Group and Mesozoic rocks at the northern end of the Stuart Lake belt, British Columbia; in Current Research, Part B, *Geological Survey of Canada*, Paper 73-1B, pages 31-42.

Porter, E.W. and Ripley, E. (1985): Petrologic and stable isotope study of the gold-bearing breccia pipe at the Golden Sunlight Deposit, Montana; *Economic Geology*, Volume 80, pages 1689-1706.

Ray, G., Webster, I., Megaw, P., McGlasson, J. and Glover, K. (2002): The Lustdust Property in central British Columbia: a polymetallic zoned porphyry-skarn-manto-vein system; in Geological Fieldwork, *British Columbia Ministry of Energy and Mines*, Paper 2002-1, pages 257-280.

Richards, J.P. (1995): Magmatic-epithermal transitions in alkalic systems: Porgera gold deposit, Papua New Guinea; *Geology*, Volume 23, pages 547-550.

Schiarizza, P., compiler (2000): Old Hogem (Western Part) (NTS 93N/11, 12, 13) Bedrock Geology; B.C. *Ministry of Energy and Mines*, Open File 2000-33, Scale 1:100 000.

Schroeter, T.G. and Cameron, R. (1996): Alkalic intrusion-associated Au-Ag; in Lefebure, D.V. and Hõy, T., eds., B.C. Mineral Deposit Profiles, Volume 2; *British Columbia Ministry of Energy, Mines and Petroleum Resources*, Paper 1996-13, pages 49-51.

Sillitoe, R.H., Grauberger, G.L. and Elliott, J.E. (1985): A diatreme-hosted gold deposit at Montana Tunnels, Montana; *Economic Geology*, Volume 80, pages 1707-1721.

Stevenson, D.B. (1991): A geological, geochemical, geophysical and diamond drilling report on the Hawk property, Germansen Landing area, central British Columbia, Omineca Mining Div.; *British Columbia Ministry of Energy, Mines and Petroleum Resources*, Assessment Report 21012, 20 pages.

Struik, L.C., Schiarizza, P., Orchard, M.J., Cordey, F., Sano, H., MacIntyre, D.G., Lapierre, H. and Tardy, M. (2001): Imbricate architecture of the upper Paleozoic to Jurassic oceanic Cache Creek Terrane, central British Columbia; *Canadian Journal of Earth Sciences*, Volume 38, pages 495-514.

Taylor, A.B. (1987): Geology of the central Verdigold Property, B.C. *Ministry of Energy and Mines*, Assessment Report 15936, for Imperial Metals Corporation, 20 pages.

Thompson, T.B., Trippel, A.D. and Dwelley, P.C. (1985): Mineralized veins and breccias of the Cripple Creek district, Colorado; *Economic Geology*, Volume 80, pages 1669-1688.

Winchester, J.A. and Floyd, P.A. (1977): Geochemical discrimination of different magma series and their differentiation products using immobile elements; *Chemical Geology*, Volume 20, pages 325-343.

Woodsworth, G.J. (1976): Plutonic rocks of McConnell Creek (94D West Half) and Aiken Lake (94C East Half) map-areas; in Current Research Part A, *Geological Survey of Canada*, Paper 76-1A, pages 69-73.

Woodsworth, G.J., Anderson, R.G. and Armstrong, R.L. (1991): Plutonic regimes, Chapter 15; in Geology of the Cordilleran Orogen in Canada, H. Gabrielse and C.J. Yorath, eds., *Geological Survey of Canada*, Geology of Canada, no. 4, pages 491-531 (also *Geological Society of America*, The Geology of North America, v. G-2).

Use of Spinel in Mineral Exploration: The Enigmatic Giant Mascot Ni-Cu-PGE Deposit – Possible Ties to Wrangellia and Metallogenic Significance

By Graham T. Nixon

KEYWORDS: Giant Mascot, spinel, [illegible]

INTRODUCTION

[illegible]

[illegible]

THE PETROGENETIC SPINEL DATABASE

[illegible]

GIANT MASCOT Ni-Cu-PGE DEPOSIT

[illegible]

[illegible]

[illegible]

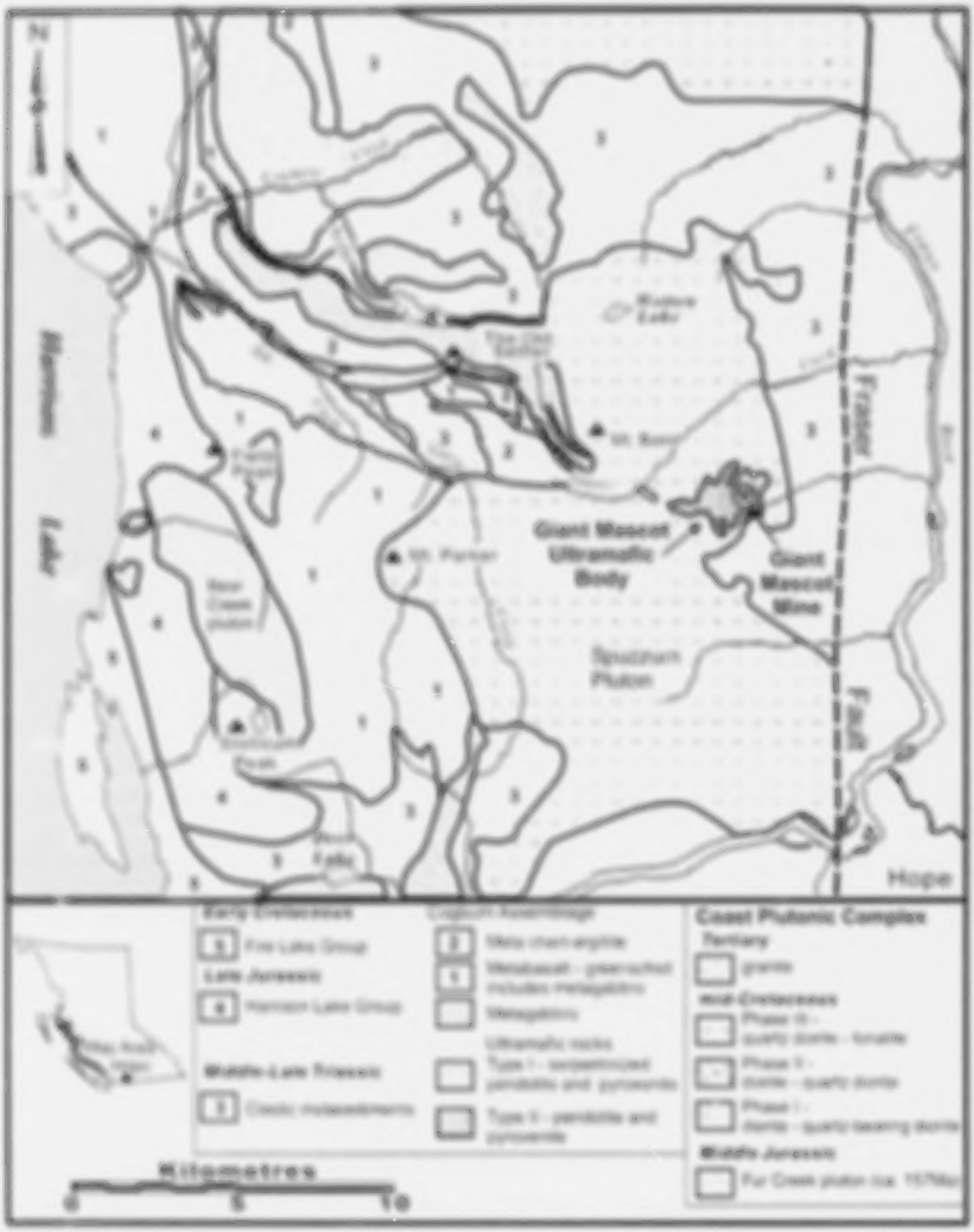

Harrison Lake
Fraser Fault
Giant Mascot Ultramafic Body
Giant Mascot Mine
Spuzzum Pluton
Hope
Bear Creek pluton
Early Cretaceous
5 Fire Lake Group
Late Jurassic
4 Harrison Lake Group
Middle-Late Triassic
3 Clastic metasediments
Cogburn Assemblage
2 Meta chert-argillite
1 Metabasalt - greenschist includes metagabbro
Metagabbro
Ultramafic rocks
Type I - serpentinized peridotite and pyroxenite
Type II - peridotite and pyroxenite
Coast Plutonic Complex
Tertiary
granite
mid-Cretaceous
Phase III - quartz diorite - tonalite
Phase II - diorite - quartz diorite
Phase I - diorite - quartz-bearing diorite
Middle Jurassic
Fir Creek pluton (ca. 157Ma)
Kilometres
0
5
10

Figure 1. Location and geologic setting of the former Giant Mascot Ni-Cu-PGE mine, southern British Columbia (after Ash, 2002).

Cockfield and Walker, 1933; Aho, 1956; McLeod *et al.*, 1976); and the ultramafic rocks were once considered to be an early differentiate of the calc-alkaline Spuzzum Pluton (*e.g.* McLeod *et al.*, 1976). This conclusion appears difficult to reconcile with the common association of Ni-Cu-PGE sulphide ores with tholeiitic magmatic environments (*e.g.* Hulbert, 2001). The most recent geological investigations have concluded that the Giant Mascot ultramafic body is intruded by, and therefore older than, Spuzzum diorite, and represents either a partially engulfed ophiolite fragment analogous to those farther west (*i.e.* the Cogburn Assemblage (Ash, 2002; Fig. 3); or serves as a host to "gabbro-related" magmatic sulphide ores of unknown age and origin (Pinsent 2002).

PETROTECTONIC SETTING OF GIANT MASCOT

SPINEL DATA

The compositions of chrome spinels occurring in ultramafic rocks and ores at Giant Mascot provide information that is directly relevant to the origin of the ultramafic body and thus independent of interpretations regarding external geological relationships.

In his study of the 4600 Level ore body, Muir (1971) made a number of electron-microprobe analyses of spinel grains in both ore-bearing and barren pyroxenites and peridotites, including olivine- and clinopyroxene-bearing hornblende orthopyroxenites and hornblende harzburgites and their sulphide-rich equivalents. The amount of amphibole in these rocks appears unique to the 4600 Level orebody when compared to the more olivine-enriched ores described by Aho (1956). The mineralized samples contain variable proportions of ferromagnesian silicates and Fe-Ni and Cu sulphides, and ores typically exhibit semi-massive to blebby to net-textured sulphides. The analyzed spinels include euhedral grains in unaltered olivine and orthopyroxene as well as a random sampling of grains whose host mineral is not specified. The quality of the electron-probe analyses is difficult to assess: some minor elements were not determined (Mn, Zn and V); oxide totals are generally high (range = 98.3-104.2 wt %; arithmetic mean = 101.3 wt %) but vary slightly depending on the details of the Fe_2O_3 recalculation procedure; at the very least, the analyses do appear to be consistent with spinel stoichiometry.

SPINEL PLOTS

The compositions of Giant Mascot (GM) spinels are shown below in three diagrams based on standard projections of the spinel prism: a triangular Cr-Al-Fe^{3+} plot representing projection onto the face of the prism and cation ratio plots of $Cr/(Cr+Al)$ (or Cr#) and $Fe^{3+}/(Cr+Al+Fe^{3+})$ (or Fe3#) vs $Fe^{2+}/(Mg+Fe^{2+})$ (or Fe2#), and a fourth plot of TiO_2 vs $Fe^{2+}/(Mg+Fe^{2+})$ (Ti plot). Data density contours for selected categories or subcategories of spinel compositions in the global database are also shown at the 50th and 90th percentiles (*i.e.* 50% and 90%, respectively, of analyses in the category/subcategory of the database fall within these contours).

Figure 2 compares GM spinels with the composition of spinels in metamorphic terranes at greenschist, amphibolite and higher grades of metamorphism. From details of compositional zoning given by Muir (1971), it is clear that some GM spinel grains support rims and/or areas of secondary magnetite and "ferritchromit" that fall at the Fe3+ apex or close to the Cr-Fe3+ join, respectively, in the triangular plot, and have similar compositions to metamorphic spinels (Fig. 2d provides the best discriminant).

Spinels that last equilibrated with Fe-Ni sulphides are compared to GM spinel compositions in Figure 3. The latter are clearly displaced from the global array in the triangular and Cr# plots, and very few GM spinel grains appear to have equilibrated with magmatic sulphide. Clearly, the overall curvilinear trends of GM spinels in these plots appear consistent with trends formed at high temperatures during crystal-liquid equilibration and subsolidus exchange reactions between spinel and its host silicate phase. It is valid, therefore, to compare the trends of GM spinels with those in the global database to derive information regarding their igneous affiliation.

Figures 4-6 show the compositional fields for spinels derived from ultramafic-mafic rocks in selected oceanic environments and include ocean floor (abyssal) peridotites, ophiolites (including tectonized peridotites and ultramafic-mafic cumulates), and high-pressure, high-temperature "Alpine" peridotites. Relative to oceanic rocks, GM spinels contain significantly higher Fe^{3+}, and in the Cr# and Fe3# plots spinel compositions are displaced to higher Fe^{2+}.

Figure 7 examines potential relationships with Alaskan-type ultramafic intrusions. Although the Ti plot shows a reasonable correspondence with GM spinels, the latter trend is displaced towards higher Fe2# on the Cr# and Fe3# plots. In addition, the triangular plot shows a clear distinction between GM and Alaskan-type spinels which lie closer to the Cr-Fe^{3+} join. This observation is also supported by the presence of cumulus orthopyroxene at Giant Mascot since this phase is typically absent in Alaskan-type ultramafic complexes.

Comparisons with spinels from layered intrusions are shown in Figure 8. All of these plots (Fig. 8a-d) show a close overall correspondence between spinels from layered intrusions and the GM spinel trend. Small aberrations are apparent in the Cr# plot where three GM spinel analyses fall outside the 90th percentile contour (Fig. 8c), and on the Ti plot where a cluster of spinel analyses fall within a population density minimum (Fig. 8b).

The fields for subvolcanic intrusions in flood basalt provinces are shown in Figure 9. As with layered intrusions, there is good overall agreement between the GM spinel trend and the global array. The population density minimum in the Ti plot is no longer evident although there is a slightly greater discrepancy in the Cr# plot for low Cr# GM spinels. This category of spinels, and those from layered intrusions, represent the closest analogues to the compositions of GM spinels.

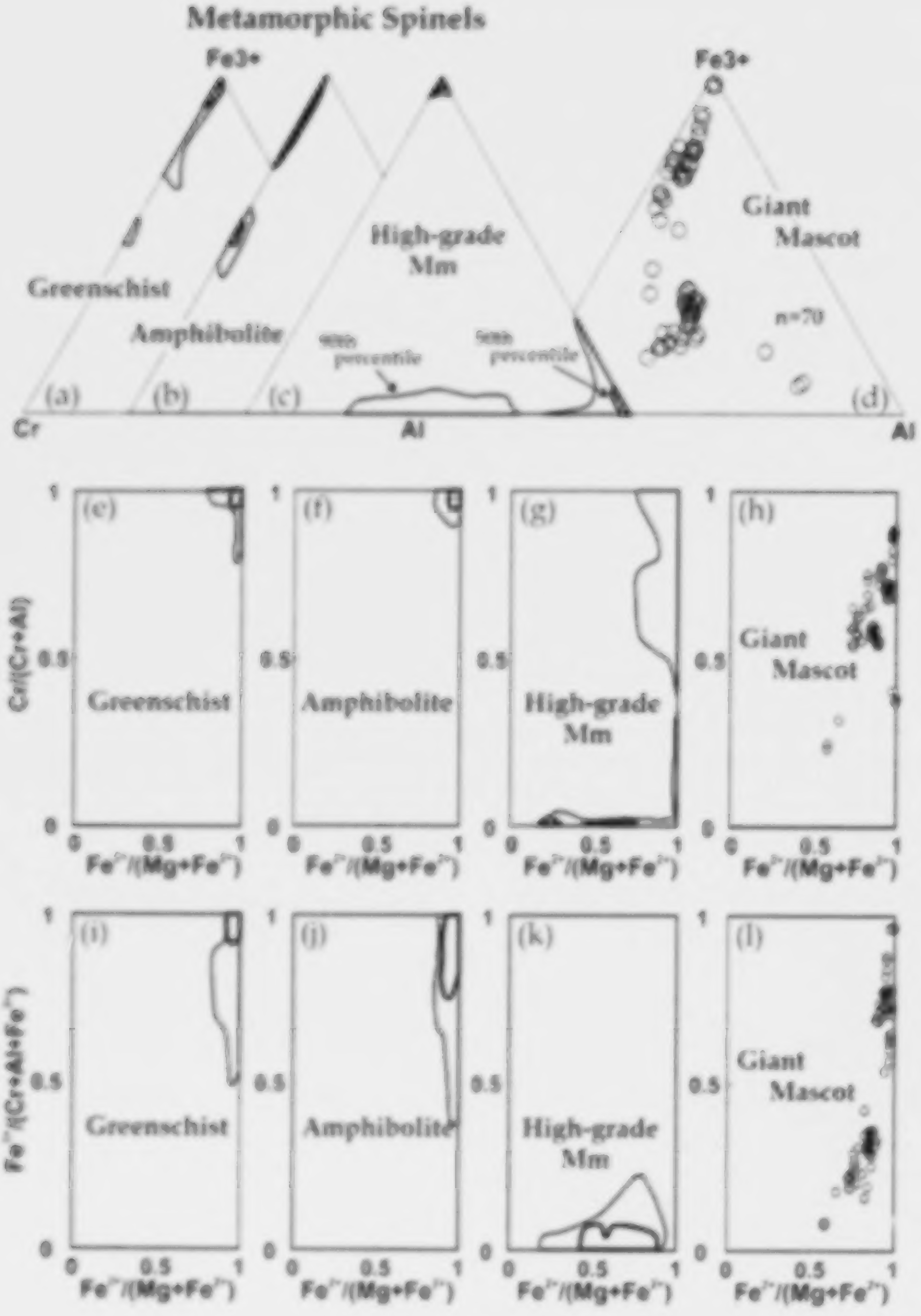

Figure 2. Trivalent cation, Cr/(Cr+Al) vs $Fe^{2+}/(Mg+Fe^{2+})$ and $Fe^{3+}/(Cr+Al+Fe^{3+})$ vs $Fe^{2+}/(Mg+Fe^{2+})$ plots for spinel compositions in greenschist (a, e, i), amphibolite(b, f, j) and high-grade metamorphic rocks (c, g, k) from various protoliths (including komatiites) compared to spinels from Giant Mascot (d, h, l). The field outlines represent contours of the density of spinel populations for the subcategory in the global database of Barnes and Roeder (2001) given at the 50th and 90th percentiles (*i.e.* 50%s and 90%s of analyses in the subcategory fall within the 50th (thick line) and 90th (thin line) percentile contours, respectively). Note that the curvilinear trends of Giant Mascot spinel analyses taken from Muir (1971) are readily distinguished from spinel compositions at each grade of metamorphism when all three plots are taken into account.

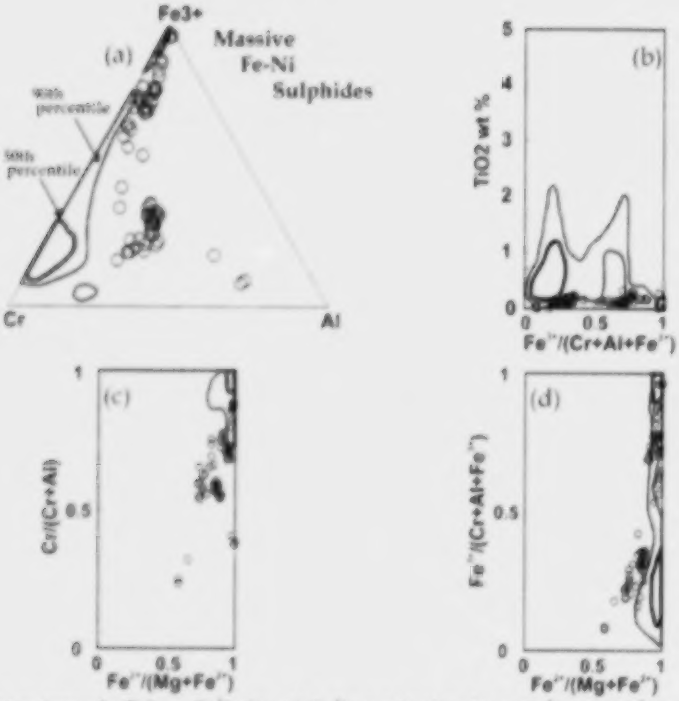

Figure 3. Plots of (a) trivalent cations, (b) TiO_2 vs $Fe^{3+}/(Cr+Al+Fe^{3+})$, (c) $Cr/(Cr+Al)$ vs $Fe^{2+}/(Mg+Fe^{2+})$ and (d) $Fe^{3+}/(Cr+Al+Fe^{3+})$ vs $Fe^{2+}/(Mg+Fe^{2+})$ for Giant Mascot spinels showing data density contours (as in Fig. 2) for spinels at the margins of massive Fe-Ni ore bodies taken from the global database. The lack of equilibration between Giant Mascot spinels and sulphides is clearly evident in plots (a) and (c).

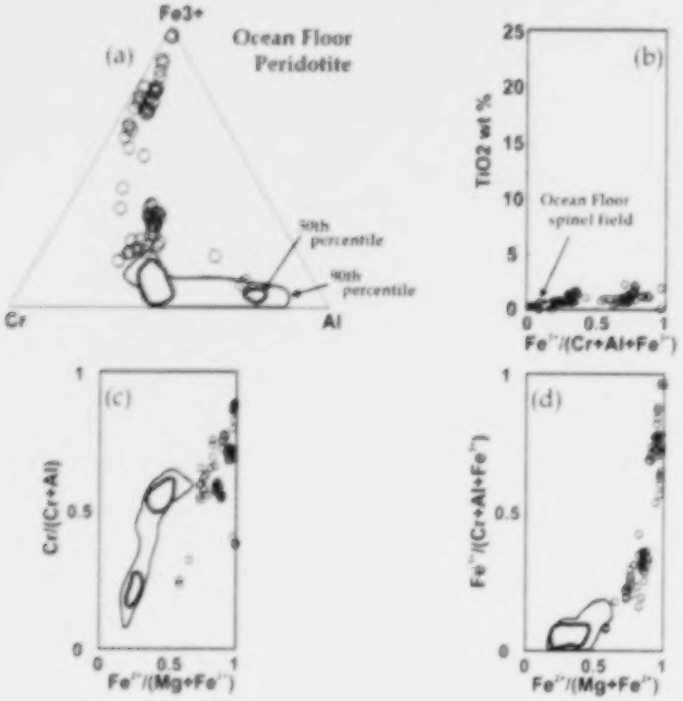

Figure 4. Plots of (a) trivalent cations, (b) TiO_2 vs $Fe^{3+}/(Cr+Al+Fe^{3+})$, (c) $Cr/(Cr+Al)$ vs $Fe^{2+}/(Mg+Fe^{2+})$ and (d) $Fe^{3+}/(Cr+Al+Fe^{3+})$ vs $Fe^{2+}/(Mg+Fe^{2+})$ for Giant Mascot spinels showing data density contours for spinels from ocean floor (abyssal) peridotites. Note the overall higher Fe^{3+} and TiO_2 contents, and higher $Fe/(Mg+Fe)$ ratios of Giant Mascot spinels.

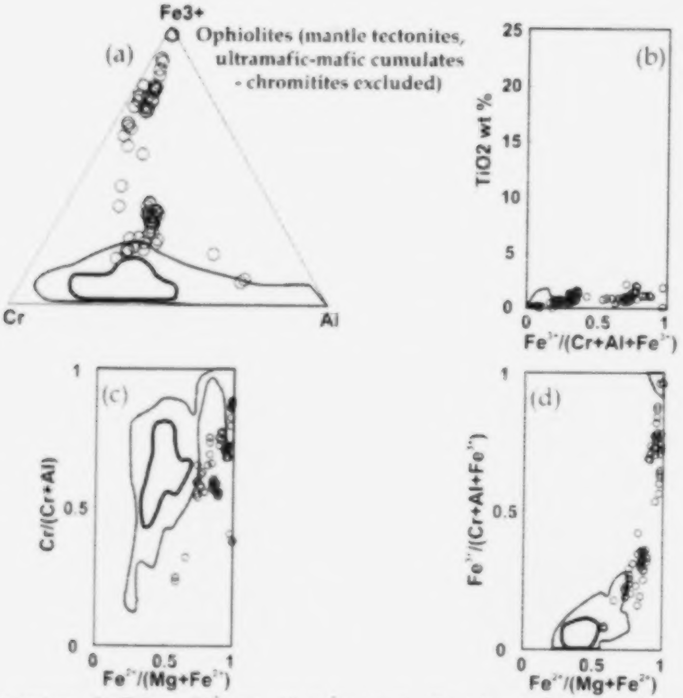

Figure 5. Plots of (a) trivalent cations, (b) TiO_2 *vs* $Fe^{3+}/(Cr+Al+Fe^{3+})$, (c) $Cr/(Cr+Al)$ *vs* $Fe^{2+}/(Mg+Fe^{2+})$ and (d) $Fe^{3+}/(Cr+Al+Fe^{3+})$ *vs* $Fe^{2+}/(Mg+Fe^{2+})$ for Giant Mascot spinels showing data density contours for spinels from ophiolite complexes including tectonized ultramafic rocks and ultramafic-mafic cumulates (chromitite seams excluded). Note that Giant Mascot spinels generally have higher Fe^{3+} contents and $Fe/(Mg+Fe)$ at equivalent $Cr/(Cr+Al)$ ratios.

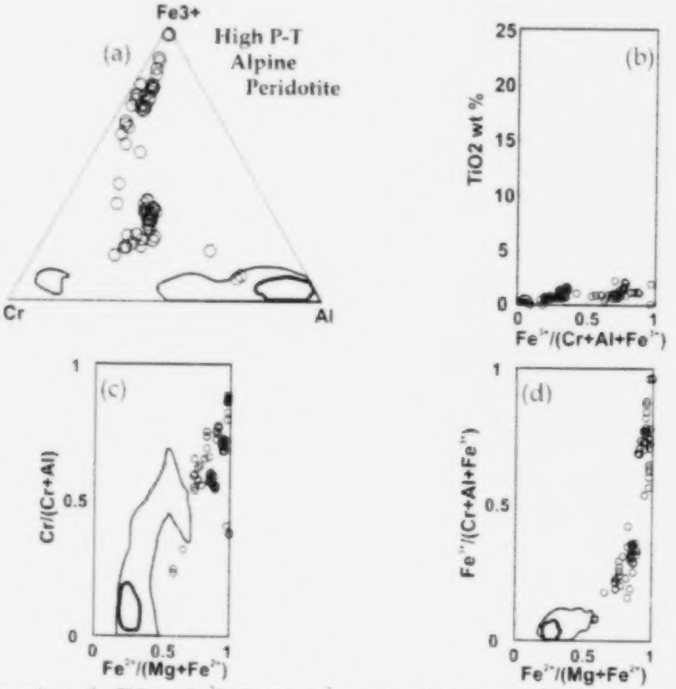

Figure 6. Plots of (a) trivalent cations, (b) TiO_2 *vs* $Fe^{3+}/(Cr+Al+Fe^{3+})$, (c) $Cr/(Cr+Al)$ *vs* $Fe^{2+}/(Mg+Fe^{2+})$ and (d) $Fe^{3+}/(Cr+Al+Fe^{3+})$ *vs* $Fe^{2+}/(Mg+Fe^{2+})$ for Giant Mascot spinels showing data density contours for spinels from tectonically emplaced, high-pressure, high-temperature "Alpine" ultramafic bodies of probable ophiolitic affinity in orogenic belts. Note the overall higher Fe^{3+} contents and $Fe/(Mg+Fe)$ ratios of Giant Mascot spinels.

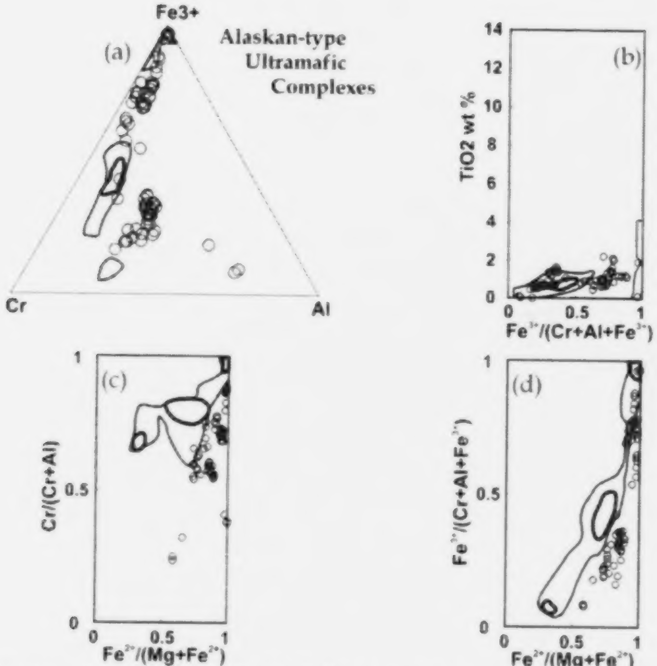

Figure 7. Plots of (a) trivalent cations, (b) TiO_2 *vs* $Fe^{3+}/(Cr+Al+Fe^{3+})$, (c) $Cr/(Cr+Al)$ *vs* $Fe^{2+}/(Mg+Fe^{2+})$ and (d) $Fe^{3+}/(Cr+Al+Fe^{3+})$ *vs* $Fe^{2+}/(Mg+Fe^{2+})$ for Giant Mascot spinels showing data density contours for spinels from Alaskan-type ultramafic complexes. Note that Giant Mascot spinel trends are slightly but systematically displaced to higher Fe/(Mg+Fe) in plots (c) and (d); and are best distinguished from Alaskan-type complexes on the Cr-Al-Fe^{3+} plot.

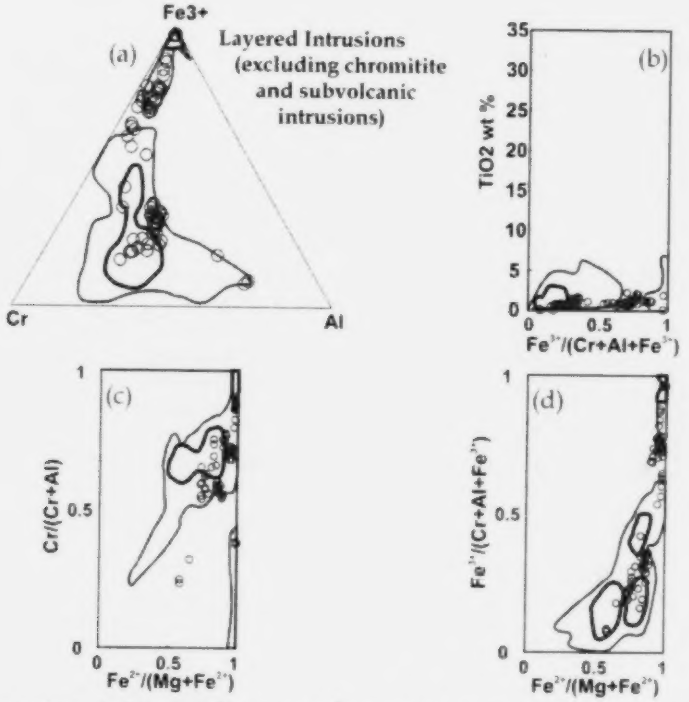

Figure 8. Plots of (a) trivalent cations, (b) TiO_2 *vs* $Fe^{3+}/(Cr+Al+Fe^{3+})$, (c) $Cr/(Cr+Al)$ *vs* $Fe^{2+}/(Mg+Fe^{2+})$ and (d) $Fe^{3+}/(Cr+Al+Fe^{3+})$ *vs* $Fe^{2+}/(Mg+Fe^{2+})$ for Giant Mascot spinels showing data density contours for spinels from layered continental mafic-ultramafic intrusions (excluding chromitite seams and subvolcanic intrusion subcategories). Note the close correspondence between layered intrusion and Giant Mascot spinel trends.

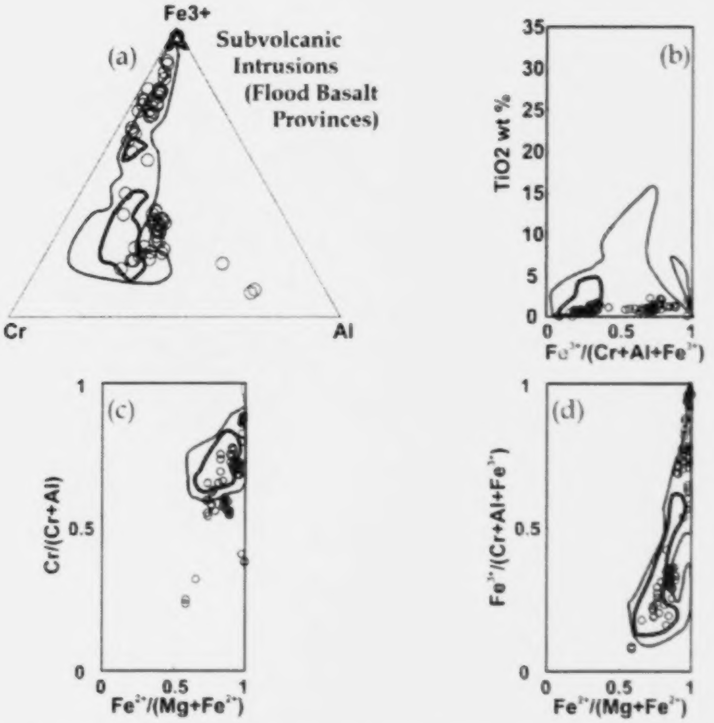

Figure 9. Plots of (a) trivalent cations, (b) TiO_2 *vs* $Fe^{3+}/(Cr+Al+Fe^{3+})$, (c) $Cr/(Cr+Al)$ *vs* $Fe^{2+}/(Mg+Fe^{2+})$ and (d) $Fe^{3+}/(Cr+Al+Fe^{3+})$ *vs* $Fe^{2+}/(Mg+Fe^{2+})$ for Giant Mascot spinels showing data density contours for spinels from continental mafic-ultramafic subvolcanic intrusions in flood basalt provinces. As in Fig. 8, note the close correspondence between subvolcanic intrusion and Giant Mascot spinel trends.

SIGNIFICANCE OF SPINEL DATA

Comparisons of the composition of GM spinels with the global spinel database indicate that the ultramafic rocks which host the Ni-Cu-PGE deposits are not derived from an obducted oceanic terrane, nor are they related to Alaskan-type ultramafic intrusions such as the Tulameen complex. Instead, the spinels at Giant Mascot exhibit a strong affinity with the major continental layered intrusions and smaller subvolcanic intrusions in flood basalt provinces, both of which have a tholeiitic magmatic association. The only igneous province in the northern Cordillera currently recognized to contain a component of tholeiitic flood basalt volcanism, the Late Triassic Karmutsen-Nicolai province, is Wrangellia. This correlation also satisfies the most recent interpretations that the Giant Mascot ultramafic body is intruded by mid-Cretaceous plutonic rocks. According to the compositions of chrome spinels in host rocks and ores, therefore, the Giant Mascot ultramafic body represents a high-level intrusive fragment of the Late Triassic accreted terrane of Wrangellia accidently incorporated in the Spuzzum Pluton. This conclusion may be tested geologically, and, if correct, has important tectonic and metallogenic ramifications as discussed below.

TECTONIC IMPLICATIONS

The boundaries of Wrangellia in the southern Coast Belt are not well known at present (Fig. 10). Currently defined limits are based on vestiges of distinctive Wrangellian stratigraphy, as typified by Late Triassic Quatsino limestone and Karmutsen basalts (Jones *et al.* 1977), which are found as scattered pendants and septa of marble and greenschist to amphibolite-grade metabasalts in Middle to Late Jurassic and Cretaceous granitoid rocks of the Coast Plutonic Complex. The southern margin of Wrangellia appears to be buried by northwesterly verging, early Late Cretaceous structures of the San Juan – Cascade thrust system (Brandon *et al.*, 1988), and by structurally stacked oceanic basin and arc terranes in the southeastern Coast Mountains (*i.e.* east of Harrison Lake; and *see* Ash (2002) for a different structural interpretation of surface exposures in this region). Based on seismic refraction and reflection profiles, Wrangellia appears to form much of the lower and middle crust of the southwestern Coast Belt, and may extend into the 30 km-thick, complexly deformed crust of the southeastern Coast Belt (Zelt *et al.*, 1993; Monger and Journeay, 1994). These arguments have been used to infer the southern limit of Wrangellia in the subsurface shown in Figure 10. Note that this inferred boundary is essentially coincident with the location of Giant Mascot. Thus, the interpretation of the spinel data offered above is consistent with the inferred continuation of Wrangellia to the east where it is

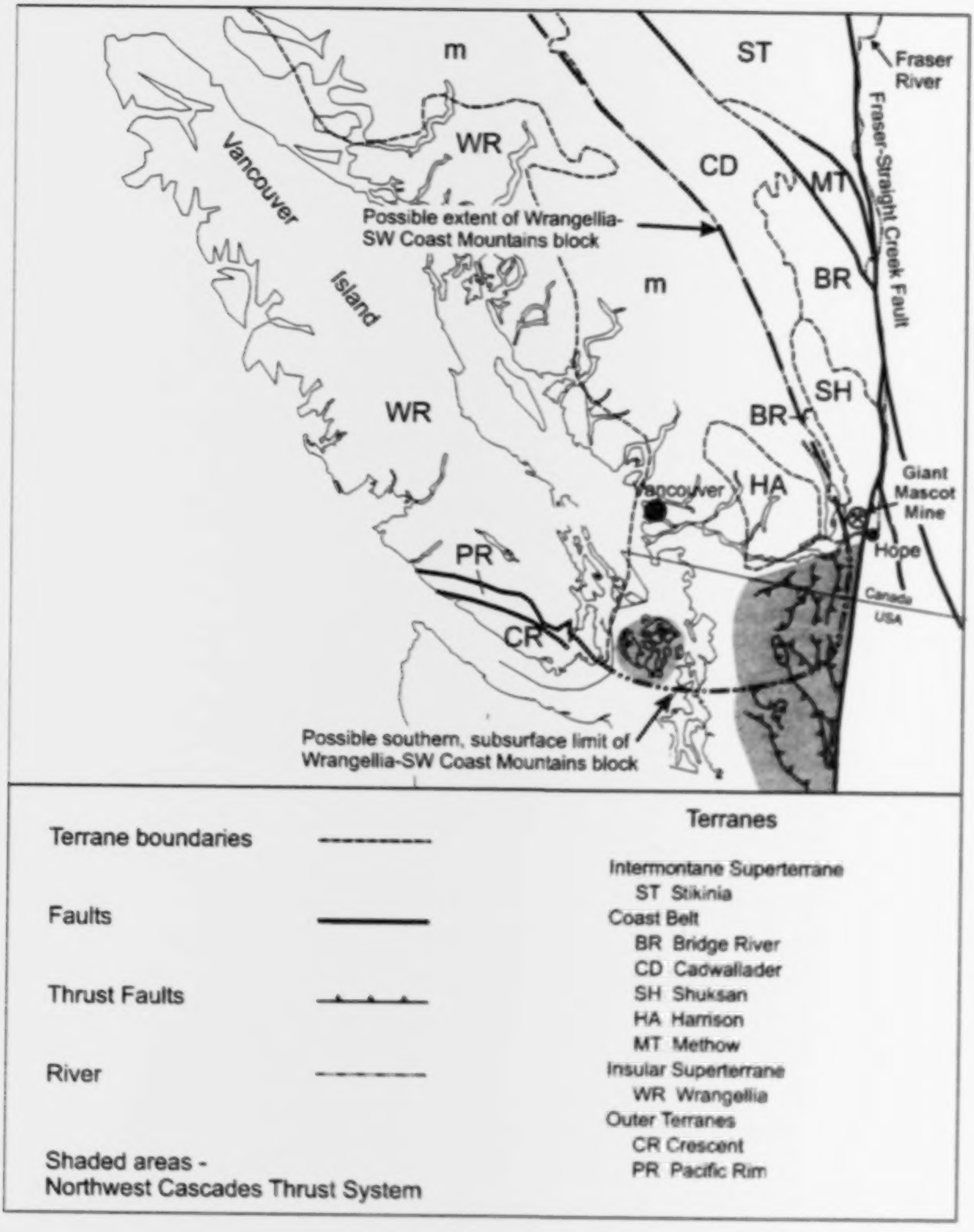
m
ST
Fraser River
WR
Fraser-Straight Creek Fault
Vancouver
CD
MT
Possible extent of Wrangellia-SW Coast Mountains block
Island
m
BR
SH
WR
BR
Giant Mascot Mine
Vancouver
HA
Hope
PR
Canada
USA
CR
Possible southern, subsurface limit of Wrangellia-SW Coast Mountains block
Terrane boundaries
Faults
Thrust Faults
River
Shaded areas - Northwest Cascades Thrust System
Terranes
Intermontane Superterrane
ST Stikinia
Coast Belt
BR Bridge River
CD Cadwallader
SH Shuksan
HA Harrison
MT Methow
Insular Superterrane
WR Wrangellia
Outer Terranes
CR Crescent
PR Pacific Rim

Figure 10. Terrane assemblage map of the southern Coast Belt showing the location of the Giant Mascot ultramafic body in relation to known and inferred boundaries for Wrangellia (modified from Monger and Journeay, 1994).

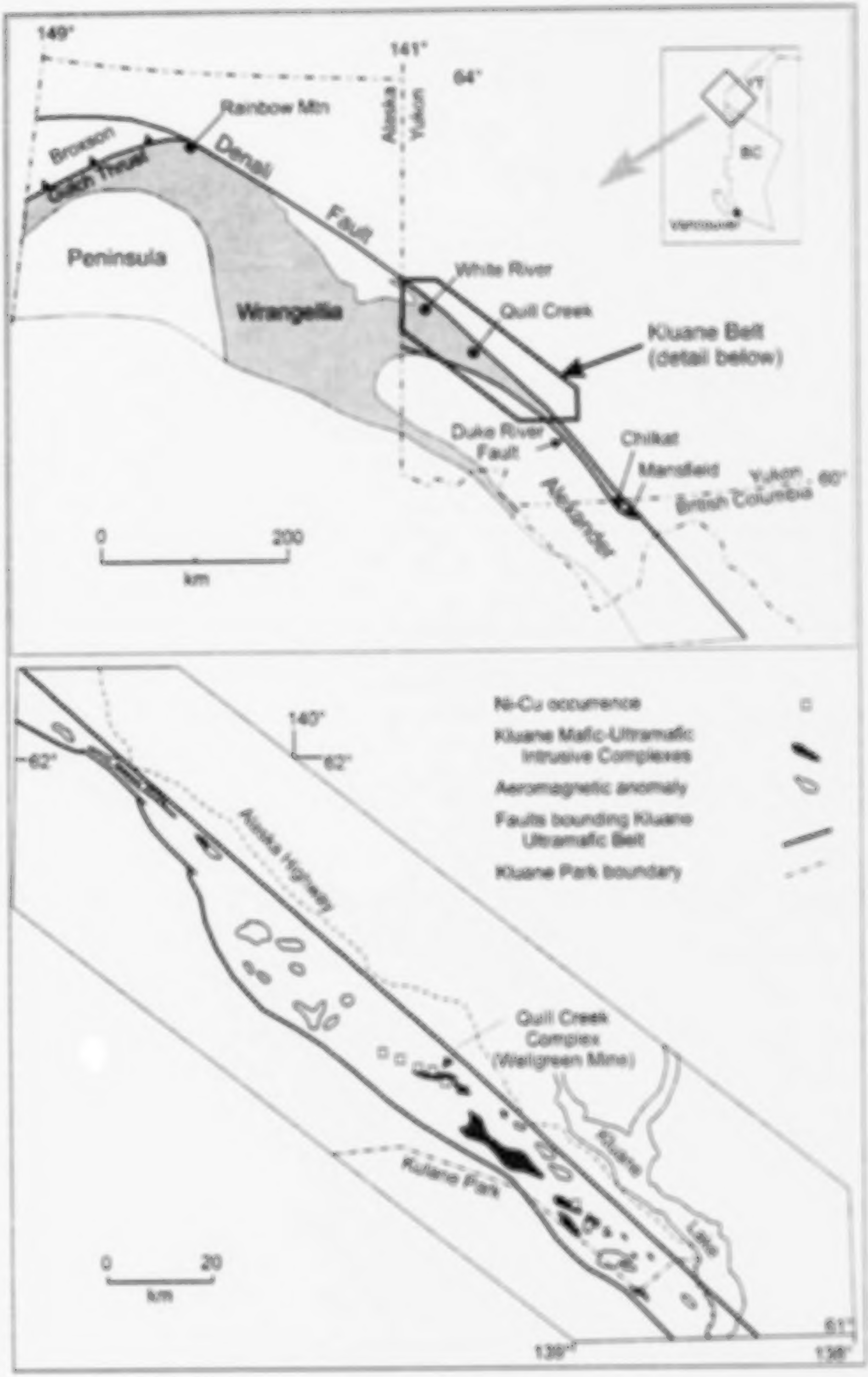
149°
141°
64°
Alaska
Yukon
YT
BC
Vancouver
Rainbow Mtn
Broxson
Gulch Thrust
Denali
Fault
Peninsula
Wrangellia
White River
Quill Creek
Kluane Belt
(detail below)
Duke River
Fault
Chilkat
Mansfield
Yukon
British Columbia
60°
Alexander
0
200
km
Ni-Cu occurrence
Kluane Mafic-Ultramafic
Intrusive Complexes
Aeromagnetic anomaly
Faults bounding Kluane
Ultramafic Belt
Kluane Park boundary
140°
62°
62°
Alaska Highway
Quill Creek
Complex
(Wellgreen Mine)
Kluane
Lake
Kluane Park
0
20
km
61°
139°
138°

Figure 11. Generalized tectonic setting of the Kluane ultramafic belt in the Yukon showing the location of ultramafic-mafic intrusive complexes at the eastern margin of the Wrangellia accreted terrane and their associated Ni-Cu-PGE deposits (after Hulbert, 1997).

probably truncated by the Fraser - Straight Creek fault system.

METALLOGENIC SIGNIFICANCE

Mafic-ultramafic intrusions that host magmatic Ni-Cu-PGE sulphide deposits and prospects are known in northern Wrangellia along the Denali (Shakwak) fault system in Alaska and the Yukon Territory (Fig. 11). The Kluane mafic-ultramafic belt contains the largest known concentration of these intrusions and their mineral deposits, and coincidently(?), occupies a setting analogous to Giant Mascot at the eastern margin of Wrangellia. The southern extension of this belt crosses into northernmost British Columbia in the form of the Chilkat and Mansfield complexes (Fig. 11). The largest mafic-ultramafic bodies form sill-like subvolcanic intrusions (≤600m thick) preferentially emplaced in pyritic metasedimentary strata of Pennsylvanian-Permian age and comagmatic with Middle(?) to Late Triassic Nicolai volcanic rocks (Hulbert 1997). One of the largest intrusions in the Kluane belt, the Quill Creek complex, hosts the former Wellgreen mine, the only past-producer of Ni-Cu ore in the Yukon. Of the initial reserves of 669 150 tonnes of ore, only 171 652 tonnes were mined (1972-73) with an average grade of 2.23% Ni, 1.39% Cu, 0.073% Co and 2.15 ppm Pt and Pd (Hulbert 1997). The sulphide ores have similar mineralogy (pyrrhotite-pentlandite-chalcopyrite-pyrite) and textures (massive, semi-massive and disseminated sulphides) to those at Giant Mascot, and with respect to the PGE, over 20 species of platinum-group minerals have been identified (Barkov *et al.*, 2002). Further details of the Kluane intrusions and their mineral deposits may be found in Hulbert (1997).

The similarities noted above between the petrotectonic setting and nature of Ni-Cu-PGE deposits in mafic-ultramafic rocks of the Kluane belt and Giant Mascot also extend to their spinel compositions. Chromites in Kluane ultramafic-mafic intrusions are compared with the global data array for layered intrusions and subvolcanic intrusions in flood basalt provinces in Figures 12 and 13, respectively. In all these plots, Kluane spinels are coincident with the global data density maxima for spinels from continental tholeiitic intrusions. The compositions of spinels from Giant Mascot are plotted with Kluane spinels in Figure 14. Note the similarity of Kluane and GM spinel compositions at the Fe^{3+}-poor end of the spinel populations, and the more extensive Fe^{3+}-enrichment of GM spinels (Figs. 14c and d). The divergence in Kluane and GM spinel trends in the Ti plot (Fig. 14b) may be a function of different crystal-liquid fractionation histories or reflect variable TiO_2 contents of parental magmas in the Kluane belt. Notwithstanding these details, the overall similarity of spinel compositions in ultramafic rocks at Kluane and Giant Mascot is striking and strengthens arguments advanced above for a similar petrotectonic and metallogenic setting.

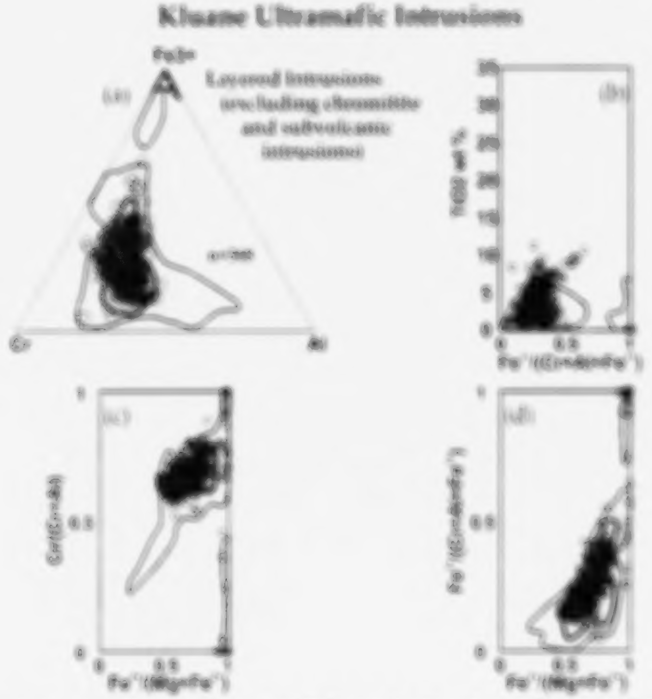

Figure 12. Plots of (a) trivalent cations, (b) TiO_2 vs $Fe^{3+}/(Cr+Al+Fe^{3+})$, (c) $Cr/(Cr+Al)$ vs $Fe^{2+}/(Mg+Fe^{2+})$ and (d) $Fe^{3+}/(Cr+Al+Fe^{3+})$ vs $Fe^{2+}/(Mg+Fe^{2+})$ for spinels from mafic-ultramafic intrusions at the eastern margin of Wrangellia in the Yukon and Alaska (spinel data from Hulbert, personal communication, 2002, and see Hulbert 1997). Data density contours are for spinels in layered intrusions (Fig. 9). Note the correspondence of data density maxima in all plots.

Kluane Ultramafic Intrusions

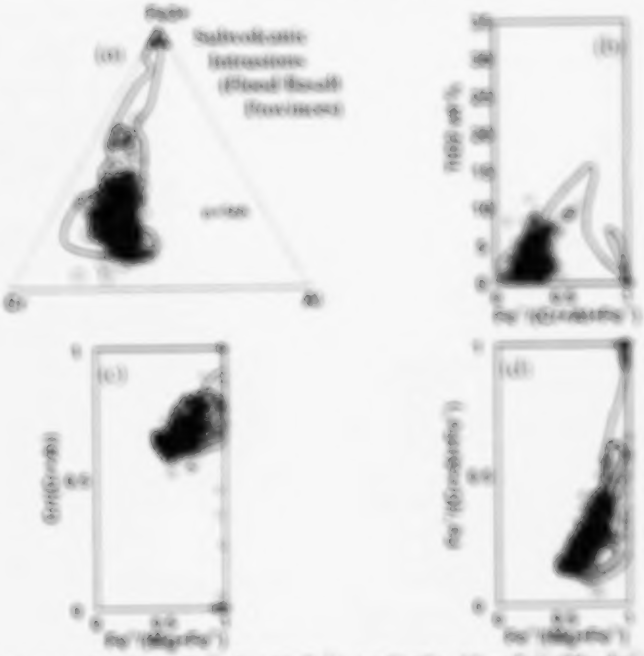

Figure 13. Plots of (a) trivalent cations, (b) TiO2 vs Fe3+/(Cr+Al+Fe3+), (c) Cr/(Cr+Al) vs Fe2+/(Mg+Fe2+) and (d) Fe3+/(Cr+Al+Fe3+) vs Fe2+/(Mg+Fe2+) for Giant Mascot spinels showing data density contours for spinels from continental mafic-ultramafic subvolcanic intrusions in flood basalt provinces. As in Fig. 12, note the correspondence of data density maxima in all plots.

Giant Mascot vs Kluane Ni-Cu-PGE

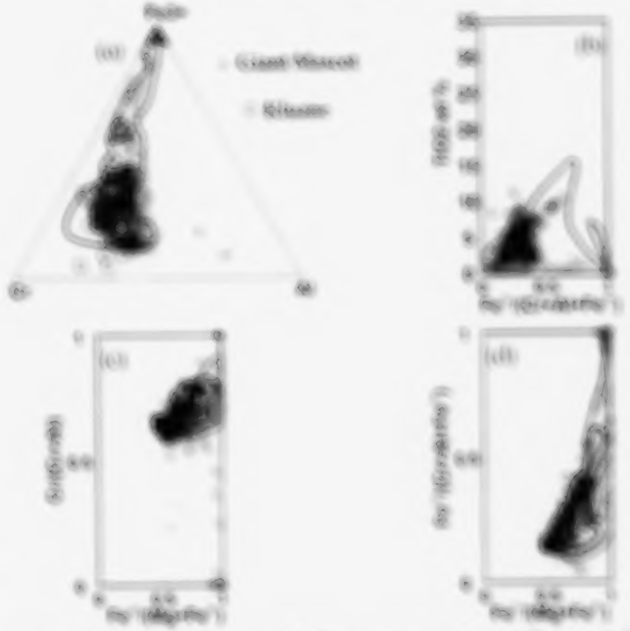

Figure 14. Plots of (a) trivalent cations, (b) TiO2 vs Fe3+/(Cr+Al+Fe3+), (c) Cr/(Cr+Al) vs Fe2+/(Mg+Fe2+) and (d) Fe3+/(Cr+Al+Fe3+) vs Fe2+/(Mg+Fe2+) for Giant Mascot and Kluane spinels showing data density contours for spinels from subvolcanic intrusions in flood basalt provinces. Note the close correspondence between the datasets and the more extensive Fe enrichment of Giant Mascot spinels along the global data array.

Based on these spinel compositions, therefore, the mineral deposit model that most closely approximates Giant Mascot appears to be the world-class (Russia) Noril'sk-Talnakh Ni-Cu-PGE ores which are hosted by subvolcanic intrusions associated with the Triassic Siberian flood basalt province (deposit type 5b of Cox and Singer, 1986). Differences between this deposit type and Giant Mascot include the fact that the latter ores are hosted by ultramafic rocks, and these lithologies carry igneous amphibole as an important constituent. The gabbroid-associated Ni-Cu-PGE deposit type favoured for Giant Mascot by Eckstrand (1984; deposit type 12.2) for rocks like the intrusions seems inappropriate because these deposits are considered to be associated with orogenic as opposed to extensional or plume-related tectonic settings.

CONCLUDING REMARKS

It has been shown above that spinels can be usefully employed as "indicator minerals" in the search for economically attractive ultramafic-mafic-hosted Ni-Cu-PGE deposits in the Cordillera. In the case of Giant Mascot, the available spinel data provide new insight into the petrotectonic setting and metallogenic significance of this seemingly unusual deposit type. Spinel compositions indicate that the Giant Mascot ultramafic body and its associated ore deposits represent a fragment of the Late Triassic Wrangellian flood basalt province. Furthermore, the Ni-Cu-PGE sulphide ores at Giant Mascot are not unique but related to similar deposits described in Alaska and the Yukon which share the same tectonic setting and mineral deposit type. If correct, this interpretation presents new opportunities for base and precious metal mineral exploration in the southern Insular Belt, particularly along the poorly defined eastern margin of Wrangellia where most documented occurrences in the northern Cordillera are concentrated.

As a caveat, it must be emphasized that: 1) these conclusions are based on a single set of electron-microprobe analyses made by Muir (1971) over 30 years ago; and 2) the analyzed chromites represent samples collected from ultramafic rocks associated with just one (4600) out of at least 28 different ore shoots. A more comprehensive suite of samples is currently being analyzed in order to check the spinel compositions on which this paper is based in an attempt to corroborate these conclusions.

ACKNOWLEDGMENTS

Thanks are extended to Kirk Hancock for drafting some of the figures. Any errors or omissions are the sole responsibility of the author.

REFERENCES

Aho, A.E. (1956): Geology and genesis of ultrabasic nickel-copper-pyrrhotite deposits at the Pacific Nickel property, southwestern British Columbia; *Economic Geology*, Volume 51, pages 444-481.

Ash, C.H. (2002): Geology of the East Harrison Lake Belt, southwestern British Columbia; *in* Geological Fieldwork 2001, *British Columbia Ministry of Energy and Mines*, Paper 2002-1, pages 197-210.

Barkov, A.Y., Laflamme, J.H.G., Cabri, L.J. and Martin, R.F. (2002): Platinum-group minerals from the Wellgreen Ni-Cu-PGE deposit, Yukon, Canada; *Canadian Mineralogist*, Volume 40, pages 651-669.

Barnes, S.J. and Roeder, P.L. (2001): The range of spinel compositions in terrestrial mafic and ultramafic rocks; *Journal of Petrology*, Volume 42, pages 2279-2302.

Brandon, M.T., Cowan, D.S. and Vance, J.A. (1988): The Late Cretaceous San Juan thrust system, San Juan Islands, Washington; *Geological Society of America*, Special Paper 221, 81 pages.

Cockfield, W.E. and Walker, J.F. (1933): The nickel-bearing rocks near Choate, British Columbia; *Geological Survey of Canada*, Summary Report 1932, Part A, pages 62-68.

Cox, D.P. and Singer, D.A., Editors (1986): Mineral deposit models; *United States Geological Survey*, Bulletin 1693, 379 pages.

Eckstrand, O.R., Editor (1984): Canadian mineral deposit types: a geological synopsis; *Geological Survey of Canada*, Economic Geology Report 36, 86 pages.

Hulbert, L.J. (1997): Geology and metallogeny of the Kluane mafic-ultramafic belt, Yukon Territory, Canada: eastern Wrangellia – a new Ni-Cu-PGE metallogenic terrane; *Geological Survey of Canada*, Bulletin 506, 265 pages.

Hulbert, L.J. (2001): GIS maps and databases of mafic-ultramafic hosted Ni, Cu-Ni, Cr ± PGE occurrences and mafic-ultramafic bodies in British Columbia; *British Columbia Ministry of Energy and Mines*, Geoscience Map 2001-2.

Irvine, T.N. (1965): Chromian spinel as a petrogenetic indicator; Part 1, Theory; *Canadian Journal of Earth Sciences*, Volume 2, pages 648-672.

Irvine, T.N. (1967): Chromian spinel as a petrogenetic indicator; Part 2, Petrologic applications; *Canadian Journal of Earth Sciences*, Volume 4, pages 71-103.

Jones, D.L., Silberling, N.J. and Hillhouse, J. (1977): Wrangellia – a displaced terrane in northwestern North America; *Canadian Journal of Earth Sciences*, Volume 14, pages 2565-2577.

McLeod, J.A. (1975): The Giant Mascot ultramafite and its related ores; unpublished M.Sc. thesis, *The University of British Columbia*, 123 pages.

McLeod, J.A., Vining, M. and McTaggart, K.C. (1976): Note on the age of the Giant Mascot ultramafic body, near Hope, B.C.; *Canadian Journal of Earth Sciences*, Volume 13, pages 1152-1156.

Monger, J.W.H. and Journeay, J.M. (1994): Basement geology and tectonic evolution of the Vancouver region; *in* Geology and Geologic Hazards of the Vancouver Region, southwestern British Columbia, J.W.H. Monger, Editor, *Geological Survey of Canada*, Bulletin 481, pages 3-25.

Muir, J.E. (1971): A study of the petrology and ore genesis of the Giant Nickel 4600 ore body, Hope, British Columbia; unpublished M.Sc. thesis, *The University of Toronto*, 123 pages.

Nixon, G.T., Cabri, L.J. and Laflamme, J.H.G. (1990): Platinum-group element mineralization in lode and placer deposits associated with the Tulameen Alaskan-type complex, British Columbia; *Canadian Mineralogist*, Volume 28, pages 503-535.

Nixon, G.T., Hammack, J.L., Ash, C.H., Cabri, L.J., Case, G., Connelly, J.N., Heaman, L.M., Laflamme, J.H.G., Nuttall, C., Paterson, W.P.E. and Wong, R.H. (1997): Geology and platinum-group-element mineralization of Alaskan-type ultramafic-mafic complexes in British Columbia; *British*

Columbia Ministry of Employment and Investment, Bulletin [illegible], [illegible] pages.

[illegible] (2004): [illegible] of the [illegible] and [illegible] [illegible]; British Columbia Ministry of Energy and Mines, Paper 2005-1, pages [illegible].

[illegible] (1990): [illegible]; Canadian Mineralogist, Volume [illegible], pages [illegible].

Stevens, R. E. (1944): Composition of some chromites of the western hemisphere; American Mineralogist, Volume [illegible], pages [illegible].

[illegible] and [illegible] (1991): [illegible]; Canadian Journal of Earth Sciences, Volume [illegible], pages [illegible].

Iron Mask Project, Kamloops Area

By James M. Logan

[illegible]

INTRODUCTION

[illegible]

[illegible]

[illegible]

[illegible]

[illegible]

[illegible]

[illegible]

REGIONAL GEOLOGY

[illegible]

[illegible]

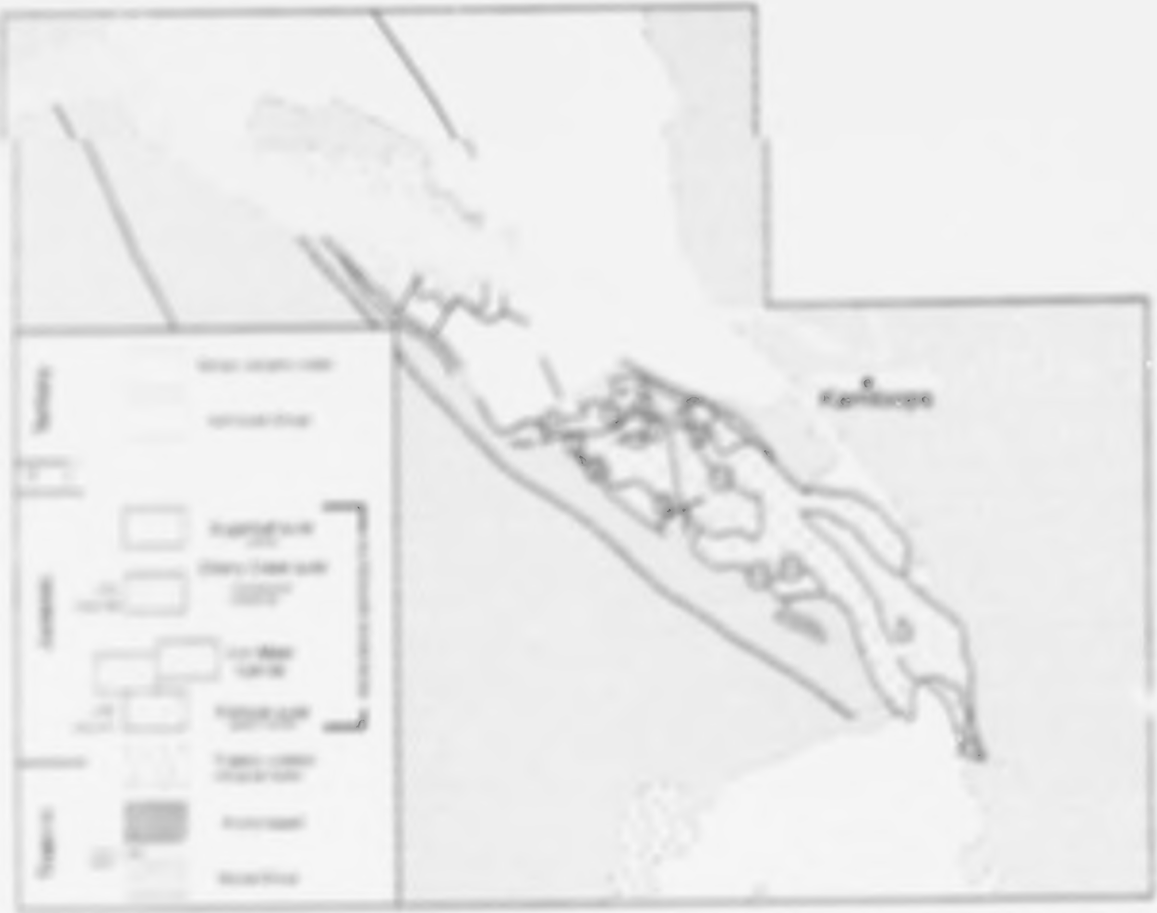

Figure 1. Location of project area, showing geology after Kwong (1987), Snyder (1994) and this study. Legend is after Snyder (1994). Location of past producing Cu-Au mines (1. Afton; 2. Pothook; 4. Crescent; 11. Ajax West, Ajax East) and Cu-Au mineral occurrences (3. DM; 5. Big Onion; 6. Iron Mask; 7. Iron Cap; 8. Coquihalla East; 9. Rainbow No.1, No.2 zones; 10. Galaxy).

Mask batholith was shown to be equivalent to arc-derived ultramafic basalts which regionally overlie the Nicola Group stratigraphy (Snyder and Russell, 1993). Middle Eocene volcanic rocks of the Kamloops Group unconformably overlie the Nicola Group and Iron Mask rocks (Figure 1).

Intrusive phases are separated by "fundamental faults" which control mineralization and alteration, and no significant mineralization has been delineated outside the batholith in the Nicola volcanic rocks. Mineralization consists primarily of fracture-controlled chalcopyrite and bornite associated with pyrite, pyrrhotite and magnetite. Lang et al. (1994) show unit specific alteration assemblages comprising: magnetite-apatite-actinolite in the Pothook and hybrid units; potassic in the Cherry Creek monzonite; and sodic alteration of the Sugarloaf diorite.

Evaluation of the geophysical response of these known mineralized and altered assemblages, may provide a predictive geophysical response that can be modeled and applied to covered areas in the southern portion of the batholith.

EXPLORATION ACTIVITY

Exploration activities in the area of the Iron Mask Batholith includes work around the Afton pit, where DRC Resources is currently drilling deep holes to test the continuity and geometry of the remaining resources of the Afton deposit. The company is evaluating a possible underground operation for the remaining southwest plunging, higher grade Cu-Au-Pd-Ag mineralization. Indicated mineral resources for the main zone are 34.3 Mt of 1.55% Cu, 1.14 g/t Au, 0.125 g/t Pd and 3.42 g/t Ag (DRC corporate website, 2002).

Abacus completed 3,500 metres of drilling on its Rainbow property in June. Results from this first phase drill program extends the known zones and has intersected mineralized sections of copper-gold and in places palladium mineralization. Mapping and sampling between the 42 Zone (Rainbow) and the Pothook pit has recognized structures, alteration and copper mineralization that will refine drill target selection for the second phase of drilling. Along strike, and within the northwest-trending structural corrdor that hosts Afton, Pothook and the Rainbow showing, is the Coquihalla East zone. This gold-rich, copper-poor style of mineralization was first recognized by Teck Cominco in the 1990's. Surface sampling of the Coquihalla East and the Iron Cap zone (located south of the Crescent deposit), returned gold-rich assays of 6.36 g/t Au, 0.83 g/t Pd and 1.0% Cu (Abacus News release, Dec 17, 2002) and as high as 30.9 g/t Au over 2.0 m (Abacus News release, Nov 7, 2002) respectively.

SUMMARY

The initial phase of geological compilation and a brief field orientation for the Iron Mask Project has been completed. Incorporation of the digital geophysical data and refining the geology map remains to be done. The ultimate product is envisioned to be an interactive, web-based map showing the geology and mineral occurrences with separate geophysical overlays and marginal interpretive notes. This will provide exploration geologist with the spatial distribution of some of the important controls for copper-gold and platinum-palladium mineralization in the Iron Mask Pluton.

ACKNOWLEDGMENTS

The Iron Mask project was one of a number of Public-Private Partnerships that were conducted across the province this year. The project was conceived through discussions between Abacus Mining and Exploration Corp. and the Ministry of Energy and Mines and jointly funded. I would like to thank Teck Cominco Ltd. and Abacus Mining and Exploration Corp. for permission and access to study the deposits and mineral occurrences in the Kamloops area.

Special thanks also to Graeme Evans of Teck Cominco Ltd. who shared his knowledge of the geology and mineralization of the batholith together with some of the unresolved geological relationships. Robert Darney, Scott Weeks and Robert Friesen are acknowledged for their logistical support, field visits and helpful geological discussions with the author.

REFERENCES

Cockfield, W.E. (1948): Geology and Mineral Deposits of Nicola Map-area, British Columbia; *Geological Survey of Canada*, Memoir 249.

Ghosh, D. (1995): Uranium-Lead Geochronology, *in* Porphyry Copper-Gold Systems of British Columbia; *Mineral Deposit Research Unit, The University of British Columbia*, Annual Technical Report, pages 11.1-11.28.

Kwong, Y.T.J. (1987): Evolution of the Iron Mask Batholith and its Associated Copper Mineralization; *B.C. Ministry of Energy, Mines and Petroleum Resources*, Bulletin 77, 55 pages.

Lang, J.R., Stanley, C.R., Thompson, J.F.H. and Dunne, K.P.E. (1995): Na-K-Ca Magmatic-Hydrothermal Alteration Associated with Alkalic Porphyry Cu-Au Deposits in British Columbia; *in* Magmas, Fluids and Ore Deposits, Edited by Thompson, J.F.H., *Mineralogical Association of Canada*, Short Course Volume 23, Victoria, 1995, pages 339-366.

Mortimer, N. (1987): The Nicola Group: Late Triassic and Early Jurassic subduction-related volcanism in British Columbia; *Canadian Journal of Earth Sciences*, Volume 24, pages 2521-2536.

Northcote, K.E. (1976): Geology of the Southeast Half of the Iron Mask Batholith, *in* Geological Fieldwork 1976, *B.C. Ministry of Energy, Mines and Petroleum Resources*, Paper 1977-1, pages 41-46.

Northcote, K.E. (1977): Geological Map of the Iron Mask Batholith (92I/9W and 10E); *B.C. Ministry of Energy, Mines and Petroleum Resources*, Preliminary Map No. 26 and accompanying notes, 8 pages.

Preto, V.A.G. (1967): Geology of the Eastern Part of the Iron Mask Batholith; *B.C. Minister of Mines and Petroleum Resources*, *Annual Report 1967*, pages 137-147.

Preto, V.A. (1977): The Nicola Group: Mesozoic Volcanism Related to Rifting in Southern British Columbia; *in* Volcanic Regimes in Canada, Baragar, W.R.A., Coleman, L.C. and Hall, J.M., Editors, *Geological Association of Canada*, Special Paper No. 16, pages 39-57.

Preto, V.A. (1979): Geology of the Nicola Group between Merritt and Princeton; *B.C. Ministry of Energy, Mines and Petroleum Resources*, Bulletin 69, 90 pages.

Shives, R.B.K. (1994): Airborne Geophysical Survey, Iron mask Batholith, British Columbia; *Geological Survey of Canada*, Open File 2817, 1:50 000 scale.

Snyder, L.D. (1994): Petrological studies within the Iron Mask batholith, south-central British Columbia; unpublished M.Sc. thesis, *The University of British Columbia*, 192 pages.

Snyder, L.D. and Russell, J.K. (1994): Petrology and Stratigraphic Setting of the Kamloops Lake Picritic Basalts, Quesnellia Terrane, South-central B.C., *in* Geological Fieldwork 1993, Grant, B. and Newell, J.M., Editors, *B.C. Ministry of Energy, Mines and Petroleum Resources*, Paper 1994-1, pages 297-309.

Snyder, L.D. and Russell, J.K. (1995): Petrogenetic Relationships and assimilation processes in the alkalic Iron Mask batholith, south-central British Columbia; *in* Porphyry Deposits of the Northwestern Cordillera of North America, Edited by T.G. Schroeter, Canadian Institute of Mining and Metallurgy, Special Volume 46, pages 593-608.

Kena Mountain Gold Zone, Southern British Columbia

By James M.Logan

KEYWORDS: Gold, Silver King intrusions, Rossland Group, Elise volcanic rocks, porphyry mineralization, structural-controlled, tourmaline, synkinematic, Silver King Shear Zone.

INTRODUCTION

The discovery of a new style of gold mineralization on the Kena Gold property has resulted in a resurgence of exploration in a historical gold-copper mineral belt located south of Nelson. The Gold Mountain Zone (GMZ) was discovered in 2000 by follow-up trenching of gold-in-soil anomalies which straddle the contact between Rossland Group volcanic rocks and the "previously considered to be unmineralized" Silver King pluton. The Silver King pluton is one of six intrusive bodies that comprise a north to northwest trending, 4 x 20 km long prospective, and largely untested, magmatic belt that extends from Ymir north to Nelson (Figure 1). The regional geology and mineralization are described by Höy and Dunne (2001); however, the ages and controls of the different styles of mineralization and alteration on the Kena property are not fully understood.

The Kena Gold project is a private-public partnership developed between the Ministry of Energy and Mines and Sultan Minerals Inc. The main objectives of the project are: 1) map and sample exposures of Silver King intrusions (magnetic susceptibility, density and structural fabric measurements) along the length of the magmatic belt to assess the mineral potential of the suite as a whole; 2) log and sample core from the GMZ to characterize alteration and mineralization; 3) constrain age of deformation and/or mineralization; 4) establish a metallogenic model that accounts for the variety of mineralization types, and ultimately can be used to direct exploration along the length of this belt of early Middle Jurassic magmatic rocks.

A total of ten days were spent in the field mapping and sampling along the length of the prospective magmatic belt as well as examining drill core on the Kena property. This report summarizes the results of this work.

LOCATION

Mapping, sampling and deposit studies where conducted between Nelson and Ymir in southeastern British Columbia, NTS map sheet 82F/6. The Gold Mountain Zone is situated in the northern portion of the Kena property, approximately 5 km south of Nelson (Figure 1).

PREVIOUS WORK

Previous geological mapping of the Nelson map sheet was conducted by the Geological Survey of Canada, between 1948 and 1952 (Mulligan, 1952; Little, 1960), and the British Columbia Ministry of Energy, Mines and Petroleum Resources between 1987 and 1990 (Höy and Andrew, 1989a; Höy and Dunne, 1991). More detailed, property-scale mapping and deposit specific studies have been completed by various mining companies, and are available in provincial assessment reports.

Mineralization on the property was first described by G.M. Dawson of the Geological Survey of Canada, in the Annual Report for 1888-89. Old prospect pits, trenches and underground workings attest to early exploration on the claims, but little is recorded prior to 1973 when Otto Janout staked the Kena claims. Thereafter the Kena claims were optioned and explored by various companies for poly-metallic volcanic-hosted massive sulphide deposits, porphyry copper deposits, copper-silver±gold veins and copper-gold replacement mineralization, up until 1991 (Dandy, 2001). The property lay dormant until 1999 when a number of the known showings were acquired (Kena Gold Zone, Kena Copper Zone and Shaft/Cat Zone) and amalgamated by Sultan Minerals Inc. under the name Kena property (Figure 2).

Initial work by Sultan Minerals focused on two areas: the Kena Gold and Gold Mountain zones.

At the Kena Gold Zone previously drilled core was re-logged and untested intervals were split and sampled for analyses. The results from this work indicated that wide zones of low-grade gold mineralization are present throughout the Kena Gold Zone. Previous work looked for a relatively narrow, but higher-grade, gold target and had not recognized the lower-grade bulk tonnage potential of the Kena Gold.

At the Gold Mountain Zone, grid lines from earlier work were extended 900 m to the southwest to evaluate the high gold in soil samples and high chargeability present at the ends of the old grid lines. Soil sampling, magnetometer surveys and geological mapping were carried out over this grid, which for the first time tested the potential of the Silver King pluton. Rock chip sampling, followed by excavator trenching delineated a 120 m by 90 m area, centered on L11N, 3E that averaged 1.43 g/t Au from 3 m chip samples of altered Silver King intrusive rocks (Dandy, 2001).

In 2001 work continued at the Gold Mountain Zone, where a detailed alteration and mineralogy study by Kathryn Dunne and a structural geology study by David

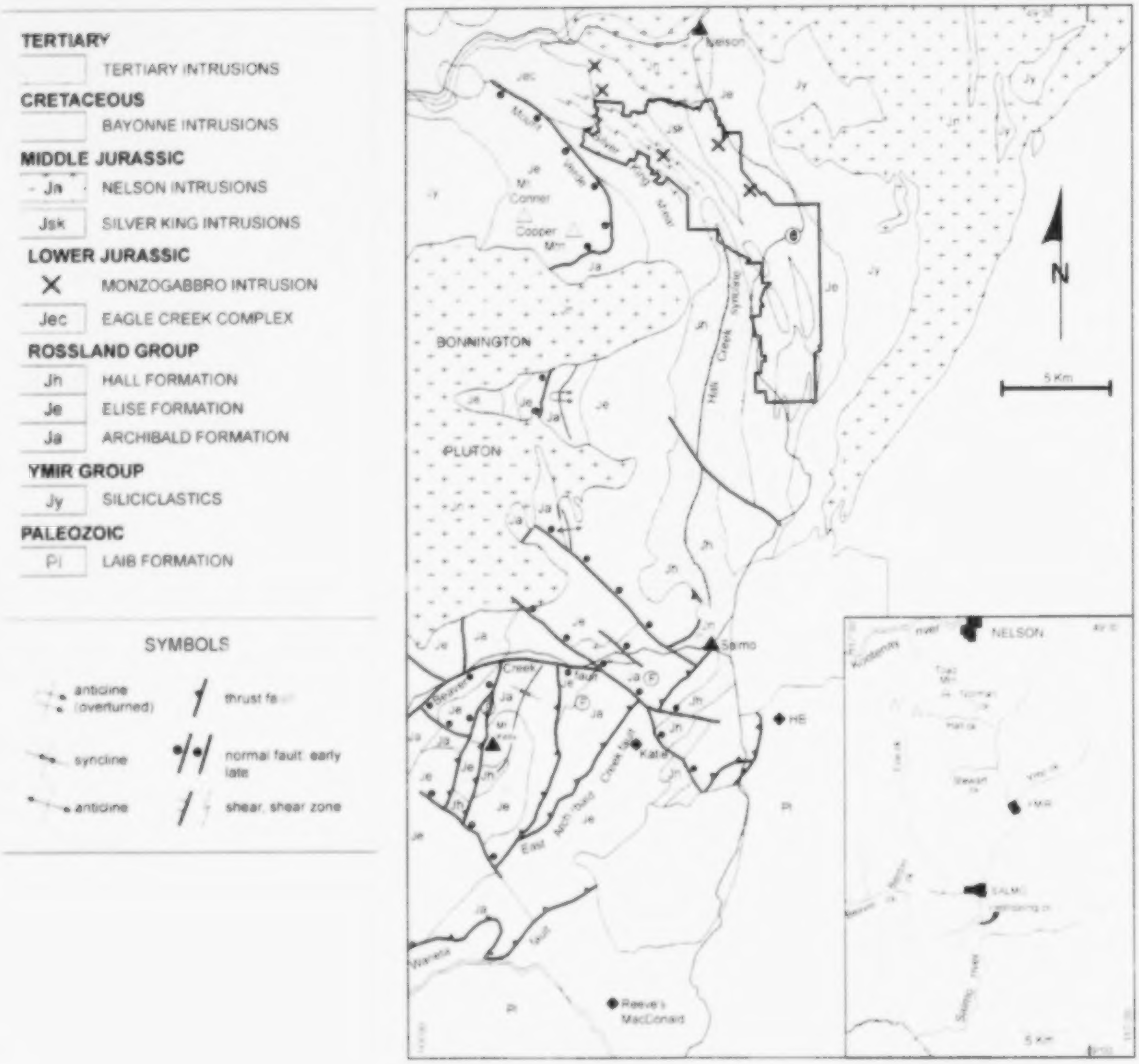
TERTIARY
TERTIARY INTRUSIONS
CRETACEOUS
BAYONNE INTRUSIONS
MIDDLE JURASSIC
Jn NELSON INTRUSIONS
Jsk SILVER KING INTRUSIONS
LOWER JURASSIC
MONZOGABBRO INTRUSION
Jec EAGLE CREEK COMPLEX
ROSSLAND GROUP
Jh HALL FORMATION
Je ELISE FORMATION
Ja ARCHIBALD FORMATION
YMIR GROUP
Jy SILICICLASTICS
PALEOZOIC
Pl LAIB FORMATION
SYMBOLS
anticline (overturned)
thrust fault
syncline
normal fault: early late
anticline
shear, shear zone
Nelson
Salmo
BONNINGTON
PLUTON
Mt Conner
Cooper Mtn
Mount Verde
Silver King Shear
Hall Creek syncline
Beaver Creek fault
East Archibald Creek fault
Waneta fault
Kate
HB
Reeve's MacDonald
N
5 Km
NELSON
Kootenay river
YMIR
SALMO
Salmo river
5 Km

Figure 1. Geology map of the Nelson-Salmo area, southeast British Columbia (082F/SW) shows location of Silver King magmatic belt, extent of the Kena property and select deposits (after Höy and Dunne, 1997, 2001).

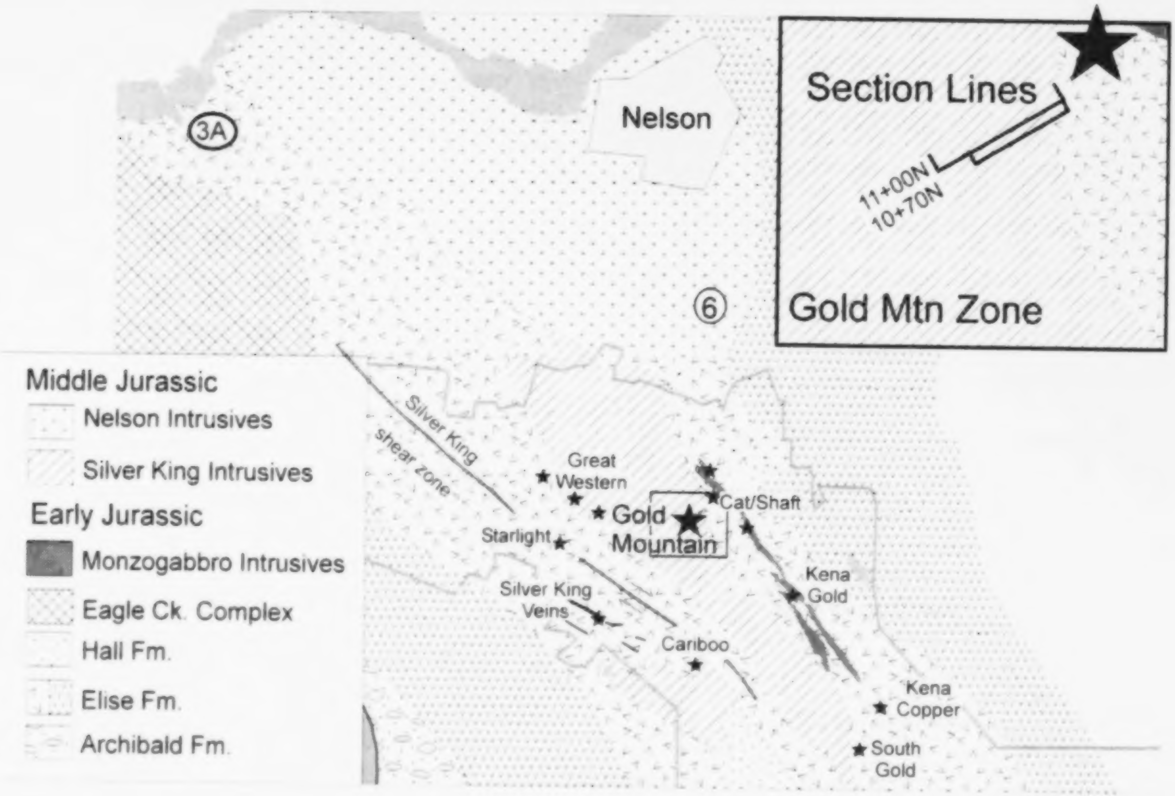
Section Lines
11+00N
10+70N
Gold Mtn Zone
Nelson
3A
6
Middle Jurassic
Nelson Intrusives
Silver King Intrusives
Early Jurassic
Monzogabbro Intrusives
Eagle Ck. Complex
Hall Fm.
Elise Fm.
Archibald Fm.
Silver King shear zone
Great Western
Gold Mountain
Cat/Shaft
Starlight
Silver King Veins
Kena Gold
Cariboo
Kena Copper
South Gold

Figure 2. Geology map of the northern part of the Kena property, showing location of mineral deposits described in text. Inset shows location of section lines for Figure 6 (after Höy and Dunne, 1998).

Rhys were undertaken. An additional six trenches and seven diamond drill holes were completed in the immediate vicinity of the discovery trenches (Dandy, 2001). Assay results from drilling were encouraging enough to warrant a second drill program in the fall that completed an additional 23 holes.

A two-phase exploration program began in early spring of 2002 with a 15-hole diamond drill program on two additional section lines through the Gold Mountain zone. All holes encountered significant widths of ~1g/t Au mineralization and many intersected narrower high-grade zones. On going soil geochemistry, geophysics and rock chip sampling was carried out over the newly acquired claims as well as follow-up on the gold soil geochemical anomalies recognized from the 2000 and 2001 fieldwork. The II Phase continued definition drilling over the Gold Mountain zone, completing another 5 holes and traced mineralization to the south and north of the main discovery zone. Assays are pending (vg noted). An additional 3 holes were drilled on the Starlight claim and a single hole tested the vein structure of the Great Western showings.

Recently Sultan Minerals has entered into an agreement with Kinross Gold whereby Kinross will finance not less than CAD $500,000 in expenditures on or before Dec. 31, 2002, and an additional CAD $500,000 by Sept. 4, 2003, to acquire an option to earn a 60% in the Kena gold-copper property owned by Sultan Minerals (News release, Mon. Sept. 9, 2002). Following this announcement drilling began again on the property and continued late into the fall of 2002. An additional 5696m of diamond drilling was completed in 31 holes.

REGIONAL GEOLOGICAL SETTING

The Omineca belt (Kootenay terrane) of southern British Columbia is the exhumed metamorphic-plutonic hinterland to the foreland, fold and thrust belt. It consists of variably metamorphosed and polydeformed Proterozoic to Tertiary rocks and marks the boundary between accreted terranes and rocks of the North American miogeocline.

Obduction of Quesnellia in the southern Canadian Cordillera began in the earliest Middle Jurassic in response to collision and thrusting of the Intermontane Superterrane over the western margin of North America (Monger *et al.*, 1982; Brown *et al.*, 1986; Murphy *et al.*, 1995). Archibald *et al.* (1983) document Barrovian metamorphism and major deformation circa 165-175 Ma in the Kootenay Arc, followed by exhumation and rapid cooling to <300°C prior to the end of the Jurassic. Leclair *et al.* (1993) constrain a second, regional penetrative deformation and metamorphic event in mid-Cretaceous, west of Kootenay Lake. Contraction appears to have continued until the latest Paleocene (Parrish *et al.*, 1988; Carr, 1992) at which time the southern Omineca underwent extension.

The character of magmatism along the North America margin at this latitude evolved from subduction-generated metaluminous, granitic melts emplaced prior to and accompanying the accretion of Quesnellia (in the Jurassic) to anatectic, peraluminous melts, produced (in the Cretaceous and Paleocene), in response to crustal thickening, metamorphism and partial melting. Widespread mafic volcanism and alkaline magmatism accompanied regional extension in the Eocene.

PROPERTY GEOLOGY

The Kena property is underlain by mafic, shosonitic volcanic and sedimentary rocks of the Rossland Group, an Early Jurassic volcanic arc succession that developed along the eastern margin of Quesnellia. The stratigraphy and tectonic setting of the Rossland Group have been well documented by Höy and Dunne (1997), who describe a tripartite subdivision (after Frebold and Little, 1962) including the Archibald, Elise and Hall formations, for the Nelson area (Figure 1 and 2).

The Early Jurassic, Sinemurian Rossland Group, in the Nelson area is intruded by comagmatic (Eagle Creek plutonic complex, Cat/Shaft monzogabbro complex), synkinematic (Silver King intrusions) and post-tectonic plutons (Nelson suite, Bayonne suite and Coryell syenites) as well as numerous mafic and felsic dikes (Little, 1960; Höy and Dunne, 1997, 2001). It is the mafic volcanic and synvolcanic intrusive rocks of the Elise Formation and younger synkinematic intrusions, which host mineralization on the Kena property.

ELISE FORMATION

A complete stratigraphic section of the Elise Formation is exposed along Highway 6 (Figure 1), south of Nelson, where the rocks have been subdivided into a lower unit of mafic flows and upper unit of predominantly mafic to intermediate pyroclastic rocks (Höy and Andrew, 1988, 1989b; Höy and Dunne, 1997).

The lower Elise is a sequence of primarily mafic flows and flow breccias, minor lahars and tuffs up to one kilometre thick. Coarse-grained augite porphyry flow breccias typically 0.5 to 1.0 m thick comprise the dominant lithology of the lower unit. It lies with apparent conformity on sedimentary rocks of the Ymir Group (Höy and Dunne, 1997). The upper Elise is a sequence of mafic to intermediate flows, tuffs and minor epiclastic deposits up to 2500 metres thick (Figure 4-5, in Höy and Dunne, 1997). A number of cyclical, sequences of mafic to intermediate, typically fining-upwards pyroclastic rocks characterize the Highway 6 section. In contrast to the mafic flows in the lower unit where augite phenocrysts dominate, tuffs in the upper unit are characterized by up to 20% plagioclase phenocrysts.

Geochemistry of the Elise Formation (Beddoe-Stephens and Lambert, 1981, Höy and Dunne, 1997) indicates both alkaline and subalkaline basalt, andesite, trachyandesite and hawaiite compositions. The subalkaline rocks show calcalkaline trends. The high alkalinity and trace element data indicate a shoshonitic affinity and an oceanic island arc setting (Beddoe-Stephens and Lambert, 1981). However, high concentrations of low field strength elements, and REE data are more comparable with values typical of continental margin arc basalts and andesites (Höy and Dunne, 1997, 2001).

EARLY JURASSIC - MONZOGABBRO INTRUSIONS

Small monzogabbro sills or stocks occur throughout the Elise Formation (Figure 1). These are interpreted to be high-level synvolcanic intrusions and locally are associated with copper-gold-magnetite mineralization (Höy and Dunne, 1997). The Shaft mafic intrusive complex is one of these monzogabbro intrusions. It follows the regional foliation, is up to 50 m in width and is more than 5 km long (Figure 2). Andrew and Höy (1989) describe the intrusion as a fine to medium grained porphyritic quartz diorite to monzodiorite. Petrographic examinations report 30 to 45 % plagioclase of labradorite composition, 5 to 10 % orthoclase, rare microcline and 2 to 3% quartz (op. cited, 1989). Biotite (10 to 25%), epidote (<10%) and chlorite (<5%); with or without carbonate and quartz, have replaced all of the primary mafic minerals. These minerals occur as irregular intergrowths and are pseudomorphic after amphibole and/or pyroxene. The feldspars have been altered to sericite. Opague minerals include disseminations, blebs and foliation parallel streaks of magnetite, pyrite and chalcopyrite. Andrew and Höy (1989) noted, "the biotite is widely distributed and occurs as sheaves of tabular crystals that have grown parallel to the schistosity", inferring that alteration was synkinematic. Biotite is part of the pervasive potassic alteration that hosts the copper-gold±magnetite mineralization at the Shaft, Cat and Kena Copper showings.

In addition to the Shaft mafic complex, a number of other sill-like bodies intrude the 1 km wide zone of volcanic rocks located adjacent to the eastern contact of the Silver King pluton (Figure 2). Lewis and Silversides (1991) describe a subvolcanic andesite porphyry unit with varying abundances of plagioclase phenocrysts. Where phenocrysts exceeded 10%, it resembles the Silver King porphyry and where phenocrysts are less, the unit resembles monzodiorite of the Shaft complex. The unit is dike-like and extends 2 km southeast from the Kena Gold zone following the regional foliation. Höy and Dunne (1997) present major oxide chemistry and grouped it with their monzogabbro unit.

There are also a number of narrow (2-20 m) sill-like bodies of Silver King (?) porphyry that intrude the areas northeast and southwest of the main Silver King pluton (Gold Creek and Giveout Creek areas). These are typically highly sheared and altered (epidote-chlorite-calcite±pyrite) and follow the regional foliation.

EARLY- MIDDLE JURASSIC SILVER KING INTRUSIONS

Six, north to northwest elongate quartz monzodiorite to granodiorite plagioclase porphyritic plutons of Early Middle Jurassic age intrude Early Jurassic volcanic strata along the overturned eastern limb of the Hall Creek syncline (Figure 1). Contact relationships with the Rossland Group rocks are either sharply discordant or complexly interdigitated and often intensely sheared. The contact generally follows the regional northwest structural fabric; in the vicinity of the Gold Mountain Zone the contact has variable northerly-trending orientations. In road exposures north of the GMZ the contact zone is sheared and steeply dipping, however, 200 to 300 metres south, the contact is comprised of metre-wide apophyses of porphyry that interfinger with strongly pyritized Elise volcanic rocks. Altered and partially digested xenoliths of metavolcanic rocks occur within the porphyry and are exposed in trenches at the "discovery zone". These relationships indicate that the porphyry is intrusive into the volcanic sequence.

The Silver King intrusions form white-weathering, resistant outcrops that for the most part conform to the dominant regional foliation. In hand sample the rock is characterized by 20 to 60 % white plagioclase phenocrysts in a variable dark green, grey or white matrix. Green actinolite and/or biotite have replaced hornblende. Coarse (0.5 mm), euhedral sphene is commonly visible in handspecimen.

Earlier petrographic studies characterized the Silver King intrusions as quartz diorite porphyry (Mulligan, 1952), leuco-diorite porphyry (Höy and Dunne, 1997) and quartz monzonite to quartz monzodiorite (Höy and Dunne, 2001; Wells, 2001). Thin sections show 30 to 60 % sodic plagioclase of andesine to labradorite composition, 5 % orthoclase, and 1 to 2% rounded, resorbed quartz. The plagioclase is extensively sericitized, particularly along outer zones of the phenocrysts and/or sausseritized (epidote+sericite±carbonate±chlorite), chiefly in the interior of the phenocrysts. Primary mafic minerals are rarely preserved. Irregular crystal aggregates and prismatic pseudomorphs after amphibole, of secondary biotite, epidote, carbonate, pyrite and chlorite have replaced the primary mafic minerals. The groundmass consists chiefly of plagioclase, orthoclase, quartz and alteration minerals (sericite-epidote-carbonate ±chlorite). Opague minerals comprise generally less than 1.5 % and include, in order of abundance, coarse euhedral sphene and fine disseminations of magnetite and pyrite.

The margins of the Silver King pluton, and specifically the narrow Silver King intrusive sills present in the Gold Creek area, are strongly sheared and altered. In thin section a cataclastic fabric is typically visible (Höy and Dunne, 1997, and this study). This fabric varies from an anastamosing foliation defined by sericite-quartz-calcite±biotite±chlorite minerals to protomylonite zones where plagioclase phenocrysts have been rotated (Plate 6-8, page 82; Höy and Dunne, 1997) together with grain size reduction. In samples from the Great Western showing, the foliation has transposed quartz-biotite-pyrite, and quartz-calcite±pyrite veinlets and as well, rotated plagioclase phenocrysts and boudins of sericite-carbonate altered groundmass. These relationships imply that the alteration and mineralization(?) of the Silver King pluton coincide with or predate the main phase of regional deformation.

Dunne and Höy (1992) interpreted the contact relationships and the foliated to massive nature of the intrusions as evidence to suggest the Silver King intrusions are a pre to synkinematic suite. Discordant uranium-lead zircon data indicates crystallization ages of the intrusions to be Aalenian (*ca.* 174-179 Ma), (Höy and Dunne, 1997).

MAFIC DIKES

Dark green lamprophyre dikes intrude the Elise Formation greenschists and metavolcanic rocks generally parallel to the main foliation. Fine-grained mafic and biotite lamprophyre dikes also cut the Silver King pluton and follow northwest and north trending shear zones in the monzodiorite. Higher-grade gold intersections commonly coincide with hangingwall and footwall sections adjacent to the mafic dikes, but the dikes themselves do not carry elevated gold values. Dikes typically return less than 0.05 g/t Au, immediate wall rocks to the dikes contain at least an order of magnitude higher gold. For example, 2 m intersections from drill hole 01GM-10 returned: 0.58 g/t Au from the footwall to a 2.04 m dike intersected at 58.96m, and 1.15 g/t Au and 0.86 g/t Au from hangingwall and footwall sections respectively of a second 2 m dike intersected at 117 m depth. Shear-hosted lamprophyre dikes were noted in workings at the Great Western, and in greenschsist units at the Starlight showing (*see* below).

GEOCHEMISTRY

Silver King intrusions define a 20 km long magmatic belt extending from Nelson south to Ymir (Figure 1). The northern most intrusion (Silver King pluton) hosts the Gold Mountain Zone (GMZ) and has received the most study to date (Dandy, 2001; and references therein). Porphyry Au-Cu mineralization and hydrothermal alteration overprint much of the primary composition of this intrusion. Sampling of additional intrusions from the belt was carried out to evaluate their potential to host similar Au-Cu mineralization and to characterize the major and trace element chemistry of the Silver King intrusive suite. A suite of 8 samples from 6 separate Silver King intrusions were collected and analyzed for major and trace element abundances. Major oxides were determined by lithium borate fusion and XRF analysis and trace element geochemistry was determined using pressed pellet and XRF analysis at Cominco Research Labs, Vancouver. The results are list in Table 1. The analyses are plotted together with data from twelve monzogabbro intrusive samples (Höy and Dunne, 1997) and six samples of monzodiorite from the Silver

TABLE 1
MAJOR OXIDE AND TRACE ELEMENT ABUNDANCES FOR INTRUSIVE ROCKS IN THE NELSON AREA

Sample	Intrusives	Easting	Northing	SiO2	TiO2	Al2O3	Fe2O3	MnO	MgO	CaO	Na2O	K2O	P2O5	Cr2O3	Ba	LOI	Total
01GM-15	SK pluton	478459	5476204	63.58	0.38	17.29	3.57	0.09	0.75	4.8	4.57	2.86	0.15	*	678	1.39	99.5
01GM-17	SK pluton	478652	5476315	61.63	0.38	16.43	3.77	0.05	0.73	4.17	4.82	3.57	0.12	*	189	3.59	99.34
01GM-18	SK pluton	478741	5476134	61.65	0.38	16.94	3.28	0.05	0.75	4.21	5.15	3.41	0.11	*	424	3.34	99.34
01GM-7	SK pluton	479470	5475670	61.95	0.4	16.88	3.63	0.05	0.83	3.08	4.9	4.73	0.11	*	171	2.83	99.52
02JLO2-7	SK suite	479457	5473679	62.09	0.5	17.04	4.84	0.14	1.35	4.98	4.53	1.83	0.2	*	954	2.07	99.66
02JLO4-25	SK suite	483667	5461045	57.31	0.58	19.37	5.19	0.12	1.22	5.03	5.76	1.99	0.21	*	659	2.58	99.42
02JLO4-28	SK suite	480505	5474806	57.06	0.69	16.45	6.59	0.11	2.51	5.75	3.59	3.45	0.25	*	712	2.92	99.44
02JLO4-30	SK pluton	480418	5474158	62.84	0.38	17.11	3.73	0.1	0.75	4.46	4.8	2.59	0.11	*	839	2.48	99.43
02JLO5-33	SK pluton	477544	5477235	63.54	0.37	17.25	3.72	0.03	0.75	4.51	4.8	2.81	0.11	*	677	1.66	99.62
02JLO6-44-2	SK suite	482349	5469945	63.34	0.43	17.28	3.75	0.07	1	4.8	4.8	1.25	0.15	*	657	2.73	99.67
02JLO6-44-3	SK suite	482349	5469945	63.22	0.4	15.05	2.58	0.09	0.75	5.07	4.67	1.63	0.12	*	555	5.48	99.11
02JLO6-45	SK suite	482754	5468130	62.74	0.43	17.23	3.74	0.05	1.05	4.44	4.96	1.63	0.15	*	649	3.11	99.59
*01GM01	SK pluton	479346	5475910	63.39	0.25	15.21	5.28	0.02	0.38	1.75	4.44	5.07	0.07	0.036	100	4.04	99.96
*01GM10	SK pluton	479130	5475786	61.97	0.38	16.9	3.89	0.07	1.07	4.04	4.79	4.72	0.16	0.018	800	1.95	100
*01GM11	SK pluton	479132	5475902	63.03	0.39	16.6	3.14	0.03	0.86	3.17	5.22	4	0.12	0.018	700	2.37	100
*01GM11	SK pluton	479132	5475902	63.83	0.38	16.82	3.18	0.06	0.79	3.65	5.62	3.78	0.07	0.023	700	2.1	100.37
*01GM14	SK pluton	479329	5475553	64.73	0.4	17.86	2.92	0.04	0.74	3.34	5.46	3	0.08	0.018	800	1.33	99.99
*01GM15	SK pluton	478459	5476204	64.13	0.36	16.98	3.65	0.1	0.86	4.8	4.45	2.64	0.14	0.028	100	1.78	99.92
**R137-9	SK suite	478469	5473764	62.72	0.54	17.31	5.24	0.11	1.38	4.15	4.42	1.79	0.2	*	618	2.11	99.97
**R47-2	SK suite	483880	5461150	62.22	0.54	17.28	4.87	0.14	1.17	4.47	3.94	2.41	0.18	*	685	2.99	100.21
**R50-20	SK pluton	478716	5477323	63.6	0.42	17.31	3.46	0.06	0.79	4.05	4.7	3.3	0.12	*	614	2.46	100.27
**R78-2	SK suite	477274	5476245	65.05	0.38	16.48	2.31	0.08	1.02	3.54	2.41	3.78	0.15	*	1554	3.79	98.99
**R79-1	MNGB	479706	5475849	52.9	0.54	16.71	7.71	0.2	1.73	5.67	2.91	5.79	0.28	*	989	4.61	99.05
**R79-10	MNGB	479706	5475849	50.97	0.79	16.55	10.67	0.25	4.2	5.55	3.72	3.56	0.37	*	768	2.58	99.21
**R79-17	MNGB	479706	5475850	51.94	0.55	15.57	8.32	0.27	2.29	5.85	2.6	5.48	0.29	*	1106	6.47	99.63
**R79-21	MNGB	479706	5475850	55.5	0.62	18.08	7.99	0.22	2.62	2.71	4.62	4.39	0.31	*	925	2.45	99.51
**R79-3	MNGB	479706	5475849	54.77	0.61	17.32	7.62	0.18	2.62	5.32	3.56	4.76	0.59	*	1245	2.32	99.67
**R80-1b	MNGB	479714	5475852	55.6	0.57	17.15	7.32	0.12	2.3	3.16	4.87	5.07	0.33	*	916	2.89	99.38
**R80-6	MNGB	479712	5475849	54.29	0.57	16.91	7.44	0.14	2.45	3.91	4.52	5.27	0.32	*	891	3.4	99.22
**R82-3	MNGB	480854	5474376	52.67	0.82	16.07	10.17	0.24	3.68	5.24	4.49	3.09	0.31	*	436	2.68	99.46
**R82-8	MNGB	480854	5474376	52.07	0.72	16.5	9.67	0.05	4.08	0.49	1.9	8.92	0.31	*	1977	0.47	99.18
**R86-11	SK suite	481421	5473498	56.33	0.74	16.01	7.11	0.13	2.67	5.17	3.59	2.86	0.26	*	521	4.91	99.78
**R86-18	SK suite	481222	5473589	64.01	0.42	17.46	3.89	0.13	0.79	4.3	5.21	1.53	0.12	*	591	2.1	99.96
**R86-24	SK suite	481471	5473446	60.75	0.58	18.31	5.54	0.1	1.81	3.58	4.34	2.36	0.22	*	666	2.33	99.92
**R92-10	MNGB	481920	5473316	55.38	0.48	17.38	3.97	0.04	1.56	4.35	4.71	5.78	0.32	*	714	5.07	99.04
**R92-4	MNGB	481699	5473620	57.32	0.37	16.52	4.34	0.06	1.19	4.95	4.4	4.6	0.21	*	744	5.14	99.1
**R92-5	MNGB	481790	5473538	54.94	0.37	16.05	4.58	0.06	2.13	4.52	4.67	5.16	0.21	*	869	6.4	99.09

* Data from Wells, 2001

** Data from Höy and Dunne, 1997

King pluton (Wells, 2001). The chemical data is presented in three subgroups: samples of monzogabbro intrusions from the Kena area (Höy and Dunne, 1997); Silver King intrusives (with the exception of the Silver King pluton); and samples of the Silver King pluton (Figure 3).

The samples are from an area, which was metamorphosed to lower greenschist grade. In addition, many of the samples are from mineralized zones that are strongly altered by hydrothermal processes. As a result, losses on ignition (LOI) values are high and major element mobility has occurred for some samples. Petrographic studies reveal varying degrees of alteration.

Analyses of the Silver King intrusive suite fall in the subalkaline field on the total alkali-silica plot (Höy and Dunne, 1997; and this study) in marked contrast to the alkaline nature of the subvolcanic, monzogabbro intrusive suite (Figure 3-A). In detail, altered samples of the Silver King intrusive suite straddle positions transitional to the alkaline field. The alkaline nature of the monzogabbro intrusions is due mainly to the high potassium content of these rocks; a reflection of their comagmatic relationship with the shoshonitic Elise volcanic suite (Höy and Andrew, 1989b). Analyses of samples from the Silver King pluton also show elevated potassium content relative to most of the other feldspar porphyry bodies analyzed from the Silver King magmatic belt (Figure 3-B). Both, potassium and sodium enrichment of samples from the Gold Mountain and peripheral mineralized zones can be related to hydrothermal alteration processes, but the majority of samples of the Silver King pluton have consistently elevated potassium content (relative to other Silver King intrusives) that cannot be entirely related to secondary alteration. Separation of the intrusive suites and the isolation of the Silver King pluton data from the other feldspar porphyry bodies in the belt are shown clearly on a Na_2O K_2O vs. SiO_2 plot (Figure 3-D).

Previous petrographic and chemical studies characterized the Silver King intrusions as leuco-diorite porphyry (Höy and Dunne, 1997) and quartz monzonite to quartz monzodiorite (Wells, 2001). Using data from the earlier studies in addition to the new data reported here the intrusive rock samples are classified according to CIPW normative mineral calculations using the QAP diagram (LeMaitre, 1989), which uses the same classification as Streckeisen (1976). The monzogabbro samples plot along the lower axis in the monzonite and syenites fields. The Silver King intrusive data define three distinct clusters: 1) a subset of samples from peripheral dikes (Cu *Zone*) or separate feldspar porphyry plutons (Cariboo, Three Friends, Salmo River) - cluster at the borders of granodiorite-monzogranite-quartz monzonite and monzodiorite, 2) least altered samples from within the Silver King pluton but distal from the GMZ - plot as quartz monzonite and 3) drill core samples of potassium and sodium enriched (altered) rocks from the GMZ - are displaced towards the alkali feldspar apex (P) into the quartz syenite field (Figure 3).

The intrusions are metaluminous and show Nb and Y trace element signatures of volcanic arc and syn-collisional granites (Figure 3-E and 3-F). Low (<100 ppm) Rb values are more characteristic of volcanic arc granites than syn-collisional granite (Y+Nb vs. Rb plot) (Höy and Dunne, 1997).

STRUCTURE

The structures in the Nelson area are predominantly north trending broad, east-verging folds and associated shears (Höy and Andrew, 1989b; Höy and Dunne, 2001). The Kena property (Figure 2) lies on the eastern limb of the Hall Creek syncline, a south plunging, west dipping overturned fold that deforms Early Jurassic Rossland Group rocks (~182 Ma) and Early Middle Jurassic Silver King intrusive rocks. Regional foliation trends northwest, dips steeply to the southwest and is axial planar to the Hall Creek syncline. Northwest of the closure of the Hall Formation the synclinal core *zone* is replaced by a kilometre wide shear *zone*, referred to as the Silver King shear (Höy and Dunne, 2001). This shear *zone* bounds the Silver King pluton and much of the Kena property to the west. The north-trending structures are cut and therefore constraint by the Middle Jurassic Bonnington and Nelson intrusions (~165 Ma).

In the vicinity of the Kena Gold *zone* and surrounding areas the dominant foliation (S_n) strikes 120-160° and dips moderately southwest, with local dip reversals in the headwaters of Noman Creek. Foliation varies from typically penetrative in the metavolcanic rocks to a spaced foliation or lacking entirely in the Silver King pluton. Rhys (2000) recognized a second, more northerly trending spaced cleavage (S_{n+1}) and several north-striking, west-dipping shear *zones* up to 10 m thick, within and along the margin of the Silver King pluton. Asymmetric foliations and pressure shadows surrounding plagioclase phenocrysts suggest a sinistral shear sense on 2 of these structures but conflicting shear sense indicators have been obtained along strike (Rhys, 2000).

Crenulation of the dominant foliation S_n about west-trending, westerly plunging axis is well developed in greenschists and metatuffs within the Silver King shear *zone*, located southwest of the Silver King pluton (Figure 2).

MINERAL OCCURRENCES

The Kena property hosts a number of gold and gold-copper occurrences (Dandy, 2000, 2001), covering a large area located south of the town of Nelson (Figure 1 and 2). Mineralization occurs within the early Jurassic, Elise Formation metavolcanic rocks (Silver King, Starlight, Cariboo) and subvolcanic intrusive rocks (Shaft Cat, Kena); early Middle Jurassic, Silver King intrusive rocks (Gold Mountain *zone*, Great Western), and is locally concentrated along the north-northwesterly trending contact *zone* between these units (Gold Mountain *zone*). The main focus of this study was to document the style and relationships of mineralization alteration at the Gold Mountain *Zone*, however because Au-Cu porphyry systems can be large, peripheral showings were examined and their regional relationships are summarized below. Deposits pe-

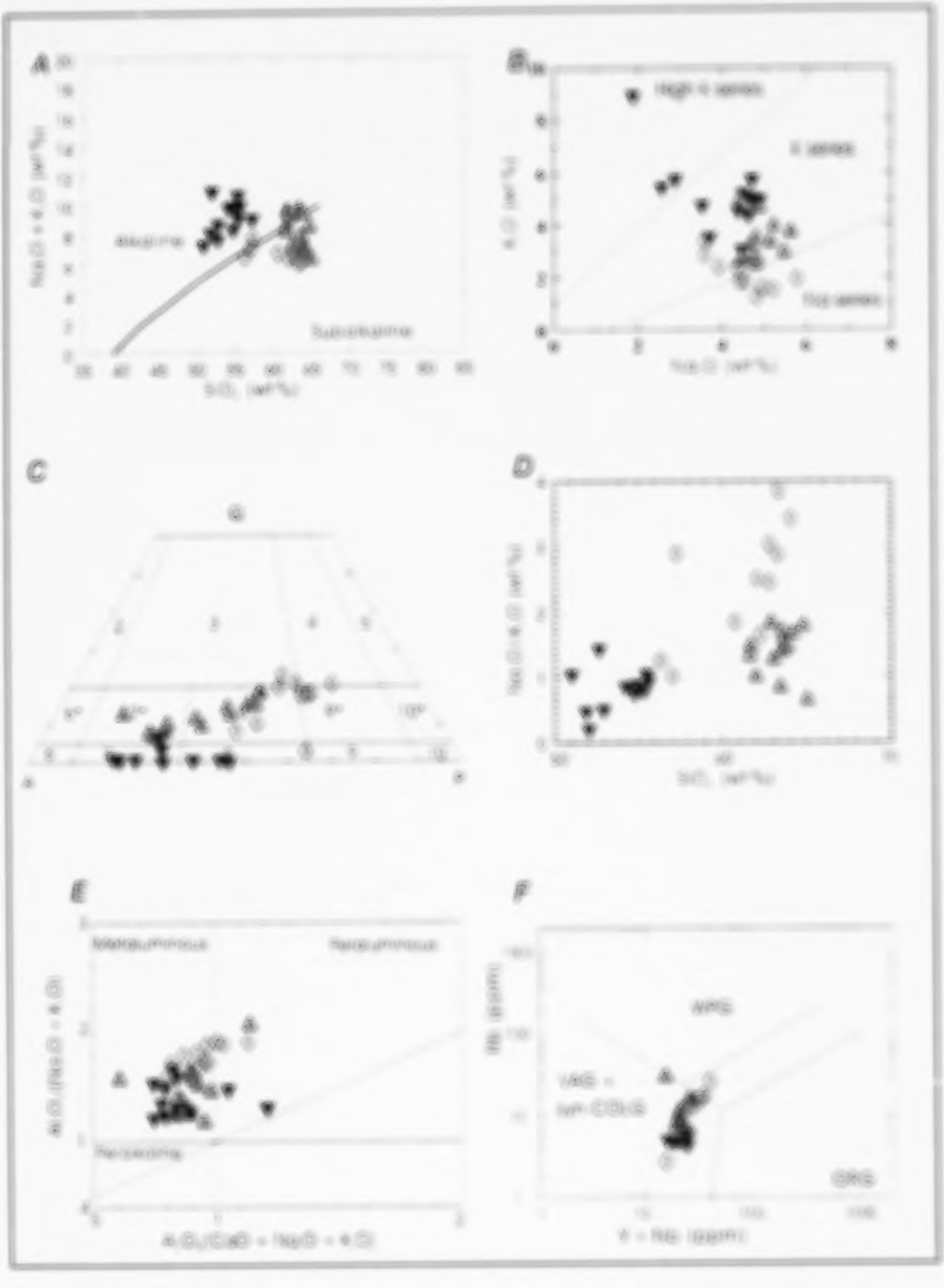

Figure 5. Major and trace element geochemical plots for Silver King intrusions (diamonds), metagabbro intrusions (inverted filled triangle; data from Hoy and Dunne, 1997), Silver King pluton (filled triangle). A) total alkali versus silica (after Irvine and Baragar, 1971); B) K_2O versus Na_2O (after Middlemost, 1975); C) plot of normative quartz-alkali feldspar-plagioclase compositions, projected onto the modal classification of Streckeisen (1976); D) Na_2O/K_2O versus silica; E) Shand's index diagram showing relative alumina saturation (after Shand, 1951); F) plot of Rb versus Y+Nb (after Pearce *et al.*, 1984).

ripheral to the Gold Mountain zone occur primarily NE and SW of the Silver King pluton. The NE contact zone extends 2 km north of Giveout Creek and 5 km south and contains foliation parallel shears and zones of intense brittle fracturing that have localized alteration and copper-gold mineralization at the Shaft, Cat, Kena Gold and Kena 0 copper mineral showings. The SW contact zone extends approximately 5 km north from the headwaters of Giveout Creek and is characterized by intense zones of foliation parallel shearing (Silver King shear zone) and hosts the Silver King, Starlight, Caribou and Giveout Creek mineral showings.

GOLD MOUNTAIN ZONE (82F/SW 379)

The Gold Mountain Zone is located 8 kilometres south of Nelson. It straddles the eastern contact of the Silver King pluton and Elise Formation metavolcanic rocks, but lies mainly within the pluton (Figure 2).

Exploration Parameters

The Gold Mountain Zone has a well defined gold-in-soil geochemical signature (1500 m x 1000 m) that exhibits a northwesterly trend (Dandy, 2002). Gold values in soils overlying the Silver King pluton and contact zone are enriched relative to the values overlying the Elise volcanic rocks, and within the pluton there are specific large anomalous zones with significant elevated gold values. Along the northwest-trending, eastern contact zone between the intrusion and volcanic rocks soil values are generally <50 ppb Au. Gold values >100 ppb in soils define the Gold Mountain, Kena Gold and the South Gold zones that together are aligned in a northwest trend, parallel to the regional foliation.

Results from a magnetometer survey that was carried out over the Gold Mountain grid (Dandy, 2001), indicated a strong response with generally higher magnetic susceptibility for areas located at the northern and northwestern portions of the pluton. Vein stockwork, disseminated and locally magnetite breccias (Dunne, 2001; this study) have been mapped in the north and southern sections of the pluton. Relatively lower magnetic readings define a wide belt overlying the discovery area where pervasive potassium-silica-pyrite alteration is evident.

An Induced Polarization survey was conducted over the discovery area to test the response of the auriferous sulphide mineralization in the Silver King pluton. After a strong chargeability response was obtained over the "discovery" area, IP was completed over the rest of the grid and defined a number of additional geophysical anomalies (Walcott, 2001). Areas of high chargeability and coincident high resistivity correlate well with the gold soil geochemical anomalies (Dandy, 2002) and reflect pyrite content of mineralization and accompanying potassic-silica alteration.

Mineralization-Alteration

Hydrothermal alteration mineral assemblages present in drill core in and around the Gold Mountain zone are similar to the principal alteration types developed around gold-rich porphyry deposits of the Pacific rim (Sillitoe, 1979, 2000). These alteration types include potassium silicate (K-spar, quartz), propylitic (chlorite, epidote, calcite, albite), intermediate argillic (sericite, clay, chlorite, hematite) and sericitic (quartz, sericite, pyrite). Not present on the Kena property is an advanced argillic alteration zone, which is commonly developed in the upper, volcanic-hosted parts of a porphyry system (Sillitoe, 1993). A study of rocks in the vicinity of the Kena Gold Mountain Zone identified six (6) alteration mineral assemblages (Dunne, 2001). These include tourmaline stockwork, magnetite dominant and magnetite-pyrite assemblages (potassic); magnetite + quartz assemblage (propylitic); pyrite dominant assemblage (sericitic); and quartz stockwork alteration zones (Table 2). A systematic mapping program of the alteration assemblages and their distribution in and around the Silver King pluton remains to be undertaken. The following describes the assemblages but controls on their distribution have not been established.

POTASSIC

Potassium alteration of the rocks on the Kena property is subtle and recognized chiefly by staining samples with sodium cobaltinitrite (Dunne, 2001; this study). Pervasive alkali flooding affects the finer-grained volcaniclastic rocks and the groundmass of the quartz monzonite porphyry in particular. It generally consists of fine-grain aggregates of potassium feldspar, plagioclase, quartz and lesser fine sericite. The alteration is primarily microfracture-controlled and only rarely is alteration evident from potassium feldspar-quartz veinlets. Locally plagioclase phenocrysts are fractured and cut by secondary orthoclase veinlets and variably altered by fine dustings of sericite

TABLE 2
MAJOR ALTERATION TYPES AND MINERAL ASSEMBLAGES FROM THE GOLD MOUNTAIN ZONE (AFTER DUNNE, 2001)

Potassic	
tourmaline stockwork	tourmaline-quartz ± K-spar-pyrite
magnetite dominant	magnetite ± K-spar-biotite [illegible] ± [illegible]
magnetite + pyrite	magnetite-pyrite ± K-spar-biotite [illegible] [illegible]
Propylitic	
magnetite + quartz dominant	magnetite-quartz-chlorite-sericite-[illegible]
Sericitic	
pyrite dominant	pyrite-sericite ± K-spar [illegible] [illegible]
quartz stockwork	quartz-pyrite-sericite ± K-spar [illegible] [illegible] [illegible]

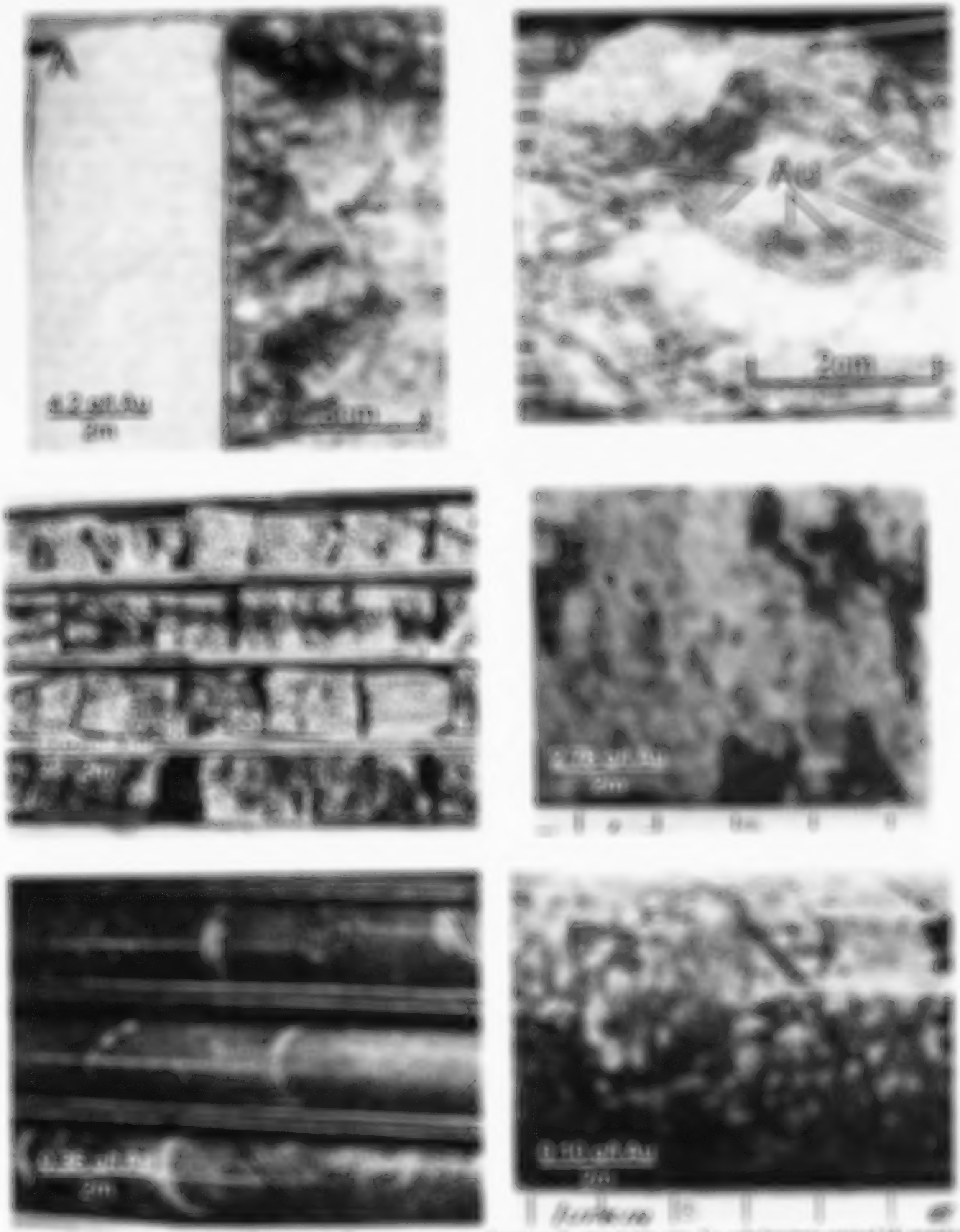
4.2 g/t Au
2m
5cm
Au
2cm
0.78 g/t Au
2m
2m
0.35 g/t Au
2m
0.10 g/t Au
2m

[illegible]

[illegible]

[illegible]

[illegible]

[illegible]

[illegible]

[illegible]

[illegible]

[illegible]

[illegible]

[illegible]

[illegible]

from drill hole 93GM-7. Trace amounts of molybdenum are also present in quartz-sericite veinlets.

Gold occurs primarily as fine grains but in a variety of relationships and mineral associations. Grain size varies from very fine "micro-flake" gold (Wells, 2001) to millimetre-sized blebs of visible gold (Figure 10). Gold always occupies late fractures. It occurs as fine, sub-rounded inclusions in veinlet pyrite, as fracture fillings in brecciated veinlet pyrite and as colloidal grains in quartz and a late calcite (?) gangue. Gold also occurs together with pyrite and magnetite in a veinlet (93GM-4, 84.3m) that crosscuts pervasive potassium alteration.

Gold Distribution

Gold and trace metal abundances were determined by neutron activation analyses for a limited suite (12) of Silver King intrusives. All six samples of quartz monzodiorite collected from separate plutons across the Silver King magmatic belt contain less than 2 ppb Au, while most samples of Silver King pluton contain elevated gold values and show variable alteration. Two of the least altered samples of Silver King pluton, however contained less than 2 ppb Au, indicative that mineralization is closely associated with alteration.

Mineralization at the GMZ consists primarily of disseminated blebs of pyrite-chalcopyrite and rare pyrrhotite (Rhys, 2000; Dunne, 2001) and lesser stringers and fracture veinlets. At the "discovery" zone (GMZ) gold values of 1 to 3 g/t Au correspond directly with intervals of pervasive potassium alteration and pyritization, which coincide with higher fracture and veinlet densities. Pyrite-quartz-tourmaline-calcite veinlet density varies positively with gold concentration, particularly in holes 93GM-1 and 93GM-3 (Rhys, 2001). Measurements of pyrite coated fractures, joints, cleavage, quartz-pyrite veins and iron oxide coated

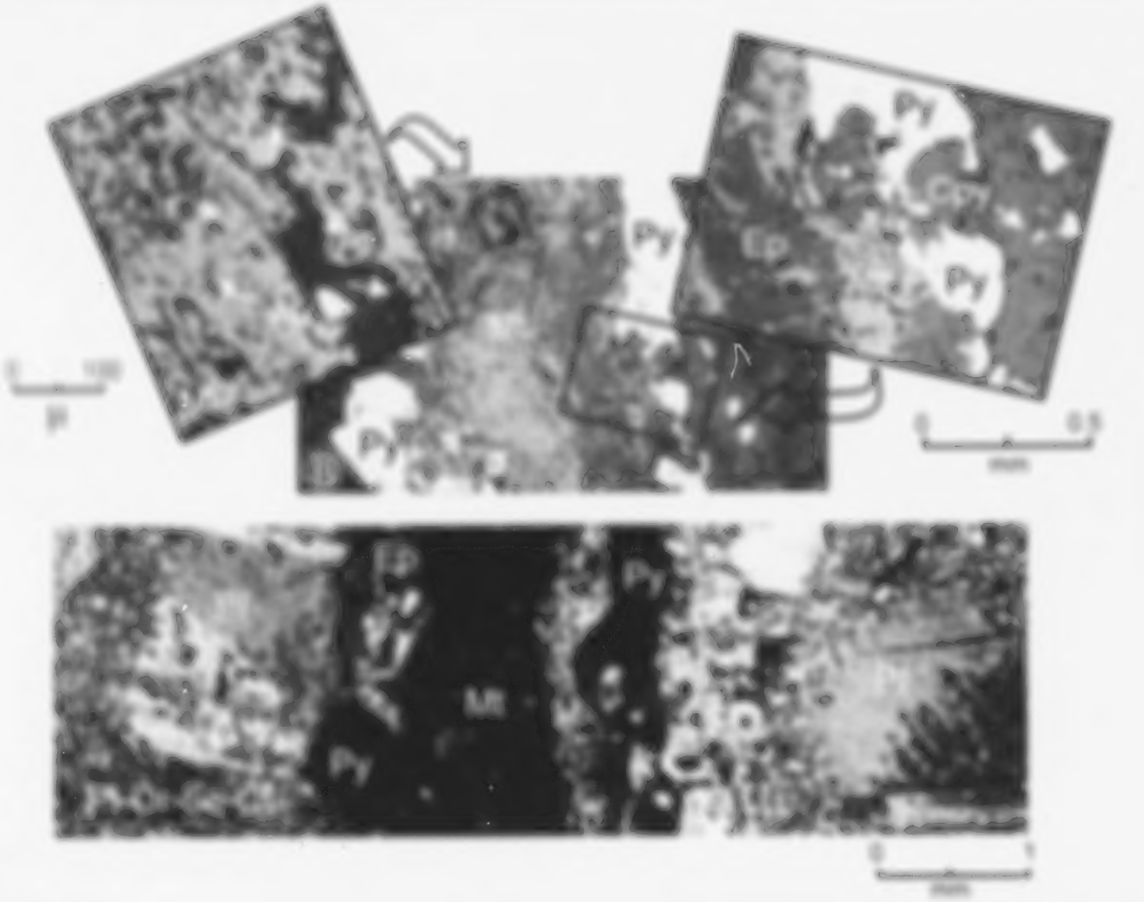

Figure 11. Photomicrograph of auriferous magnetite veinlet cutting quartz monzonite from the Gold Mountain Zone (93GM-04, 84.3 m). A) Characteristic porphyry texture of Silver King pluton, large plagioclase phenocrysts in a fine-grained plagioclase-orthoclase-sericite-quartz matrix, cut by a magnetite-pyrite-gold vein. The vein is mantled by epidote-pyrite-chalcopyrite and chloritic alteration envelope (transmitted light, x-nicols). B) Field of view reduced to show the distribution of opaque minerals in the vein. Insets show the grain size and relationships between gold and magnetite mineralization in the center of the vein, and the chalcopyrite-pyrite-quartz (-gold and pyrite) assemblages that is present along the margins of the vein (reflected light).

joints from surface trench exposures of the GMZ (Rhys, 2001), show a consistent veinlet and fracture orientation, which have steep to moderate southerly dips, with strikes ranging between 330-150°. Shallow dipping features and those with north to north-northeast trends were rare. These orientations are the same at the Great Eastern/Western showings (see below) and as peripheral mineralized veins contained within the metavolcanic rocks (Kena Gold).

Definition drilling of the Gold Mountain Zone shows wide zones of alteration and gold mineralization, which hosted within the pluton and locally, extend beyond the contact zone into the metavolcanic country rocks. Section 11+00N and Section 10+70N reproduced and modified from Dandy (2002), show the geology and gold assays from 2000 and 2001 diamond drilling at the GMZ (Figure 6). Drill core was sampled on 2 metre intervals and analyzed for gold and other metals. From this raw assay data, continuous intervals of greater than 1 g/t Au were isolated, the assay values combined and an average grade determined. This average grade was then applied to the entire intersection, grouped into populations of greater than 1, >2, >3, >5 or >10 g/t Au and plotted onto the section lines (Figure 6).

On section L11+00N, higher-grade and wider intersections of gold mineralization occur in a zone below the "discovery" trenches (3+00E), giving continuity to, and expanding the area of anomalous gold values outlined by surface chip sampling. A second zone of higher-grade intersections straddles and follows the porphyry metavolcanic contact zone. Some of the highest gold assays have come from intervals of porphyry and metavolcanic rocks located within 20 m above and below this contact zone. It is difficult to project the higher-grade intersections from one section line to the next or to determine their prospective orientations.

Great Eastern and Western (82FSW 171,172)

The Great Eastern/Western showings are located east of the Gold Mountain Zone close to the western contact of the Silver King pluton. Gold mineralization occurs in quartz veins and shear zones hosted entirely within the Silver King pluton. The shear zones, like those in the adjacent greenstones and metavolcanic rocks are northwest trending, parallel to the dominant foliation, while the quartz veins trend easterly with generally steep north and south dips. Early exploration and development work focused on three veins, "A", "B", and "C" (Fahrni, 1946). The three veins are located along a single(?) or multiple foliation parallel shears, with "A" at the southern end, "B" located 215 m northwest and "C" located a further 275 m northwest. At its southern end the shear zone strikes 116/63° SW and at its northwestern end the same(?) northwest-trending shear dips 80° SW and contains two narrow lamprophyre dikes. The shear zone and wallrock to the veins are extensively altered and bleached. Pyritic, carbonate and sericite alteration assemblages replace the sheared monzonite and envelope narrow quartz-pyrite-sericite veins and quartz-calcite-pyrite veins. Samples of schistose monzonite from the shear at "A" vein returned 1.71 g/t Au, from the shear at "B" vein returned 0.32 g/t Au, and from the shear at "C" vein, two samples returned 1.37 g/t Au and 0.32 g/t Au (Fahrni, 1946).

Vein orientations are highly discordant to the northwest trending shear(s). The "A" vein strikes 72/90° SE, the "B" vein 290/85° N and the "C" vein 260/85° N. The "C" vein cuts and offsets the northwest-trending shear zone that contains the lamprophyre dikes (Fahrni, 1946) and narrow east-trending, sheeted quartz± tourmaline veins, located east of the "A" portal, appear to crosscut the dominant southeast-trending foliation (Figure 7). Deposition of the "C" vein and sheeted quartz veins crosscut the dominant foliation and therefore post-date it's development. Exposures in all of the old workings have generally narrow widths of quartz material (5 cm) with similar widths of altered pyritized, quartz monzonite wallrock. A 33 cm sample of quartz and wallrock from the face of the "A" vein returned 6.17 g/t Au (Fahrni, 1946). Quartz-tourmaline-sericite breccias and narrow quartz-pyrite veins cut quartz monzonite at the "B" vein workings.

A single hole was drilled (121.92 m) to test the area of the "C" vein (August 2002). Alteration and mineralization of the porphyry is controlled by narrow fractures. Fracture density increases down section where sericite-quartz-pyrite-calcite stockworks have bleached and destroyed the igneous texture and rarely host auriferous quartz-pyrite-calcite veinlets. Visible gold is present in core, but gold assays returned only three widely separated 2 m intervals containing 1-2 g/t Au.

Narrow, mineralized quartz veins at the Great Eastern and Western workings contain visible gold in east-trending structures that locally, post-dates development of the foliation and define a structural corridor that when project further east intersects the "discovery" area at the Gold Mountain Zone.

PERIPHERAL MINERALIZATION

The Kena Gold Zone (82FSW 237)

The Kena Gold Zone has been the focus of most of the earlier work on the Kena Property. The mineralized showings (Main and Neil) are located 3 km southeast of the Gold Mountain Zone in Elise Formation metatuff and metabasalt units, approximately 500 m northeast of the Silver King pluton. A large number of synvolcanic diorite and monzogabbro intrusions, sill-like bodies of younger, intermediate to felsic plutons and lamprophyre dikes intrude the volcanic rocks in this northwest-trending zone adjacent to the Silver King pluton. The area contains foliation-parallel shears and zones of intense brittle fracturing that have localized potassic (orthoclase and biotite) and sericitic (sericite, quartz and carbonate) alteration assemblages and associated copper-gold mineralization.

Initial percussion drilling (4 holes, 250 m total) by Ducanex Resources Ltd. recognized an east trending, south dipping mineralized zone that contained 1.37 to 1.70 g/t Au over 6 to 10 m thick intervals in potassic, sericitic altered volcanic rocks (Johnson, 1974; 1975). Subsequent work on the Kena Gold Zone includes trenching, geophysical-, geo-

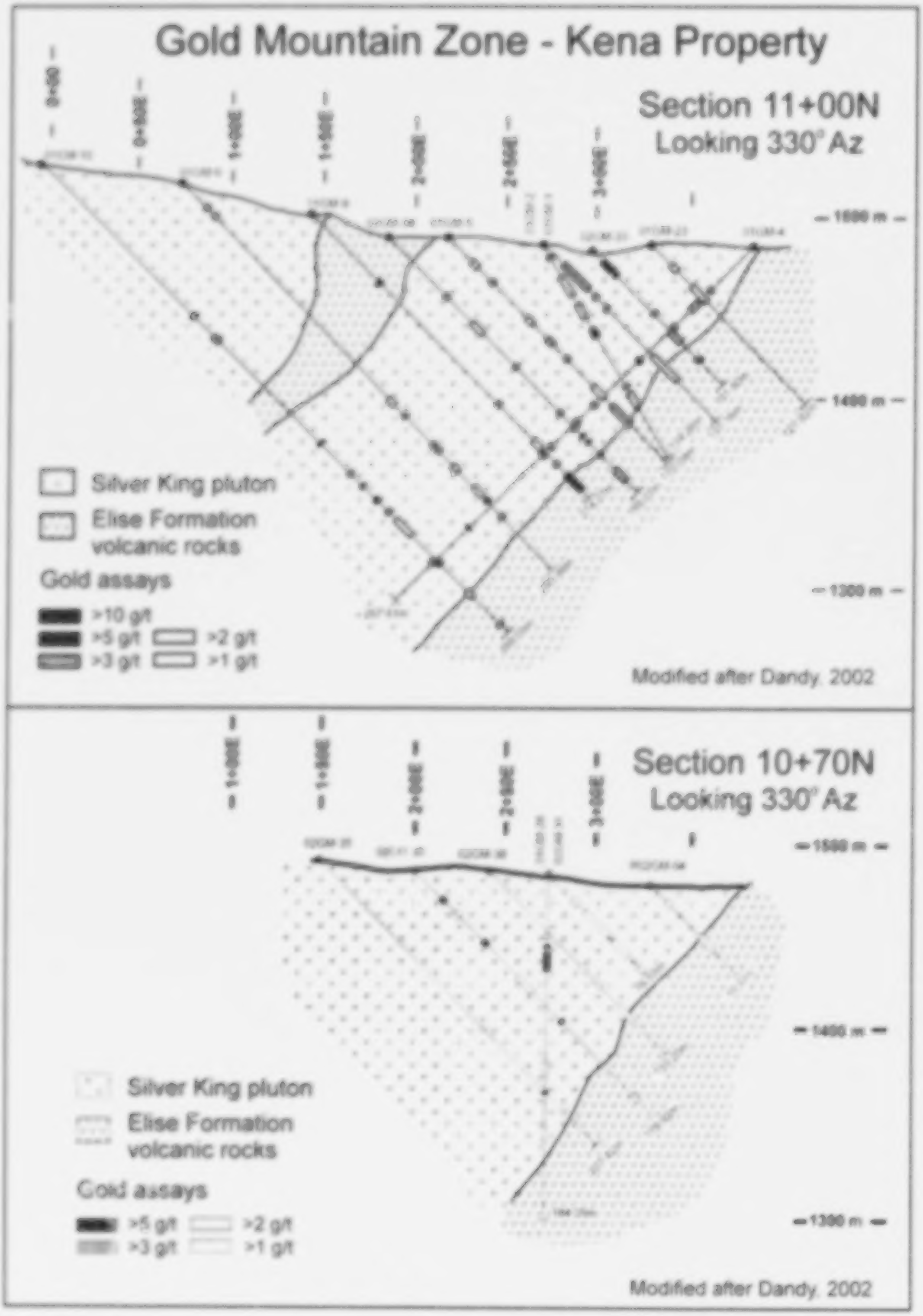
Gold Mountain Zone - Kena Property
Section 11+00N
Looking 330° Az
0+00
0+50E
1+00E
1+50E
2+00E
2+50E
3+00E
1500 m
1400 m
1300 m
Silver King pluton
Elise Formation volcanic rocks
Gold assays
>10 g/t
>5 g/t
>3 g/t
>2 g/t
>1 g/t
Modified after Dandy, 2002
Section 10+70N
Looking 330° Az
1+00E
1+50E
2+00E
2+50E
3+00E
1500 m
1400 m
1300 m
Silver King pluton
Elise Formation volcanic rocks
Gold assays
>5 g/t
>3 g/t
>2 g/t
>1 g/t
Modified after Dandy, 2002

Figure 6. Section Line 11+00N and Line10+70N showing geology (from Dandy, 2002) and calculated average gold grades of the Gold Mountain Zone. The gold assays were calculated from continuous, 2m intersections grading >1 g/t Au.

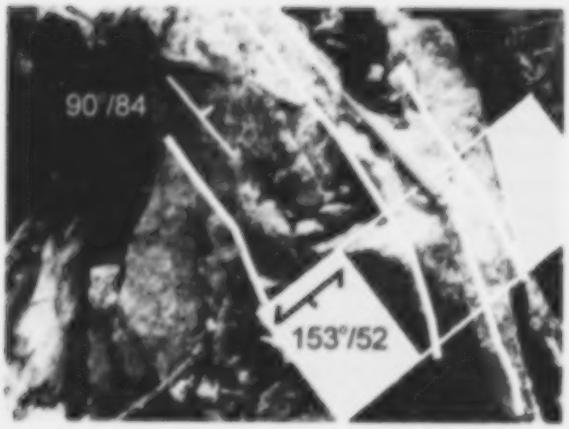

Figure 7. Narrow, east-trending sheeted quartz veinlets cutting the dominant foliation S$_1$ (153/52°) in the Silver King pluton. Outcrop located east of the "A Vein" portal, Great Western showings.

chemical- and geological surveys and forty-seven drill holes aggregating 6 502 m (Sirola, 1982; Johnston, 1985, 1986; Black, 1987; Lewis and Silversides, 1991; Lisle, 1991).

Alteration and mineralization are spatially associated with subconcordant, mafic (monzogabbro suite) and intermediate (Silver King suite) intrusions and replace fracture and crackle breccia zones that have developed in both the intrusive and volcanic country rock (Johnston, 1986). The broad northwest-trending zone of alteration and mineralization follows brecciated, lithologic contacts and the dominant foliation, evidence that both played an important role in controlling the distribution of alteration and gold mineralization. East-striking subvertical fracture sets are conspicuous in the vicinity of the Main Zone (Johnston, 1985) and quartz-pyrite veins with potassium, sericite, quartz and calcite alteration following this trend consistently carry >2 g/t Au (Rhys, 2000). East-trending fracture sets are prominent at the Gold Mountain Zone and host the majority of the mineralization (Rhys, 2001).

At the main showing orthoclase-biotite-silica alteration assemblages have bleached the metavolcanic rocks to a pale grey-brown colour. Pyrite, chalcopyrite, lesser malachite and bornite, occur as foliation parallel blebs and stringers, filling fractures or as matrix to breccias within the alteration zones. Johnston (1986) suggested that the gold at the Kena is associated with a fine-grained "yellow pyrite" distinct from the variety disseminated throughout the metavolcanic rocks. Bimodal gold grades and pyrite types might be specific to the exploration target; with "silvery pyrite" associated with the newly recognized wide zones of lower grade gold mineralization that surround, narrower higher-grade ("yellow pyrite?") intersections at the Kena Gold zone (Dandy, 2000). Late, (sulphide-free) fractures filled with calcite and specular hematite cut the potassic and sericitic alteration.

Shaft/Cat Zone (82FSW 331)

The Shaft and Cat mineralized zones are spatially associated with an early mafic intrusive complex that intrudes augite porphyry flows and tuffs of the upper Elise Formation (Andrew and Höy, 1989). The Shaft lies within 500 m of the eastern contact zone of the Silver King pluton adjacent to the Gold Mountain Zone, and the Cat, approximately 500 m to the northwest. The mafic intrusive is up to 50 m in width, 5 km long and parallels the regional foliation and eastern margin of the Silver King pluton.

Mineralization consists of disseminations and stringers of pyrite-chalcopyrite-magnetite and pyrite±chalcopyrite-quartz-epidote-calcite veins. Alteration of the diorite/monzogabbro is biotite-dominant (Andrew and Höy, 1989), and the association with magnetite and secondary potassium feldspar is typical of potassic alteration (Rhys, 2000). Local zones of intense chlorite-sericite-carbonate±quartz had been interpreted to represent a late sericite alteration overprint of an earlier (?) propylitic alteration (Andrew and Höy, 1989). Gold and copper mineralization occurs mainly within the monzodiorite complex but also in the Elise volcanic rocks and in the margins of the Silver King porphyry (Andrew and Höy, 1989). If the monzodiorite complex was the mineralizer, the Shaft/Cat gold-copper mineralization would predate the gold mineralization at Gold Mountain Zone hosted in the Silver King porphyry. The similar alteration and mineralization assemblages present suggest a single event related to the youngest host (Silver King porphyry). From the distribution of mineralization, alteration and intense shearing parallel to the regional foliation, Andrew and Höy (1989) suggested the likelihood of strong structural control; Rhys (2000) on the other hand, thought that the principal control of mineralization was lithology and alteration rather than structure.

Silver King Mine (82FSW 176)

The Silver King mine is located 7 km south of Nelson, on the northeast side of Toad Mountain. The Hall brothers first staked the Silver King claims in 1886. The property produced high-grade silver-copper ore continuously between 1889 and 1910 and then intermittently from 1913 to 1948. Production from 1889 to 1958 totaled 202 049 tonnes yielding 138.2 tonnes of silver, 8.8 kgs gold, 6 790 tonnes copper, 15.23 tonnes of lead and 4.07 tonnes of zinc. All of the production came from the Main Silver King vein structure.

The Silver King property is dominated by thoroughly sheared Elise Formation volcanic rocks and sill-like apophyses of Silver King intrusives which host three main mineralized structures; the Main Silver King Vein, the Iroquois Vein and the Kohinoor Vein. The veins dip steeply south and sub-parallel the northwest-trending Silver King Shear Zone. The silver/copper mineralization appears to be controlled by cross-structures intersecting the Iroquois Vein. The mineralization consists of pyrite-chalcopyrite-galena±sphalerite±tetrahedrite±bornite in quartz-calcite-siderite veins. W.R. Baragar (personal communication, in Little, 1960) describes a rare copper-silver sulphide mineral, stromeyerite that is associated with bornite in the veins.

The productive ore bodies were found at the intersection of the northwest veins and E-striking cross structures.

Starlight (82FSW 174)

The Starlight showings lie southwest of the Great Western workings on the west side of Giveout Creek. Surface stripping and underground workings explore a wide quartz vein which on surface has an apparent width of 2 metres. The vein strikes southeast and dips shallower than the regional schistosity. Approximately 25 m below the surface exposure, the vein is explored underground by 100 m of crosscuts and 45 m of drifting. Within the drift the vein is narrow and discontinuous (Fahrni, 1946) but reported to carry values in gold.

Three holes were drilled on the Starlight vein structure in August 2002. Drill intersections of the vein structure showed varied, and substantially narrower widths (<1.0 m), than exposed at surface and generally low gold grades, but visible gold was noted. A 12 m intersection in drill hole 02SL-02 (85-97 m) returned elevated gold grades (1.97 g/t Au) from a quartz stockwork zone in strongly foliated, altered metavolcanics rocks in the footwall section of the vein. Gold grades in the other two holes returned generally low values, with one or two slightly elevated values over less than metre intervals.

North Star (82FSW 276, 333)

North of the Starlight and adjacent to the Great Western claims are three volcanic-hosted, conformable Au±Cu mineralized alteration zones: Giveout Creek North, Giveout Creek South and Black Witch (Höy and Andrew, 1989c). These are associated with sheared and foliated intrusions of probable Silver King affinity (Höy and Dunne, 2001), and have mineralogy and alteration assemblages similar to the Kena Gold zone located on the east side of the Silver King pluton. The mineralization consists primarily of pyrite with minor chalcopyrite, as foliation parallel stringers and disseminations distributed throughout a pervasive carbonate-quartz-sericite alteration zone and have been informally classified as "conformable gold" mineralization (Höy and Andrew, 1989b). Gold values do not correlate with other metals, but Cu-Ag-Pb has a strong positive correlation (Höy and Andrew, 1989c), an assemblage found at the Silver King mine. In addition, some mineralization occurs in late, post-kinematic, crosscutting quartz veins (Höy and Andrew, 1989c).

CONTROLS ON MINERALIZATION

Gold mineralization on the Kena property occurs within early Jurassic, Elise Formation metavolcanic and subvolcanic intrusive rocks, early Middle Jurassic, Silver King intrusive rocks, and is locally concentrated along the north-northwesterly trending contact zone between these units (Gold Mountain zone).

Mineralization within the metavolcanic rocks occupies structures that generally parallel the dominant northwest-trending foliation, but may have steeper dips. These occurrences fall into the synkinematic shear-related or conformable gold category of (Höy and Dunne, 1989b). The zones/structures have pervasive iron-carbonate±sericite±chlorite alteration envelopes. In detail the northwest-trending contact zone between porphyry and metavolcanic rocks (Gold Mountain Zone) varies in strike and character from sheared or interdigitated to sharp. It is pervasively potassium-altered and variably pyritized. Higher-grade intervals are localized above and below this contact (Figure 6).

Highly discordant to the regional foliation shears are east-trending quartz-pyrite veins that are well developed at the Kena Gold zone in altered metavolcanic rocks and within the Silver King pluton at the Gold Mountain and Great Western zones. The easterly-trending quartz-pyrite veins at the Kena Gold consistently carry >2 g/t Au (Rhys, 2000). Mineralization hosted within the Silver King pluton occupies fractures and veinlets, which show a preferred easterly trend and steep south dip (Gold Mountain Zone, Rhys, 2001 and Great Western area, this study).

The productive ore bodies at the Silver King mine, albeit Cu-Ag rich, ±Zn±Pb replacements, occurred at the intersection of northwest-trending veins and an E-directed shear (Aylward, 1983). Gold values are not recorded for greater than 90 % of production from the Silver King mine (prior to 1913), but when under development by Consolidated Mining and Smelting Company of Canada (Limited) between 1913 and 1914, a totaled of 15,500 tonnes grading about 261 g/t Ag, 1.8% Cu and 0.5 g/t Au were produced. Ore mineralogy at the Silver King is unique to many of the other deposits in the area, but if the production figures from these two years are correct they suggest that gold was deposited in parts of the system, possibly on younger cross structures.

The steep, east-trending zone of higher-grade gold mineralization at the Kena Gold Zone (Johnston, 1985; Rhys, 2000; this study), the preferred easterly trend and steep southerly dips of mineralized fractures at the Gold Mountain Zone (Andrew, 2000; Rhys, 2001) and Great Western showings (Fahrni, 1946; this study) and the repeated reference to (E-W) cross-structures as the control for mineralization at the Silver King mine (Little, 1960), indicate structural controls particularly east-trending structures are important hosts for some of the higher grade gold mineralization on the Kena property. The identification of these potential higher-grade targets and/or structural corridors has important economic significance for some of the larger lower-grade zones.

AGE OF MINERALIZATION

Gold-copper mineralization in the Rossland Group includes stratiform massive sulphides, skarns and shear-related veins, and is generally interpreted as coeval with Early Jurassic volcanism. On the Kena property the monzogabbro intrusive suite and the Silver King pluton host intrusion-related porphyry-style alteration and gold mineralization (Dandy, 2000; Dunne, 2001). The early

Middle Jurassic intrusions are deformed (synkinematic, Dunne and Höy, 1992) and post-date the Elise Formation volcanism by ca 10 Ma. The dominant northwest-trending foliation and deformation of rock units as young as 174-179 Ma are truncated by Nelson suite intrusive rocks that constrain the main deformation event to pre 170-166 Ma. Petrographic studies indicate that the gold emplacement was either pre or syn-kinematic (Rhys, 2000; Wells, 2001; and this study). Mineralization at the Kena, Shaft/Cat, Great Western and Gold Mountain zones has all been affected by the main deformational event and development of S_n (regional foliation). Veinlets cutting the volcanic rocks are frequently folded and transposed; those within the Silver King pluton are less affected. Hydrothermal biotite associated with mineralization at the Shaft/Cat is aligned parallel to S_n suggesting that potassic alteration was synkinematic (Andrew and Höy, 1989). Rhys (2000) has recognized isolated pyrite-chalcopyrite stringers at the Gold Mountain Zone that he interprets to represent late remobilization of disseminated sulphides.

Early to Middle Jurassic deformation is well constrained in Southern British Columbia and is related to the late collision of the eastern edge of Quesnellia with the North American craton between 184 and 174 Ma (Murphy *et al.*, 1995; Colpron *et al.*, 1996). A suite of synkinematic felsic dikes and sills at Kootenay Lake (Fyles, 1964) yielded a U-Pb zircon age of 173±5 Ma (Smith *et al.*, 1992) and at the north end of the Kootenay Arc the Kuskanax batholith (173±5 Ma, Parrish and Wheeler, 1983) intrudes northeast-verging structures associated with the emplacement of Quesnellia.

SUMMARY

The Silver King pluton is chemically distinct; with relatively higher alkali content than the other Silver King intrusions as well as a quartz monzonite composition.

Hydrothermal alteration mineral assemblages present in drill core in and around the Gold Mountain zone are similar to the principal alteration types developed around gold-rich porphyry deposits (*i.e.* potassic, propylitic, intermediate argillic and sericite).

Age of mineralization is equivocal. Au-Cu mineralization is hosted by Sinemurian volcanic rocks and synvolcanic monzogabbro intrusions, Aalenian (Silver King pluton) intrusives and in synkinematic (*ca.* Aalenian) structures (shears, fractures and vein stockworks) that are truncated by Bajocian (170-166 Ma) intrusions .

Adjacent to the GMZ are higher-grade, mineralized quartz vein systems (Starlight and Great Western), which contain visible gold and some historically limited production. These appear to lie along an east-trending structural corridor that intersects the GMZ discovery area.

CONCLUSIONS

The 2002 Kena project carried out reconnaissance mapping, sampling and deposit studies within a relatively focused belt (4 x 20 km) of early Middle Jurassic magmatic rocks in southern British Columbia. Results from Pb-isotopic studies, polished section and SEM work are pending but field observations, thin section studies and geochemistry support an intrusion-related Au-Cu porphyry system, related to the early Middle Jurassic Silver King pluton as causative to the alteration and gold mineralization at the Gold Mountain zone. Mineralization at some of the peripheral showings (*i.e.* Kena, Shaft/Cat) may also be related to this same system.

Gold mineralization occurs in areas of pervasive pyritized Silver King pluton and within 20 m of the contact with volcanic rocks. It consists primarily of disseminated blebs of pyrite±chalcopyrite and lesser stringers and veinlets. The latter follow a preferred easterly trend, and similar oriented structures at the Kena, Great Western and Silver King mine have localized consistently higher-grades of mineralization. The identification of these potential higher-grade targets and/or structural corridors has important economic significance for the larger lower-grade zones.

ACKNOWLEDGMENTS

I wish to thank Linda Dandy for her insightful introduction to the geology of the Kena property, logistical help and enthusiastic geological discussions in the field and over maps in the office. Work was carried out with the help of Linda Dandy and field assistance of Jarrod Brown and Otto Janout. Jarrod provided cheerful assistance and shared extensive knowledge about the alteration and mineralization styles present in the core and over the property. Jack Denny and his entire family are thanked for their gracious hospitality. Brian Grant visited the property during the course of fieldwork. He also reviewed and improved an earlier version of this manuscript.

This project was one of a number of P3s that were conducted this year. I would like to thank Sultan Minerals Inc. for the opportunity to work together with them on the Kena property and for their logistical and financial support.

REFERENCES

Andrew, K.P.E. and Höy, T. (1988): Preliminary Geology and Mineral Deposits of the Rossland Group between Nelson and Ymir, Southeastern British Columbia; *B.C. Ministry of Energy, Mines and Petroleum Resources*, Open File 1988-1.

Andrew, K.P.E. and Höy, T. (1989): The Shaft Showing, Elise Formation, Rossland Group; *in* Exploration in British Columbia 1988; *B.C. Ministry of Energy, Mines and Petroleum Resources*, pages B21-28.

Archibald, D. A., Glover, J. K., Price, R. A., Farrar, E. and Carmichael, D. M. (1983): Geochronology and Tectonic Implications of Magmatism and Metamorphism, Southern Kootenay Arc and Neighbouring Regions, Southeastern British Columbia. Part I: Jurassic to mid-Cretaceous; *Canadian Journal of Earth Sciences*, Volume 20, p. 1891-1913.

Aylward, P.S. (1983): Silver King Property - Drilling, Trenching and Compilation of Previous work; *B.C. Ministry of Energy, Mines and Petroleum Resources*, Assessment Report 12611.

Beddoe-Stephens, B. and Lambert, R. St. J. (1981): Geochemical, Mineralogical and Isotopic Data Relating to the Origin and Tectonic Setting of the Rossland Volcanic Rocks, Southeastern British Columbia; *Canadian Journal of Earth Sciences*, Volume 18, pages 858-868.

Black, P.T. (1987): Tournigan Mining Explorations Ltd. 1987 - Drilling Project, Kena Mineral Claims; *B.C. Ministry of Energy, Mines and Petroleum Resources*, Assessment Report 16594.

Brown, R. L., Journeay, M. J., Lane, L. S., Murphy, D. C. and Rees, C. J. (1986): Obduction, Backfolding and Piggyback Thrusting in the Metamorphic Hinterland of the Southeastern Canadian Cordillera; *Journal of Structural Geology*, Volume 8, pages 255-268.

Carr, S.D. (1992): Tectonic setting and U-Pb geochronology of the early Tertiary Ladybird leucogranite suite, Thor-Odin-Pinnacles area, southern Omineca Belt, British Columbia; Tectonics, v. 11, p. 258-278.

Colpron, M., Price, R.A., Archibald, D.A. and Carmichael, D.M. (1996): Middle Jurassic Exhumation along the Western Flank of the Selkirk Fan Structure: Thermobarometric and Thermochronometric Constraints from the Illecillewaet Synclinorium, Southeastern British Columbia; Geological Society of America, Bulletin, 108, pages 1372-1392.

Dandy, L. (2001): Geological Geochemical Geophysical and Trenching Report on the Kena Property; *B.C. Ministry of Energy, Mines and Petroleum Resources*, Assessment Report 26503.

Dandy, L. (2001): Geology, Trenching and Diamond Drilling Report on the Kena Property; *B.C. Ministry of Energy, Mines and Petroleum Resources*, Assessment Report 26699.

Dandy, L. (2002): Geology, Geochemistry, Geophysics, Trenching and Diamond Drilling Report on the Kena Property; Unpublished Report for Sultan Minerals Inc., 60 pages.

Dawson, G. M. (1889): Report on a portion of the West Kootenai District, British Columbia; *Geological Survey of Canada*, Annual Reports 1888-1889.

de Rosen Spence, A.F. (1985): Shoshonites and Associated Rocks of Central British Columbia; *B.C. Ministry of Energy, Mines and Petroleum Resources*, Geological Fieldwork 1984, Paper 1985-1, pages 426-442.

Dunne, K.P.E and Höy, T. (1992): Petrology of Lower and Middle Jurassic Intrusions in the Rossland Group, Southeastern British Columbia; *in* Geological Fieldwork 1991, *B.C. Ministry of Energy, Mines and Petroleum Resources*, Paper 1992-1, pages 9-19.

Dunne, K.P.E (2001): Alteration Mapping Study of the Gold Mountain Zone, Kena Property, Unpublished Report for Sultan Minerals Inc. 7 pages.

Fahrni, K.C. (1946): Report on the Giveout Creek Group of Claims; Unpublished Report, 12 pages.

Frebold, H. and Little, H.W. (1962): Paleontology, Stratigraphy, and Structure of the Jurassic Rocks in Salmo Map-area, British Columbia; *Geological Survey of Canada*, Bulletin 81.

Ghosh, D. K. (1986): Geochemistry of the Nelson-Rossland Area, Southeastern British Columbia; Unpublished Ph.D thesis, *University of Alberta*, Edmonton, Alberta, 310 pages.

Ghosh, D.P. (1995a): Nd and Sr Isotopic Constraints on the Interactions of the Intermontane Superterrane with the Western Edge of North America in the Southern Canadian Cordillera; *Canadian Journal of Earth Sciences*, Volume 32, pages 1740-1758.

Höy, T. and Andrew, K.P.E. (1988): Preliminary Geology and Geochemistry of the Elise Formation, Rossland Group, between Nelson and Ymir, Southeastern British Columbia; *in* Geological Fieldwork 1987, Newell, J.M and Grant, B., Editors, *B.C. Ministry of Energy, Mines and Petroleum Resources*, Paper 1988-1, pages 19-30.

Höy, T. and Andrew, K.P.E. (1989a): Geology of the Rossland Group, Nelson Map-area, Southeastern British Columbia; *B.C. Ministry of Energy, Mines and Petroleum Resources*, Open File Map 1989-1.

Höy, T. and Andrew, K.P.E. (1989b): The Rossland Group, Nelson Map Area, Southeastern British Columbia; *in* Geological Fieldwork 1988, Newell, J.M. and Grant, B., Editors, *B.C. Ministry of Energy, Mines and Petroleum Resources*, Paper 1989-1, pages 33-43.

Höy, T. and Andrew, K.P.E. (1989c): The Great Western Group, Elise Formation, Rossland Group; *in* Exploration in British Columbia 1988, *B.C. Ministry of Energy, Mines and Petroleum Resources*, pages B15-19.

Höy, T. and Andrew, K.P.E., (1991b): Geology of the Rossland -Trail Area, Southeastern British Columbia (82F/4); *B.C. Ministry of Energy, Mines and Petroleum Resources*, Open File 1991-2.

Höy, T. and Dunne, K.P.E. (1997): Early Jurassic Rossland Group, Southern British Columbia Part I - stratigraphy and tectonics: *B.C. Ministry of Energy and Mines*, Bulletin 109, 196 pages.

Höy, T. and Dunne, K.P.E. (2001): Metallogeny and Mineral Deposits of the Nelson-Rossland Map Area: Part II: The Early Jurassic Rossland Group, Southern British Columbia; *B.C. Ministry of Employment and Investment*, Bulletin 102, 124 pages.

Irving, T.N. and Barager, W.R.A. (1971): A Guide to the Chemical Classification of the Common Rocks; *Canadian Journal of Earth Sciences*, Volume 8, pages 523-548.

Johnson, D. L. (1974): Percussion Drilling Report on the Kena 7 Claim Group, Gold Creek, Nelson area; *B.C. Ministry of Energy, Mines and Petroleum Resources*, Assessment Report 5222.

Johnston, D. L. (1975): Geological, Geochemical and Geophysical Report on the Kena Claim Group, Toad Mountain, Nelson Area; *B.C. Ministry of Energy, Mines and Petroleum Resources*, Assessment Report 5665.

Johnson, R.J. (1985): Report on Trenching and Diamond Drilling Kena 7, 18-25, Gold Mtn 1-3, 6-8 Gold Mtn Fr, Linde 1, 2, Mac 1, Mac Fr, Keno, Kena Fr Claims; *B.C. Ministry of Energy, Mines and Petroleum Resources*, Assessment Report 14023.

Johnston, R.J. (1986): Summary Report on 1986 Work - Kena Property; *B.C. Ministry of Energy, Mines and Petroleum Resources*, Assessment Report 15767.

LeBas, M.J., LeMaitre, R.W., Streckeisen, A. and Zanettin, B. (1986): A Chemical Classification of Volcanic Rocks Based on the Total Alkali-Silica Diagram; *Journal of Petrology*, Volume 27, Part 3, pages 745-750.

Leclair, A.D., Parrish, R.R. and Archibald, D.A., 1993, Evidence for Cretaceous deformation in the Kootenay Arc based on U-Pb and 40Ar/39Ar dating, southeastern British Columbia: *in* Current Research, Part A: Geological Survey of Canada, Paper 93-1A, p. 207-220.

Le Maitre, R.W. (1989): A Classification of Igneous Rocks and Glossary of Terms; *Blackwell, Oxford Press*, 193 pages.

Lewis, W.J. and Silversides, D.A. (1991): Kena Project - 1990 Diamond Drilling Report on the K Group, Drill Holes K90-1 to 90-4; *B.C. Ministry of Energy, Mines and Petroleum Resources*, Assessment Report 20894.

Lisle, T.E. (1991): Geological, Geochemical and Drilling Report on the K Group of Mineral Claims; *B.C. Ministry of Energy, Mines and Petroleum Resources*, Assessment Report 21917.

Little, H.W. (1960): Nelson Map-area, West-half, British Columbia; *Geological Survey of Canada*, Memoir 308, 205 pages.

Little, H.W. (1982a): Geology, Bonnington Map Area, British Columbia; *Geological Survey of Canada*, Map 1571A.

Monger, J.W.H., Price, R.A. and Tempelman-Kluit, D.J. 1982, Tectonic accretion and the origin of the two major metamorphic and plutonic welts in the Canadian Cordillera: *Geology*, Volume 10, pages 70-75.

Mulligan, R. (1952): Bonnington Map Area, British Columbia; *Geological Survey of Canada*, Paper 52-13, 37 pages.

Murphy, C.M., Gerasimoff, M., Van der Hedyden, P., Parrish, R.R., Klepacki, D.W., McMillan, W.J., Struik, L.C. and Gabites, J. (1995): New Geochronological Constraints on Jurassic Deformation on the Western Edge of North America, Southeastern Canadian Cordillera; *in* Jurassic Magmatism and Tectonics of the North American Cordillera, Miller, D.M. and Busby, C., Editors, *Geological Society of America*, Special Paper 299, pages 159-171.

Parrish, R.R., Carr, S.D. and Parkinson, D.L. (1988): Eocene Extensional Tectonics and Geochronology of the Southern Omineca Belt, British Columbia and Washington; *Tectonics*, Volume 7, pages 181-212.

Parrish, R.R. and Wheeler, J.O. (1983): A U-Pb Zircon Age from the Kuskanax Batholith, Southeastern British Columbia; *Canadian Journal of Earth Sciences*, Volume 20, pages -548.

Pearce, J.A., Harris, N.B.W. and Tindle, A.G. (1984): Trace Element Discrimination Diagrams for the Tectonic Interpretation of Granitic Rocks; *Journal of Petrology*, Volume 25, pages 956-983.

Rhys, D. (2000): Kena Property Structural Geology Study: Unpublished Report for Sultan Minerals Inc., 12 pages

Rhys, D. (2001): Structural Geology Study of the Gold Mountain Zone, Kena Property: Unpublished Report for Sultan Minerals Inc., 14 pages

Sevigny, J.H. and Parrish, R.R. (1993): Age and Origin of Late Jurassic and Paleocene Granitoids, Nelson Batholith, Southern British Columbia; *Canadian Journal of Earth Sciences*, Volume 30, pages 2305-2314.

Sillitoe, R.H. (1979): Some Thoughts on Gold-Rich Porphyry Copper Deposits; Mineralium Deposita, Volume 14, pages 161-174.

Sillitoe, R.H. (1993): Gold-rich Porphyry Copper Deposits: Geological Model and Exploration Implications; in Kirkham, R.V., Sinclair, W.D, Thorpe, R.I and Duke, J.M., eds., Mineral Deposit Modeling; Geological Association of Canada, Special Paper 40, p. 465-478.

Sillitoe, R.H. (2000): Gold-rich Porphyry Deposits: Descriptive and Genetic Models and Their Role in Exploration and Discovery; Society of Economic Geology Reviews, Volume 13, p. 313-345.

Sirola, W. M. (1982): Nelson Project, Toad Mountain Area, Nelson M.D. - Report on 1981 Exploration for Kerr Addison Mines Ltd.; *B.C. Ministry of Energy, Mines and Petroleum Resources*, Assessment Report 9593.

Streckeisen, A. (1976): To Each Plutonic Rock its Proper Name; *Earth Science Reviews*, Volume 12, pages 1-33.

Tipper, H.W. (1984): The Age of the Jurassic Rossland Group of Southeastern British Columbia; *in* Current Research, Part A, *Geological Survey of Canada*, Paper 84-1A, pages 631-632.

Walcott, P.E. (2001): A Geophysical Report on Electromagnetic and Induced Polarization Surveying; Unpublished Report for Sultan Minerals Inc., 25 pages.

Wells, R.C. (2001): Petrographic, Lithogeochemical and Interpretative Report on drill core samples taken from the Kena Property; Unpublished Report for Sultan Minerals Inc., February 2001, 20 pages

Wheeler, J.O. and McFeely, P. (1991): Tectonic Assemblage Map of the Canadian Cordillera and Adjacent Parts of the United States; *Geological Survey of Canada*

National Geochemical Reconnaissance Surveys in the BC Cordillera Identify New Mineral Exploration Targets

By Ray Lett[1] and Peter Friske[2]

KEYWORDS: Geochemistry, mineral exploration, multi-element, stream sediment, stream water, National Geochemical Reconnaissance Program, Regional Geochemical Survey, RGS, Fort Fraser, Bella Coola

INTRODUCTION

Since 1976 the British Columbia Ministry of Energy and Mines (MEM) has been involved in reconnaissance-scale stream sediment and stream water surveys under Canada's National Geochemical Reconnaissance (NGR) program. British Columbia continues to independently manage the Regional Geochemical Survey (RGS) in the Province and maintains the sample collection and preparation and analytical standards established by the Geological Survey of Canada. Currently, the RGS database covers close to 65 percent of British Columbia and contains field and analytical information for over 46 000 sample sites. Multi-element data, generated by regional surveys, are used by the mining industry to identify areas of higher mineral potential and to focus on exploration targets.

Program highlights this year were the publication of results from a 1:250 000 scale stream sediment and water survey covering parts of the Bella Coola (NTS 93D) and Laredo Sound (NTS 103A) map sheets (Lett *et al.*, 2002) and completion of a new survey covering parts of the Fort Fraser (NTS 93K) map sheet. The Geological Survey of Canada Targeted Geoscience Initiative (TGI) and the BC Ministry of Energy and Mines funded both surveys. Results of a detailed survey covering the Triumph Bay area (parts of NTS 103H) and funded by the Corporate Resource Inventory Initiative (CRII), were published in April (Jackaman, 2002). Instrumental neutron activation (INAA) data, produced by reanalysis of archived samples from previous RGS surveys covering the Prince George (NTS 93G) and McBride (NTS 93H) maps sheets, were also released. These surveys (Figure 1) are described in this paper.

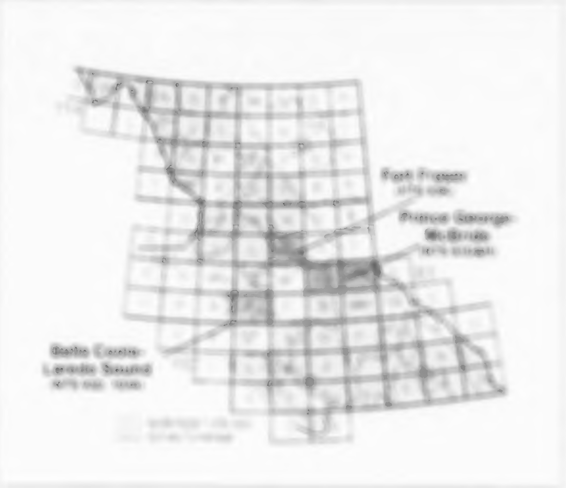

Figure 1. Location map of surveys.

BELLA COOLA-LAREDO SOUND DATA RELEASE

New field and analytical results for 1180 sediment and water samples, collected in the Bella Coola-Laredo Sound area, were published in August 2002 (Lett *et al.*, 2002). Stream sediment samples were analysed for more than 40 parameters (Table 1), including base and precious metals. Water samples were analysed for pH, uranium and fluoride. In addition 232 filtered and acidified stream water samples were analysed for over 40 trace and major elements.

The western part of the Bella Coola survey area is underlain by Paleozoic to Jurassic metavolcanic and metasedimentary rocks and Eocene intrusive rocks which together form the Coast Complex. This assemblage is separated from Middle Jurassic Hazelton Group volcanic and sedimentary rocks to the east by the Coast Shear zone. Hazelton Group submarine silica-bimodal volcanic rocks and sedimentary rocks, interpreted by Diakow *et al.*, 2002 as a Stikinia magmatic arc, have the potential for hosting porphyry Cu-Au deposits associated with subvolcanic plutons, epithermal Au-Ag deposits in sub aerial volcanic rocks and stratiform massive sulphide deposits. One example of volcanic-associated stratiform sulphide mineralization is the Nifty Pb-Zn-barite prospect (MINFILE 93D007) in the eastern part of the survey area. The Coast Complex has the potential to host gold-quartz veins associated with major faults such as the Surf Inlet occurrence (MINFILE 103H 027) and volcanogenic massive sulphide (VMS) mineralization in metavolcanic rocks such as the Ecstall deposit (MINFILE 103H 011).

---

[1] *BC Geological Survey Branch*
[2] *Geological Survey of Canada*

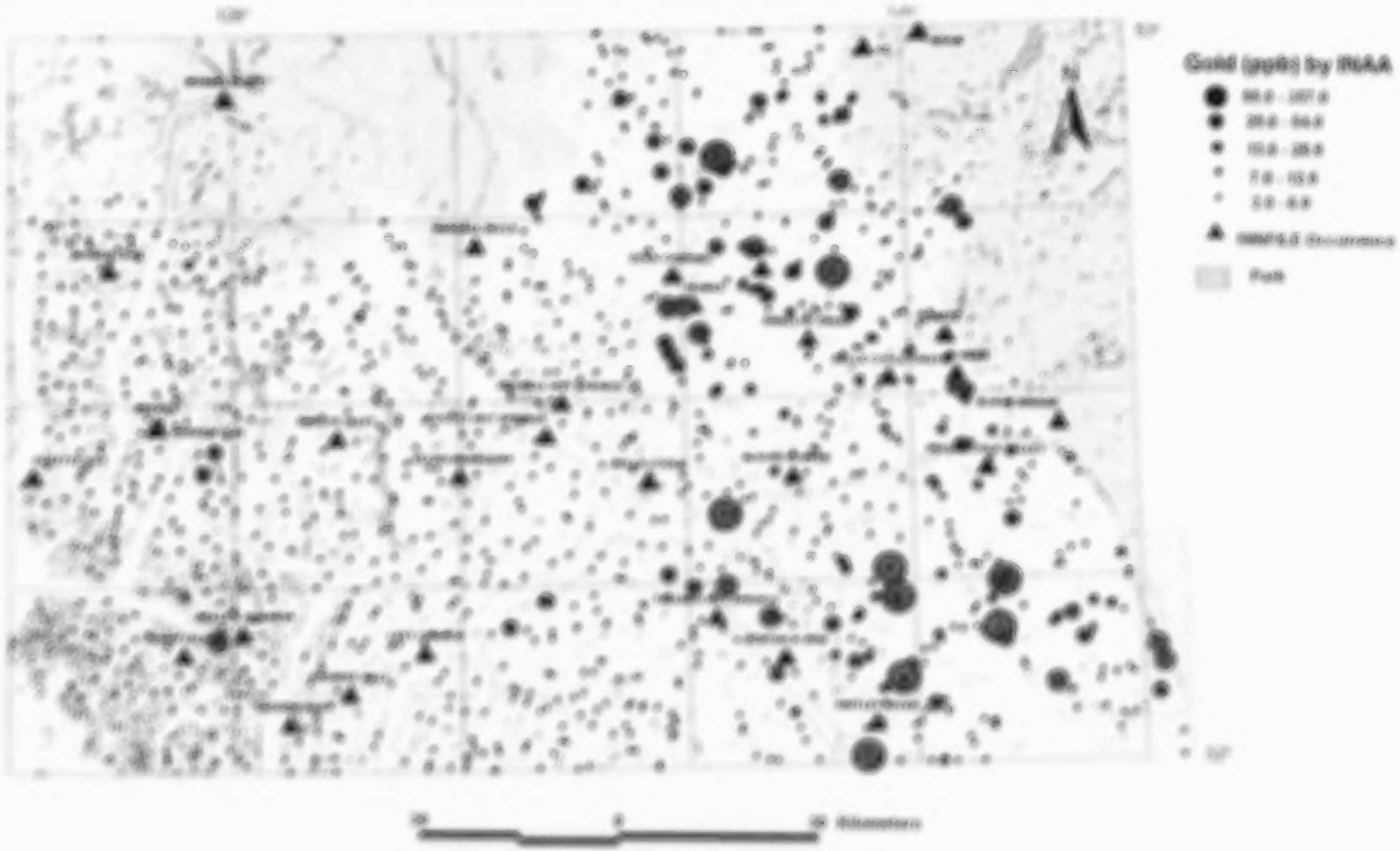
Gold (ppb) by INAA
55.0 - 107.0
28.0 - 54.0
15.0 - 28.0
7.0 - 15.0
2.0 - 6.0
MINFILE Occurrences
Park
128°
126°
52°
20
0
20 Kilometres

Figure 2. Distribution of gold in stream sediments by INAA in the Bella Coola-Laredo Sound survey area.

TABLE 1
[illegible]

Element	Detection	Units	Method
Aluminum	0.01	%	ICP-MS
Antimony	0.02/0.1	ppm	ICP-MS / INAA
Arsenic	0.1/0.5	ppm	ICP-MS / INAA
Barium	0.5/50	ppm	ICP-MS / INAA
Bismuth	0.02	ppm	ICP-MS
Bromine	0.5	ppm	INAA
Cadmium	0.01	ppm	ICP-MS
Calcium	0.01/1	%	ICP-MS / INAA
Cerium	3	ppm	INAA
Cesium	0.5	ppm	INAA
Chromium	0.5/5	ppm	ICP-MS / INAA
Cobalt	0.1/5	ppm	ICP-MS / INAA
Copper	0.01	ppm	ICP-MS
Europium	1	ppm	INAA
Gallium	0.2	ppm	ICP-MS
Gold	0.2/2	ppb	ICP-MS / INAA
Hafnium	1	ppm	INAA
Iron	0.01/0.2	%	ICP-MS / INAA
Lanthanum	0.5/2	ppm	ICP-MS / INAA
Lead	0.01	ppm	ICP-MS
Lutetium	0.2	ppm	INAA
Magnesium	0.01	%	ICP-MS
Manganese	1	ppm	ICP-MS
Mercury	5	ppb	ICP-MS
Molybdenum	0.01	ppm	ICP-MS
Nickel	0.1	ppm	ICP-MS
Phosphorus	0.001	%	ICP-MS
Potassium	0.01	%	ICP-MS
Rubidium	5	ppm	INAA
Samarium	0.1	ppm	INAA
Scandium	0.1/0.1	ppm	ICP-MS / INAA
Selenium	0.1	ppm	ICP-MS
Silver	2	ppb	ICP-MS
Sodium	0.001/0.02	%	ICP-MS / INAA
Strontium	0.5	ppm	ICP-MS
Sulphur	0.02	%	ICP-MS
Tantalum	0.5	ppm	INAA
Tellurium	0.02	ppm	ICP-MS
Terbium	0.5	ppm	INAA
Thallium	0.02	ppm	ICP-MS
Thorium	0.1/0.2	ppm	ICP-MS / INAA
Titanium	0.001	%	ICP-MS
Tungsten	0.2/1	ppm	ICP-MS / INAA
Uranium	0.1/0.5	ppm	ICP-MS / INAA
Vanadium	2	ppm	ICP-MS
Ytterbium	2	ppm	INAA
Zinc	0.1/50	ppm	ICP-MS / INAA
Fluorine	10	ppm	ION
Loss on Ignition	0.1	%	GRAV
Fluoride (waters)	20	ppb	ION
Uranium (waters)	0.05	ppb	LIF
pH (waters)	0.1		GCE

There are numerous base and precious metal stream sediment geochemical anomalies in the Bella Coola-Laredo Sound survey area. For example, Au values exceed [illegible] ppb in sediment at nine sites in the eastern part of the survey area (Figure 2). Sample sites where there are different multi-element anomalies are shown in Figure 3. The element associations were chosen to reflect VMS-type mineralization (Ag-Ba-Cu-Pb-Sb-Zn), porphyry-type mineralization (Cu-Mo) and epithermal vein-type mineralization (Au-Sb-Hg-As). Lefebure *et al.* (2002) used a similar procedure for interpreting stream sediment multi-element anomalies west of Dease Lake, BC. There are clusters of samples with a VMS-type signature in the area between Dean and Burke Inlets (93D/06 and 93D/06), north of Laredo Inlet (93D/12) and in the northern half of NTS 93D/15. Two sites with a VMS-type signature occur in NTS 103A/08 along a northwest trending belt of Paleozoic age sedimentary volcanic rocks in the Coast Complex. Another site with a VMS-type signature is a stream draining the area of the Nifty prospect. Sample sites with anomalous Cu-Mo values are located predominantly in the eastern part of the survey area. Those sites showing an Au-Sb-Hg-As geochemical signature are grouped in NTS 93D/15 and 93D/11. In NTS 103A/08 one Au-Sb-Hg-As site has a spatial association with a VMS-type anomaly on a northwest trend. Samples with elevated Ag-Ba-Cu-Pb-Sb-Zn, Cu-Mo and Au-Sb-Hg-As values are listed in Tables 2, 3 and 4.

Sample sites with a Ag-Ba-Cu-Pb-Sb-Zn signature have been ranked by calculating Ag, Ba, Cu, Pb, Sb, Zn normalized values from raw element data and plotting the sum of normalized values as symbols (Figure 4). The largest cluster of sites with high normal values is in the area between Dean and Burke Inlets.

PRINCE GEORGE AND MCBRIDE ARCHIVE DATA RELEASE

Since 1993 over 21 000 archived stream sediment samples have been analysed by instrumental neutron activation analysis (INAA) for Au and 27 other metals. These sediment samples were saved from reconnaissance-scale stream sediment and water surveys conducted from 1976 to 1985. The original RGS publications contained analytical data for a small number of key ore-indicator metals (e.g. Ag, Cu, Co, Hg, Fe, Mn, Pb, Ni, Mo, U). New INAA data for twenty-one 1:250 000 NTS map sheet areas have been published to date.

The new archive data were released for the Prince George (NTS 93G) and McBride (NTS 93H) map sheets. Conducted in 1986, the Prince George and McBride RGS programs comprised a total of [illegible] sediment samples and [illegible] water samples collected from [illegible] sites over a 30 000 square kilometre area. The distribution of Au by INAA in the stream sediments (Figure 5) clearly shows a cluster of anomalies in the southwest part of the McBride sheet corresponding to the Wells-Barkerville area. However, the highest Au values (up to 1050 ppb) are in southeast part of the Prince George sheet. Samples with Au values above 170 ppb are listed in Table 5.

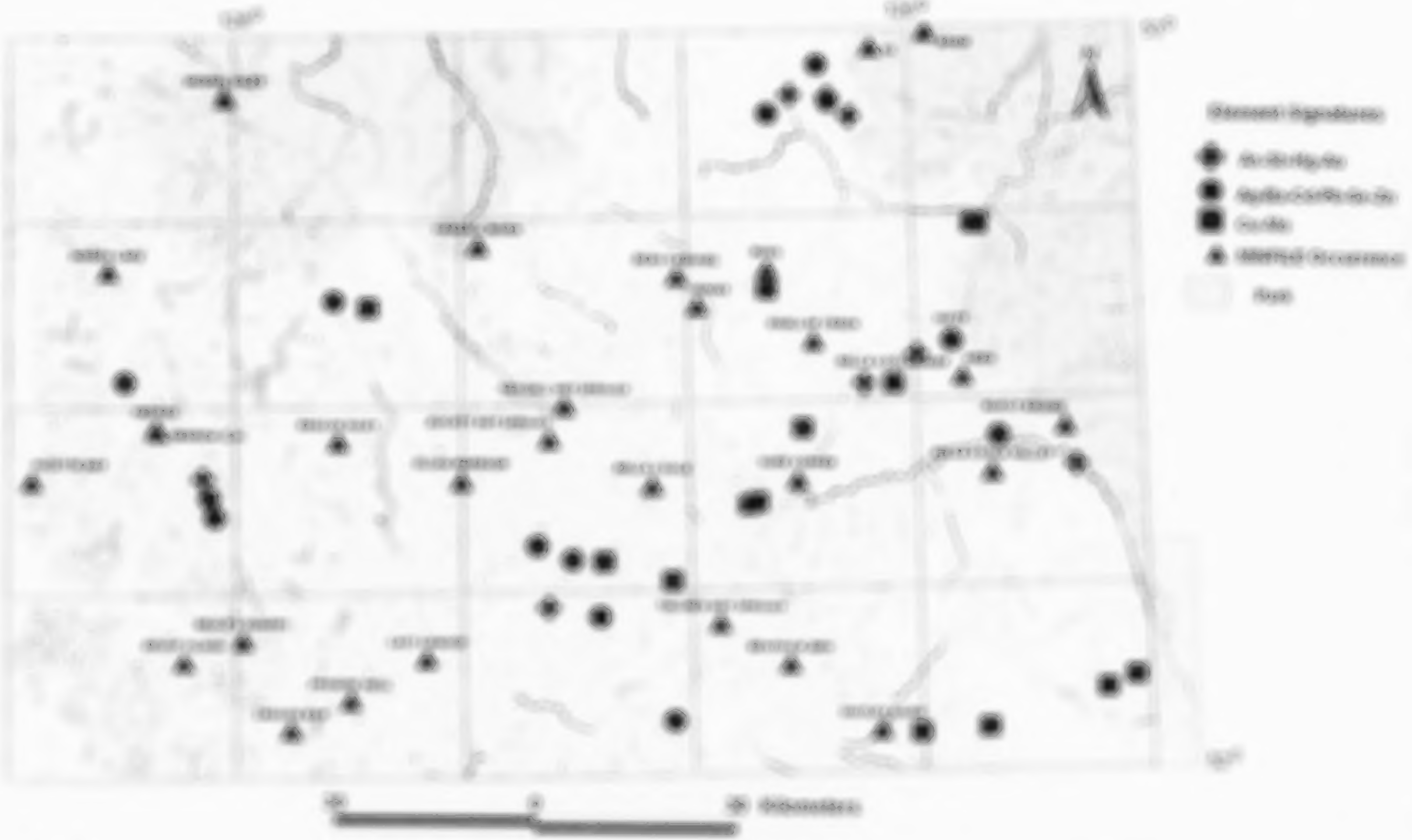

[illegible]

[illegible]
[illegible]

[illegible]	[illegible]	[illegible]	[illegible]	[illegible]	[illegible]	[illegible]	[illegible]	[illegible]	[illegible]	[illegible]
[illegible]	[illegible]	[illegible]	[illegible]	[illegible]	[illegible]	[illegible]	[illegible]	[illegible]	[illegible]	[illegible]
[illegible]	[illegible]	[illegible]	[illegible]	[illegible]	[illegible]	[illegible]	[illegible]	[illegible]	[illegible]	[illegible]
[illegible]	[illegible]	[illegible]	[illegible]	[illegible]	[illegible]	[illegible]	[illegible]	[illegible]	[illegible]	[illegible]
[illegible]	[illegible]	[illegible]	[illegible]	[illegible]	[illegible]	[illegible]	[illegible]	[illegible]	[illegible]	[illegible]
[illegible]	[illegible]	[illegible]	[illegible]	[illegible]	[illegible]	[illegible]	[illegible]	[illegible]	[illegible]	[illegible]
[illegible]	[illegible]	[illegible]	[illegible]	[illegible]	[illegible]	[illegible]	[illegible]	[illegible]	[illegible]	[illegible]
[illegible]	[illegible]	[illegible]	[illegible]	[illegible]	[illegible]	[illegible]	[illegible]	[illegible]	[illegible]	[illegible]
[illegible]	[illegible]	[illegible]	[illegible]	[illegible]	[illegible]	[illegible]	[illegible]	[illegible]	[illegible]	[illegible]
[illegible]	[illegible]	[illegible]	[illegible]	[illegible]	[illegible]	[illegible]	[illegible]	[illegible]	[illegible]	[illegible]
[illegible]	[illegible]	[illegible]	[illegible]	[illegible]	[illegible]	[illegible]	[illegible]	[illegible]	[illegible]	[illegible]
[illegible]	[illegible]	[illegible]	[illegible]	[illegible]	[illegible]	[illegible]	[illegible]	[illegible]	[illegible]	[illegible]
[illegible]	[illegible]	[illegible]	[illegible]	[illegible]	[illegible]	[illegible]	[illegible]	[illegible]	[illegible]	[illegible]
[illegible]	[illegible]	[illegible]	[illegible]	[illegible]	[illegible]	[illegible]	[illegible]	[illegible]	[illegible]	[illegible]
[illegible]	[illegible]	[illegible]	[illegible]	[illegible]	[illegible]	[illegible]	[illegible]	[illegible]	[illegible]	[illegible]
[illegible]	[illegible]	[illegible]	[illegible]	[illegible]	[illegible]	[illegible]	[illegible]	[illegible]	[illegible]	[illegible]

[illegible]

[illegible]
[illegible]
[illegible]

[illegible]	[illegible]	[illegible]	[illegible]	[illegible]	[illegible]	[illegible]
[illegible]	[illegible]	[illegible]	[illegible]	[illegible]	[illegible]	[illegible]
[illegible]	[illegible]	[illegible]	[illegible]	[illegible]	[illegible]	[illegible]
[illegible]	[illegible]	[illegible]	[illegible]	[illegible]	[illegible]	[illegible]
[illegible]	[illegible]	[illegible]	[illegible]	[illegible]	[illegible]	[illegible]
[illegible]	[illegible]	[illegible]	[illegible]	[illegible]	[illegible]	[illegible]
[illegible]	[illegible]	[illegible]	[illegible]	[illegible]	[illegible]	[illegible]
[illegible]	[illegible]	[illegible]	[illegible]	[illegible]	[illegible]	[illegible]
[illegible]	[illegible]	[illegible]	[illegible]	[illegible]	[illegible]	[illegible]
[illegible]	[illegible]	[illegible]	[illegible]	[illegible]	[illegible]	[illegible]
[illegible]	[illegible]	[illegible]	[illegible]	[illegible]	[illegible]	[illegible]
[illegible]	[illegible]	[illegible]	[illegible]	[illegible]	[illegible]	[illegible]
[illegible]	[illegible]	[illegible]	[illegible]	[illegible]	[illegible]	[illegible]
[illegible]	[illegible]	[illegible]	[illegible]	[illegible]	[illegible]	[illegible]
[illegible]	[illegible]	[illegible]	[illegible]	[illegible]	[illegible]	[illegible]

[illegible]

TABLE 4
RGS SITES WITH ANOMALOUS (>95 PERCENTILE) AU-AS-HG-SB VALUES

NTS Map	Sample ID Number	UTM Zone	UTM East 83	UTM North 83	As ppm	Au ppb	Hg ppb	Sb ppm
[illegible]	[illegible]	[illegible]	[illegible]	[illegible]	[illegible]	[illegible]	[illegible]	[illegible]
[illegible]	[illegible]	[illegible]	[illegible]	[illegible]	[illegible]	[illegible]	[illegible]	[illegible]
[illegible]	[illegible]	[illegible]	[illegible]	[illegible]	[illegible]	[illegible]	[illegible]	[illegible]
[illegible]	[illegible]	[illegible]	[illegible]	[illegible]	[illegible]	[illegible]	[illegible]	[illegible]
[illegible]	[illegible]	[illegible]	[illegible]	[illegible]	[illegible]	[illegible]	[illegible]	[illegible]
[illegible]	[illegible]	[illegible]	[illegible]	[illegible]	[illegible]	[illegible]	[illegible]	[illegible]
[illegible]	[illegible]	[illegible]	[illegible]	[illegible]	[illegible]	[illegible]	[illegible]	[illegible]
[illegible]	[illegible]	[illegible]	[illegible]	[illegible]	[illegible]	[illegible]	[illegible]	[illegible]
[illegible]	[illegible]	[illegible]	[illegible]	[illegible]	[illegible]	[illegible]	[illegible]	[illegible]

[illegible]

TABLE 5
STREAM SEDIMENT AU ANOMALIES IN THE PRINCE GEORGE, NTS [illegible] MAP SHEETS [illegible] ABSORPTION SPECTROMETRY

Map	Sample	UTM	UTM83 Easting	UTM83 Northing	Ag ppm	As ppm	Au ppb	Ba ppm	Cr ppm	Cu ppm	Fe %	Hg ppb	Mn ppm	Mo ppm	Pb ppm	Sb ppm	Zn ppm
[illegible]	[illegible]	[illegible]	[illegible]	[illegible]	[illegible]	[illegible]	[illegible]	[illegible]	[illegible]	[illegible]	[illegible]	[illegible]	[illegible]	[illegible]	[illegible]	[illegible]	[illegible]
[illegible]	[illegible]	[illegible]	[illegible]	[illegible]	[illegible]	[illegible]	[illegible]	[illegible]	[illegible]	[illegible]	[illegible]	[illegible]	[illegible]	[illegible]	[illegible]	[illegible]	[illegible]
[illegible]	[illegible]	[illegible]	[illegible]	[illegible]	[illegible]	[illegible]	[illegible]	[illegible]	[illegible]	[illegible]	[illegible]	[illegible]	[illegible]	[illegible]	[illegible]	[illegible]	[illegible]
[illegible]	[illegible]	[illegible]	[illegible]	[illegible]	[illegible]	[illegible]	[illegible]	[illegible]	[illegible]	[illegible]	[illegible]	[illegible]	[illegible]	[illegible]	[illegible]	[illegible]	[illegible]
[illegible]	[illegible]	[illegible]	[illegible]	[illegible]	[illegible]	[illegible]	[illegible]	[illegible]	[illegible]	[illegible]	[illegible]	[illegible]	[illegible]	[illegible]	[illegible]	[illegible]	[illegible]
[illegible]	[illegible]	[illegible]	[illegible]	[illegible]	[illegible]	[illegible]	[illegible]	[illegible]	[illegible]	[illegible]	[illegible]	[illegible]	[illegible]	[illegible]	[illegible]	[illegible]	[illegible]
[illegible]	[illegible]	[illegible]	[illegible]	[illegible]	[illegible]	[illegible]	[illegible]	[illegible]	[illegible]	[illegible]	[illegible]	[illegible]	[illegible]	[illegible]	[illegible]	[illegible]	[illegible]
[illegible]	[illegible]	[illegible]	[illegible]	[illegible]	[illegible]	[illegible]	[illegible]	[illegible]	[illegible]	[illegible]	[illegible]	[illegible]	[illegible]	[illegible]	[illegible]	[illegible]	[illegible]
[illegible]	[illegible]	[illegible]	[illegible]	[illegible]	[illegible]	[illegible]	[illegible]	[illegible]	[illegible]	[illegible]	[illegible]	[illegible]	[illegible]	[illegible]	[illegible]	[illegible]	[illegible]
[illegible]	[illegible]	[illegible]	[illegible]	[illegible]	[illegible]	[illegible]	[illegible]	[illegible]	[illegible]	[illegible]	[illegible]	[illegible]	[illegible]	[illegible]	[illegible]	[illegible]	[illegible]
[illegible]	[illegible]	[illegible]	[illegible]	[illegible]	[illegible]	[illegible]	[illegible]	[illegible]	[illegible]	[illegible]	[illegible]	[illegible]	[illegible]	[illegible]	[illegible]	[illegible]	[illegible]
[illegible]	[illegible]	[illegible]	[illegible]	[illegible]	[illegible]	[illegible]	[illegible]	[illegible]	[illegible]	[illegible]	[illegible]	[illegible]	[illegible]	[illegible]	[illegible]	[illegible]	[illegible]
[illegible]	[illegible]	[illegible]	[illegible]	[illegible]	[illegible]	[illegible]	[illegible]	[illegible]	[illegible]	[illegible]	[illegible]	[illegible]	[illegible]	[illegible]	[illegible]	[illegible]	[illegible]
[illegible]	[illegible]	[illegible]	[illegible]	[illegible]	[illegible]	[illegible]	[illegible]	[illegible]	[illegible]	[illegible]	[illegible]	[illegible]	[illegible]	[illegible]	[illegible]	[illegible]	[illegible]
[illegible]	[illegible]	[illegible]	[illegible]	[illegible]	[illegible]	[illegible]	[illegible]	[illegible]	[illegible]	[illegible]	[illegible]	[illegible]	[illegible]	[illegible]	[illegible]	[illegible]	[illegible]
[illegible]	[illegible]	[illegible]	[illegible]	[illegible]	[illegible]	[illegible]	[illegible]	[illegible]	[illegible]	[illegible]	[illegible]	[illegible]	[illegible]	[illegible]	[illegible]	[illegible]	[illegible]
[illegible]	[illegible]	[illegible]	[illegible]	[illegible]	[illegible]	[illegible]	[illegible]	[illegible]	[illegible]	[illegible]	[illegible]	[illegible]	[illegible]	[illegible]	[illegible]	[illegible]	[illegible]
[illegible]	[illegible]	[illegible]	[illegible]	[illegible]	[illegible]	[illegible]	[illegible]	[illegible]	[illegible]	[illegible]	[illegible]	[illegible]	[illegible]	[illegible]	[illegible]	[illegible]	[illegible]
[illegible]	[illegible]	[illegible]	[illegible]	[illegible]	[illegible]	[illegible]	[illegible]	[illegible]	[illegible]	[illegible]	[illegible]	[illegible]	[illegible]	[illegible]	[illegible]	[illegible]	[illegible]
[illegible]	[illegible]	[illegible]	[illegible]	[illegible]	[illegible]	[illegible]	[illegible]	[illegible]	[illegible]	[illegible]	[illegible]	[illegible]	[illegible]	[illegible]	[illegible]	[illegible]	[illegible]
[illegible]	[illegible]	[illegible]	[illegible]	[illegible]	[illegible]	[illegible]	[illegible]	[illegible]	[illegible]	[illegible]	[illegible]	[illegible]	[illegible]	[illegible]	[illegible]	[illegible]	[illegible]
[illegible]	[illegible]	[illegible]	[illegible]	[illegible]	[illegible]	[illegible]	[illegible]	[illegible]	[illegible]	[illegible]	[illegible]	[illegible]	[illegible]	[illegible]	[illegible]	[illegible]	[illegible]
[illegible]	[illegible]	[illegible]	[illegible]	[illegible]	[illegible]	[illegible]	[illegible]	[illegible]	[illegible]	[illegible]	[illegible]	[illegible]	[illegible]	[illegible]	[illegible]	[illegible]	[illegible]
[illegible]	[illegible]	[illegible]	[illegible]	[illegible]	[illegible]	[illegible]	[illegible]	[illegible]	[illegible]	[illegible]	[illegible]	[illegible]	[illegible]	[illegible]	[illegible]	[illegible]	[illegible]
[illegible]	[illegible]	[illegible]	[illegible]	[illegible]	[illegible]	[illegible]	[illegible]	[illegible]	[illegible]	[illegible]	[illegible]	[illegible]	[illegible]	[illegible]	[illegible]	[illegible]	[illegible]
[illegible]	[illegible]	[illegible]	[illegible]	[illegible]	[illegible]	[illegible]	[illegible]	[illegible]	[illegible]	[illegible]	[illegible]	[illegible]	[illegible]	[illegible]	[illegible]	[illegible]	[illegible]
[illegible]	[illegible]	[illegible]	[illegible]	[illegible]	[illegible]	[illegible]	[illegible]	[illegible]	[illegible]	[illegible]	[illegible]	[illegible]	[illegible]	[illegible]	[illegible]	[illegible]	[illegible]
[illegible]	[illegible]	[illegible]	[illegible]	[illegible]	[illegible]	[illegible]	[illegible]	[illegible]	[illegible]	[illegible]	[illegible]	[illegible]	[illegible]	[illegible]	[illegible]	[illegible]	[illegible]

[illegible]

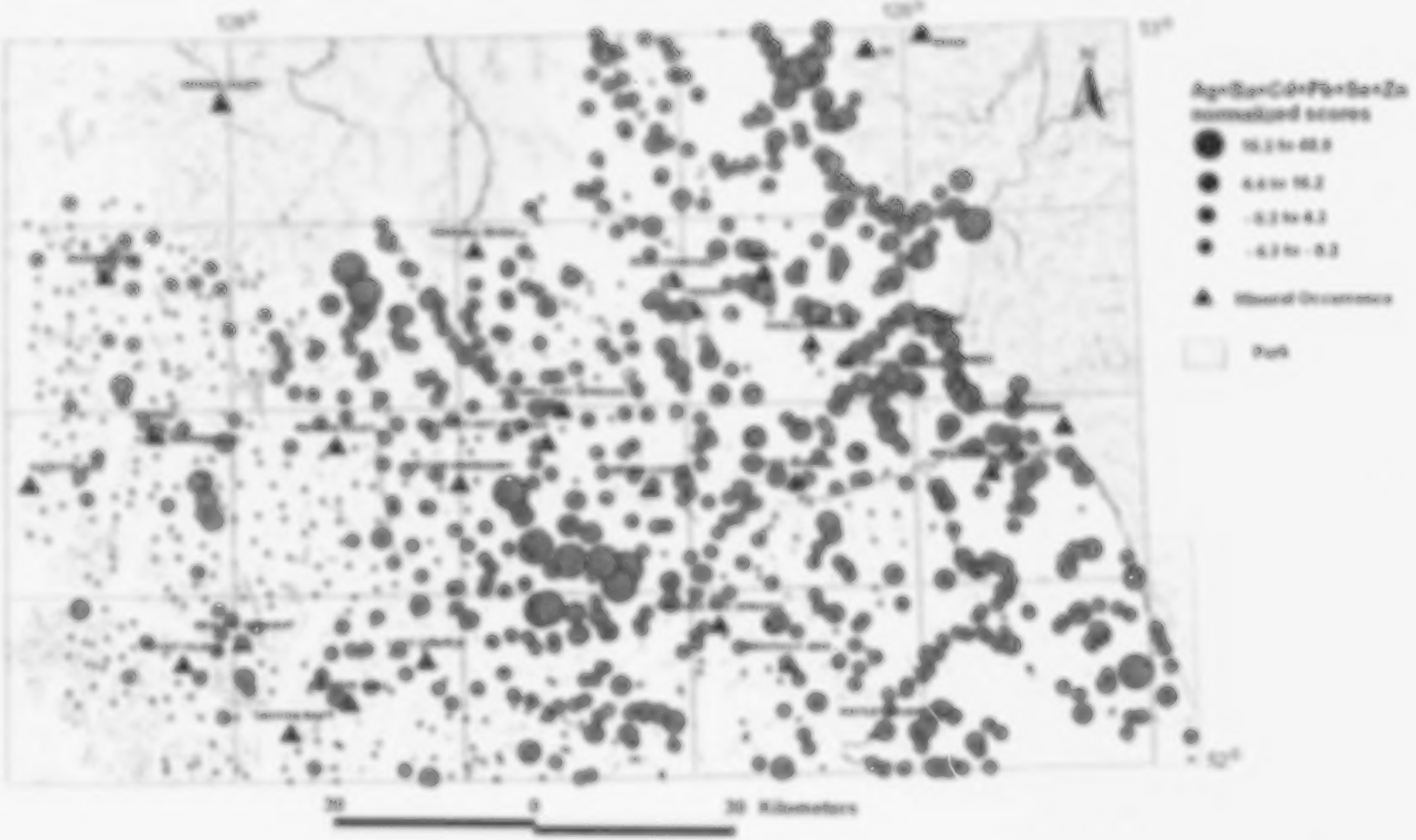
Ag+Ba+Cd+Pb+Se+Zn normalized scores
Mineral Occurrence
Park
20
0
20 Kilometers

Figure 4. Normalized Ag-Ba-Cd-Pb-Se-Zn values in stream sediments in the Bella Coola-Laredo Sound survey area.

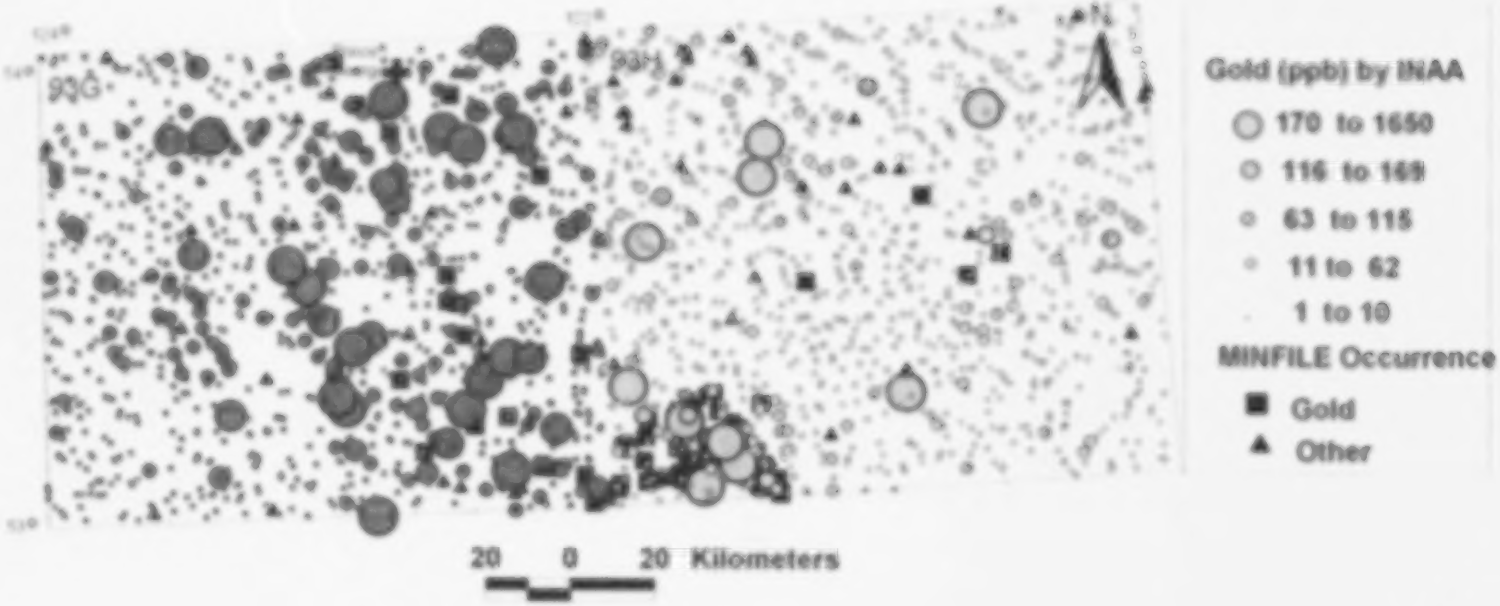
93G
93H
N
Gold (ppb) by INAA
170 to 1650
116 to 169
63 to 115
11 to 62
1 to 10
MINFILE Occurrence
Gold
Other
20
0
20
Kilometers

Figure 5. Distribution of gold in stream sediment, Prince George and McBride map sheets.

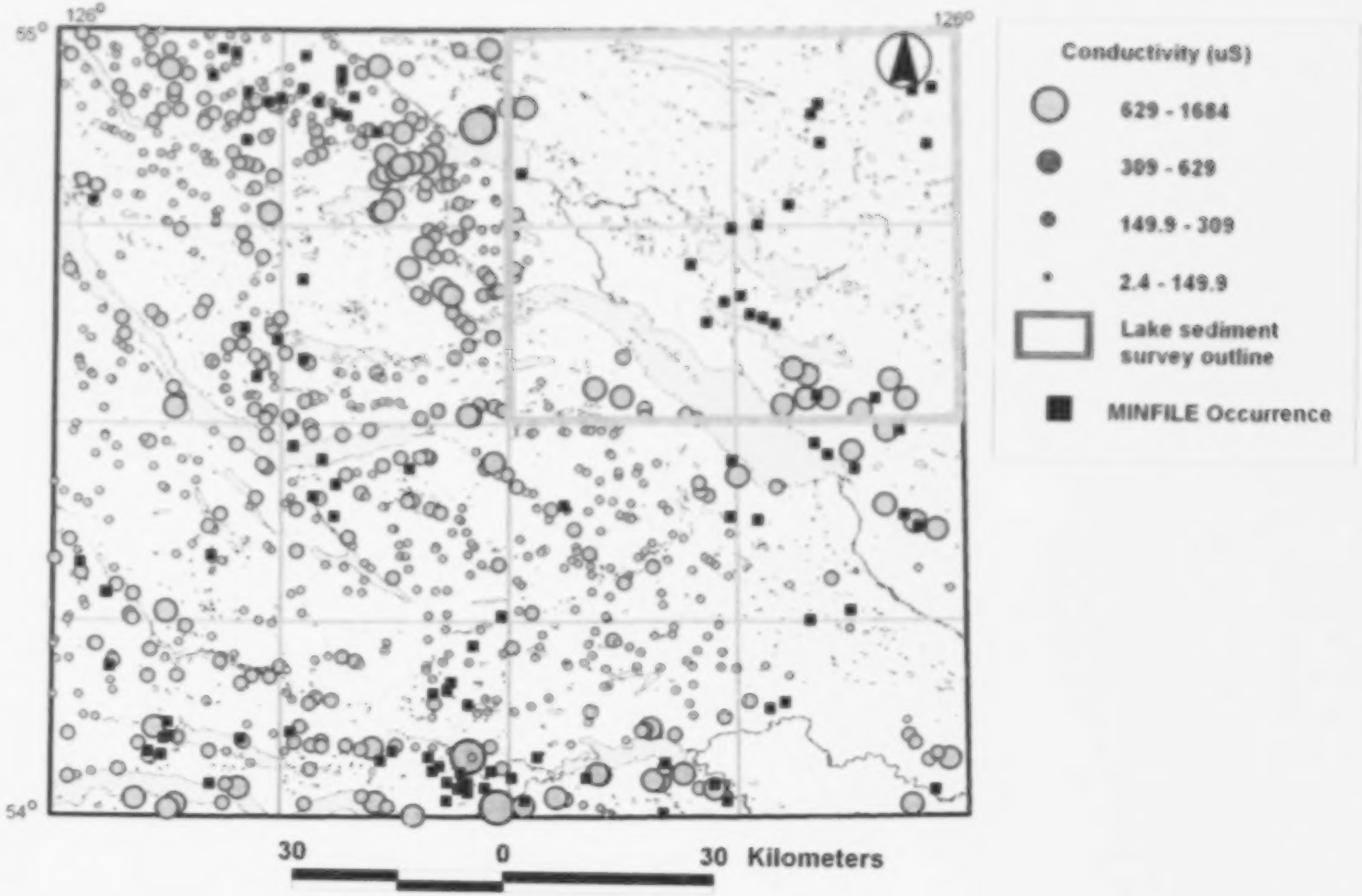
126°
126°
55°
54°
30
0
30 Kilometers
Conductivity (uS)
629 - 1684
309 - 629
149.9 - 309
2.4 - 149.9
Lake sediment survey outline
MINFILE Occurrence

Figure 6. Stream water conductivity in the Fort Fraser Map Sheet.

TABLE 6
STREAM AND MOSS MAT SEDIMENT DATA FOR SELECTED RGS SITES

Sample		002RL002	002RL003	002RL007	002RL008	002RL017	002RL018
UTM	East	365200	365200	360905	360905	363200	363200
UTM	North	6010250	6010250	6008550	6008550	6031300	6031300
Type		SEDIMENT	MOSS MAT	SEDIMENT	MOSS MAT	SEDIMENT	MOSS MAT
Ag	ppb	398	313	56	48	177	136
Al	%	1.23	1.02	0.9	0.84	1.44	1.2
As	ppm	1.7	1.4	3.4	3.4	4.1	3.3
Au	ppb	-0.2	-0.2	0.2	-0.2	0.2	0.2
B	ppm	1	1	1	1	-1	1
Ba	ppm	247.9	198.3	147.8	132.9	143.5	112
Bi	ppm	0.41	0.32	0.07	0.07	0.22	0.12
Ca	%	0.72	0.69	0.5	0.53	0.84	0.79
Cd	ppm	0.35	0.29	0.12	0.12	0.34	0.32
Co	ppm	6.4	5.7	8.3	8.4	13.6	10.3
Cr	ppm	16.5	19.2	23.8	36.6	43.2	41.5
Cu	ppm	16.3	13.03	13.28	13.42	32.8	26.78
Fe	%	2.37	2.86	2.9	3.95	2.92	2.63
Ga	ppm	4.2	3.7	3.4	3.6	5.4	4.5
Hg	ppb	33	25	11	12	32	31
K	%	0.08	0.07	0.05	0.06	0.06	0.08
La	ppm	28.3	28.9	14	16.3	14.9	13.2
LOI	%	9.9	9.2	4.6	5.4	10.8	10.6
Mg	%	0.4	0.33	0.35	0.32	0.71	0.61
Mn	ppm	590	443	508	432	883	682
Mo	ppm	9.01	6.26	0.45	0.6	1.85	1.34
Na	%	0.011	0.01	0.014	0.014	0.013	0.013
Ni	ppm	9.6	8.1	11.4	12	28.4	23.4
P	%	0.096	0.115	0.079	0.101	0.08	0.082
Pb	ppm	14.24	11.18	6.93	6.13	7.31	6.21
S	%	0.03	0.03	0.01	0.02	0.03	0.04
Sb	ppm	0.13	0.13	0.28	0.32	0.31	0.3
Sc	ppm	2.9	2.4	3	3	4.8	4.1
Se	ppm	0.4	0.2	0.4	0.5	0.8	0.9
Sr	ppm	89	75.7	48.3	47.2	67.6	58.6
Te	ppm	0.02	0.02	-0.02	-0.02	0.03	0.02
Th	ppm	7.1	5.6	2.2	2.6	1.5	1.4
Ti	%	0.049	0.046	0.068	0.078	0.067	0.067
Tl	ppm	0.09	0.07	0.05	0.04	0.06	0.05
U	ppm	6.9	5.3	1.8	1.5	0.9	0.8
V	ppm	57	78	92	134	64	63
W	ppm	-0.1	-0.1	-0.1	-0.1	-0.1	0.3
Zn	ppm	61.7	55.2	43	45.5	93.3	79.9

FORT FRASER

Covering approximately 11 500 square kilometres of the Interior Plateau (Figure 1), the eastern part of the survey area is a rolling plateau with numerous lakes and swamps becoming more mountainous to the west. The area is underlain by Mesozoic to Tertiary volcanic and sedimentary rocks intruded by monzonite to granodiorite plutons. There are over sixty known mineral occurrences including the Endako molybdenum mine and the area has the potential for VMS, epithermal Au-Ag vein and porphyry Cu-Mo deposits. A regional till survey (Plouffe, 1995) and a lake sediment survey (Cook *et al.*, 1995) cover parts of the map sheet. A Geoscape map (Hastings *et al.*, 1999), produced from data compiled by Struik *et al.*, 2001, displays the relationships between bedrock geology, surficial geology and existing geochemistry for the Fort Fraser map sheet.

Truck, boat and helicopter-supported sample collection started in late July 2002 and was completed by early September. A total of 842 stream sediment and 800 water samples were collected from 795 sites (Figure 6). Despite the low summer rainfall in the area only five percent of the streams were dry. Additional 125 ml water samples, collected from 138 of the sites, were filtered and acidified in the field. All water samples were analysed in the field for pH and conductivity. Stream water conductivity is shown in Figure 6. Stream sediment samples were air dried and sieved to -18 mesh (<1 mm) in a Fraser Lake preparation laboratory. The - 80 mesh (< 0.177 mm) fraction of the sediment samples will be analyzed for metals by aqua regia-ICPMS and by INAA. Water samples are being analyzed for elements including U and F.

ORIENTATION GEOCHEMISTRY

Orientation surveys aim to establish the characteristics of geochemical dispersion from a mineralized source so that optimum sampling density and preferred sample media can be selected for future surveys. Although stream sediments are the preferred sample type for large scale reconnaissance surveys other media such as moss mat sediment, heavy mineral and lake bottom sediments can be used depending on survey area topography (*e.g.* moss mat sediment in mountainous terrain) and commodity sought (*e.g.* heavy mineral for Au). Moss mat and stream sediment pairs were collected from several streams (Figure 7) during the regional survey and the - 80 mesh (< 0.177 mm) fraction analysed by aqua regia digestion and ICPMS to compare the geochemistry of the two media. Results, shown in Table 6, indicate that most ore indicator (*e.g.* Cu, Mo) and pathfinder elements are higher in stream sediment compared to the moss mat sediment.

CONCLUSIONS

In the Bella Coola-Laredo Sound area multi-element stream sediment anomalies suggest the presence of VMS, porphyry Cu-Mo and epithermal Au-vein type mineralization. Many of the multi-element anomalies are not related to known mineral occurrences.

New data from re-analysis of archived sediment samples by instrumental neutron activation reveals numerous Au anomalies in the Prince George and McBride map sheets. The highest Au value, exceeding one part per million, occurs in sediment is from a stream in the southeast part of the Prince George map sheet.

Orientation studies in the Fort Fraser survey area reveal that element values are higher in stream sediment than in moss mat sediment.

ACKNOWLEDGMENTS

The authors would like to thank Brian Grant for reviewing a preliminary draft of this paper. Management of the Fort Fraser regional geochemical survey by Wayne Jackman, McElhanney Consulting Services, Vancouver, B.C. was greatly appreciated. Orientation survey samples were analysed by ACME Analytical, Vancouver, B.C.

REFERENCES

Cook, S.J., Jackaman, W., Lett, R.E., McCurdy, W. and Day, S.J. (1999): Regional lake water geochemistry of the Nechako Plateau, central British Columbia (NTS 93F/02,03; 93K/09,10,15,16; 93L/09,16; 93M/01,02,07,08), *BC Ministry of Energy and Mines*, Open File 1999-5.

Diakow, L.J., Mahoney, J.B.,Gleeson, T.G., Hrudey, M.G., Struik, L.C. and Johnson, A.D. (2002): Middle Jurassic stratigraphy hosting volcanogenic massive sulphides mineralization in Eastern Bella Coola map area, southwest British Columbia. *in* Geological Fieldwork 2001, *BC Ministry of Energy and Mines*, Paper 2002-1, pages 119-134.

Hastings, N., Plouffe, A., Struik, L.C., Turner, R.J.W., Anderson, R.G., Clague, J.J., Williams, S.P., Kung, R. and Taccogna, G. (1999): Geoscape Fort Fraser, British Columbia, *Geological Survey of Canada*, Miscellaneous Report 66, 1 sheet.

Jackaman, W. (2002): Stream sediment and water geochemistry of the Triumph Bay area (NTS 103H /07,08,09,10,15,16), *BC Ministry of Energy and Mines*, Open File 2002-8.

Jackaman, W. (2002): Archived stream sediment and water geochemistry data for the Prince George (NTS 93G) and McBride (NTS 93H) map sheets, *BC Ministry of Energy and Mines*, Open File 2002-6.

Lett, R.E.W., Jackaman, W. and Friske, P.W.B. (2002): Regional stream sediment and water data - Bella Coola (NTS 93D) and Laredo Sound (NTS 103A), *Natural Resources Canada and the BC Ministry of Energy and Mines*, BC RGS 56, GSC Open File 4014.

Lefebure, D.V., Jackaman, W., Mihalynuk, M.G. and Nelson, J. (2002): Anomalous RGS survey results west of Dease Lake - new massive sulphide targets. *in* Geological Fieldwork 2001, *BC Ministry of Energy and Mines*, Open File 2002-1, pages 383-388.

Plouffe, A. (1995): Geochemistry, mineralogy and visible gold grain content of till in the Manson River and Fort Fraser map areas, central British Columbia (NTS 93K and N); Geoscape Fort Fraser, British Columbia, *Geological Survey of Canada*, Open File 3194, 119 pages.

Struik, L.C., MacIntyre, D. and Hastings, N. (2001): Geochemical Data - Nechako Project, *BC Ministry of Energy and Mines*, Open File 2001-9, *Geological Survey of Canada*, Open File 4356.

Marilla Perlite - Volcanic Glass Occurrence, British Columbia

By Melissa Rotella[1] and George Simandl[2]

ABSTRACT

Perlite is a natural hydrated volcanic glass that displays concentric 'onion-skin-like' fractures in hand sample or in thin section. It can occur as silicic lava domes, lava flows, welded ash-flow tuffs, glassy plugs, laccoliths and dikes, but most commercial perlite production comes from domes. There are two main hydration processes of perlite. Primary hydration occurs during formation of the rock before it has cooled. Secondary hydration occurs after the rock has cooled and is the more important of the two processes. Perlite has a number of industrial and agricultural applications. There are at least 23 known occurrences in British Columbia, which are listed in MINFILE (a British Columbia computer based mineral inventory system). Currently there are no producing perlite mines in Canada.

The Marilla perlite occurrence is located approximately 170 km west of Prince George, directly south of Cheslatta Lake, and outcrops for 65 m along the eastern side of Marilla Road. It consists mainly of aphyric or porphyritic biotite-plagioclase-bearing rhyolite typical of the Ootsa Lake Group, which outcrops sporadically throughout the area. Geochemical analysis confirms that the six identified lithological units are rhyolite or rhyodacite in composition. Expansion tests, using a propane torch, showed at least some degree of expansion in each sample, with a boulder found near the occurrence expanding readily. This study confirms the exploration potential in the Prince George area for expanding perlite deposits, however the distance to the market should be taken into consideration during a conceptual study before selecting this area for a major exploration program.

BACKGROUND INFORMATION

DEFINITION

Petrographically, perlite is defined as a hydrated natural rhyolite glass with perlitic texture (Bates and Jackson, 1987). It consists of 2-5% total water held within the glass structure, which is considerably higher than average obsidian water content. Industry defines perlite as any hydrated felsic rock which through rapid thermal expansion increases in volume to form a white porous lightweight cellular aggregate (McPhie *et al.*, 1993; Breese and Barker, 1994; Simandl *et al.*, 1996).

Perlite is expanded by heating crushed perlite rock to the softening temperature of glass in a furnace. At temperatures ranging from 870 to 1100°C the glass becomes soft enough for the water it contains to expand into steam resulting in a cellular structure and an increase in volume of up to 20 times. The result is a frothy particle with extremely low density, high surface area and light or white colour (Breese and Barker, 1994).

ORIGIN OF PERLITE

The water content of obsidian is typically less than 1 weight percent and is considered to be "primary" magmatic water. The higher water content of perlite (up to about 5%) is attributed to the addition of "secondary" water from external sources, such as ground water or surface water (Ross and Smith, 1955; Friedman *et al.*, 1966; Lofgren, 1971). Primary hydration occurs during the formation of a volcanic rock or glass until the first stages of metamorphogenetic changes, or rock weathering, in which hydration becomes secondary (Nasedkin, 1988). Secondary hydration occurs after emplacement and late in the cooling history of the glass, or after complete cooling to surface temperatures (Nasedkin, 1988). Secondary hydration takes place at the conditions of zeolite facies in the processes of metamorphism and rock weathering (Nasedkin, 1988). Zeolite facies metamorphism and rock weathering typically occur below 2.5 kb and 300°C.

PERLITE APPLICATIONS/USES

In the building and construction industry, expanded perlite is mixed in mortar, concrete and plaster to utilize its thermal, acoustic, lightweight and fire resistant properties. Its thermal insulation properties and low density make it highly effective in roof insulation board, pipe insulation, and refrigerator insulation. Its sonic insulation properties make it an ideal material for acoustical ceiling tile (Breese and Barker, 1994).

The ability of expanded perlite to retain water in its cellular structure makes it desirable in horticultural applications, and it is therefore used to condition soil. Expanded perlite adds loft, reduces compaction, and facilitates water drainage and moisture retention in soils due to its ability to retain water in its cellular structure (Simandl *et al.*, 1996). It is commonly used as a propagating medium for seedlings and for the packaging and storage of bulbs and plants

---

[1] *University of Victoria*

[2] *BC Geological Survey Branch and adjunct professor at University of Victoria*

(Breese and Barker, 1994). Expanded perlite can also be used as a substrate in hydroponic farming, and as a fertilizer-carrying matrix (Lin, 1989).

The internal cellular structure of expanded perlite makes it advantageous in filtration aids and oil absorbents. Expanded perlite offers high porosity and does not interfere chemically with the liquid filtered (Shackley and Allen, 1992).

Expanded perlite is used extensively in livestock applications, for the absorption of nutrients, liquid chemicals such as pesticides, fertilizers, oils, and pharmaceuticals. It is used as an additive in animal feed mixtures to aid in digestion and for growth promotion (Lin, 1989), and also can be used as an absorbent in litter padding for chicken coops (Lin, 1989).

Unexpanded perlite can be used in ceramics, glass, explosives as well as several other applications (Lin, 1998).

GENERALIZED CHARACTERISTICS OF PERLITE DEPOSITS

Perlite has many modes of occurrence including silicic lava domes and lava flows, welded ash-flow tuffs, glassy plugs, laccoliths, and dikes (Breese and Barker, 1994). Most commercial production comes from flows associated with thick accumulations of tuffs and lava flows, and from lava domes (Chesterman, 1966).

A single perlite flow can range in thickness from less than a metre to several metres and may be traced along the length of the outcrop for more than a kilometer. Silicic lava flows commonly display internal textures and structures such as flow banding, aligned elongate phenocrysts, and stretched vesicles (McPhie *et al.*, 1993). Perlite domes can range from 100 m to 2 km in diameter, and can extend vertically more than 100 m from their base (Chesterman, 1966). Rhyolite domes are usually flat or gently sloping on the upper surfaces, with steep sides and flow fronts (Figure 1). Upper parts of the dome may exhibit steep flow foliations and ramp structures with ridges on the surface (McPhie *et al.*, 1993). These silicic lava flows and domes consist of a typical zonation shown in Figure 1, in which a texturally zoned exterior glass unit encompasses a partially devitrified and crystallized inner glass unit. This zonation is produced by rapid quenching of exterior surfaces and crystallization of the interior (Breese and Barker, 1994).

PERLITE MARKETS

There are no producing perlite mines in Canada causing sized and expanded perlite to be imported mostly from the United States and Greece. Greece is by far the largest exporter of perlite, from its deposits on the island of Milos in the Aegean Sea (White, 2002). The United States exports about 10% of its production, the majority of which goes to Canada. Crushing and sizing is generally done at facilities located close to the pits. To reduce transportation costs the unexpanded perlite is shipped directly from the pits to local markets where it is expanded and processed for distribution to end users (Breese and Barker, 1994).

The total world production of perlite is over two million tonnes per year (Coope, 1999). The market value for high-quality raw perlite in British Columbia, Alberta, Washington, and N.W. Oregon in 1994 was estimated at $2.9 million Canadian dollars, and the total market for perlite in the same region in 1994 was estimated at 42 000 tonnes (Gunning and McNeil, 1994). Of this amount, 35 000 tonnes were sized ore and 7 000 tonnes were expanded perlite. Coated perlite microspheres represented 2 700 tonnes and $2.5 million Canadian dollars (Gunning and McNeil, 1994).

PERLITE IN BRITISH COLUMBIA

There are at least 23 known perlite occurrences in BC, with the Prince George area hosting several of these occurrences within the Ootsa Lake Group, including the Marilla perlite occurrence (Figure 2). These occurrences are described in MINFILE (a computer based mineral inventory system) <www.em.gov.bc.ca/Mining/Geolsurv/Minfile/search/>. Perlite resources in BC were previously described by White (1990), Morin and Lamothe (1991), Hora and Hancock (1995), Simandl *et al.* (1996) and White (in press). The Francois and Frenier deposits are two past producing perlite mines in British Columbia. Approximately 1589 tonnes were mined from Francois from 1949-1953 by Western Gypsum Products Ltd.. The Frenier deposit produced 6 000 tonnes of crude perlite from 1983 through 1985. The Frenier mine has been inactive since 1986 in part due to a low-capacity bridge across the Fraser River.

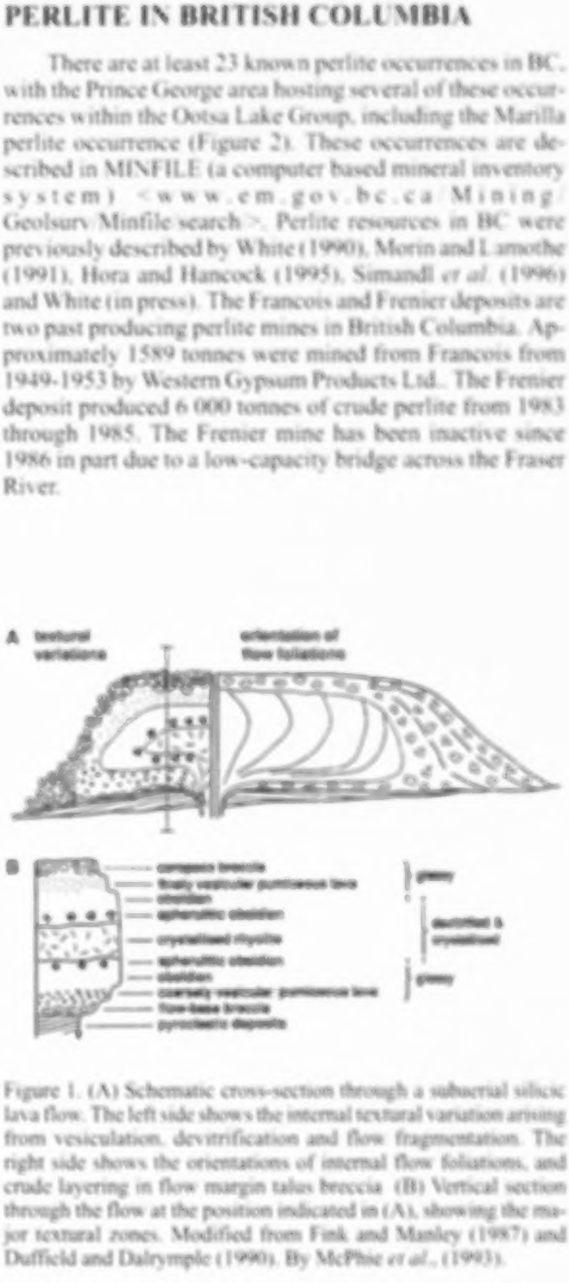

Figure 1. (A) Schematic cross-section through a subaerial silicic lava flow. The left side shows the internal textural variation arising from vesiculation, devitrification and flow fragmentation. The right side shows the orientations of internal flow foliations, and crude layering in flow margin talus breccia. (B) Vertical section through the flow at the position indicated in (A), showing the major textural zones. Modified from Fink and Manley (1987) and Duffield and Dalrymple (1990). By McPhie *et al.*, (1993).

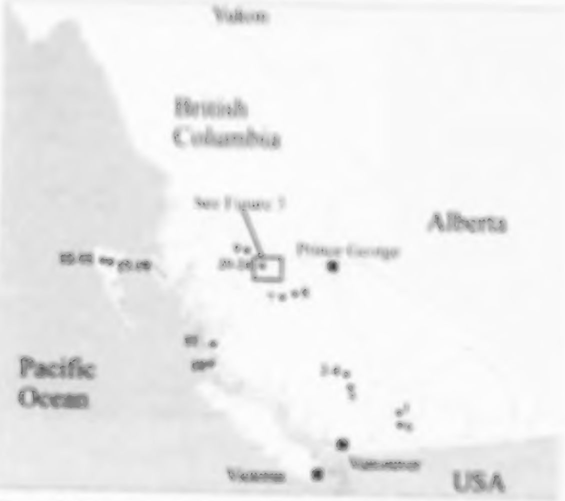
Yukon
British Columbia
Alberta
See Figure 3
Prince George
Pacific Ocean
Vancouver
Victoria
USA

Figure 2. Location of perlite occurrences in BC listed in MINFILE <www.em.gov.bc.ca/Mining/ Geolsurv/Minfile/search/>with location of the map shown in Figure 3. 1-Prospect Creek; 2-Empire Valley; 3-Moore Lake; 4-Fremier; 5-French Bar Creek; 6-Terrace Mountain; 7-Anahim Peak; 8-Narko; 9-Tasalit Mountain; 10-Denny Island; 11-Lagoon Bay; 12-Ironside Mountain; 13-Coutes Creek; 14-Skelu Bay; 15-Blackwater Creek; 16-Canoe Creek; 17-Slip Kenta Island; 18-Juskatla Inlet; 19-Florence Creek; 20-Cheslatta Lake; 21-Henson Hills; 22-Uncha Lake; 23-Francois; 24-Marilla. Modified from White (2002).

ARILLA PERLITE SHOWING

The Marilla perlite showing is located approximately 170 km west of Prince George, directly south of Cheslatta Lake N53° 42.588' and W125° 19.371' (Figures 2 and 3). It outcrops along the eastern side of Marilla Road for 65 m. The showing was mapped and sampled in 2000 by the British Columbia Geological Survey. The deposit consists mainly of an aphyric or porphyritic biotite-plagioclase-bearing rhyolite, typical of the Ootsa Lake Group as described by Duffell (1959), Tipper (1963), Diakow *et al.* (1997), and Grainger and Anderson (1999). The Ootsa Lake Group is composed of rhyolitic flows and domes, crystal and lithic-crystal tuffs, pyroclastic and autoclastic breccias, and minor dacite and andesite flows (Grainger and Anderson, 1999). The predominant rock type is a flow-laminated rhyolite, that occurs as flows and less commonly as domes. Its colour varies from red to white to grey, and locally purple or green. Textures within the Ootsa Lake group can vary within metres. Monolithic breccias, containing flow-laminated clasts, are found associated with rhyolite flows and domes. The rocks are aphyric or sparsely plagioclase-phyric. Biotite, alkali feldspar, quartz, and/or rare hornblende are minor phenocryst phases. Several exposures of buff, flow-laminated rocks have black, glassy, perlitic flow bases (Grainger and Anderson, 1999). The Ootsa Lake Group is host to occurrences such as the Cheslatta Lake, Henson Hills, Uncha Lake and

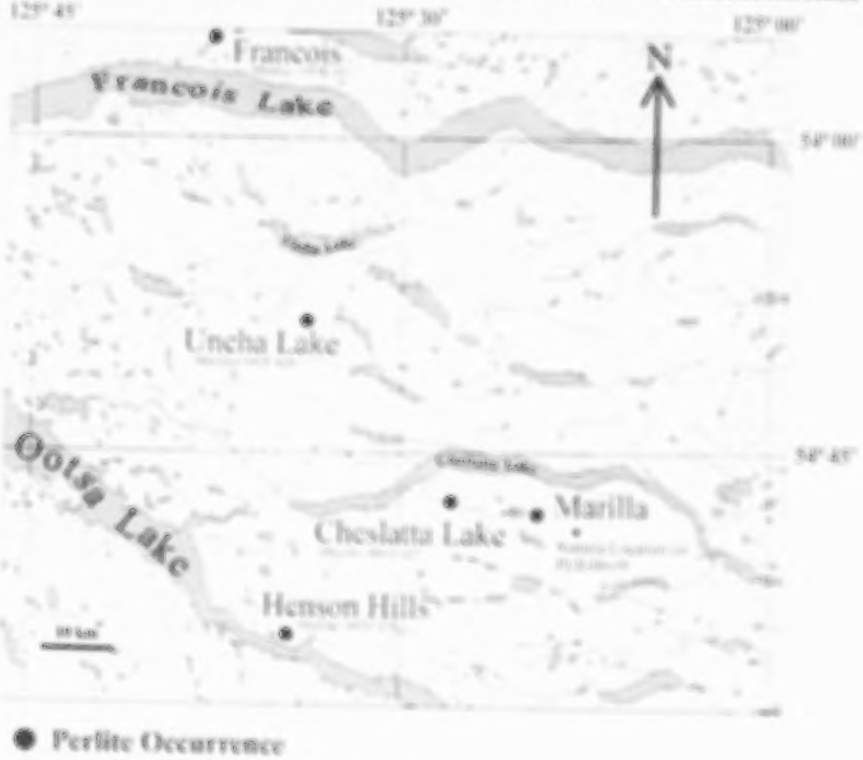
125° 45'
125° 30'
125° 00'
Francois
Francois Lake
N
54° 00'
Uncha Lake
Uncha Lake
Ootsa Lake
Cheslatta Lake
53° 45'
Cheslatta Lake
Marilla
Henson Hills
10 km
Perlite Occurrence

Figure 3. Perlite occurrences in the Prince George area Ootsa Lake Group with location of the newly discovered Marilla perlite occurrence. See Figure 2 for location of map within BC.

François occurrences, as well as the Marilla occurrence (Figure 5).

Six lithologies of the Marilla perlite showing were distinguished in the field (Figure 6). These are: Banded Spherulitic Rhyolite Breccia, Flow-Banded Perlite, Rhyolite with Biotite Phenocrysts, Spherulitic Amygdaloidal Perlite, Spherulitic Rhyolite, and a Grey Perlite Breccia described below. Sample MAR-00-09, from the Flow Banded Perlite Obsidian unit, was taken from a loose angular boulder about one meter in diameter found on the roadside 200 m west of the showing. Sample PER-00-01, from the Perlite with Amoeba-like Spherulite unit, was taken from a small flat outcrop in the ditch approximately 4 km east of the Marilla perlite showing. The coordinates for this unit are N53° 42.211' and W125° 16.42'.

PERLITE ROCK UNITS

Banded Spherulitic Rhyolite Breccia (MAR-00-01)

This rock is layered grey and cream, with maroon spherulites on a fresh surface. Altered surfaces are grey with beige bleaching in 2-5 mm thick zones. Common opal fills open spaces in the rock, with some opal forming veinlet swarms. Major constituents consist of 5-10% subhedral partially dissolved plagioclase grains averaging 1mm in diameter and 2% biotite averaging 0.4 mm in longest dimension. Spherulites make up 40-45% of the rock and are up to 1 cm in diameter, consisting of plagioclase microlites (Figure 5). The spherulite's brown colour is due to the presence of palagonite, which is a low temperature hydration and alteration mineral of sideromelane. Some spherulites are nucleated on plagioclase phenocrysts. Minor constituents are epidote (<1%, 0.25 mm in diameter) and iron oxides (2%) possibly consisting of hematite or magnetite and pyrite. There are relatively few plagioclase microlites in the glass matrix. Perlitic texture is common throughout the glass matrix. The rock expands by less than 30% when heated with a propane torch.

Flow-Banded Perlite (MAR-00-02)

This unit is layered dark grey and orange red with maroon spherulites. Layers are up to 3 cm thick, with flow banding and spherulites following the flow banding. There

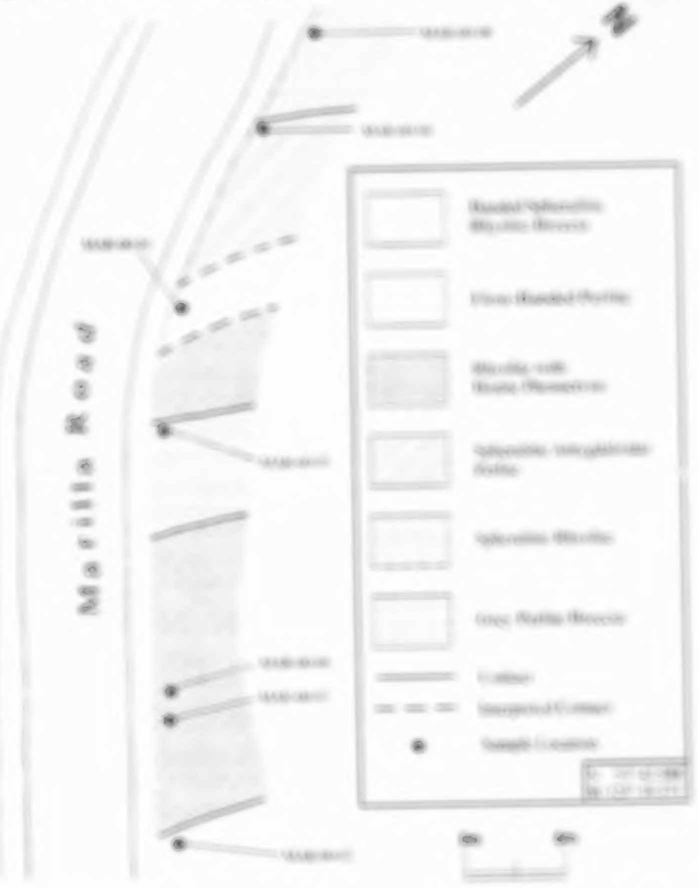

Figure 6. The Marilla perlite outcrop in plan view showing the six major lithological units.

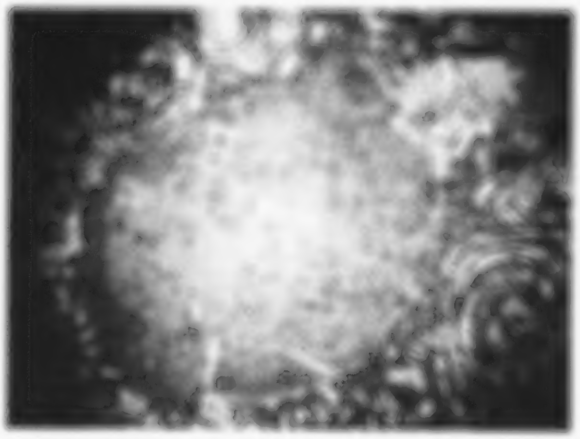

Figure 5. Spherulite of sample [illegible] (Banded Spherulitic Rhyolite Breccia) in plane polarized light.

is a pearly lustre on the [illegible] glass fractured surface. Major constituents are spherulites (40%) which are up to 1 cm in diameter, subhedral partially dissolved plagioclase grains (5-10%) averaging 0.7 mm in diameter and biotite phenocrysts (2%) averaging 0.5 mm in longest dimension with some biotite phenocrysts reaching 0.9 mm in longest dimension. Minor constituents are opaques (<1%) averaging 0.08 mm in diameter, epidote (<1%) averaging 0.1 mm in diameter, and amygdules of silica, agate and common opal (1-2%) that averages 6 mm in longest dimension. Large areas of alteration are common, displaying remnant perlitic texture. The rock made some popping noises when heated with a propane torch, but expansion was minimal at less than 5%.

Rhyolite with Biotite Phenocrysts ([illegible])

This rhyolite is beige pink grey with 2 mm black biotite phenocrysts that have a copper coloured reflection on a fresh surface. The altered surfaces appear lighter coloured than the fresh surfaces. Major constituents are plagioclase and orthoclase phenocrysts (5%) averaging 0.5 mm in diameter with some up to 2 mm, and bright orange-red coloured biotite (2%) averaging 0.25 mm in longest dimension. Amygdules (2%) infilled with carbonates that display fan textures are present and averaged 2 mm in longest dimension. Embayed feldspar grains are cemented with a glassy matrix, and flamme texture is evident throughout the rock. No expansion was observed when heated with a propane torch.

Spherulitic Amygdaloidal Perlite ([illegible])

This rock is dark grey green with maroon spherulites averaging 0.5 cm in diameter on a fresh surface, and light brown and green with maroon spherulites exposed on a weathered surface. Major constituents are spherulites (85%) up to 0.75 cm in diameter, partially dissolved embayed plagioclase phenocrysts (8%) averaging 0.6 mm in diameter, and biotite (1%) averaging 0.2 mm in longest dimension. Minor constituents are epidote (<1%) averaging 0.5 mm in diameter, opaques (<1%) averaging 0.1 mm in diameter, amygdules (1%) averaging 5 mm in diameter and swallow tails of plagioclase (<1%). Most of the perlitic textured glass is altered and has been taken over by spherulitic texture. Most spherulites are round but some are fan or plumose shaped. The lighter coloured portion of the rock popped, but no evident expansion occurred when heated with a propane torch.

Spherulitic Rhyolite ([illegible])

This rock is light grey with abundant maroon spherulites on a fresh surface. It breaks apart easily on altered surfaces due to fracture networking, beige bleaching and swarming of veinlets. No layering or banding is evident. Major constituents are spherulites (55%) up to 2.5 cm in diameter, partially dissolved plagioclase phenocrysts (5%) averaging 0.75 mm in diameter and biotite (2%) averaging 0.5 mm in longest dimension. Opaques (possibly hematite, magnetite or ilmenite) consist 1% and are 0.1 mm in diameter. The spherulites are nucleated mainly on plagioclase or biotite phenocrysts, and some have reaction rims between them and the glass. The glass matrix displays perlitic texture in which microlites have grown in the perlitic fractures (Figure 6). There was expansion of the rock by 35% when heated with a propane torch.

Rhyolite with Biotite Phenocrysts ([illegible])

This sample was taken from the same lithological unit as sample [illegible] (Rhyolite with Biotite Phenocrysts unit) and is similar in hand sample and thin section. The thin section has a slightly darker appearance in cross polarized light than [illegible], which may be the result of slightly more alteration, denser compaction, or a slightly thicker cut slide. Swallow tails of plagioclase occur, and zoned feldspars are common. The rock expanded by less than 5% when heated with a propane torch.

Grey Perlitic Breccia ([illegible])

On a fresh surface this rock has dark grey fragments averaging 2 cm in diameter surrounded by cream coloured matrix and smaller brecciated pieces of light grey rock. The

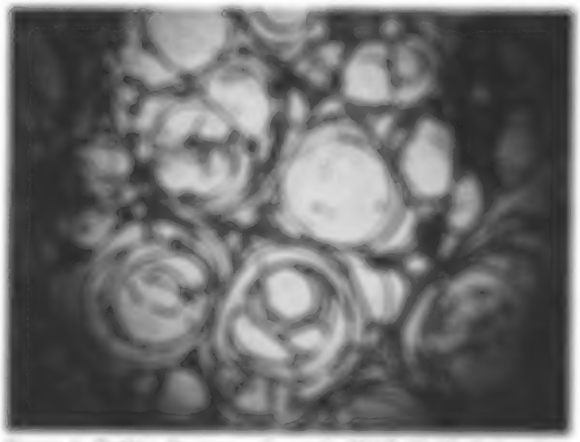

Figure 6. Perlitic fractures of sample [illegible] (Spherulitic Rhyolite unit) in plane polarized light.

[illegible]

[illegible]

[illegible]

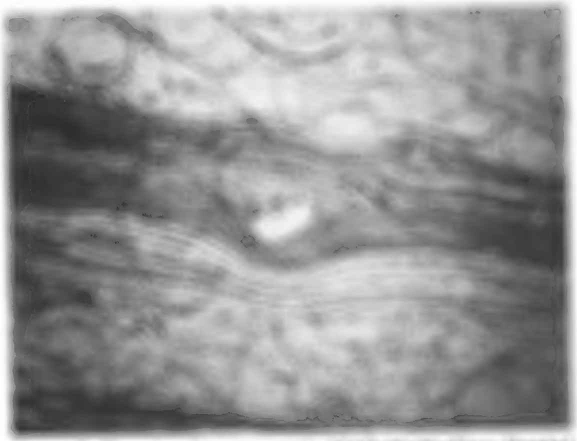

[illegible]

[illegible]

[illegible]

[illegible]

[illegible]

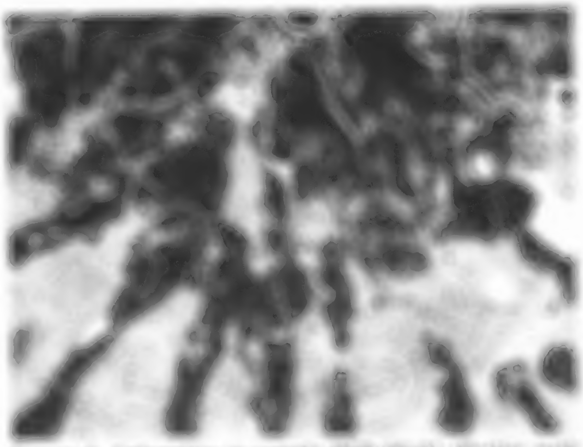

[illegible]

[illegible]

[illegible]

[illegible]

	SiO_2 %	TiO_2 %	Al_2O_3 %	Fe_2O_3 %	MnO %	MgO %	CaO %	Na_2O %	K_2O %	P_2O_5 %	LOI %	[illegible] ppm	[illegible] ppm	[illegible] ppm	[illegible] ppm	[illegible] ppm	[illegible] ppm	[illegible] ppm	[illegible] ppm
[illegible]	[illegible]	[illegible]	[illegible]	[illegible]	[illegible]	[illegible]	[illegible]	[illegible]	[illegible]	[illegible]	[illegible]								
[illegible]	[illegible]	[illegible]	[illegible]	[illegible]	[illegible]	[illegible]	[illegible]	[illegible]	[illegible]	[illegible]	[illegible]								
[illegible]	[illegible]	[illegible]	[illegible]	[illegible]	[illegible]	[illegible]	[illegible]	[illegible]	[illegible]	[illegible]	[illegible]	[illegible]	[illegible]	[illegible]	[illegible]	[illegible]	[illegible]	[illegible]	[illegible]
[illegible]	[illegible]	[illegible]	[illegible]	[illegible]	[illegible]	[illegible]	[illegible]	[illegible]	[illegible]	[illegible]	[illegible]	[illegible]	[illegible]	[illegible]	[illegible]	[illegible]	[illegible]	[illegible]	[illegible]
[illegible]	[illegible]	[illegible]	[illegible]	[illegible]	[illegible]	[illegible]	[illegible]	[illegible]	[illegible]	[illegible]	[illegible]	[illegible]	[illegible]	[illegible]	[illegible]	[illegible]	[illegible]	[illegible]	[illegible]
[illegible]	[illegible]	[illegible]	[illegible]	[illegible]	[illegible]	[illegible]	[illegible]	[illegible]	[illegible]	[illegible]	[illegible]	[illegible]	[illegible]	[illegible]	[illegible]	[illegible]	[illegible]	[illegible]	[illegible]
[illegible]	[illegible]	[illegible]	[illegible]	[illegible]	[illegible]	[illegible]	[illegible]	[illegible]	[illegible]	[illegible]	[illegible]								
[illegible]	[illegible]	[illegible]	[illegible]	[illegible]	[illegible]	[illegible]	[illegible]	[illegible]	[illegible]	[illegible]	[illegible]								

[illegible]

[illegible]

[illegible]

	SiO_2 %	TiO_2 %	Al_2O_3 %	Fe_2O_3 %	MnO %	MgO %	CaO %	Na_2O %	K_2O %	P_2O_5 %	LOI %
[illegible]	[illegible]	[illegible]	[illegible]	[illegible]		[illegible]	[illegible]	[illegible]	[illegible]		[illegible]
[illegible]	[illegible]	[illegible]	[illegible]	[illegible]		[illegible]	[illegible]	[illegible]	[illegible]		[illegible]
[illegible]	[illegible]	[illegible]	[illegible]	[illegible]		[illegible]	[illegible]	[illegible]	[illegible]		[illegible]
[illegible]	[illegible]	[illegible]	[illegible]	[illegible]		[illegible]	[illegible]	[illegible]	[illegible]		[illegible]
[illegible]	[illegible]	[illegible]	[illegible]	[illegible]		[illegible]	[illegible]	[illegible]	[illegible]		[illegible]
[illegible]	[illegible]	[illegible]	[illegible]	[illegible]		[illegible]	[illegible]	[illegible]	[illegible]		[illegible]
[illegible]	[illegible]	[illegible]	[illegible]	[illegible]		[illegible]	[illegible]	[illegible]	[illegible]		[illegible]
[illegible]	[illegible]	[illegible]	[illegible]	[illegible]		[illegible]	[illegible]	[illegible]	[illegible]		[illegible]
[illegible]	[illegible]	[illegible]	[illegible]	[illegible]		[illegible]	[illegible]	[illegible]	[illegible]		[illegible]
[illegible]	[illegible]	[illegible]	[illegible]	[illegible]	[illegible]	[illegible]	[illegible]	[illegible]	[illegible]	[illegible]	[illegible]
[illegible]	[illegible]	[illegible]	[illegible]	[illegible]	[illegible]	[illegible]	[illegible]	[illegible]	[illegible]	[illegible]	[illegible]

[illegible]

[illegible]

[illegible]

average [illegible]% and [illegible]% respectively (Breese and Barker, 1994).

Method of analysis was x-ray fluorescence. Typical (classical) compositions of perlite sites and average compositions of perlite and rhyolite are given for comparison to the Marilla perlite values.

Major and minor elements are plotted on three different discrimination diagrams (Figures 9, 10, and 11). The %SiO2 - (%Na2O+%K2O) diagram shows all units plotting in the rhyolite field with the exception of the Rhyolite with Biotite Phenocrysts unit (sample MAR-00-03). This unit contains carbonate amygdules and falls into the dacite field (Figure 9). The samples taken from the Marilla perlite showing were relatively pristine with little alteration. Due to this, the major element plot of %SiO2 - (%Na2O+%K2O) is considered to be accurate in the classification of most units being rhyolite.

Four of the eight samples were sent for trace element analyses (Table 1). These samples are plotted on a Zr/TiO2 - %SiO2 graph (Figure 10). Three of these samples plotted in the rhyodacite-dacite field with one sample falling in the trachyte field. The same four samples were also plotted on a Nb/Y - Zr/TiO2 graph (Figure 11). This plot shows all the samples falling near the rhyolite, rhyodacite-dacite, and trachy-andesite boundaries. Diagrams using immobile element ratios such as Nb/Y and Zr/TiO2 are useful in determining the original composition of volcanic rocks affected by alteration. Elements such as Zr, Ti, Nb, and Y are relatively immobile and remain in the rock when alteration occurs.

ECONOMIC POTENTIAL

Subject to a torch flame, most samples display at least some degree of expansion. More rigorous testing using standard laboratory equipment is needed before confirming the potential as raw material for an expanding perlite plant.

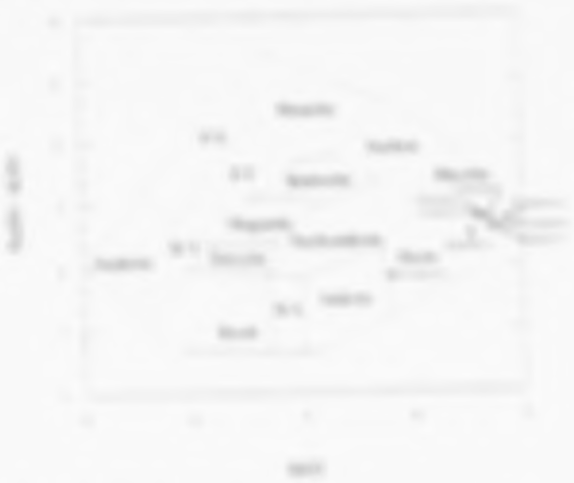

Figure 9. (%SiO2 - (%Na2O+%K2O)) discrimination diagram for volcanic rocks (Cox *et al.*, 1979).

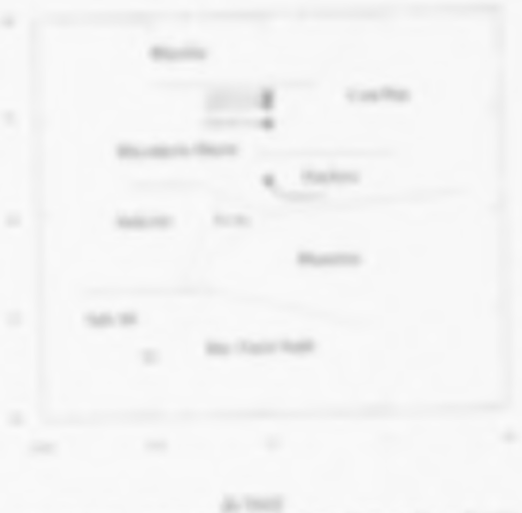

Figure 10. (Zr/TiO2 - %SiO2) discrimination diagram for volcanic rocks. Abbreviations: Com = comendite, Pan = pantellerite, TrAn = Trachy Andesite, AB = andesite basalt, Bas-Trach-Neph = basalt-trachyte-nephelinite (Winchester and Floyd, 1977).

The *Flow Banded Perlitic Obsidian* unit (sample MAR-00-09 from the boulder found 200m west of the showing), expanded to about 75%, which merits special attention. It is possible that the source of this perlite, or more highly expanding perlite, may be found in the area covered by overburden. The direction of ice flow during the last glaciation was estimated at 60° NE (Plouffe, 1999), and the angularity of this boulder suggests the source of the *Flow Banded Perlitic Obsidian* boulder (sample MAR-00-09) would be relatively nearby, and southwest of the Marilla perlite showing.

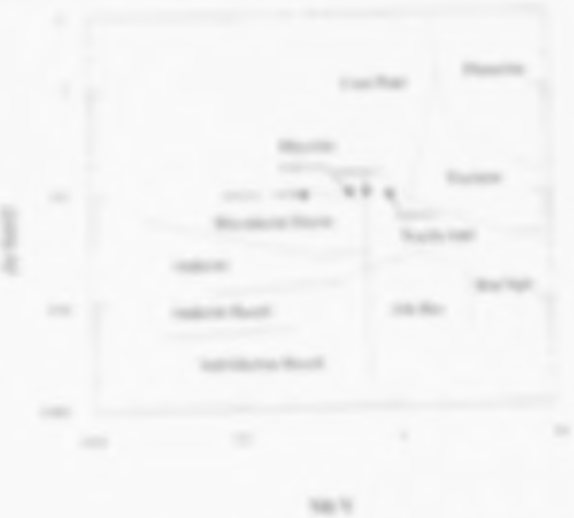

Figure 11. (Nb/Y - Zr/TiO2) discrimination diagram for volcanic rocks. Abbreviations: Com = comendite, Pant = pantellerite, Bsn = basanite, Nph = nephelinite, Alk-Bas = alkali basalt (Winchester and Floyd, 1977).

Testing of known volcanic glass occurrences and exploration in the Ootsa Lake Group is justified as it is a favourable host for expandable perlite. The Francois occurrence (Figure 3) has proven that perlite satisfying industry specifications can be found in the Prince George area. Approximately 1389 tonnes were mined from 1949-1953 by Western Gypsum Products Ltd.. Several of the volcanic glass and perlite localities in this area have been previously described by Tipper (1963), Duffel (1959), Grangier and Anderson (1999), White (1990) and White (in press). Distance of the deposit from perlite consumers should be taken into consideration before investing heavily into exploration of this geologically favourable area, as a potential source of expanding perlite may be found closer to the market.

ACKNOWLEDGEMENTS

We would like to thank Bob Lane for showing us the site, Amy Boulton and Dan Marshall for assisting in the fieldwork, and Mike Fournier for his help in drafting figures. Suzanne Paradis of the Geological Survey of Canada and Jennifer Beauregard of the University of Victoria reviewed an earlier version of this manuscript.

REFERENCES

Bates, R.L., and Jackson, J.A. (1987): *Glossary of Geology*, American Geological Institute, Alexandria, Virginia, 3rd edition, page 494.

Breese, R.O.Y., and Barker J.M. (1994): Perlite; *in* Industrial Minerals and Rocks, 6th Edition, *Society for Mining, Metallurgy and Exploration Inc.*, pages 735-749.

Chesterman, C. W. (1966): Pumice, Pumicite, Perlite, and Volcanic Cinders; *Mineral Resources of California*, Bull. 191, pg. 336-341.

Coope, B. (1999): Perlite; *in* Mining Annual Review 1999, *Mining Journal Ltd.*, Page B136.

Cox, K.G., Bell, J.D., and Pankhurst, R.J. (1979): The Interpretation of Igneous Rocks; *George Allen and Unwin*, London.

Diakow, L.J., Webster, I.C.L., Richards, T.A., and Tipper, H.W. (1997): Geology of the Fawnie and Nechako Ranges, southern Nechako Plateau, Central British Columbia (93F/2, 3, 6, 7); *in* Interior Plateau Geoscience Project: Summary of Geological, Geochemical and Geophysical Studies, *British Columbia Ministry of Energy, Mines and Petroleum Resources*, Paper 1997-2, pages 7-30.

Duffell, S. (1959): Whitesail Lake Map-area, British Columbia; *Geological Survey of Canada*, Memoir 299, 119 p.

Duffield W.A., and Dalrymple G.B. (1990): The Taylor Creek Rhyolite of New Mexico: a rapidly emplaced field of lava domes and flows; *Bulletin of Volcanology*, vol. 52, pages 475-487.

Fink J.H., and Manley C.R. (1987): Origin of Pumiceous and Glassy Textures in Rhyolitic Flows and Domes; *Geological Society of America*, Special Paper 212, pages 77-88.

Friedman, I., Smith, R. L., and Long, W. D. (1966): Hydration of Natural Glass and Formation of Perlite; *Geological Society of America*, Bulletin, vol. 77, pages 323-328.

Grainger N.C., and Anderson R.G. (1999): Geology of the Eocene Ootsa Lake Group in Northern Nechako River and Southern Fort Fraser map areas, central British Columbia; *in* Current Research 1999-A, *Geological Survey of Canada*, pages 139-148.

Gunning, D.F. and McNeal & Associates Consultants Ltd. (1994): Perlite Market Study for British Columbia; *BC Ministry of Energy and Mines and Petroleum Resources*, Open File 1994-21, 44 pages.

Hora, Z. D., and Hancock, K. D. (1995): Nazko Cinder Cone and a New Perlite Occurrence; *in* Geological Field Work 1994, *B.C. Ministry of Energy, Mines and Petroleum Resources*, Paper 1995-1, pages 405-407.

Kadey, F.L. Jr (1983): Perlite; *in* Industrial Minerals and Rocks, 5th edition, pages 997-1015.

Le Maitre, R.W. (1976): The Chemical Variability of Some Common Igneous Rocks; *Journal of Petrology*, vol. 17, part4, pages 589-637.

Lin, I. J. (1989): Vermiculite and Perlite For Animal Foodstuff & Crop Farming; *Industrial Minerals*, page 44-49.

Lin, I.J. (1990): Perlite and Vermiculite: Crudely speaking, the potential is good; *Industrial Minerals*, pages 55-59.

Lofgren, G. (1971): Experimentally Produced Devitrification Textures in Natural Rhyolitic Glass; *Geological Society of America*, Bulletin, vol 82, pages 111-124.

McPhie, J., Doyle, M., and Allen, R. (1993): Volcanic Textures: A guide to the interpretation and textures in volcanic rocks; Center for Ore Deposit and Exploration Studies, *University of Tasmania*, 198 pages.

MINFILE (2001): <www.em.gov.bc.ca/Mining/Geolsurv/Minfile/search/>

Morin, J., and Lamothe, J. (1991): Testing on Perlite and Vermiculite Samples from British Columbia; *in* Geological Field Work 1990, *B.C. Ministry of Energy, Mines and Petroleum Resources*, Paper 1991-1, pages 265-268.

Naumkin, V.V. (1988): Hydration Types, Minerals and Geology of Volcanic Glasses; *in* Second International Conference on Natural Glasses, *Prague*, J. Konta ed., pages 65-71.

Plouffe, A. (1999): New Data on Till Geochemistry in the Northern Section of the Nechako River Map Area, British Columbia; *in* Current Research 1999-A, *Geological Survey of Canada*, pages 169-178.

Ross, C.S., and Smith, R.L. (1955): Water and Other Volatiles in Volcanic Glasses; *American Mineralogist*, vol. 40, pages 1071-1089.

Shackley, D. (1989): Characterization and Expansion of Perlite; Ph.D thesis, Nottingham University, 1988.

Shackley, D., and Allen, M.J. (1992): Perlite and the Perlite Industry; Minerals Industry International, *Institution of Mining and Metallurgy*, 1008, pages 13-22.

Simandl, G. J., Church, N. B., and Hodgson, W. (1996): "Perlite" From Terrace Mountain, Vernon Area: Possible Industrial Applications; *in* Geological Field Work 1995, *B.C. Ministry of Energy, Mines and Petroleum Resources*, Paper 1996-1, pages 223-226.

Tipper, H.W. (1963): Nechako River Map-area, British Columbia; *Geological Survey of Canada*, Memoir 324, 59 pages.

White, G.V. (1990): Perlite and Vermiculite Occurrences in British Columbia; *in* Geological Field Work 1989, *B.C. Ministry of Energy, Mines and Petroleum Resources*, Paper 1990-1, pages 481-487.

White G.V. (2002): Perlite in British Columbia; *Canadian Institute of Mining, Metallurgy and Petroleum*, *in*: Special Volume #53, Suzanne Dunlop and George Simandl, editors, Industrial Minerals in Canada, pages 59-63..

Winchester, J.A., and Floyd, P.A. (1977): Geochemical Discrimination of Different Magma Series and their Differentiation Products Using Immobile Elements; *Chemical Geology*, vol., 20, pages 325-343.

Feldspathic Sandstone Flagstone from Near Hudson Hope, Northern British Columbia - Potential for Sandstone Production in British Columbia

By Z.D. Hora

INTRODUCTION

Throughout the fall of 2001 and following winter months I had the opportunity to study the sandstone quarry site located about 15 kilometres southwest of Hudson Hope in northeastern British Columbia.

This report summarizes my observations and conclusions on the potential for producing flagstone and sandstone dimension stone in the province of British Columbia.

DIMENSION STONE AND FLAGSTONE

Dimension stone is natural stone which has been selected and fabricated to specific sizes or shapes. In British Columbia it means a rock or stone product that is cut or split on 2 or more sides and includes, without limitations, tiles, facing stone, monument and ornamental stone, but does not include stone in structural applications.

Flagstone is a type of dimension stone usually of sedimentary origin (but may also be metamorphic), which splits into thin slabs from 1 to 5 cm (0.4 to 2 inches) in thickness.

There are a number of well-established flagstone and dimension stone producers supplying the existing market in Western Canada and adjacent US states. Such products are distributed in pallets of approximately 1 cubic metre (around 2 metric tonnes) (Photos 1, 2), sorted by thickness and degree of processing, such as with or without sharp edges, random or square shapes, etc. The BC and Alberta products are complemented by imported stone types not available from local producers.

Photo 1. Typical pallets of split stone - lithified volcanic ash from the Okanagan area. Kettle Valley Stone Ltd product.

Photo 2. Typical pallets of split stone - granite from Beaverdell Quadra Stone Company Ltd product.

The basic requirements for any building stone are durability, soundness, uniformity and chemical stability. Dimension stone should also be attractive and easy to process and shaped according to specifications, without producing uneconomic quantities of waste.

Chemical stability means that the stone should not react with mortars or cement. When exposed to weather, it should not produce unsightly stains (rust for example), nor be susceptible to crystallization of soluble salts. A recently published article on the restoration of the Parliament Buildings in Ottawa describes how, for example, the Ohio sandstone, which had been used , exhibits salt crystallization damage resulting in fracturing, surface erosion and overall crumbling (exfoliation).

The decision to use a particular stone may be dictated by price, but very often is based on personal taste. Even construction fashion of the time may play an important role.

SANDSTONE AND ITS USE IN BRITISH COLUMBIA

Sandstone was the first building stone used commercially in this province and its use dates to about 1870: varieties of blue, brown and yellow types were quarried from

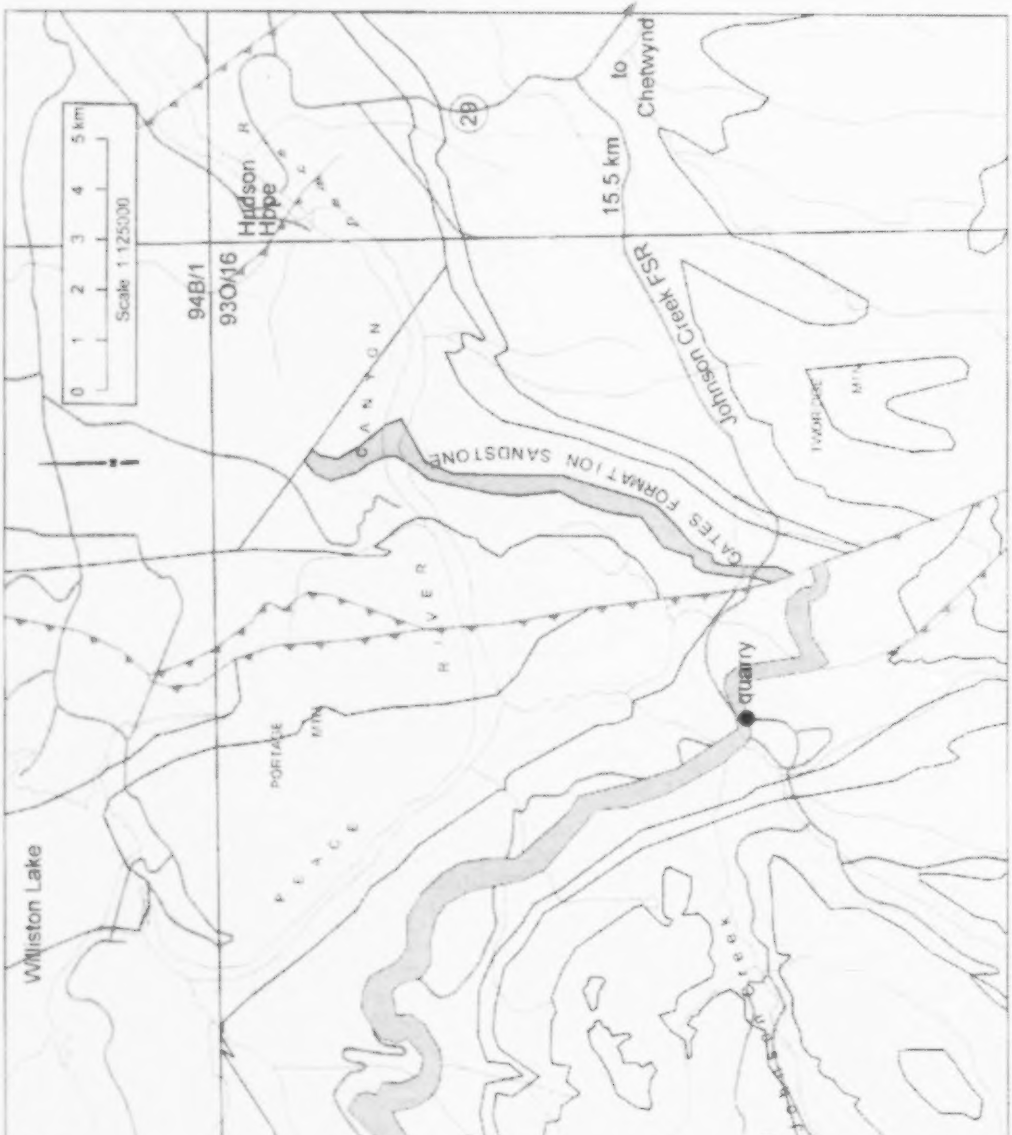
Williston Lake
Scale 1:125000
0 1 2 3 4 5 km
94B/1
93O/16
Hudson Hope
29
to Chetwynd
15.5 km
Johnson Creek FSR
CANYON
GATES FORMATION SANDSTONE
PEACE RIVER
PORTAGE MTN
quarry
Johnson Creek

Figure 1. Gates sandstone and Johnson Creek quarry location.

sites on Vancouver Island and most of the Gulf Islands. The quarry locations, quality and performance records of these sandstones are well documented. Many of the structures in which these sandstones were used are still standing in downtown areas of Vancouver, Nanaimo and Victoria (Parks,1917).

In Alberta, similar sandstones were quarried in the Foothills from sites located between Red Deer and Lethbridge. Edmonton and Calgary still have buildings with sandstone from these Alberta quarries. These sandstones were used as masonry blocks and ashlar, lintels, sills, window and door frames and similar products. However, it was not split in sheets for general flagstone applications. Stone producers one hundred years ago concentrated their attention to produce a sound structural sandstone and completely ignored sites with stone of flaggy development.

This once flourishing industry was replaced by the use of quarried granite, andesite (a volcanic rock from Haddington Island north of Nanaimo), concrete and steel, and the quarries were abandoned many years ago with plenty of resource still available.

Commercially available sandstone in the Pacific Northwest currently comes from the Hercules Quarry in Washington State through Marenacos Stone Center, Issaquah, WA. It can be obtained in up to 10-ton blocks and is marketed as cut and split product in a variety of shapes and sizes. Some sandstone is also produced by Wilkeson Sandstone Quarry LLC. located in Wilkeson, WA.

Recent geological studies of Nanaimo Group sandstones on Vancouver and Gulf Islands by Peter Mustard, and his graduate students of Simon Fraser University in Vancouver, identified a number of sites, where the sandstone splits readily into thin slabs. With the increased industry interest in flaggy sandstones, some of those sites merit examination for development potential.

Thinly bedded sandstone turbidites are observed at following sites (Mustard, personal communication, 2002):

Denman Island:

- Cedar District Formation along southwest shoreline near the ferry dock, and for about 5 kilometres to the southeast.
- Northcumberland Formation along the northeast shoreline, from about 1 kilometre southeast of Fillongley Park to about 2 kilometres northwest of the Hornby Island ferry dock.

Hornby Island:

- Spray Formation on east side of the island. In particular the Sandpiper Beach area and the northeast facing coastline on southwest side of Tribune Bay near Dunlop Point and the coast to the northwest.

Mayne Island:

- Bennett Bay and Horton Bay on the east side of the island.
- Gabriola Island:
- Gabriola Formation at Descano Bay, to the southwest of ferry dock.
- Northcumberland Formation near beach along False Narrows on the south coast.

The required material characteristics, physical requirements and testing procedures for building stone are covered by industry standards specified in American Society for Testing and Materials (ASTM) and Canadian Standards Association (CSA) designations.

ASTM and CSA specifications are very often identical and ASTM standards are widely used by industry in Canada. These designations apply to dimension stone used for general building and structural purposes. Minimum characteristics of sandstone suitable for commercial use are listed in "Standard Specification for Quartz-Based Dimension Stone, ASTM C 616-99.

JOHNSON CREEK QUARRY

The quarry site is located east of Williston Lake within the Rocky Mountains Foothills, the eastern part of the Rocky Mountains Thrust and Fold Belt.This eastern part of the Thrust and Fold Belt is more distal of the maximum deformation and adjacent to the tectonically undisturbed Interior Platform. But it is still affected by wide, low angle folds and subsequent faulting. A major north to south thrust fault truncates the Gates sandstone only 3 kilometres east of the quarry (Figure1). Such deformations cause the close jointing pattern observed on the quarry face.

The site was opened in 1981 as a quarry to provide stone for construction of Johnson Creek Forest Service Road (FSR). During 1995 some stone was removed for flagstone application and in 1996 the site was a source of riprap for local use. Since 1996 the site has been left inactive. Some of B.C. stonesmasons compared the Hudson Hope sandstone to the so called "Pennsylvania Bluestone", a very popular feldspathic flagstone produced in New York state and Pennsylvania and sold all over the USA and Canada.

The Johnson Creek quarry can be accessed from Highway 29 driving west 15.5 kilometres on Johnson Creek Forest Service Road (FSR) (Fig.1).

There are a variety of sandstones exposed in the quarry which belong to the "Gates Formation" sandstones of the Early Cretaceous age. This sandstone unit has been named after The Gates - a site on the Peace River 5 kilometres downstream of Hudson Hope, where the sandstone outcrop was first described in detail.

The Gates Formation is described as fine-grained, marine and non-marine sandstones (Stott,1982). The sandstones extend upstream from The Gates to Steamboat Island at the lower end of the Peace River canyon. From there they can be traced southward to Pine River and as far south as Deadhorse Meadows, near Kakwa River, over a distance of over 300 kilometres.

Sandstone beds of 18 – metres thickness, are exposed at The Gates; over 61 metres are present at Steamboat Island, and the Formation increases to a maximum of 263 metres thickness at Mount Belcourt.

Gates sandstones are described as generally brownish grey, and they weather to a light brown to lightly rusty colour. Most are laminated, the brittle laminations developed by mica minerals, clay, or finely comminuted carbonaceous material. The most common occurrence is in thin to thick - bedded units which weather in stacks of plates.

Sedimentary structures found within the Gates sandstones include cross-bedding, ripplemarks, mud cracks and various irregular forms called "tracks and trails". These include rounded, elongated features which are artifacts of the burrows and castings of worm-like animals (Stott, 1975; 1982). These features can also be found on the Johnson Creek quarry site.

The quarry face consists of a main rock cut with a vertical wall of varied height rising from about 1 metre at each end to approximately 7 metres in the centre. The length of this wall is approximately 30 metres (Photo 3). Numerous important geological features are exposed on the quarry face.

The rock is a well-stratified fine-grained arenite. Individual bed thickness is very irregular, from less that 1 centimetre up to approximately 20 centimetres.

They are separated by fragile, thin layers of clay, mica and detrital coal (Photo 4), and split easily in slabs and sheets along these layers. Some layers appear to be sealed to percolating meteoric water, but many have brown zones as a result of ground water *see*page (Photo 5). The units exhibit almost horizontal bedding dipping 5 to 10 degrees to the southeast in some parts of the quarry face, to 5 to 10 degrees to the south and southwest in others. Some beds contain cross- stratification features; wedge shaped layers resulting from deposition in a deltaic environment. Some beds exhibit a very rough, irregular surface with ripplemarks, worm burrows, mud cracks, carbonized root and wood remnants and similar irregularities. There is no uniformity in the appearance of the bed surface.

The sandstone weathers brown where it has been in contact with percolating meteoric waters. This is due to slow, but gradual oxidation of iron originally present in bi-valent form and causing "blue" (or to some people "green") coloration, into the tri-valent form, which is rusty brown. Water and frost have also softened the less solidified partings and finely laminated layers. Therefore, close to the surface, the Gates sandstone in the quarry area occurs in stacks of easily separable slabs and plates (Photo 7).

White stains occur locally on the quarry face (Photo 6, 7). These are clearly recent features and are located along coal - rich ledges where water percolating through the strata

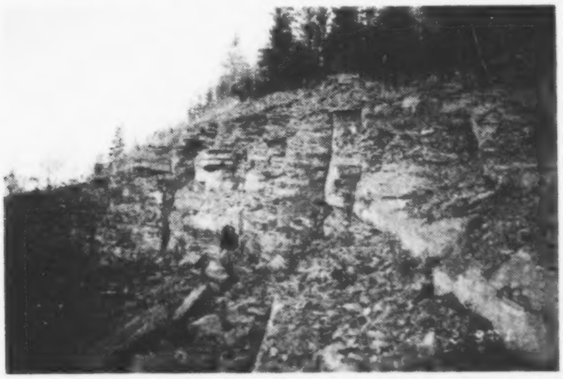

Photo 3. Johnson Creek quarry. Horizontal and vertical continuity of steep fractures and bedding plane system. View from the south.

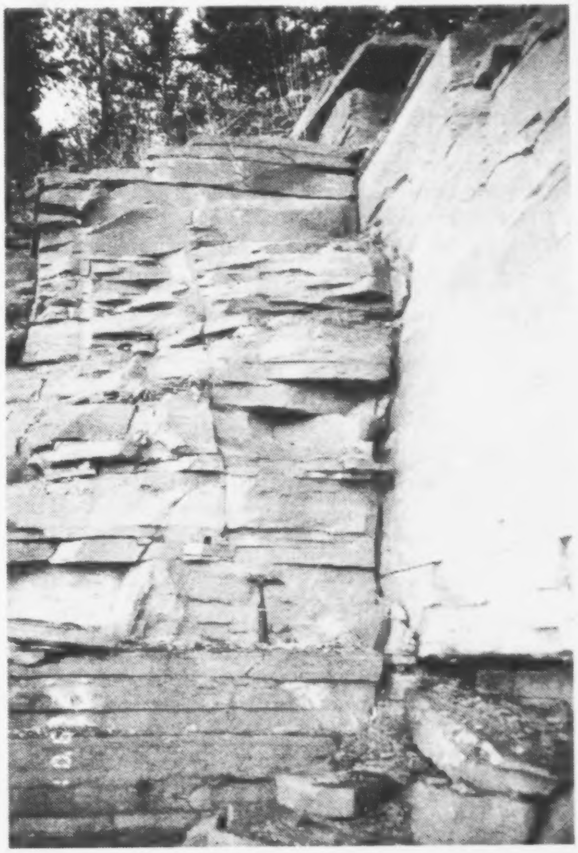

Photo 4. Fracture frequency results in quarrying slabs up to 1 metre in size. Hammer for scale is approximately 30 centimetres.

Photo 5. Brown colouration (oxidation) from percolating water along bedding planes.

Photo 6. Large patches of white staining, below some bedding planes, indicate soluble salts problem in the sandstone . Seepage comes periodically from many bedding planes after the spring break-up or rainy periods.

Photo 7. Detail look as above.

seeps out from the quarry wall. This white substance is probably leachate from coal layers, rich in pyrite, which is precipitated when water comes in contact with air.

TABLE 1
ASTM ABSORPTION TESTS ON SAMPLES FROM HUDSON HOPE

Sample #	As Received Weight	Oven Dry Weight	Soaked Weight	Percent Absorption
1	634.6	632.5	634.6	0.3
2	211.7	208.7	214.7	2.9
3	1539.9	1521.8	1543.7	1.4
4	165.2	163.1	166.3	2
5	505.8	498.8	510.3	2.3
6	155.6	153.5	158.6	3.3

Note: The unit of measurement for all weights shown above is grams.

When examined closely, the individual beds exposed in the quarry face, while having a very similar look, exhibit distinct properties. Some, when hit by a standard geological hammer have a sharp, metallic sound, while others sound dull and hollow. Some are hard, while others scratch easily. Six samples, taken at about 50 - centimetre intervals from bottom up, and numbered #1 to #6, were collected from the quarry face. The samples were tested for absorption, to identify the stone's porosity, which can provide clues as to homogeneity, and how the stone produced from the quarry site will potentially perform. The absorption test was done by Thurber Engineering Ltd geotechnical laboratory in Victoria and results confirmed the lack of homogeneity, as suspected from the hollow to metallic sound of the stone. The values range from 0.3 % in sample #1 to 3.3 % in sample # 6 (Table 1). This is well within the ASTM limits for quartz – based dimension stone.

The thin section study was undertaken by Vancouver Petrographics Ltd. of Langley, BC. The study identified the rocks as feldspathic sandstone lithified mostly by compaction; only sample # 1 has a calcite matrix. A carbonaceous substance and very fine-grained pyrite are identified, disseminated throughout the rock . No evidence of microfractures or enhanced cleavage in feldspar was noticed in any of the samples.

Samples 2 to 6 were found to be fine - grained lithic arenites, texturally mature in that they are generally well sorted and contain little or no original clay component, however, clasts are angular. Composition consists of approximately 30 – 40 % angular lithic fragments, 25 – 30 % angular quartz fragments and roughly 15 – 25 % feldspar or clay and sericite after feldspar. Minor mica as individual flakes and fragments of carbonaceous material are also noted. The rocks appear lithified by compaction, with a pseudomatrix consisting of altered and squashed (compacted) lithic and feldspar clasts.

Sample 4 is finely laminated.

Sample 1 differs from the others as it has a calcite matrix (visually estimated at slightly more that 20 % of the sample) and shows little if any evidence of compaction prior to introduction of the cement. Relative proportions of lithic fragments, quartz and feldspar are approximately the same as other samples of the suite, and clasts have similar size range and are similarly angular.

Opaque materials cannot be positively identified in thin section, as the slides are covered.

However examination of offcuts indicates that most of the opaque material is carbonaceous matter. There are also traces of very fine pyrite (grains <0.1 mm in diameter) scattered in each sample, most commonly observed within lithic or feldspathic fragments. The pyrite appears to be most abundant in sample 3, where it is estimated at less than 0.5 %. In many cases pyrite shows some partial oxidation to hematite around grain edges.

Other than bedding features, the quarry face exhibits numerous steeply dipping fractures (Photo 3). The most prominent is about 20 degrees to the general direction of the quarry wall. It consists of continuous parallel faults, approximately 5 to 7 metres apart (Photo 3). These faults have a direction from 60 to 70 degrees and dip at 70 to 80 degrees northwest. The faults are exposed on the quarry wall and can be traced along the quarry floor. There are numerous less pronounced and less continuous subordinate parallel fractures as a part of the system, together with many irregular fractures in all directions without a pattern. But all show the rusty brown coating. The rusty brown staining demonstrates that the Gates sandstone in the Johnson Creek quarry area had a well developed system of vertical fractures and open bedding planes through which the ground water circulated for many millennia, well before the quarry was opened.

The stone has been used on a trial basis in construction of a house built 5 years ago on Bowen Island, which was described in Canadian House and Home magazine. A variety of stone was used in its construction, and for landscaping.

While the retaining walls, chimneys and other structures use irregular size and shape blocks of imported "Montana Stone" – a mixture of crystalline igneous and metamorphic rocks, the deck around the house is paved with approximately 5 centimetre (2 inches) thick slabs of cut sandstone taken from the Hudson Hope site. The slabs are of very irregular size and shape (Photo 8). The average size is approximately 1 square foot (900 square centimeters); some of the slabs are smaller, some may be up to 2 square feet in size. The colour is not uniform, ranging from light bluish green to dark brown. The surface is not uniformly smooth; some slabs are very smooth, but many have slight irregularities like small blobs sticking out or irregular hollows (Photo 8). Many slabs exhibit a coarse, pitted, and almost rasp - like surface. Physical deterioration was noted in several places as a result of chipped out fragments along the edges of individual slabs. The size of such holes is in the order of a quarter to a one - dollar coin. In general, the stone has a very pleasing look.

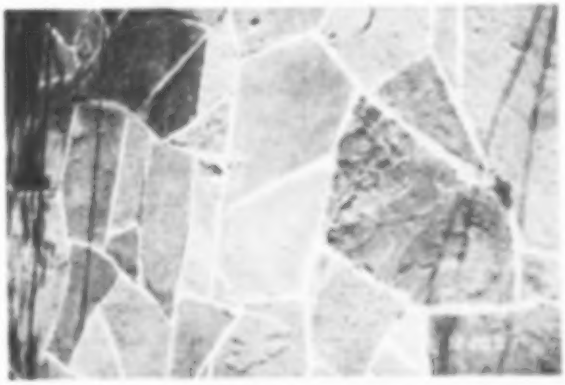

Photo 8. Bowen Island home patio floor. Cut, irregular shape slabs of 1 to 2 square feet (900 to 1800 square centimeters) in size.

The availability of Gates sandstone in this part of BC is practically unlimited. It outcrops over a large area of the Rocky Mountain Foothills from Peace River southeast to the BC – Alberta border, and similar deltaic development is certainly not unique.

Within the quarry area there is no doubt that flaggy sandstone can be produced from the existing site by opening an east – west oriented face at the south end of the present quarry wall and gradually progressing to the north. That will offer the advantage of processing first, the easily separable stacks of slabs and plates in the surficial layer.

Aside from aesthetic appeal, responsible marketability of the Hudson Hope sandstone will depend on its physical and chemical properties, long-term performance in potential end use and competitive pricing with alternative products available from stone distributors.

Three samples of sound, massive sandstone beds collected from the present face of the quarry were subjected to compressive strength test according to ASTM specifications. The sandstone slabs were drilled with a 2 inch (5 centimeter) bit (Photo 9) and the resulting core was cut into cylinders of equal length. Five cylinders from each sample were then crushed to measure the load under which they fail. The result gives the strength of the stone, which is com-

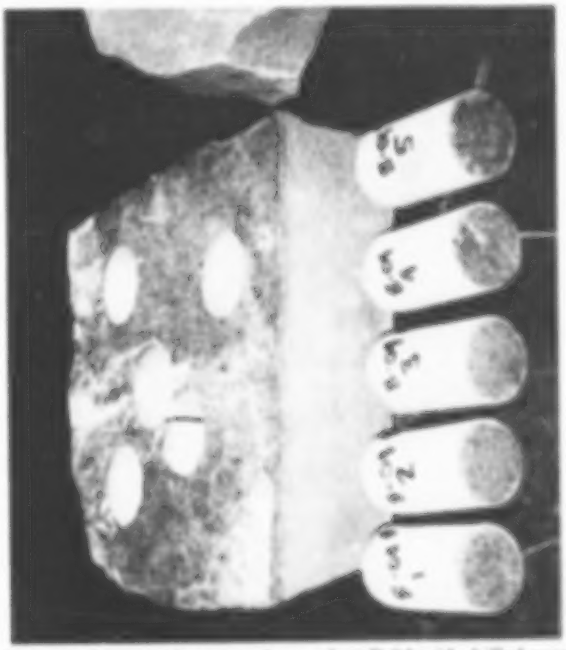

Photo 9. Compressive strength sample # B-04 with drilled core segments.

TABLE 2
COMPRESSIVE STRENGTHS OF CORED SANDSTONE

Location	Core No	Tested Length (mm)	Diameter (mm)	Corr. Factor	Load kN	Uncorrected Strength mPa	Corrected Strength mPa	Corrected Strength psi
B-04	1	47.5	45.6	1.0000	295	180.7	180.7	26,211
	2	48.5	45.6	1.0000	318.4	195.1	195.1	28,298
	3	48.7	45.6	1.0000	330.4	202.4	202.4	29,357
	4	50.7	45.6	1.0000	314.4	192.6	192.6	27,935
	5	50.2	45.6	1.0000	319.8	195.9	195.9	28,413

Location	Core No	Tested Length (mm)	Diameter (mm)	Corr. Factor	Load kN	Uncorrected Strength mPa	Corrected Strength mPa	Corrected Strength psi
B-05	1	52.6	45.6	1.0000	340.5	208.6	208.6	30,256
	2	52.8	45.6	1.0000	325.3	199.3	199.3	28,906
	3	50.1	45.6	1.0000	307.6	188.4	188.4	27,331
	4	50.1	45.6	1.0000	334.7	205	205	29,738
	5	50.4	45.6	1.0000	319.5	195.7	195.7	28,388

Location	Core No	Tested Length (mm)	Diameter (mm)	Corr. Factor	Load kN	Uncorrected Strength mPa	Corrected Strength mPa	Corrected Strength psi
B-06	1	48	45.6	1.0000	360.5	220.9	220.9	32,051
	2	49.7	45.6	1.0000	342.6	209.9	209.9	30,441
	3	50.4	45.6	1.0000	364.2	223.1	223.1	32,360
	4	49.3	45.6	1.0000	335.9	205.8	205.8	29,845
	5	51.2	45.6	1.0000	348.6	213.6	213.6	30,978

parable with other stones and specifications required for a particular application.

All 15 samples produced very similar results, which are provided in Table 2.

The average strength measured was 193 megapascals (mPa) in metric units or 28042 pounds per square inch (psi) for sample B-04; 199.4 mPa or 28923 psi for sample B-05; and, 214.7 mPa or 31130 psi for sample B-06 (Table 2).

These values are the highest, ever recorded in British Columbia. Most of B.C. sandstone quarried in the past has a reported strength between 8256 psi and 16505 psi. Only the stone from Saltspring Island has a similar strength of 27229 psi (Parks, 1917).

FLAGSTONE AND BRITISH COLUMBIA MARKETS

Producing flagstone is a labour- intensive enterprise. In a typical scenario, one central BC producer brings stone blasted by standard explosive from the quarry site to the yard by truck, for further splitting and sorting. Split and sorted by thickness, the stone is stacked onto 1- square - metre wooden pallets. Depending on the slab thickness, a complete pallet weighs between 1.5 and 2 metric tones (Photos 1, 2). It takes an average skilled worker one day to split and sort one pallet. At the quarry site, about 50% of the blasted rock is rejected as waste; at the yard, rejected unusable stone is about 25 % of the processed material.

In another case the quarry is easily reached by a flat bed truck. There, the blasted rock is split, sorted and stacked on the quarry floor. Total stone recovery in this example is about 50 %, but this is mainly because the stone splits more evenly. Productivity here is about the same - one pallet a day per person.

There are a number of well-established flagstone facing stone producers supplying the existing market in Western Canada and adjacent US states.

- Kootenay Stone Centre of Salmo is producing quartzite in a variety of brown, beige, yellow or green colours, in thicknesses of 0.25 to 0.5 inch (0.8 to 1.25 centimetres), 1 inch (2.5 centimetres), 2 inches and 4 inches thick, at a price of $ 2 to $ 4 per square foot.
- Revelstoke Flagstone Quarries Ltd. of Revelstoke is producing a silvery grey, mica schist, in thicknesses of 0.5 inch, 1 inch, 2 inches, at a price of $ 4 per square foot.

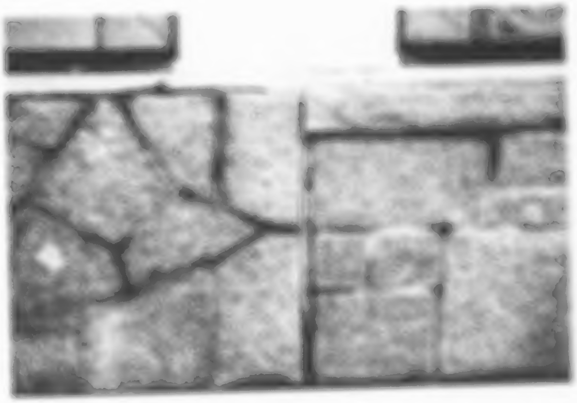
Photo 10: Typical use of split stone in wall facing. BC granite from Fox Island. Quadra Stone Company Ltd. product.

- Kettle Valley Stone of Kelowna is producing lithified white and red green banded volcanic ash, in thicknesses of 1 inch and 4 inches, at a price of $ 2 to $ 7 per square foot. Kettle Valley Stone also sells split basalt.
- A variety of split granite is also produced in BC in square shapes and in some areas competes with flagstone (Photo 10).
- Garibaldi Granite Group in Squamish is producing a variety of sizes of 2 and 4- inch -thick slabs of white, grey and beige granite at $ 2.50 to $ 8 per square foot; a specialty product without sharp edges at $ 12 per square foot; and 4- inch sawn basalt at $ 8 per square foot.
- Margranite Industries Limited of Surrey, Quadra Stone Company Limited of Vancouver and Adera Natural Stone Supply Ltd of Burnaby also offer a small selection of BC split square granite products at a competitive price.
- Margranite Industries Limited is also producing about ten different colours of BC cut and polished or flamed granite tile in two sizes – 1 and 1½ foot squares. The price of BC stone tiles is from $ 12.75 to $ 14.95 per square foot.
- Marix Marble Corporation of Duncan is selling black and white BC marble varieties as square paving blocks (Photo 11) for $ 9 per square foot and tile for $ 12 per square foot.

The prices quoted are retail, as sold from the producer's yard or a distribution center.

A very popular so called "Rundle Stone" or "Rundle Rock", dark grey to black silty sandstone is quarried in Alberta near Canmore by Thunderstone Quarries Ltd. It is used in rough split pieces as a patio stone, facing stone, etc. It can be seen in Banff on many structures including the Banff Springs Hotel. It retails in Vancouver in 2 inch thick slabs for $ 6.99 per square foot.

The transportation cost of BC flagstone products to Vancouver is between $ 45 to $ 100 per pallet or $ 600 to $ 800 for a 25 tonne trailer from eastern BC locations on Highway #1 or #3.

Photo 11. Vancouver Island marble varieties. Mosaic floor assembled of 10 by 10 centimetres square cut pavers (tiles). Marix Marble Corporation product.

Photo 12. Typical use of stone chips (rubble) in wall facing. BC granites from Fox Island (left) and Beaverdell (right). Quadra Stone Company Ltd. product.

Throughout the BC interior, and probably elsewhere, many local contractors operate small-scale intermittent quarries for their own use. Some of the stone comes from blasted rock in road construction, road cuts and natural cliffs and is usually available at no cost. There is no control or documentation of such local stone production and furthermore much of it is not really a flagstone, but just irregular rubble, or "chips" (Photo 12). This type of stone partic-

Photo 15. Quartzite flagstone, 'Kootenay Rainbow' trade name, as a column facing in Vancouver airport building. Kootenay Stone Centre product.

cially one used in interior application, is transportation sensitive. Very rarely such stone is shipped to more distant locations. One exception is the so called "Golden Fern" stone from Grand Forks, a coarse - grained crystalline quartzite which is occasionally quarried on the east side of the town and shipped to Vancouver stone distributors. This stone has an unusual look and appeal due to its colour and texture.

Although many highrise structures were built in downtown Vancouver during the last 20 years with an extensive use of natural stone, all is highly processed granite and marble. None of it is split flagstone. One of the few exceptions is the newly expanded Vancouver Airport Terminal with its minor use of quartzite, mica schist, basalt and granite in its interiors (Photos 15, 16).

About 20 000 housing units are built every year in British Columbia. Of these, only a few percent are custom built houses with a demand for stone. Standard houses with a fireplace use stone as wall facing and/or the hearth, but due to a 1991 ban against wood-burning fireplaces in the Vancouver area, this market disappeared

Photo 16. Split columnar basalt from Whistler as a wall facing, Vancouver airport building. Garibaldi Group product.

FLAGSTONE

Kootenay Stone Centre
Revelstoke Flagstone Quarries
Kettle Valley Stone Ltd
Thunderstone Quarries Ltd
Total ~12000 tonnes

CUT AND SPLIT GRANITE AND MARBLE

Garibaldi Group
Margranite Industries Limited
Adera Natural Stone Supplies Ltd
Quadra Stone Company Ltd
Matrix Marble Corporation
Total ~ 2500 tonnes

overnight. Most of the split stone (of all varieties) used in recent years has been in recreational areas, with more use in architecture. Whistler, Blackcomb and Banff are representative examples of this high-end niche market, not residential dwellings.

The following are estimates of split stone production in BC and Alberta:

The rest of reported production tonnage is in the form of small chips / waste from splitting the stone blocks, sold as landscaping stone, for road maintenance, etc., or possibly as raw material for cement manufacture.

Almost all producers sell up to 50% of their production to other parts of Canada, as well as to the United States.

A significant quantity of stone products is also imported. These are, in part, stone types not available from local producers, or different shapes and sizes produced elsewhere and required for special projects.

In recent years there has been competitive pressure on BC producers from very low priced imports from overseas, particularly from China.

In conclusion, it is my estimate that including imports, the BC market for flagstone and similar facing stone products is approximately 10 thousand tonnes per year.

MARKET POTENTIAL FOR [illegible] CREEK QUARRY SANDSTONE

Responsible marketing of sandstone from the quarry site near Hudson Hope would require good physical and chemical characterization of the stone to establish its competitive position in the marketplace. The distribution in the deposit of different qualities of the stone, as well as the distribution of its dimensional properties will have to be established. The production cost needs to address issues of effective quarrying and labour intensive processing. Transportation costs from quarry to the marketplace will also be a factor.

It is known the stone varies in some physical properties (namely absorption) and some of it reacts with [illegible] water, producing potential problems with [illegible], stains and soluble salts. While there is always room for a new product, as has been shown most recently by [illegible] Valley Stone Ltd., such new products must offer [illegible] competitive price, reliability and quality, if it is to replace an already established product with a good reputation. If the product fails only in one of the expected or required properties and specifications, the market potential drops to zero.

The Hudson Hope stone can be used safely in interior applications that are not exposed to weather conditions. Its use is to be established. However, the pieces of the Hudson Hope [illegible] seem to be doing well, considering five years of being exposed to the BC coastal climate.

SUMMARY

The Hudson Hope sandstone is not unique. Gates Formation sandstones outcrop over a large area between the Peace and [illegible] rivers in northeastern British Columbia.

- 100 years ago, western Canada had a flourishing sandstone industry on the B.C. coast and in the Alberta foothills. The stone in these quarries has not been depleted and has a reasonable performance record in masonry pieces.
- The use of statistics for market projections may be misleading. Split stone (flagstone and ashlar) can only be 20 to 25% of total reported production volume.
- The petrographic study confirmed that some beds have a different texture or composition from others.
- The fracture pattern and bedding planes exposed in the quarry face exhibit [illegible] fracture cutting and stacking, which must have developed over many millennia. The spacing between individual fractures [illegible] that [illegible] can be easily quarried from this site.
- Three samples taken from different massive beds exposed in the quarry face and tested for compressive strength are proof that the stone has excellent physical properties, superior to most of BC sandstones quarried in the past.

While the Hudson Hope location may have a significant logistical drawback, a similar sedimentary environment in Lower Cretaceous formations occurs over large areas of Rocky Mountain Foothills and further east. Also, similar flaggy sandstones occur in Triassic rocks of [illegible] Formation, between Peace and [illegible] rivers of northeastern British Columbia ([illegible] and [illegible], [illegible]).

Recent studies of Nanaimo Group sandstones on Vancouver and Gulf Island identified a number of potential sites on Gulf Islands, which should be examined by an experienced quarry master for flagstone production.

ACKNOWLEDGMENTS

The author would like to thank a number of individuals who helped in collecting the data and preparation of this report. Namely, Brian Grant of [illegible] Engineering Ltd., [illegible], Andrew Legun and [illegible] of BC Government, [illegible] of Vancouver Petrographics Ltd. and several BC stone producers [illegible].

Thanks are extended to Dave Lefebure and Brian Grant for editorial comments and improving the manuscript.

BIBLIOGRAPHY

Barton, W.R. (1968): Dimension Stone. Information Circular 8391, US Bureau of Mines, 147 pages.

Bowles, O. and Barton, W.R. (1963): Sandstone as Dimension Stone. Information Circular 8182, US Bureau of Mines, 31 pages.

Currier, L.W. (1960): Geologic Appraisal of Dimension-Stone Deposits. Bulletin 1109, US Geological Survey, 78 pages.

Kennedy, R. (2001): Inspection Report [illegible] Ministry of Energy and Mines, [illegible] pages.

[illegible] (2000): Building Stones of Canada's Federal Parliament Buildings; [illegible] Canada, Vol. [illegible], No. [illegible], pages [illegible].

Parks, W.A. (1917): Report on the Building and Ornamental Stones of Canada, Vol. V: Province of British Columbia; No. [illegible], Canada Department of Mines, [illegible] pages.

[illegible] and [illegible] (1995): [illegible]

[illegible] (1994): [illegible], pages [illegible].

[illegible] (1989): [illegible] An Introduction; [illegible] pages.

[illegible] (1975): [illegible] Geological Survey of Canada, [illegible] pages.

[illegible] (1988): [illegible] Geological Survey of Canada, [illegible] pages.

[illegible] (1988): [illegible] pages [illegible].

Atlin TGI, Part VI: Early to Middle Jurassic Sedimentation, Deformation and a Preliminary Assessment of Hydrocarbon Potential, Central Whitehorse Trough and Northern Cache Creek Terrane

By Joseph M. English[1], Mitchell G. Mihalynuk[2], Stephen T. Johnston[1], Michael J. Orchard[3], Martin Fowler[4] and Lucinda J. Leonard[1]

KEYWORDS: *Cache Creek terrane, Laberge Group, Sinwa Formation, Nakina, Tulsequah, regional geology, forearc basin, accretionary complex, hydrocarbon potential, organic maturation*

INTRODUCTION

The Whitehorse Trough is an Early to Middle Jurassic marine basin, which extends from southern Yukon to Dease Lake in British Columbia. It flanks oceanic crustal rocks to the east, including thick platformal carbonate and argillaceous chert successions of the northern Cache Creek terrane (Figure 1). Early studies recognised the low metamorphic grade of these sedimentary rocks (*e.g.* Monger, 1975) and their potential to host hydrocarbon accumulations (*e.g.* Gilmore, 1985; Hannigan *et al.*, 1995; National Energy Board, 2001). However, early assessments were based on data from samples collected in southern Yukon (Gilmore, 1985; National Energy Board, 2001); these data indicate that the Whitehorse Trough in the Yukon is gas-prone. It is not known if potential hydrocarbon traps were filled and preserved, as none have been drilled. Structural complexity and metamorphic grade decreases in the British Columbia portion of the Trough. On the basis of flat-lying Eocene volcanic rocks, no widespread deformation post-dates Early Eocene time (Mihalynuk, 1999). Indeed, undeformed Middle Jurassic plutons cut all major fabrics within the Whitehorse Trough in BC. Deformation is therefore constrained in age to between about 172 and 170 Ma - the age of youngest deformed strata and oldest cross-cutting plutons (*e.g.* Mihalynuk *et al.*, 1999). Such a simple deformational history limits the possibility of hydrocarbon escape subsequent to generation, during successive deformational events. An uncomplicated history also simplifies thermal maturation modeling. Previous assessments in BC were based on extrapolation from the Yukon portion of the Trough.

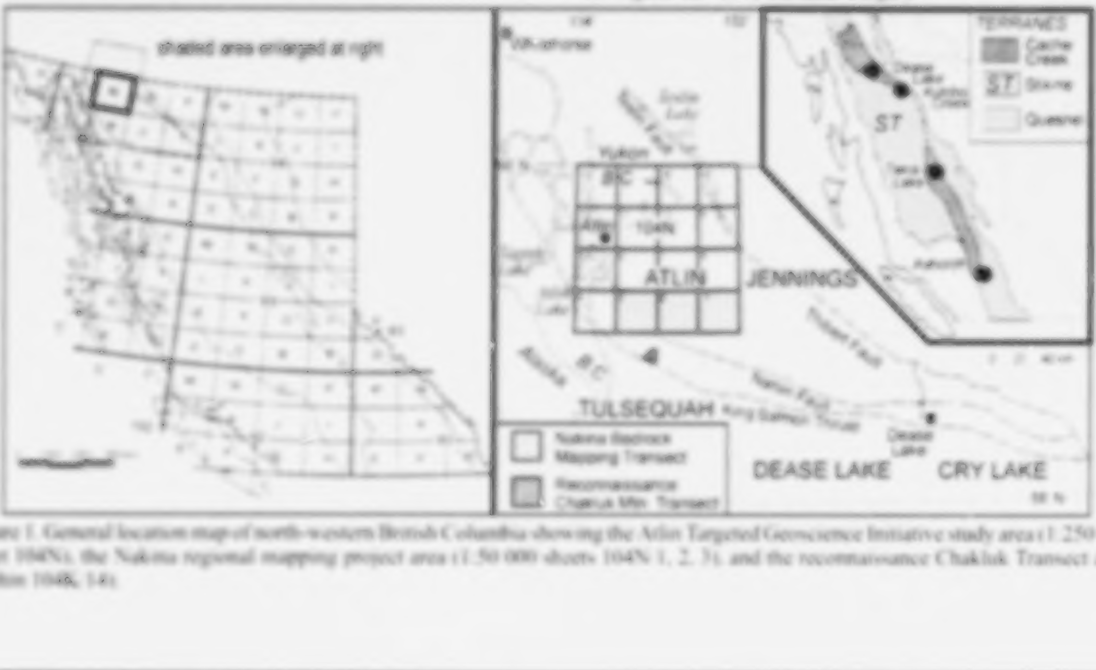

Figure 1. General location map of north-western British Columbia showing the Atlin Targeted Geoscience Initiative study area (1:250 000 sheet 104N), the Nakina regional mapping project area (1:50 000 sheets 104N/1, 2, 3), and the reconnaissance Chakluk Transect area (within 104K/14).

---

[1] *University of Victoria*
[2] *BC Geological Survey Branch*
[3] *Geological Survey of Canada*
[4] *Geological Survey of Canada, Calgary*

We report here on the first results of a preliminary hydrocarbon assessment of the BC portion of the Whitehorse Trough and the adjacent Cache Creek terrane that was conducted as a partnership between the New Ventures Branch of the BC Ministry of Energy and Mines, and the Atlin Targeted Geoscience Initiative (TGI). The Atlin TGI is a joint Geological Survey of Canada - BC Geological Survey project aimed at providing mineral exploration incentive through provision of an enhanced geoscience database for the Atlin area (mapsheet 104N; Lowe and Mihalynuk, 2002). A component is a 1:50,000 map transect across the southern part of the sheet 104N/1, 2 & 3 in 2001 and 2002 (Figure 1). This ~90km long transect spans the Cache Creek-Whitehorse Trough contact, providing an opportunity to sample and evaluate hydrocarbon potential as part of the mapping program. Initial observations from mapping within the Cache Creek terrane are reported in Mihalynuk *et al.* (2002; 2003, this volume). A preliminary report on the geology of the Whitehorse Trough, which constitutes the southwestern portion of mapsheet 104N/3, is presented in this paper (Figure 1). In addition, a reconnaissance transect of the southwestern side of the Whitehorse Trough, near the Taku River, was mapped and sampled in order to provide continuity of hydrocarbon assessment across the Trough (Figure 1). In this report, stratigraphic and structural observations are combined with petrographic analyses, programmed pyrolysis data and conodont alteration indices (CAI's) in order to provide a preliminary assessment of hydrocarbon potential in the central Whitehorse Trough and northern Cache Creek terrane.

GEOLOGICAL BACKGROUND

The Cache Creek terrane is a belt of oceanic rocks that occupies a central position within the accreted terranes of the northern Cordillera (Coney *et al.*, 1980). Fossil data suggest an age range from Mississippian through to Lower Jurassic for these rocks (Monger, 1975; Cordey *et al.*, 1991; Orchard, 1991). The terrane is characterised by tectonically imbricated slices of chert, argillite, volcaniclastic rocks, carbonate and wacke, as well as ultramafics, gabbro and basalt. These lithologies represent two distinctive lithotectonic elements: a Middle Triassic to Lower Jurassic, subduction-related accretionary complex, and a dismembered oceanic basement assemblage (Terry, 1977; Monger *et al.*, 1982; Ash, 1994; Mihalynuk, 1999). Preliminary geochemical investigations of Upper Permian (Devine, 2002) igneous rocks associated with the Nahlin ultramafic body indicate that they were produced in a primitive island-arc setting (English *et al.*, 2002). The Cache Creek terrane also includes a Permo-Triassic island-arc assemblage, the Kutcho Assemblage (Childe and Thompson, 1997), which lies to the SW of the Nahlin Fault and forms basement to the Lower Jurassic Laberge Group in the Dease Lake/Cry Lake area (Thorstad and Gabrielse, 1986; Gabrielse, 1998; Figure 1). The northern Cache Creek terrane (N of 58°) was emplaced over the Stikine terrane and Laberge Group during the closure of an ocean basin in the Middle Jurassic (Thorstad and Gabrielse, 1986; Mihalynuk, 1999).

The Whitehorse Trough is a ~500 km long, early Mesozoic marine basin, which extends from southern Yukon to Dease Lake in British Columbia. Lower - Middle Jurassic sediments of the Trough are known as the Laberge Group. In BC, the Trough is bounded by the Nahlin Fault to the east and by the King Salmon Thrust to the southwest, although south of the King Salmon Thrust, conglomeratic facies onlap onto the Upper Triassic volcanic and carbonate rocks of the Stikine terrane (*e.g.* Souther, 1971; Figure 1). The Laberge sediments range in age from Lower Sinemurian to Middle Bajocian, and are believed to represent submarine-fan deposition in an arc-marginal setting (*e.g.* Tempelman-Kluit, 1979; Dickie and Hein, 1995; Hart *et al.*, 1995; Johannson *et al.*, 1997). The sediments are deposited on the Stuhini Group throughout much of the length of the Whitehorse Trough in British Columbia (*e.g.* Monger *et al.*, 1991), and overlie the equivalent strata - Lewes River Group - in the Yukon (*e.g.* Wheeler, 1961). However, further south in the Dease Lake area, the Laberge sediments overlie the Kutcho Assemblage of the Cache Creek terrane (*e.g.* Thorstad and Gabrielse, 1986; Gabrielse, 1998).

CACHE CREEK TERRANE

The geology of the Cache Creek terrane in the Nakina area is described in Mihalynuk *et al.* (2002; 2003, this volume), and will not be discussed in detail here. Within this region, speculative hydrocarbon plays have focused on the Mississippian - Permian carbonates of the Horsefeed Formation (Hannigan *et al.*, 1995). These carbonate sequences were deposited upon volcanic pediments within the Cache Creek ocean basin (Monger, 1977; English *et al.*, 2002), and were subsequently incorporated into the Cache Creek subduction complex during closure of an ocean. A potential gas source within the Horsefeed Formation is provided by shallow water back-reef algal laminites and dark, fetid argillaceous limestones (*e.g.* National Energy Board, 2001). However, a lack of maturation data has previously precluded a rigorous assessment of the hydrocarbon potential of this region.

LABERGE GROUP

Laberge Group strata are well exposed in the mountains west of the Sloko River in 104N/3. Estimates of total stratigraphic thickness are difficult to determine due to thrust fault repetition and the absence of biogeochronological constraints. Basal units have been observed during this study at one location north of Mount Headman, and uppermost units have not been identified.

Laberge Group lithologies within the Nakina area include greywacke, sandstone, siltstone, argillite and minor conglomerate. The dominant lithology is blue-grey to green-grey medium-grained massive wacke with subordinate interbedded argillites (Photo 1). Greywacke beds are 1-2 m thick, while subordinate argillaceous intervals reach 20 cm in thickness. Interbedded siltstone and sandstone couplets display a characteristic banded appearance, and commonly weather an orange-brown colour (Photo 2). Couplet intervals reach 200 m in thickness, although they

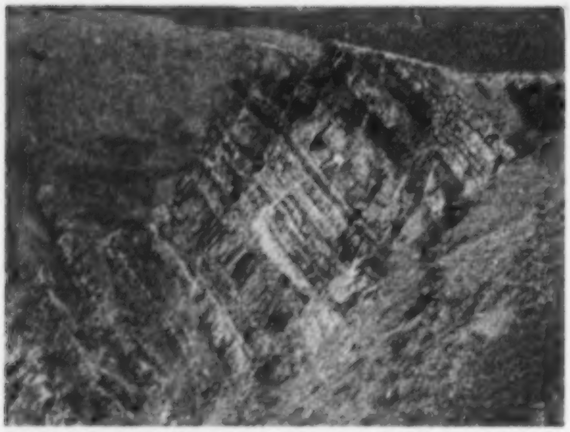

Photo 1. Laberge Group strata exposed NE of Paradise Peak. The succession is dominated by well-bedded greywacke with subordinate argillaceous interbeds. A brick-red columnar jointed sill of the Sloko Group here intrudes Laberge Group strata.

Photo 2. Dark grey siltstone and pale brown sandstone couplets exposed south of the Nakonake River. These lithologies are interpreted to dominate the lowermost strata of the Laberge Group in this region. The hammer lies on a contact with overlying greywacke.

are commonly minor (~ 1 m) components of greywacke dominated successions. Conglomerates are a minor constituent of the Laberge Group in this region and are laterally discontinuous reflecting deposition in channels (Photo 3). These conglomerates are matrix-supported and reach 10 m in thickness.

STRATIGRAPHY ALONG THE CHAKLUK TRANSECT

A transect with continuous exposure extends from Mount Headman to Chakluk Mountain, herein referred to as the Chakluk Transect (Figures 1 and 2). The oldest strata on the Chakluk Transect are the Upper Triassic carbonates of the Sinwa Formation (Figure 3). These carbonates are composed of fine-grained, medium brownish-grey limestone, commonly with a bioclastic component of gastropods and bryozoans. No bedding was discernible.

The Sinwa Formation is overlain disconformably by the Laberge Group (Souther, 1971), the contact was not exposed along the Chakluk Transect. The basal unit of the Laberge Group is a coarsening-upward sequence that is approximately 1000 m thick (Figure 3). The sequence grades from beds of siltstone and argillite to rhythmically bedded couplets of siltstone and sandstones, and finally up into beds of massive greenish greywacke.

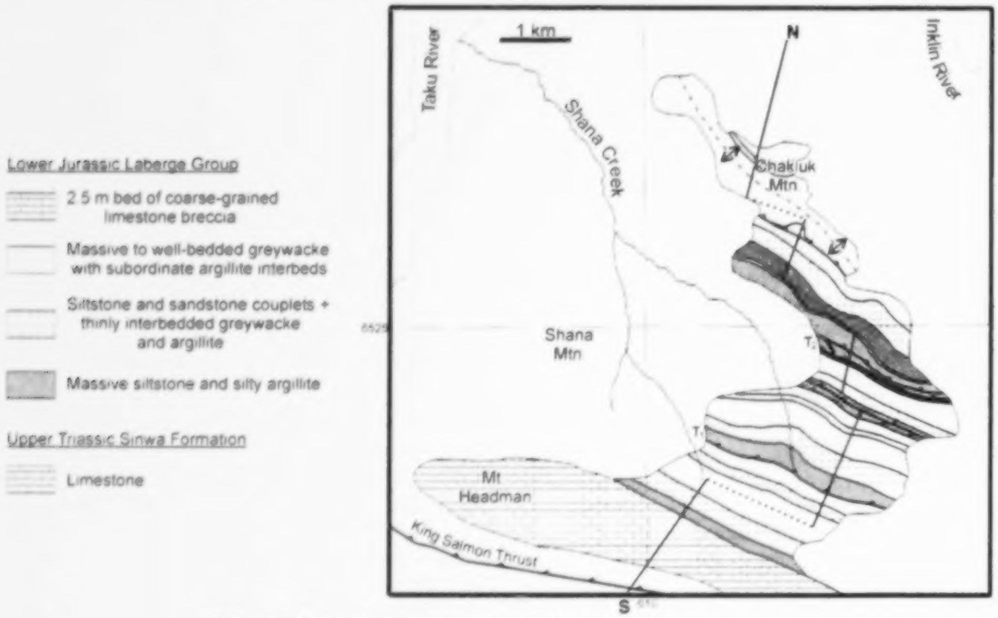
Lower Jurassic Laberge Group
2.5 m bed of coarse-grained limestone breccia
Massive to well-bedded greywacke with subordinate argillite interbeds
Siltstone and sandstone couplets + thinly interbedded greywacke and argillite
Massive siltstone and silty argillite
Upper Triassic Sinwa Formation
Limestone
1 km
N
S
Taku River
Inklin River
Shana Creek
Chakluk Mtn
Shana Mtn
Mt Headman
King Salmon Thrust
T2
T1
6525

Figure 2. Generalised geologic map of the Chakluk Transect area.

Photo 3. Matrix-supported conglomerate exposed SE of Paradise Peak. Well-rounded granitoid clasts reach 30 cm in size at this locality.

Overlying the wacke is a succession of fine-grained siltstone with subordinate greywacke (Figure 3). These strata include a single, 2.5 metre marker bed of limestone breccia containing bioclasts of crinoid ossicles and bivalves (Photo 4). This bed becomes laminated toward its top. This fine-grained sequence grades upwards into coarser-grained facies, with a predominance of medium-grained greenish greywacke around Chakluk Mountain. This succession of 1 m greywacke beds and subordinate argillite is at least 350 m thick.

Slatey cleavage is commonly developed along the transect, and in one outcrop, folded, fine-grained metasediments display a phyllitic sheen (Photo 5).

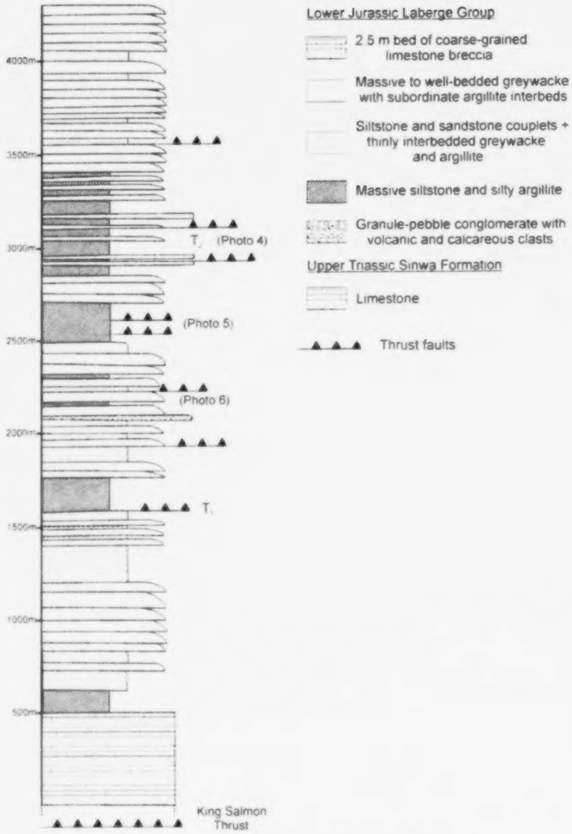
4000m
3500m
3000m
2500m
2000m
1500m
1000m
500m
T₂ (Photo 4)
(Photo 5)
(Photo 6)
T₁
King Salmon Thrust
Lower Jurassic Laberge Group
2.5 m bed of coarse-grained limestone breccia
Massive to well-bedded greywacke with subordinate argillite interbeds
Siltstone and sandstone couplets + thinly interbedded greywacke and argillite
Massive siltstone and silty argillite
Granule-pebble conglomerate with volcanic and calcareous clasts
Upper Triassic Sinwa Formation
Limestone
Thrust faults

Figure 3. Stylised stratigraphic column for the Chakluk Transect.

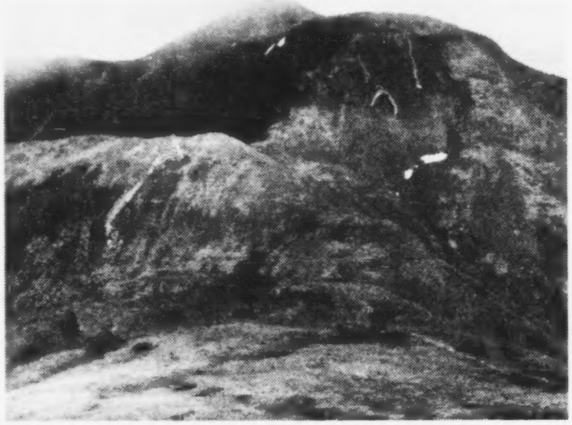

Photo 4. 2.5m bed of limestone breccia exposed on the ridges south of Chakluk Mountain. This carbonate unit has been truncated and repeated by a series of NW trending thrust faults.

STRATIGRAPHY IN NAKINA MAP-AREA

Stratigraphic correlation within the Laberge Group is hampered by frequent lateral facies changes and a lack of marker horizons and macrofossils. Nevertheless, a tentative stratigraphic column is presented in Figure 4. This stratigraphic column includes a complete section from SW to NE. The degree of structural repetition remains unconstrained.

Southwest of thrust fault T_3 (Figure 5), the lowermost strata in the core of anticline A_1 comprise couplets of 10-30 mm, fine-grained sandstones grading into ~ 10-30 mm of darker siltstone layers (Photo 2). These intervals reach 200 m in thickness, and weather a characteristic orange-tan colour, possibly as a consequence of pervasive dolomitisation of the matrix. These strata grade upwards into a succession dominated by massive blue-grey wacke interleaved with 1-5 m thick intervals of sandstone and siltstone couplets. The stratigraphically highest strata south of thrust fault T_3 are dominated by a monotonous succession of medium-grained blue-grey to green-grey epidote-bearing wacke and occasional ~ 100 m intervals of dark grey siltstone. Sparse tabular to lensoid bodies of matrix-supported cobble conglomerate contain clasts dominated by limestone, volcanic and felsic intrusive lithologies (Figure 4). Sinwa Formation and the Stuhini Group are probable sources. Granitic clasts may signal exhumation of plutonic roots of the Stuhini arc.

Photo 5. Folded metasediments display a phyllitic sheen at some localities south of Chakluk Mountain. Elsewhere, Laberge Group strata do not display any signs of significant thermal metamorphism.

Strata interpreted as the lowest stratigraphic levels in the hanging wall of thrust fault T_3 are lithologically similar to those in the footwall. Once again, the succession is dominated by ubiquitous blue-grey to green-grey wacke interleaved with intervals of sandstone and siltstone couplets and subordinate cobble conglomerate. The lack of marker horizons hinders estimation of structural repetition. These wacke dominated successions pass into finer grained facies dominated by interbedded argillite and greywacke (1 m thick on average). This sequence is at least 300 m in thickness.

These strata grade upwards into a series of coarsening upwards cycles (Figure 4). They are 25 m in thickness; there are thinly interbedded sandstone and siltstone at the base, with sandstone beds becoming thicker (up to 1-2 m) and more massive towards the top. At least 5 cycles are counted, although the number of cycles varies along strike. Above these cycles, significant intervals of siltstone and sandstone couplets are conspicuous by their absence, as once again the stratigraphy becomes dominated by a monotonous succession of medium-grey to green-grey wacke and rare ~100 m intervals of dark grey siltstone. Fine-grained argillaceous interbeds within the greywacke are commonly rich in woody fragments and plant-detritus.

The uppermost part of the stratigraphy within the Nakina area consists of sets of light grey-tan coloured wacke and sandstones that overlie a silty shale interval (Figure 4). One of these sets (~ 50-100 m) is mainly coarse sandstone and granule conglomerates containing up to 3% vitreous orange garnet (1-5 mm) and sparse, unusually fresh olivine grains. As is typical of other wacke units, a high percentage of the grains are derived from fine to medium grained hornblende-feldspar porphyry. This unit has a magnetic susceptibility of > 20×10^{-3} SI, and consequently shows up as an anomaly on the aeromagnetic map of the Atlin area. This has allowed extrapolation of this unit into areas of poor exposure.

One of the structurally highest units within the Laberge Group may also be one of the stratigraphically youngest. It occurs along the Sloko River below the confluence with the Nakonake (Figure 5). Petrographic analysis of a sample reveals a single grain of very fine-grained dark blue to tan-violet pleochroic crystals that may be blueschist. If correct, this unit may record the influx of Cache Creek detritus in the Whitehorse Trough.

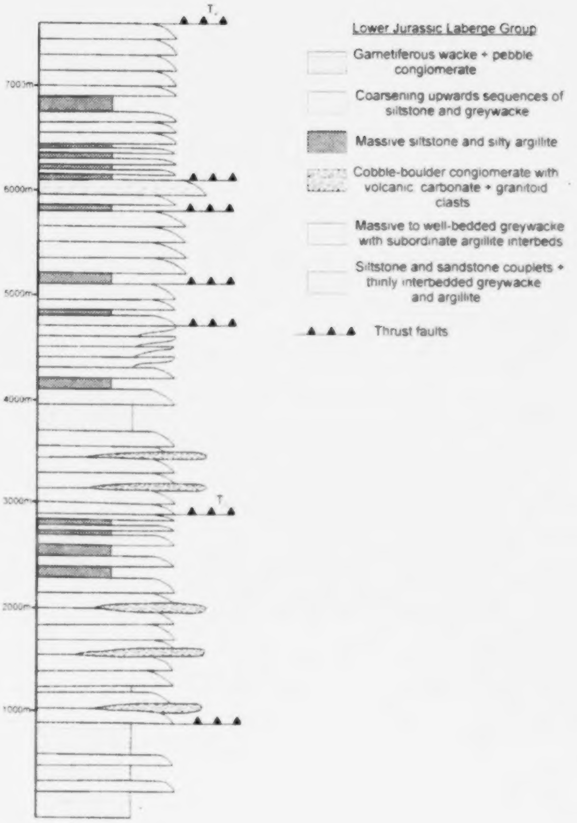
T_4
T_3
7000m
6000m
5000m
4000m
3000m
2000m
1000m
Lower Jurassic Laberge Group
Garnetiferous wacke + pebble conglomerate
Coarsening upwards sequences of siltstone and greywacke
Massive siltstone and silty argillite
Cobble-boulder conglomerate with volcanic carbonate + granitoid clasts
Massive to well-bedded greywacke with subordinate argillite interbeds
Siltstone and sandstone couplets + thinly interbedded greywacke and argillite
Thrust faults

Figure 4. Stylised stratigraphic column for the Nakina area. T_3 and T_4 correspond to thrust faults on Figure 5.

STRUCTURE OF THE LABERGE GROUP

Laberge sediments overlie the Upper Triassic Sinwa Formation (Souther, 1971) or are carried in the hanging wall of the crustal-scale King Salmon Thrust together with the Sinwa Formation, and are thrust over the more proximal facies of the Laberge Group to the south (Takwahoni Formation; Figure 1). Subsidiary thrust faults in the Chakluk and Nakina areas mimic the orientation and vergence of this major structure (Figures 6 and 7 respectively). Average dips of 40°-60° suggest syn-to-post deformational steepening of these thrust faults. Displacement on thrust faults is difficult to constrain due to a lack of marker horizons and age-control.

Laberge Group sediments predominantly dip to the northeast. Locally, bedding does flatten to horizontal or

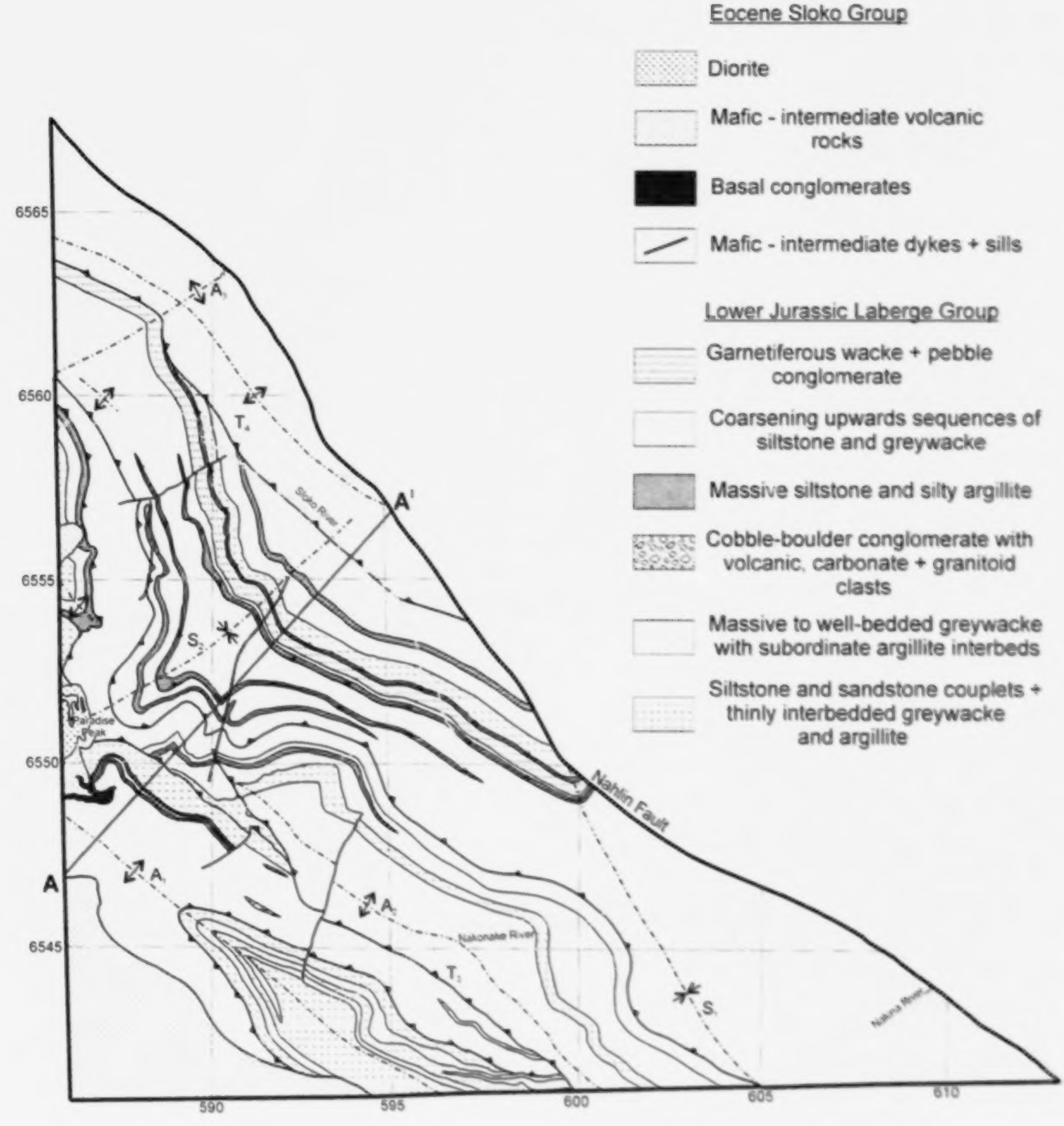
Eocene Sloko Group
Diorite
Mafic - intermediate volcanic rocks
Basal conglomerates
Mafic - intermediate dykes + sills
Lower Jurassic Laberge Group
Garnetiferous wacke + pebble conglomerate
Coarsening upwards sequences of siltstone and greywacke
Massive siltstone and silty argillite
Cobble-boulder conglomerate with volcanic, carbonate + granitoid clasts
Massive to well-bedded greywacke with subordinate argillite interbeds
Siltstone and sandstone couplets + thinly interbedded greywacke and argillite
6565
6560
6555
6550
6545
A
A'
A₁
A₂
A₃
T₁
T₄
S₁
S₂
Sloko River
Paradise Peak
Nakonake River
Nakina River
Nahlin Fault
590
595
600
605
610

Figure 5. Generalised geologic map of the Nakina area, NTS 104N/3 with a 5km UTM grid superimposed.

even SW-dipping, commonly forming the western limb of antiforms interpreted as occurring above hanging wall ramps in underlying thrust faults. Planes of parting dip steeply to the SW.

NW-SETRENDING THRUST FAULTS

Along the Chakluk Transect, the King Salmon Thrust décollement is within or at the base of the Sinwa Formation. Another major thrust fault (T_1) is believed to cause structural repetition of the basal (Sinemurian?) Inklin Formation (Figure 6), although biogeochronological evidence to support this is lacking. Fine-grained intervals both regionally and locally form décollement horizons. One such contorted fine-grained interval is structurally underlain and overlain by coherent wacke-dominated successions (Photo 6). A limestone breccia unit occurs within the fine-grained succession that has been sliced by a multitude of thrust faults, which are interpreted to sole into a single thrust fault (T_2) (Figure 6). Age constraints and regional mapping along strike are required to confirm or refute these structural geometries.

In the Nakina area, strata dominantly strike northwest, except north of the Sloko River where they swing to a westerly orientation (Figure 5). A major thrust (T_3) occurs within the Laberge Group in this region (Figures 5 and 7). T_3 dips steeply to the NE and is associated with a hanging-wall anticline along most of its length within the map-area. A number of subsidiary thrust faults occur in the hanging wall of T_3. These subsidiary thrust faults display bedding-parallel orientations along most of their length, and cumulative structural repetition of stratigraphy is unconstrained. A second major thrust fault (T_4) in the Nakina area is interpreted on the basis of discordant bedding (Figure 7).

Photo 6. Décollement horizon within a fine-grained interval south of Chakluk Mountain. At this locality, a number of thrust faults cut through this sequence of interbedded sandstone and siltstone, while greywacke-dominated succession on either side remain relatively undisturbed.

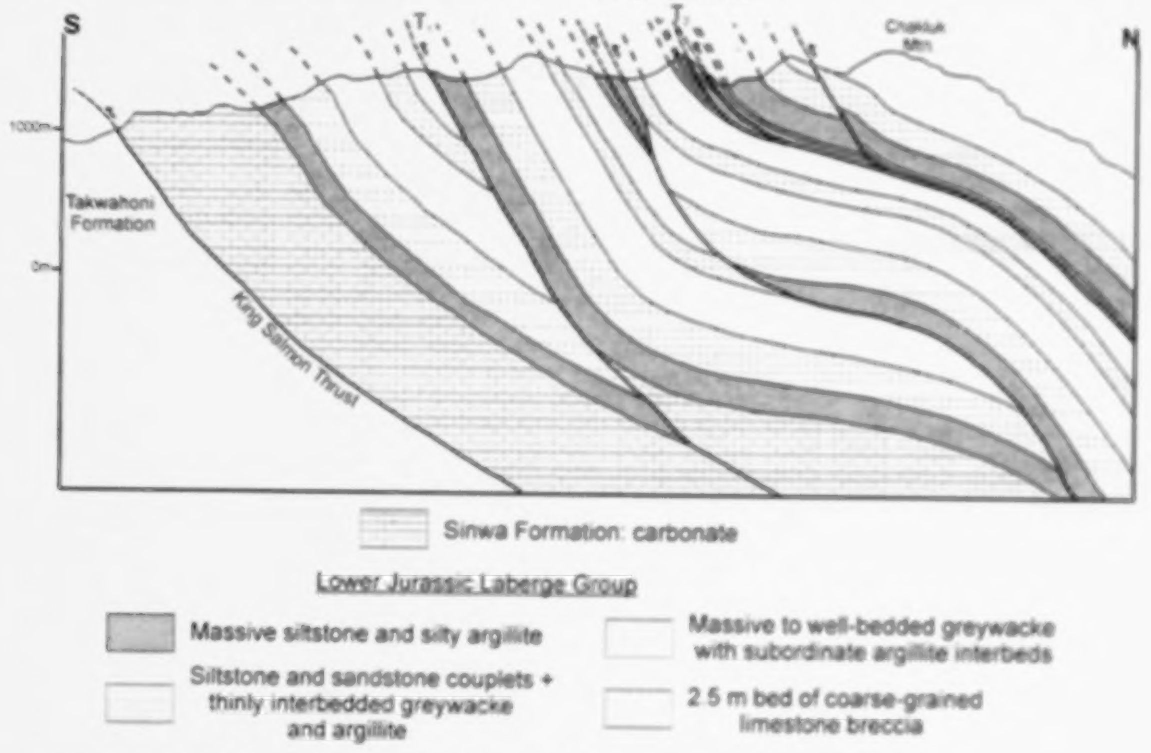
S
N
T_1
T_2
Chakluk Mtn
1000m
0m
Takwahoni Formation
King Salmon Thrust
Sinwa Formation: carbonate
Lower Jurassic Laberge Group
Massive siltstone and silty argillite
Siltstone and sandstone couplets + thinly interbedded greywacke and argillite
Massive to well-bedded greywacke with subordinate argillite interbeds
2.5 m bed of coarse-grained limestone breccia

Figure 6. Composite cross-section of the Chakluk Transect area; *see* Figure 2 for section line.

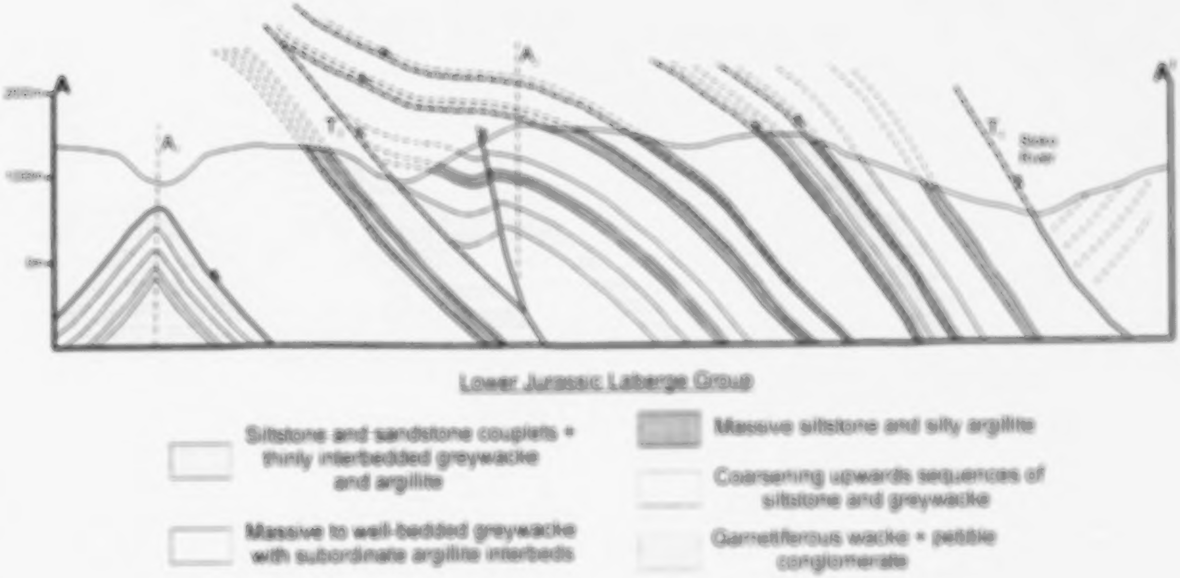
2000m
1000m
0m
A
A'
A₁
A₂
T₂
T₁
Sloko River
Lower Jurassic Laberge Group
Siltstone and sandstone couplets + thinly interbedded greywacke and argillite
Massive to well-bedded greywacke with subordinate argillite interbeds
Massive siltstone and silty argillite
Coarsening upwards sequences of siltstone and greywacke
Garnetiferous wacke + pebble conglomerate

Figure 7. Cross-section of the Nakina area; see Figure 5 for section line.

NW-TRENDING FOLDS

There are a number of NW-trending folds in the Nakina map-area (Figure 5). An open anticline (A_1) in the southwestern corner of the map-sheet plunges gently towards 310°. Another anticline (A_2) is carried in the hanging wall of thrust fault T_2. Subsidiary thrust faults may terminate in the core of these anticlines. Another anticline (A_3) and syncline (S_1) are interpreted in the western portion of the Laberge Group in the Nakina area to explain changes in bedding attitude, although faulted contacts cannot be ruled out due to poor exposure.

NE-TRENDING OPEN FOLDS

NE-trending open folds were also mapped in the Nakina area. The major northeast structure is an open syncline (S_2) that runs through Paradise Peak (Figure 5). NW-trending folds to the north of this syncline plunge ~40° to the south, whereas similar structures to the south plunge in the opposite direction. The orientations of Laberge strata and thrust faults swing from ~ 300° to ~ 330° across this synclinal structure. A broad anticline is tentatively interpreted north of the Sloko River on the basis of a similar swing in the orientation of strata.

LATE BLOCK FAULTS

The structure of the Laberge Group has been modified by Eocene block faults, and dike sill emplacement related to Sloko volcanism. Diking and block faulting is particularly well developed in the Paradise Peak area, and appears to crosscut all folds and thrust faults in the region. Subvertical block faults vary in orientation from NNE to ENE and may be extensional in origin. Dikes related to Sloko volcanism follow similar orientations. Sloko volcanic and intrusive rocks are described in Mihalynuk *et al.* (2003).

THERMAL MATURATION

Thermal maturation can be determined by a number of different techniques including: metamorphic mineral assemblages, colour alteration indices (CAI's), vitrinite reflectance, fission-track dating, cooling ages and programmed pyrolysis. In this report, metamorphic grade and conodont colour alteration indices are utilised to assess the hydrocarbon potential of the northern Cache Creek terrane, while new programmed pyrolysis data is presented for the Laberge Group.

CACHE CREEK TERRANE + REGIONAL CAI DATA

Regional metamorphic grade of the Cache Creek rocks in the Atlin area is prehnite-pumpellyite facies. The level of organic maturation (LOM) corresponding to prehnite-pumpellyite facies metamorphism is generally considered to be above the oil-window (Table 1). Metamorphic grade increases in the aureoles of post-emplacement plutons.

Conodont colour alteration index (CAI) values are also available for the Cache Creek terrane, Sinwa Formation and from clasts of Upper Triassic carbonate within Laberge Group conglomerates (Table 2, Figure 8). The CAI is based on a calibration of the colour change of a conodont element

TABLE 1
COMPARISON OF VARIOUS INDICATORS OF THERMAL MATURITY WITH ZONES OF OIL AND GAS GENERATION

Oil and Gas generation	Tmax	Romax	Conodont CAI's	Metamorphic assemblage
			7	Biotite + Garnet zones
			6	Chlorite zone
			5	
		4	4	Prehnite-Pumpellyite facies
dry gas		~2.5		
generation		1.5	3	
oil +	~465	~1.35		
wet gas		1.1	2	
generation	~430	~0.5		Zeolite facies
		0.40	1	

compiled from Peters (1986), Allen and Allen (1990), and Greenwood *et al.* (1991)

with time. The oil-window lies at CAI values of 1.5-2.8. In the Atlin area, including the Nakina Transect, CAI values are typically in the 5-6 range, corresponding to the chlorite to biotite zone. This apparent discrepancy with observed metamorphic grade (prehnite-pumpellyite) may be due to the comparison of metamorphic grade for different protoliths. These data preclude the preservation of hydrocarbons within the Cache Creek terrane.

CAI values from the Sinwa Formation and from clasts of Sinwa limestone within the Inklin Formation in the Tagish Lake area fall in the range of 5-6. In the Tulsequah region, CAI values from these same lithologies fall in the 2-4 range, and hence may be prospective for hydrocarbon exploration (Figure 8). No data from Laberge Group conglomerates within the Nakina area is available yet, although results from 26 samples are pending.

LABERGE GROUP – NAKINA AND CHAKLUK AREAS

Systematic sample collection for programmed pyrolysis was undertaken in the Chakluk and Nakina Transect areas in order to assess the hydrocarbon potential of the central Whitehorse Trough. Programmed pyrolysis of whole rock using the Rock-Eval VI system provides information on the type, maturity and quantity of associated organic matter (Espitalié *et al.*, 1977). Aliquots of sediment samples were dried and powdered for Rock-Eval TOC analysis at the Geological Survey of Canada Calgary (GSCC). A Vinci Technologies Rock-Eval VI instrument was used. Duplicate analyses of samples were carried out to test reproducibility of data. Each sample of finely ground source rock is put in a furnace at 250°C, raised to 550°C, and then allowed to cool. The hydrocarbons liberated during heating are analysed by a flame ionisation detector, which separates the components into three peaks (Figure 9). The first peak, denoted S_1 (mg $_{HC}$/g $_{rock}$), indicates 'free bitumen' already in the sample. The second peak, denoted S_2 (mg $_{HC}$/g $_{rock}$), results from thermal breakdown of kerogen, while the third peak, S_3 (mg $_{CO2}$/g $_{rock}$), represents the oxygen-bearing compounds released at high temperature. The temperature of the S_2 peak (T_{max}) is an indicator of source rock maturity, although this value is only reliable when $S_2 > 0.2$ (Peters, 1986), and is also affected by organic matter type. ($S_1 + S_2$) gives an indication of source rock richness. Other determined parameters include the Hydrogen Index (S_2/TOC) and the Oxygen Index (S_3/TOC); these parameters are used to determine the type of organic matter present in the potential source rock.

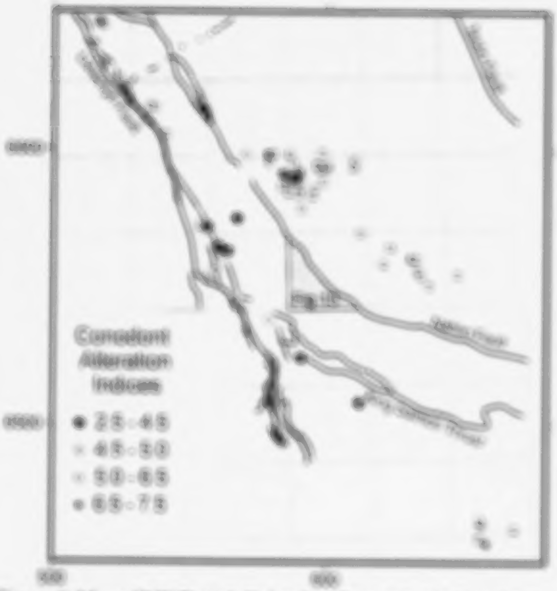

Figure 8. Map of NW British Columbia illustrating the distribution of CAI values. The Whitehorse Trough lies between the Llewellyn Fault/King Salmon Thrust and the Nahlin Fault.

A select sample of the Rock-Eval pyrolysis data is presented in Table 2 (the complete dataset may be obtained at the BCGS website: GeoFile 2003-1; Fowler, 2003). Source

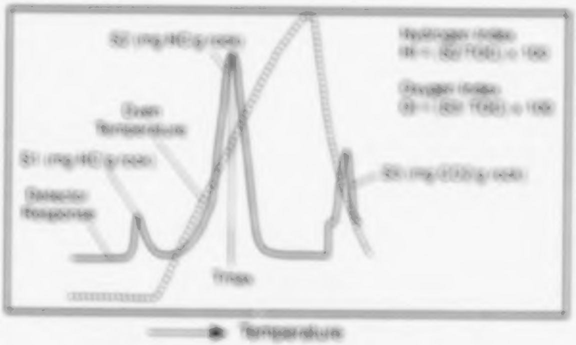

Figure 9. Schematic pyrogram illustrating the liberation of hydrocarbon during heating of the rock sample. Determined parameters include S_1, S_2, S_3, T_{max} and the hydrogen and oxygen indices.

TABLE 3
COMPILATION OF CAI VALUES AVAILABLE FOR
NW BRITISH COLUMBIA

Conodont Alteration Indices					
Sample No.	Rock Unit	Age	CAI	Easting	Northing
[illegible]	Cache Creek Group	Lower Carboniferous: late Visean-Serpukhovian	[illegible]	[illegible]	[illegible]
[illegible]	Cache Creek Group	Upper Carboniferous: Bashkirian-Moscovian	[illegible]	[illegible]	[illegible]
[illegible]	Cache Creek Group	Upper Carboniferous: Bashkirian-Moscovian	[illegible]	[illegible]	[illegible]
[illegible]	[illegible]	Upper Triassic: late Norian [illegible]	[illegible]	[illegible]	[illegible]
[illegible]	Sinwa Formation	[illegible] - Triassic	[illegible]	[illegible]	[illegible]
[illegible]	Sinwa Formation	Upper Triassic: late Norian [illegible]	[illegible]	[illegible]	[illegible]
[illegible]	[illegible]	Upper Triassic: late Norian [illegible]	[illegible]	[illegible]	[illegible]
[illegible]	Cache Creek Group	Permian	[illegible]	[illegible]	[illegible]
[illegible]	Cache Creek Group	Carboniferous-Permian	[illegible]	[illegible]	[illegible]
[illegible]	Cache Creek Group	Upper Carboniferous: Bashkirian-Moscovian	[illegible]	[illegible]	[illegible]
[illegible]	Cache Creek Group	Upper Triassic: late Carnian	[illegible]	[illegible]	[illegible]
[illegible]	Cache Creek Group	probably Permian	[illegible]	[illegible]	[illegible]
[illegible]	Cache Creek Group	[illegible] - Triassic	[illegible]	[illegible]	[illegible]
[illegible]	Cache Creek Group	Permian [illegible] Triassic	[illegible]	[illegible]	[illegible]
[illegible]	Cache Creek Group	[illegible] - Triassic	[illegible]	[illegible]	[illegible]
[illegible]	Cache Creek Group	Permian	[illegible]	[illegible]	[illegible]
[illegible]	Cache Creek Group	Lower Carboniferous: Serpukhovian	[illegible]	[illegible]	[illegible]
[illegible]	Cache Creek Group	Lower Carboniferous: Serpukhovian	[illegible]	[illegible]	[illegible]
[illegible]	Cache Creek Group	Lower Carboniferous: Visean-Serpukhovian	[illegible]	[illegible]	[illegible]
[illegible]	Cache Creek Group	Lower Carboniferous: Serpukhovian	[illegible]	[illegible]	[illegible]
[illegible]	Cache Creek Group	Lower Carboniferous: Visean-Serpukhovian	[illegible]	[illegible]	[illegible]
[illegible]	Cache Creek Group	[illegible] - Triassic	[illegible]	[illegible]	[illegible]
[illegible]	Stuhini Group	Upper Triassic: Carnian	[illegible]	[illegible]	[illegible]
[illegible]	Cache Creek Group	Upper Carboniferous	[illegible]	[illegible]	[illegible]
[illegible]	Cache Creek Group	Upper Carboniferous?	[illegible]	[illegible]	[illegible]
[illegible]	Cache Creek Group	Lower Carboniferous: Serpukhovian	[illegible]	[illegible]	[illegible]
[illegible]	Cache Creek Group	Upper Carboniferous: Bashkirian-Moscovian	[illegible]	[illegible]	[illegible]
[illegible]	Cache Creek Group	Upper Carboniferous: Bashkirian-Moscovian	[illegible]	[illegible]	[illegible]
[illegible]	Cache Creek Group	probably Upper Carboniferous	[illegible]	[illegible]	[illegible]
[illegible]	Cache Creek Group	Permian	[illegible]	[illegible]	[illegible]
[illegible]	Cache Creek Group	Permian	[illegible]	[illegible]	[illegible]
[illegible]	Cache Creek Group	Permian	[illegible]	[illegible]	[illegible]
[illegible]	Cache Creek Group	probably Triassic	[illegible]	[illegible]	[illegible]
[illegible]	Cache Creek Group	Permian	[illegible]	[illegible]	[illegible]
[illegible]	Cache Creek Group	Permian	[illegible]	[illegible]	[illegible]
[illegible]	Cache Creek Group	Upper Triassic: early Norian	[illegible]	[illegible]	[illegible]
[illegible]	Cache Creek Group	Permian - Triassic	[illegible]	[illegible]	[illegible]
[illegible]	Cache Creek Group	probably Triassic	[illegible]	[illegible]	[illegible]
[illegible]	Cache Creek Group	Upper Carboniferous - Lower Permian	[illegible]	[illegible]	[illegible]
[illegible]	Cache Creek Group	Upper Carboniferous - Lower Permian	[illegible]	[illegible]	[illegible]
[illegible]	Cache Creek Group	[illegible] - Triassic	[illegible]	[illegible]	[illegible]
[illegible]	Cache Creek Group	Permian - Lower Triassic	[illegible]	[illegible]	[illegible]
[illegible]	Cache Creek Group	Upper Triassic: early-mid Norian	[illegible]	[illegible]	[illegible]
[illegible]	Cache Creek Group	Permian - [illegible] Triassic	[illegible]	[illegible]	[illegible]
[illegible]	Cache Creek Group	Middle-Upper Triassic	[illegible]	[illegible]	[illegible]
[illegible]	Cache Creek Group	Upper Triassic: late Carnian-early Norian	[illegible]	[illegible]	[illegible]
[illegible]	Cache Creek Group	Upper Carboniferous - Permian	[illegible]	[illegible]	[illegible]
[illegible]	Cache Creek Group	Upper Carboniferous - Permian	[illegible]	[illegible]	[illegible]
[illegible]	Stuhini Group: [illegible] Fm.	Upper Triassic: early Norian	[illegible]	[illegible]	[illegible]

[illegible]

Sample No.	Rock Unit	Age	CAI	Easting	Northing
[illegible]	[illegible]	[illegible]	[illegible]	[illegible]	[illegible]
[illegible]	Sinwa Formation	[illegible]	[illegible]	[illegible]	[illegible]
[illegible]	Sinwa Formation	[illegible]	[illegible]	[illegible]	[illegible]
[illegible]	Sinwa Formation	[illegible]	[illegible]	[illegible]	[illegible]
[illegible]	Sinwa Formation	[illegible]	[illegible]	[illegible]	[illegible]
[illegible]	[illegible]	[illegible]	[illegible]	[illegible]	[illegible]
[illegible]	[illegible]	[illegible]	[illegible]	[illegible]	[illegible]
[illegible]	[illegible]	[illegible]	[illegible]	[illegible]	[illegible]
[illegible]	[illegible]	[illegible]	[illegible]	[illegible]	[illegible]
[illegible]	[illegible]	[illegible]	[illegible]	[illegible]	[illegible]
[illegible]	Cache Creek Group	[illegible]	[illegible]	[illegible]	[illegible]
[illegible]	[illegible]	Triassic	[illegible]	[illegible]	[illegible]
[illegible]	[illegible]	[illegible]	[illegible]	[illegible]	[illegible]
[illegible]	[illegible]	[illegible]	[illegible]	[illegible]	[illegible]
[illegible]	[illegible]	Triassic	[illegible]	[illegible]	[illegible]
[illegible]	[illegible]	[illegible]	[illegible]	[illegible]	[illegible]
[illegible]	[illegible]	Triassic	[illegible]	[illegible]	[illegible]
[illegible]	Sinwa Formation	[illegible]	[illegible]	[illegible]	[illegible]
[illegible]	[illegible]	Upper Triassic	[illegible]	[illegible]	[illegible]
[illegible]	Cache Creek Group	Triassic	[illegible]	[illegible]	[illegible]
[illegible]	Cache Creek Group	[illegible]	[illegible]	[illegible]	[illegible]
[illegible]	Cache Creek Group	[illegible]	[illegible]	[illegible]	[illegible]
[illegible]	Cache Creek Group	Permian	[illegible]	[illegible]	[illegible]
[illegible]	Cache Creek Group	Permian	[illegible]	[illegible]	[illegible]
[illegible]	Cache Creek Group	Triassic	[illegible]	[illegible]	[illegible]
[illegible]	Cache Creek Group	[illegible]	[illegible]	[illegible]	[illegible]
[illegible]	Cache Creek Group	Permian	[illegible]	[illegible]	[illegible]
[illegible]	Cache Creek Group	Triassic	[illegible]	[illegible]	[illegible]

Based on M.J. Orchard's reports of conodont collections at GSC Vancouver

[illegible]

[illegible]

[illegible]

rocks with 0-0.5% total organic carbon (TOC) are considered poor, those with 0.5-1% TOC are fair, those with 1-2% TOC are good and finally those with >2% TOC are considered to be very good (Peters, 1986). Figure 10 shows a plot of TOC versus residual carbon. Most samples are classified as poor to fair source rocks, with 23% classified as good and 9% classified as very good. However, Figure 10 also illustrates that TOC is almost equal to residual carbon in the majority of samples, i.e. there is little generative potential left in these rocks (pyrolysable carbon (PC) is low). Therefore, depending on organic matter type, these samples may have had much higher TOC originally. All samples from the [illegible] have no generative potential remaining.

The organic matter type in a source rock can be determined by plotting Hydrogen Index against the Oxygen Index (Espitalie *et al.*, 1977; Figure 11). Figure 11 suggests that some of the potential source rocks sampled here are oil prone; the majority are inert (low Hydrogen Index) due to the lack of any generative potential, while the rest are gas prone. The lack of generative potential may be due to the high thermal maturity. From a spatial standpoint, samples that are gas prone and have some generative potential left are almost entirely from the northern part of the [illegible] map area. They are also interpreted to be the [illegible] and stratigraphically highest units within the [illegible] Group in the region.

T_{max} can be used as an indicator of thermal maturation as long as $S_2 > 0.2$. Unfortunately, for the majority of samples, the quantities [illegible] on the interpretation of the [illegible] data for maturation purposes. Once again, qualifying samples tend to come from the northern part of the [illegible] map area, and these samples are within the oil and gas window (Table 3; Figure 12). Although T_{max} values of samples with $S_2 < 0.2$ must be viewed cautiously, it can be

[illegible]

[illegible]

[illegible]	[illegible]	[illegible]	[illegible]	[illegible]	[illegible]	[illegible]	[illegible]	[illegible]	[illegible]	[illegible]	[illegible]	[illegible]	[illegible]	[illegible]	[illegible]	[illegible]	[illegible]	[illegible]	[illegible]
[illegible]	[illegible]	[illegible]	[illegible]	[illegible]	[illegible]	[illegible]	[illegible]	[illegible]	[illegible]	[illegible]	[illegible]	[illegible]	[illegible]	[illegible]	[illegible]	[illegible]	[illegible]	[illegible]	[illegible]
[illegible]	[illegible]	[illegible]	[illegible]	[illegible]	[illegible]	[illegible]	[illegible]	[illegible]	[illegible]	[illegible]	[illegible]	[illegible]	[illegible]	[illegible]	[illegible]	[illegible]	[illegible]	[illegible]	[illegible]
[illegible]	[illegible]	[illegible]	[illegible]	[illegible]	[illegible]	[illegible]	[illegible]	[illegible]	[illegible]	[illegible]	[illegible]	[illegible]	[illegible]	[illegible]	[illegible]	[illegible]	[illegible]	[illegible]	[illegible]
[illegible]	[illegible]	[illegible]	[illegible]	[illegible]	[illegible]	[illegible]	[illegible]	[illegible]	[illegible]	[illegible]	[illegible]	[illegible]	[illegible]	[illegible]	[illegible]	[illegible]	[illegible]	[illegible]	[illegible]
[illegible]	[illegible]	[illegible]	[illegible]	[illegible]	[illegible]	[illegible]	[illegible]	[illegible]	[illegible]	[illegible]	[illegible]	[illegible]	[illegible]	[illegible]	[illegible]	[illegible]	[illegible]	[illegible]	[illegible]
[illegible]	[illegible]	[illegible]	[illegible]	[illegible]	[illegible]	[illegible]	[illegible]	[illegible]	[illegible]	[illegible]	[illegible]	[illegible]	[illegible]	[illegible]	[illegible]	[illegible]	[illegible]	[illegible]	[illegible]
[illegible]	[illegible]	[illegible]	[illegible]	[illegible]	[illegible]	[illegible]	[illegible]	[illegible]	[illegible]	[illegible]	[illegible]	[illegible]	[illegible]	[illegible]	[illegible]	[illegible]	[illegible]	[illegible]	[illegible]
[illegible]	[illegible]	[illegible]	[illegible]	[illegible]	[illegible]	[illegible]	[illegible]	[illegible]	[illegible]	[illegible]	[illegible]	[illegible]	[illegible]	[illegible]	[illegible]	[illegible]	[illegible]	[illegible]	[illegible]
[illegible]	[illegible]	[illegible]	[illegible]	[illegible]	[illegible]	[illegible]	[illegible]	[illegible]	[illegible]	[illegible]	[illegible]	[illegible]	[illegible]	[illegible]	[illegible]	[illegible]	[illegible]	[illegible]	[illegible]
[illegible]	[illegible]	[illegible]	[illegible]	[illegible]	[illegible]	[illegible]	[illegible]	[illegible]	[illegible]	[illegible]	[illegible]	[illegible]	[illegible]	[illegible]	[illegible]	[illegible]	[illegible]	[illegible]	[illegible]
[illegible]	[illegible]	[illegible]	[illegible]	[illegible]	[illegible]	[illegible]	[illegible]	[illegible]	[illegible]	[illegible]	[illegible]	[illegible]	[illegible]	[illegible]	[illegible]	[illegible]	[illegible]	[illegible]	[illegible]
[illegible]	[illegible]	[illegible]	[illegible]	[illegible]	[illegible]	[illegible]	[illegible]	[illegible]	[illegible]	[illegible]	[illegible]	[illegible]	[illegible]	[illegible]	[illegible]	[illegible]	[illegible]	[illegible]	[illegible]
[illegible]	[illegible]	[illegible]	[illegible]	[illegible]	[illegible]	[illegible]	[illegible]	[illegible]	[illegible]	[illegible]	[illegible]	[illegible]	[illegible]	[illegible]	[illegible]	[illegible]	[illegible]	[illegible]	[illegible]
[illegible]	[illegible]	[illegible]	[illegible]	[illegible]	[illegible]	[illegible]	[illegible]	[illegible]	[illegible]	[illegible]	[illegible]	[illegible]	[illegible]	[illegible]	[illegible]	[illegible]	[illegible]	[illegible]	[illegible]
[illegible]	[illegible]	[illegible]	[illegible]	[illegible]	[illegible]	[illegible]	[illegible]	[illegible]	[illegible]	[illegible]	[illegible]	[illegible]	[illegible]	[illegible]	[illegible]	[illegible]	[illegible]	[illegible]	[illegible]
[illegible]	[illegible]	[illegible]	[illegible]	[illegible]	[illegible]	[illegible]	[illegible]	[illegible]	[illegible]	[illegible]	[illegible]	[illegible]	[illegible]	[illegible]	[illegible]	[illegible]	[illegible]	[illegible]	[illegible]
[illegible]	[illegible]	[illegible]	[illegible]	[illegible]	[illegible]	[illegible]	[illegible]	[illegible]	[illegible]	[illegible]	[illegible]	[illegible]	[illegible]	[illegible]	[illegible]	[illegible]	[illegible]	[illegible]	[illegible]
[illegible]	[illegible]	[illegible]	[illegible]	[illegible]	[illegible]	[illegible]	[illegible]	[illegible]	[illegible]	[illegible]	[illegible]	[illegible]	[illegible]	[illegible]	[illegible]	[illegible]	[illegible]	[illegible]	[illegible]
[illegible]	[illegible]	[illegible]	[illegible]	[illegible]	[illegible]	[illegible]	[illegible]	[illegible]	[illegible]	[illegible]	[illegible]	[illegible]	[illegible]	[illegible]	[illegible]	[illegible]	[illegible]	[illegible]	[illegible]
[illegible]	[illegible]	[illegible]	[illegible]	[illegible]	[illegible]	[illegible]	[illegible]	[illegible]	[illegible]	[illegible]	[illegible]	[illegible]	[illegible]	[illegible]	[illegible]	[illegible]	[illegible]	[illegible]	[illegible]
[illegible]	[illegible]	[illegible]	[illegible]	[illegible]	[illegible]	[illegible]	[illegible]	[illegible]	[illegible]	[illegible]	[illegible]	[illegible]	[illegible]	[illegible]	[illegible]	[illegible]	[illegible]	[illegible]	[illegible]
[illegible]	[illegible]	[illegible]	[illegible]	[illegible]	[illegible]	[illegible]	[illegible]	[illegible]	[illegible]	[illegible]	[illegible]	[illegible]	[illegible]	[illegible]	[illegible]	[illegible]	[illegible]	[illegible]	[illegible]
[illegible]	[illegible]	[illegible]	[illegible]	[illegible]	[illegible]	[illegible]	[illegible]	[illegible]	[illegible]	[illegible]	[illegible]	[illegible]	[illegible]	[illegible]	[illegible]	[illegible]	[illegible]	[illegible]	[illegible]
[illegible]	[illegible]	[illegible]	[illegible]	[illegible]	[illegible]	[illegible]	[illegible]	[illegible]	[illegible]	[illegible]	[illegible]	[illegible]	[illegible]	[illegible]	[illegible]	[illegible]	[illegible]	[illegible]	[illegible]
[illegible]	[illegible]	[illegible]	[illegible]	[illegible]	[illegible]	[illegible]	[illegible]	[illegible]	[illegible]	[illegible]	[illegible]	[illegible]	[illegible]	[illegible]	[illegible]	[illegible]	[illegible]	[illegible]	[illegible]

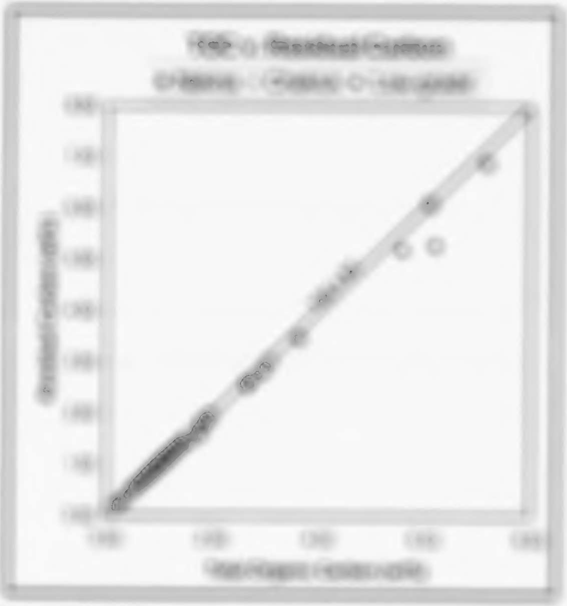

[illegible]

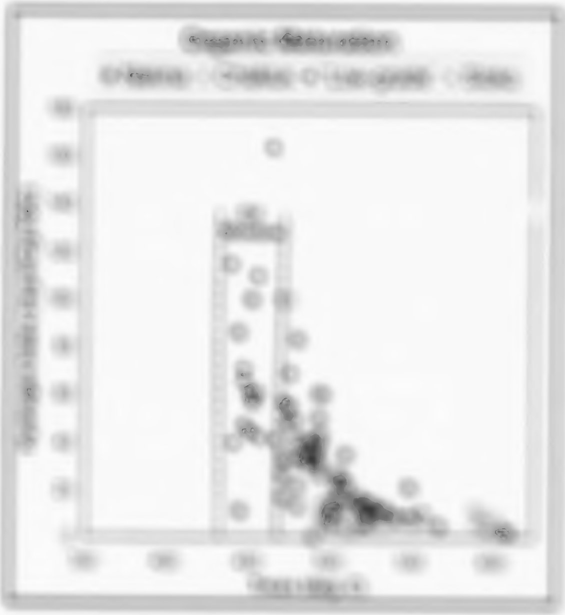

[illegible]

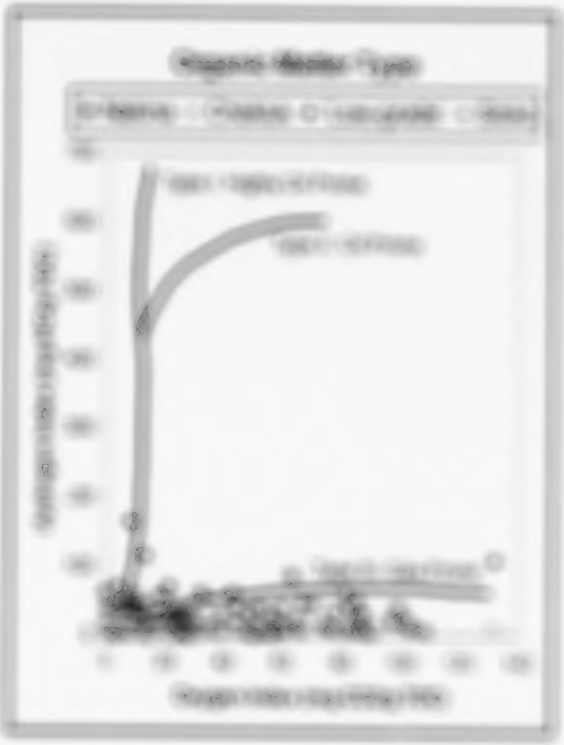

[illegible]

[illegible]

[illegible]

[illegible]

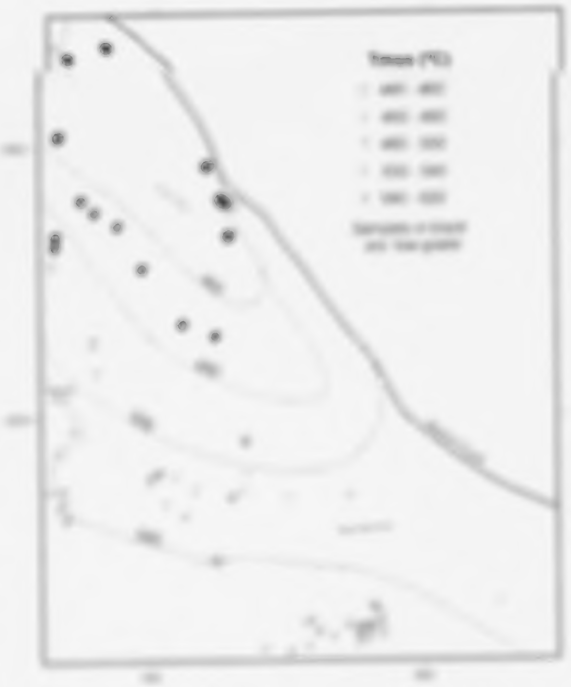

Figure 13. Contoured thermal maturation map for NTS 104N/1 based on T_{max} values. Note: T_{max} values are poorly constrained for relatively 'high-grade' samples due to the low S_2 values.

Structural style within the central Whitehorse Trough is analogous to the Rocky Mountain fold and thrust belt, where structural traps are important for accumulating hydrocarbons. Gas has been generated during basin burial and deformation within the Trough; whether any of this gas is still present remains unknown. A more rigorous assessment of gas potential necessitates constraints on the timing of hydrocarbon generation and also on the timing of burial, heating, and deformation. It is possible that some hydrocarbon generation may have occurred within the oldest strata due solely to sedimentary burial, prior to Middle Jurassic deformation. However, structural burial of sediments during this contractional event likely caused a major pulse of gas generation. The hydrocarbon potential of the central Whitehorse Trough hinges on the persistence of gas traps that may have been filled during its deformational history.

FUTURE WORK

- The thermal maturation of a select group of samples will be investigated using vitrinite reflectance in order to augment maturation data from programmed pyrolysis.
- A number of samples will be submitted for palynological investigation to acquire age constraints on the Laberge stratigraphy in this region. Age constraints are of vital importance in attempting to correlate stratigraphy, as well as in assessing the displacement and geometry of thrust faults, and in interpreting structural burial.
- Additional mapping of the stratigraphy and structure of the Laberge Group in this region is planned. It will help to constrain the geometry of structures, and allow a more efficient assessment of possible traps within the basin.

CONCLUSIONS

The first results of a preliminary hydrocarbon assessment of the BC portion of the Whitehorse Trough and the adjacent Cache Creek terrane are reported here. Cache Creek rocks in the Nakina area are prehnite-pumpellyite grade and have CAI's > 4. This indicates that they are overmature and not prospective for hydrocarbon exploration. Potential source rocks within the Laberge Group in the Nakina and Chakluk areas are gas-prone, although many are overmature and have no remaining generative potential. Mature organic-rich, gas prone source rocks occur in the northern part of the Nakina map-area. A major phase of gas generation probably occurred during structural burial of the Laberge sediments associated with a Middle Jurassic deformational event. The hydrocarbon potential of the central Whitehorse Trough hinges on the preservation of structural and stratigraphic traps that may have been filled at this time.

ACKNOWLEDGEMENTS

Thanks to the remaining members of Team Nakina: Adam Bath, Jacqueline Blackwell, Fabrice Cordey, Oliver Roenitz and Fionnuala Devine, who gave their all and sometimes a little bit more for the cause. Full credit goes to Norm and Larry Graham of Discovery Helicopters in Atlin for ensuring that we lived to see the end of the summer, despite our best/worst efforts! To the rest of the TGI family: Bob Anderson, Carmel Lowe, Lyle Hansen, Margaret Harder, Valerie Cameron, Dante Canil, Kelly Russell, Hiro Sano, Toshio Igawa and Tetsuji Onoue. This paper has benefited from reviews and comments by Brian Grant, Fil Ferri, Mark Hayes and Dave Richardson.

REFERENCES CITED

Allen, P.A. and Allen, J.R. (1990): Basin analysis: principles and applications; Blackwell Science, 451 pages.

Ash, C.H. (1994): Origin and tectonic setting of ophiolitic ultramafic and related rocks in the Atlin area, British Columbia (NTS 104N); B.C. Ministry of Energy, Mines and Petroleum Resources, Bulletin 94, 48 pages.

Childe, F.C. and Thompson, J.F.H. (1997): Geological setting, U-Pb geochronology, and radiogenic isotopic characteristics of the Permo-Triassic Kutcho Assemblage, north-central British Columbia; Canadian Journal of Earth Sciences, Volume 34, pages 1310-1324.

Coney, P.J., Jones, D.L. and Monger, J.W.H. (1980): Cordilleran suspect terranes; Nature, Volume 288, pages 329-333.

Cordey, F., Gordey, S.P. and Orchard, M.J. (1991): New biostratigraphic data from the northern Cache Creek terrane, Teslin map area, southern Yukon; in Current Research, Part E, Geological Survey of Canada, Paper 91-1E, pages 67-76.

Devine, F.A.M. (2002): U-Pb geochronology, geochemistry, and tectonic implications of oceanic rocks in the northern Cache Creek Terrane, Nakina area, northwestern British Columbia;

unpublished B.Sc. thesis, *The University of British Columbia*, 49 pages.

Dickie, J.R. and Hein, F.J. (1995): Conglomeratic submarine fans of the Jurassic Laberge Group, Whitehorse Trough, Yukon Territory: sedimentation and unroofing of a volcanic arc complex; *Sedimentary Geology*, Volume 98, pages 263-292.

English, J.M., Mihalynuk, M.G., Johnston, S.T., and Devine, F.A.M. (2002): Atlin TGI Part III: Geology and petrochemistry of mafic rocks within the northern Cache Creek Terrane and tectonic implications; *in* Geological Fieldwork 2001, *B.C. Ministry of Energy and Mines*, Paper 2002-1, pages 19-30.

Espitalie, J., Madec, M., Tissot, B., Mennig, J.J. and Leplat, P. (1977): Source rock characterization method for petroleum exploration; *Proceedings of the 9th Annual Offshore Technology Conference*, Volume 4, pages 439-448.

Fowler, M. (2003): Rock-Eval VI analysis of samples from the central Whitehorse Trough by the Geological Survey of Canada in partnership with the BC Ministry of Energy and Mines; *BC Ministry of Energy and Mines*, Geofile 2003-1.

Gabrielse, H. (1998): Geology of Cry Lake and Dease Lake map areas, north-central British Columbia; *Geological Survey of Canada*, Bulletin 504, 147 pages.

Gilmore, R.G. (1985): Whitehorse field party, unpublished report, *Petro-Canada*, 16 pages.

Hannigan, P., Lee, P.J. and Osadetz, K.G. (1995): Oil and gas potential of the Bowser - Whitehorse area of British Columbia; unpublished report, *Institute of Sedimentary and Petroleum Geology*, 47 pages plus appendices.

Hart, C.J.R., Dickie, J.R., Ghosh, D.K. and Armstrong, R.L. (1995): Provenance constraints for Whitehorse Trough conglomerate: U-Pb zircon dates and initial Sr ratios of granitic clasts in Jurassic Laberge Group, Yukon Territory; *in* Jurassic magmatism and tectonics of the North American Cordillera, Miller, D.M., and Busby, C., Boulder, Colorado, *Geological Society of America*, Special Paper 299, pages 47-63.

Johannson, G.G., Smith, P.L. and Gordey, S.P. (1997): Early Jurassic evolution of the northern Stikinian arc: evidence from the Laberge Group, northwestern British Columbia; *Canadian Journal of Earth Sciences*, Volume 34, pages 1030-1057.

Lowe, C. and Mihalynuk, M.G. (2002): Overview of the Atlin Integrated Geoscience Project, northwestern British Columbia; *Geological Survey of Canada*, Current Research 2002-A6, 7 pages.

Mihalynuk, M.G. (1999): Geology and mineral resources of the Tagish Lake area (NTS 104M/8, 9, 10E, 15 and 104N/12W) northwestern British Columbia; *B.C. Ministry of Energy, Mines and Petroleum Resources*, Bulletin 105, 217 pages.

Mihalynuk, M.G., Meldrum, D., Sears, W.A. and Johannson, G.G. (1995): Geology of the Stuhini Creek Area (104K/11); *in* Geological Fieldwork 1994, Grant, B., and Newell, J.M., Editors, *B.C. Ministry of Energy, Mines and Petroleum Resources*, Paper 1995-1, pages 321-342.

Mihalynuk, M.G., Erdmer, P., Ghent, E.D., Archibald, D.A., Friedman, R.M., Cordey, F., Johannson, G.G. and Beanish, J. (1999): Age constraints for emplacement of the northern Cache Creek terrane and implications of blueschist metamorphism; *in* Geological Fieldwork 1998, *B.C. Ministry of Energy, Mines and Petroleum Resources*, Paper 1999-1, pages 127-141.

Mihalynuk, M.G., Johnston, S.T., Lowe, C., Cordey, F., English, J.M., Devine, F.A.M., Larson, K. and Merran, Y. (2002): Atlin TGI Part II: Preliminary results from the Atlin Targeted Geoscience Initiative, Nakina Area, Northwest British Columbia; *in* Geological Fieldwork 2001, *B.C. Ministry of Energy and Mines*, Paper 2002-1, pages 5-18.

Mihalynuk, M.G., Johnston, S.T., English, J.M., Cordey, F., Villeneuve, M.E., Rui, L. and Orchard, M.J. (2003): TGI Part II- Regional and economic geology of the Nakina Transect, northwest British Columbia; *in* Geological Fieldwork 2002, *B.C. Ministry of Energy and Mines*, Paper 2003-1, this volume.

Monger, J.W.H. (1975): Upper Paleozoic rocks of the Atlin terrane; *Geological Survey of Canada*, Paper 74-47, 63 pages.

Monger, J.W.H. (1977): Upper Paleozoic rocks of the northwestern British Columbia; *Geological Survey of Canada*, Paper 77-1A, pages 255-262.

Monger, J.W.H., Price, R.A. and Tempelman-Kluit, D.J. (1982): Tectonic accretion and the origin of the two major metamorphic and plutonic welts in the Canadian Cordillera; *Geology*, Volume 10, pages 70-75.

Monger, J.W.H., Wheeler, J.O., Tipper, H.W., Gabrielse, Harms, H. T., Struik, L.C., Campbell, R.B., Dodds, C.J., Gehrels, G.E. and O'Brien, J. (1991): Cordilleran terranes; *in* Geology of the Cordilleran orogen in Canada, Gabrielse, H. and Yorath, C.J. (Editors), *Geological Survey of Canada*, Geology of Canada, Volume 4, pages 281-327.

National Energy Board (2001): Petroleum resource assessment of the Whitehorse Trough, Yukon Territory, Canada; *Yukon Energy Resources Branch*, 50 pages.

Orchard, M.J. (1991): Conodonts, time and terranes: An overview of the biostratigraphic record in the western Canadian Cordillera; *in* Ordovician to Triassic conodont palaeontology of the Canadian Cordillera, Orchard, M.J. and McCracken, A.D., Editors, *Geological Survey of Canada*, Bulletin 417, pages 1-25.

Peters, K.E. (1986): Guidelines for evaluating petroleum source rock using programmed pyrolysis; *The American Association of Petroleum Geologists Bulletin*, Volume 70, pages 318-329.

Greenwood, H.J., Woodsworth, G.J., Read, P.B., Ghent, E.D. and Evenchick, C.A. (1991): Metamorphism; *in* Geology of the Cordilleran Orogen in Canada, Gabrielse, H. and Yorath, C.J. (Editors), *Geological Survey of Canada*, Geology of Canada, Volume 4, pages 533-570.

Souther, J.G. (1971): Geology and mineral deposits of Tulsequah map-area, British Columbia; *Geological Survey of Canada*, Memoir 362, 84 pages.

Tempelman-Kluit, D.J. (1979): Transported cataclasite, ophiolite and granodiorite in Yukon: Evidence of arc-continent collision; *Geological Survey of Canada*, Paper 79-14, 27 pages.

Terry, J. (1977): Geology of the Nahlin ultramafic body, Atlin and Tulsequah map-areas, northwestern British Columbia; *Geological Survey of Canada*, Paper 77-1A, pages 263-266.

Thorstad, L.E., and Gabrielse, H. (1986): The Upper Triassic Kutcho Formation, Cassiar Mountains, north-central British Columbia; *Geological Survey of Canada*, Paper 86-16, 53 pages.

Wheeler, J.O. (1961): Whitehorse map-area, Yukon Territory, (105D); *Geological Survey of Canada*, Memoir 312, 156 pages.

Pseudovitrinite: Possible Implications for Gas Saturation in Coals and Surrounding Rocks

By Barry Ryan
New Ventures Branch

INTRODUCTION

Coal Petrography is for many a black science using terms that are for some not only incomprehensible but also in flux. For utilization purposes, the organic component of coal is generally broken down into reactive and non-reactive macerals, often with little further differentiation of the macerals. The main incentive to differentiate further is the recognition that the degree of reactivity in vitrinite macerals and the degree of non-reactivity in inert macerals, both vary.

In terms of coalbed methane (CBM) studies it is important to consider separately gas generation, adsorption capacities and actual present gas contents (desorbed gas) in terms of the different macerals. Some CBM studies have divided coal into maceral groups that generally have different gas generation and adsorption capacities (Lamberson and Bustin, 1993). A host of environmental, as well as physical, parameters influence actual gas contents and there is no clear evidence that gas contents are strongly influenced by coal petrography (Bustin and Clarkson, 1998). Gurba *et. al.* (2001) have attempted to outline a more subtle maceral control on actual gas content in Permian Australian coals from the Gloucester basin, New South Wales. To date it appears that there is nothing in the form or texture of macerals that provides specific information about adsorption ability, actual gas contents or the environment in which coal macerals generated or retained gas.

This note proposes that a sub maceral of vitrinite called pseudovitrinite may flag changes in coal that influence its adsorptive capacity and maybe also influence its actual gas content. Pseudovitrinite is derived from grey textureless vitrinite (Photo 1) that is used for reflectance measurements and under present classification is referred to as collotelinite. It differs from collotelinite because of the presence of small elliptical slits of different sizes and different orientations (Photo 2). Pseudovitrinite is considered to be an alteration product of collotelinite derived by devolatilization, desiccation or oxidation or a combination of these processes. It is for this reason that it might at least flag changes in the adsorptive capacity of coal.

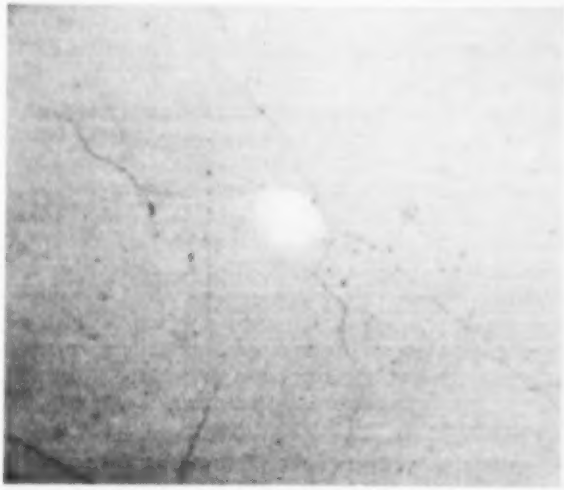

Photo 1. Collotelinte "normal vitrinite" used for rank determinations.

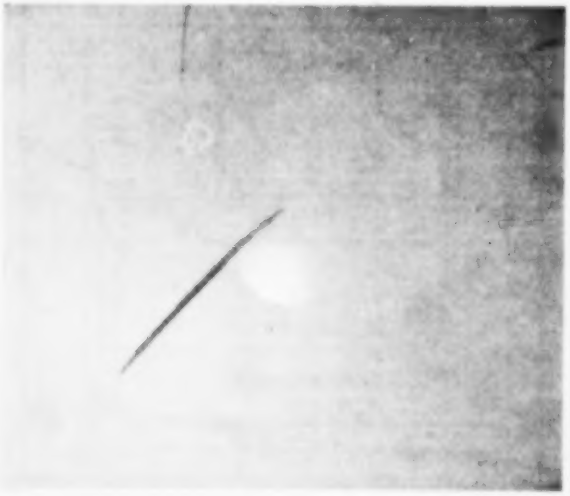

Photo 2. Pseudovitrinite in Comox and Gething Formation coals.

PRESENT VIEWS ON THE ORIGIN OF PSEUDOVITRINITE

The origin of pseudovitrinite has been attributed to early oxidation, forming when vitrinite was still in a gel state (Benedict *et al.* 1968). They considered it to act like an inert maceral during carbonization, but to be a separate sub maceral and different from oxyvitrinite, which forms during weathering of coal seams at surface. Kaegi (1985) considered pseudovitrinite to form insitu after coalification. Hagemann and Wolf (1989) considered it to form early in the maturation of coal and attributed it to gel desiccation and shrinkage. Lamberson (1993) states that none of the above explanations adequately explain the presence of pseudovitrinite in Gates Formation coals in northeastern British Columbia. Her data indicate that the ratio pseudovitrinite/vitrinite increases with the amount of total vitrinite in the samples (Figure 1). This might indicate a relationship between seam permeability and development of pseudovitrinite.

Kaegi (1985) demonstrated that pseudovitrinite formed in a sample heated in air in an oven at 50°C. Obviously this would initially dry the sample so that the production of pseudovitrinite that was seen may in part be caused by desiccation. Unfortunately Kaegi did not repeat the experiment at the same temperature in an inert atmosphere in order to distinguish between the effects of desiccation and oxidation. However his control samples, which were maintained at 23°C in an inert atmosphere, registered small increases in the amount of pseudovitrinite. It is apparent that some pseudovitrinite is formed by desiccation alone and does not require oxidation. Also it can form in vitrinite after coalification.

Pseudovitrinite is different from surface weathering of vitrinite, which produces low reflecting halos and fracturing. Kaegi (1985) suggests that pseudovitrinite becomes oxyvitrinite with progressive oxidation. It is certainly possible for vitrinite to become oxidized without going through the stage of first becoming pseudovitrinite, because there are lots of examples of weathered coals from the Mist Mountain Formation in southeastern British Columbia that do not contain pseudovitrinite.

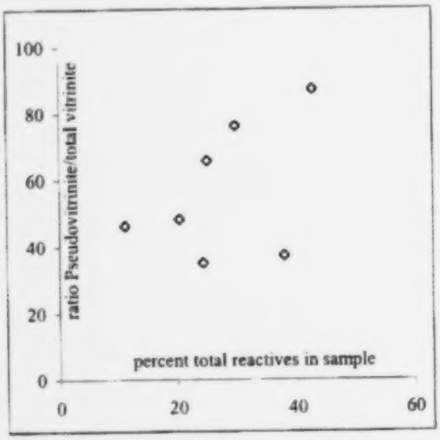

Figure 1. Relationship between amount of pseudovitrinite and total vitrinite in Gates coals from northeastern British Columbia data from Lamberson (1993).

Taylor, *et. al.* (1998) conclude that pseudovitrinite is formed by mild long-term oxidation that can occur at depth in mines especially where coal is in contact with permeable sandstone roofs. They state that pyrite is not present in pseudovitrinite grains because it has been removed by oxidation. This is not always the case for samples from drill holes on Vancouver Island (Photo 3).

Diessel and Gammidge (1998) consider pseudovitrinite to form by drying under relatively shallow overburden. They suggest that coal once dried cannot regain its original moisture on re wetting possibly because of dewatered and collapsed pores. They also noted that in their study of Gates Formation coals and coals collected from the Bowen and Sydney coal basins, pseudovitrinite was only seen in Gates coals.

The reflectance of pseudovitrinite is typically 0.025% higher than that of vitrinite (Stach, *et. al.*, 1982). Small increases in reflectance are also characteristic of low rank coals that have been dried (DeVanney, 2001). High temperature oxidation of coal increases reflectance where as low temperature weathering lowers reflectance. Surface oxidation is usually associated with a decrease in reflectance and some times a swelling of vitrinite grains producing micro fracturing.

DESCRIPTION AND OCCURRENCE OF PSEUDOVITRINITE

Most authors consider pseudovitrinite to be a form of collotelinite characterized by elliptical slits. Other criteria mentioned by Kaegi (1985) include higher reflectance, stepped fracture patterns, higher relief and absence of pyrite inclusions. By far the most obvious characteristic is the presence of elliptical slits and for the purpose of this paper, they are the only criteria used to distinguished pseudovitrinite from collotelinite. In practical terms, when viewing a grain of collotelinite using a reflecting microscope, if a number of slits are present within a small viewing area of about 0.1 mm square, then the grain-count is

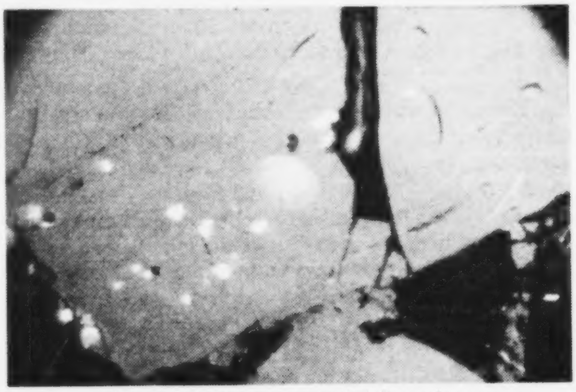

Photo 3. Pyrite in pseudovitrinite grains.

considered to be pseudovitrinite. Slits can be of any size ranging in length up to 2 x10-5 metres long and up to 1 x10-6 metres wide. They are often weakly aligned along one or 2 directions in the grains (Photo 4) and are therefore not always parallel to remnant layering in macerals. The angle between the two orientations appears to be variable. Generally slits do not show evidence of deformation such as s or z shapes. The slits only form in homogeneous macerals and ones that have higher volatile and moisture contents. They are therefore seen mainly in collotelinite and sometimes in collodetrinite but never in the inert macerals such as macrinite.

Samples from Vancouver Island, Gething and Gates formations in northeastern British Columbia and the Tulameen deposit in south central British Columbia were studied using an optical microscope and a Scanning Electron Microscope (SEM) at the University of British Columbia. Under reflected light the slits appear black and it is very difficult to determine if they are mineral filled. However using an SEM and back scattered electron images it is obvious which slits are mineral filled and which are not. In fact in many respects SEM images are the negative of reflecting microscope images. In the former mineral grains are bright and coal dark and in the latter the reverse is true.

Preliminary SEM work indicates that the majority of the slits are filled with minerals (Photo 5). EDS scans allow semi quantative identification of some elements present in minerals. Scans indicated that most of the slits are filled with kaolinite (Figure 2) and some of the larger slits filled with calcite or dolomite (Figure 2). Slits in the high-volatile A coals from the Comox Formation often form 2 directions one parallel compositional layering and one across it. The slits parallel layering are filled with kaolinite and those across layering with carbonate, indicating the possibility of 2 generations of slits. In the low-volatile bituminous Gething Formation coals, slits are generally smaller and are filled mainly with kaolinite. It was difficult to identify any unfilled slits and those that were tentatively identified could be original cell structure and not slits, consequently it appears that of the Gething and Comox samples examined nearly all the slits are mineral filled. Any slit-like structure in collotelinite not parallel to remnant layering almost certainly indicates pseudovitrinite.

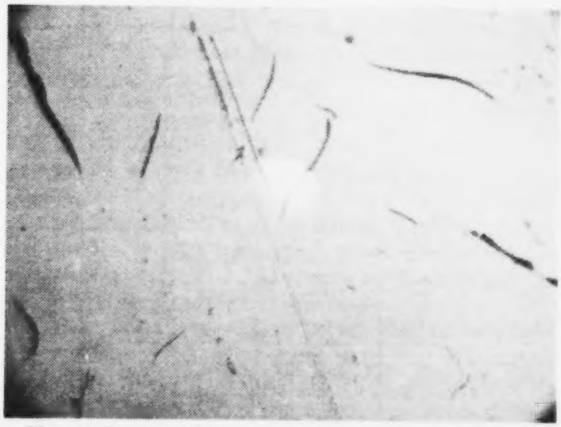
Photo 4. Pseudovitrinite with multiple orientations of slits.

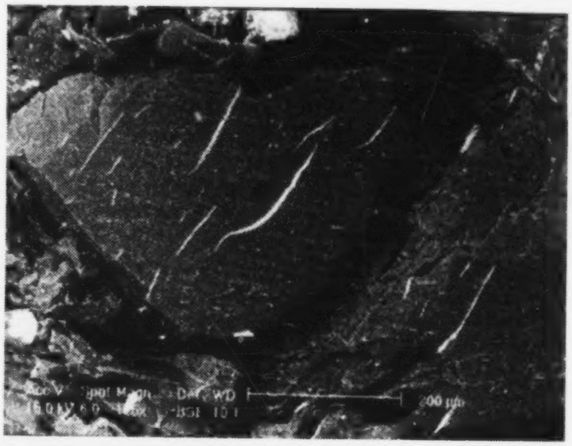
Photo 5. Mineralized slits back scattered electron images scanning electron microscope.

COMMENTS ON THE APPARENT ORIGIN OF PSEUDOVITRINITE

The occurrence of pseudovitrinite in "fresh coal" from mines and open pits in the Gates and Gething formations coals from northeast British Columbia has been documented by many authors (Lamberson, 1993 and Diessel and Gammidge, 1998). Most of the samples in which pseudovitrinite was identified came from near surface exposures either test pits or surface mines. However samples from the Comox Formation discussed in this paper came from drill holes intersecting coal at depths up to 500 metres and though the amount of pseudovitrinite decreases with depth it is still present at a depth of 486 metres (Figure 3). A

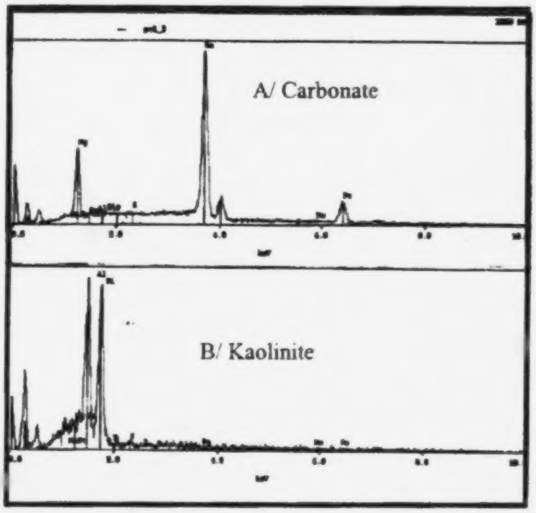

Figure 2. EDS scans of minerals in slits: A/carbonate and B/kaolinte.

similar pattern of decreasing pseudovitrinite with depth is seen in samples of Gething coal collected from a shallow drill hole in northeastern British Columbia (Figure 3). The amount of pseudovitrinite correlates in part with the amount of vitrinite in the sample, which is also seen in the Gates samples from Lamberson (1993). The Comox samples are close to 100% vitrinite macerals on a mineral matter free basis so there is no relationship between the amounts of pseudovitrinite and vitrinite in the samples.

Samples of Gates coals from a number of deep holes were provided to the author by industry. Initial petrography on these samples measured the percentage of pseudovitrinite compared to the total of collotelinite plus pseudovitrinite. Pseudovitrinite is present in samples covering a depth range of 600 to 2000 metres with little relationship to depth. The percent of collotelinite classified as pseudovitrinite varies from 39% to 14% in the samples (Figure 4).

The presence of slits in collotelinite collected from a range of depths indicates that they are not necessarily formed close to surface. Also the presence of mineral filling in slits indicates that they did not form recently and have not formed as a result of bringing the drill core to surface and suddenly relaxing the insitu stress. Spears and Caswell (1986) studied mineralization on cleats. They state that kaolinite forms at temperatures in the range of 55° to 100°C and calcite at around 100°C or at higher temperatures. This would suggest that kaolite is deposited in slits as the coal traverses the ranks sub bituminous to high volatile bituminous and calcite and other carbonates at ranks of high volatile bituminous or higher. Dating the filling of slits does not necessarily date the time of formation of slits with reference to coalification, but it is unlikely that slits would remain open unless mineral filled soon after formation.

Slits do not reveal evidence of excessive deformation, which seems to dispel the idea of early formation. They may form as a result of oxidation or desiccation of vitrinite (Kaegi, 1985) or by devolatilization. In that all coals loose volatile matter as rank increases and not all medium-volatile bituminous coals contain pseudovitrinite it appears that if slits form by devolatilization it is not a normal process. The process could be unusually rapid coalification or rapid degassing of adsorbed gas. The latter possibility is unlikely because un mineralized slits are not ubiquitous in degassed core samples. The former possibility cannot be proved or disproved based on the data at hand.

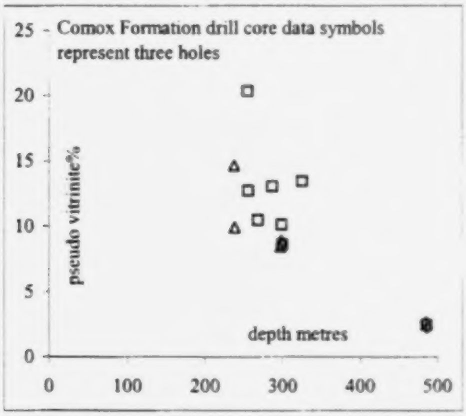

Figure 3. Depth *versus* percent pseudovitrinite for Comox coals and Willow Creek coals.

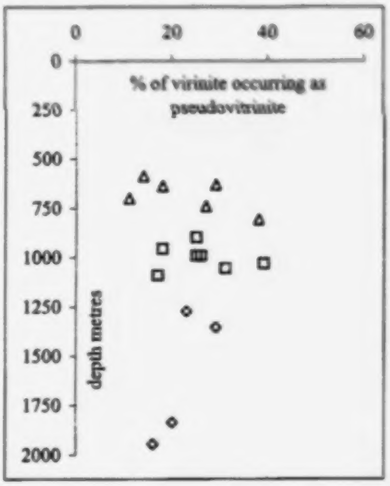

Figure 4. Depth *versus* percent pseudovitrinite in collotelinite Gates Formation coals.

Data indicates or at least leaves open the possibility that slits form at depth after the coal has reached ranks at which it is generating thermogenic methane. It is possible that either or both oxidation and desiccation are operating at depths in excess of 1000 metres in some but not all formations, because pseudovitrinite is much less common in coals from the Mist Mountain Formation in the southeast British Columbia than in coals in the Gates and Gething formations.

Coal is sometimes washed using froth floatation, which uses the difference in hydrophobicity of rock and coal to float the coal. Rock and oxidized coal sink (have high wetability low hydrophobicity) and un oxidized coal floats. In fact vitrinite macerals float better than the inert macerals and studies have shown (Arnold and Aplan, 1988) that pseudovitrinite floats better than vitrinite. This indicates that pseudovitrinite is not an oxidized variety of vitrinite.

Desiccation of coals at depth can only occur if the seam is gas saturated. The ability of gases to retain water varies with the conditions and the gas composition. The solubility of water in CH_4 is generally low and increases as the temperature increases or as the pressure falls. In order to estimate the solubility of water in CH_4 at depth it is necessary to superimpose a geothermal gradient on a solubility plot (McKetta and Wehe, 1958), in this case re plotted using linear scales (Figure 5). It appears that at about 3000 metres one cubic metre of CH_4 can hold about 3 grams of water in solution based on a geothermal gradient of 25°C/Km. The effect of this on coal depends on the volume of gas adjacent to the seam. Figure 6 illustrates the amount of water in solu-

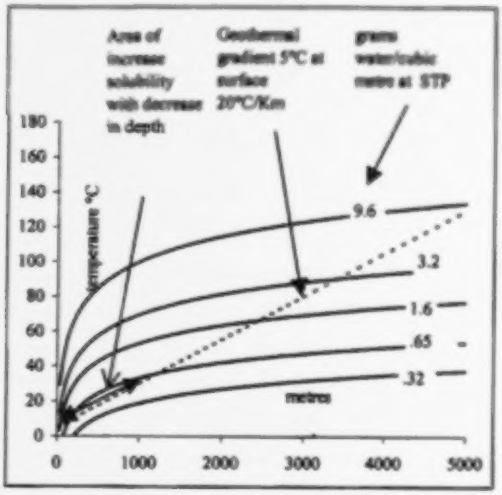

Figure 5. Solubility of water in CH_4 adapted from McKetta and Wehe (1958).

tion in gas pressured into a rock with 5% porosity as hydrostatic pressure increases. The volume of rock was calculated to be the same as the volume of 1 tonne of coal. It therefore appears that at 3000 metres the gas in a porous rock adjacent to the tonne of coal can hold 25 grams of water. In order to have an appreciable drying effect there would have to be at least 10 cubic metres of gas filled porous rock for every cubic metre of coal.

There is also a rule-of- thumb used in the industry that assumes that up to 22 barrels of water can be dissolved in one million cubic feet of gas. This is equivalent to 124 grams per cubic metre, which is more than is indicated by the graphs of McKetta and Wehe (1958). Using this estimate the gas in the 5% porous rock could hold 4.76 kilograms of water at a depth of 3000 metres. It would not take many cubic metres of gas-saturated rock adjacent to a coal seam to hold much of the free water in the seam. The solubility of water in CO_2 is much higher so that if the coal is in contact with a mixture of gases it would be much easier to remove water from the coal.

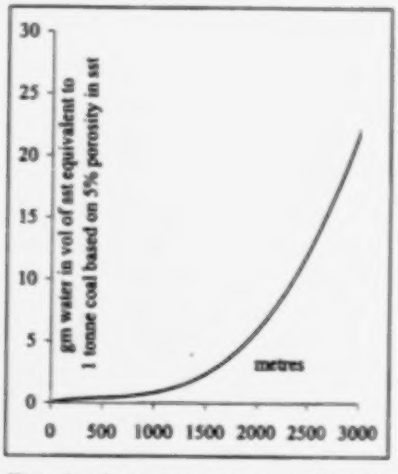

Figure 6. Water in solution in 1 cubic metre of sandstone with 5% porosity.

The ability of gas to hold water in solution does not mean that it has the ability to extract water from the coal because the gas may already be saturated. However when a burial uplift tract constructed assuming a normal geothermal gradient is superimposed on the diagram of McKetta and Wehe (1958), it forms a curve (Figure 7). Traversing along the curve provides values of water solubility in gas during progressive burial or uplift. It is apparent that above a depth of about 1000 metres the ability of gas to hold water starts to increase and below this depth the ability of gas to hold water decreases. The equilibrium moisture content of coal decreases with increasing temperature and therefore depth (Bustin and Clarkson, 1998)(Figure 8) so that at depths of less than 1000 metres, as coal is uplifted, equilibrium moisture value is increasing but the ability of gas to hold water is also increasing. The coal is attempting to regain moisture to reach equilibrium moisture content at the

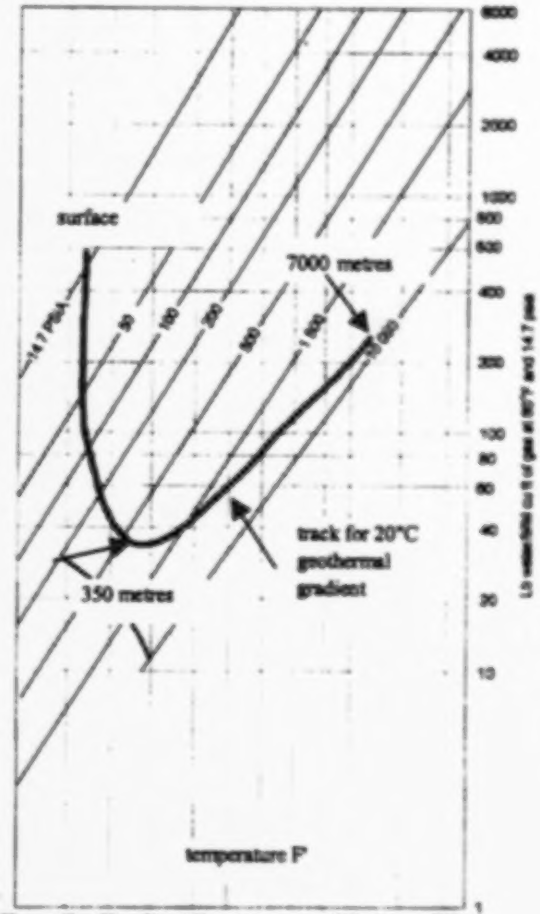

Figure 7. Burial tract superimposed on the solubility curves of Mcetta and Wehe (1958)

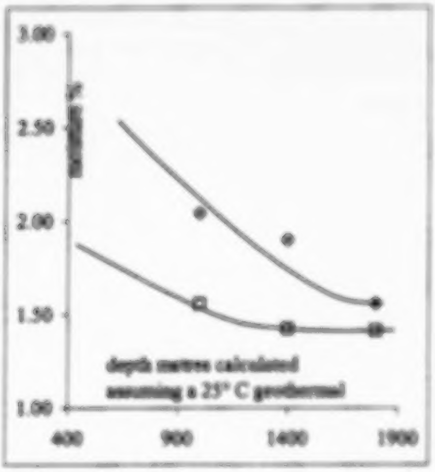

Figure 8. Variation of Equilibrium moisture with depth. Data from Bustin and Clarkson (1998).

same time that the gas has the ability to hold more water in solution. This environment may produce mild desiccation of the coal. Conditions for desiccation are improved if the geothermal gradient is low.

There are provisional arguments that indicate the possibility of drying coal below equilibrium moisture at depths of 1000 metres. Slits were seen in Gates coals at depth greater than this depth so it is certainly not proved that desiccation at depth is the only process forming pseudovitrinite. However there are enough data to indicate the possibility.

RELATIONSHIP OF PSEUDOVITRINITE TO ADSORPTION CAPACITY AND GAS CONTENT

Before discussing the implications of pseudovitrinite on adsorption it is interesting to note that all isotherm analyses are performed on coals that have adsorbed oxygen on exposure to the atmosphere and they may therefore not be the same as isotherms that would be obtained on coal at depth in an oxygen deficient environment.

The presence of pseudovitrinite may indicate desiccation that precedes oxidation and or early stages of oxidation. There are a number of papers that document the effects of oxidation and desiccation on the adsorption characteristics of coal. Ettinger *et. al.* (1967) discusses the effects of mild oxidation on the adsorption and desorption of carbon dioxide and methane. Initial oxidation produces a surface effect that makes it harder for CH_4 to desorb and easier for coal to adsorb CO_2. This might explain the initial release of CO_2 from desorption canisters. The effect may not influence the amount of CH_4 previously adsorbed on the coal but could slow down desorption making it the rate controlling process for production. Clarkson (1992) found that laboratory oxidation slightly decreased adsorption capacity. Vessay (1999) quoting a number of authors states that surface oxidation causes a slight decrease in adsorptive capacity but that laboratory oxidation resulted in an increase in adsorptive capacity. It is possible that high temperature oxidation that occurs in the absence of water is not the same as low temperature oxidation occurring at surface under moist conditions (Huggins *et. al.*, 1983).

The effect of moisture on adsorption was investigated by Joubert *et. al.* (1973) who measured CH_4 adsorption isotherms on a number of coals of different rank and at different moistures ranging from 0% to equilibrium moisture. They considered equilibrium moisture to be independent of pressure though they did not consider the effects of temperature. Bustin and Clarkson (1998) indicate that equilibrium moisture of Permian Australian coals decreases as temperature increases (Figure 8). The best estimate of the effect of natural desiccation of coal is probably obtained by calculating the difference between the equilibrium moisture isotherm and one measured at or about air-dried moisture. This is done for three coals studied by Joubert *et. al.* (1973) (Figure 9, 10). At low to intermediate rank a small amount of

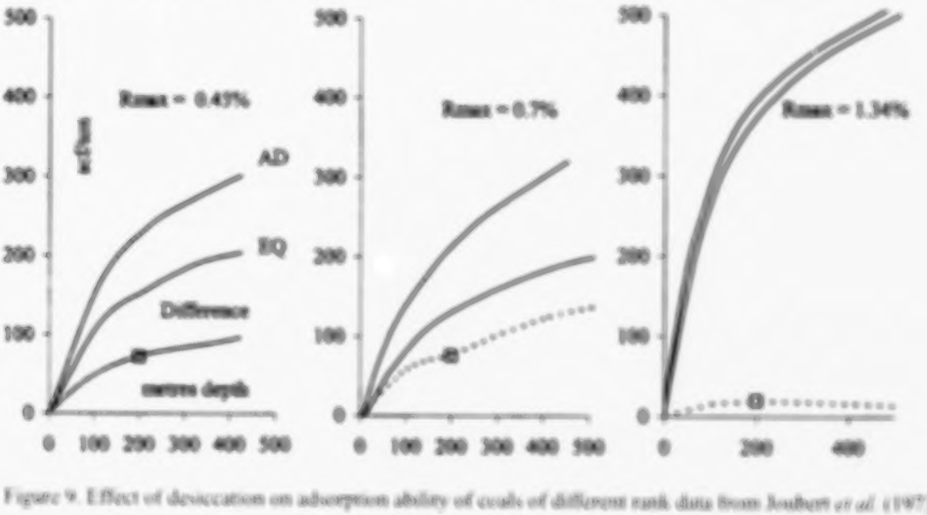

Figure 9. Effect of desiccation on adsorption ability of coals of different rank data from Joubert *et al.* (1973).

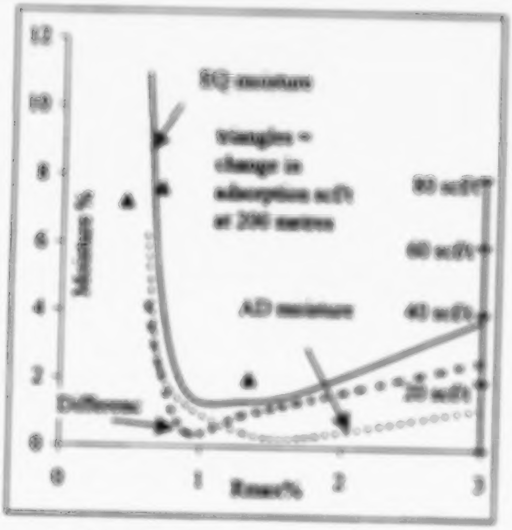

Figure 10. Relationship between the difference equilibrium moisture and air-dried moisture *versus* rank and for the difference in adsorption ability for equilibrium moisture and air dried samples *versus* rank.

desiccation can increase adsorption capacity by up to 100 scf/t at depths less than 500 metres. At medium-volatile ranks the increase is much less. However the difference between equilibrium and air-dried moisture increases again at higher ranks above 1.5 Rmax, which would impact some of the Gething coals in northeast British Columbia.

At constant rank, equilibrium moisture is strongly dependent on vitrinite content. There is insufficient data to attempt to unravel the relationship between vitrinite and pseudovitrinite contents on an ash-free basis and equilibrium moisture available for this study but this is an obvious direction to pursue in the future.

No data have been located that address directly the effect of pseudovitrinite on adsorption. Re interpreting existing data indicates that the presence of pseudovitrinite may improve adsorption of coals, based on using Gething Formation adsorption data (Ryan and Lane, 2002) and re doing the petrography of the samples to estimate the amount of pseudovitrinite present. A tertiary plot of vitrinite pseudovitrinite and inertinite on a mineral matter free basis (Figure 11) indicates a possible increase in Langmuir volumes with increasing pseudovitrinite content. The rank of these coals is high (1.6% Rmax) so a difference in adsorption capacity is possible based on the results from Figures 9 and 10. Obviously these samples were not collected from a gas saturated environment, but when coal is dried below equilibrium moisture the micro porous structure is irreversibly altered and rewetting the coal will not undo the damage and presumably the increase in adsorptive capacity remains.

Unfortunately the paired adsorption isotherms from Comox and Tulameen coals were obtained from coal samples with very similar contents of pseudovitrinite.

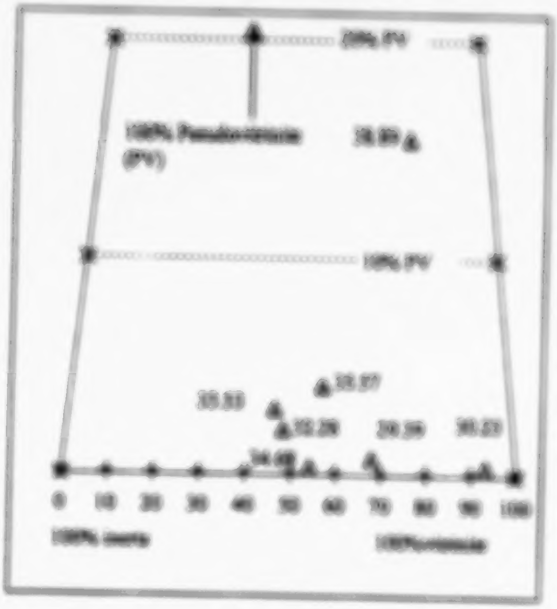

Figure 11. Tertiary plot of vitrinite, pseudovitrinite and inert macerals, indicating adsorption capacity on a dry-ash-free basis.

Desorption data for Comox coals reported previously (Ryan, 2002) exists for samples with varying amounts of pseudovitrinite. It is possible to plot gas contents on a daf basis *versus* percent pseudovitrinite for samples collected from adjacent depths (Figure 12). The samples all have high vitrinite contents on a mineral-matter-free basis, so it

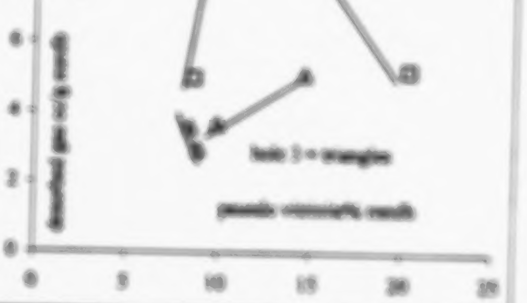

Figure 12. Plot of desorbed gas contents *versus* percent pseudovitrinite content for samples collected from similar depths, Comox Formation.

is not necessary to consider other petrographic variables. Five pairs of data exist. Based on grouping data by depth, of these pairs two have very little change in gas contents and three have significant changes in gas content and pseudovitrinite content. Of these, two show a marked increase in desorbed gas content with increase in pseudovitrinite content and one a decrease. The data is obviously inconclusive but the process demonstrates a way that could prove or disprove a connection between desorbed gas content and amount of pseudovitrinite.

DISCUSSION

In terms of the importance of pseudovitrinite to CBM exploration there are a number of considerations.

Firstly, does pseudovitrinite occur at a depth where one would hope to extract CBM? If it develops during uplift at shallower depths, then its effect on gas adsorption is irrelevant in terms of CBM production. However if it affects adsorption it will cause samples to produce adsorption curves that are not characteristic of their adsorption behaviour at depth. Pseudovitrinite occurs at depths of over 200 metres in Comox Formation coals. In northeast British Columbia pseudovitrinite occurs in the Gething and Gates formations. In the Gething Formation it is documented in a shallow drill hole and in a test pit; in Gates coals it is found in the active mines, some distance below the original topography (Diessel, 1998) and in drill holes to depths of about 2000 metres. Pseudovitrinite is definitely not restricted to shallow coals.

Secondly if pseudovitrinite occurs at depth and affects adsorption then the amount of pseudovitrinite should be considered when interpreting isotherm data. No data are presented that proves a connection between the amount of pseudovitrinite in coal and its adsorption ability or desorbed gas content. However the Gething coal data leave open the possibility. Certainly desiccation increases adsorption ability though the effect is probably a minimum for medium rank coals. There is no direct evidence that pseudovitrinite is in part caused by desiccation but there is circumstantial evidence. Pseudovitrinite does not form exclusively as coal is uplifted close to the present surface because it is present at depth. It must form at depth in which case oxidation seems unlikely.

Thirdly does the environment in which pseudovitrinite forms have implications for the gas potential of the stratigraphic package in which the coal occurs? If it is accepted that pseudovitrinite forms at depth by partial desiccation of coal, then this obviously implies that at some time the coal was in a gas-saturated environment. Coal cannot be under saturated in a gas-saturated environment based on existing pressure and temperature. Also within the volume that is gas saturated there is effectively no pressure gradient and the only thing varying the adsorption capacity is temperature. The presence of pseudovitrinite can be detected from a small sample of coal chips so information about its presence is easy to obtain from drill hole chips. Compiling this type of information may be useful in locating natural gas fields.

If the adsorptive capacity of coal increases with pseudovitrinite content, then the potential desorbed gas content and micro permeability of the coal may also improve. However the coal must be able to scavenge gas. This is obviously possible if pseudovitrinite forms in a gas-saturated environment. The degree of saturation of coal may depend on the depth that the pseudovitrinite formed and the amount of subsequent uplift. If it formed at depths much greater than 2000 metres and the coal was subsequently uplifted, then adsorptive ability may increase markedly leaving the coal under saturated. If on the other hand the pseudovitrinite forms at a depth close to the present depth and in a depth production window for CBM, then the coal should be close to saturated with excellent adsorptive capacity. The coal section may be gas saturated at depth and experience partial desiccation. Later the stratigraphy may become water saturated but the coal will not be able to regain its original equilibrium moisture level nor will the pseudovitrinite revert to normal vitrinite and the coal will retain an improved adsorption capacity.

If development of pseudovitrinite in coals is accompanied by an improvement in adsorption capacity, then this has interesting implications in a dynamic situation of a producing well. In the situation where desiccation or oxidation has not occurred prior to production, but commences during production from a well, any increase in adsorption capacity will hinder production. This could occur because, over a period of months to years, pumping water out of the coal seam may introduce oxygen or cause some drying of the coal seams.

The limited amount of data discussed in this paper does not prove, but does leave open the possibility that the presence of pseudovitrinite may be a useful indicator to consider when analyzing adsorption and desorption data. It may also be of interest to those studying natural gas reservoirs because of the assumed association with gas-saturated stratigraphy.

REFERENCES

Arnold, B.J. and Aplan, F.F. (1989): The hydrophobicity of coal macerals; *Fuel*, Volume 68, pages 651-658.

Benedict, L.G., Thompson, R.R., Shigo, J.J. and Aikman, R.P. (1968): Pseudovitrinite in Appalachian coals; *Fuel*, Volume 47, pages 125-143.

Bustin, R.M. and Clarkson, C.R. (1998): Geological controls on coalbed methane reservoir capacity and gas content; *International Journal of Coal Geology*, Volume 38, pages 3-26.

Bustin, R.M. (2001): Characterizing CBM and gas shale reservoirs for reserves booking: implications for western Canada; Coalbed methane Forum Calgary.

Clarkson, C.R. (1992): Effect of low temperature oxidation on micropore surface area, pore distribution and physical chemical properties of coal; MSc. thesis Geological Sciences, *The University of British Columbia*.

DeVanney, N. (2001): Impact of sample desiccation on the mean maximum vitrinite reflectance for various ranks of coal; TSOP Annual Conference, pages 15-20.

Diessel, C.F.K. and Gammidge, L. (1998): Isometamorphic variations in reflectance and fluorescence of vitrinite – a key to depositional environments; *International Journal of Coal Geology*, Volume 36, pages 167-222.

Ettinger, I., Eremin, I., Zimakov, B. and Yanovskaya, M. (1967): Natural factors influencing coal sorption properties II – gas sorption properties of coals formed in conditions free of coal deposits; *Fuel*, Volume 46, pages 277-282.

Gurba, L.W. and Weber, C.R. (2001): The relevance of coal maceral type to coalbed methane evaluation using the Gloucester Basin, Australia as a Model; International Coalbed Methane Symposium, 2001 Tuscaloosa, Alabama, pages 371-382.

Huggins, F.E., Huffman, G.P. and Lin, M.C. (1983): Observations on low-temperature oxidation of minerals in bituminous coals; *International Journal of Coal Geology*, Volume 3, pages 157-182.

Joubert, J.I., Grein, C.T. and Bienstock, D. (1973): Sorption of methane in moist coal; *Fuel*, Volume 52, pages 181-185.

Kaegi, D.D. (1985): On the identification and origin of Pseudovitrinite; *International Journal of Coal Geology*, Volume 4, pages 309-319.

Lamberson, M.N. and Bustin, R.M. (1993): Coalbed methane characteristics of the Gates Formation coals, northeastern British Columbia: effect of maceral composition; *American Association of Petroleum Geologists*, Bulletin Volume 77, pages 2062-2076.

Lamberson, M.N. (1993): Composition and facies variations in mid-Cretaceous Gates Formation coals, Northeastern British Columbia: implications for interpretation of paleo-environments and assessment of coalbed methane characteristics; Ph.D. thesis, The University of British Columbia, Canada.

[illegible] and [illegible] (1976): Hydrocarbon Processing, page [illegible].

Taylor, G.H., Teichmüller, M., Davis, A., Diessel, C.F.K., Littke, R. and Robert, P. (1998): Organic Petrology; Gebrüder Borntraeger, Berlin, page 198.

Ryan, B.D. and Lane, B. (2002): Adsorption characteristics of coals from the Gething Formation northeast British Columbia; B.C. Ministry of Energy and Mines, Geological Fieldwork 2001, Paper 2002-1, pages 83-98.

Ryan, B.D. (2002): Coalbed methane desorption results of Comox Formation coals from the Courtenay area, Vancouver Island, British Columbia; B.C. Ministry of Energy and Mines, Geological Fieldwork 2001, Paper 2002-1, pages 63-75.

Spears, D.A. and Caswell, S.A. (1986): Mineral matter in coals: Cleat minerals and their origin in some coals from the English Midlands; *International Journal of Coal Geology*, Volume 6, pages 107-125.

Stach, E., Mackowsky, M., Teichmüller, M., Taylor, G.H., Chandra, D. and Teichmüller, R. (1982): Coal Petrography; Gebrüder Borntraeger, Berlin, Stuttgart.

Vessey (1999): Coalbed methane characteristics of Mist Mountain formation southern Canadian Cordillera: Effect of heating and oxidation; MSc. Thesis, The University of British Columbia, Canada.

Overview of the Coalbed Methane Potential of Tertiary Coal Basins in the Interior of British Columbia

By Barry Ryan
New Ventures Branch

INTRODUCTION

[illegible]

[illegible]

[illegible]

[illegible]

[illegible]

UNIQUE CHARACTERISTICS OF TERTIARY BASINS

[illegible]

[illegible]

TABLE 1
STRATIGRAPHY OF TERTIARY BASINS IN BRITISH COLUMBIA THAT CONTAIN COAL

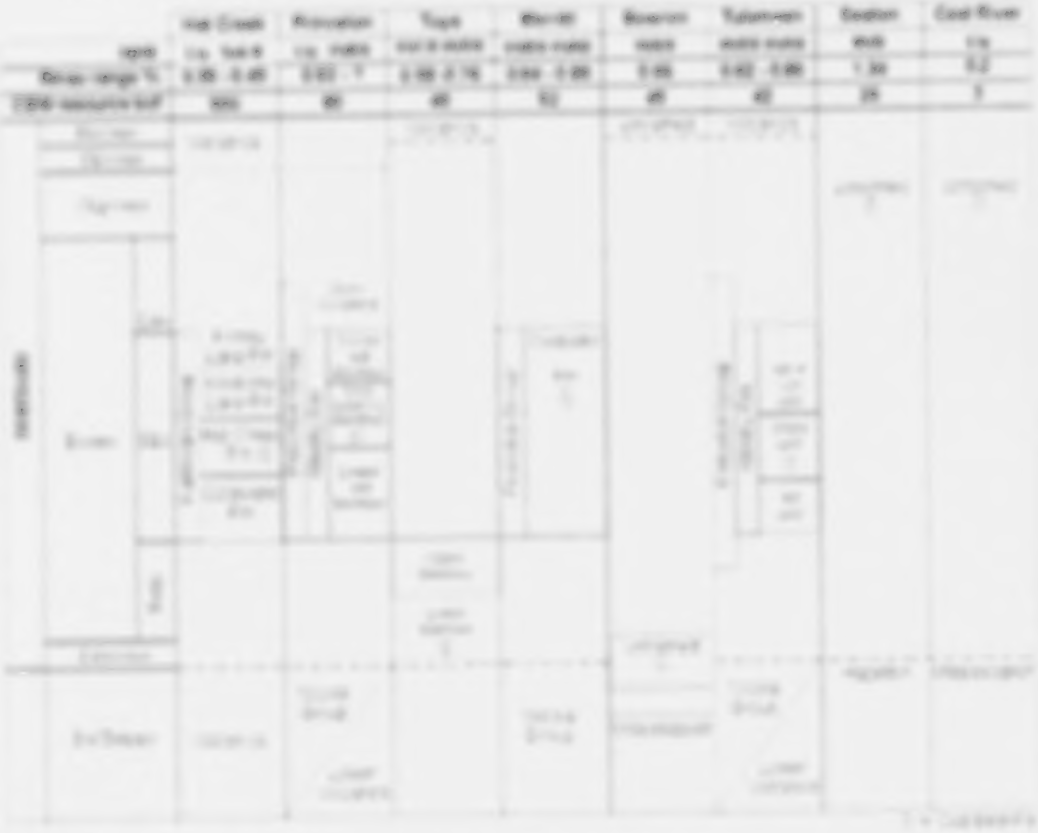

which because of Eocene volcanism may have been high. Coal rank is therefore dependent on depth and not position in folds. The high heat flow in some basins probably resulted in a coalification gradient characterized by high temperature and low pressure, very different from that experienced by Cretaceous coals in the Rocky Mountains.

One could speculate that coals that attain their rank in an environment dominated more by temperature and less by pressure may have a more micro porous structure than coals that attain the same rank in an environment dominated more by pressure. The result may be that Tertiary coals, on an equivalent rank basis, may have higher adsorption abilities than other coals. To some extent this might be a circular argument because the higher adsorption would be reflected in a lower moisture content, which in turn would give the appearance of a higher rank. Also rank is estimated using different parameters and one persons rank estimated using calorific value or carbon content (dry ash-free basis) may not be the same as another person's rank estimated using vitrinite reflectance.

Tertiary coals are generally of low rank often well cleated (Ryan, 2002) and are contained in immature sediments, consequently in some situations the coals will be harder than the surrounding lithologies. They should have and maintain good permeability even at considerable depth. Thicker coal seams should respond well to fracing as long as they are deep enough. If the surrounding sediments are poorly consolidated or bentonite rich they may not propagate fractures and remain as aquatards. Some coal zones may respond well to cavitation as long as enclosing sediments are consolidated.

Generally Tertiary basins influenced by Eocene volcanic activity have high geothermal gradients. Coal rank in some basins may increase rapidly with depth and vary along strike because of high and variable geothermal gradients in the basins. The general low rank of Tertiary coals will limit adsorption capacity. Also the present geothermal gradient may be high and this will have the effect of decreasing the adsorptive capacity of coals at depth as temperatures increase.

Sediments in most Tertiary basins are non-marine (Graham, 1990) with no marine association one can expect formation water to be non-saline. Basin shapes, combined with impermeable sediment layers such as bentonite bands, may be ideal to restrict water movement through the sediments allowing accumulation of biogenic methane. Some of the basins are in the form of major synclines with limbs tending to outcrop on the sides of valleys making for ideal artesian over pressured environments in the cores of the basins. Bentonite layers may respond to dewatering by swelling and therefore help to inhibit water movement across the stratigraphy.

The presence of basement volcanic rocks may effect the gas composition, providing sources for thermogenic carbon dioxide (CO_2) and nitrogen (N_2). Carbon dioxide is generated at low rank during coal maturation and may still be present in the stratigraphic section. The low rank and poor compaction of the sediment pile may allow easy migration of gases from the basement.

Coals of sub-bituminous to high-volatile bituminous rank have not generated much thermogenic methane. Meissner (1984) states that thermogenic methane generation starts when the volatile matter (dry, ash-free basis) is less than 37.8 %, equivalent to a rank of high-volatile A bituminous or a mean maximum reflectance of vitrinite (Rmax% value) of 0.73%. Dow (1977) suggests that thermogenic methane generation starts at a Rmax value of 1.0% however Snowden and Powell (1982) suggest that oil and condensates can be generated from coals rich in resinite at Rmax% values in the range 0.4% to 0.6%. Some of the Tertiary basins such as Hat Creek, Tuya and Bowron contain significant amounts of amber a form of resinite.

Tertiary coals in British Columbia generally have higher vitrinite contents than Cretaceous coals in the province. This probably indicates an absence of paleofires that characterized the Early Cretaceous (Lamberson, 1991). Also in part because of low rank, they contain more liptinite. Based upon these petrographic characteristics Tertiary coals should generate thermogenic methane at lower temperatures and have better adsorption characteristics at equivalent ranks compared to Cretaceous coals in British Columbia.

COAL RANK DETERMINATIONS

For some of the basins, rank determinations in the form of vitrinite reflectances either as mean maximum (Rmax) or as mean random (Rrand) are available. For low rank coals the difference between Rmax and Rrand is minimal but for higher rank coals Rmax is distinctly higher than Rrand and an empirical correction should be applied before comparing data sets. Grieve (1993) uses Rmax=1.0809*Rrand - 0.0306 and Diessel (1998) uses Rmax=1.07*Rrand - 0.01. In some basins the only data available are old proximate analyses. It is possible to estimate rank from volatile matter corrected to an ash-free basis (VM daf). Meissner (1984) uses a series of equations to cover the range of VM daf and Rmax data. Before using this approach to estimate rank it is important to remove the effects of ash from the VM daf value and to consider the effect of petrography on the VM daf value. A true VM daf value is obtained by plotting VM daf values versus ash and projecting to zero ash to obtain VM daf(zero ash). This removes the contribution of volatile matter by ash to the VM daf value. Vitrinite contains more volatile matter than inert macerals and this has to be considered when using VM daf data to estimate Rmax values. A limited data set of VM daf and petrography data was used to derive the equation

Rmax=-1.2124*ln(VM daf)-0.00731*R%+4.4851

Where R is percent vitrinite on a mineral matter free basis and VM daf is volatile matter dry ash-free derived from a plot of data and projected to zero ash.

Using this approach it is possible to derive approximate rank determinations for a lot of the basins and to determine if rank increases with depth. In the future an extended database will be used to improve the equation.

FRACTURE POROSITY

Low rank coals have limited ability to adsorb gas so that the free gas may be a major percent of the total gas recovered. It is difficult to estimate fracture porosity in coals but it is possible to estimate it using bulk washability data (Ryan and Takkinen, 1999). Washability data may be available if there has been active mining in an area and the data can be useful for CBM studies. It is possible to derive some information on fracture porosity by careful inspection of the different sizes washed and the average ash in each SG split of the wash matrix. For larger size consists the ash concentration of material in each SG split is higher than for smaller size consists. This is because there is greater fracture porosity associated with the larger coal fragments. The porosity is estimated by converting ash concentration to average density. The density equation in Ryan and Takkinen (1999) can then be used to predict the porosity in the larger size consist.

HAT CREEK

GENERAL

The Hat Creek area is about 20 kilometers west of Cache Creek. G.M. Dawson of the Geological Survey of Canada first reported coal in the area in 1877. There was some drilling and development of coal outcrops along Hat Creek in the early 1900,s and from 1933 to 1945 a few hundred tonnes of coal were mined. In 1959 the property was purchased for 2 million dollars by the for-runner of BC Hydro as a potential source of coal for a coal fired power plant. There was not much exploration on the property till 1974, when BC Hydro initiated a series of major exploration and engineering projects.

GEOLOGY

Middle Eocene rocks of the Coldwater Group are preserved between 2 north trending faults that define a graben about 6 kilometres wide and 25 kilometres long (Figure 2). The Group is subdivided into three members a lower member 1400 metres thick is composed of coarse-grained sediments and is overlain by a member composed of fine-grained sediments and coal. This member, which is 1,200 metres thick, contains up to 550 metres of intermixed coal (70%) and rock partings (30%). An upper unit 600 metres thick is composed of fine-grained sediments and contains no coal. Two coal deposits referred to as the Number 1 and Number 2 deposits have been explored within the graben. A major negative gravity anomaly (Figure 2) over-

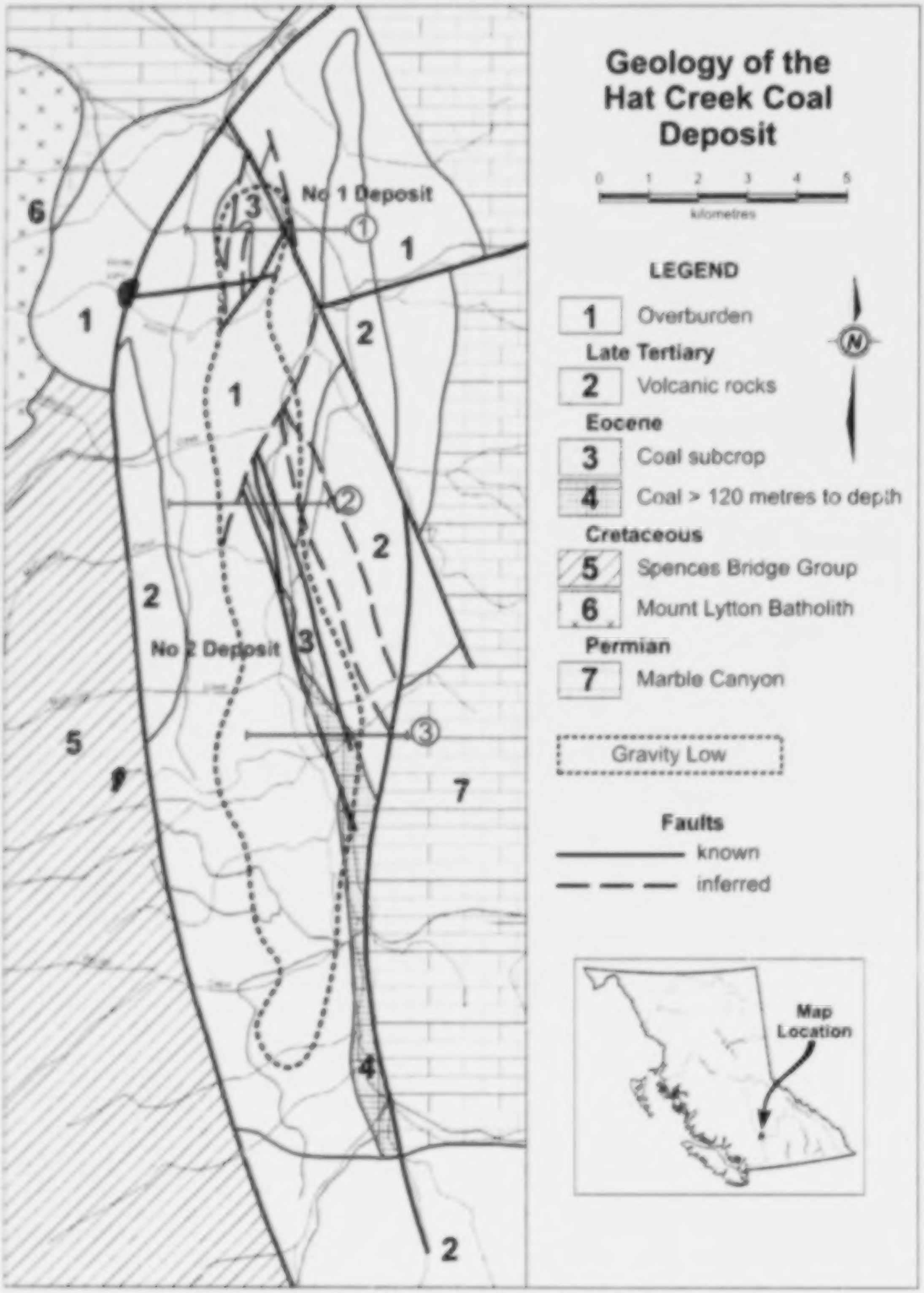
Geology of the Hat Creek Coal Deposit
0
1
2
3
4
5
kilometres
LEGEND
1 Overburden
Late Tertiary
2 Volcanic rocks
Eocene
3 Coal subcrop
4 Coal > 120 metres to depth
Cretaceous
5 Spences Bridge Group
6 Mount Lytton Batholith
Permian
7 Marble Canyon
Gravity Low
Faults
known
inferred
N
Map Location
No 1 Deposit
No 2 Deposit
①
②
③
1
2
3
4
5
6
7

Figure 2. General Geology of the Hat Creek deposit adapted from Church (1975).

lies both deposits and extends south of the Number 2 deposit (Church, 1975).

The northern Number 1 deposit was extensively explored because of its low strip ratio and potential as an open pit mine. 474 holes were drilled into the deposit, which contains lignite A to sub bituminous C coal. The deposit comprises two synclines plunging 15° - 17° south-southwest separated by an anticline. The synclines are truncated on the southeast end by northeast trending gravity faults (Graham 1989) (Figure 3). The folds are truncated in the south by a fault and in places beds are steepened or overturned by reverse faults.

The second and potentially larger Number 2 deposit is 10 kilometres south of the Number 1 deposit. It has experienced less exploration and only 64 holes have been drilled to date. Most of these holes failed to penetrate the full thickness of the deposit. The deposit occurs within a graben bounded on the east and west by north-trending normal faults. Displacements on the western faults appear to be more than on the eastern faults causing a rotation and a 25° western dip of the sediments. The deposit appears to be folded into a broad anticline, which trends north and is dis-

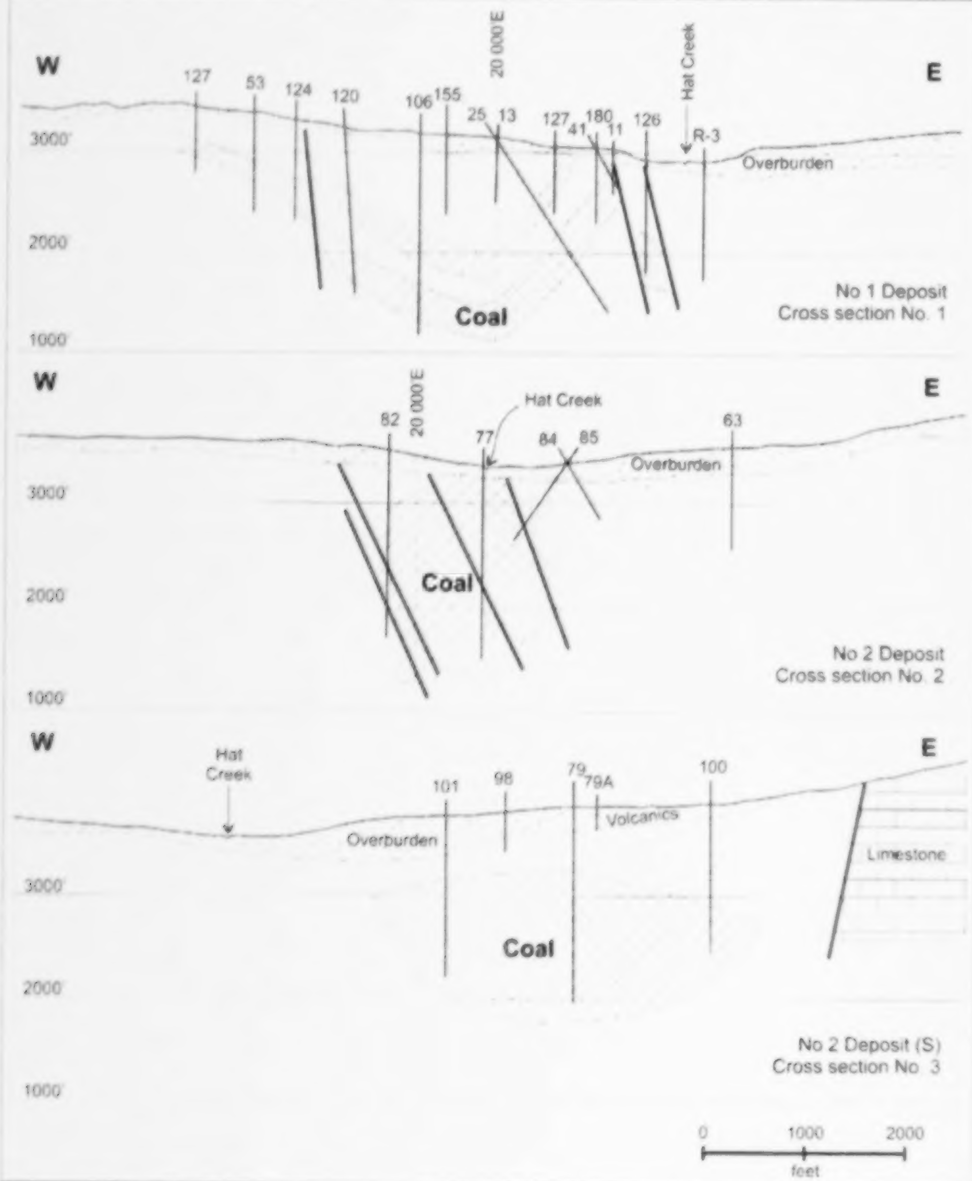
W
E
20 000'E
Hat Creek
127
53
124
120
106
155
25
13
127
41
180
11
126
R-3
3000'
2000'
1000'
Overburden
Coal
No 1 Deposit
Cross section No. 1
W
E
20 000'E
Hat Creek
82
77
84
85
63
Overburden
Coal
3000'
2000'
1000'
No 2 Deposit
Cross section No. 2
W
E
Hat Creek
101
98
79
79A
100
Volcanics
Overburden
Limestone
Coal
3000'
2000'
1000'
No 2 Deposit (S)
Cross section No. 3
0
1000
2000
feet

Figure 3. Schematic cross sections of the Number 1 and 2 deposits, Hat Creek; from Campbell *et. al.* (1977).

rupted by faulting on its eastern edge. The deposit is divided into 4 coal units numbered from A at the top to D at the bottom; thicknesses are respectively 185, 100, 150 and 80 metres (Goodarzi and Gentzis, 1987) though they may well be minimum as it is not clear if any holes drilled the complete coal section. Coal unit D is described as consisting almost entirely of coal.

COAL RANK

Coal at Hat Creek is composed of almost 100% vitrinite macerals (Goodarzi and Gentzis, 1987). Rank of the Number 1 deposit varies from a random reflectance (Rrand%) of 0.38% to 0.5% over a depth of 600 metres (Goodarzi, 1985), which indicates a rank gradient of about 0.06%/100 metres. At these ranks the difference between random reflectance and mean maximum reflectance is minimal. This gradient is similar to those in southeast BC (Hacquebard and Cameron 1989) and at Seaton and is not noticeably compressed. The rank of the larger Number 2 deposit (Figures 4 and 5) is slightly lower than that of the number 1 deposit and varies from 0.35% to 0.45% over a depth of 500 metres (Goodarzi and Gentzis, 1987). There is no clear trend of increasing rank with depth.

COAL RESOURCE

Estimates of the mineable reserves in the Number 1 deposit range from 200 to 750 million tonnes (mt). Kim (1979) estimates a reserve of 740 million tonnes. Of this total, over 500 mt are within of 200 metres of the surface. The resource of the No 2 deposit to a depth of 460 metres is estimated to be over 2 billion tonnes (Papic, *et. al.*, 1977).

The potential resource in the whole graben is estimated at over 10 billion tonnes by Campbell *et al.*, (1977) and in the two known pit areas to be 10 billion tonnes (7 in pit 2 and 3 in pit 1, Papic, *et al.*, 1977). Church (1975) refers to gravity data that indicates that 3000 hectares (30 square kilometers or 11.6 square miles) of the central part of the graben may be underlain by coal. Depending on the thickness of coal assumed, the potential resource could easily exceed 10 billion tonnes

CBM RESOURCE

CBM in Hat Creek coals will be of biogenic origin because of the low rank. Based on experience in the Powder River Basin where coal ranks and ash contents are lower, it is unlikely that adsorbed gas contents will exceed 2 cc/g even at depth. Gas contents in the Powder River Basin range from 0.1 to 1 cc/g (Larsen, 1989) for coal with ranks ranging from 0.28% to 0.4%, which are a little lower than those at Hat Creek. Adsorption characteristics are very variable for low rank coals and appear to increase rapidly with small increases in rank as seen in Figure 6, which includes an isotherm from a coal of rank 0.67%. Figure 6 also illustrates the effect of a 5% gas filled porosity on the total gas available for production. The adsorption of Hat Creek coal should be somewhat better than that of Powder River on an ash free basis though generally Hat Creek coal contains more ash than Powder River coals. In the absence of any adsorption or desorption data, estimates of the CBM resource are made using 1 cc/g and 2 cc/g (30-70 scf/ton) applied to the resource estimate of pit 2 which is 7 billion tonnes. This provides a potential resource in the range of 0.2 tcf to 0.65 tcf.

The possible anticline structure of the Number 2 deposit in conjunction with the many bentonite layers may form ideal traps for adsorbed or free gas. The bentonite layers may make it possible to produce CBM from different stratigraphies in the deposit at different times. If this is the case, water extracted from one layer could be injected into a layer, which had already been depleted of CBM by production. This would mean that after an initial period of production, produced water could be re injected with minimal disruption of production. It is also conceivable that if a surface power plant were constructed that CBM produced water could be used as cooling water in the plant. Final costs of water disposal would be shared by both developments.

There are some data on ground water composition from the Number 1 deposit. BC Hydro conducted an Environmental Impact Study in 1978 (Beak Consultants, 1978) in which there are some analyses of water from holes drilled into the Number 1 deposit (Table 2). The drill hole water meets the standards for toxic chemicals required by Canadian standards for drinking water and for cations only exceeds the limits for sodium. It is apparent that the water would need very little treatment before surface discharge.

COMPARISON OF HAT CREEK TO POWDER RIVER BASIN

Ranks of coals in the Powder River range from 0.28% to 0.4% (Pratt *et al*, 1997) and are similar to, though slightly lower than ranks at Hat Creek. Desorbed gas contents are 0.6 to 0.7 cc/g (20-25 scf/ton) at depths of 175-200 metres. Both Hat Creek and Powder River coals are vitrinite rich

TABLE 2
PERMEABILITY DATA HAT CREEK NUMBER 1 DEPOSIT

Lith Unit	No of tests	milli Darcies	
		low	high
Upper Siltstone	13	0.0001	3
A zone siltstone and coal	6	0.001	0.03
B zone coal	3	20	50
C zone siltstone and coal	13	0.003	3
D zone coal	12	0.6	100
Lower Siltstone sandstone	15	0.0002	0.5
Conglomerate	4	0.0095	0.3
Limestone	7	0.12	10 000

The B and D coal zones may have reasonable permeability

Data from Hat Creek Mining report, Volume 1, 1979 BC Hydro

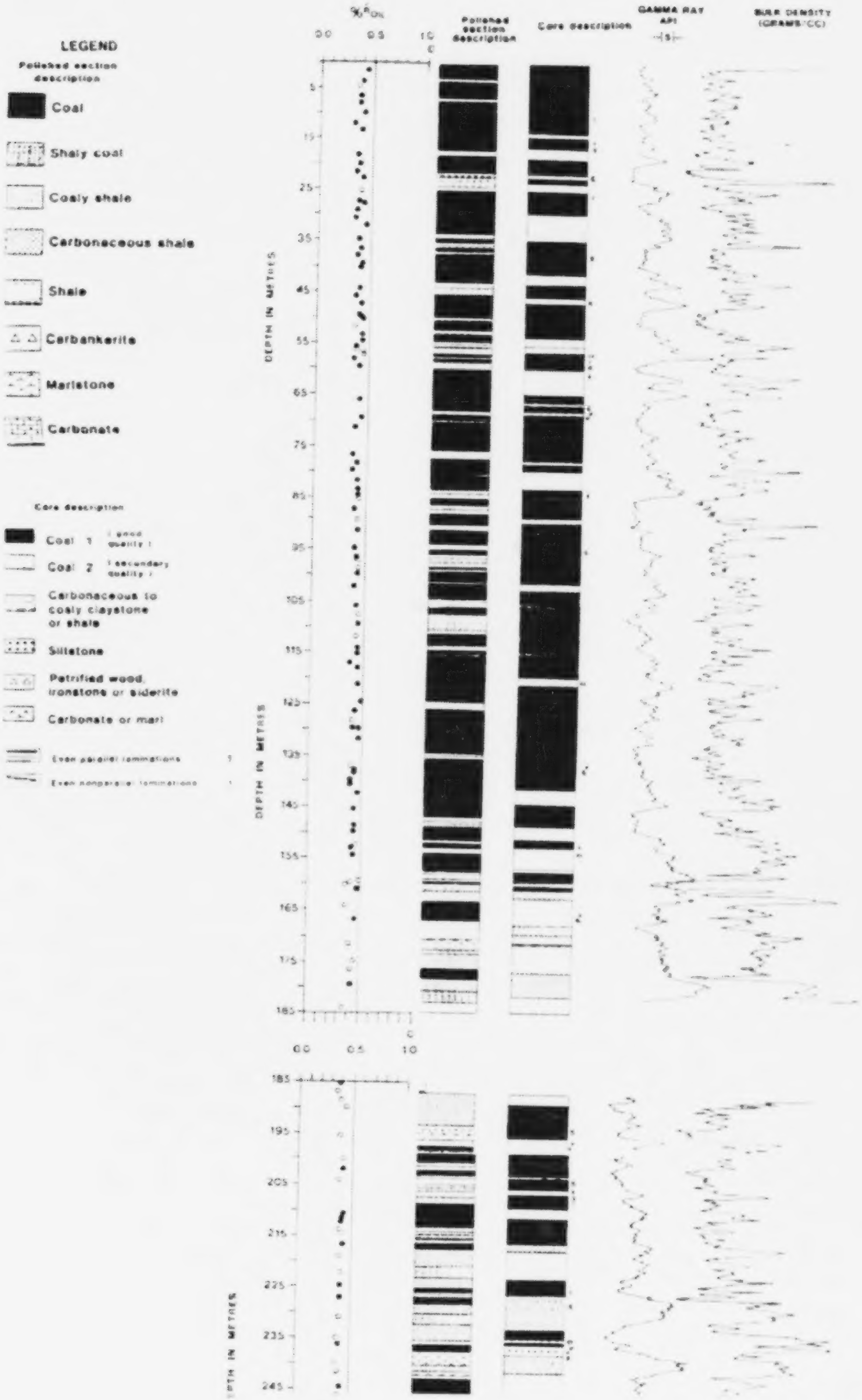

Figure 4. Rank and geophysical logs from the Number 2 deposit; data from Goodarzi and Gentzis (1987).

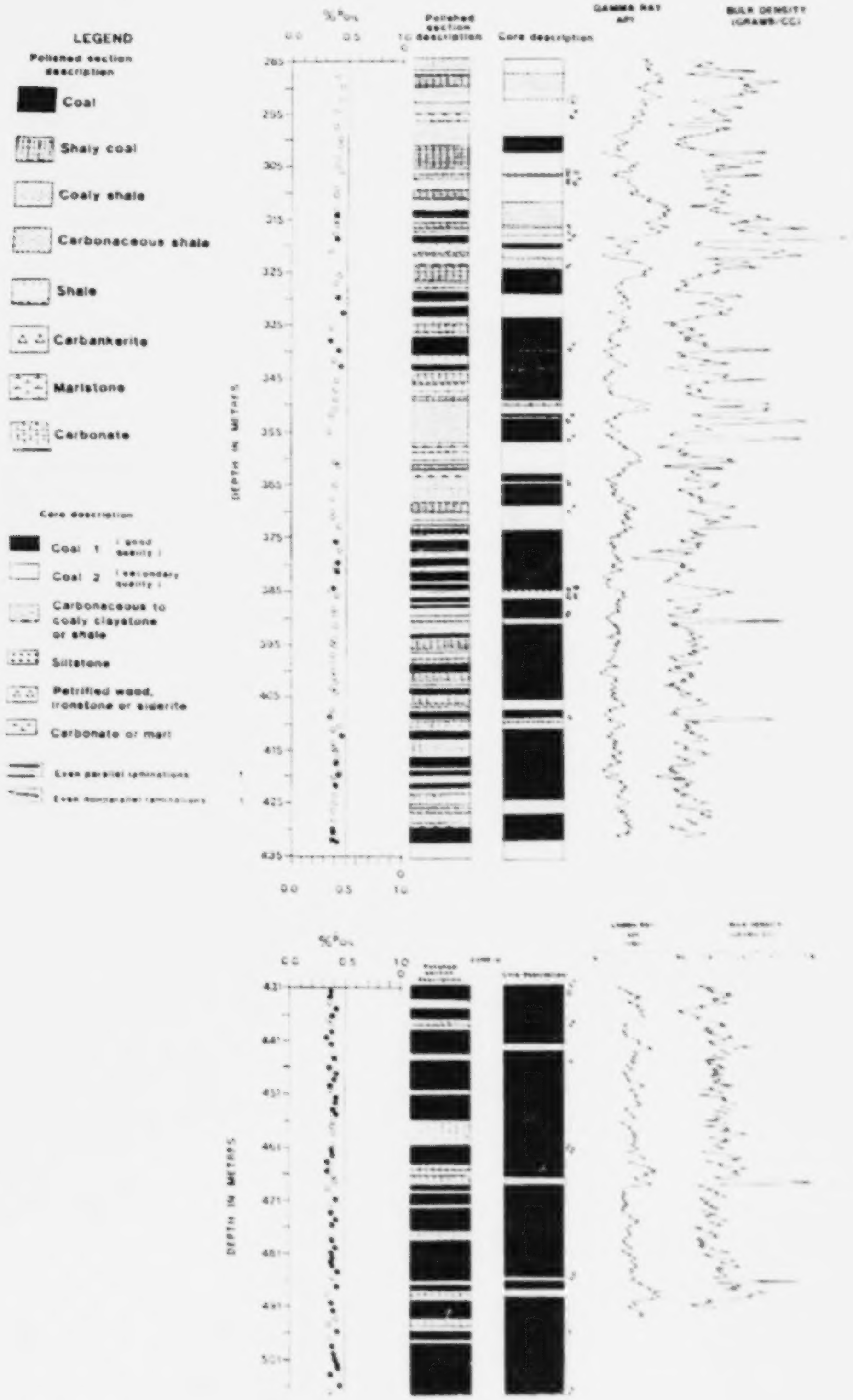

Figure 5. Rank and geophysical logs from the Number 2 deposit; data from Goodarzi and Gentzis (1987).

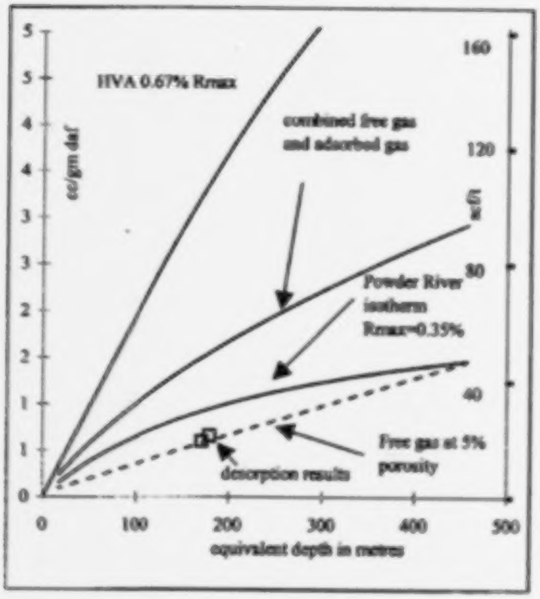

Figure 6. Adsorption isotherms for the Powder River Basin data from Mavor *et. al.* (1999).

with the Powder River coals containing more inertinite (15% to 25% mmfb) compared to Hat Creek coals that contain almost no inertinite (Goodarzi and Gentzis, 1987). Hat Creek coals generally contain a lot of rock splits and the intervening coal probably averages about 30% ash. In comparison the Powder River coals generally have low ash contents of less than 10% % (Pratt *et al*, 1997).

Permeability is high in the Powder River coals and values range from the milli Darcies to Darcies. Some conductivity data, available for the Number 1 deposit at Hat Creek is converted to milli Darcies (Table 3). The upper coal zone A has low permeability but the two lower zones B and D appear to have good permeabilities (averaging 40 and 50 milli Darcies) though not as good as Powder River.

One of the reasons that the Powder River Basin is successful is that the desorbed gas content appears to account for less than half of the recoverable gas per tonne of coal. It has been suggested (Bustin and Clarkson, 1999) that in low rank coals a significant amount of the gas in a volume of coal (up to 70%) may be stored as free gas in the matrix porosity. There is no information on the fracture porosity of Hat Creek coal but it may be possible to extract some useful information from washability data that exists for the property. It may also be possible to use moisture analyses to indicate if the coal is gas saturated. If equilibrium moisture values are greater than as -received moisture values obtained from core samples, then this might indicate that cores were partially gas saturated. This assumes that the core samples were sealed and not allowed to dry out prior to as-received moisture analyses.

TABLE 3
PETROGRAPHY OF TULAMEEN AND TUYA RIVER SAMPLES

	telinite	collotelinite	collodetrinite	vitrodetrinite	gelinite	corpogelinite	total reactives	semifusinite	fusinite	macrinite	micrinite	inertodetrinite	total inerts
A	15	34	45	1	4	1	99	1	0	0	0	0	1
B	7	41	43	3	2	3	100	0	0	0	0	0	0
C	6	33	50	3	8	0	100	0	0	0	0	0	0
D	57	10	15				97						3

A Tulameen HW B Tulameen FW
C Tuya River D Hat Creek

Hat Creek data from Goodarzi (1985)

MERRITT

GENERAL

The Merritt Coal Basin (also referred to as the Nicola Basin) comprises several isolated Eocene (Coldwater Formation) sedimentary areas (Figure 7) (Read, 1988) that outcrop within a radius of 15 kilometres. The main area, which covers about 80 square kilometers is centered on the town of Merritt and includes the mining areas of Coal Gully, Coldwater Hill and Diamond Vale. A second area 15 kilometres to the east overlies Quilchena Creek and covers about 25 square kilometers. It hosts the Diamond Valle prospect. The Tertiary rocks in the area unconformably overly the Triassic Nicola Group and Coast Range intrusive rocks.

The limits of the Merritt Basin to the southwest follow the Coldwater Creek and to the northeast the Nicola River and in both areas are obscured by valley fill. The basin is filled with sediments belonging to the Coldwater Formation that are in part overlain by Miocene-Pliocene basalts in the east. The coal measures are up to 300 metres thick on the western edge of the basin where seams tend to be thicker and more continuous (Matheson, 1992). Structure is dominated by a series of northwest trending normal faults and folds (Figure 8). The folds are described as plunging to the southeast (Dolmage and Campbell, 1975) but the map of Swaren (1979) implies a northwest plunge. Dips steepen and the structure becomes more complicated to the west near the contact with the basement. The northeastern part of the basin is overlain by Pliocene basalt flows that separate the Normandale mine from the rest of the basin. Overall the basin has not been extensively explored; much of it is overlain by alluvium with potential coal seams at depth and therefore not of interest as resources for surface or shallow underground mining.

In the past mining occurred in three areas in the Merritt Basin. Most occurred in the Coal Gulch area (Figure 7), which produced about 2.5 mt of high-volatile C to A bituminous coal in the period 1906 to 1963. In this area Swaren (1977) identified seven coal zones (not numbered in strati-

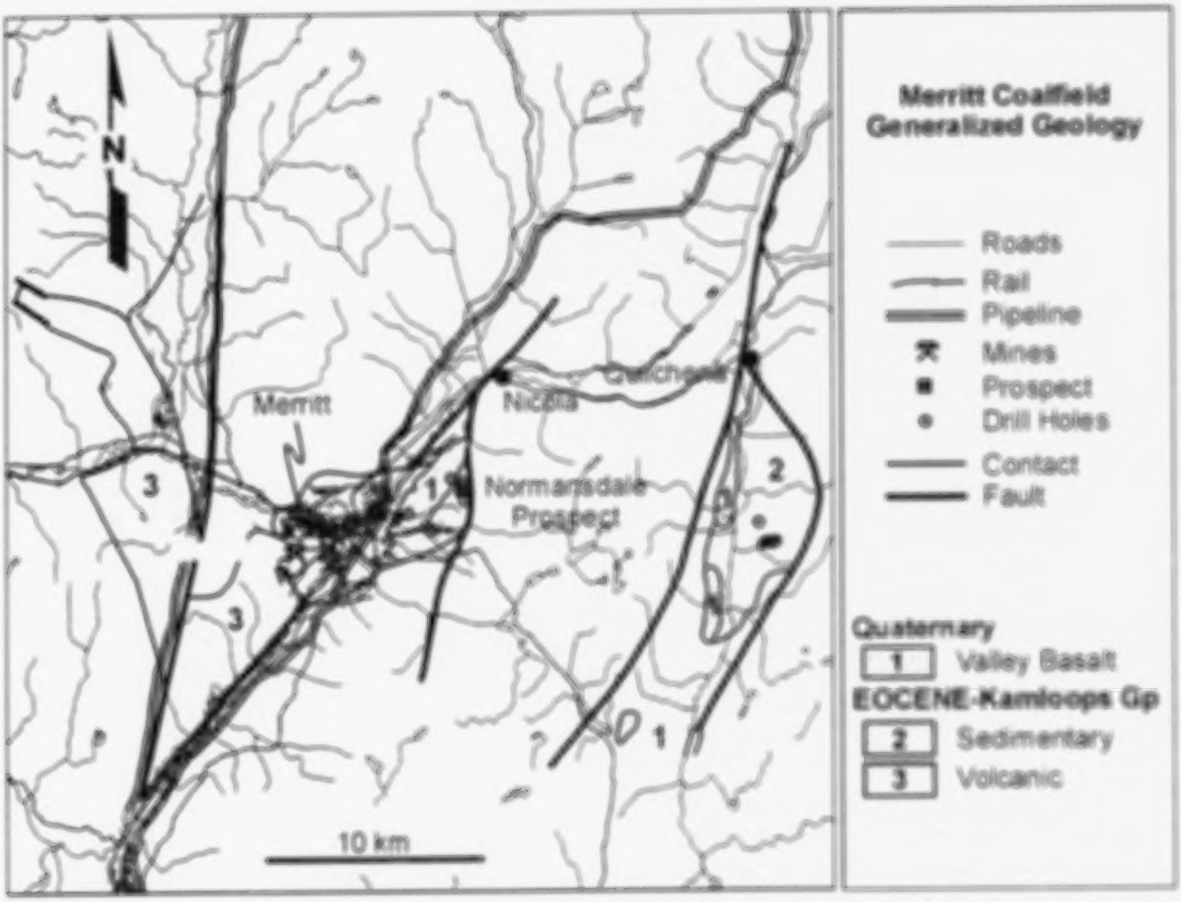
Merritt Coalfield
Generalized Geology
N
Roads
Rail
Pipeline
Mines
Prospect
Drill Holes
Contact
Fault
Quaternary
1 Valley Basalt
EOCENE-Kamloops Gp
2 Sedimentary
3 Volcanic
Merritt
Nicola
Quilchena
Normansdale Prospect
1
2
3
10 km

Figure 7. General geology of the Merritt Basin from Read (1988) and Matheson (1992).

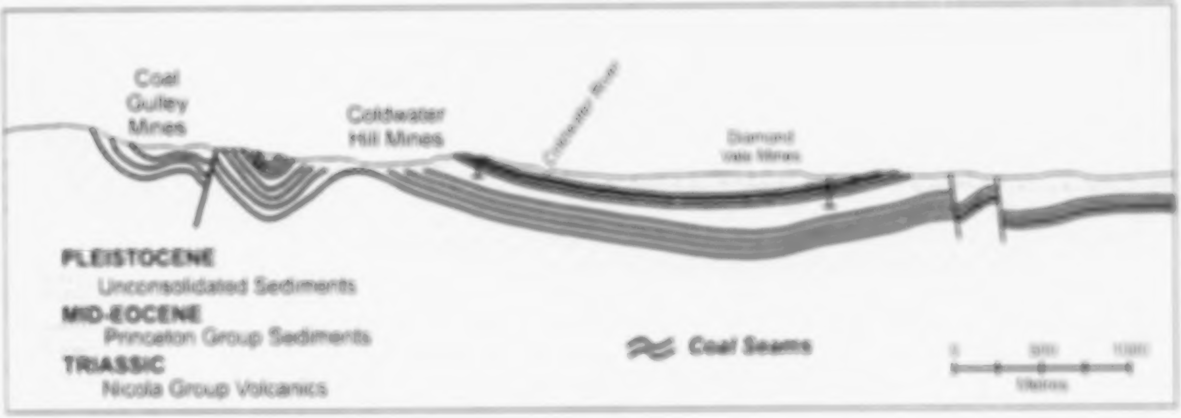
Coal Gulley Mines
Coldwater Hill Mines
Coldwater River
Diamond Vale Mines
PLEISTOCENE
Unconsolidated Sediments
MID-EOCENE
Princeton Group Sediments
TRIASSIC
Nicola Group Volcanics
Coal Seams
0
500
1000
Metres

Figure 8. Generalized cross section through the Merritt Basin from Matheson (1992).

graphic order) in the 300 metres coal section. The lowest No 1 is 7.9 metres, No 5 is 1.5 metres, No 4 is 7.6 metres, No 8 is 2.44 metres, No 6 is 1.8 metres, No 3 is 0.76 and the top seam (No 2) is 1.8 metres thick for a cumulative thickness of 23.76 metres. On Coldwater Hill one kilometer northeast of the Coal Gully mines, ten seams with cumulative coal thickness of 6.4 metres occur in a 140 metre section.

In the Diamond Vale Mine, which is 2 kilometers east of the Coldwater Mines, seams 2, 3 and 6 were mined, seams lower in the section were not mined because of depth. Five seams are described with a cumulative thickness of 5.3 metres over a stratigraphic interval of 95 metres. Seams dip to the southwest outlining a northwest trending syncline between the Diamond Vale and Coal Gully mines. The fold projects the coal seams under the town of Merritt and the Nicola River. The depth to the top of the coal measures in the core of the syncline is projected to be greater than 450 metres (Swaren, 1977). A single seam 1.5 metre thick was explored and mined briefly at the Normandale Mine, which is on the eastern edge of the Merritt Basin. Beds in the area dip to the southeast and it is not clear how this relates to the westerly dips at the Dips at the Diamond Vale mine.

In the Quilchena area, where the Diamond Valle prospect is described, coal seams rarely exceed of 1.5 metres (Ellis, 1905). Thicker seams 2 to 4.5 metres thick were apparently found in the northern part of the sub basin (Ellis, 1905). Drilling in 1981 did not intersect additional seams and it appears that either there is much less coal in the section than in the Merritt area or the drill holes missed the coals seams because of faulting.

COAL QUALITY

Coal rank in the Merritt area spans the range high-volatile C to A bituminous with random reflectances ranging from 0.62% to 0.82% (Rmax 0.64% to 0.86%). There does not appear to be any relationship to depth but rank may be increasing in a northeasterly direction (Matheson *et al*, 1994). Reflectance values of 0.745% and 1.44% were obtained from Coal Gully (Kilby, personal communication 1987). Proximate data (Matheson *et. al.* 1994) predict a rank of 0.75% based on the equation discussed in the introduction. The volatile matter data is used to predict the Volatile matter dry ash-free value at zero ash and this with an assumption of vitrinite content is used to predict Rmax% values (Figure 9).

COAL AND CBM RESOURCE

In the western part of the Merritt Basin, Swaren (1977) estimates the speculative underground mining resource of 180 million tonnes. The area considered does not extend north under the town of Merritt or northeast along the Nicola valley. Including these areas in a potential resource calculation increases the tonnage to about 300 million tonnes. The calculation used 20 metres of accumulated coal in the western part of the basin progressively thinning to 5 metres in the northeast and no tonnage was assigned to the Normandale Prospects area where only one 1.5 metre thick seam has been mapped.

Coal rank averages about 0.75% Rmax. Isotherms for coals of rank 0.8% and 0.67% as well as the predicted gas content for Rmax 0.75% (Ryan Equation, Ryan 1992) bracket the possible gas content for Merritt coal (Figure 10). The isotherms were obtained from coals with close to 100 % vitrinite on a mineral-matter free basis and in conjunction with the calculated isotherm have been recalculated to a 25% ash basis. The coal resource of 300 million tonnes is assumed to be evenly distributed from 0 to 800 metres and appropriate gas contents assigned to each block of coal. The potential CBM resource of the coal is then estimated to be about 52 bcf. The best potential is west and under the town of Merritt. Areas that have untested potential include the Nicola Valley to the northeast and under the Miocene-Pliocene valley basalts on the eastern side of the Merritt Basin.

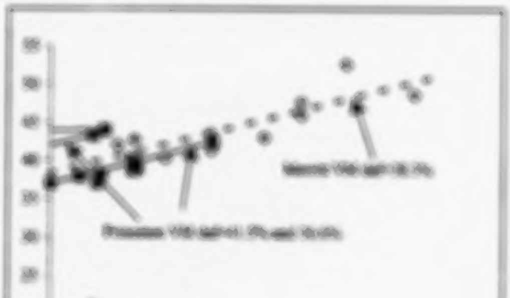

Figure 9. Rank determination for the Merritt and Princeton basins.

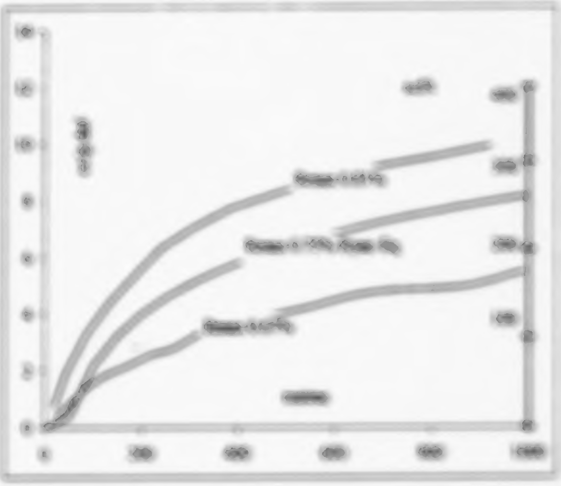

Figure 10. Possible adsorption isotherms for Merritt coals.

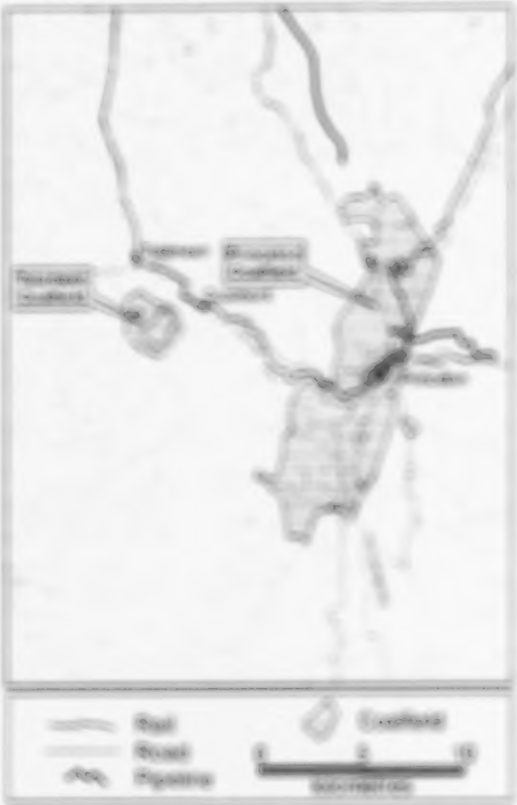

Figure 11. Similkameen coalfields and location of the Tulameen and Princeton Basins.

PRINCETON BASIN

GENERAL

The Similkameen Coalfield (Figure 11) contains a number of basins. The two most important are the Princeton and Tulameen. The Princeton Basin is a northerly elongated basin approximately 6 to 7 kilometres wide and 26 kilometres long, covering a total area of about 170 square kilometres and centered on the town of Princeton (Figure 12). The basin is a half graben bounded on the east by a north-northeasterly trending west dipping extension fault that has a minimum separation of 1400 metres (McMechan, 1983). The basin is filled with mid Eocene strata of the Princeton Group, which rest unconformably on volcanic rocks of the Upper Triassic Nicola Group. The Princeton Group is divided into 2 formations. The Lower Volcanic Formation, which is 1570 metres thick (Cedar Formation, Read, 1987) is overlain by the coal-bearing Allenby Formation, which is 1700 metres thick (Shaw, 1952). This formation is divided into 3 members, a lower member containing volcanic tuffs and flows, a middle member containing non-marine sediments and tuffs and an upper member containing non-marine sediments and coal. Four coal zones occur in the basal 530 metres of the coal-bearing member, other coal zones occur higher in the member. Sediments in the northern part of the basin north of the town of Princeton coarsen and coal zones may not be present possibly because paleocurrent direction was from the north or northeast (McMechan, 1983).

The basin is divided east-west by the Similkameen River and a northwest trending open anticline. The southern part of the basin, which contains most of the potential coal resources, forms an east plunging syncline truncated by the boundary fault to the east. A maximum thickness of about 1700 metres of Allenby Formation is preserved. The basin is shallower in the north and consists of a homocline dipping east at 15° to 25°, truncated by the boundary fault. A gravity survey (Agar, 1975) confirmed that the thickness of sediments in the northern part of the basin is much less than that in the south where the survey indicated a maximum thickness of 1200 to 1700 metres. The survey did not indicate a major gravity low that might be associated with a deposit similar to Hat Creek.

COAL RESOURCES

Coal mining started in the basin in 1909 and over the next 52 years, 15 small underground and one surface mine operated in the central part of the basin. Mining activity finished in the basin in 1961, by which time 1.9 million tonnes of sub-bituminous coal had been mined. From 1971 to 1982 there was renewed exploration and 26 short holes were drilled mainly in the northern part of the basin but no major coal seams were intersected and the coal licenses were subsequently dropped.

In the southern part of the basin, coal seams are difficult to correlate and 'lens out' over fairly short distances. Four major coal zones, numbered from 1 at the top to 4 at the base of the section (Holmage and Campbell, 1975), have been recognized in a 530 metre section. The lowest zone (Number 4) is represented by the Blue Flame, Black

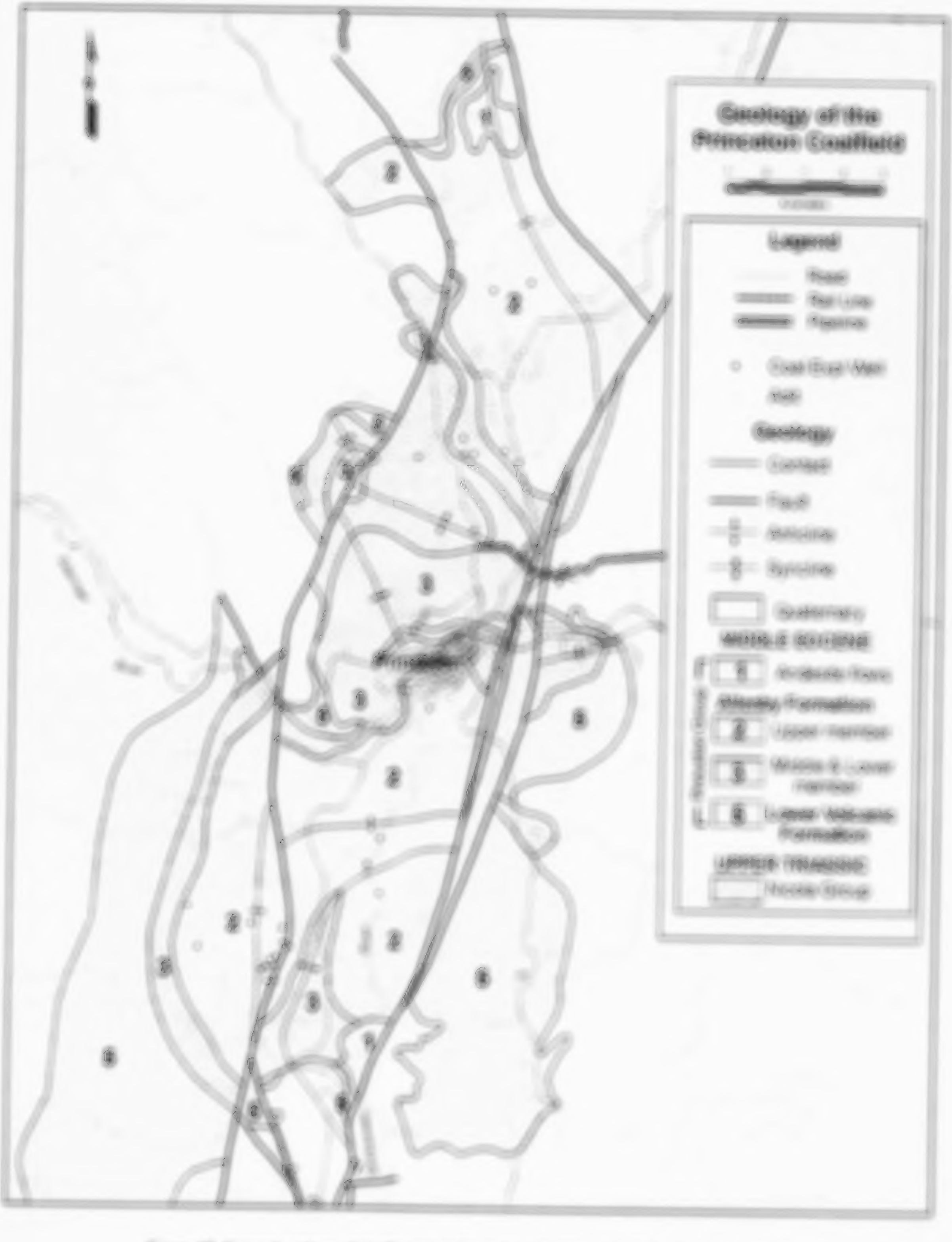
Geology of the Princeton Coalfield
Kilometres
Legend
Road
Rail Line
Pipeline
Coal Expl Well
Adit
Geology
Contact
Fault
Anticline
Syncline
Quaternary
MIDDLE EOCENE
Princeton Group
1 Andesite Flows
Allenby Formation
2 Upper Member
3 Middle & Lower Member
4 Lower Volcanic Formation
UPPER TRIASSIC
Nicola Group
Princeton
1
2
3
4

Figure 12. General geology of the Princeton Basin from McMechan (1983) and Read (1987).

[illegible]

COAL QUALITY

[illegible]

COAL AND GAS RESOURCES

[illegible]

[illegible]

[illegible]

[illegible]

[illegible]

PEACE RIVER

GENERAL

[illegible]

[illegible]

TABLE 4
[illegible] RIVER CBM RESOURCES

depth	coal	adsorption gas		resource
metres	m	scf/ton	cc/g	bcf
0	30.0	0.0	0.0	0.0
100	30.0	8.8	0.3	0.3
200	30.0	39.0	1.4	1.8
300	30.0	69.1	2.7	2.7
400	30.0	108.8	3.4	3.3
500	30.0	124.9	3.9	3.8
600	30.0	139.1	4.3	4.2
700	30.0	149.2	4.7	4.6
800	30.0	158.8	5.0	4.9
900	30.1	167.3	5.2	5.1
1000	30.0	174.9	5.5	5.4
1100	30.0	181.8	5.7	5.6
1200	30.0	188.1	5.9	5.8
total sq.	400.0			47.6

at various depths to 1600 metres and gas contents predicted using six isotherms from a Quinsam coal (Rmax 0.67%) or using the Ryan Equation Rmax 0.72% and 25% ash. The two methods produce the same potential resource of about 60 bcf.

The basin is very isolated but could provide energy to the local communities of Dease Lake or Telegraph Creek. It could also provide energy for any other resource development in the area.

TULAMEEN BASIN

GENERAL

The Tulameen basin, which is about 20 kilometres northwest of Princeton, forms an elliptical sedimentary basin 5.4 by 3.6 kilometres that contains two well-developed thick coal seams (Figure 14). The area underlain by coal is about 10 square kilometres.

Gold was discovered in Granite Creek in 1885 adjacent to coal outcrops. However, the first references to the coal potential of the area is found in the GSC Summary Reports for 1908 and 1909 by W.F. Robertson describing in part a 1901 observation. Coal analyses are reported in the Geo-

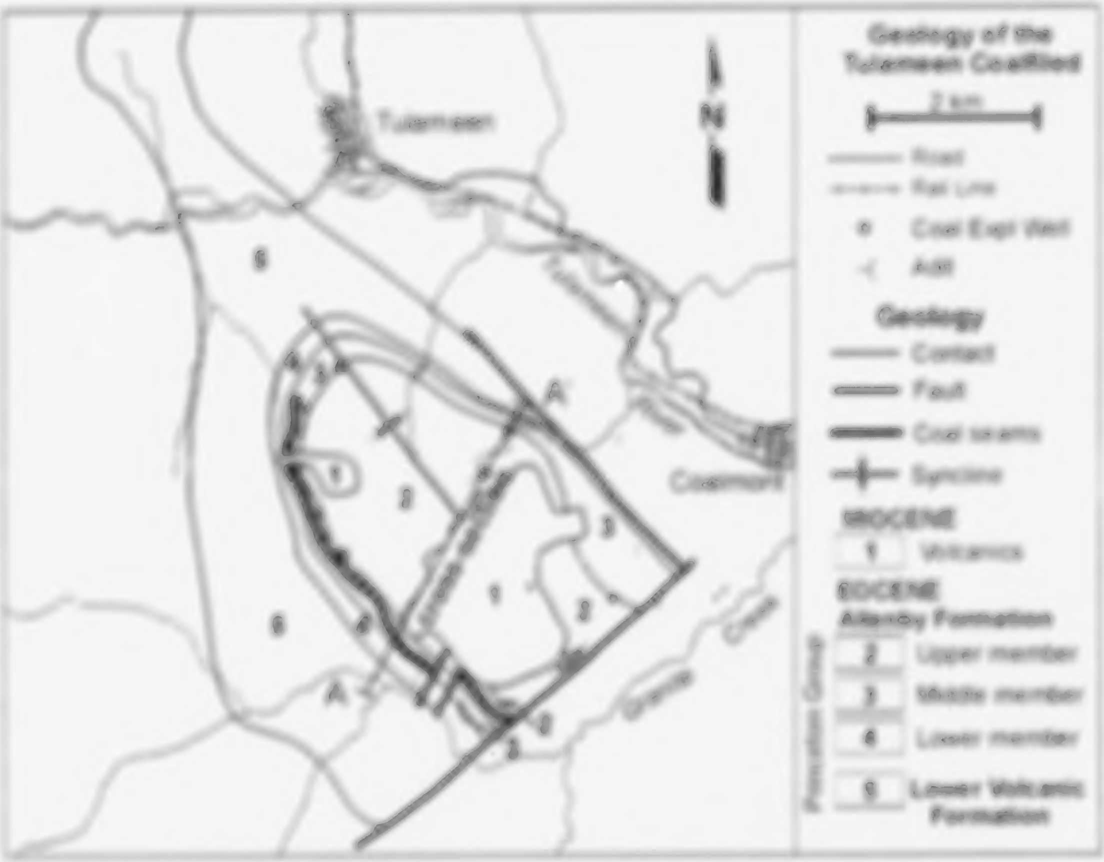
Tulameen
N
Coalmont
A
A'
Granite Creek
1
2
3
4
5
Geology of the
Tulameen Coalfield
2 km
Road
Rail Line
Coal Expl Well
Adit
Geology
Contact
Fault
Coal seams
Syncline
MIOCENE
1 Volcanics
EOCENE
Allenby Formation
2 Upper member
3 Middle member
4 Lower member
5 Lower Volcanic Formation
Princeton Group

Figure 14. Generalized geology of the Tulameen Basin.

logical Survey Report for 1899. Mining started in 1904 in the Blakeburn Creek area with the development over the next 30 years of 5 underground mines. In 1913 Coalmont Collieries developed the No 1 and No 2 mines. The No 3 and No 4 mines were developed in mid 1920's, but closed in the mid 1930's because of fires and flooding. In fact the No 4 mine closed after a disastrous explosion on August 13, 1930, which killed 45 men. Up until that time the mines had been described as gas free with almost no mention of methane by the fire bosses. The cause of the explosion was not clear, but it was suggested that gas built up as a result of spontaneous combustion in an area closed off from active mining. The gas broke out into the active mine area because of low atmospheric pressure associated with a violent thunderstorm. Once mixed with air the gas became explosive and was probably ignited by the reactivated spontaneous combustion. The explanation indicates that desorbing methane was not a major contributing factor. The No 5 mine opened in 1931 and operated for 9 years.

In the period 1900 to 1940 about 2.2 million tonnes were produced from the basin. A small strip mine operated in 1954 to 1957 and produced about 240 000 tonnes. The basin has seen sporadic exploration since 1960 and at present Compliance Coal Mining is planning to develop a small mine. The main limitation on underground mining was the increase in crushing of the coal with depth. Possibly caused by movement within the bentonite bands. Also, in some mines, deterioration in coal quality caused mining to stop.

In 2000 a small test was excavated into the upper coal zone and coal shipped for test washing. The coal is hard and well cleated in outcrop with numerous bentonite or clay partings (Ryan, 2002).

GEOLOGY

The stratigraphy in the basin is subdivided into 5 units (Anderson, 1976) that consist of a lower conformable volcanic unit, three sedimentary units and an uppermost non conformable volcanic unit. The lower 4 units are probably contemporaneous with the Princeton Group to the southeast and the 3 sedimentary units with the Allenby Formation, though stratigraphic nomenclature has not been established. The lower sedimentary unit is composed of sandstones and is 100 to 150 metres thick. The middle unit contains shales and 2 major coal seams and is about 130 metres thick (Anderson, 1976). The upper sedimentary unit consists of conglomerates sandstones and is at least 400 metres thick. The depositional environment for the sediments is described as a slowly subsiding valley influenced by intermittent volcanic activity but distant from salt water.

The Tertiary sediments of the Princeton group rest unconformably on volcanic and sedimentary rocks of the Upper Triassic Nicola group. Beds appear to be folded into a southeast trending syncline with beds on the southwest limb dipping shallowly to the northeast (20°-25°) and beds on the northeast limb dipping steeply southwest (40°-65°) (Figure 15). The maximum thickness of sediments in the basin is about 850 metres and the maximum depth to the top of the coal-bearing unit is about 700 metres based on sections by Evans (1978). The plunge of the syncline was estimated by Evans (1978) to be 15° in a direction 138°. A gravity survey (Church and Bassett, 1983) did not find evidence of a south plunging syncline and Anderson (1976) describes the structure as an asymmetric northwest trending syncline and does not assign a plunge.

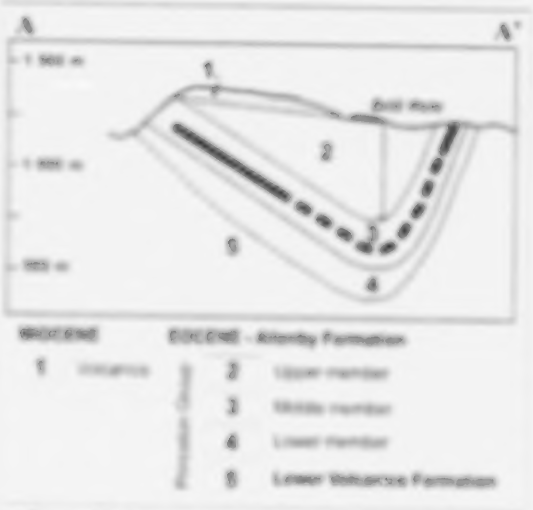

Figure 15. Cross section through the Tulameen Basin.

The area is cut by a number of vertical faults that trend north to northeast (Anderson, 1976). One fault mapped by Shaw (1952) had a down drop on the west of about 150 metres and another of 40 metres both faults trended northeast. Other faults are mapped that generally trend northeast with down drop to the east or west.

COAL QUALITY

Two coal zones are present in the basin; the lower, which is generally less well developed, is 120 metres above the volcanic unit. It is 7 to 7.6 metres thick and averages 52% ash (Anderson, 1976). There is not a lot of coal quality or rank information available for the lower seam because most exploration concentrated on the upper coal zone. This zone, which is 25 to 40 metres above the lower coal zone, is better developed and attains thicknesses ranging from 15 to 21 metres. Bentonite rich partings make up from 10% to 60% of the seam generally increasing in percentage to the northeast. The coal bands are vitrinite rich and well cleated with face and butt cleats. Ankerite sometimes coats butt cleats.

The rank of Tulameen coal is high-volatile B bituminous and it contains over 90% vitrinite on an ash free basis. The low rank means that any rank variation may have a significant impact on the potential CBM resource. Rank increases from 0.62% in the north to 0.86% in the south but there does not seem to be any relationship to depth (Williams and Ross, 1979). Other authors have found that rank varies from 0.69% to 0.81% over 19 metres in the upper part of the main seam, but below this depth remains constant at about 0.8% (Donaldson, 1972). No rank determinations exist for coal in the central part of the basin. If rank was superimposed after folding then it should be higher at depth in the center of the basin.

COAL AND CBM RESOURCE POTENTIAL

The area of the basin is about 6 square kilometres and based on average thicknesses for the two coal zones and the percent of coal in the zones the potential coal resource is in the range of 300 million tonnes.

Two adsorption isotherms are available for the upper coal zone (Figure 16). They are typical of low rank coals in that isotherm slopes are flat at low pressures and only at high pressures or depth does the adsorptive capacity increase markedly, reaching 8 to 10 cc/g daf basis at about 1000 metres. There is no obvious reason for the better adsorption of the footwall sample. Both samples have similar petrography and rank (Table 4).

The CBM potential resource is estimated by distributing the coal resource evenly between 0 and 800 metres and assigning gas contents for each depth increment, based on the adsorption isotherms. The estimated total potential CBM resource is 42 bcf. A zero gas content is assigned to coal less than 100 metres. This is conservative but is meant to take into account the fact that the Tulameen Basin occupies relatively high ground between the drainages of Blackburn Creek and the Tulameen River. Probably the height of the old mines above Blakeburn Creek explains the apparent absence of gas in them.

BOWRON BASIN

GENERAL

The Bowron River graben, which is 50 kilometres east of Prince George, is 2.5 kilometres wide and 19 kilometres long (Figure 17). Coal was discovered in the area in 1871 by G.M. Dawson and has been intermittently explored from period 1914 to 1981. The lower 85 meters of the late Cretaceous to Paleocene sedimentary section (Graham, 1980), which is over 700 metres thick (Klein, 1978), is coal-bearing. The area of the basin could be up to 47.5 square kilometers based on aero-magnetic maps (Verzosa, 1981) so that there is potential for a moderately large CBM resource. The underground mineable resource calculated, based on an area of 3.6 square kilometres, is reported as 81 mt.

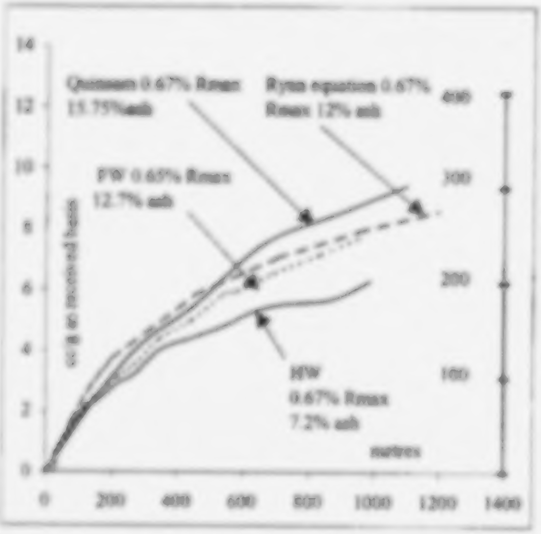

Figure 16. For hanging wall and footwall upper coal zone, Tulameen Basin.

Outcrop is sparse and most is found in an 11 kilometre stretch along the west bank of the Bowron River. Ninety-five holes were drilled From 1967 to 1981. The description of the stratigraphy, which is characterized by rapid changes in lithology, is based mainly on drill hole data. The coal measures are interpreted to rest unconformably on the Antler Formation and to be folded into a southeast plunging syncline, which intersects the northwest trending fault that defines the eastern edge of the basin (Verzosa, 1981). Information in the northern half of the basin is sparse and there is no structural interpretation.

There are a number of coal zones in the section but only the lowest appears to be persistent. It is between 50 and 100 metres above the Antler Formation and is up to 35 metres thick (Graham, 1980) of which up to 6.7 metres is coal. In places there may be a single seam up to 5 metres thick in others multiple thinner seams. There is a coal zone that occurs about 50 metres above the lower coal zone that is less persistent and averages 4.75 metres of coal and rock partings.

COAL QUALITY

The coal is high-volatile B bituminous in rank and is characterized by a high (8%) resin content. The average rank of the lower seam is 0.65% (Campbell 1973). The raw ash content of a number of proximate analyses of drill core averages 35.7% (Verzosa, 1981).

CBM RESOURCE

Any CBM potential will depend on presence of biogenic methane though the presence of amber may help initiate generation of thermogenic methane at a lower rank. The synclinal structure in the southern part of the basin indicates that the coal intersects the eastern fault at depths ranging from less than 100 metres to over 1500 metes. Matheson and Sadre (1991) estimate a potential resource of 400 mt down to a depth of 1200 metres considering only the lower seam. There is some indication in the volatile matter analyses that the rank increases over the depth covered by the drilling (0 to 350 metres). Using a rank of 0.65%, an ash content of 35% and distributing the resource over 1200 metres produces a potential CBM resource of 47.6 bcf (Table 5).

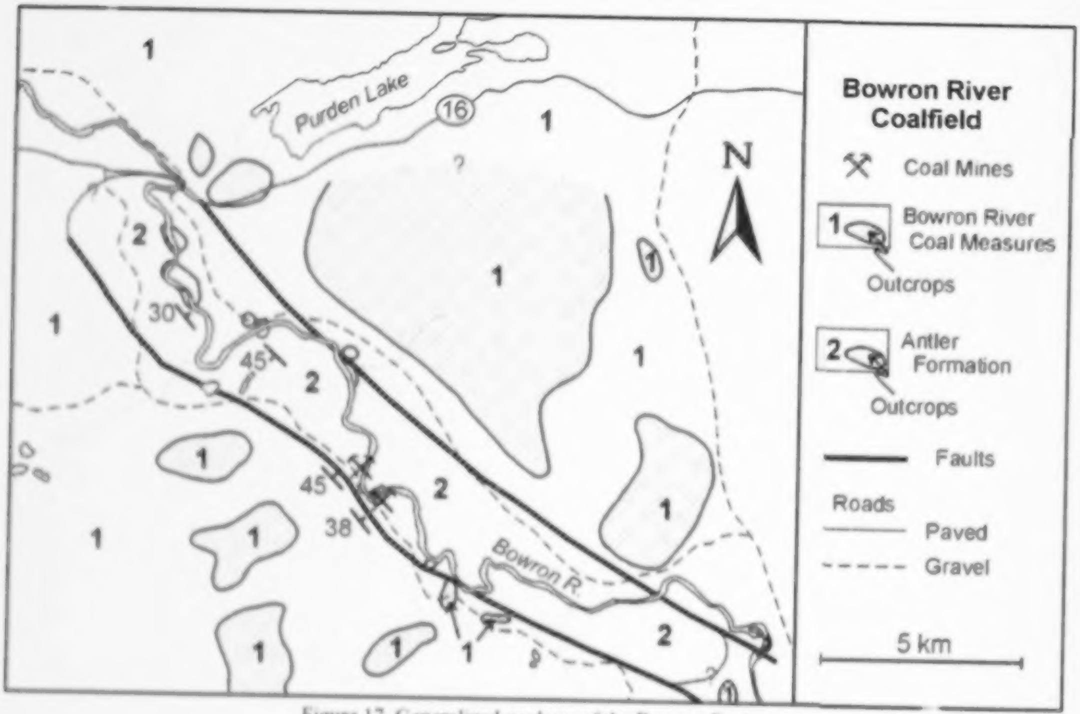
1
Purden Lake
16
1
?
N
2
1
1
30
45
2
1
1
1
45
2
38
1
1
Bowron R.
1
1
1
2
1
Bowron River Coalfield
Coal Mines
Bowron River Coal Measures
Outcrops
Antler Formation
Outcrops
Faults
Roads
Paved
Gravel
5 km

Figure 17. Generalized geology of the Bowron Basin.

SEATON COAL BASIN

GENERAL

The Grand Trunk British Columbia Rail Line (now the CN line) was constructed in the Bulkley Valley in 1910. This stimulated exploration for coal and a number of small coal basins were found including the Tertiary Seaton Basin 42 kilometres north of Smithers, others older than Tertiary include one in the Zymoetz River and Denys Creek in the Smithers area. Only the Lower Cretaceous Telkwa Basin sustained commercial mining and by 1930 most of the other basins including Seaton had been abandoned. Exploration activity briefly resumed in the Seaton Basin in the period 1986 to 1988.

The Bulkley Valley is a graben in the vicinity of the Seaton Basin defined by faults trending north or northwest with throws of over 1000 metres on each side of the valley (Figure 18). The valley, which is flat and generally filled with alluvium, is about 5 kilometres wide. Surrounding mountains rise to 1000 to 1500 metres above the valley and are comprised of Cretaceous rocks of the Skeena Group and Jurassic rocks of the Bowser Lake Group. The valley-fill al-

TABLE 5
SUMMARY OF INFORMATION ON THE TERTIARY BASINS

Basin	Area Km^2	Rank Rmax %	Coal million tonnes	CBM bcf total	CBM scf/t ton	CBM bcf section
Hat Creek	35	0.35-0.45	10000	500	50	37.0
Merritt	105	0.64-0.86	312	52	167	1.3
Princeton	170	0.52	800	80	100	1.2
Tulameen	19.4	0.62-0.86	300	42	140	5.6
Bowron	47.5	0.65	400	48	120	2.6
Tuya	150	0.68-0.76	460	66	143	1.1
Seaton	25	1.34	100	25	250	2.6
Coal River	35	0.20	200	3	15	0.2

luvium is interspersed with scattered outcrops as young as Paleocene.

The first reference to coal in the Seaton Coal Basin was by Dawson (1881). Dowling (1915) summarized work in the area up to 1915. Activity was in three areas. A 3.4 metre thick section of carbonaceous shale and coal was trenched and tunneled in one area. Elsewhere eleven thin coal seams were found in a 150 metres section. Ash contents were high but the coal was reported to produce a firm coke. In another area six seams varying in thickness up to 1 metre thick were described. Analyses indicate that seams are medium-volatile bituminous rank with moderate ash contents. Further exploration in 1916 and 1927 describes exploration in three widely dispersed areas that located three seams: Number 1, 1.4 metres thick, Number 2, 0.43 metres and Number 3, 1.0 metre thick. Two diamond core holes were drilled in 1987 and three in 1988 for a total length of 794 metres. A geological report (Perry 1986) was prepared for the company and a single petrographic analysis was made (Pearson 1987).

GEOLOGY

There appears to be at least 400 metres of Tertiary sediments in the basin. Sediments consist of a number of fining upward cycles, which are from 5 to 30 metres thick. Cycles start with chert-pebble conglomerate, grit or coarse sandstone deposited on an erosional surface and are overlain in succession by sandstone, siltstone, mudstone and sometimes carbonaceous mudstone with coal. Coal seams are usually less than 1 metre thick. Sediments generally dip shallowly to the east with variable strike. Paleonology on mudstone samples indicate a Late Eocene to Early Oligocene age (Sweet; personal communication 1991). The unexpectedly high coal rank of the samples made extraction of spores and pollen difficult. Some of the samples appear to contain material reworked from a Campanian aged source.

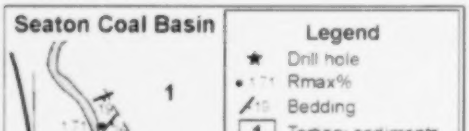

Figure 18. Geology of the Seaton Basin.

COAL QUALITY

The average raw ash of the coal is 30.5%. Thirteen Rmax values average 1.34% indicating a rank of medium-volatile bituminous that extends for 9 kilometres along the Bulkley River. This represents a large area of unusually high rank for Tertiary coal. This could indicate a combination of high geothermal gradient and/or removal of a lot of overlying sediment. Reflectance values for samples from a 1988 drill hole indicate a vertical reflectance gradient of 0.38%/100 metres, which is high. A single Rmax measurement (0.65%) on Tertiary rocks 40 kilometres to the south indicates a rank of high volatile bituminous B, considerably lower than the rank at Seaton and similar to the rank in other Tertiary coal basins.

COAL AND CBM RESOURCE

Seams are generally thin the thickest located was 1.4 metres and only about 3.5 metres of cumulative coal was located in a 100 metres section of nearly continuous outcrop. Thicker seams could exist in the basin much of which remains untested, especially the lower parts of the section. Potential resource in basin is about 100 million tones, based on an area of 25 square kilometers and a cumulative coal thickness of about 3 metres. Sediments accompanying the coal are at least 50 per cent sandstones and conglomerates with good permeability and porosity. The cycles of coarse to fine sediments probably produces permeability barriers between the sediments of each cycle.

The high rank gradient and Rmax values indicate that considerable cover must have been removed from the basin. Rapid uplift may help coals to maintain gas saturation. The cyclical nature of the sediments may trap gas generated during coalification, so that it can be re-adsorbed by the coal during uplift, as temperatures decrease. A medium-volatile coal generates enough gas during coalification to saturate between 20 and 40 times its volume of sediments with free gas. If sediment packages including coal are isolated from overlying and under lying packages by impermeable mudstone layers, then gas may remain adjacent to seams and be available to be re-adsorbed when the adsorption capacity of coal increases as temperature decreases during uplift.

Raw coal analyses average 30.5% and the rank averages 1.34%. Based on these values and a depth of 200 metres a potential gas content of 8.25 cc/g is predicted. This provides a potential CBM resource of about 25 bcf. Because of the steep reflectance gradient any coal deep in the

Tertiary section could be very gassy, especially considering its high vitrinite content.

COAL RIVER

GENERAL

The Coal River area was mapped in 1991 (Ryan, 1996) (Figure 19). The river flows south joining the Liard River approximately 150 kilometres east of Watson Lake and 40 kilometres south of the Yukon border. The river crosses the Alaska Highway at kilometre 858. The area is marked by subdued topography and elevations range from about 550 to 600 metres. McConnel (1891) was the first to reported coal in the area. He located lignite boulders, at the mouth of Coal River, which he describes as being of inferior quality. The source of the lignite was located by Williams and DeLeen prior to 1944 (Williams, 1944) about 10 kilometres as the crow flies up river from the Alaska Highway. At about the same time crews building the Alaska Highway were using lignite boulders, washed down from the outcrop, for heating in an army camp. Williams found an outcrop of 4.6 metres of lignite dipping to the southwest at about 25 degrees on the west bank of the river. He did not expose the footwall and part of the seam was on fire. Williams describes foul smelling gases and the presence of tar at the surface. A partial map of the area was produced in 1950 by McLearn and Kindle (1950) who outlined an area of about 50 square kilometres possibly underlain by Tertiary lignite-bearing sediments. The area was mapped in 1958 and 1960 by Gabrielse (1962) who mapped a small area of Tertiary lignite bearing sediments on Coal River but found no other occurrences in the vicinity.

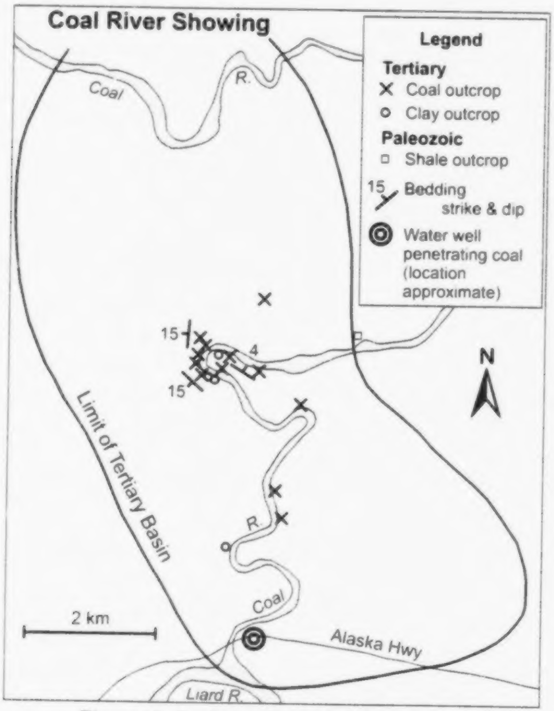

Figure 19. Geology of the Coal River Basin.

Generally Tertiary outcrops are restricted to the bank of Coal River, trees, swamp and a burn zone cover the rest of the area. The area around the river is marked by large crescent shaped slumps, presumably where younger sediments have slid on a prominent clay layer. A number of lignite outcrops were located along Coal River. The lignite is well cleated with two sets developed. The full thickness of the seam is not observed in any of the outcrops found and where exposed thicknesses range up to over 8 metres. Generally 3 to 4 metres of lignite are exposed in outcrops on the west side of the river, where lignite is overlain by about 10 metres of white to light grey clay. The clay contains occasional iron stained surfaces but otherwise appears to be quite pure.

On the east side of the river, the topography is flatter, outcrops less well developed and no thickness estimates were obtained. Here the lignite is underlain by grey clay. It is assumed that the lignite outcrops on the west and east sides of the river are of the same seam. The clay will make a very good seal above the lignite to contain any biogenic methane formed in the seam. A water-well drilled near where the river crosses the Alaska Highway, intersected 15 metres of coal at a depth of 15 metres. This may or may not be the same seam that outcrops 10 kilometres up Coal River.

COAL QUALITY

Lignite samples were analyzed by Williams (1944) and Ryan (1996). Rmax% measurements are difficult to make because of the very low rank. In fact the average of five values is 0.2%, which classifies the material as a peat rather than lignite. This is supported by the average volatile matter on a dry ash free basis, which is 75% but is not supported by the heat value or the as-received moisture measurements, both of which are characteristic of a coal with a higher rank. Ash is generally less than 10% and sulphur averages 0.3% both on a dry basis.

COAL AND CBM RESOURCE

The basin has a possible area of about 35 square kilometers and appears to be underlain by at least 5 metres of lignite, which provides a potential resource of about 200 mt at shallow depth.

The rank is too low for the lignite to have generated thermogenic methane. However the lignite could contain reasonable quantities of biogenic methane in part as free gas. The overlying clay would act as a perfect trap to contain the methane. There are no data on gas contents of lignite coals but a value of 0.5 cc/g or 16 scf/t for adsorbed and free gas should be conservative. This would predict a potential resource of about 3 bcf. A resource of this size is of no interest to a major company but might be very useful in supporting local development on the Alaska Highway.

SUMMARY

The potential CBM resources of Tertiary basins in British Columbia range from over 0.5 tcf to less than 10 bcf (Table 6). In all cases these estimates are based on minimal data and there is a lot of room for re interpretation that may indicate the possibility of a greatly increased CBM resource in some of the basins. The rank of the coal in the basins is moderately well defined at least at surface. Information about rank at depth is generally not available but can be estimated from coal quality data. There is very little CBM data available.

There is no published desorption data and not much anecdotal data from old underground mines in the basins. It is feasible to collect samples for adsorption isotherms and this paper presents two for the Tulameen Basin. However for low rank coals adsorption isotherms may give a miss-leading estimate of the potential of the basin because of the importance of free gas, as is the case in the Powder River Basin.

Tertiary coal basins in British Columbia have unique characteristics compared to older coal basins in the province. They are generally fault bounded and more likely to have experienced extensional tectonics combined with rapid subsidence. Geothermal gradients may have been and may still be high as indicated by the evidence of volcanism contemporaneous with deposition of the coal zones. This is a plus in terms of increasing rank with depth but could be a negative in terms of a high present temperature gradient that could limit adsorption capacity at depth.

The basins are filled with lacustrine sediments and therefore the ground water is probably fresh.

The low rank and simple tectonic history ensures that in most cases the coals are hard, well cleated and will not generate fines. They should be amenable to fracing or cavitation depending on the cohesion of the surrounding sediments. The cyclic deposition of fining upwards units may ensure good permeability and sealing of each unit. Bentonite layers, which represent time lines in the stratigraphy may be the perfect seals for ensuring no inflow of water from hanging walls and foot walls of seams during dewatering.

The coal seams are often in coal zones containing a lot of carbonaceous material and the whole zone should be considered for its ability to adsorb methane and not just the low ash components.

REFERENCES

Adamson, T.J. (1978): Tulameen coal project; *Coal Assessment Report 200*, Ministry of Energy and Mines, British Columbia.

Ager, C.A. (1975): Princeton Basin gravity survey; *Private Report* by C.A. Ager and Associates Ltd.

Beak Consultants Limited (1978): Hat Creek Project: Detailed Environmental Studies, Inventory Volume 2; Environmental, Impact Statement Reference Number 19b, British Columbia Hydro and Power Authority.

Bustin, R.M. and Clarkson, C.R. (1999): Free gas storage in matrix porosity: a potentially significant coalbed resource in low rank coals; *1999 International Coalbed Methane Symposium*, Tuscaloosa, Alabama, pages 197-214.

Campbell, R.B. (1973): Geology of the McBride Map Area; *Geological Survey of Canada*, Paper 72-35.

Campbell, D.D., Jory, L.T., and Saunders, C./R. (1977): Geology of the Hat Creek Coal deposits; *Canadian Institute of Mining and Metallurgy*, pages 99-108.

Camsell, C. (1913): Geology and mineral deposits of the Tulameen District , B.C. : *Canada Department of Mines, Geological Survey Memoir 26*.

Church, B.N., Ewing, T.E. and Hora, Z.D. (1983): Volcanology, structure, coal and mineral resources of Early Tertiary Outliers in south-central British Columbia; *Geological Association of Canada*, May 7-10, 1983 Field trip Guide.

Church, B.N. and Basnett, D. (1983): Geology and gravity survey of the Tulameen Coal Basin; *British Columbia Ministry of Energy and Mines*, Geological Fieldwork 1982, Paper 1983-1, pages 47-55.

Church, B.N. (1975): Geology of the Hat Creek Coal Basin; Summary of Field Activities, *B.C. Department of Mines*, pages 104-108..

Dawson, G.M. (1881): Report on Exploration from Port Simpson on the Pacific Coast to Edmonton on the Saskatchewan; *Geological Survey of Canada*, Report of Progress 1878-80.

Diessel, C.F.K. and Gammidge, L. (1998): Isometamorphic variations in reflectance and fluorescence of vitrinite - a key to depositional environment; *International Journal of Coal Geology*, Volume 36, pages 167-222

Dolmage, Campbell and Associates Ltd (1975): Coal Resources of British Columbia; BC Hydro Report.

Donaldson, R.J. (1973): The petrography of the coal from the Blakeburn strip mine in the Tulameen Coal Area, British Columbia; *Geological Survey of Canada*, Paper 72-39.

Dowling, D.B. (1915): Coal Fields of British Columbia; *Geological Survey of Canada*, Memoir 69, pages 189-222.

Dowling, D.B. (1915): Coal Fields of British Columbia; Geological Survey of Canada, Memoir 69, pages 179-181.

Dow, W.G. (1977): Kerogen Studies and Geological Interpretations; *Journal of Geochemical Exploration*, Volume 7, pages 79-99.

Ells, R.W. (1905): Nicola Coal Basin, British Columbia; *Geological Survey of Canada*, Annual Report 10904, pages A42-A74.

Evans, S.H. (1977): Geology of the Tulameen Coal Basin; *Paper 1978-1*, B.C. Ministry of Energy, Mines and Petroleum Resources, pages 76-88.

Gabrielse, H. (1962): Rabbit River; *Geological Survey of Canada*, Preliminary Map 2-1961.

Goodarzi, F. (1985): Organic Petrology of Hat Creek Coal Deposit No. 1, British Columbia; *International Journal of Coal Geology*, Volume 5, pages 377-396.

Goodarzi, F., and Gentzis, T. (1987): Depositional setting determined by organic petrography of the middle Eocene Hat Creek No 2 Coal Deposit, British Columbia; *Bulletin of Canadian Petroleum Geology*, Volume 35 pages 197-211.

Graham, P.S.W. (1980): Geology and coal potential of Tertiary sedimentary basins, interior of British Columbia; *Alberta Research Council Information Series* No. 103, Advances in Western Canadian Coal Geoscience - Forum Proceedings, April 1989, pages. 70-89.

Grieve, D. (1993): Geology and rank distribution of the Elk Valley Coalfield, Southeast British Columbia; *B.C. Ministry of Energy, Mines and Petroleum Resources*, Bulletin 82.

Hacquebard, P.A. and Cameron A.R. (1989): Distribution and coalification patterns in Canadian bituminous and anthracite coals; *International Journal of Coal Geology*, Volume B, pages 207-260.

Kim, H. (1979): Depositional environment and stratigraphic subdivision; Hat Creek Number 1 Deposit, British Columbia; 4th Annual Meeting *Canadian Institute of Mining and metallurgy*, Vancouver British Columbia, pages 1-10.

Klein, G.H. (1978): Bowron Basin, (93H/12,13); *British Columbia Ministry of Energy and Mines*, Geological Fieldwork 1977, Paper 78-1, page 63.

Lamberson, M.N., Bustin, R.M., and Kalkreuth, W.D. (1991): Lithotype maceral composition and variation as correlated with paleo-wetland environments; Gates Formation Northeastern British Columbia, Canada; *International Journal of Coal Geology*; Volme18, pages 87-124.

Larsen, V.E. (1989): Preliminary evaluation of coalbed methane geology and activity in the Recluse area Powder River Basin Wyoming; *in* Methane from Coal Seams Technology, June 1989, pages 2-9.

Long, D.G.F. (1981): Dextral strike slip faults in the Canadian Cordillera and depositional environments of related fresh-water intermontane coal basins; *Geological Association of Canada*, Special Paper 23, pages 153-186.

Matheson, A. (1992): Subsurface thermal coal sampling survey, Merritt coal deposits south-central British Columbia (92I/2); *Ministry of Energy and Mines*, Geological Fieldwork, Paper 1992-1, pages 427-432.

Matheson, A., Grieve, D.A., Goodarzi, F. and Holuszko, M.E. (1994): Selected thermal coal basins of British Columbia; *Ministry of Energy and Mines*, Paper 1994-3.

Matherson, A. and Sadre, M. (1991): Subsurface coal sampling survey, Bowron River coal deposits, Central British Columbia; *British Columbia Ministry of Energy and Mines*, Geological Fieldwork, 1990, Paper 1991-1, pages 391-397.

Mavor, M., Pratt, T. and DeBruyn, R.P. (1999): Study quantifies Powder River coal seam properties; *Oil and Gas Journal Special*, April 26^{th} 1999, pages 35-42.

McMechan, R.D. (1983): Geology of the Princeton Basin; *British Columbia Ministry of Energy, Mines and Petroleum resources*, Paper 1983-3.

McConnell, R.G. (1891): Report on exploration in the Yukon and Mackenzie Basins; *Geological Survey of Canada*, Annual Report 1888, 1889, Volume IV, Part D.

McLearn, F.H. and Kindle, E.D. (1950): Geology of Northern British Columbia; *Geological Survey of Canada*, Memoir 259.

Meissener, F.F. (1984): Cretaceous and Lower Tertiary coals as sources for gas accumulations in the Rocky Mountain Area; *in* Hydrocarbon Source Rocks of the Greater Rocky Mountain Region; Woodward, J. Meissener, F.F. and Clayton, J.L. Editors, *Rocky Mountain Association of Geologists*, 1984 Symposium, pages 401-431.

Papic, M.M., Warren, I.H. and Woodley, R.M. (1977): Hat Creek coal utilization; *Canadian Institute of Mining and metallurgy*, Bulletin November 1977, pages 99-105

Pearson, D.E. (1987): Petrographic analysis of Bulkley Valley Sample #2; Unpublished Report for Atna Resources Limited.

Perry, J.H. (1986): Coal Project West-Central British Columbia Bulkley River Property; Unpublished report for Atna Resources Limited.

Pratt, J.T., Mavor, M.J. and DeBruyn, R.P. (1997): Coal gas resource and production potential of sub bituminous coal in the Powder River Basin; *1997 International Coalbed Methane Symposium* Tuscaloosa Alabama, pages 23-34.

Read, P.B. (1987): Tertiary stratigraphy and industrial minerals, Princeton and Tulameen Basins, British Columbia; *Ministry of Energy and Mines*, Open File 1987-19

Read, P.B. (1988): Tertiary stratigraphy and industrial minerals, Merritt Basin Southern, British Columbia; *Ministry of Energy and Mines*, Open File 1988-15

Richards, T.A. (1981): Hazelton Map Sheet, 93M; *Geological Survey of Canada*, Open File Map 720.

Ryan, B.D. (1991): Geology and potential coal and coalbed methane resources of the Seaton Coal Basin (93M/3,7); *in* Exploration in British Columbia 1990, *B.C. Ministry of Energy, Mines and Petroleum Resources*, Paper 1991-1, pages 153-167.

Ryan, B.D. (1991): Geology and potential coal and coalbed methane resource of the Tuya River Coal basin; *B.C. Ministry of Energy, Mines and Petroleum Resources*, Paper 1991-1, pages 419-427.

Ryan, B.D. (1992): An equation for estimation of maximum coalbed-methane resource potential; *BC Ministry of Energy, Mines and Petroleum Resources*, Geological Fieldwork 1991, Paper 1992-1, pages 393-396.

Ryan, B.D. (1996): Lignite occurrences on the Coal River Northern British Columbia (94M/10); *in* Geological Fieldwork 1996, *B.C. Ministry of Energy and Mines*, Paper 1996-1, pages 271-275.

Ryan, B.D. and Takkinen, M. (1999): Insitu fracture porosity and specific gravity of highly sheared coals from southeast British Columbia (82G/7); *B.C. Ministry of Energy and Mines*, Geological Fieldwork 1999, Paper 2000-1, pages 359-371.

Ryan, B.D. (2002): Cleat development in some British Columbia coals; In press); *B.C. Ministry of Energy and Mines*, Geological Fieldwork 2002, Paper 2003-1.

Swaren, R. (1997): Merritt Coalfield preliminary evaluation; Coal Assessment report 760, *Ministry of Energy and Mines*.

Shaw, W.S. (1952): The Princeton Coalfield, British Columbia; *Geological Survey of Canada*, Paper 52-19.

Smitheringale, W.Y. (1953): Report on coal occurrences, Tuya and Thaltan Rivers, Telegraph Creek area, B.C.; Coal Assessment Report 245, *Ministry of Energy and Mines*.

Snowden, L.R and Powell, T.G. (1982): Immature oil and condensate-modification of hydrocarbon generation model for terrestrial organic matter; *American Association of Petroleum Geologists*, Bulletin, Volume 66, pages 775-788.

Verzosa, R. (1981): Geological summary ant thermal coal potential of the Bowron River Coal property of Norco Resources Ltd; Coal Assessment report 760, *Ministry of Energy and Mines*.

Vincent, (1979): Geological mapping, Tuya River Property, British Columbia, Esso Minerals Canada; Coal Assessment Report 246, *Ministry of Energy and Mines*.

Williams, M.Y. (1944): Geological reconnaissance along the Alaska Highway from Fort Nelson, British Columbia to Watson Lake, Yukon; *Geological Survey of Canada*, Paper 44-28.

Williams, V.E. and Ross, C.A. (1979): Depositional setting and coal petrology of Tulameen Coalfield south-central British Columbia; *American Association of Petroleum Geologists* Bulletin, Volume 63, pages 2058-2069.

Cleat Development in Some British Columbia Coals

By Barry Ryan
New Ventures Branch

INTRODUCTION

Many coal seams contain coalbed methane (CBM) yet most of the world's production comes from the San Juan Basin in the United States. In fact CBM production from this basin of about 0.9 tcf/yr accounts for about 80% of the CBM production in the US (1.2 tcf/yr) and about 60% of world production. Success in the San Juan Basin is not because of increased gas content in the coals compared to coals in other basins, rather it is because of permeability. Permeability of CBM through coal seams is generally the most important coal seam property affecting the viability of a CBM field and it is controlled mainly by the degree of cleat development. Cleats are orthogonal closely spaced tension fractures characteristic of coal seams and their importance in controlling permeability in coal seams is documented and discussed in numerous papers.

This paper discusses cleats and describes cleating and other structural features seen in a number of coal outcrops in British Columbia. A version of the paper containing numerous photos of cleats in British Columbia coals is available on CD from the Ministry of Energy and Mines.

All coalmines in operation in British Columbia in the last few years were visited, as well as a number of properties where good coal exposures exist. Also notes are provided on some other properties that the author has visited over the years. The mines and properties discussed are located in Figure 1.

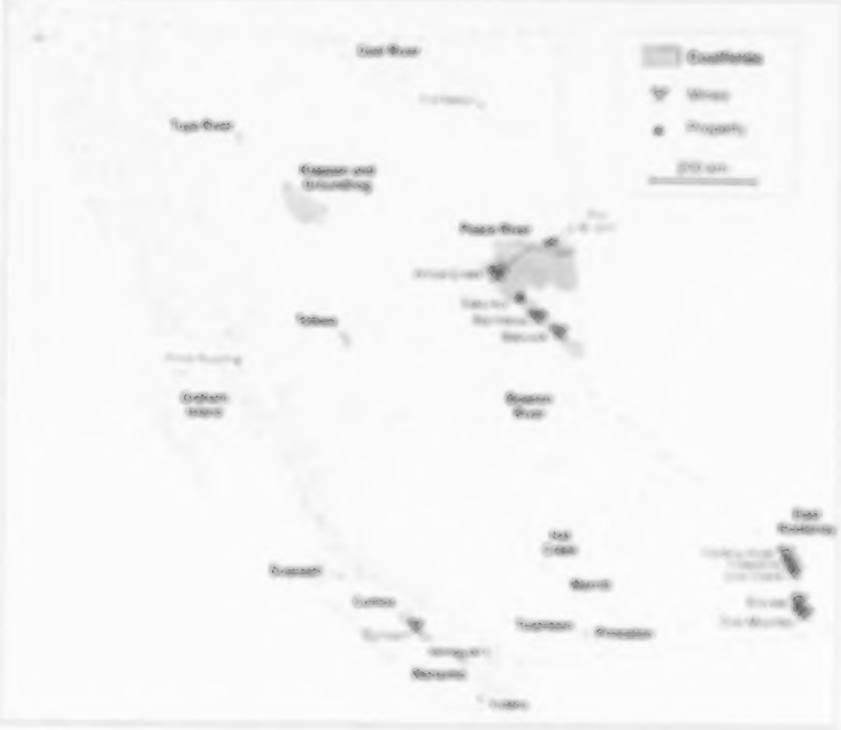

Figure 1. Regional map locating areas visited during this study.

In general there are three tectonic settings useful for describing cleat development and preservation in coals in British Columbia.

- Coals in the northeast and southeast coalfields and the Bowser Basin (Klappan and Groundhog coalfields) have experienced varying degrees of folding and thrusting. Coals are variously cleated, shear jointed or fragmented.
- Cretaceous coals at Telkwa and on Vancouver Island in general experienced only mild folding and steep angle faulting. Coals are well cleated when not close to faults.
- Coals in a number of Tertiary basins are generally of low rank and have experienced simple tectonic histories. Coals are generally well cleated.

SOME GENERAL COMMENTS ON CLEATS

A number of authors have described cleats in coal and Laubach *et al.* (1998) provide a comprehensive summary. The approach taken in papers may be purely descriptive, describing the geometry of cleats and degree of development, or may attempt a genetic classification by outlining possible origins of cleats.

A descriptive or geometric classification is used by a number of authors (Ferm, 2002) and to some extent in this paper. The simplest descriptive classification refers to cleats as face or butt cleats depending on degree of development and then records their spacing and planar extent. This can usually only be estimated by measuring height of cleats as it is generally not possible to measure cleat development into the outcrop. Surface coating of cleats indicates that at one time they were open, though they may now be cemented. Otherwise it is difficult in outcrop to estimate the relative openness of cleats, especially in mines where most outcrops are the result of blasting and excavation in the immediate area, both of which tend to open cleats.

The degree of cleat development varies through seams depending on lithotypes. Dull lithotypes (inertinite rich layers) tend to be massive and poorly cleated whereas bright lithotypes (vitrain rich layers) are often finely banded and well cleated. The best descriptive approach involves measuring and describing cleat sets, where developed, but also attempts to provide a description of the seam as a whole in terms of degree of fragmentation. This approach is used by Frodsham and Gayer (1999) in their description of deformed coals in South Wales, UK. Using their approach, it is possible to recognize a progression in the degree of fragmentation and shearing of the whole coal seam as indicated below.

1. Parts of the seam are massive and preserve original compositional banding, if present, and maybe some widely spaced cleats. Other parts that are vitrain rich contain closely spaced cleats.
2. The seam is cleated though out with cleats that are perpendicular to bedding but it also contains sets of shear joints that are not perpendicular to bedding. These inclined joints break the seam into random sized and shaped fragments.
3. The seam is highly fractured into fragments less than 1 centimeters caused by folding or shearing. Any early cleating is destroyed and late forming cleats do not form because the seam is already fragmented. Fragments may reveal minor (drag ?) folds in the seam.
4. The degree of shearing increases and vitrain rich zones are reduced to a grit or powder consistency. Some bands of powdered coal form at acute angles to hanging wall and footwall.
5. The original layering in the seam is largely destroyed. Finely crushed coal is compacted and cut by closely spaced shear surfaces of variable orientation. The surfaces are fluted or striated with lineations having a variable orientation. The surfaces are curved rather than planar and have a greasy luster. They are similar to surfaces described by Bustin (1982a, 1982b) who compared some of them to cone in cone structure or shatter cones (Bustin (1982a)).

This type of descriptive approach is useful because it emphasizes the overall appearance of the seam rather than concentrating on those areas where well preserved cleats are visible and only recording their orientation and appearance.

Ammosov and Eremin (1963) used a genetic classification. A detailed study by these authors classified fractures in coal as endogenetic (related to coal maturation) or exogenetic (related to tectonism). Endogenetic fractures in coal are the classic "cleats" that form under tension probably in response to dewatering and shrinkage of the coal matrix as coal rank increases. Exogenetic fractures are formed by regional stress fields and their orientations are controlled by these fields. There is therefore no reason why they should be restricted to coal seams.

ENDOGENETIC CLEATS AND COAL MATURATION

Law (1993) describes a relationship between cleat spacing and coal rank, with cleat spacing decreasing as rank increases, in the same fashion as the moisture content of coal decreases with increasing rank. The implication is that cleat spacing is related to the loss of water as rank increases. Alternatively cleat spacing at a particular rank could be related to the strength or compressibility of coal at that rank. The first explanation for endogenetic cleats leads to an early origin related to progressive maturation. The second leads to a late origin associated with uplift and decompression.

Formation of early formed endogenetic cleats is probably related to shrinkage of the bulk coal caused by loss of water and volatile matter during progressive coal maturation. It is possible to estimate the loss of mass of coal, as rank increases, by using average inherent water and as-received volatile matter contents for different ranks starting with lignite. The required coal quality data are available in coal petrology textbooks such as Taylor *et al.* (1998). It is assumed as a first approximation that the amount of fixed carbon in a sample does not decrease as rank increases. It is then possible, using matching values of volatile matter (daf) and rank (mean maximum reflectance Ro values) to track the decrease in coal mass and mass or volume of water and volatile matter expelled as rank increases. The volume occupied by the expelled volatile matter is estimated by converting rank into temperature using relationships in Taylor *et al.* (1998) and then using a geothermal gradient to derive depth and hydrostatic pressure. This method of estimating coal mass loss with rank probably provides a minimum estimate because some fixed carbon is converted to volatile matter as rank increases.

It is possible once weight loss is calculated to use standard estimates of coal density for different ranks, to calculate the volume decrease of the coal mass generated by the loss of volatile matter and water. In-situ coal density is difficult to measure (Ryan, 1991) but values do not change much as rank increases and are in the range of 1 to 1.4 (corrected to an ash-free basis). This volume is the volume available for the water and volatile matter to occupy.

Obviously there are a lot of assumptions and approximations made in the calculations; however by the time lignite is converted to a rank of Rmax 0.7%, it is estimated that its volume has decreased by over 50% (Figure 2). In the calculations the starting coal is lignite to sub-bituminous coal from Hat Creek (British Columbia), which has a rank of Rmax = 0.30% to 0.5% over a depth of range 600 metres (Goodarzi and Gentzis, 1987). It is possible plot the incremental coal mass loss as rank increases (Figure 3). The curve has 2 maxima at temperatures of about 50°C and 100°C and these temperatures correspond approximately with the production of CO_2 and water at low temperature and CH_4 at higher temperature (Rightmire, 1984). The effect of adsorption onto the coal of gases distilled out of the coal as rank increases, does not have much effect because at the temperatures in effect, adsorption capacity is low compared to the amount of gas generated.

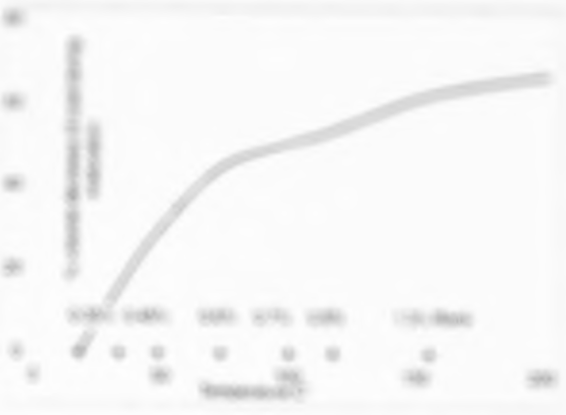

Figure 2. Estimates of percent volume decrease versus rank.

The first maxima accounts for most of the volume decrease of the solid coal and is probably accompanied by the formation of face cleats. There will be a lot of water movement along these cleats and there may be precipitation of low temperature minerals such as kaolinite on the cleat surfaces (Spears and Caswell, 1986). The higher temperature maxima corresponds with the volume decrease associated with the production of methane and only a little water by the coal. It is possible that this dry volume decrease is associated with the formation of butt cleats. Butt cleats are cleats that form at 90° to and terminate against face cleats. In this model butt cleats may not be present in low rank coals that had not reached sufficient rank to generate large volumes of methane. Because the butt cleats form after most of the water has been driven off the coal they are less likely to be mineral coated. Minerals likely to form on butt cleats at high temperature include calcite (Spears and Caswell, 1986).

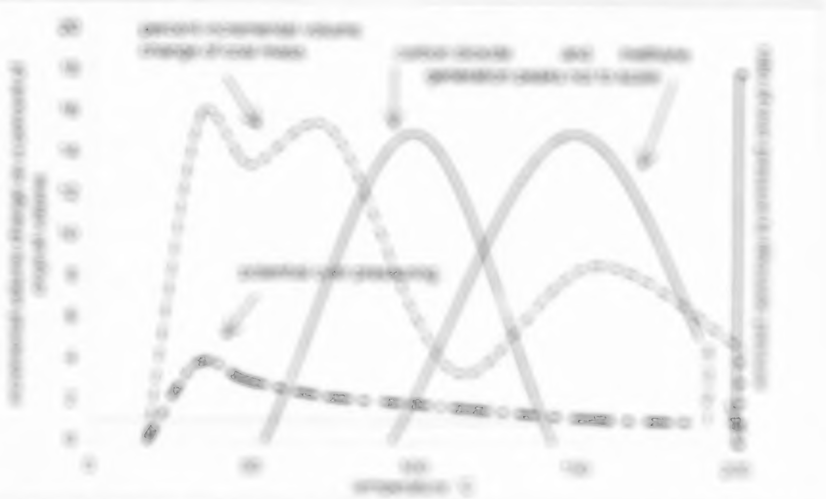

Figure 3. Incremental volume decrease during coalification, potential cleat spacing and approximate temperatures for generation of carbon dioxide and thermogenic methane.

[illegible]

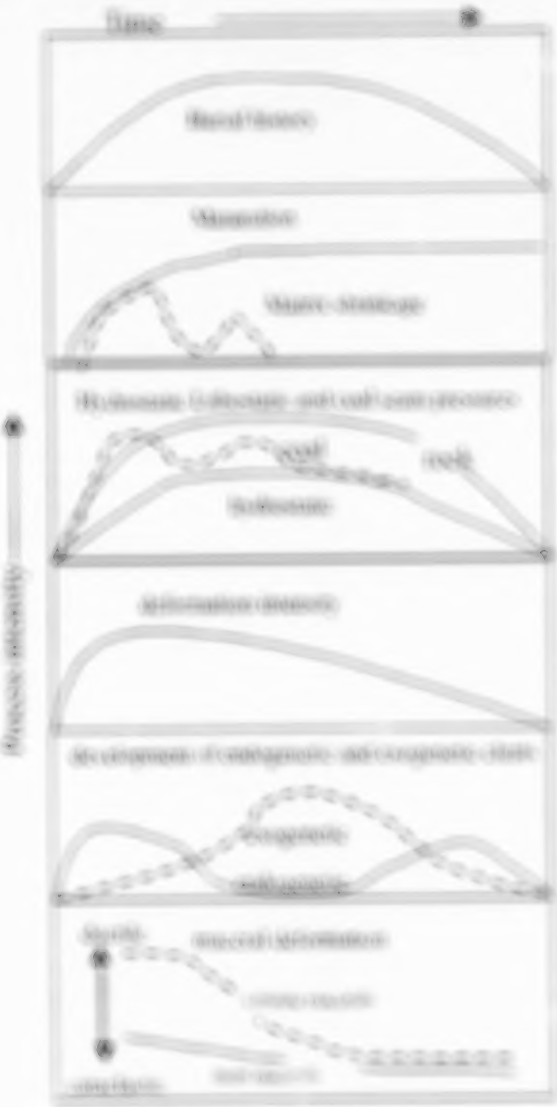
Time
Burial history
Maturation
Matrix shrinkage
Hydrostatic, lithostatic, and coal seam pressures
coal
rock
hydrostatic
deformation intensity
Development of endogenetic and exogenetic cleats
exogenetic
endogenetic
shallow
deep
Process intensity

Figure 9. Schematic of various processes that influence cleat development.

[illegible]

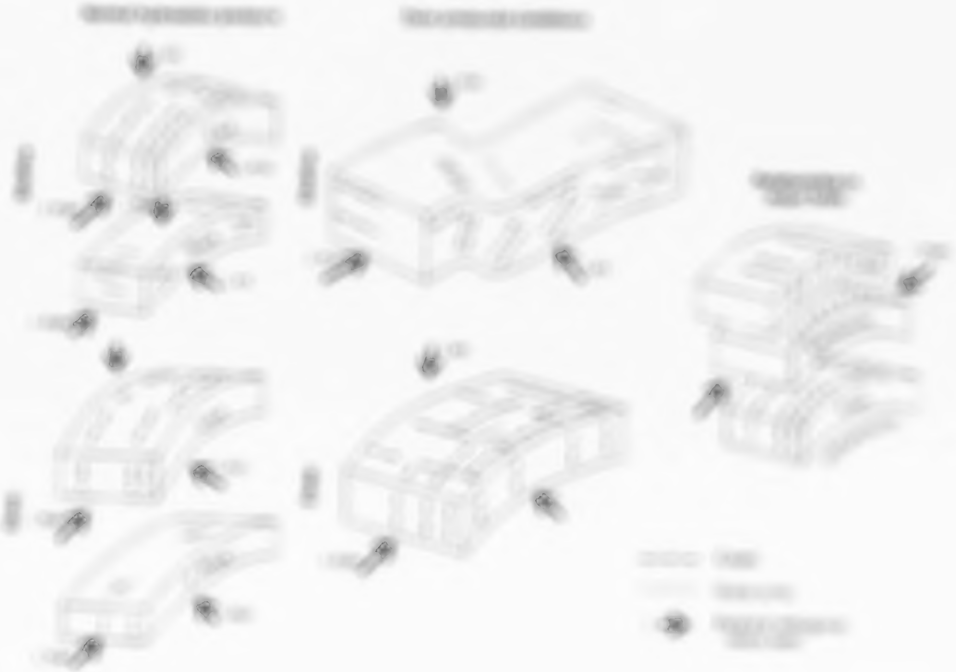

[illegible]

[illegible]

[illegible]

[illegible]

[illegible]

[illegible]

[illegible]

are annealed at higher ranks. Xianbo *et al.* (2001) also describe annealed cleats in higher rank coals.

Face cleats or the better developed endogenetic cleats are often perpendicular to the regional fold/basinal axis, for example the San Juan Basin (Close and Mavor, 1991), the Mississippian and Pennsylvanian anthracite fields (Levine and Edmunds, 1993) and the Greater Green River basin (Laubach *et al.*, 1993). They are considered to form parallel to the direction of regional compression (Tyler, 2001). Butt cleats, which terminate against the face cleats, are therefore generally oriented parallel the basin axis and often intersect bedding to form a line parallel the strike of the bedding.

EXOGENETIC CLEATS AND COAL MATURATION

Exogenetic fractures (fractures of tectonic origin) in coal are obviously of prime concern in the northeast and southeast coalfields of British Columbia. They are not necessarily perpendicular to bedding and their geometries are controlled by regional stress fields. In contrast to endogenetic cleats, they may form under compression and therefore tend to generate powdered coal, which can migrate and damage permeability. Experience in Russia (Ammosov and Eremin, 1963) indicated that increased development of exogenetic fractures in coal progressively decreased permeability to the point that it was difficult to drain methane (CH_4) from underground mining blocks. Development of exogenetic fractures in coal is in part dependent on the strength of the litho types that make up the seam. Ammosov and Eremin (1963) indicate that coal strength is a minimum for medium rank coals and consequently coals of this rank will tend to develop a greater frequency of exogenetic fractures as well as endogenetic cleats. Hardgrove Index is a measure of the friability of coal (high numbers equal friable coals) and is a measurement used to appraise coals for mining and handling characteristics. It varies with rank indicating a minimum hardness at medium rank (Figure 6 from Yancy and Geer, 1945). The variation is not as extreme as the variation in cleat spacing with rank (Law, 1993) and this might be interpreted as evidence for an early endogenetic origin for many cleats.

Hardgrove Index values often exist in the literature separate of CBM studies. If they indicate that a coal is more friable than expected for its rank then the coal is probably fragmented and not cleated. If numbers are lower than expected, then the coal is hard considering its rank and may contain a predominance of inertinite. It is likely to be less fragmented and well cleated compared to coals of similar rank with higher Hardgrove Index values.

It is important to remember that exogenetic cleats owe their origin to regional or local stress fields and not coal maturation. They are therefore more likely to extend across hanging wall and footwall boundaries. This may make it difficult to dewater and de-pressure a coal seam without also accessing the surrounding lithologies. As mentioned, coal maturation may occur before the surrounding rocks are coherent enough to fracture. Therefore exogenetic fractures in coal and surrounding rocks may form after endogenetic cleats in seams.

CLEATS AND MATRIX SHRINKAGE CAUSED BY DEGASSING

Matrix shrinkage, initiated by gas desorption, has been discussed by a number of authors (Harpalani and Chen, 1997). Coal that over its life desorbs 500 scf/t (15.6 cc/g) actually looses about 11 kg of mass per tonne (1.1 wt%). If the gas was held in the coal with the density of a liquid then this accounts for about 3% of the volume of the coal. The coal may or may not shrink to accommodate this volume loss. Obviously if the 500 scf/t of gas is concentrated in only part of the coal (vitrain rich bands), then the shrinkage in some layers will be much greater. Matrix shrinkage increases permeability as long as the rate of shrinkage is greater than the strain rate induced in the coal as a consequence of the decrease of hydrostatic pressure resulting from pumping the water out of the seam. Reducing hydrostatic pressure increases deviatoric stress and initiates a strain response in the coal.

Some coals are substantially under saturated. This may be the result of degassing at their present location or indicate that the coal was unable to adsorb gas, as temperature decreased and adsorption capacity increased, during uplift. If under saturation is the result of degassing, then it must be accompanied by matrix shrinkage that might leave evidence in the form of cleats or micro fractures. There is sometimes a correlation between vitrinite content and micro permeability (Clarkson and Bustin, 1997) and between permeability and degree of under saturation (Bustin, 1997). In situations where ground water movement starts to strip gas from coal, the accompanying matrix shrinkage may form micro cleats and accelerate the process. It might be possible to recognize micro fractures associated with matrix shrinkage under an optical microscope or scanning electron microscope.

In the more deformed seams in northeast and southeast British Columbia, coal has flowed into fold hinges, along thrusts or along duplex surfaces within seams. Movement of coal into lower pressure areas may trigger desorption and

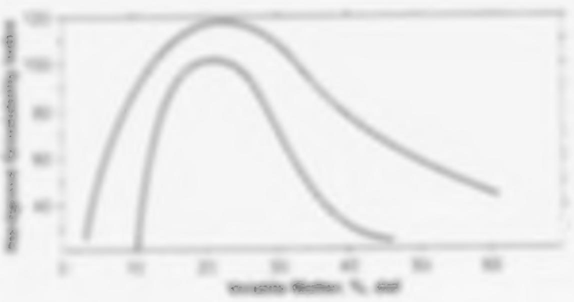

Figure 6. Variation of Hardgrove Index with rank from Levine (1993).

matrix shrinkage and generally aid the flow process. Unfortunately this will produce sheared and degassed coal. As the structural regime changes and pressure increases, coal will be under saturated and may adsorb methane or carbon dioxide. It is important, that once desorption and matrix shrinkage start, that the desorbed gas can migrate. If this is the case, then there may be rapid desorption with a half life for desorption approaching that of coals in a canister where half lives are often less than 1 day. Half life is obviously related to pressure drop and gas content and together both provide information on the stain rate produced by matrix shrinkage. Matrix shrinkage associated with pressure drop and degassing, may, to some extent, be countered by elastic expansion. The strain rate induced by a rapid decrease in pressure can be estimated from the relationship of (delta Volume) / Volume to pressure and pressure to gas content (isotherms). For example if pressure decreases by 4 MPa (equivalent to about 400 metres) and coal looses half its gas in 1 day for a 1% shrinkage then this could indicate a strain rate of 1.16×10^{-7} Sec^{-1}. This rate is much faster than geological strain rates. There may be situations where deformation and changes in hydrostatic pressure can initiate degassing and matrix shrinkage in coals, with the accompanying strain rate greater than normal geological strain rates.

SOME COMMENTS ON THRUST AND FOLD GEOMETRIES

Thrust thickening of coal, seams is more prevalent in seams low in the Mist Mountain Formation in southeast British Columbia than in the Gething and Gates formation coals in northeast British Columbia. Seams are thickened by combinations of thrusting, duplexing and cataclastic flow. It is important to consider the mechanisms of these processes and to understand the implications on coal quality and permeability. In simple terms the three processes re arrange the internal layering or coal quality variations in different ways. Thrusting produces a repetition of any quality variations within the seam (*i.e.* higher ash or inertinite in the upper part of a seam). Duplexing increases the seam thickness but does not totally destroy the original quality layering within the seam. Cataclastic flow, in the extreme, homogenizes any quality variations in the seam. All three processes probably destroy or damage any regional flow paths along seams in terms of through going cleat systems.

Thrusts may traverse footwalls or hanging walls of seams, but on close inspection it is obvious in many seams that there is also a lot of internal deformation, which in some cases appears to have developed into duplexing within seams. Geometries of this type of deformation are described by (Boyer and Elliott, 1982), Gayer (1993) and Frodsham and Gayer (1999). Gayer (1993) described polished, closely spaced, sigmoidal surfaces oriented at 30° to 45° to bedding that result from internal deformation in seams experiencing progressive easy slip thrusting (PEST). Surfaces of this type are prevalent in seams in southeast British Columbia. The intersection of these shear fractures with the hanging walls usually defines the regional fold axis trend. If they are not pervasively developed then regional permeability will be anisotropic and best along fold axis directions. Bedding plane slip and duplexing have been described in seams in China (Li, 2001) and are responsible for increased risk of mine outbursts. The sheared and powdered coal has low permeability and tends to seal in gas until mining reduces most of the confining pressure. It is not clear if the shearing increases the ability of coal to adsorb gas. Studies in southeast British Columbia appear to indicate that shearing does not affect coal adsorption capacity (Vessey, 1999).

The combination of thrusting and duplexing may destroy permeability in seams but it can generate tension fractures in the hanging wall rocks. The process of developing horses within seams and differential movement between footwall and hanging wall forms an anticline and syncline pair in roof rocks that migrates forward as thrusting and duplexing develop (Boyer and Elliott, 1982). The forward propagation of these folds produces extensional features in the hanging wall rocks and dilation of the coal as they pass. As they migrate forward fluid pressure in the local area may be reduced and coals partially degassed. This is not important in terms of CBM resource because the process probably occurs during the early stages of coal maturation and before generation of thermogenic methane. If the coal is not already fragmented, folding and decrease in hydrostatic pressure may allow fold axis normal cleats to form, however the predominant orientation of cleats will probably be axial planar. Because of fold migration in the hanging wall rocks in the thrust direction, these rocks may be extensively fractured out of keeping with the present fold style and intensity.

Folds in adjacent lithologies can cause extension or compression in coal seams. Competent units fold by flexural slip or buckling, in which case regions of extension and compression are controlled by the neutral surface (surface of zero strain). A seam folded into an anticline may experience extension (above neutral surface) or compression (below neutral surface), depending on its relative position with respect to the neutral surface in an adjacent competent sandstone. Identifying these regions may outline fold axis oriented areas of improved permeability. In a tectonic regime where seams are developing folds and are not over pressured, regional cleats will form normal to the fold axis direction (Figure 6) though local cleats may form parallel the fold axis in local regions of extension.

RELATIONSHIP BETWEEN COAL MATURATION AND DEFORMATION

Coalfields in the northeast and southeast of British Columbia have experienced varying degrees of thrusting and folding. This needs to be considered when exploring in the coalfields for CBM. It is important to match coal maturation and the accompanying shrinkage of the coal mass, with the deformation history in order to understand the interplay between the formation of endogenetic and exogenetic fractures in seams. Coal shrinkage during maturation influences the formation of face cleats (and maybe butt cleats) and the formation of larger structures in seams.

There is probably a strong linkage between thrusting and early coal maturation (ranks from lignite to high-volatile bituminous) in coal sequences, where thrusting forms part of the deformation history. Gayer (1993) suggests that fluid over pressuring in seams causes thrusting. He has built on the descriptions of thrust geometries by Boyer and Elliott (1982) to explain thrust geometries seen in seams and describes progressive easy slip thrusting (PEST) imitated in coals because of fluid over pressuring. Over pressuring is a direct result of dewatering and de-volatilization associated with increasing coal rank. There is therefore a close relationship between the environment in which coal progresses through the ranks of lignite to high-volatile bituminous and the initiation of thrusts associated with thick seams.

Over pressuring within a seam provides the ideal conditions for thrust development. Even with the escape of some fluid, if hydrostatic pressure is equal to lithostatic pressure, then after a coal mass volume decrease of 50%, the coal will be effectively floating and experiencing no deviatoric stress. In these conditions over pressuring probably causes extension in the vertical direction, rather than the horizontal, and horizontal tension fractures form. It may also be responsible for the generation of coal fines rather than a coherent set of cleats.

Thrusts initiated in coal seams by over pressuring form at moderately shallow depths and at these depths over pressuring will produce bedding parallel fractures that will participate in thrusting and not aid in the development of cleats. This may explain in part why some seams can be a mixture of highly sheared zones and fairly massive coal. The development of the duplexing and or thrusts may produce, in bands of coal that escape shearing, cleats that are parallel to the axial plane of thrust ramps (Figure 6). In this tectonic regime the orientation of face cleats will vary somewhat between thrust blocks and they will owe their origin to the temporary generation of extension as folds migrate forward during thrusting.

Once the geometries of cleats and fractures in seams are documented, it is important to relate their orientations to that of the present stress field. There are some obvious and important considerations. The contact between coal seams and hanging wall and footwall lithology is probably a surface with low cohesion and therefore principle stress axes will tend to be parallel and perpendicular to these surfaces whatever the dip of the seam. If the present minimum stress direction is perpendicular to the main cleat direction, then there will be a tendency for the cleats to remain or be opened. The magnitude and orientation of the present day stress field described in terms of effective stresses and stress gradients combined with the orientation of cleats and fractures in seams together are by far the most important factors controlling permeability. In fact studies in the Black Warrior Basin indicate that ultimate gas recovery correlates better with the magnitude of the minimum stress within the bedding surface (Shmin) than gas in place (Sparks *et al.*, 1995).

Water disposal is usually one of the costs associated with CBM production. It may be possible to use water disposal from one seam to aid in CBM production from another by enhancing its permeability. If water is injected into one horizon isolated in terms of permeability from a second, then the increase volume in the second zone may open cleats and improve permeability in it. This may help production in shallow buried seams. In more deeply buried seams dewatering a lower seam may produce enough subsidence in an overlying seam to increase permeability. Staged dewatering of a stack of seams may increase produceability in upper seams. In coal sections where seams are isolated by impermeable layers such as bentonites it may be possible to re inject water into depleted seams to stimulate production in other seams and thus gain the double advantage of cheep water disposal and improved permeability.

MICRO DEFORMATION AND COAL MATURATION

The style of deformation of macerals, as seen under the microscope, should reveal something about the timing of deformation relative to coal maturation. To some extent coal is made up of two structural components, one of which is brittle, hard and of unchanging characteristics during maturation (inert macerals) and one that is initially ductile but becomes progressively more brittle as coal rank increases (vitrinite macerals). Evidence for deformation that occurs early during coal maturation will include compaction and rotation effects in vitrinite (collodetrinite) around inert fragments and the general impression of flow structures in collodetrinite. Deformation that occurs later in coal maturation will take the form of micro fracturing, strain shadows and cataclastic flow.

There may also be tendencies towards different microstructures in coal based on whether it was over pressured or not at the time of deformation. If the coal was over pressured at shallow depth in a thrusting environment, in which horizontal cleats were forming, then compaction effects may be perpendicular to cleats and therefore probably act along bedding. The effects would not be very conspicuous but would tend to be visible against the sides of inert fragments buried in collodetrinite. There may also be evidence of flow and rotation of inert fragments in collodetrinite. If the coal is not over pressured, then there may not be signs of rotation and compaction may operate across bedding.

COMMENTS ON COAL SEAM POROSITY

Some geophysical logs measure seam density. If the ash content of seams is determined later when core is recovered, then it is possible using a simple equation (Ryan, 1991 and Ryan and Takkanin, 1999) to calculate porosity. An even simpler way of estimating seam porosity in outcrop is to collect outcrop samples where the seam is water saturated. Seal the sample and send it to a laboratory for a determination of as-received and air-dried moistures. The difference the two moisture analyses will provide a weight of surface water, which if the fracture porosity was saturated can be converted into a volume percent porosity. In small diameter holes drilled to collect coals for desorption, careful use of density logs and coal analyses can provide useful and cheep information about coal porosity, which may correlate with permeability.

COMMENTS ON INDIVIDUAL LOCATIONS

All the mines and a number of coal properties were visited during the study. A lot of photos were taken at the various sites and these are available with the text in the form of a CD from the ministry.

PEACE RIVER COALFIELD

There are two coal-bearing formations in the coalfield (Figure 7). The lower Gething Formation contains coal over an extensive area, though the best development is in the area between the Sukunka and Pine rivers. The formation is enclosed by the underlying Cadomin conglomerate and the overlying Bluesky conglomerate, above which is the marine Moosebar Formation. This formation is overlain by the coal-bearing Gates Formation, which contains coal from the Sukunka River southeast to the Alberta border.

The deformed belt of the coalfield (inner foothills), which trends northwest, is defined by the outcrop of the Gething Formation on the west and a number of major thrusts on the east; the main one being the Gwillam Lake Thrust. East of the thrusts Cretaceous beds dip into the trough of the western Canadian Sedimentary Basin and are in places too deep to be of interest for CBM development. Fold style is generally chevron with well-developed flat limbs and shorter steep dipping limbs. Regional thrusts are west dipping, though at least at Willow Creek (Figure 7) reverse faults and axial planes dip steeply to the east. Locating fold hinges at depth may require knowledge of the dip of axial surfaces.

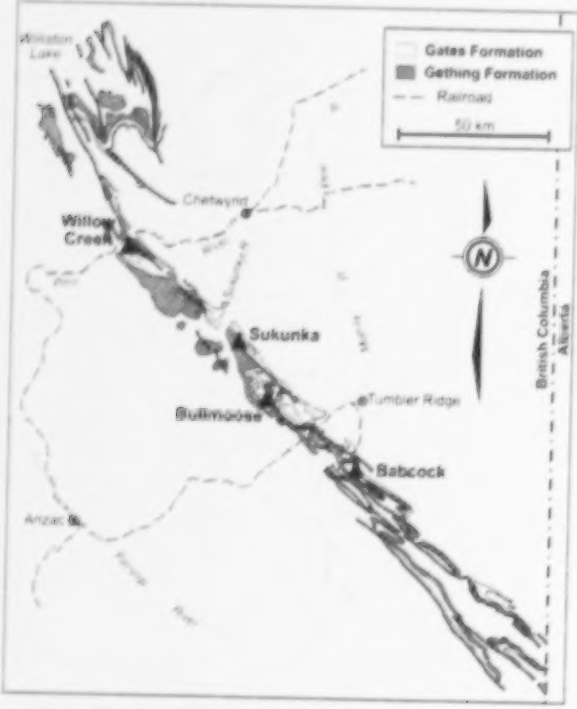

Figure 7. Distribution of Gething and Gates formations northeast British Columbia.

Bachu (2002) studied the present insitu stress regime in the coal-bearing strata of the northeastern plains area of British Columbia and data in his paper may be applicable to coals in the deformed belt to the west in the Peace River Coalfield. Shmin is oriented northwest southeast in the study area (Bachu, 2002) and is therefore following the trend of the regional structures. Permeability will be enhanced in a direction northeast southwest and fractures or cleats with this orientation will have more chance of being open. Langenberg (1990) found that face cleats in the Rocky Mountain Front Ranges are oriented northeast southwest and are therefore perpendicular to the fold axis trends and to the present day Shmin. As mentioned below face cleats in the Gething in the north in the deformed belt appear to be parallel the regional fold trend and face cleats in the Gates to the south tend to be fold axis normal. If these orientations are maintained regionally, then the Gates coals may have better permeability than the Gething coals. However the regional structural trend indicates that drainage areas around individual wells will be elongated in a northwest southeast direction. The ideal situation would be where permeability is also enhanced in this direction.

GATES FORMATION COALS

BULLMOOSE MINE

Coal at the Bullmoose Mine is contained in the lower Cretaceous Gates Formation. Seams at the mine are numbered from A seam at the base of the section, which is about 90 metres thick, upwards to E seam. The cumulative thickness of coal is about 12 metres with B seam being the thickest at about 4.8 metres. Seams A, B and C were observed. The mine will close in 2003 and is now only mining seams A and B.

Seam A is divided into an upper coal, A2 separated from A1 by a parting that can be up to 1.5 metres thick. The seam contains more vitrain than B seam. Face cleats are well developed in vitrain bands and are fold axis normal in the upper and lower zones (Figure 8). Some of the cleats are calcite coated. Low angle shear surfaces dip to the southwest and intersect bedding parallel to the regional fold trend.

Seam B, which is the thickest seam on the property, is generally high in inertinite but has a low ash content of 12%. Cleats strike northeast and southeast. Closely spaced cleats in vitrain bands strike southeast whereas more widely spaced cleats in inertinite rich bands strike northeast. The seam can be massive in places with occasional cleats appearing tight. There is no indication of cement on cleat surfaces.

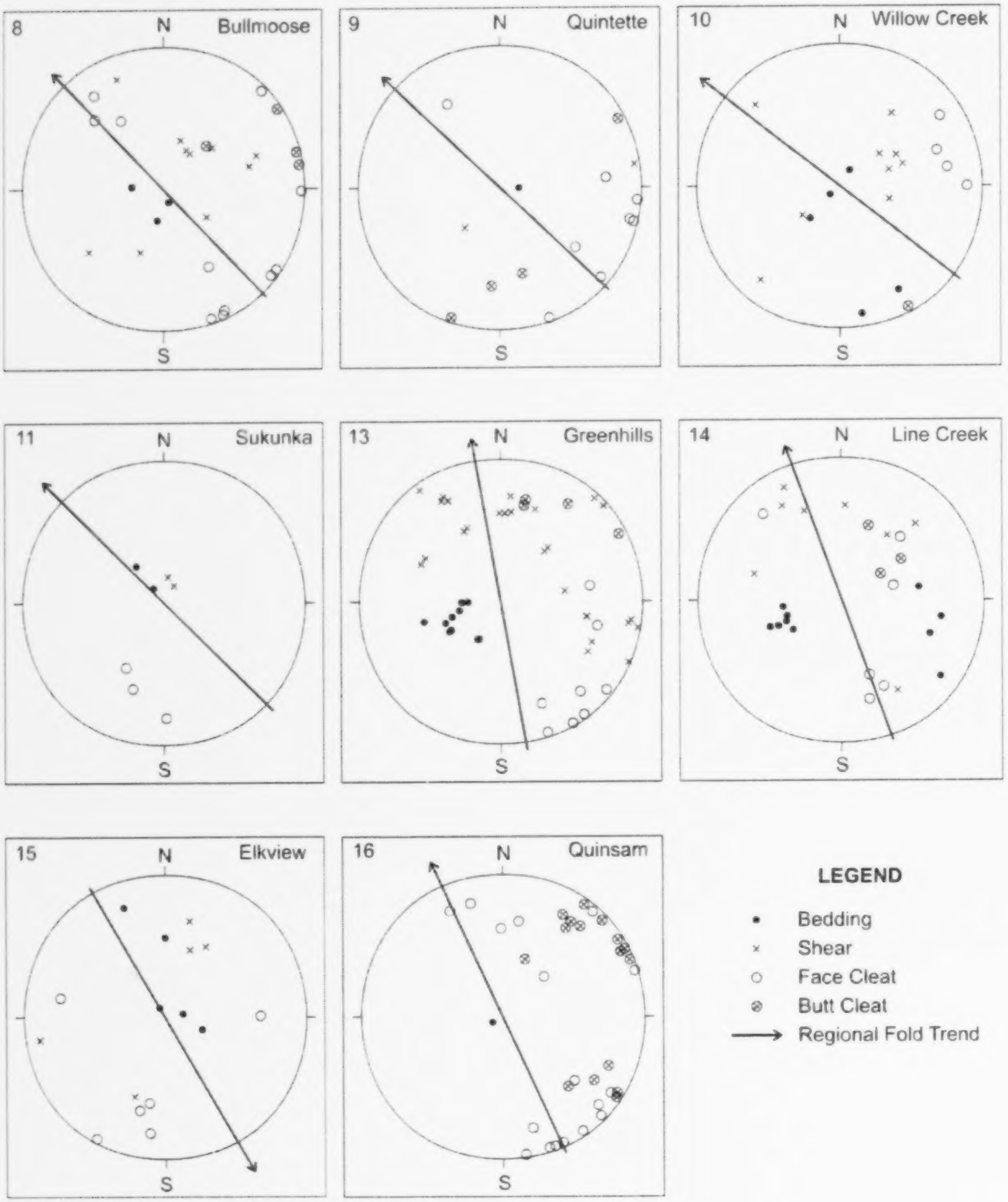

Figures 8 to 11 and 13 to 16. Steriographic plots of poles to bedding, shear joints and cleats for data from the Bullmoose Mine, Quintette Mine, the Willow Creek Mine, the Sukunka property, the Greenhills Mine, the Line Creek Mine, the Elkview Mine and the Number 1 seam Comox Formation Quinsam Coal Mine.

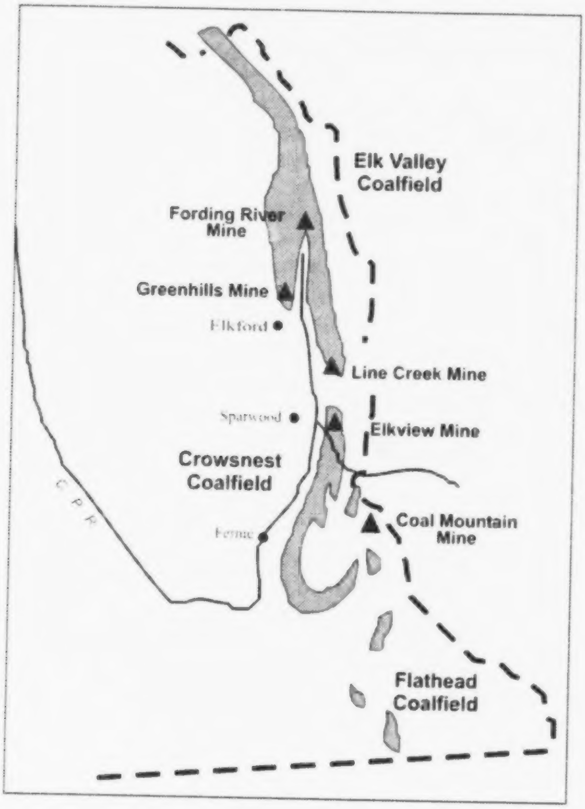

Figure 12. Coalmines and coalfields in southeast British Columbia.

Seam C, which is 1.8 metres thick, has a fairly high ash content (35%) and is inertinite rich. The seam is generally broken into blocks with intervening shear or fragmented zones. Face cleats strike 040° and dip 90° and therefore trend perpendicular to the regional fold trend. Butt cleats strike 135° and dip 47° to the southwest.

Based on limited measurements (Figure 8) the best-developed cleats tend to be fold axis normal as is common in other coalfields.

QUINTETTE MINE

The Quintette Mine extracted coal from the Gates Formation, but to ensure a level of confusion with reference to the Bullmoose Mine, seams are numbered from the base of the section starting at K and decreasing in letter to D at the top of the section, which varies in thickness up to 85 metres. Cumulative coal in the section varies from 14 to 23 metres. The mine is now closed and being reclaimed. During its life a number of deposits were mined in three areas each with different intensities of deformation. Coal on Mesa Mountain is extensively folded and faulted. In the Shikano pit, close to the wash plant, the coal measures are folded into a tight syncline with planar limbs. On Babcock Mountain, the Gates Formation is folded into a broad northwest trending anticline and this is probably the only perspective type of geology for CBM development in the area.

Cleats were measured in a number of seams on Babcock Mountain (Figure 9). K seam, which is the base of the section and thin, appears to be massive but is cut by numerous shear joints that intersect bedding parallel the regional fold direction (Figure 9). Cleats are poorly developed and restricted to small un-sheared blocks of coal between shear joints. J seam is about 4 metres thick and has about 20% raw ash. Cleats are normal or parallel the fold trend and it is not clear which trend formed first or is more persistent as the degree of development of the cleats changes along the outcrop. Seam F, which is 2.5 metres thick, is finely cleated with closely spaced cleats trending north and sub-parallel the fold axis trend. More widely spaced cleats trend east west. Seams E and D appear blocky with interspersed fracture zones.

GETHING FORMATION COALS

WILLOW CREEK PROPERTY

Pine Valley Coal Limited is developing a small open pit mine on the Willow Creek Property, which is 45 kilometres west of Chetwynd. The area is underlain by the Gething Formation, which in its upper 270 metes contains 8 seams numbered from 1 at the top of the section to 8 in the middle of the formation (personal communication, Kevin James, 1999). Cumulative coal in the section ranges from 21.2 metres at Willow Creek central to 16.1 metres at Willow Creek north. To date the company has excavated test pits in seams 6 and 7, which have exposed good outcrops of the seams.

Outcrops of 7 Seam form a monocline with an extensive flat limb and a short near vertical limb that breaks the surface. The steep limb appears to be duplexed with horses formed at an acute angle to bedding in the hanging wall. Cleating is not visible in the seam on the steep limb where slip surfaces intersect the hanging wall along a line parallel the regional fold axis (Figure 10). On the flat limb, 7 Seam contains cleats in occasional vitrain bands but is otherwise fairly massive. Cleats strike sub parallel to the regional fold axis trend. In places low angle southwest dipping shear joints are developed, which destroy cleats. These shears are evidence of the pervasive northeast thrusting and if they continue to develop probably lead to duplexing within seams. It is possible that the duplexing seen in the steep limb predated the folding and the zone of thickening it produced acted as a locus for the development of the fold hinge and steep limb.

The overlying 6 Seam, where exposed, is flat dipping and inertinite rich and consequently fairly massive. Closely spaced cleats are restricted to a single vitrain band and are oriented parallel the fold axis trend. Southwest dipping shear surfaces are also present but not pervasive. The seam is not well cleated where exposed but would probably fracture well under stimulation at the right depth. Inertinite tends to have higher diffusivity than vitrinite and this could compensate for the more widely spaced cleats in the inertinite rich parts of the seam.

In contrast to the Gates Formation in to the southeast the predominant cleats in the Gething in the Willow Creek area are fold axis parallel however the same southwest shear joints are present and in one area have developed to the extent of obliterating the original fabric of the seam.

SUKUNKA PROPERTY

The Sukunka Property is located about 60 kilometres south of Chetwynd and 35 kilometres west of Tumbler Ridge (Figure 1). The main seams are in the Upper Gething and are the Bird seam near the top of the formation and the underlying Chamberlain and Skeeter seams. The Chamberlain seam, which is split into an upper and lower member, is well exposed on the north side of Chamberlain Creek where a number of adits were constructed in the 1970's. The seam is blocky with widely spaced cleats that strike east southeast, approximately parallel the regional fold axis (Figure 11). In places southwest dipping shear surfaces break up the coal. They have similar geometries to those seen at Willow Creek and are evidence of incipient northeast directed thrusts. In general the seam does not contain extensive shear zones and the dip is flat. It is overlain by a prominent sandstone, which may limit the break out of thrusts from the coal seam but may also be permeable allowing for movement of gas and water across the seam boundary.

SOUTHEAST COALFIELDS

Coal is mined in five mines in the 2 major coalfields (Crowsnest and Elk Valley) in southeast British Columbia (Figure 12). Coal in the coalfields is contained in the Mist Mountain Formation, which in the mines varies in thickness from 150 metres at Coal Mountain Collieries to 550 metres at the Fording River Mine. The coalfields are in the upper plate of the Lewis Thrust. Folds in both coalfields trend north to northwest and in part postdate west-dipping thrusts with the same trend. Extension occurred in the Tertiary when the major north trending Erickson Fault formed. It down drops beds on the west and is responsible for the preservation of part of the Elk Valley Coalfield. The western boundary of both coalfields is partially defined by the Bourgeau Thrust.

There have been a number of studies of coal seam deformation in the Crowsnest Coalfield. Norris (1965) studied A seam in underground A-North Mine at the north end of the Crowsnest Coalfield. This seam is approximately 420 metres above the basal Balmer or 10 Seam in the Mist Mountain Formation. He describes the seam as being highly sheared with abundant shear surfaces and intrastratal folds. Joints tended to strike north or northwest with evidence of early minor extension faults cut off by renewed bedding plane slip. He does not directly discuss cleats or the degree of shearing in the seam but the impression is left that the seam is highly sheared and fragmented.

Bustin (1982b) studied the lowest seam in the Mist Mountain Formation in a number of underground coal-mines (Balmer North, Five Panel and Six Panel) at the north end of the Crowsnest Coalfield. In the Balmer North Mine, the best-developed cleats formed acute angles to bedding, striking northwest and dipping shallowly to the southeast. Cleat surfaces were polished and striated. Other cleat sets were measured but did not have a consistent orientation through the mine. Cleats in the Five and Six Panel mines are more consistent with a set striking north to northwest with a steep dip to the west. These cleats are sub perpendicular to bedding and trend parallel to the regional fold axis. All fractures and most cleats in the seam appear to have a tectonic influence, with surfaces polished and often showing evidence of shearing. However their orientations are not easily related to a regional stress field. Thrusting probably started with differential movement between the roof and floor (Norris, 1965) that disrupted earlier extension faults. As seam thickening and thrusting progressed exogenetic fractures with fold axis parallel trends and variable dips to the west developed in the coal.

A number of authors have studied the relationship of coal maturation to thrusting and folding. Bustin and England (1989) studied a number of deep drill holes in southeast British Columbia and concluded that in 7 out of 11 holes a significant component of maturation postdated emplacement of over thrust sheets. In the Crowsnest Coalfield, Pearson and Grieve (1977, 1978) considered a large component of coalification to post-date folding. In that folding was probably synchronous or post dated thrusting, coal maturation must have continued after thrusting. This to be expected based on the correlation of possible over pressuring with low rank coals (Figure 3). In this case a seam could have different ranks in different thrust sheets, depending on depth of burial after thrusting and possibly folding. Obviously it would be very dangerous to generalize about the cleating or permeability in a seam across thrust blocks.

The number of seams in the Mist Mountain Formation ranges from 3 at Coal Mountain Collieries to over 30 at the Greenhills Mine. Unfortunately seam nomenclature varies between the 2 coalfields and between mines. Exploration in the Crowsnest coalfield has generally numbered the seams starting at seam 1at the base of the section. At the northern end on the coalfield mines in the Michel Valley referred to the thick basal seam as the Balmer Seam or at the Elk Valley Mine as the Number 10 Seam. Seam numbers decreased up section until the numbering system is forced to use letters. The same nomenclature is used in the southern end of the Elk Valley Coalfield at Line Creek Mine. In the northern part of the Elk Valley Coalfield seams are numbered 1 at the base of the section with numbers increasing up section. Seams are generally thicker lower in the Mist Mountain Formation and generally contain more inertinite than seams higher in the formation. Often the third seam up in the section has the highest inertinite content.

There has not been a regional study of present day stress fields in the Mist Mountain Formation. Local studies did not find a strong relationship between cleat orientation and regional stresses (Bustin, 1979, 1982).

GREENHILLS MINE

The Greenhills Mine occupies the core of the Greenhills Syncline, which plunges gently to the north. In the pit, seams on the west limb dip at 20° to 40° to the east and on the east limb beds dip 20° to 60° to the west. The east limb is cut off by the north-trending Erickson normal fault. On the regional scale the syncline is not broken by major thrusts but on the local scale there are a number of sub horizontal thrusts with minor offsets.

Up to 33 seams are exposed in the Mist Mountain section, which is about 560 metres thick. Seams are numbered as 1 at the base of the formation with numbers increasing up section. Seams 1 to 6 are not well exposed in the mine at the moment. Previously, where mined, 1 Seam was finely powdered and devoid of cleats. Polished sections of the seam indicate pervasive micro fracturing. A number of seams from 10 Seam up were examined for cleats and fracturing in the northern most footwall of one of the active pits.

Seam10, which is about 6 metres thick is moderately to highly fractured but does contain closely spaced face and butt cleats (Figure 13). Face cleats range in strike from 010° to 060° and are consistently perpendicular to bedding. They appear to be roughly fold axis normal but rotated anticlockwise. Butt cleats seem to have a more consistent orientation and strike parallel the fold axis.

Seam 1, which is about 1.5 metres thick, is generally moderately to highly sheared with only a few zones retaining closely spaced cleats that appear to be approximately fold axis normal. Sheared zones are welded and contain numerous grooved or lineated sigmoidal surfaces similar to the surfaces described by Bustin (1982a). The lineations have variable orientation. Seam 12 is 1.5 metres thick and is similar to seam 11 being highly sheared with remnant cleating that is approximately fold axis normal.

Seams 14 and 16 are fragmented and sheared and in some places coal is welded into a hard dull mass that breaks exposing sigmoidal surfaces with a greasy luster. Seam 17, which is 2 metres thick, is highly fragmented with occasional areas where closely spaced cleating survives.

Seam 18 is 1.5 metres thick. There is no cleating in the seam, which contains pervasive shear surfaces parallel bedding with no clear movement direction. Seam 19 is generally fragmented with a few surviving face cleats that are approximately fold axis normal. In contrast seam 20 seam, which is also fragmented and sheared, has cleats that are approximately parallel the fold axis trend in areas that have escaped shearing. Seam 21 is similar to seam 20.

In places seam 29-2 appears to contain original layering that has not developed cleats. In contrast, Seam 29-3 is sheared and welded with sigmoidal and grooved surfaces. Seam 30 contains original bedding in places but no cleats are present. Seam 31-0 is generally massive with no cleating though there are partings, which parallel bedding. There are areas within the seam, which are sheared to powder along zones parallel the footwall.

Despite the over all appearance of minimal deformation seams generally are fragmented or sheared with cleating surviving in only a few layers within seams. Seams observed occupy the mid to upper part of the section. Shear surfaces within them are either parallel the hanging wall or intersect bedding to define a direction that tends to be perpendicular to the fold axis trend. The shearing therefore has not increased the seam thicknesses and appears to have been directed along the fold axis direction rather than across it. The best-developed cleats form an oblique angle to the fold axis trend but appear to be rotated to the west off a fold axis normal trend. Butt cleats are also rotated westwards off a fold axis parallel trend. Possibly the initial stress field was directed more from the southwest and rotated to a westerly direction after formation of the face cleats.

LINE CREEK MINE

Coal in the Line Creek Mine is mined in a number of pits that occupy the west and east limbs of the north-trending Alexander Creek Syncline, which is truncated by the Ewin Creek Thrust. The syncline extends to the north to the Fording River Mine where it is referred to as the Eagle Mountain Syncline. Coal ranks appear to be lower in the lower thrust block. Seam numbering starts with 10 Seam at the base of the section with numbers decreasing upwards with the upper seams given letter designations. Seams on both limbs of the Alexander Creek Syncline were observed (Figure 14).

On the west limb of the Alexander Syncline, 9 Seam contains cleats in vitrain bands in the lower part. The mid part of the seam is fairly massive and the upper part is sheared and welded. Up section, 8 Seam is composed predominantly dull litho types and is generally massive with about one third of the seam sheared.

About one third of the 7 Seam is massive with no cleats, one third is sheared into small fragments and one third (the lower part of the seam) is massive with vitrain bands that contain some cleating. The top one third of 6 Seam is sheared and does not contain cleats, while the lower two thirds is blocky with shear joints that have shallow plunging lineations. Seam 6 is overlain by a coal-spar rich sandstone that could contain better permeability than normal bedded sandstones and mudstones.

A number of seams were examined on the east limb of the Alexander Creek Syncline below the Ewin Pass Thrust. Seam nomenclature is the same as on the west limb. Seams dip steeply to the west and are noticeably more sheared than on the west limb. Cleating is generally destroyed and where developed tends to be fold axis normal. Seam 8, which contains pyrite disseminated on fractures, is split into at least three members by rock splits. The lower part of the seam contains disseminated spherulites of pyrite or siderite.

ELKVIEW MINE

The mine is at the northern end of the Crowsnest Coalfield. The main pit occupies the Elk Syncline, which trends north on the west side of the Erickson normal fault. Seams are numbered as at Line Creek, though the basal 10 Seam at

Elkview is slightly higher in the stratigraphy than 10 Seam at Line Creek. Only two of the lower seams in the section were observed (Figure 15).

Seams 10 and 8 were examined at different locations in the mine. In general both seams are highly sheared with only a few areas where original banding or cleating survive. Shear surfaces have fragmented the seams into ellipsoidal chips often with striated curved surfaces with a greasy luster. The striations have variable orientations that are not consistently parallel or perpendicular to the fold axis trend. The few cleats measured tend to be fold axis normal.

Seam 10 in the Elk Pit has been thickened by thrusting or duplexing and is completely fragmented or sheared except for lower part where original banding is preserved. In places small-scale thrusts break out of the hanging wall and insert wedges of 10 seam in the overlying rocks. Striations in the sheared part of the seam trend roughly at 90° to the fold axis direction. Seam 8 is completely sheared, in places into ellipsoidal chips that are then folded into small drag folds. Often the slip surfaces have near horizontal striations with variable orientations though some trend 150° roughly parallel the fold axis trend.

FORDING RIVER MINE

Mining is taking place in the Eagle Mountain Syncline, which is the northern extension of the Alexander Syncline at Line Creek and east of the Erickson normal fault, which separates the active pits at Fording River from the Greenhills Mine. There are approximately 15 seams in the section numbered from 1 at the base to 15 near the top. No cleat measurements were made at the mine. The degree of shearing and seam fragmentation is similar to that at the Greenhills Mine.

COAL MOUNTAIN OPERATIONS

The Coal Mountain Mine occupies an outlier east of the Crowsnest Coalfield. Most of the coal is contained in the basal seam of the Mist Mountain Formation. The seam has been folded, thrusted and sheared and original bedding is often obliterated. Coal in some fold hinges has been mobilized to the extent of becoming diapers disconnected from the original fold hinges (personal communication, Pisony 2002). Cleats have not survived and outcrop structures were not documented.

Cretaceous Intermontane and Vancouver Island Coalfields

Coal on Vancouver Island is contained in the Upper Cretaceous Nanaimo Group, which survives in two coalfields. In the north, in the Comox Coalfield, coal is in the Comox Formation and in the south (Nanaimo Coalfield) in the Extension and Protection formations. Coal seams generally dip gently to moderately to the east and northeast. They are broken by north-trending steep-dipping faults and are un-folded to moderately folded. The Quinsam Mine in the northern part of the Comox Coalfield was visited. There are few references to cleats in the rest of the Comox coalfield. Cathyl Bickford (2002) describes cleats in the Comox Number 3 Mine (Number 2 seam) that strike 028° to 033° and dip 70° to 80° to the northwest. Butt cleats strike 115° to 125°.

QUINSAM MINE

There are 4 seams, in the Comox Formation numbered from 1at the base to 4 at the top of the coal section. Surface and underground mining has taken place in seams 1 and 3. Data were collected from the underground mine in 1 Seam and in small surface pits. Seam 1 is blocky and well cleated with cleats generally perpendicular to bedding. Face cleats are spaced between 0.5 and 10 cm apart and individual cleats having visible surface areas of over 1 metre square. Face cleats, which in 1 Seam tend to be calcite coated, strike northeast across the trend of the regional bedding and the basin. Butt cleats strike northwest parallel the strike of the regional bedding and generally are not calcite coated (Figure 16). Cleats are closer spaced and better developed in vitrain-rich coal. Cleats in the upper seams were not systematically observed but the calcite coating is restricted to the lower seam. The east west trending face cleats formed first and the tectonic history allowed them to remain open. Later east west compression tended to close the southeast trending butt cleats. Calcite could therefore have been introduced onto the east west trending face cleats at any time. Spears and Caswell (1986) suggest that calcite is deposited from diagenetic fluids at temperatures of about 100°C.

Early tensional faults, some times associated with calcite veining, trend east west (Kenyon *et al.*, 1991 and Gardner and Lehtinen, 1992). These faults are responsible for graben structures and at surface are identified by low swampy ground. They also appear to act as channels for water into the underground mine. The calcite coated cleat set is either related to these faults or is related to early stresses that formed the north to northwest trending basin.

Gardner and Lehtinen (1992) identify a later period of pull-apart faulting that is largely restricted to 1 Seam zone. These faults are parallel the strike of the beds and are down dropped by a few metres on the down dip side with respect to the regional bed dip. The faults are shallow dipping and consequently produce a barren zone up to 20 metres wide where they cut seams. They probably represent ductile response of the incompetent 1 Seam to buckling and down warping of the sedimentary package. Kenyon *et al.* (1991) describe a later period of northeast to southwest compression. This deformation produced some folds and southwest verging thrusts. They also identify tear faults, trending northeast to east, that are probably post Late Eocene.

TELKWA PROPERTY

Ryan and Dawson (1994) summarized the CBM potential of the Telkwa coalfield (Figure 1) based on exploration data up to 1994 and the following is based on that paper. Since then Manalta Coal Limited conducted a number of exploration programs so that more data are available in coal assessment reports in the Ministry of Energy and Mines, Victoria.

Coal at Telkwa is broken by steep faults but has not experienced much folding and consequently seams are blocky and well cleated. They generally strike northwesterly and dip to the east. northwest-striking east-dipping reverse and thrust faults break the coal measures into numerous fault blocks. Folds are locally associated with these early faults. There are at least two episodes of later normal faulting. Older normal faults trend northerly. A few outcrops of andesite dikes, striking northwest, are apparently associated with these faults. Younger normal faults trend east-west. Folds trend north or northwest with shallow plunges to the northwest or southeast.

Outcrop is sparse but joints were measured in a test pit constructed in 1982. Joints tend to intersect bedding at large angles along a line of intersection trending northwest (fold axis trend) or intersect bedding at large angles along a line, which is perpendicular to the fold axis trend.

Subsurface bed orientations are available from dip meter logs and subsurface joint measurements were made in 1982 during a geotechnical program (Telkwa Stage Two report, 1982). Joint orientations were measured in core relative to bedding. Using dip meter logs to provide bed orientation, it is possible to rotate the joints into their "true orientation" using a stereonet. The technique is approximate because only a single average bed orientation is used to rotate all the joints in a hole. Joint data from 22 holes are summarized in Figure 18, which does not depict the true joint frequency because vertical holes tend not to intersect vertical fractures, despite this, it appears that the joints tend to form a great circle girdle about the northwest trending fold direction. Eigen vectors provide a pole to the great circle girdle trending 316° with a plunge of 1°. This means that the joints intersect the bedding surface along a line parallel to the northwest trending fold axis direction.

It is probable that the face cleats in the coal seams strike northwest and dip steeply east or west, based on the joint data from surface outcrops and drill holes. The surface joint pattern identifies a northeast trending joint set which is perpendicular to the fold trend. This may be the orientation of butt cleats in the coal.

Permeability will be improved in direction trending 315° to 360° (face cleats) and probably to a lesser extent in a direction trending 30° to 60° (butt cleats).

Faults observed in the test pit are generally tight and may block the flow of methane in an northeast direction along seams but probably will also not discharge a lot of water into seams as they are dewatered. The area in each coal seam available to be drained will be limited in a northeast to southwest direction but may extend further in a northwest southeast direction because of the improved permeability in this direction and the absence of cross cutting faults.

To ensure good permeability coal must have sufficient strength to resist overburden stresses and maintain some porosity along the joint surfaces. Data on the uniaxial compressive of rock types (Ryan and Dawson, 1994) indicates that the coal is as strong as the mudstone and weaker than other rock types. Compared to many coals from other areas in British Columbia, Telkwa coal is strong. This is substantiated by the Hardgrove Index values of Telkwa coal, which range from 45 to 65 compared to values of coal from southeast British Columbia that range from 90 to 110. At appropriate depths the coal will respond well to fracing or cavitation.

Permeability measurements were made as part of the Telkwa Stage Two study (Ryan and Dawson, 1994). Permeabilities of seam numbers 2 to 8 in three drill holes in the east Goathorne area were measured at depths ranging from 29 to 158 metres. Permeabilities do not correlate with depth and values range from 0.5 to 50 millidarcies. This range is considered to be excellent for coal, considering the depth of the measurements. Data were reported as hydraulic conductivity (metres per second) and converted to millidarcies.

The permeability of sections of mudstone, siltstone and sandstone interburden varying in thickness from 14 to 27 metres were measured in drill holes north of the Telkwa River. Permeabilities range from 15 to 35 millidarcies. At the depths of less than 200 metres permeabilities of interburden rock and coal are moderate. The permeability of the interburden is on average greater than that of the coal. In order to be able to drain water from seams it will be important to have impermeable hanging wall and footwall material. This information is available in the core descriptions and geophysical logs included in the assessment reports submitted to the British Columbia government.

BOWSER BASIN KLAPPAN AND GROUNDHOG COALFIELDS

The rank of coals in the two coalfields, which are contained within the Skeena fold belt (Evenchick, 1991), is low-volatile bituminous to anthracite. These coalfields have been visited in the past but not in the context of a cleat study. Coal in the Klappan Coalfield has experienced a similar tectonic history to that of coals in northeast BC though the rank is higher. The coal has probably experienced some shearing and fragmentation. In 1982 Gulf Canada Limited excavated a test pit and some undocumented photos of the test pit and outcrops in the region survive (Jahak Koo, personal communication, 1986). The coal at Klappan has fairly high CaO concentrations, which indicates the possible presence of calcite coating on fractures or cleats.

TERTIARY BASINS

Most of the Tertiary basins are relatively undeformed. Exceptions are parts of the Merritt Coalfield and the Hat Creek Basin. Three Tertiary basins were visited.

COAL RIVER PROPERTY

The Coal River property is in the north-east of the province adjacent to the Alaska Highway and 40 kilometres south of the Yukon border. The property contains a resource of up to 200 million tonnes of lignite. A single seam in excess of 5 metres thick, with sub horizontal dip, is exposed either side of Coal River. The seam contains two sets of

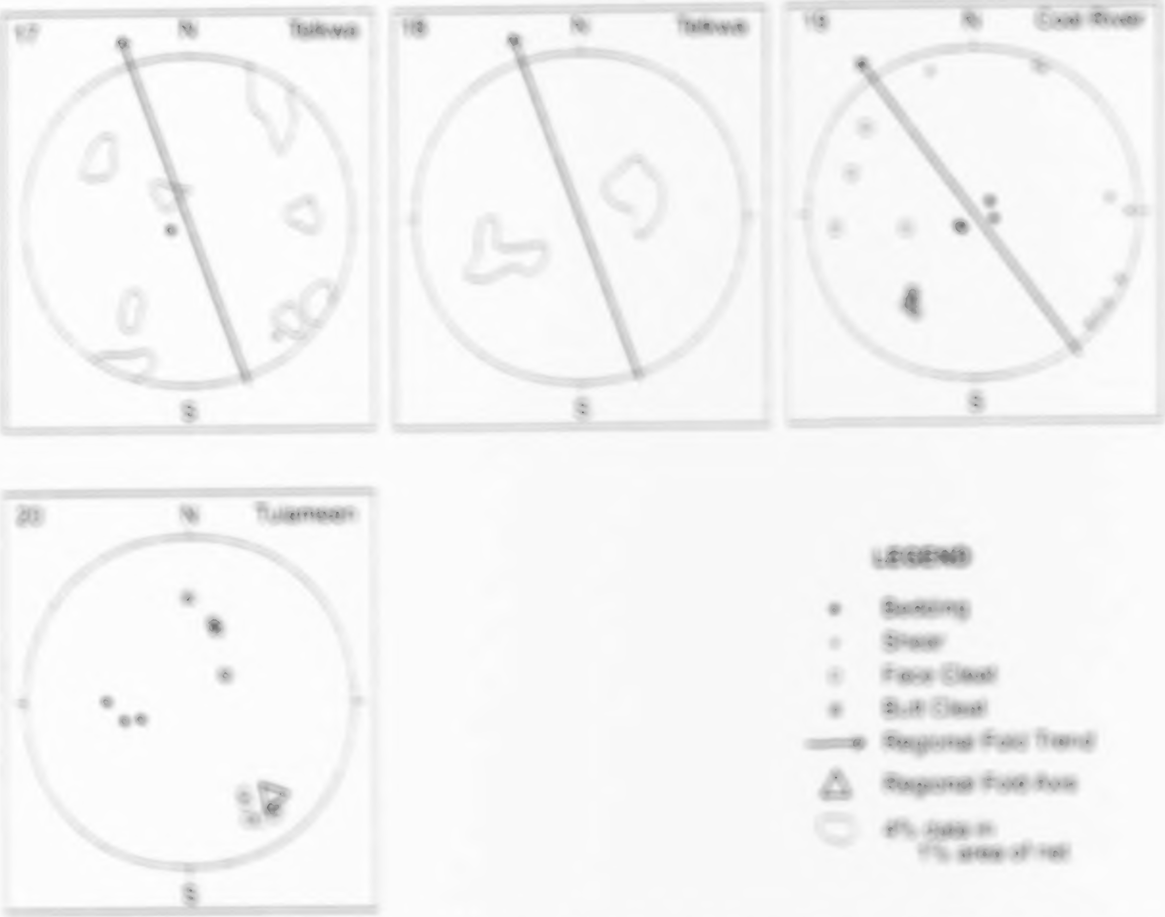

Figures 17 to 20. Stereographic plots of poles to joints from the test pit at the Telkwa Property, from drill core, Telkwa Property, from the Coal River Property and from the Tulameen Property.

cleats. The better-developed set has an average strike of 020° and an 80° dip to the east; the second set has a more consistent orientation and strikes 125° and dips 68° to the northeast (Figure 19). The bedding surfaces contain a strong lineation that appears to either derive from the original vegetation or water movement in the compacting vegetation. It varies in orientation but tends to be oriented between 120° and 180°. Cleats are widely spaced and have the appearance of tension fractures.

TUYA RIVER

The Tuya River property, which is northwest of the town of Dease Lake, was mapped in 1988 by the author (Ryan, 1991). The coal zone is folded into a broad syncline that is cut by normal faults. The coal is massive with well-developed cleats. No cleat measurements were taken.

TULAMEEN PROPERTY

The Tulameen Basin, which is about 20 kilometres northwest of Princeton, forms an elliptical sedimentary basin 5 by 3.6 kilometres that contains two well-developed thick coal seams of high-volatile B bituminous rank. The upper zone, which is 25 to 40 metres above the lower coal zone, is better developed and attains thicknesses ranging from 15 to 21 metres. The lower zone, which is generally less well developed, is 7 to 7.6 metres thick and averages 52% ash.

The basin is part of the Princeton group, which rests unconformably on volcanic and sedimentary rocks of the Upper Triassic Nicola group. Beds appear to be folded into a southeast trending syncline with beds on the southwest limb dipping shallowly to the northeast (20°-25°) and beds on the northeast limb dipping steeply southwest (40°-65°). The plunge of the syncline was estimated by Evans (1978) to be 15° in a direction 130°. Anderson (1978) describes the structure as an asymmetric northwest trending syncline and does not accept a plunge. The area is cut by a number of vertical faults that trend north to northeast (Anderson, 1978).

The upper seam was observed on the west limb in a test pit excavated on 2000 (Figure 20). Bentonite rich partings make up from 10% to 60% of the seam, generally increasing in percentage to the northeast. Coal bands are extreme rich and well cleated with face and butt cleats. Vitrinite sometimes contains cleats. Face cleats are well developed and are oriented perpendicular to the fold axis. Butt cleats appear to be approximately perpendicular to bedding and face cleats and therefore may form an axial plane fan around the fold axis. There are no shear joints in the coal though there is some shearing along the contacts of bentonite bands in the coal seam.

CONCLUSIONS

Coal proximate data gives some indication of the ability of coal to generate over pressure and the amount of volume decrease of the coal mass associated with rank increase. Over pressuring occurs at low rank and may play a part in initiating fracturing. The volume decrease versus rank (or temperature) plot indicates that there are maxima at low and intermediate ranks. The first may be associated with formation of face cleats and possibly fracturing and predates generation of thermogenic methane. The latter may be associated with formation of butt cleats and generation of thermogenic methane.

Possibly useful insights into cleats can be derived if they are considered in the context of forming in over pressured or normal hydrostatic pressured environments. Other important parameters are depth, stress field and timing of coal maturation. Data on cleat development and orientation, as well as mineral textures observed under the microscope, may lead to an understanding of the interrelationships of hydrostatic pressure, depth, stress fields and coal maturation. The intent is to gain useful insights into development of permeability and anything that influences anisotropy of permeability in terms of direction. Permeability of the coal, more than the size of the CBM resource available in a basin, controls the economic potential of the basin.

Permeability decreases exponentially with depth. It increases with cleat development up to the point that the degree of fracturing decreases the ability of the skeletal structure of the seam to withstand lithostatic pressure once hydrostatic pressure is decreased. It also decreases as generation of fine coal increases, because migration of fines blocks flow pathways. It is improved if the present day stress regime is extensional and especially if the direction of extension is perpendicular to cleat surfaces.

The structural geology in northeast and southeast British Columbia is complicated and the conditions supporting improved permeability may be structurally controlled. Many of the fractures are syngenetic and therefore may not be restricted to coal seams. Development of fractures at shallow depth and under conditions of over pressuring produces shear surfaces either parallel to bedding or at small angles to bedding. These surfaces and the over pressuring are responsible for generating fines in coal seams. Generally, the best developed cleats are normal to the regional fold trend. In areas where thrusting predominates, cleats if present may be parallel the regional fold trend and less consistent in orientation.

In coalfields where deformation has not been extensive such as Vancouver Island and Tofino, it is important to identify areas where there is an expectation of a present day stress field that is extensional along the regional fold trend. This may take the form of culminations or depressions along the plunge of folds, draping over buried structures or development of sedimentary wedges. In areas where thrusting predominates one should look for areas where present day extension is normal to the regional fold trend. This may take the form of normal faults following the same trend as earlier thrust faults. Because cleats developed in the over-pressured environment are less consistent in orientation the best permeability direction may be different in different thrust sheets.

In areas where fracturing and permeability are related to the deformation it is important to match CBM economics to classic structural geology domain analysis. If the rationale for good permeability is cleating developed on a flat limb of

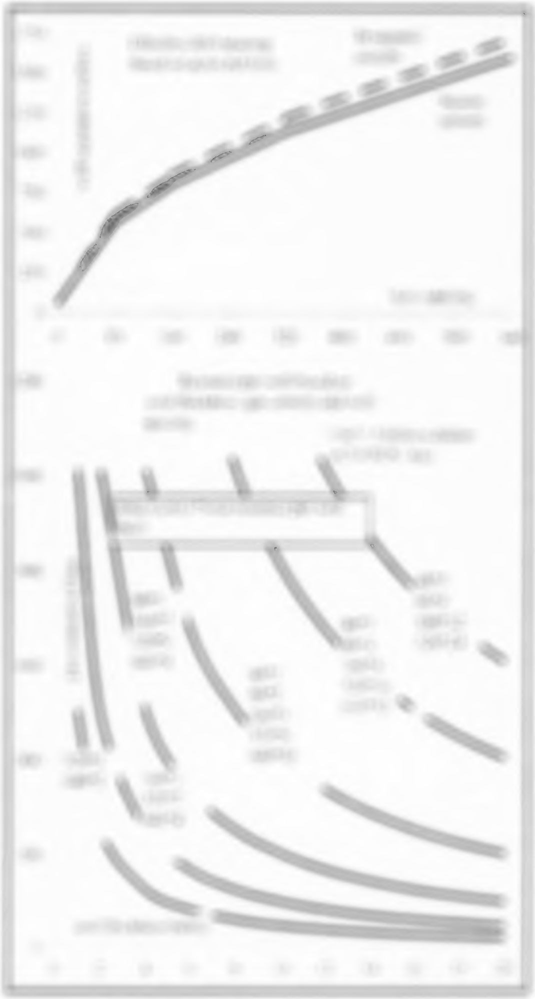

Figure 21. Relationship between cumulative coal thickness, gas content, total potential resource and well spacing.

[illegible]

REFERENCES

[illegible]

[illegible]

[illegible]

[illegible]

[illegible]

[illegible]

[illegible]

[illegible]

[illegible]

[illegible]

[illegible]

[illegible]

[illegible]

[illegible]

[illegible]

[illegible]

[illegible]

[illegible]

Indications for Effective Petroleum Systems in Bowser and Sustut Basins, North-Central British Columbia

By K.G. Osadetz[1], C.A. Evenchick[2], F. Ferri[3], L.D. Stasiuk[1] and N.S F.Wilson[1]

KEYWORDS: Bowser Basin, Sustut Basin, Bowser Lake Group, Sustut Group, Skeena Group, hydrocarbons, petroleum, oil, gas, thermal maturity, organic.

ABSTRACT

Field work in the Bowser and Sustut basins has found "live" oil stains in Bowser Lake Group sedimentary rocks. This provides direct evidence that there is an effective petroleum system in the Bowser Lake Group, specifically, and in the Bowser and Sustut basins, generally. Other, anecdotal evidence suggests that natural gas is seeping from sub-Bowser Lake Group rocks, suggesting that they may also be targets for petroleum exploration. These conclusions are consistent with revised models of thermal maturity in Bowser and Sustut basins, that illustrate large lateral and stratigraphic variations in organic and thermal maturity. As a result of these developments existing petroleum assessments need to be expanded to capture both the reduced play level risks in Bowser Lake Group plays and to add the potential of lower rocks, the latter of which are not currently attributed any petroleum potential. Much additional work is needed to improve the characterization of petroleum potential in the Bowser and Sustut basins.

INTRODUCTION

Indications for an effective petroleum system provide positive evidence for the generation, migration, entrapment and preservation of hydrocarbons in sedimentary basins. This study examines new evidence for an effective petroleum system in the Bowser and Sustut basins of north-central British Columbia. Previous studies indicated that the highest stratigraphic levels of the Bowser Basin succession contain anthracite and semi-anthracite coals. This led many to infer that the stratigraphically lower parts of the Bowser Basin had little petroleum potential, as Hilt's law commonly follows stratigraphic position, with maturity increasing down section. A geographically more comprehensive study of thermal maturity indicated that the initial pessimistic view of petroleum potential was incorrectly founded because of large lateral and stratigraphic variations in thermal maturity (Evenchick *et al.*, 2002).

Subsequent field work this summer tested the re-evaluation of the thermal history and its implications for the petroleum potential of Bowser Basin. Indications for an active petroleum system, manifest as both observed stains of "live" petroleum in Bowser Lake Group sediments and anecdotal indications for active petroleum seepages, are clear indications of effective petroleum systems for both natural gas and crude oil. These observations are consistent with the more optimistic assessment of thermal maturity variations.

SETTING

The Bowser and Sustut basins are located in the Intermontane Belt of north-central British Columbia, between 55° N and 58° N latitude, and occupy an area of more than 60,000 km^2 (Figure 1). These basins lie between the metamorphic and plutonic Omineca and Coast belts (Wheeler and McFeely, 1991). Bowser and Sustut basins are vast, effectively unexplored regions, that are prospective for petroleum accumulation and development. They overlie Devonian to early Middle Jurassic strata of Stikinia, an allochthonous terrane that accreted to the western margin of North America in the Early Jurassic to early Middle Jurassic. Broadly then, the Bowser and Sustut basins are successor basins, like the Sverdrup Basin. The Sverdrup Basin contains approximately 25% of the natural gas and 10% of the crude oil reserve in Canada (Chen *et al.*, 2002).

REGIONAL STRATIGRAPHIC FRAMEWORK

The region is underlain by three broad, partly overlapping, stratigraphic successions: Bowser Lake Group, Skeena Group and Sustut Group. Bowser Lake Group is the oldest, and most widespread succession. It includes upper Middle Jurassic to mid-Cretaceous clastic strata deposited in a variety of marine and nonmarine environments (*e.g.* Tipper and Richards, 1976; Evenchick *et al.*, 2001). Bowser Lake Group was deposited directly on the allochthonous terrane Stikinia, and is composed primarily of clasts derived from the oceanic Cache Creek terrane, although Stikinia was a major source in the southern basin. Syntheses of Bowser Lake Group stratigraphy include those by Eisbacher (1974a; 1981), Tipper and Richards

---

[1] *Geological Survey of Canada, Calgary*

[2] *Geological Survey of Canada, Vancouver*

[3] *New Ventures Branch, BC Ministry of Energy and Mines*

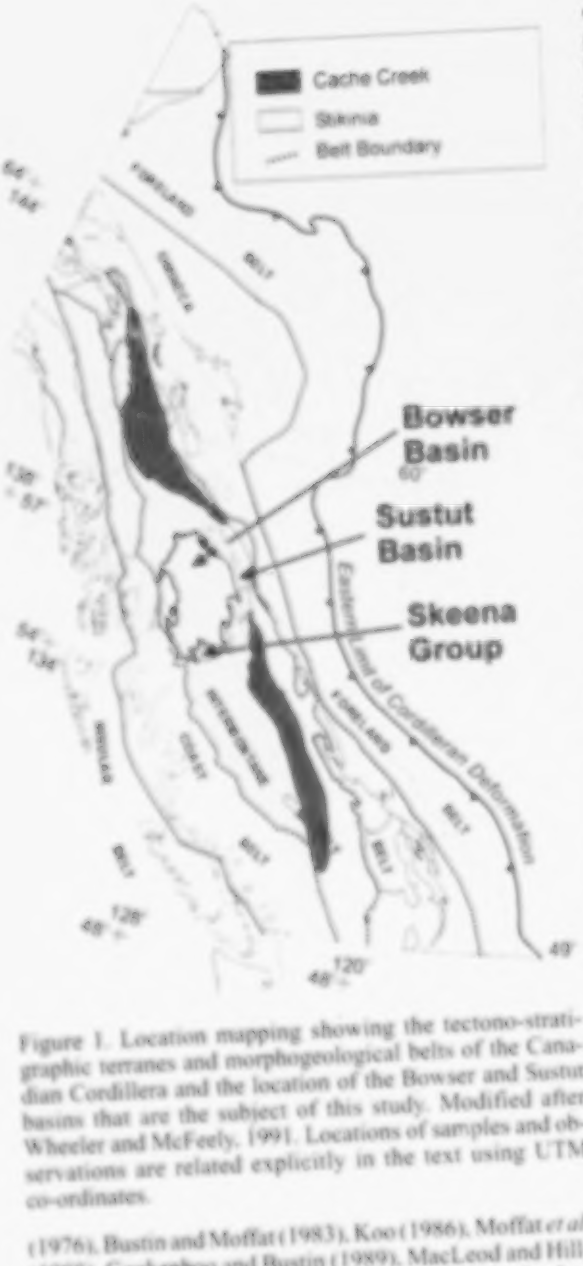

Figure 1. Location mapping showing the tectono-stratigraphic terranes and morphogeological belts of the Canadian Cordillera and the location of the Bowser and Sustut basins that are the subject of this study. Modified after Wheeler and McFeely, 1991. Locations of samples and observations are related explicitly in the text using UTM co-ordinates.

(1976), Bustin and Moffat (1983), Koo (1986), Moffat *et al.* (1988), Cookenboo and Bustin (1989), MacLeod and Hills (1990), Green (1992), Evenchick *et al.* (1992), Cookenboo (1993), Ricketts and Evenchick (1999), Evenchick (2001), Evenchick *et al.* (2000), Evenchick *et al.* (2001).

The Bowser Lake Group is divided into several lithofacies assemblages defined using lithologies, successions, and sedimentary structures. Each is interpreted to represent a dominant depositional environment in submarine fan, slope, shallow marine shelf, deltaic, and fluvial environments. This framework has been integrated with a comprehensive fossil database, permitting the regional interpretation of Bowser Basin depositional history (Evenchick, 2001; Evenchick *et al.*, 2001). Mapped at reconnaissance scale, the distinctive lithofacies assemblages provide a major improvement that enhances petroleum system analysis, facilitates the search for reservoirs and traps, and identifies regions suitable for advanced geophysical prospect generation.

The Lower to mid- Cretaceous Skeena Group occurs south of the Bowser Basin. Its stratigraphic relationship to Bowser Lake Group is not clear. Skeena Group sediments were deposited in a range of marine to nonmarine environments, which locally included a volcanic provenance (Tipper and Richards, 1976; Bassett and Kleinspehn, 1997; Haggart *et al.*, 1998). Mid-Cretaceous to Upper Cretaceous Sustut Group rocks occur along the northeast side of the Bowser Basin. Sustut sediments were deposited in fluvial and lacustrine environments, with possibly minor marine influence. On the southwest side of the Sustut Basin, these strata overlie deformed Bowser Lake Group and Stikine Terrane strata whereas to the northeast they overlie Stikine Terrane strata (Eisbacher, 1974b; Bustin and McKenzie, 1989; Evenchick *et al.*, 2001).

REGIONAL STRUCTURAL FRAMEWORK

Strata of Stikinia and the three overlying successions are folded and thrust faulted in contractional structures of the Skeena Fold Belt, a thin-skinned fold and thrust belt of Cretaceous age (Evenchick, 1991a). The dominant structures are open to close folds hundreds of metres to kilometer-scale wavelengths. Larger wavelength folds are associated with structural culminations of competent volcanic rocks of Stikinia. The dominant fold trend is northwest, but domains of northeast trending structures occur locally on the west side of the fold belt. Large-scale features of the fold belt are presented by Evenchick (1991a,b; 2001). Structural studies of more restricted areas include those by Moffat and Bustin (1993), and Bone (2002).

First order characteristics of the fold belt are (Evenchick, 1991a,b; 2001):

1. Folds in most of the belt trend northwest, are close to tight, and upright to inclined to the northeast;
2. Thrust faults are present, but difficult to recognize because Bowser Lake Group lacks distinctive regional stratigraphic markers;
3. Contractional structures affect underlying volcanic, clastic, and carbonate successions of Stikinia; the fold belt accommodated a minimum of 44% horizontal shortening;
4. It terminates to the northeast in a triangle zone within Sustut Group; and it is rooted in the Coast Belt to the west.

The scale of folds is controlled by the proximity to mechanically strong volcanic units in the Stikine Terrane. The relationships between structures and stratigraphic units indicate that orogenic shortening began prior to Albian (mid-Cretaceous) time, and continued into the

Maastrichtian (latest Cretaceous) or later (Evenchick, 1991a; 2001). Provenance and basin analysis link Sustut Basin subsidence to Skeena Fold Belt formation (Eisbacher, 1974b). Sustut Group and Devils Claw Formation are both inferred to be synorogenic deposits linked to Skeena Fold Belt deformation (Evenchick, 2001). The revised structural model, especially the identification of a triangle zone, has important implications for a revised petroleum assessment.

PREVIOUS WORK

PREVIOUS ASSESSMENT OF PETROLEUM POTENTIAL

Bowser and Sustut basins were assessed using a probabilistic play-based volumetric method (Hannigan *et al.*, 1995; Canadian Gas Potential Committee, 2001). The method (Lee, 1993) employs distributions of potential petroleum field parameters, constrained by available data, to calculate a conditional petroleum accumulation size distribution. By estimating both the number of potential prospects and the prospect-level risk it is possible to infer the likely number of petroleum accumulations to be found. This is used to produce a set of distributions that describe the probability of pool size for a pool of a given size rank. The play-level risk modifies the calculated total play potential. Because of the very large size of the basin and its untested structures, the basin was attributed a significant undiscovered potential, although this was significantly affected by play-level risks. Resource potentials were calculated for five anticlinal plays (Hannigan *et al.*, 1995).

Skeena Group gas play has a mean in-place natural gas potential of 7.19 x 1010 m^3 (2.54 TCF - trillion cubic feet). The median largest field size is 1.47 x 1010 m^3 (519 BCF - billion cubic feet) in place. It is expected that about 19 Skeena Group gas fields will be found. Skeena Group oil play has a mean in-place potential of 2.01 x 108 m^3 or 1264 million barrels. The largest Skeena Group oil field is estimated to be between 1.00 x 107 m^3 and 1.42 x 108 m^3 or 63.1 to 893.3 million barrels. The expected number of Skeena Group oil fields is 16. Bowser Lake Group gas play has a total mean in-place gas potential of 5.78 x 1010 m^3 or 2.0 TCF. The median largest undiscovered field size (in-place) is 1.80 x 1010 m^3 (637 BCF). The assessment identified significant play level risks, especially for the preservation of Bowser Lake Group reservoirs. If gas fields exist in Bowser Lake Group then the expected number of fields is 173. No oil potential was assigned to Bowser Lake Group plays, because of the now-outdated thermal maturity model that prevailed at the time of the assessment. Sustut Group gas play is among the most attractive, despite significant concerns including the relative timing of trap formation to hydrocarbon generation. The mean in-place play potential is 5.27 x 1010 m^3 or 1.86 TCF of gas. The median largest Sustut Group field size is 1.24 x 1010 m^3 (438 BCF). The expected number of Sustut Group gas fields is 14. Sustut Group structural oil play has play parameters and risks similar to its gas play. The mean in-place Sustut oil potential is 1.84 x 108 m^3 (1158 million barrels) and the median largest field size is 4.17 x 107 m^3 or 262 million barrels. The expected number of oil fields in the Sustut Group is 14.

Revised stratigraphic and structural frameworks are key elements in improved calculations of Bowser and Sustut basin petroleum potential. Primary among these are division of the Bowser Lake Group into a number of lithofacies assemblages so that stratigraphic components of entrapment may be considered, and the revision of the structurally defined plays to consider a foreland fold and thrust belt that includes a frontal triangle zone. It is believed that the existing assessments (Hannigan *et al.*, 1995; CGPC, 2001) have underestimated the petroleum potential because of perceptions that observed levels of thermal maturity in some of the highest stratigraphic levels were unfavorable for both the diagenesis of reservoirs (a play-level risk) and the function of the petroleum systems. Changes in the description of organic maturity history have had a profound impact on how the petroleum resource potential of the basin is perceived and risked.

REVISED THERMAL MATURITY MODEL

Petroleum resource potentials of these basins must be re-assessed using new stratigraphic and tectonic models which consider the physical environment, primarily temperature, and temporal relationships between hydrocarbon generation, migration, entrapment, and preservation. The first widespread thermal maturity data set for the Bowser and Sustut basins illustrates that large regions have sufficiently low organic maturity levels, that the generation and preservation of hydrocarbons and the diagenetic history of reservoirs are favourable for the formation and preservation of a significant petroleum resource (Evenchick *et al.*, 2002). These results are a substantial change from the previous view that the high thermal maturity of some of the highest Bowser strata is a negative indication for hydrocarbon potential in all stratigraphic levels and regions of the basin. Although parts of the study area are at very high thermal maturity levels, there are clear regional variations in the thermal maturity of outcrops such that even the lowest stratigraphic units are marginally to fully mature in select regions of the basin.

The presence of type 2 migrabitumen, identified in the thermal maturity study, is a positive indication for the generation and migration of liquid petroleum within the Bowser Basin. Together the revised patterns and levels of thermal maturity, combined with positive indications for the generation and migration of liquid petroleum, provides a much more positive indication for petroleum system function and petroleum preservation than was held previously. The preliminary thermal maturity data show a number of first-order patterns not previously recognized.

1) The highest levels of thermal maturity (Ro max > 2.5%) underlie a broad area and cross a wide range of stratigraphic units. This region coincides approximately with a broad aeromagnetic high. The high thermal maturity and aeromagnetic anomaly are possibly a result of bur-

ied Late Cretaceous and/or Tertiary plutons similar to those that outcrop in the southeast-most part of the study area. In this interpretation the plutons are the source of increased heat flow.

2) The northwest limit of the region described above coincides with areas of highest thermal maturity reported by Bustin and Moffat (1983). Although we recognize the same general pattern of reduced thermal maturity to the northwest, as noted by Bustin and Moffat (1983), in several areas, we observe and report lower thermal maturity than Bustin and Moffat (1983). This difference will be addressed in future analyses.
3) Significant portions of the northwest and western Bowser Basin are within the range of Ro max values compatible with oil and gas preservation. These regions were not previously recognized, and the lower thermal maturation than assumed indicates a greater possibility for oil and gas generation and preservation, and reduced exploration risk.
4) A broad band of strata in the northeast Bowser Basin and southwest Sustut Basin, coinciding with the roof of the triangle zone and regions structurally below the roof, reached peak thermal maturity in the main stage of oil generation. These relationships are highly favourable for a potential triangle zone play.
5) Northeast of the triangle zone, samples in the Sustut Group are consistently in the main stages of hydrocarbon generation. Although data are sparse, they are widespread in a large area of favourable stratigraphic and structural traps, and suggest reduced play-level risk. The combination of thermal maturity and structural position in the triangle zone are most favourable revisions of the geological parameters constraining petroleum potential. Not only was the triangle zone play not explicitly considered in the previous assessments (Hannigan *et al.*, 1995; CGPC, 2001), but it presents a clear analogue to some of the most prospective and productive settings in the thrust and fold belt of the Foreland Belt of the southern Canadian Cordillera (Stockmal *et al.*, 2001).

INDICATIONS FOR EFFECTIVE PETROLEUM SYSTEMS

OIL STAINS

A sample of an ammonite in a very fine grained chert arenite was collected from Muskaboo Creek assemblage marine succession at the "Tsatia Mountain" reference section , 02-OE-36 (NAD 27, UTM Zone V E442468 N6380068), during 2002 fieldwork. The sample was notable because material, initially suspected to be pyrobitumen, occurred as a cast in an anatomical sinus of the fossil. Subsequent and more careful examination indicates that the cast material is calcite blackened by numerous primary and secondary petroleum fluid inclusions. Petrographically these fluid inclusions are composed of a sky-blue fluorescing "live" oil (Figure 2). Some fluid inclusions in this material may also contain petroleum condensate. These

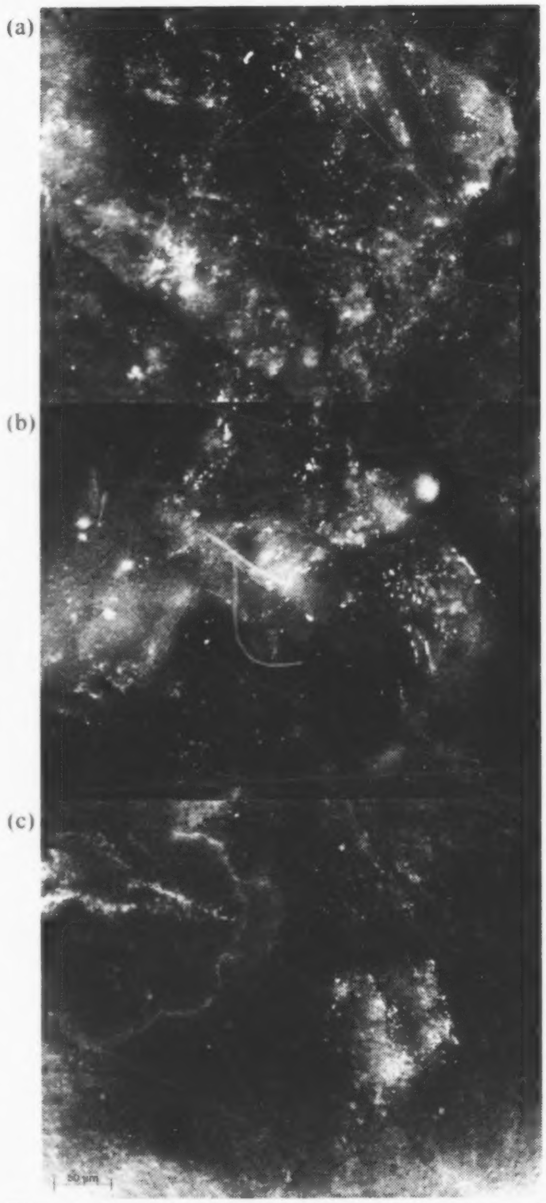

Figure 2. Photomicrographs of petroleum fluid inclusions from Muskaboo Creek Assemblage Rocks, Bowser Lake Group, at the "Tsatia Mountain" reference section , (NAD 27, UTM Zone V E442468 N6380068). Sample field number 02-OE-36; and GSC Calgary Collection Number C-428547. Organic Petrology Pellet Number 575/02, calcite 'vein' filling material in an ammonite fossil. Figure 2a, (top) and 2b, (middle) and 2c, (bottom). Abundant blue fluorescing crude oil inclusions, predominantly in coarse grained calcite, occur as both primary fluid inclusions and within micro-fractures within the calcite. Also present is an orange fluorescing fine grained botryoidal carbonate that may be fossil infill. The fluid inclusions are two-phase hydrocarbon fluid inclusions that might be suitable for the determination of homogenization temperatures. In colour the petroleum fluid inclusions are both bright yellow and blue, in black and white both populations of petroleum fluid inclusions are white. Scales as indicated.

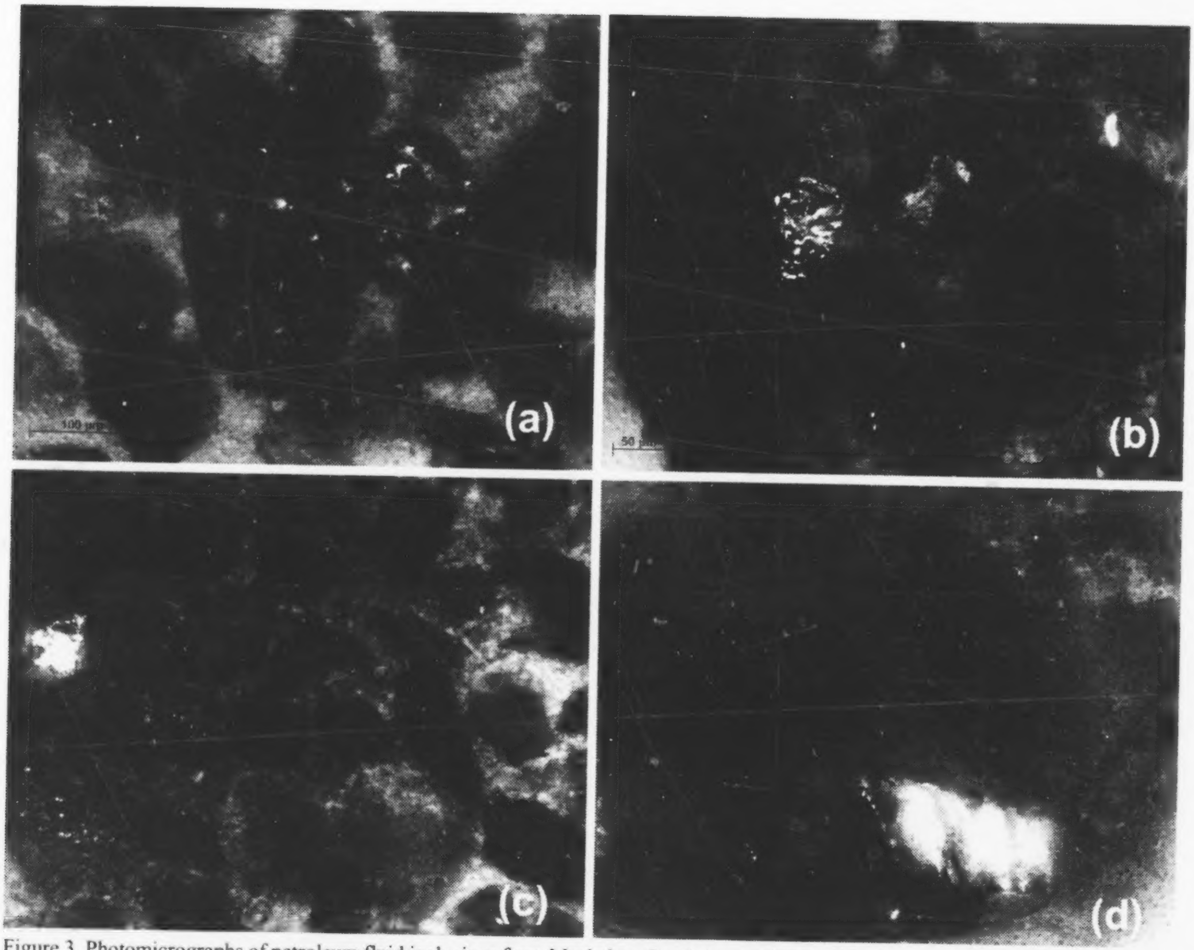

Figure 3. Photomicrographs of petroleum fluid inclusions from Muskaboo Creek Assemblage Rocks, Bowser Lake Group, at the "Tsatia Mountain" reference section , (NAD 27, UTM Zone V E442468 N6380068). Sample field number 02-OE-36; and GSC Calgary Collection Number C-428547. Organic Petrology Pellet Number 576/02, Muskaboo Creek Assemblage chert arenite, Figure 3a) and 3b) (top row, left to right) and 3c) and 3d) (bottom row, left to right) Abundant orange to yellow to white yellow crude oil inclusions within microfractured grains that occur with sparse blue fluorescing crude oils and condensate fluid inclusions. These petroleum fluid inclusions appear to be restricted to the mineral grains and do not occur in the fine-grained matrix and inter-particle regions. In colour the petroleum fluid inclusions are both bright yellow and blue, in black and white both populations of petroleum fluid inclusions are white. Scales as indicated.

petrographic characteristics indicate a petroleum composition consistent with an unaltered, low density, high thermal maturity crude oil, >45° API. The occurrence mode and its position in the paragenetic sequence indicates that the oil in these petroleum fluid inclusions resulted from an indisputable secondary migration of petroleum into the fossil.

In addition, and quite unexpectedly, a large number of detrital chert grains from the host rock also contain fluorescing inclusions of "live" petroleum. The fluid inclusions have two dominant sets of petrographic characteristics and compositions whose mode of occurrence is similar. Typically the petroleum fluid inclusions occur as sub-parallel fine, linear to planar inclusions within individual grains, possibly following original bedding laminations, which are chaotically oriented within the chert arenite rock mass. The two sets of petroleum fluid inclusions contain distinctively different petroleum compositions. One set is composed of yellow to green fluorescing petroleum. This represents an inferred unaltered medium density petroleum of moderate thermal maturity, 30-35° API. The other set is composed of sky blue fluorescing petroleum. This set is inferred to be compositionally similar to the petroleum in the ammonite cast filling material. It too is inferred to be composed of an unaltered, low density, high thermal maturity crude oil, >45° API. The siliceous matrix of the sandstone does not appear to have petroleum fluid inclusions.

From these observations we infer that the detrital chert grains themselves are carrying two different petroleums of distinctive thermal maturity. The preservation of this difference is a strong indication that the local level of thermal maturity is equal to or less than that of the yellow-green fluorescing inclusions, or less than ~0.8 vitrinite reflectance equivalent. This is consistent with the maturities reported locally from other petrographic samples (Evenchick *et al.*, 2002). It confirms that the basin contains regions of thermal maturity suitable to the generation and preservation of crude oil. When and where the petroleum fluid inclusions in the detrial chert grains originated is not yet determined. They may represent an in-situ generation of petroleum, in which case the petroleum generation would have to predate their formation as detrital grains. Alternatively, they might be composed of oils generated during multiple phases of secondary migration, or some combination of autochthonous and allocthtonous petroleum generation. The secondary stained calcite in the ammonite, the "vein filling", has a much higher thermal maturity than the sedimentary rocks it hosts, suggesting secondary migration of an oil of greater than 45° API through the Bowser sediments at this locality.

The details of the diagenesis and the significance of the absence of petroleum fluid inclusions in the cement of the arenite are currently the subject of additional study. As well, it may be possible to perform a solvent extraction on the sample for the purpose of characterizing the bulk and molecular composition of the petroleum. The extent of these stains in the basin should be examined in greater detail and more petrography should be done on available samples.

ANECDOTAL INDICATIONS FOR SEEPAGES

In the course of fieldwork this season, local residents Mr. Hal and Mrs. Bunty Althaus, proprietors of the Tatogga Lake Resort, on the eastern shore of Tatogga Lake, volunteered knowledge of a persistent possible natural gas seepage adjacent to their dock. Mr. And Mrs. Althaus characterized the possible gas seep as:

- Persistent. They had been aware of the seepage in the same location for about ten years, 'ever since they had owned the place';
- Of noticeable volume. They had observed anomalous freezing and melting behaviour in the lake over the possible seepage, identical to petroleum gas seepages that one of us (Osadetz) had observed elsewhere, and;
- Flammable. Mr. Althaus recounted how he had once ignited gas from the seepage.

The site of the possible seepage, (NAD 27, UTM Zone V E440380 N6396997 ~+825m elev.), was visited by two of us (Osadetz and Ferri) that day, but conditions on the lake, including a considerable chop, and the recovery efforts at a crashed floatplane adjacent the dock, were not conducive to successfully observing a seepage free of contamination.

The possible seepage, at this locality, occurs in a region of Hazelton or Stuhini group outcrop and the pattern of local thermal maturity is consistent with a possible natural gas seepage from these rocks. The manner in which the information was volunteered, the consistency of the recounting by both Mr. And Mrs. Althaus, and the description of anomalous freezing and melting behaviour at the site of the possible seepage were consistent with it being a natural seepage of thermogenic petroleum. Additional work, at the site of the possible seepage accompanying the early days of freezing on the Lake, and elsewhere in the vicinity, as well as additional interviews of local residents, is warranted.

DISCUSSION

The observation of "live" petroleum stains, both in "vein-filling" material and "detrial" clasts of Bowser Lake Group occur within the region where the revised thermal maturity model suggests that the Bowser Lake Group is within the main stage of petroleum generation. The different petrographic characteristics of the inclusions are a clear indication that at least some of the higher maturity, sky blue fluorescing, petroleum fluid inclusions have migrated into these rocks. When these observations are combined with the anecdotal indications for a natural gas seepage from sub-Bowser rocks at Tatogga Lake it is clear that there is an effective petroleum system, or systems, operating in the Bowser and Sustut basins of the Intermontane Belt. These observations, and the composition of the petroleum at each occurrence, are consistent with the revised thermal maturity observations and patterns reported by Evenchick *et al.* (2002). The corroboration of this much larger data set of thermal maturity indicators suggests that the general inferences of that report are correct. Together these observations reduce play level risks that were applied to the existing petroleum assessments. This suggests that the assessments should be revised to consider these new, more favourable data. The impact of such a revision can be inferred qualitatively to increase both the size and certainty of the mean petroleum resource potential in the Bowser and Sustut basins. Most important, the indications for possible gas seepage in regions of sub-Bowser Lake Group outcrops suggests that there may be petroleum potential in lower strata. These new plays need to be defined and should be used to augment the existing set of petroleum plays in subsequent reassessments of the petroleum potential of Bowser and Sustut basins.

There is a general tendency to consider regions of high thermal maturity as unfavourable for petroleum preservation and occurrence. However, data from the United States shows that petroleum potential and production remains even where rocks have been buried to very great depths and reached high temperatures (Dymond and Osadetz, 2002). In the U.S.A., 20,715 wells have been drilled to depths greater than 15,000 feet, or ~5 kms. 11,522 of these deep wells are producing petroleum wells and 5,119 of these wells are producing from the deepest formation penetrated. In 1999 more than 1.5 TCF of natural gas was produced from wells completed deeper than ~5 kms. Acknowledging the increased risk with complicated and deep burial, it is valuable to consider that the limits and margins of petroleum production from sedimentary rocks are best proved by the drill bit than by inferences and models that are often valid only in specific geographic regions.

CONCLUSIONS

Field work in the Bowser and Sustut basins has found migrated and possibly indigenous 'live' oil stains in Bowser Lake Group sedimentary rocks. This provides direct evidence that there is an effective petroleum system in the Bowser and Sustut basins. Anecdotal evidence suggests that flammable, probably petroleum, natural gas is seeping from sub-Bowser rocks near the edge of Tatogga Lake. This suggests another target for petroleum exploration. As a result of these developments, existing petroleum assessments need to be expanded to capture both the reduced play level risks in Bowser Lake Group plays and to add the potential of sub-Bowser Lake Group rocks, the latter of which are not currently attributed any petroleum potential. These conclusions are consistent with revised models of thermal maturity in Bowser and Sustut basins (Evenchick *et al.*, 2002), which are much more favourable for petroleum preservation and entrapment than previous, still locally valid, models (Bustin and Moffat, 1983). Much additional work is needed to improve the characterization of petroleum potential in this region.

REFERENCES

Bassett, K.N. and Kleinspehn, K.L. (1997): Early to Middle Cretaceous paleogeography of north-central British Columbia: stratigraphy and basin analysis of the Skeena Group; *Canadian Journal of Earth Sciences*, Volume 34, pages 1644-1669.

Bone, K. (2002): Relative timing and significance of folding in the western Skeena Fold Belt, northwestern Bowser Basin, British Columbia: Interpretation of structural and seismic reflection data; M.Sc. Thesis, *The University of British Columbia*.

Bustin, R.M. and McKenzie, K.J. (1989): Stratigraphy and depositional environments of the Sustut Group, southern Sustut Basin, north central British Columbia; *Bulletin of Canadian Petroleum Geology*, Volume 37, pages 210-223.

Bustin, R.M. and Moffat, I. (1983): Groundhog coalfield, central British Columbia: reconnaissance stratigraphy and structure; *Bulletin of Canadian Petroleum Geology*, Volume 31, pages 231-245.

Canadian Gas Potential Committee. (2001): West Coast and Interior Assessment Region; in: Anonymous ed.; Natural Gas Potential *in* Canada 2001: A report by the Canadian Gas Potential Committee. ISBN 0- 9682125-1-4, *The Canadian Gas Potential Committee*, Calgary, 2001, Chapter 15, pages 1-6, with 11 Figures.

Chen, Z., Osadetz, K. G., Embry, A. F., Gao, H., and Hanningan, P. K. (2000). Petroleum potential in western Sverdrup Basin, Canadian Arctic Archipelago. *Bulletin of Canadian Petroleum Geology*, Volume 48, pages 323-338.

Cookenboo, H.O. (1993): Lithofacies, provenance, and diagenesis of Jura-Cretaceous strata of the northern Bowser Basin, British Columbia; Ph.D. Thesis, *The University of British Columbia*, 216 pages.

Cookenboo, H.O. and Bustin, R.M. 22 (1989): Jura-Cretaceous (Oxfordian to Cenomanian) stratigraphy of north-central Bowser Basin, northern British Columbia; *Canadian Journal of Earth Sciences*, Volume 26, pages 1001-1012.

Dyman, T.S., and Osadetz, K.G. (2002): Deep natural gas potential of North American Basins (abstract) in: B. Law (ed.), *World Energy Consortium Workshop*, Denver, October 8th and 9th, 2002.

Eisbacher, G.H. (1974a): Deltaic sedimentation in the northeastern Bowser Basin, British Columbia; *Geological Survey of Canada*, Paper 73-33, 13 pages.

Eisbacher, G.H. (1974b): Sedimentary history and tectonic evolution of the Sustut and Sifton basins, north-central British Columbia; *Geological Survey of Canada*, Paper 73-31, 57 pages.

Eisbacher, G.H. (1981): Late Mesozoic-Paleogene Bowser Basin molasse and Cordilleran tectonics, western Canada; *in* Sedimentation and Tectonics in Alluvial Basins, (ed.) A.D. Miall; *Geological Association of Canada*, Special Paper 23, pages 125-151.

Evenchick, C.A. (1991a): Geometry, evolution, and tectonic framework of the Skeena Fold Belt, north-central British Columbia; *Tectonics*, Volume 10, pages 527-546.

Evenchick, C.A. (1991b): Structural relationships of the Skeena Fold Belt west of the Bowser Basin, Northwest British Columbia; *Canadian Journal of Earth Sciences*, v. 28, 973-983.

Evenchick, C.A. (2001): Northeast-trending folds in the western Skeena Fold Belt, northern Canadian Cordillera: a record of Early Cretaceous sinistral plate convergence; *Journal of Structural Geology*, Volume 23 pages 1123-1140.

Evenchick, C.A., Hayes, M.C., Buddell, K.A., and Osadetz, K.G.(2002): Vitrinite reflectance data and preliminary organic maturity model for the northern two thirds of the Bowser and Sustut basins, north-central British Columbia. *Geological Survey of Canada*, Open File 4343 and *B.C. Ministry of Energy and MInes*, Petroleum Geology Open File 2002-1.

Evenchick, C.A., Mustard, P.S., Porter, J.S., and Greig, C.J. (1992): Regional Jurassic and Cretaceous facies assemblages, and structural geology in Bowser Lake map area (104A), British Columbia; *Geological Survey of Canada*, Open File 2582.

Evenchick, C.A., Mustard, P.S., Greig, C.J., Porter, J.S., and McNeill, P.D. (2000): Geology, Bowser Lake, (104A) British Columbia; *Geological Survey of Canada*, Open File 3918.

Evenchick, C.A., Poulton, T.P., Tipper, H.W., and Braidek, I. (2001): Fossils and facies of the northern two-thirds of the Bowser Basin, northern British Columbia; *Geological Survey of Canada*, Open File 3956.

Gabrielse, H. (1991): Late Paleozoic and Mesozoic terrane interactions in north-central British Columbia; *Canadian Journal of Earth Sciences*, Volume 28, pages 947-957.

Green, G.M. (1992): Detailed sedimentology of the Bowser Lake Group, northern Bowser Basin, north-central British Columbia; M.Sc. Thesis, *Carleton University*, 197 pages.

Haggart, J.W., Woodsworth, G.J., and Justason, A. (1998): Update on geological mapping, southeast Nass River map area, British Columbia; in Current Research, 1998-A, *Geological Survey of Canada*, pages 69-77.

Hannigan, P., Lee, P. J., and Osadetz, K. G. (1995): Oil and gas resource Potential of the Bowser-Whitehorse area of British Columbia; Internal Report Prepared for *B.C. Ministry of Energy, Mines and Petroleum Resources*.

Koo, J. (1986): Geology of the Klappan coalfield in northwestern British Columbia (104H/2,3,6,7); *in* Geological fieldwork, 1985; *B.C. Ministry of Energy Mines and Petroleum Resources*, Paper 1986-1, pages 225-228.

Lee, P.J. (1993): Two decades of petroleum resource assessments in the Geological Survey of Canada; *Canadian Journal of Earth Sciences*, Volume 30, pages321-332.

MacLeod, S.E. and Hills, L.V. (1990): Conformable Late Jurassic (Oxfordian) to Early Cretaceous strata, northern Bowser Basin, British Columbia: a sedimentological and paleontological model; *Canadian Journal of Earth Sciences*, Volume 27, pages 988-998.

Moffat, I.W. and Bustin, R.M. (1993): Deformational history of the Groundhog Coalfield, northeastern Bowser Basin, British Columbia; styles, superposition and tectonic implications; *Bulletin of Canadian Petroleum Geology*, Volume 41, pages1-16.

Moffat, I.W., Bustin, R.M., and Rouse, G.E. (1988): Biochronology of selected Bowser Basin strata; tectonic significance; *Canadian Journal of Earth Science*, Volume 25, pages 1571-1578.

Ricketts, B.D. and Evenchick, C.A. (1999): Shelfbreak gullies; products of sea-level lowstand and sediment failure: examples from Bowser Basin, northern British Columbia; *Journal of Sedimentary Research*, Volume 69, pages 1232-1240.

Ricketts, B.D., Evenchick, C.A., Anderson, R.G., Murphy, D.C. (1992): Bowser Basin, northern British Columbia: constraints on the timing of initial subsidence and Stikinia-North America terrane interactions; *Geology*, Volume 20, pages 1119-1122.

Stockmal, G. S., Osadetz, K. G., Lebel, D., and Hannigan, P. K. (2001): Structure and hydrocarbon occurrence, Rocky Mountain Foothills and Front Ranges, Turner Valley to Waterton Lakes – Field Trip Guidebook, *Geological Survey of Canada*, Open File 4111, 161 pages.

Tipper, H.W. and Richards, T.A. (1976): Jurassic stratigraphy and history of north-central British Columbia; *Geological Survey of Canada*, Bulletin 270, 73 pages.

Wheeler, J.O. and McFeely, P.1991: Tectonic assemblage map of the Canadian Cordillera and adjacent parts of the United States of America; *Geological Survey of Canada*, Map 1712A, scale 1:2 000 000.

Geological and Mineral CO$_2$ Sequestration Options: A Technical Review

By Danae A. Voormeij[1] and George J. Simandl[2]

INTRODUCTION

This review results from directed studies at the University of Victoria by the senior author and it covers the main technical aspects of the Greenhouse Gas Sequestration methodology.

The Kyoto Agreement may or may not be ratified, however, the following text highlights those options that British Columbia will have if a need for geological, mineral or deep ocean sequestration arises. Of the six greenhouse gases covered by the Kyoto protocol, carbon dioxide (CO$_2$) is the greatest contributor to Canada's total GHG emissions (Table 1). Fossil fuel combustion is the main source of anthropogenic CO$_2$, and it currently supplies over 85% of the global energy demand (Figure 1). The main engineering effort for reduction of CO$_2$ emissions is therefore aimed at increased efficiency of fossil energy usage, development of energy sources with lower carbon content and increased reliability on alternative energy sources such as wind, solar, geothermal and nuclear. It is not likely that the reduction of CO$_2$ emissions, in an order of magnitude similar to the Kyoto agreement, could be met using these measures alone. CO$_2$ sequestration methods that are currently considered, or being evaluated by industrialized countries, are part of the global plan. Each method has its weaknesses and strengths. The methods that we will cover in this review are:

- Storage in Oil and Gas Reservoirs
- Storage in Deep Coal Seams
- Storage in Deep, Saline Aquifers
- Storage in Deep Ocean
- Storage in Salt Caverns
- Mineral Carbonation

Since all geological and mineral CO$_2$ sequestration methods involve the capture and extraction of CO$_2$ from flue-gases or industrial streams, transportation of CO$_2$ and its disposal in an appropriate sink, the next stage of our study will identify the main stationary point sources of CO$_2$ emissions and the main potential carbon or CO$_2$ sinks in British Columbia.

TABLE 1
CANADIAN GREENHOUSE GAS EMISSIONS

Carbon Dioxide (CO$_2$)	**78.00%**
Methane (CH$_4$)	**12.40%**
Nitrous Oxide (N$_2$O)	**7.40%**
Other (HFCs*, PFCs^{+} and SF$_6$$^{\wedge}$)	**1.30%**

*Hydrofluorocarbons

$^{+}$Perfluorocarbons

$^{\#}$ As Carbon Dioxide Equivalent

$^{\wedge}$Sulphur hexafluorides

(Source: Environment Canada, 2002)

Geographic relationships between the main stationary point CO$_2$ sources and sinks is an essential piece of the puzzle for CO$_2$ sequestration planning in British Columbia since transportation is one of the important cost factors.

PHYSICAL PROPERTIES OF CARBON DIOXIDE

It is important to know the main properties of carbon dioxide to understand carbon sequestration methods. Carbon dioxide (CO$_2$) is an odourless, colourless gas that occurs naturally in the atmosphere. Current ambient atmo-

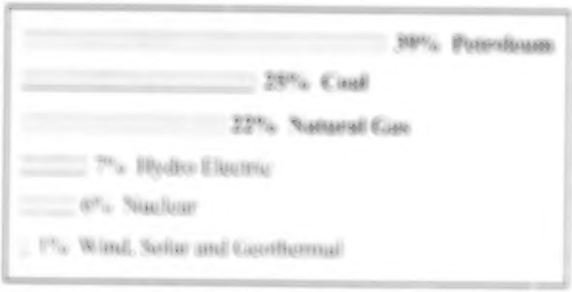

Figure 1. Global energy demand. Fossil fuels supply over 85% of the world's energy. (Source: McKee, 2002)

spheric concentrations of CO_2 are around 370 ppm (0.037%). Benson *et al.* (2002) summarizes the effects of high concentrations of CO_2 on humans and other life forms.

---

[1] *University of Victoria*

[2] *BC Geological Survey Branch and adjunct professor at University of Victoria*

Depending on pressure and temperature, CO_2 can take on three separate phases (Figure 2). CO_2 is in a supercritical phase at temperatures greater than 31.1°C and pressures greater than 7.38 MPa (critical point). Below these temperature and pressure conditions, CO_2 will be either a gas or a liquid. Depending on in situ temperature and pressure, CO_2 can be stored as a compressed gas or liquid, or in a supercritical (dense) phase.

CO$_2$ STORAGE IN OIL AND GAS RESERVOIRS

Both depleted and active fossil fuel reservoirs are potential storage space for CO_2 in underground formations. CO_2 may be injected directly into a depleted or inactive reservoir without expectation of any further oil production, or the CO_2 injection may result in enhanced oil gas recovery and simultaneous CO_2 sequestration. CO_2 may also be injected into producing oil and gas reservoirs, where CO_2 enhanced oil recovery (EOR) and CO_2-enhanced gas recovery (EGR) will offer an economic benefit. Typically, oil reservoirs have undergone a variety of production and injection processes during primary and secondary recovery (*e.g.* gas, water or steam injection), as described by Jimenez and Chalaturnyk (2002). As a tertiary recovery process, CO_2 can be injected into the reservoir to improve the mobility of the remaining oil (van der Meer, 2002), thereby extending the production life of the reservoir. Injection of CO_2 into producing gas reservoirs for EGR was previously believed to risk contaminating the natural gas reserve (Stevens *et al.*, 2000). However, recent studies by Oldenburg and Benson (2002, 2003) suggest that mixing of the CO_2 and methane (CH_4) in a gas reservoir would be limited due to the high density and viscosity of CO_2 relative to the natural gas. Furthermore, significant quantities of natural gas can be produced by repressurization of the reservoir. According to Davison *et al.* (2001), it is possible that improved oil and gas recovery could more than offset the cost of CO_2 capture and injection.

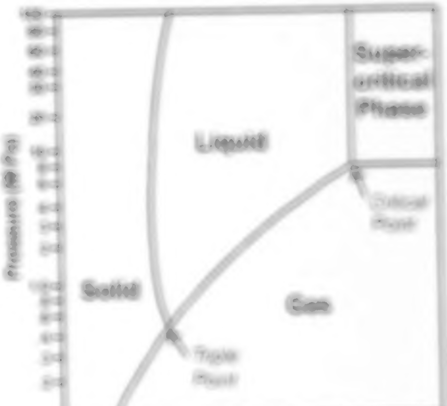

Figure 2. Carbon dioxide phase diagram. The critical point for CO_2, when it reaches supercritical state, is 31.1°C and 7.38 MPa (Adapted from Koide *et al.*, 1996).

For the purpose of this paper, the term "depleted fossil fuel reservoirs" refers to abandoned oil and gas reservoirs. These reservoirs have undergone primary and secondary recovery and CO_2-enhanced oil recovery is not currently envisaged to generate positive cashflow.

ACTIVE OIL RESERVOIRS

The petroleum industry has been injecting CO_2 into underground formations for several decades (Gentzis, 2000) to improve oil recovery from light and medium oil reservoirs, even before climate change became an issue (Bachu, 2000a). CO_2 injected into suitable oil reservoirs can improve oil recovery by 10-15% of the original oil in place in the reservoir (Davison *et al.*, 2001). When CO_2 is injected into a reservoir above its critical point (typically a reservoir depth greater than 800 m), the gas acts as a powerful solvent. If the pressure is high enough and the oil gravity is greater than 25° API (Bachu, 2001), the CO_2 and oil become completely miscible. According to Aycaguer *et al.* (2001), the miscible flood reduces the oil's viscosity thereby enabling the oil to migrate more readily to the producing wells (Figure 3). At lower pressures CO_2 and oil are not completely miscible, however some fraction of the CO_2 will dissolve in the oil. This is known as immiscible displacement and also enhances oil recovery. CO_2-enhanced oil recovery is now considered as a mature technology (Gentzis, 2000). If EOR is the main objective of CO_2 injection, then the operation is optimized to minimize the cost of CO_2 used and maximize the oil recovery. CO_2 sequestration differs from EOR by CO_2; its main objective is to sequester as much CO_2 in the reservoir as possible for geological time (van der Meer, 2002; Benson, 2000).

A life cycle assessment study on EOR with injection of CO_2 in the Permian Basin of West Texas (Aycaguer *et al.*, 2001) suggests that the amount of CO_2 injected, not includ-

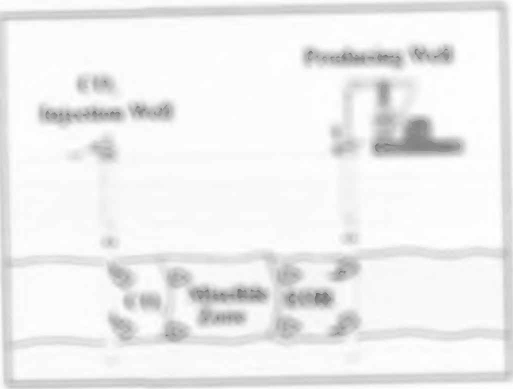

Figure 3. Simplified diagram of a CO_2-enhanced oil recovery (EOR) operation. (Modified from IEA R&D Programme, 2001).

ing the recycled CO_2, may balance the amount of CO_2 in emissions that ultimately are produced by combustion of the extracted hydrocarbon product. To reduce atmospheric CO_2 and preserve natural CO_2 reservoirs, the source of CO_2 for EOR should come from anthropogenic sources. Most of the existing CO_2 EOR projects in the world use natural CO_2 sources (Whittaker and Rostron, 2002). The CO_2 comes from natural carbon dioxide reservoirs where the infrastructure for distribution is already present, providing delivery without major capital costs (Koogan *et al.*, 2001) and without processing (Smith, 1998). Of the 70 CO_2 EOR projects in the USA, only four use anthropogenic CO_2 (Whittaker and Rostron, 2002). A Canadian study done by Tontiwachwuthikul *et al.* (1998) on the economics of CO_2 production from coal-fired power plants concluded that flue gas extraction could be an economically viable CO_2 supply source for CO_2 EOR projects in Western Canada, should oil prices increase substantially. Currently, in Weyburn, Canada, a large-scale project for CO_2 EOR has been developed with the aim at implementing a guideline for geological storage of anthropogenic CO_2 (Moberg, 2001; Whittaker and Rostron, 2002; Srivastava and Huang, 1997). The Weyburn project is sponsored by a number of Governments and industries from North America, Europe and Japan.

DEPLETED OIL AND GAS RESERVOIRS

Following more than a century of intensive petroleum exploration, thousands of oil and gas fields are approaching the ends of their economically productive lives (Davison *et al.*, 2001). Some of these exhausted fields could act as storage sites for CO_2. As in the case of producing fields, the general concept of CO_2 disposal in depleted oil and gas reservoirs is that the hydrogeological conditions that allowed the hydrocarbons to accumulate in the first place will also permit the accumulation and trapping of CO_2 in the space vacated by the produced hydrocarbons (Hitchon *et al.*, 1999; Gentzis, 2000). The caprock that prevented the escape of oil and gas over geological time, should retain the sequestered CO_2 for thousands of years (Bachu, 2001), as long as it is not damaged as a result of overpressuring during the CO_2 injection (van der Meer, 1993), by the presence of unsealed, improperly completed or abandoned wells (Hitchon *et al.*, 1999), tectonic activity or pH change.

About 80% of the world's hydrocarbon fields are at depths greater than 800m (IEA website) thus meeting the criteria for the pressure and temperature needed to efficiently store CO_2 as a supercritical fluid (van der Meer, 1993). Existing infrastructure and reservoir properties make storage of CO_2 in depleted oil and gas reservoirs a simpler option than other forms of CO_2 sequestration (Bachu, 2000a).

Closed, underpressured **oil reservoirs** that have not been invaded by water should have good sequestration capacity (Bachu, 2001). Oil field primary recovery varies from 5% to 40% (van der Meer, 2002); thus, depending on the extraction technology used and economic conditions that prevailed during the active life of the reservoir (Bachu *et al.*, 2000), significant oil reserves may remain in the reservoir. Therefore, if exhausted oil fields were used for CO_2 storage, substantial amounts of oil could be recovered (van der Meer, 2002). Depleted hydrocarbon reservoirs that are filled with connate water (fully water saturated reservoirs) offer limited storage capacity. The injected CO_2 would have to displace the connate water of the reservoir. Storage of CO_2 in water-saturated reservoirs would in practice amount to aquifer storage (Bachu, 2000a; van der Meer, 2002) as described later in this paper.

Closed, underpressured, depleted **gas reservoirs** are excellent geological traps for CO_2 storage. Firstly, primary recovery of gas fields usually removes as much as 95% of the original gas in place (Bachu, 2001), creating large storage potential. Secondly, the injected CO_2 can be used to restore the reservoir to its original pressure (Bachu *et al.*, 2000), thereby preventing possible collapse or man-induced subsidence. Thirdly, the trapping mechanism that retained hydrocarbons in the first place should ensure that CO_2 does not reach the surface (Bachu *et al.*, 2000). And lastly, the existing surface and downhole infrastructure used for production of gas is ideally suited for transportation and injection of supercritical CO_2.

Spatial association between hydrocarbon production and the presence of reservoirs suitable for CO_2 sequestration may result in shared infrastructure and reduction of transportation costs. Furthermore, depleted hydrocarbon fields commonly have an established geological database and as such, reservoir characteristics are well known. Currently, the petroleum industry is reluctant to consider storage of CO_2 in depleted hydrocarbon reservoirs, because abandoned fields will still contain oil and gas resources (U.S. Dept of Energy, 2002), which potentially have economic value if oil prices were to rise enough or new EOR techniques were developed in the future (Davison *et al.*, 2001; Bachu *et al.*, 2000). Today, sequestration of CO_2 in depleted oil reservoirs offers little or no economic benefit for the oil companies; however these reservoirs may become a base of the future CO_2 disposal industry.

CO_2 STORAGE IN COALBEDS

Coalbeds are a potential storage medium for CO_2. British Columbia has abundant coal resources, some of them lie at depths too great to be considered for conventional mining. CO_2 can be injected into suitable coal seams where it will be adsorbed onto the coal, stored in the pore matrix of the coal seams, and locked up permanently. An alternative to CO_2-only storage is injection of flue gas, a mixture of CO_2 and nitrogen (N_2) into coalbeds. According to Reeve (2000), flue gases account for 80% of CO_2 emissions in western Canada. Although in British Columbia flue gases represent much smaller percentage of total emissions, the injection of flue gas may avoid the high cost of CO_2 separation (Law *et al.*, 2002).

CO2-ENHANCED COALBED METHANE RECOVERY

[illegible]

[illegible]

[illegible]

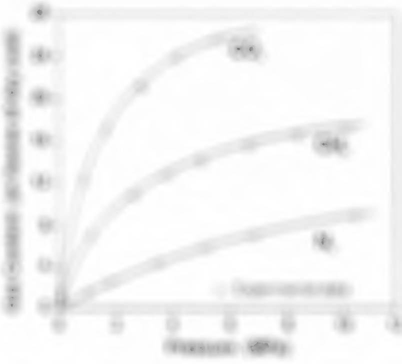

[illegible]

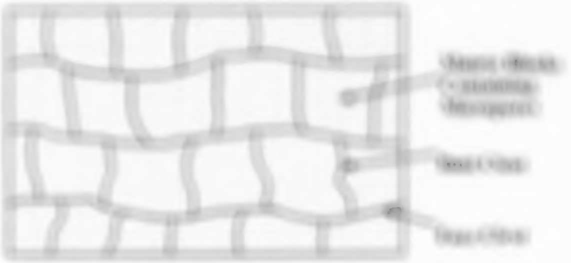
Matrix Blocks Containing Micropores
Butt Cleat
Face Cleat

[illegible]

[illegible]

[illegible]

[illegible]

- [illegible]

[illegible]

- [illegible]
- [illegible]

[illegible]

CO₂ STORAGE IN DEEP AQUIFERS

[illegible]

[illegible]

TABLE 1
[illegible]

Storage Option	Global Capacity	
	Gt CO₂	[illegible]
Depleted oil and gas fields	920	45
Deep saline aquifers	400–10,000	20–500
Unminable coal seams	>15	>1

[illegible]

[illegible] **hydrodynamic trapping** [illegible]

[illegible] **mineral trapping** [illegible]

[illegible]

[illegible]

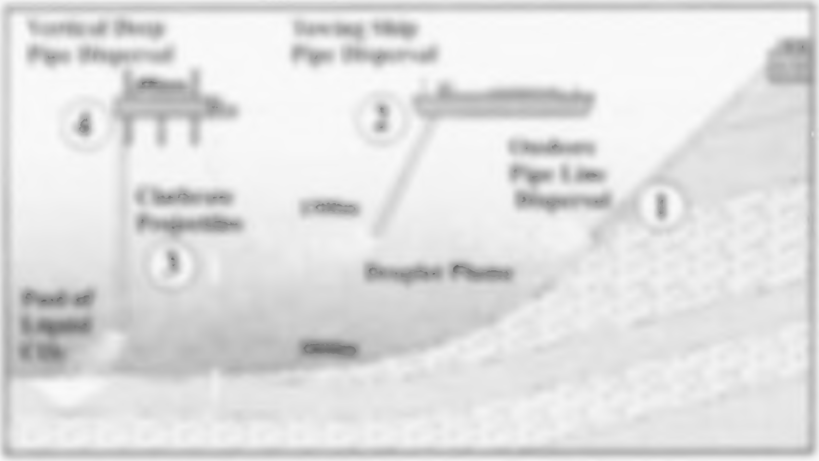

Figure 6. Compilation diagram of proposed methods for ocean disposal of CO_2. Method 1 and 2 dispose of CO_2 by injecting a droplet plume, which dissolves into the ocean water. Method 3 and 4 involve sequestration of CO_2 as clathrate hydrates.

Injection of CO_2 into deep saline aquifers relies on existing technology. Since 1996, Statoil injects about 1 million tonnes of CO_2 per year into a deep aquifer offshore Norway (Chadwick *et al.*, 2002). Sequestration of the CO_2 waste, a by-product of natural gas production, saves the company from paying a Norwegian CO_2 tax (Gentzis, 2000).

DEEP OCEAN DISPOSAL OF CO_2

The ocean is the largest sink available for disposal of CO_2 with a residence time of four to five hundred years (Gentzis, 2000). The oceans contain a stratified thermocline, which is located between the surface layer and the deep ocean. Its waters circulate between surface and deep layers on varying time scales from 250yrs in the Atlantic Ocean to 1000yrs for parts of the Pacific Ocean (Wigmore *et al.*, 2002; Ormerod *et al.*, 2002). The atmosphere and the ocean are in contact over 70% of the globe and there is a continuous exchange of inorganic carbon between them. Oceans are, at present time, removing about six gigatonnes CO_2/year from the atmosphere (Ormerod *et al.*, 2002). Disposing anthropogenic CO_2 in the deep ocean would accelerate a natural process. CO_2 could be injected as a liquid below the thermocline at depths greater than 1500m and be sequestered either by dissolution in the water column or by formation of CO_2 hydrates (Figure 6).

STORING CO_2 BY DISSOLUTION

One approach involves transporting liquid CO_2 from shore by pipeline and then discharging it from a manifold lying on the ocean bottom, forming a **droplet plume**. Since liquid CO_2 is less dense than seawater, the CO_2 droplets will rise until they are dissolved into the seawater and the CO_2-charged solution spreads laterally into the (stratified) surrounding seawater. The dissolved CO_2 may travel in the thermocline, and eventually (after hundreds of years) circulate back into the atmosphere. The deeper the CO_2 is injected, the more effectively it is sequestered, but injecting deeper requires more advanced technologies (Ormerod *et al.*, 2002). The oil and gas industry have established technology to construct vertical risers in deep water and to lay seabed oil and gas pipelines in depths down to 1600m (Ormerod *et al.*, 2002), suggesting that this method is technically feasible.

Alternatively, liquid CO_2 could be transported by a tanker and discharged from a pipe towed by a moving ship. The Japanese R&D program for ocean sequestration of CO_2 is currently in phase II of a large-scale "moving ship" scheme in the western North Pacific to assess environmental impact and CO_2 plume behaviour (Murai *et al.*, 2002). Studies by Ozaki *et al.* (2001) have shown that CO_2 injection would be most effective at relatively slower rates (larger droplet size) and at depths greater than 1500m (Ormerod *et al.*, 2002). Such a depth is well within the capability of present day subsea pipeline technology and CO_2 could be transported by a tanker, like those used currently for transportation of liquid petroleum gas (Ormerod *et al.*, 2002).

STORING CO_2 AS CLATHRATES

Another method for ocean disposal of CO_2 involves sequestration of CO_2 at depths in excess of 3000 meters. At these depths, due to the high pressure and low temperatures (Ozaki *et al.*, 2001) CO_2 exists in the form of a clathrate hydrate, an ice-like combination of CO_2 and water (Brewer *et al.*, 2000). Pure CO_2-hydrate is denser than seawater and will generate a sinking plume, settling on the bottom of the ocean (Brewer *et al.*, 2000). CO_2 sequestered in this way would form submarine pools in hollows or trenches in the deep sea. Dissolution of CO_2 into the overlying seawater would be reduced significantly due to formation of the CO_2 hydrates. Direct disposal of CO_2 at great depths is currently not technically feasible, however, it may be possible to send cold CO_2 (dry ice) from mid-depth to the ocean floor (Aya *et al.*, 2002). With a density greater than seawater, cold CO_2 will sink to the ocean bottom and be effectively stored. The Monterey Bay Aquarium Research Institute (MBARI) has recently conducted a series of controlled experiments that involve release of cold CO_2 slurry at depths of 350-500m (Aya *et al.*, 2002).

Yet another method proposes disposal of CO_2 as **clathrate blocks**. Studies on this disposal method confirm that streamlined blocks have higher terminal velocity and thus reach the seabed faster than equidimensional blocks (Guevar *et al.*, 1996). As large as 1000 tons and shaped like a projectile, these blocks could penetrate into the deep seabed where the solid CO_2 would physically and chemically interact with the sediments before reacting with the ocean water. The retention times could, therefore, be significantly increased as compared to the gaseous or liquid CO_2 disposal methods (Guevar *et al.*, 1996). According to the IEA this method is currently not economically feasible (Ormerod *et al.*, 2002).

Further studies on ocean disposal of CO_2 include **fertilising the oceans** with additional nutrients to increase draw-down of CO_2 from the atmosphere (Ormerod *et al.*, 2002). Addition of nutrients such as nitrates and phosphates or iron may increase production of biological material, thereby drawing down additional CO_2 from the atmosphere through photosynthesis of the phytoplankton (Ormerod *et al.*, 2002). Should this method prove to be feasible, the fishing industries may benefit from the resulting increase in the fish population, with atmospheric CO_2 sequestration as a secondary benefit, however the overall impact on the marine ecosystem is not well understood.

All the above described ocean disposal methods could potentially cause at least a local change in pH of the ocean water. Marine communities are, in general, intolerant to changes in the pH. Thus, due to environmental impacts on the marine ecosystem and associated public disapproval, ocean sequestration of CO_2 is not currently considered as an attractive option. The situation may change if the development of extensive CH_4 clathrate deposits along the BC coast takes place.

STORAGE IN SALT CAVERNS

Underground caverns, such as mined salt domes, could be created to store CO_2. Salt is generally found as intrusive (domal or ridge) deposits whereby salt from a major underlying source has been forced up into overlying formations. Salt caverns are created by solution mining, a process in which water is injected down a well, to dissolve the salt, and the brine solution is pumped out, creating large cavities. These caverns can be up to 500 000 m^3 in volume (Bachu, 2000a), and since salt is highly impermeable (Marck *et al.*, 1996) these spaces could provide a long-term solution to CO_2 sequestration. Solid CO_2 (dry ice) could also be stored in these repositories, surrounded by thermal insulation to minimise heat transfer and loss of CO_2 gas (Davison *et al.*, 2001). The technology has been developed and applied for salt mining and underground storage of petroleum, compressed air and natural gas (Bachu, 2000a; Crossley, 1998; Istvan, 1983). Although salt and rock caverns theoretically have a large storage capacity, the associated costs are very high and the environmental problems relating to the mined rock and disposal of large amounts of brine are significant (Kolkas-Mossbah and Friedman, 1997). Based on current technology, storage of CO_2 in underground salt caverns is uneconomical for the time being.

MINERAL CARBONATION

Mineral carbonation is a CO_2 sequestration concept where CO_2 is chemically combined in an exothermic reaction with readily available Mg or Ca-silicate minerals to form carbonates and other stable by-products (Seifritz, 1990; Gerdemann *et al.*, 2002; O'Connor *et al.*, 2000). Both Mg and Ca carbonates are stable on geologic time-scale, potentially storing CO_2 for millions of years. Mg-silicates are favoured relative to Ca-silicates because they are more widespread, form larger bodies and contain more reactive material per tonne of rock (Lackner *et al.*, 1997; Kohlmann *et al.*, 2002). Wide variety of Mg-bearing materials, such as enstatite, asbestos tailings (Fauth and Soong, 2001), fly ash and other industrial residues were investigated as potential starting materials for the industrial carbonation process, however, in the light of recent laboratory tests, olivine [$(Mg,Fe)_2SiO_4$] and serpentine [$Mg_3Si_2O_5(OH)_4$] appear as the most promising. The two reactions below illustrate the CO_2 carbonation principle using *olivine* and serpentine as examples:

$$Mg_2SiO_4[olivine] + 2CO_2 \Rightarrow 2MgCO_3[magnesite] + SiO_2 \quad (1)$$

$$Mg_3Si_2O_5(OH)_4[serpentine] + 3CO_2 \Rightarrow 3MgCO_3[magnesite] + 2SiO_2 + H_2O \quad (2)$$

In nature, carbonation reactions involving silicates are slow (Kohlmann and Zevenhoven, 2001). Currently, a sequestration plant can be visualized as a blender operating at high temperature-pressure conditions (Figure 7). For the

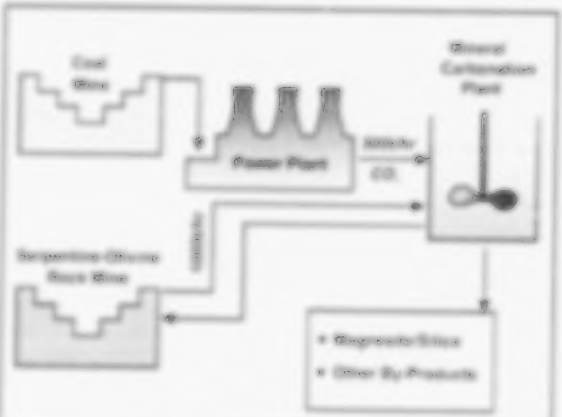

Figure 7. Idealized view of a mineral carbonation plant. (Modified from Bauer, 2001)

industrial CO_2 sequestration applications, carbonation reactions have to be accelerated by increasing surface area of the Mg-silicate, agitating the slurry (O'Connor *et al.*, 1999; Dahlin *et al.*, 2000) and by adding catalysts (for example, NaCl and $NaHCO_3$ and HCl) to the solution/slurry prior to the carbonation process (Dahlin *et al.*, 2000; Goldberg and Walters, 2002; Jia and Anthony, 2002; Fauth and Soong, 2001; Lackner *et al.*, 1998). Optimization of the carbonation process by controlling temperature and partial pressure of CO_2 (P_{CO2}) may be also a major factor (O'Connor *et al.*, 1999; Dahlin *et al.*, 2000).

Subjecting Olivine to supercritical conditions is believed to improve olivine dissolution rates (O'Connor *et al.*, 2000; 1999). Furthermore, in the case of serpentine, an energy-intensive heat pre-treatment (activation-destabilization of the crystal structures) at temperatures above 900°C is required. Such pre-treatment removes chemically bound water and increases overall porosity (Gerdemann *et al.*, 2002; Kohlmann *et al.*, 2002; Goldberg and Walters, 2002).

There is currently no mineral sequestration plant in operation, however members of the Mineral Sequestration Working Group are developing pilot-scale mineral carbonation units and according to their plan a 10 MW demonstration plant will be operational by 2008 (Goldberg and Walters, 2002). The concept is currently incorporated into the design of the coal-fuel electricity generating plant of the ZECA Corporation (New Mexico). However, it may be also applied elsewhere.

ADVANTAGES OF MINERAL CARBONATION

Serpentine and Olivine are the two most likely silicates, which could be used as starting materials in mineral sequestration. Olivine is favoured because it reacts better without the energy-intensive pretreatment that serpentine requires. In contrast to the previously described methods, once the CO_2 is locked into a carbonate (a mineral stable on geological time scales) there is no possibility for an accidental release of CO_2. Furthermore, direct carbonation does not lead to problematic by-products (Lackner *et al.*, 1998). Mineral carbonation may, therefore, benefit from public acceptance (Lackner *et al.*, 1997).

The costs of the CO_2 disposal could be higher than for the injection of CO_2 into oil and gas reservoirs or deep coal seams. These costs may be reduced if the potential for industrial applications of the product (depending on acceptable purity, form, grain size, particle shape and chemical properties), and metal recoveries could be realized. Magnesite has a wide variety of industrial applications (Simandl, 2002) and the same applies for silica. The carbonation process may also become a new source of Fe, Mn, Co, Cr and Ni recovered during the breakdown of Mg silicate's crystal structure (Haywood *et al.*, 2001; O'Connor *et al.*, 2000). Technology breakthroughs and the law of "supply and demand" will determine if, and to what extent the sequestration costs an be offset by these potential byproducts.

Large-scale CO_2 sequestration as mineral carbonates will require enormous amounts of mineral (Kohlmann *et al.*, 2002). For a typical power plant, the mass flows of fuel and carbonated mineral will be of the same order of magnitude. For example, studies suggests that for a single power plant, generating approximately 10 000 tons CO_2 per day, over 23 000 to 30 000 tons per day of Mg-silicate ore would be required (Dahlin *et al.*, 2000; O'Connor *et al.*, 2000). If mineral sequestration becomes a reality and serpentine becomes a workhorse of mineral CO_2 sequestration, no shortage of starting material is likely to occur in BC. However, if forsterite (Mg-end member of olivine) is used as starting material, supplies are limited and geographically constrained. Under ideal conditions, coal and Mg-silicate mines would be located close to each other. In most cases, serpentine is an unwanted by-product of metal and chrysotile mining, but in some locations, this waste may become a sought after commodity when its potential for CO_2 sequestration is realized. Should mineral sequestration of CO_2 become an established technology, then new opportunities will arise for potential producers of magnesium silicates and owners of magnesium silicate-rich tailings.

The British Columbia Geological Survey may not participate in the development of mineral sequestration technology, however, the inventory, characterization and documentation of potential sources of Mg-silicates is in the Survey's interest. It may attract industry to the province, should this technology become accepted.

CONCLUSIONS AND PLANS FOR FUTURE WORK

This review concentrated on the description of the main geological and mineral CO_2 sequestration methods that are currently the focus of intensive research by industrialized nations worldwide. At first glance, the most technologically mature methods are storage in active and depleted oil and gas fields, though most of the emphasis lies on maximizing oil and gas recovery rather than sequestration potential. Research relating to injection of CO_2 into deep coal seams is rapidly advancing, with CO_2-enhanced CBM recovery potentially offsetting sequestration costs. Saline aquifers provide huge storage potential in terms of volume for CO_2 sequestration, but they are much more difficult and expensive to characterize than hydrocarbon reservoirs due to the lack of an existing exploration database. The methods , which currently encounter the most resistance from the public, are storage in salt caverns and ocean sequestration. Mineral sequestration is the only method that truly disposes of CO_2 on geological time scale, with a minimum risk for an accidental CO_2 release.

The next stage of our study will expand and summarize the relative technological maturity of the methods covered in this paper and their potential applicability to British Columbia. Since all geological and mineral CO_2 sequestration methods involve the capture and extraction of CO_2 from flue-gases or industrial streams, transportation of CO_2 and its disposal in an appropriate sink, the next stage of our study will also identify the main stationary point sources of

CO_2 emissions and the main potential carbon or CO_2 sinks in British Columbia. The relative geographic relationships between the main stationary point CO_2 sources and sinks is also an essential piece of the puzzle for conceptual decision-making and a base for rigorous CO_2 sequestration planning in British Columbia if it becomes a necessity.

ACKNOWLEDGEMENTS

We would like to thank Terry, P. Mc Cullough of BC Hydro, Stefan Bachu of Alberta Energy and Utilities Board, Barry Ryan of British Columbia Ministry of Energy and Mines and Alan A. Johnson from ZECA Corporation for reviewing the earlier version of this manuscript. Brian Grant, Derek Brown and Dan Green from British Columbia Ministry of Energy and Mines greatly improved the clarity of the final version.

REFERENCES

Arri, L.E., Yee, D., Morgan, W.D. and Jeansonne, M.W. (1992): Modeling Coalbed Methane Production with Binary Gas Sorption. *Society of Petroleum Engineers Paper, No 24363*, pages 459-472.

Aya, I., Kojima, R., Yamane, K., Brewer, P.G. and Peltzer, III, E.T. (2002): In Situ Experiments of Cold CO_2 Release in Mid-Depth, *Proceedings of the 6th International Conference on Greenhouse Gas Control Technologies, Elsvier,* London UK, (A3-3).

Aycaguer, A. Lev-On, M. and Winer, A. M. (2001): Reducing Carbon Dioxide Emissions with Enhanced Oil Recovery Projects: A Life Cycle Assessment Approach. *Energy and Fuels*, Volume 15, pages 303-308.

Bachu, S. (2001): Identification of Best Sites and Means for CO_2 Sequestration in the Alberta Basin, Canada; in American Association of Petroleum Geologists 2001 Annual Meeting, *Annual Meeting Expanded Abstracts - American Association of Petroleum Geologists*, 9 pages.

Bachu, S., Brulotte, M., Brobe, M. and Stewart, S. (2000): Suitability of the Alberta Subsurface for Carbon-Dioxide Sequestration in Geological Media. *Earth Sciences Report*, Alberta Research Council, Edmonton, AB, Canada, 86 pages.

Bachu, S. (2000a): Sequestration of CO_2 in Geological Media: Criteria and Approach for Site Selection in Response to Climate Change, *Energy Conversion & Management*, Volume 41, Number 9, pages 953-70.

Bachu, S., Gunter, W. D. and Perkins, E.H. (1994): Aquifer Disposal of CO_2: Hydrodynamic and Mineral Trapping, *Energy Conversion & Management*, Volume 35, pages 269-79.

Bauer, C.O. (2001): Overview-Mineral Carbonation Workshop <www.netl.doe.gov/publications/proceedings/01/minecarb/Bauer.pdf>

Benson, S.M., Hepple, R., Apps, J., Tsang, C.F. and Lippmann, M. (2002): Comparative Evaluation of Risk Assessment, Management and Mitigation Approaches for Deep Geologic Storage of CO_2, *E.O. Lawrence Berkeley National Laboratory, LBNL-51170*, 133 pages.

Benson, S.M. (2000): An Overview of Geologic Sequestration of CO_2, *Proceedings of the 8th International Energy Forum, Presented and Published in ENERGEX*, Las Vegas, NV, pages 1219-1225.

van Bergen, F., Pagnier, H.J.M, van der Meer, L.G.H., van den Belt, F.J.G., Winthaegen, P.L.A., and Westerhoff, R.S. (2002): Development of a Field Experiment of CO_2 Storage in Coal seams in the Upper Silesian Basin of Poland (Recopol), *Proceedings of the 6th International Conference on Greenhouse Gas Control Technologies, Elsvier,* London UK, (J1-4).

van Bergen, F. and Pagnier, H.J.M. (2001): CO_2 Sequestration in Coal - a Potentially Clean Energy Cycle, *Greenhouse Issues, IEA Greenhouse Gas R&D Programme*, Volume 56.

Brewer, P.G., Peltzer, E.T., Friederich, G., Aya, I. And Yamane, K. (2000): Experiments on the Ocean Sequestration of Fossil Fuel CO_2: PH Measurements and Hydrate Formation, *Marine Chemistry*, Volume 72, pages 83-93.

Chadwick, R.A., Zweigel, P., Gregersen, U., Kirby, G.A., Holloway, S. and Johannessen, P.N. (2002): Geological Characteristics of CO_2 Storage Sites: Lessons from Sleipner, Northern North Sea, *Proceedings of the 6th International Conference on Greenhouse Gas Control Technologies, Elsvier,* London UK, (B1-3).

Crossley, N.G. (1998): Conversion of LPG Salt Caverns to Natural Gas Storage "A TransGas Experience", *Journal of Canadian Petroleum Technology*, Volume 37, Number 12, pages 37-47.

Dahlin, D.C., O'Connor, W.K., Nilsen, D.N., Rush, G.E., Walters, R.P. and Turner, P.C. (2000): A Method for Permanent CO_2 Sequestration: Supercritical CO_2 Mineral Carbonation, *Proceedings of the 17th Annual International Pittsburgh Coal Conference*, Pittsburgh, Pennsylvania.

Davison, J., Freund, P. and Smith, A. (2001): Putting Carbon Back in the Ground. *IEA Greenhouse Gas R&D Programme*, ISBN 1 898 373 28 0, pages 26.

Environment Canada (2000): . <Http://www.ec.gc.ca/pdb/ghg/factsheets/factsheet_e.cfm>

Fauth, D.J. and Soong, Y. (2001): Mineral Sequestration Utilizing Industrial By-Products, Residues, and Minerals, *National Energy Technology Laboratory (NETL), Mineral Carbonation Workshop*.

Fokker, P.A. and van der Meer, L.G.H. (2002): The injectivity of Coalbed CO_2 Injection Wells. *Proceedings of the 6th International Conference on Greenhouse Gas Control Technologies, Elsvier,* London UK, (J1-1).

Gale, J. (2002): Geological Storage of CO_2: What's Known, Where are the Gaps and What More Needs to be Done. *Proceedings of the 6th International Conference on Greenhouse Gas Control Technologies, Elsvier,* London UK, (A1-1).

Gentzis, T. (2000): Subsurface Sequestration of Carbon Dioxide - an Overview from an Alberta (Canada) Perspective. *International journal of Coal Geology*, Volume 43, pages 287-305.

Gerdemann, S.J., Dahlin, D.C. and O'Connor, W.K. (2002): Carbon Dioxide Sequestration by Aqueous Mineral Carbonation of Magnesium Silicate Minerals, *Proceedings of the 6th International Conference on Greenhouse Gas Control Technologies, Elsvier,* London UK, (K2-3).

Goldberg, P. and Walters, R. (2002): A Program to Develop CO_2 Sequestration via Mineral Carbonation, *Proceedings of the 6th International Conference on Greenhouse Gas Control Technologies, Elsvier,* London UK, (K2-1).

Guever, P., Fruman, D.H. and Murray, N. (1996): Conceptual Design of an Integrated Solid CO_2 Penetrator Marine Disposal System, *Energy Conversion & Management*, Volume 37, Numbers 6-8, pages 1053-1060.

Gunter, W.D., Bachu, S. and Benson, S.M. (in review): The Role of Hydrogeological and Geochemical Trapping in Sedimentary basins for Secure Geological Storage for Carbon Dioxide, 25 pages.

Gunter, W.D., Wiwchar, B. and Perkins, E.H. (1997): Aquifer Disposal of CO_2-Rich Greenhouse Gases: Extension of the Time Scale of Experiment for CO_2-Sequestering Reactions by Geochemical Modelling, *Mineralogy and Petrology*, Volume 59, pages 121-140.

Haywood, H. M., Eyre, J. M. and Scholes, H. (2001): Carbon Dioxide Sequestration as Stable Carbonate Minerals; Environmental Barriers. *Environmental Geology* (Berlin), Volume 41, Numbers 1-2, pages 11-16.

Hitchon, B., Gunter, W.D., Gentzis, T. and Bailey, R.T. (1999): Sedimentary Basins and Greenhouse Gases: a Serendipitous Association, *Energy Conversion & Management*, Volume 40, Number 8, pages 825-43.

International Energy Agency Greenhouse Gas R&D Programme <www.ieagreen.org.uk/>

Istvan, J.A. (1983): Storage of Natural Gas in Salt Caverns, *Proceedings of the 6th Salt Symposium*, Toronto, May 26-27th, 25 pages.

Ivory, J., Gunter, W.D., Law. D. and Wong, S. (2000): Recovery of CO_2 from Flue Gas, CO_2 Sequestration, and Methane Production from Coalbed Methane Reservoirs. *Proceedings of the International Symposium on Ecomaterials*, Ottawa, August 20-23, pages 487-501.

Jia, L. and Anthony, E.J. (2002): Mineral Carbonation and Zeca, *Proceedings of the 6th International Conference on Greenhouse Gas Control Technologies, Elsvier*, London UK, (K2-2).

Jimenez, J.A. and Chalaturnyk, R.J. (2002): Are Disused Hydrocarbon Reservoirs Safe for the Geological Storage of CO_2? *Proceedings of the 6th International Conference on Greenhouse Gas Control Technologies, Elsvier*, London UK, (G1-1).

Kohlmann, J., Zevenhoven, R. and Mukherjee, A.B. (2002): Carbon Dioxide Emission Control by Mineral Carbonation: The Option for Finland, *Proceedings of the 6th European Conference on Industrial Furnaces and Boilers*, Estoril Lisbon, Portugal.

Kohlmann, J. and Zevenhoven, R. (2001): The Removal of CO_2 from Flue Gases using Magnesium Silicates, in Finland, *Proceedings of the 11th International Conference on Coal Science*, San Francisco, California.

Koide, H., Tazaki, Y., Noguchi, Y., Iijima, M., Ito, K. and Shindo, Y. (1996): Underground Storage of Carbon Dioxide in Depleted Natural Gas Reservoirs and in Useless Aquifers, *Engineering Geology*, Volume 34, pages 175-179.

Kolkas-Mossbah, M. and Friedman, G.M. (1997): Subsurface Brine Disposal in the Cambro-Lower Ordovician of Central and Western New York: Implications for New Salt-Cavern Gas Storage Reservoirs, *AAPG Bulletin*, Volume 81, Number 8, page 1390.

Krooss, B.M., van Bergen, F., Gensterblum, Y., Siemons, N., Pagnier, H.J.M. and David, P. (2002): High-Pressure Methane and Carbon Dioxide Adsorption on Dry and Moisture-equilibrated Pennsylvanian Coals, *International Journal of Coal Geology*, Volume 51, pages 69-92.

Lackner, K.S., Butt, D.P., Wendt, C.H. and Ziock, H. (1998): Mineral carbonates as Carbon Dioxide Sinks, *Los Alamos National Laboratory*, Los Alamos, LA-UR-98-4530, 9 pages.

Lackner, K.S., Butt, D.P. and Wendt, C.H. (1997): Magnesite Disposal of Carbon Dioxide. *Proceedings of the 22nd International Technical Conference on Coal Utilization & Fuel Systems*, Clearwater Florida, pages 419-430.

Law, D.H.S., van der Meer, L.H.G. and Gunter, W.D. (2002): Comparison of Numerical Simulators for Greenhouse Gas Storage in Coalbeds, Part II: Flue Gas Injection. *Proceedings of the 6th International Conference on Greenhouse Gas Control Technologies, Elsvier*, London UK, (J1-3).

Macdonald, D., Wong, S., Gunter, B., Nelson, R. and Reynen, B. (2002): Surface Facilities Computer Model: an Evaluation Tool for Enhanced Coalbed Methane Recovery, *Proceedings of the 6th International Conference on Greenhouse Gas Control Technologies, Elsvier*, London UK, (J1-5).

Mavor, M.J., Gunter, W.D., Robinson, J.R., Law, D.H.S. and Gale, J. (2002): Testing for CO_2 Sequestration and Enhanced Methane Production from Coal, *SPE Paper 75680, Presented at the SPE Gas Technology Symposium*, May 30-June 2, Calgary, 14 pages.

McKee, B. (2002): Solutions for the 21st Century-Zero Emissions Technology for Fossil Fuels, *International Energy Agency*, 48 pages.

van der Meer, L.G.H. (2002): CO_2 Storage in the Subsurface, *Proceedings of the 6th International Conference on Greenhouse Gas Control Technologies, Elsvier*, London UK, (A1-0).

van der Meer, L.G.H. (1993): The Conditions Limiting CO_2 Storage in Aquifers. *Energy Conversion and Management*, Volume 34, pages 959-966.

Mignone, B.K., Sarmiento, J.L., Slater, R.D. and Gnanadesikan, A. (2002): Sensitivity of Sequestration Efficiency to Mixing Processes in the Global Ocean, *Proceedings of the 6th International Conference on Greenhouse Gas Control Technologies, Elsvier*, London UK, (A3-1).

Moberg, R. (2001): The Weyburn CO_2 Monitoring and Storage Project. *Greenhouse Issues, IEA Greenhouse Gas R&D Programme*, Volume 57.

Murai, S., Ohsumi, T., Nishibori, F. and Ozaki, M. (2002): The Second Phase of Japanese R&D Program for CO_2 Ocean Sequestration, *Proceedings of the 6th International Conference on Greenhouse Gas Control Technologies, Elsvier*, London UK, (A3-2).

Murck, B.W., Skinner, B.J. and Porter, S.C. (1996): Environmental Geology, *John Wiley & Sons, Inc.*, 476 pages.

O'Connor, W.K., Dahlin, D.C., Nilsen, D.N., Walters, R.P. and Turner, P.C. (2000): Carbon Dioxide Sequestration by Direct Mineral Carbonation with Carbonic Acid, *Proceedings of the 25th International Technical Conference on Coal Utilization & Fuel Systems, Coal Technology Association*, Clearwater, Florida.

O'Connor, W.K., Dahlin, D.C., Turner, P.C. and Walters, R.P. (1999): Carbon Dioxide Sequestration by Ex-Situ Mineral Carbonation, *Proceedings of the 2nd Dixy Lee Ray Memorial Symposium: Utilization of Fossil Fuel-Generated Carbon Dioxide in Agriculture and Industry*, Washington, D.C.

Oldenburg, C.M. and Benson, S.M. (2002): CO_2 Injection for Enhanced Gas Production and Carbon Sequestration, *Proceedings of the SPE International Petroleum Conference and Exhibition, Mexico, Society of Petroleum Engineers*, 10-12 February, 2002.

Oldenburg, C.M., Pruess, K. and Benson, S.M. (2001): Process Modeling of CO_2 Injection into Natural Gas Reservoirs for Carbon Sequestration and Enhanced Gas Recovery, *Energy & Fuels*, Volume 15, pages 293-298.

Ormerod, W.G., Freund, P. and Smith, A. (2002): Ocean Storage of CO_2, *IEA Greenhouse Gas R&D Programme*, ISBN 1 898 373 30 2, 26 pages.

Ozaki, M., Minamitura, J., Kitajima, Y, Mizokami, S., Takeuchi, K. and Hatakenaka, K. (2001): CO_2 Ocean Sequestration by Moving Ships, *Journal of Marine Science and Technology*, Volume 6, pages 51-58.

Reeve, D.A. (2000): The Capture and Storage of Carbon Dioxide Emissions -A Significant Opportunity to Help Canada Meet its Kyoto Targets, prepared under NRCan Contract File No. NRCan-00-0195. *Office of Energy Research and Development, Natural Resources Canada, Global Change Strategies International Inc.*, 20 pages.

Reeves, S. (2002): Coal-Seq Project Update: Field Studies of ECBM Recovery/CO_2 Sequestration in Coal Seams. *Proceedings of the 6th International Conference on Greenhouse Gas Control Technologies, Elsvier*, London UK, (J1-2).

Rice, D.D., Law, B.E., and Clayton, J.L. (1993): Coalbed gas—An Undeveloped Resource, *in* Howell, D.G., ed., The Future of

Energy Gases: *U.S. Geological Survey Professional Paper* 1570, pages 389-404.

Schraufnagel, R.A. (1993): Coalbed Methane Production, *in* Law, B.E. and Rice, D.D., eds., Hydrocarbons From Coal: *AAPG Studies in Geology*, Volume 38, pages 341-359.

Seifritz, W. (1990): CO_2 disposal by means of silicates, *Nature*, Volume 345, page 486.

Shi, J.Q., Durucan, S. and Sinka, I.C. (2002): Key Parameters Controlling Coalbed Methane Cavity Well Performance, *International Journal of Coal Geology*, Volume 49, pages 19-31.

Smith, L.K. (1998): Carbonate Cement Dissolution During a Cyclic CO_2 Enhanced Oil Recovery Treatment. *Spec. Publs int. Ass. Sediment*, Volume 26, pages 483-499.

Simandl, G.J. (2002): The Chemical Characteristics and Development Potential of Magnesite Deposits in British Columbia, Canada, *in*: Scott, P.W. & Bristow, C.M. (eds); *Industrial Minerals and Extractive Industry Geology, Geological Society*, London, pages 169-178.

Shrivastava, R. and Huang, S. (1997): Technical Feasibility of CO_2 Flooding in Weyburn Reservoir-A Laboratory Investigation, *The Journal of Canadian Petroleum Technology*, Volume 36, Number 10, pages 48-55.

Stevens, S.H., Kuuskraa, V.A. and Gale, J. (2000): Sequestration of CO_2 in Depleted Oil & Gas Fields: Global Capacity, Costs and Barriers, *Proceedings from the 5th Greenhouse Gas Control Technologies*, Elsevier, London UK

Tontiwachwuthikul, P., Chan, C.W., Kritpiphat, W., Demontigny, D., Skoropad, D., Gelowitz, D., Aroonwilas, A., Mourits, F., Wilson, M. and Ward, L. (1998): Large Scale Carbon Dioxide Production from Coal-fired Power Stations for Enhanced Oil Recovery: A New Economic Feasibility Study. *The Journal of Canadian Petroleum Technology*, Volume 37, Number 11, pages 48-55.

U.S. Department of Energy (2002): Carbon Sequestration Technology Roadmap: Pathways to Sustainable Use of Fossil Energy, *Office of Fossil energy, National Energy Technology Laboratory (NETL)*, 22 pages.

Whittaker, S.G. and Rostron, B. (2002): Geological Storage of CO_2 in a Carbonate Reservoir within the Williston Basin, Canada: An Update. *Proceedings of the 6th International Conference on Greenhouse Gas Control Technologies, Elsvier,* London UK, (D1-1).

Wong, S., MacLeod, K., Wold, M., Gunter, W.D., Mavor, M.J. and Gale, J. (2001): CO_2-Enhanced Coalbed Methane Recovery Demonstration Pilot-A Case for Australia, *Proceedings of the 2001 International Coalbed Methane Symposium*, May 14-18, Alabama, U.S., pages 75-86.

Wong, S., Gunter, W.D. and Mavor, M.J. (2000): Economics of CO_2 Sequestration in Coalbed Methane Reservoirs, *Proceedings of SPE/CERI Gas Technology Symposium 2000*, SPE 59785, April 3-5, Calgary, Alberta, pages 631-638.

Wong, S. and Gunter, B. (1999): Testing CO_2-Enhanced Coalbed Methane Recovery. *Greenhouse Issues, IEA Greenhouse Gas R&D Programme*, Volume 45.

Queen's Printer for British Columbia©
Victoria, 2003

QP403281